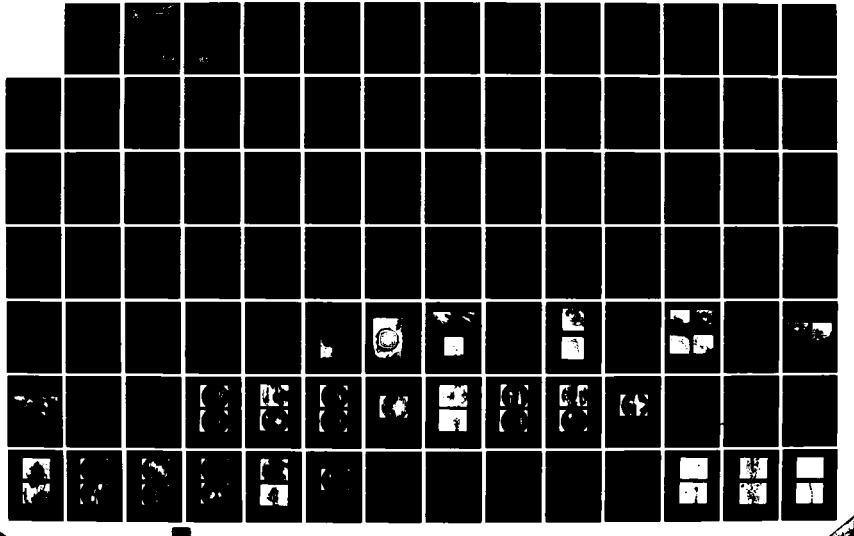
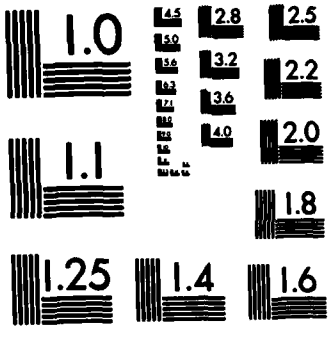
AD-A122 156 OIL ANALYSIS(U) NAVAL AIR ENGINEERING CENTER LAKEHURST 1/6
NJ SUPPORT EQUIPMENT ENGINEERING DEPT P B SENHOLZI
23 AUG 82 NAEC-92-153

UNCLASSIFIED F/G 11/8 NL





MICROCOPY RESOLUTION TEST CHART
NATIONAL BUREAU OF STANDARDS-1963-A

NAVAL AIR ENGINEERING CENTER
LAKEHURST, N.J.
08733

REPORT NAEC-92-153

OIL ANALYSIS

Advanced Technology Office
Support Equipment Engineering Department
Naval Air Engineering Center
Lakehurst, New Jersey 08733

23 AUGUST 1982

Final Report
AIRTASK A3400000/051B/1F53B7401

AD A122156

APPROVED FOR PUBLIC RELEASE:
DISTRIBUTION UNLIMITED

DTIC
ELECTE
DEC 3 1982
S D
D

Prepared for

Commander, Naval Air Systems Command
AIR-340
Washington, D.C. 20361

82 12 03 022

DTIC FILE COPY

NAEC-92-153

OIL ANALYSIS

Prepared by: Peter B. Senholzi
P. B. Senholzi

Reviewed by: P. V. Ciekurs
P. V. Ciekurs
Advanced Technology Office
(92A31)

Approved by: F E Evans
F. E. Evans
Support Equipment Engineering Superintendent

NOTICE

Reproduction of this document in any form by other than naval activities is not authorized except by special approval of the Secretary of the Navy or the Chief of Naval Operations as appropriate.

The following espionage notice can be disregarded unless this document is plainly marked CONFIDENTIAL or SECRET.

This document contains information affecting the national defense of the United States within the meaning of the Espionage Laws, Title 18, U.S.C., Sections 793 and 794. The transmission or the revelation of its contents in any manner to an unauthorized person is prohibited by law.

8-23-82 NAF

UNCLASSIFIED

SECURITY CLASSIFICATION OF THIS PAGE (When Data Entered)

REPORT DOCUMENTATION PAGE		READ INSTRUCTIONS BEFORE COMPLETING FORM
1. REPORT NUMBER NAEC-92-153	2. GOVT ACCESSION NO. A122156	3. RECIPIENT'S CATALOG NUMBER
4. TITLE (and Subtitle) OIL ANALYSIS		5. TYPE OF REPORT & PERIOD COVERED TECHNICAL
		6. PERFORMING ORG. REPORT NUMBER NAEC-92-153
7. AUTHOR(s) P. B. SENHOLZI		8. CONTRACT OR GRANT NUMBER(s)
9. PERFORMING ORGANIZATION NAME AND ADDRESS SUPPORT EQUIPMENT ENGINEERING DEPARTMENT, CODE 92A3 NAVAL AIR ENGINEERING CENTER LAKEHURST, NEW JERSEY 08733		10. PROGRAM ELEMENT, PROJECT, TASK AREA & WORK UNIT NUMBERS A3400000/051B/1F5337401
11. CONTROLLING OFFICE NAME AND ADDRESS NAVAL AIR SYSTEMS COMMAND CODE AIR-340E WASHINGTON, D.C. 20361		12. REPORT DATE 23 August 1982 13. NUMBER OF PAGES 496
14. MONITORING AGENCY NAME & ADDRESS (if different from Controlling Office) SUPPORT EQUIPMENT ENGINEERING DEPARTMENT CODE 92A31 NAVAL AIR ENGINEERING CENTER LAKEHURST, NEW JERSEY 08733		15. SECURITY CLASS. (of this report) UNCLASSIFIED 15a. DECLASSIFICATION/DOWNGRADING SCHEDULE

16. DISTRIBUTION STATEMENT (of this Report)

Approved for public release, distribution unlimited.

17. DISTRIBUTION STATEMENT (of the abstract entered in Block 20, if different from Report)

18. SUPPLEMENTARY NOTES

It is regretted that the originals of the following were lost during preparation of this report and, therefore, the quality of reproduction is not good:

Figures: 1-2, 5, 33, 35, 62, 65-68, 72, 94-97, 101-129, 134-138, 146, 148-149, 151, 154, 156-159

Tables: 27-28, 31-33

19. KEY WORDS (Continue on reverse side if necessary and identify by block number)

SPECTROMETRIC ANALYSIS
BEARING WEAR
FAILURE PROGRESSION MONITORING
WEAR DEBRIS ANALYSIS, WEAR REGIMES
GEAR WEAR
SLIDING CONTACT WEAR
SURFACE ANALYSIS, FILTRATION, LUBRICATION,
OIL ANALYSIS, FAILURE ANALYSIS, TRIBOLOGY
DIAGNOSTICS, BENCH TESTING, FERROGRAPHY
OIL SAMPLING, EQUIPMENT HEALTH MONITORING

20. ABSTRACT (Continue on reverse side if necessary and identify by block number)

The goal of the Oil Analysis Program was to place oil analysis on a firm technical basis. This goal was accomplished through an intensive experimental correlation effort relating wear debris characteristics to component surface wear condition. Such wear particle correlations served to highlight critical characteristics/parameters which reflect component surface wear condition.

Component testing was conducted for ball bearings, roller bearings, gears, and pistons/cylinders. Respective test programs were conducted by SKF Industries,

DD FORM 1 JAN 73 1473 EDITION OF 1 NOV 65 IS OBSOLETE
S/N 0102-LF-014-6601

UNCLASSIFIED

SECURITY CLASSIFICATION OF THIS PAGE (When Data Entered)

Incorporated, the Naval Air Propulsion Test Center, and Franklin Institute Research Laboratories. Test lubricant wear debris/particle analysis was conducted by SKF Industries, Incorporated, the Franklin Institute Research Laboratories, the National Bureau of Standards, Foxboro Analytical, and the Naval Air Engineering Center.

Four critical wear debris/particle characteristics were identified under the test program and respective correlation effort. These parameters include particle quantity/concentration, size distribution, elemental composition, and morphology.

The results of wear debris analysis compared to the physical examination of the component surface wear condition showed a good correlation in terms of monitoring the component wear regime/condition throughout their respective wear life. Based on these results, the present DOD Oil Analysis Program can be significantly improved in the areas of both effectiveness and cost.

Accession For	
NTIS GRA&I	☒
DTIC TAB	☐
Unannounced	☐
Justification	
By	
Distribution/	
Availability Codes	
Dist	Avail and/or Special
A	

DTIC COPY INSPECTED 2

SUMMARY

The goal of the Oil Analysis Program was to place oil analysis on a firm technical basis. This goal was accomplished through an intensive experimental correlation effort relating wear debris characteristics to component surface wear condition. Such wear particle correlations served to highlight critical characteristics/parameters which reflect component surface wear condition.

Component testing was conducted for ball bearings, roller bearings, gears, and pistons/cylinders. Respective test programs were conducted by SKF Industries, Incorporated, the Naval Air Propulsion Test Center, and the Franklin Institute Research Laboratories. Test lubricant wear debris/particle analysis was conducted by SKF Industries, Incorporated, the Franklin Institute Research Laboratories, the National Bureau of Standards, Foxboro Analytical, and the Naval Air Engineering Center.

Four critical wear debris/particle characteristics were identified under the test program and respective correlation effort. These parameters include particle quantity/concentration, size distribution, elemental composition, and morphology.

The results of wear debris analysis compared to the physical examination of the component surface wear condition showed a good correlation in terms of monitoring the company's wear regime/condition throughout their respective wear life. Based on these results, the present DOD Oil Analysis Program can be significantly improved in the areas of both effectiveness and cost.

THIS PAGE LEFT BLANK

INTENTIONALLY

TABLE OF CONTENTS

Section	Subject	Page
	SUMMARY	1
	LIST OF ILLUSTRATIONS	5
	LIST OF TABLES	14
I	INTRODUCTION	17
II	BACKGROUND	18
	A. General	18
	B. Oil Analysis Cycle	18
	C. Spectrometric Oil Analysis	20
III	PROGRAM DESCRIPTION	21
IV	PHASE I: DATA BASE	25
	A. General	25
	B. Wear Mode Categorization	26
	C. Wear Particle Categorization	26
V	PHASE II: LABORATORY STUDY	36
	A. General	36
	B. Analytical Techniques	36
	C. Bench Testing and Analysis	42
	D. Wear Particle Analysis Summary	363
VI	TEST RAMIFICATIONS	375
	A. General	375
	B. Fluid Sampling	375
	C. Wear Process	387
	D. Contamination/Filtration	390
	E. Lubricant Antiwear Properties	396
	F. Spectrometric Oil Analysis	400
	G. Analytical Ferrography	411

TABLE OF CONTENTS (Continued)

Section	Subject	Page
	H. Interrupted Testing	444
	I. Improved Oil Analysis Approach	444
VII	RECOMMENDATIONS AND CONCLUSIONS	457
VIII	BIBLIOGRAPHY	466
	APPENDIX A - SLIDING CONTACT TEST SEQUENCE "SB" FERROGRAPH DATA	475
	APPENDIX B - NAVAL AIR ENGINEERING CENTER TRIBOLOGY LABORATORY LUBRICANT SAMPLING PROCEDURE..	483
	GLOSSARY OF TERMS	489

LIST OF ILLUSTRATIONS

Figure	Title	Page
1	Schematic Drawings of Test Ball Bearing (Type 6309 Deep-Groove Ball Bearing)	43
2	SKF Type R2 Bearing Test Machine	45
3	Schematic Diagram of Closed-Loop Lubrication System for Oil Analysis Program	46
4	Oil-Wetted Components of the Recirculating Pump	47
5	Changes in Profile and Surface Texture of Bearing No. BC-028 Inner Ring Raceway With Rolling Contact Running Time	55
6	Surface Damage on Raceway of an As-Finished Ball Bearing (No. BA-025)	56
7	Interference Micrograph of a Vickers Indentation On a Rc50 Hardness Steel Substrate (Courtesy of Dr. A. W. Ruff, National Bureau of Standards)	57
8	Rolling Contact Induced Damage on Ball Bearing Raceway	58
9	Appearance of Spall Initiation Site and Spall on Bearing No. BA-025	60
10	Sketch of Inner Ring Ball Groove Showing the Location of Pure Rolling (Heathcote) and Sliding Regions	61
11	Progression of Failure at the 0° Vickers Indentation on Bearing No. BD-029	62
12	Damage at the 180° Vickers Indentation on Bearing No. BD-029	64
13	Appearance of the Leading and Lagging Edges of a Spall on Bearing No. BA-025 After 224.7 m.r.	65
14	Ball Bearing Test Sequences BQ and BX Ferrograph Density Data	67
15	Ball Bearing Test Sequence BQ Entry Deposit Low Magnification	68
16	Ball Bearing Test Sequence BX Entry Deposit Low Magnification	72

LIST OF ILLUSTRATIONS (continued)

Figure	Title	Page
17	Typical Ball Bearing Test Sequence Debris Concentration Versus Wear Life	76
18	Ball Bearing Test Sequence BA Ferrograph Density Data	78
19	Ball Bearing Test Sequence BA Entry Deposit Low Magnification	79
20	Ball Bearing Test Sequence BQ Ferrograph Density Data	88
21	Ball Bearing Test Sequence BX Ferrograph Density Data	89
22	Ball Bearing Test Sequence BQ Entry Deposit High Magnification	90
23	Ball Bearing Test Sequence BX Entry Deposit High Magnification	94
24	Ball Bearing Test Sequence BA Ferrograph Density Data	99
25	Ball Bearing Test Sequence BA Entry Deposit High Magnification	100
26	Particle Size Distribution Versus Wear Regime	106
27	Titanium Particles Detected in the Entry Deposit of a Ferrogram Made from an Oil Sample Taken from Bearing Test No. BR-002 Taken at 146 m.r.	109
28	Ball Bearing Sequence BZ Wear-In Debris (27 Million Revs.).	112
29	Typical Normal Rubbing Wear Particles	114
30	Ball Bearing Rolling Contact Fatigue Laminar Particles	115
31	Ball Bearing Rolling Contact Fatigue Spherical Particles	117
32	Ball Bearing Rolling Contact Fatigue Spall Particles	119
33	Ball Bearing Test Sequence BC (162 Million Revs.) Friction Polymer	122
34	Schematic Drawings of Test Roller Bearings LM102949/ LM102910 Tapered Roller Bearing	124

LIST OF ILLUSTRATIONS (Continued)

Figure	Title	Page
35	Changes in Surface Texture of Bearing No. RA-103 Cone Surface With Rolling Contact	132
36	Surface Defects on Components of As-Finished No. RA-103 Tapered Roller Bearing	134
37	Wear On Roller End and Flange Surfaces During Rolling Contact	135
38	Effect of Sliding in Roller End Flange Contact on Roller End Surface	136
39	Surface Damage Produced on Tapered Roller Bearing Cone Surface During Rolling Contact	137
40	Morphologies of Spalls on Tapered Roller Bearing Cone Surfaces	138
41	Emergence of Subsurface Cracks on Spall Surface Shown in Figure 40C	140
42	Roller Bearing Test Sequences RT, RU, and RY Ferrograph Density Data	142
43	Roller Bearing Test Sequence RT Entry Deposit Low Magnification	143
44	ller Bearing Test Sequence RU Entry Deposit Low Magnification	148
45	Roller Bearing Test Sequence RY Entry Deposit Low Magnification	152
46	Generalized Bearing Debris Concentration Level Comparison	157
47	Roller Bearing Test Sequence RA Ferrograph Density Data	158
48	Roller Bearing Test Sequence RA Entry Deposit Low Magnification	159
49	Roller Bearing Test Sequence RW Ferrograph Density Data	164
50	Roller Bearing Test Sequence RW Entry Deposit Low Magnification	165
51	Roller Bearing Test Sequence RT Ferrograph Density Data	175
52	Roller Bearing Test Sequence RU Ferrograph Density Data	176

TABLE OF CONTENTS (Continued)

Figure	Title	Page
53	Roller Bearing Test Sequence RY Ferrograph Density Data	177
54	Roller Bearing Test Sequence RW Ferrograph Density Data	178
55	Roller Bearing Test Sequence RT Entry Deposit High Magnification	180
56	Roller Bearing Test Sequence RU Entry Deposit High Magnification	185
57	Roller Bearing Test Sequence RY Entry Deposit High Magnification	189
58	Roller Bearing Test Sequence RW Entry Deposit High Magnification	193
59	Generalized Bearing Particle Size Distribution Versus Wear Regime	197
60	Roller Bearing Test Sequence RA Ferrograph Density Data	198
61	Roller Bearing Test Sequence RA Entry Deposit High Magnification	199
62	Similarity of Appearance of Cutting Wear Particles	204
63	Abrasive Wear Particles	205
64	Abrasive Wear Particles	208
65	Gear Test Set Configuration	214
66	Erdco Universal Tester	215
67	Cross-Section of Ryder Research Gear Machine Test Head	216
68	Shafts With Integral Slave Gears	217
69	Ryder Gear-Mesh Geometry Diagram	219
70	Ryder Gear-Mesh Velocity Vector Diagram	220
71	Schematic Diagram of Standard Closed-Loop Gear Lubrication System	221
72	Schematic Diagram of Support and Load Oil System for Ryder Gear Machine	222

LIST OF ILLUSTRATIONS (continued)

Figure	Title	Page
73	Schematic Diagram of SKF "Clean" Closed-Loop Gear Lubrication System	223
74	Gear Test Sequence GG Ferrograph Density Data	239
75	Gear Test Sequence GH Ferrograph Density Data	239
76	Gear Test Sequence GG Entry Deposit Low Magnification	240
77	Gear Test Sequence GH Entry Deposit Low Magnification	245
78	Gear Test Sequence GD Entry Deposit Low Magnification	253
79	Gear Test Sequence GE Entry Deposit Low Magnification	257
80	Gear Test Sequences GD and GE Ferrograph Density Data	261
81	Gear Test Sequence GG Ferrograph Density Data	266
82	Gear Test Sequence GH Ferrograph Density Data	266
83	Gear Test Sequence GG Entry Deposit High Magnification	267
84	Gear Test Sequence GH Entry Deposit High Magnification	272
85	Gear Test Sequence GD Ferrograph Density Data	279
86	Gear Test Sequence GE Ferrograph Density Data	280
87	Gear Test Sequence GD Entry Deposit High Magnification	281
88	Gear Test Sequence GE Entry Deposit High Magnification	285
89	Gear Test Sequence GD Scuff Versus Running Time	289
90	Gear Test Sequence GE Average Percent Scuff Versus Wear Life	290
91	Gear Test Sequence GH Average Percent Scuff Versus Running Time	291
92	Particle Size Distribution Versus Wear Regime Gear Test Sequences	293
93	Oil Analysis Program Gear Scuffing Tests	294

LIST OF ILLUSTRATIONS (Continued)

Figure	Title	Page
94	Oil Analysis Program Gear Scuffing Tests	295
95	Oil Analysis Program Gear Normal Wear/Fatigue Tests	296
96	Oil Analysis Program Gear Normal Wear/Fatigue Tests	297
97	Oil Analysis Program Gear Normal Wear/Fatigue Tests	298
98	Gear Wear-In Particles	302
99	Gear Fatigue Particles	304
100	Gear Scuffing Particles	307
101	Single-Cylinder Test Engine	309
102	Cylinder	310
103	Piston With Compression Rings and Wrist Pin in Place	312
104	SEM Micrographs of the Unrun Surface of a Cylinder Wall	317
105	Segment of the Cylinder Wall From the First Run	319
106	SEM Micrographs of a Shiny Region on the Cylinder Wall	320
107	SEM Micrographs of a Moderately Worn Area on the Surface of the Cylinder Wall at the Conclusion of the First Testing Run	321
108	SEM Micrographs of the Unrun Chrome Plated Top Piston Ring	322
109	SEM Micrographs of Wear Surface of the Top Ring After First Run	323
110	SEM Micrographs of the Surface of a New Center Piston Ring	325
111	SEM Micrographs of the Top and Bottom of the Contact Circumference of the Middle Piston Ring	327
112	Macrograph of an Unrun Bottom Piston Ring	329
113	SEM Micrographs of an Unrun Bottom Piston Ring	330
114	SEM Micrographs of the Surface of the Bottom Ring After the Completion of the Second Testing Run	331

LIST OF ILLUSTRATIONS (Continued)

Figure	Title	Page
115	SEM Micrograph of a Crack on the Wear Surface of the Bottom Ring from the Second Run	332
116	Macrograph of Wrist Pin Removed Following Completion of First Test Sequence	333
117	SEM Micrographs of an Unworn Region on the Surface of the Wrist Pin of the Previous Figure	334
118	SEM Micrographs of the Bearing Contact Surface of the Wrist Pin from Test 1 Showing a Region Which Had Been Worn Smooth	336
119	SEM Micrographs of the Bearing Contact Surface of the Wrist Pin From Test 1	337
120	SEM Micrographs of a Region of Build Up Matter on the Bearing Contact Surface of the Wrist Pin of Figure 119	338
121	SEM Micrographs of the Bearing Contact Surface of the Wrist Pin From Run 2	340
122	SEM Micrographs of the Surface of an Unrun Wrist Pin Bearing	341
123	Photograph of the Wrist Pin Bearing After Sectioning Following Completion of the First Run	342
124	Photograph of the Wrist Pin Bearing After Sectioning Following Completion of the Second Run	342
125	SEM Micrographs of the Worn Surface of the Wrist Pin Bearing After Completion of the First Run	343
126	SEM Micrographs of the Surface of the Wrist Pin Bearing After Completion of the Second Run	345
127	SEM Micrographs of the Unrun Surface of the Aluminum-Tin Crankshaft Bearing	346
128	SEM Micrographs of a Typical Region on the Crankshaft Bearing at the Completion of the First Run	347
129	Two Segments of the Crankshaft Bearing at the Conclusion of the Second Run	348
130	Sliding Contact Test Sequences SA and SB Ferrograph Density Data	351

LIST OF ILLUSTRATIONS (Continued)

Figure	Title	Page
131	Sliding Contact Test Sequence SA Ferrograph Density Data ...	352
132	Sliding Contact Test Sequence SB Ferrograph Density Data	353
133	Sliding Contact Test Sequences SA and SB Spectrometric Oil Analysis	355
134	SEM Micrographs of Ferrogram 4673 (4326) at about 50 mm Position	357
135	SEM Micrographs of 10,000X of Ferrogram 4673 (4326)	358
136	SEM Micrographs of 10,000X of Ferrogram 4673 (4326)	360
137	SEM Micrographs of Ferrogram 4759 (4329) at the 50 mm Position	361
138	SEM Micrographs of Ferrogram 89 (4277) at the 55 mm Position	362
139	Sliding Contact Rubbing Wear Debris	364
140	Prerun Piston Ring Surface	365
141	Typical Severe Sliding Contact Wear Particles	366
142	Oil Settling Rates	382
143	Antiwear Properties	398
144	Antiwear Properties	399
145	Roller Bearing Test Sequence	404
146	Gear Test Sequence Scuffing	405
147	Spectrometric Analysis	406
148	Particle Counts	407
149	Percentage Area Covered as a Function of the Test Time	409
150	Spectrometric Lag Time	410
151	Ferrograph Analyzer	414
152	Ferrogram	416
153	Ferrogram Particle Size Versus Location	417

LIST OF ILLUSTRATIONS (Continued)

Figure	Title	Page
154	Ferroscope and Densitometer	419
155	X-Ray Emission Analysis	424
156	X-Ray Emission Analysis	425
157	Sample Dilution	427
158	Size Discrimination	430
159	Size Discrimination	431
160	Ball Bearing Test Sequence BA Ferrograph Density Data	445
161	Critical Wear Particle Analysis Parameters	447
162	Wear Particle Analysis Health Monitoring Decision Process	451
163	Wear Particle Analysis Equipment Capability	454

LIST OF TABLES

Table	Title	Page
1	Ball Bearing Failure Modes	27
2	Roller Bearing Failure Modes	29
3	Gear Failure Modes	31
4	Sliding Surface Failure Modes	33
5	Analysis Technique Summary	40
6	Analytical Techniques, Advantages, and Disadvantages	41
7	Ball Bearing Test Parameters	48
8	Ball Bearing Oil Samples	50
9	Summary of Ball Bearing Test Results	52
10	Weibull Analysis of Ball Bearing Fatigure Life Results	52
11	Ball Bearing Surface Measurement Data as a Function of Million Revolutions	54
12	Spectrometric Reading, Bearing BA-025	85
13	Spectrometric Reading. Bearing Bx-020	85
14	Particle Counts - Ball Bearings Nos. BQ, BX, and BA	86
15	Ferrogram Analysis Report	107
16	Spectrometric Analysis of Oil Samples From Ball Bearing Endurance Tests	110
17	Roller Bearing Test Parameters	125
18	Roller Bearing Oil Samples	127
19	Summary of Tapered Roller Bearing Test Results	130
20	Weibull Analysis of Roller Bearing Fatigue Life Results	130
21	Roller Bearing Surface Measurement Data as a Function of Million Revolutions	131

LIST OF TABLES (Continued)

Table	Title	Page
22	Spectrometric Readings, Bearing RT-106	168
23	Spectrometric Readings, Bearing RU-107	168
24	Spectrometric Readings, Bearing RY-115	169
25	Spectrometric Readings, Bearing RW-109	169
26	Particle Counts, Roller Bearing RT Series	171
27	Particle Counts, Roller Bearing RU Series	172
28	Particle Counts, Roller Bearing RY Series	173
29	Particle Counts, Roller Bearing RW Series	174
30	Oil Analysis Program Summary of Gear Bench Tests	228
31	Particle Counts, Gear GD Series	262
32	Particle Counts, Gear GH Series	263
33	Particle Counts, Gear GG Series	264
34	Spectrometric Reading, Gear GD	299
35	Spectrometric Reading, Gear GE	299
36	Spectrometric Reading, Gear GG	300
37	Spectrometric Reading, Gear GH	300
38	Measurement of Wear in Cylinder Bore Diametral Change in Two Perpendicular Planes (Measured in .0001")	315
39	Wear Components	315
40	Sliding Contact Test Sequence Summary	349
41	Ferrograph Evaluation - Dilution Effects	429

THIS PAGE LEFT BLANK

INTENTIONALLY.

I. INTRODUCTION

A. Oil analysis has been applied for many decades as a preventive maintenance concept utilized to predict impending mechanical failure through examination of used oil samples. Initially, physical properties of oil were considered indicators of equipment wear. However, meaningful results were not obtained until examination emphasis shifted to the analysis of oil-carried wear particles. The term oil analysis has thus become synonymous with oil particle analysis or wear particle analysis.

B. The oil analysis concept is based on the premise that all mechanical systems experience the process of wear during operation. This wear process results in the production of wear debris or wear particles which are indicative of the respective wear surface condition. In the case of lubricated components these wear particles are picked up and circulated by the lubricant. Thus an examination or oil analysis of a lubricant sample can nondestructively reflect component surface wear condition.

C. Several oil analysis techniques are currently being utilized for Government and industrial applications. These techniques, however, lack a firm technical basis. They are based on assumed monitored parameters and are applied, with varying degrees of success, by trial and error.

D. The Naval Air Engineering Center (NAVAIRENGCEN), under sponsorship of the Naval Air Systems Command, initiated an ambitious research program with the goal of placing oil analysis on a firm technical basis. This goal was to be accomplished through an intensive correlation effort relating wear particle characteristics to component surface wear condition. Such wear particle correlations serve to highlight critical characteristics/parameters which are directly relatable to component surface wear condition. This report serves to summarize the results of this oil analysis research effort.

II. BACKGROUND

A. GENERAL

1. Cost effectiveness is a concept that can be defined as a measure of the benefits to be derived from, and the resources to be expended on a system. As a direct consequence of the present national condition of limited resources, coupled with excessive inflation, the optimization of equipment cost effectiveness is receiving considerable emphasis.

2. A primary element in the determination of cost effectiveness, is equipment maintainability. Maintainability is a characteristic of equipment design and installation which is expressed in terms of ease and economy of maintenance, equipment availability, safety, and accuracy in the performance of maintenance actions. In an effort to optimize equipment cost effectiveness, the concept of "on-condition" maintenance has evolved. This concept involves the performance of maintenance tasks as required, as opposed to an arbitrary time interval schedule. The prime advantage exhibited by this concept is the extension of both equipment operational and maintenance intervals. Interval extension results in substantial reductions in maintenance costs and equipment downtime, as well as subsequent reduced safety hazards.

3. "On-condition" maintenance, although desirable, can only be effective if monitoring techniques are available to support it. Techniques must be capable of detecting abnormal wear conditions before they result in equipment failure.

4. One of the prime monitoring techniques supporting "on-condition" maintenance is oil analysis. This technique serves to monitor oil lubricated component wear on a nondestructive basis.

B. OIL ANALYSIS CYCLE

1. Oil analysis can be described as a preventive maintenance concept, utilized to predict impending mechanical system failure, through the examination of

used oil samples. This concept, although varying in technique, has been applied for many decades. Initially, physical properties of oil were considered indicators of equipment wear. However, consistent results were not obtained until examination emphasis shifted to the analysis of lubricant borne wear particulates. The term oil analysis has thus become synonymous with oil particulate analysis.

2. The basic premise behind oil analysis is that wear surfaces generate wear particulates. These particulates are picked up by the lubricant (i.e., in the case of oil lubricated components) and circulated through the lubricant system. Through analysis of a lubricant sample, the circulated wear metal can be characterized and utilized to reflect component wear condition.

3. Although this premise appears to be relatively simple, the oil analysis cycle is a critical combination of techniques, test procedures, and analysis criteria. The total analysis progression can be divided into five major elements: lubricant sample, detection, diagnosis, prognosis, and prescription.

a. Sample. The sample element of the oil analysis process involves obtaining a timely, representative lubricant borne debris sample from a mechanical system.

b. Detection. The detection element provides a first cut or preliminary determination as to the health of a machine (i.e., is the machine wearing normally or abnormally?). If no abnormalities are detected, no further analysis is required until the next schedule sampled interval. If an abnormality is detected or suspected, the lubricant sample is transitioned to the next oil analysis element.

c. Diagnosis. The diagnosis element serves to further clarify the machinery wear abnormality. It provides a determination as to what machine component/components are wearing and proceeds to define what wear mode/modes are present. Based on these determinations, the analysis is transitioned to the next element.

d. Prognosis. The prognosis element of the analysis process, serves to define the course of the machinery wear abnormality. It provides a prediction of the residual life/time until failure, based on the wearing component and the wear mode progression.

e. Prescription. The last element of the analysis process serves to define a course of corrective action. It provides maintenance recommendations based on residual life, wearing component, and wear mode.

4. The sample element of the process is based primarily on technique. The elements of detection and diagnosis are based on monitored wear particle characteristics. And, lastly, the elements of prognosis and prescription rely heavily on analysis criteria.

C. SPECTROMETRIC OIL ANALYSIS

1. Spectrometric oil analysis has developed as the foremost analytical technique utilized in present Department of Defense (DOD) applications. This method involves taking a lubricant sample from a system and sending it to a spectrometric oil analysis laboratory. This laboratory determines the concentration of various elements contained in the used oil sample. Through a procedure of comparing measured results with predetermined element concentration levels, as well as comparing with concentration level measurements taken from previous oil samples on the same equipment, the laboratory arrives at required maintenance recommendations.

2. Spectrometric analysis has demonstrated that the analysis of wear metal particulate matter which accumulates and circulates in a closed cycle oil wetted system can, with varying degrees of success, be used as a means of monitoring system wear, and thus predicting impending mechanical component failure. This technique has reported success rates that vary greatly. These effectiveness variations exhibited by SOA, as well as related techniques, have not as yet been factually defined.

3. The shortcomings of the Spectrometric Oil Analysis Program were outlined in 1971, in a memo from the Assistant Secretary of Defense, B. J. Shillito, to Director of Defense Research and Engineering, Dr. J. S. Foster.

4. This memo highlighted the most important engineering requirements as follows:

a. Development of minimum sample frequency intervals.

b. Criteria for analysis of oil samples.

c. Uniform methods of developing engineering data.

d. Adjustment of equipment operating intervals based on oil analysis.

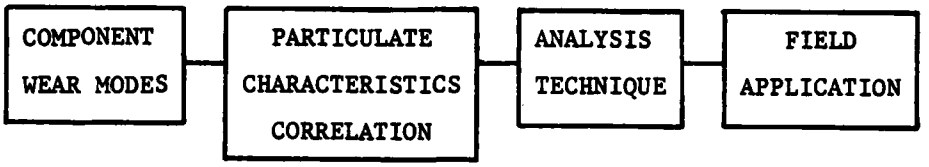
5. The memo recommended the following:

"In view of the foregoing it is requested that your office establish a project that will provide the necessary engineering research and data to accommodate the above-stated requirements and facilitate implementation of the DOD Equipment Oil Analysis Program on a realistic and systematic basis."

6. Through the Naval Air Systems Command (NAVAIRSYSCOM), AIR-340, a research program to address these requirements was established at NAVAIRENGCEN, Code 92724. This report summarized the results of this Tri-Service Oil Analysis Research and Development Program.

III. PROGRAM DESCRIPTION

A. As stated above, the Oil Analysis Program was designed in order to place oil analysis on a firm technical basis. The first step in this program design process was to consider the optimal development cycle of an oil analysis technique. This development was broken down into four distinct phases as follows:



1. COMPONENT WEAR MODES. The first element in any such development cycle is the definition and categorization of all pertinent mechanical system wear modes. This categorization lists wear modes that contribute to lubricant borne debris. It serves to define what can be monitored in a system (desirable, feasible).

2. PARTICULATE CHARACTERISTICS CORRELATION. The second element in such a development cycle is the definition of all the characteristics exhibited by the wear particles generated during component wear. These characteristics can then be correlated to surface wear progression in order to define critical parameters. The monitoring of these critical wear particulate parameters is directly related to component wear state.

3. ANALYSIS TECHNIQUE. Based on critical wear particle characteristics, the development of a required monitoring/analysis technique, or combination of techniques, is carried out. The technique definition comprises the third element.

4. FIELD APPLICATION. The fourth and final element of this program is the field application of developed techniques. This application, and resultant feedback, serves to formulate and improve analysis criteria.

B. Based on a survey of the field, the following determinations were formulated with respect to past and present oil analysis technique development cycles:

1. Numerous wear mode classification efforts have been performed.

2. Several analytical techniques have been developed.

3. All techniques have been field tested.

4. An insignificant amount of effort has been expended correlating wear modes with wear particulate characteristics.

C. These determinations revealed that a major element of the oil analysis technique development program was neglected. Very little work has been performed which serves to clarify which particle characteristic or characteristics are best reflective of surface wear conditions. Analytical techniques developed to date are based on assumed critical particulate characteristics, and have been applied by trial and error.

D. In order to bridge this technological gap, the NAVAIRENGCEN proposed and subsequently received NAVAIRSYSCOM approval for the Tri-Service Oil Analysis Research and Development Program. Its goal is to place oil analysis on a firm technical basis. Briefly the program can be described as follows: Laboratory testing to determine the feasibility of monitoring the surface wear condition of oil wetted components through the utilization of critical wear particle parameter monitoring.

E. In order to achieve the desired program goal, a three-phase effort was formulated. These phases consisted of a data base formulation phase, a laboratory study phase, and a system application phase as depicted below:



Each phase provides a critical program link and depends on the successful and meaningful completion of the preceding phase. Program phases are discussed in detail as follows:

1. DATA BASE. The data base phase of the Oil Analysis Program serves to provide information necessary to initiate meaningful laboratory testing, effectively monitor required test parameters, and thoroughly evaluate test results. Data base objectives included the development of an effective test plan and supporting analytical procedures. The initial thrust of this effort was the performance of an extensive literature search. Follow-on studies were performed to clarify such aspects as:

a. Test components
b. Test condition
c. Experimental design including test system design and analysis techniques
d. Wear surface classification
e. Wear particulate classification

2. LABORATORY STUDY. The laboratory study phase of the program involved the bench testing of prime oil lubricated components. Components were operated under equivalent field operating conditions with independent lubricant systems. Surface wear condition and the respective generated wear particle characteristics/parameters were monitored throughout the testing. Tests were continued until component failure. The objective of the laboratory study was to define critical wear particle characteristics/parameters which effectively reflect component wear condition.

3. SYSTEM APPLICATION. The third and final phase of the program involved the application of laboratory findings and conclusions to field operating equipment. The objective of the system application phase was to verify laboratory results through field equipment application. Field equipment control groups were established. These control groups periodically submitted lubricant samples to NAVAIRENGCEN for storage. Respective control group failure information was also submitted to NAVAIRENGCEN. This process created a repository of failure information combined with a respective series of preceding lubrication samples. Critical wear particle parameters, defined under the laboratory program phase,

were monitored in these series and related to respective failure information. This application of laboratory monitoring methodologies to repository oil sample failure series serves to verify the laboratory results.

F. Results of the first two program elements will be summarized in this report. The third program phase, system application, results will be summarized in a later document.

IV. PHASE I: DATA BASE

A. GENERAL

1. The Data Base Program Phase served to provide information necessary to initiate meaningful laboratory testing, effectively monitor required test parameters, and thoroughly evaluate test results. It was concluded under this phase that a major portion of mechanical systems could be broken down into four wear producing interfaces: rolling point contact, rolling line contact, sliding contact, and a combination of sliding and rolling contact. Examples of mechanical components exhibiting these interfaces are ball bearings, roller bearings, pistons/cylinders, and gears respectively. These components thus received major emphasis under the resulting testing program.

2. When component definitions were established, a complete bench test program was formulated for each component. A detailed description of bench test equipment, procedures, and parameters will be presented in Section V of this report.

3. In order to monitor both wear surface condition and wear particulate characteristics, so as to make correlation between the two possible, a categorization format was developed for each. These formats are described as follows.

B. WEAR MODE CATEGORIZATION. In order to adequately categorize pertinent test wear modes, a matrix was developed for each prime component. These matrices relate component operational parameters, wear modes, and causal factors. Ball bearing, roller bearing, gear, and piston/cylinder matrices are presented in Tables 1 through 4, respectively.

C. WEAR PARTICLE CATEGORIZATION. In order to adequately categorize wear debris/particles during laboratory testing, a categorization list was developed. This list included a number of distinct particle types and their respective characteristics. These particle types are described in the following paragraphs.

1. RUBBING WEAR PARTICLES. These particles are generated whenever two pieces of metal rub together in the presence of a lubricant. It has been found that they originate in a shear mix layer which, in the case of steel, is in the order of 1 μm thick and exhibits only a short-range crystalline order. This layer, the significance of which has only recently been appreciated, has unique properties different from those of the underlying metal. Most wear of rubbing metal surfaces is the result of flaking off of pieces of the shear mix layer, as the result of a network of cracks that gradually develop with repeated passes of the opposing surface. This type of wear is relatively benign and is fundamental to boundary layer lubrication.

2. CUTTING WEAR PARTICLES. Cutting wear particles have the appearance of tiny lathe chips or coils of fine wire. Such particles are the result of the failure of the boundary layer lubrication and are usually associated with high surface contact forces. They may also be generated by the presence of abrasives.

3. FATIGUE CHUNKS. Another type of particle is the fatigue chunk. These particles are composed of free metal, usually ferrous and show crystalline faces containing considerable detail. They are approximately as long as they are wide and are often several microns thick. Such particles are generated by certain types of gear wear and are seen in other situations where cracking perpendicular to the surface can develop.

TABLE 1. BALL BEARING FAILURE MODES

	(1) Ball - Raceway Spalling	(2) Peening - Spalling at Race Shoulder	(3) Extensive Glazing, Frosting, Microspalling of Stressed Surfaces	(4) Heavy Smear Tracks and Discoloration on Raceways and Balls	(5) Oblong Dents & Flat Spots on Balls & Raceways, Brinnelling	(6) Pattern of Oblong Scuff & Fret Marks on Raceways, False Brinnelling	(7) Heavy Cage Wear and Breakage
A) Heavy, prolonged load	Heavy load can increase incidence of fatigue damage	Very heavy thrust load can cause ball to ride over shoulder	A heavy load may cause a breakthrough of a thin film		Permanent deformations may occur if load exceeds static capacity		
B) Shock load					Can cause permanent denting		
C) Misalignment	May impose heavier loads	Wear track may run close to shoulder					Can impose heavy loads on cage pockets & land riding surfaces
D) Vibration						May cause damage when there is a lot of play and poor film damping	
E) Very light load				Insufficient tractive force can cause ball skidding			
F) Inadequate lubrication/ poor quality lubricant			May result in lack of film separation of contacting surfaces	When balls skid they may not slide on a film of oil			May prevent film separation of land riding surfaces
G) Excessive speed	Will increase stress cycles which accelerates fatiguing of surfaces			Increase the tendency to skid with light load			Cage must be balanced and land guided to withstand centrifugal forces
H) Incomplete sealing							
I) Manufacturing or material inadequacies	Soft metal, bad grain flow or size can cause spalling out of the surfaces		A rough surface finish may prevent film separation of the surfaces				
J) Incorrect design	Inadequate load carrying capability can increase fatigue damage	Shoulder height may be inadequate for load conditions		Too much internal play can contribute to skidding	Inadequate static load capacity		Cage may have inadequate strength for operating conditions
K) Improper mounting							
L) Improper handling							
M) High environmental temperature			May cause lubricant breakdown				
N) Presence of electric currents							

TABLE 1. BALL BEARING FAILURE MODES
(Continued)

	(8) Roughened, Microdented Surfaces With Increased Internal Play Abrasion	(9) Pits and Stains on Raceways and Balls, Corrosion	(10) Thermal Growth, Discoloration, and Seizure of Bearing Burnout	(11) Bands of Rust, Discoloration, Some Glazing on Pitted Surfaces Fretting	(12) Crack Formation on Rings and Balls	(13) Nicks, Dents, and Score Marks on Bearing
A) Heavy, prolonged load						
B) Shock load					Can cause cracking with thru-hardened steels	
C) Misalignment						
D) Vibration						
E) Very light load						
F) Inadequate lubrication/ poor quality lubricant		Can result in corrosive and oxidized products attacking surfaces	Inadequate heat removal capability			
G) Excessive speed			Can greatly increase heat generation			
H) Incomplete sealing	Metal contamination may cause abrasive damage to contacting surfaces	Corrosive agents such as water can destroy surfaces				
I) Manufacturing or material inadequacies					Improper heat treat can cause cracking	
J) Incorrect design						
K) Improper mounting				Too loose a fit can cause creep and fretting corrosion	Too tight a fit may cause cracking	
L) Improper handling						Abuse and rough handling may result in damage which shortens life
M) High environmental temperatures			Prevents adequate heat removal from bearing			
N) Presence of electric currents		Electric current may cause extensive pitting of surface				

TABLE 2. ROLLER BEARING FAILURE MODES

	(1) Roller and Raceway Spalling	(2) Spalling at Roller and Raceway Edge of Contact	(3) Extensive Glazing, Frosting, Microspalling of Stressed Surfaces	(4) Heavy Smear Tracks and Discoloration on Raceways and Rollers	(5) Oblong Dents & Flat Spots on Rollers & Raceways, Brinnelling	(6) Pattern of Oblong Scuff and Fret Marks on Raceways, False Brinnelling	(7) Heavy Cage Wear and Breakage
A) Heavy, prolonged load	May greatly accelerate fatigue damage		May cause a breakthrough of a thin film		Load exceeds static capacity		
B) Shock load					May cause permanent denting		
C) Misalignment		Heavy edge loading will greatly increase contact stresses	Can cause film breakdown at edges	Can cause sliding and skewing of rollers			Can impose damaging loads on cage
D) Vibration						May occur with int. clr. and poor film damping	
E) Very light load				Insufficient traction can cause roller skidding			
F) Inadequate or poor quality lubricant			Can cause a loss of film strength with metal-to-metal contact	Rollers may not slide on film of oil			May not have film separation on land riding surface
G) Excessive speed	Increase in stress cycles which accelerates fatiguing of surfaces			Increases the tendency to skid with light load			Land-guided cage required to withstand centrifugal forces
H) Incomplete sealing							
I) Manufacturing or material deficiencies	Soft metal, bad grain flow and size can increase fatigue likelihood		Poor surface finish can cause surface distress				
J) Incorrect bearing design	Insufficient load carrying capacity can cause fatigue damage	May result from an inadequate crown on rollers and raceways		Too much internal play can contribute to skidding	Inadequate capacity to resist brinnelling		
K) Improper mounting							
L) Improper handling							
M) High environmental temperatures			May cause lube breakdown with loss of film strength				
N) Presence of electric currents							

TABLE 2. ROLLER BEARING FAILURE MODES (Continued)

	(8) Roughened, Microdented Surfaces with Increased Internal Play, Abrasion	(9) Pits, Stains on Raceways and Rollers, Corrosion	(10) Thermal Growth Discoloration and Seizure of Bearing, Burnout	(11) Bands of Rust, Discoloration, Glazing of Pitted Surfaces, Fretting	(12) Crack Formation on Rings and Rollers	(13) Nicks, Dents and Score Marks on Bearings	(14) Excessive Tapered Roller End Wear at the Cone Rib
A) Heavy, prolonged load							
B) Shock load					Can occur with thru-hardened steels		
C) Misalignment							
D) Vibration							
E) Very light load							
F) Inadequate or poor quality lubricant		Damage may be caused by corrosive agents and oxidized products in oil	Inadequate heat removal capability				Can cause metal-to-metal sliding contact
G) Excessive speed			Can increase heat generation				
H) Incomplete sealing	Metal contamination may cause abrasive damage to surfaces	Corrosive agents such as water may destroy surfaces					
I) Manufacturing or material deficiencies					Improper heat treat can cause cracking		
J) Incorrect bearing design							An incorrectly specified fit-up to control end play or preload
K) Improper mounting				A loose fit may cause creep and fretting corrosion	Too tight a fit may cause ring cracking		Incorrect fit-up can increase roller end load
L) Improper handling						Abuse & rough handling may result in damage	
M) High environmental temperatures			Prevents adequate heat removal from bearing				
N) Presence of electric currents		May cause extensive pitting of surfaces					

TABLE 3. GEAR FAILURE MODES

	(1) Spalling of Tooth Surface	(15) Scoring Lines in Direction of Sliding	(16) Fatigue Fracture of Tooth With Focal Point and Contour Lines	(17) Fracture of Corner Tip of Tooth	(18) Crack Formation on Gear	(19) Crushing and Distortion Inward of the Case
A) Heavy, prolonged load	Increased contact stress promotes fatigue					
B) Shock load			May exceed bending stress limit			May damage case if severe enough
C) Misalignment	Can increase probability of fatigue damage			Can cause very heavy localized bending stress		
F) Deficient lubrication		Inadequate film strength may result in metal-to-metal sliding contact				
H) Incomplete sealing						
I) Manufacturing and material deficiencies	Soft metal, bad grain flow and size can cause spalling out of the surfaces	A rough surface finish may result in lack of film separation			Can result from bad heat treatment	Damage due to too thin a case and too soft a core
J) Incorrect gear design	Poor gear geometry may result in high stress levels		Bending stress may be insufficient for operating conditions			Required case depth may be insufficient
L) Improper handling						
K) Improper mounting		Inadequate backlash can cause gears to run hot		Can result in a misaligned gear		
M) High environmental temperatures		May result in lubricant film breakdown				

TABLE 3. GEAR FAILURE MODES
(Continued)

	(20) Rolling, Peening With Rippling and Ridging Lines on the Tooth	(8) Roughened, Microdented Surface With Increased Backlash, Abrasion	(9) Pits, Stains on Tooth Surface, Corrosion	(10) Thermal Growth, Discoloration and Softening of the Gear	(13) Nicks, Dents, Score Marks
A) Heavy, prolonged load	May produce plastic flow				
B) Shock load					
C) Misalignment	Possible localized plastic flow				
F) Deficient lubrication			Corrosive agents and oxidized products in oil can attack surfaces	May have inadequate heat removal capability	
H) Incomplete sealing		Metal contaminants can cause abrasive wear of teeth	Corrosion due to contaminants such as water can destroy surfaces		
I) Manufacturing and material deficiencies					
J) Incorrect gear design					
L) Improper handling					Abuse and mishandling may cause damage
K) Improper mounting					
M) High environmental temperatures				May prevent sufficient heat removal	

TABLE 4. SLIDING SURFACE FAILURE MODES

	(15) Smearing and Scuffing in the Sliding Direction, Adhesion	(1) Spalling of a Bearing Surface, Fatigue	(8) Roughened, Microdented Surfaces, Abrasion, Erosion	(9) Pitted, Stained Surfaces, Corrosion	(11) Fretting Corrosion	(13) Nicks, Dents, and Score Marks	(16) Cavitation Gouging of Surfaces
B) Shock load		Can cause fatigue damage to a surface subjected to repeated loading					
D) Vibration					Welding shearing and subsequent oxidation can occur ex. splines		
F) Deficient lubrication	Inadequate film strength may result in metal-to-metal sliding contact			Corrosive agents and oxidized products can attack surfaces	May allow metal-to-metal contact		
C) Misalignment	May prevent localized film separation				Can contribute to fretting corrosion in splines		
H) Incomplete sealing			Metal contamination can cause abrasive wear; also erosion of surfaces from flow of lubricant	Can allow corrosion from contaminants including water			
P) Destructive operating environment			Products of internal combustion such as carbon, sulfides will damage surfaces	Combustion products will form acids which attack surfaces			Below atmos. pressures will cause oil bubble collapse and impingement
M) High environmental temperatures	May prevent adequate film strength and cause oil breakdown			Will increase chemical activity of products in lubricant and from combustion			
I) Manufacturing and material deficiencies	Improper surface finish may prevent film separation	Material may have inadequate strength to resist fatigue cracking					
J) Incorrect design	Surface geometry may prevent adequate lube film development	System may not have sufficient strength to withstand shock load					System should be designed to prevent cavitation conditions
L) Improper handling						Abuse and mishandling can cause damage	

4. LAMINAR PARTICLES. Laminar particles are found in connection with gear and rolling bearing wear. They are exceedingly bright, free metal particles most frequently seen in connection with rolling bearing wear. The particles are thin, typically 3/4μm thick, and generally have holes in their surface. They appear to be the result of rolling out of the metal as could occur in the shear er on the ball bearing track or near the pitch line of gears.

5. SPHERICAL PARTICLES (FREE METAL SPHERES). Spherical particles are generated by the thousands in cases where micro-cracks are present in rolling bearings, such as ball bearings and roller bearings, lubricated by either oil or grease. They range in size from less than 1μm to more than 20.0μm. The smaller sizes are much more numerous. Up to several million spheres can be generated in the course of a bearing fatigue failure. These spherical particles are not to be confused with polymer spheres or oxide spheres. The polymer spheres are thought to be the result of polymerization of oil around wear particles which serve as a nucleating catalyst. Oxide spheres are produced in a variety of ways, but probably the most common is fretting of steel surfaces. The non-free metal spheres are easily distinguished from free metal spheres by virtue of the reflectivity and opacity of the free metal.

6. CORROSIVE WEAR PARTICLES. Corrosive wear particles are those particles which have been digested by the lubricant. They are distinguished from red and black oxides of iron because they are generally colorless and much more transparent. They may be chlorides of the wearing material.

7. OXIDE PARTICLES. Some wearing systems show large quantities of the red oxide of iron, hematite, Fe_2O_3. These particles are the result of rusting in the machine and generally indicate the presence of moisture or moist conditions which permit the rusting to occur. The rust is usually not generated at the wearing surface, but is simply material flaked off of shafts, the insides of pipes, and many other places. (The oxides of other metals may be white, bl , green, or yellow, depending on the metal.)

8. DARK METALLO-OXIDE PARTICLES. Another category consists of dark metallo-oxide particles which are thought to be principally Fe_3O_4, magnetite. These particles are non-stoichiometric oxides and may be thought of as oxides with iron dissolved in them. They are surprisingly more opaque than would be expected from pure Fe_3O_4. These particles appear as black or very dark chunk-like particles, similar to pieces of hard coal. It is postulated that they are sufficiently hard to cause surface denting and subsequent micro-cracking of the surfaces of rubbing elements in bearings. A second type of dark, chunk-like particle has been found, usually accompanied by dark, flat platelets with straight sides. They appear to be the wear product from carbon seals or separators. The chunk-like particles do not have the sharp edges characteristic of magnetite; the fracture surfaces are conchoidal, similar to that of glass.

9. NONFERROUS METALLIC PARTICLES. These particles may belong to any of the first five categories.

10. HYBRID PARTICLES. Hybrid particles are composed of nonferrous material which also contains some iron. They result from the wearing of some non-ferrous alloy, such as bronze, against steel.

11. NONMETALLIC CRYSTALLINE PARTICLES. Nonmetallic crystalline particles are common, the most familiar example being sand. However, other oxides and carbides, such as silicon carbide, are also frequently seen. The significance of such particles depends on local conditions. The presence of sand, for example, can indicate an air filter failure or a bearing seal that is leaking.

12. AMORPHOUS MATERIAL. Amorphous material consists of deposits of material which do not have a specific shape. The material is usually translucent but often contains thousands of metal particles. Various contaminant polymers such as gasket material and plasticizers are the major sources of this material.

V. PHASE II: LABORATORY STUDY

A. GENERAL. The Laboratory Study Program Phase served to provide actual test data related to bench testing of ball bearings, roller bearings, gears, and piston/cylinders. A series of tests was conducted under each group in which components were run to failure under simulated field operating conditions. In order to simplify the analysis, each component was run in its own individual lubricant system. Component surface condition/wear was regularly monitored during testing. Wear debris was also characterized during testing through the analysis of withdrawn lubricant samples. Results of both surface wear monitoring and respective wear debris monitoring were then correlated.

B. ANALYTICAL TECHNIQUES. During the Laboratory Phase various monitoring techniques were utilized during component bench testing. These techniques served to assess operational parameters, wear surfaces, and wear debris characteristics. These three groups will be discussed separately.

1. OPERATIONAL PARAMETERS. Techniques that fall under this category were used to monitor test conditions utilized in component bench testing. Operating conditions such as load, speed, vibration, and temperature were monitored. Conventional techniques were utilized to monitor these operational parameters, and therefore a detailed discussion of these techniques is not necessary in this report.

2. WEAR SURFACES. In order to thoroughly monitor the wear surfaces before, during, and after bench testing, several techniques were utilized:

a. Profilometer
b. Optical Microscope
c. Scanning Electron Microscope (SEM)
d. Transmission Electron Microscope (TEM)
e. Direct Measuring Devices (Micrometers, Gauges, etc.)

These techniques are rather standard and as such they warrant no further elaboration.

3. WEAR DEBRIS. The assessment of wear debris/particulate characteristics proved to be most challenging. A total assessment effort was implemented through the utilization of a combination of both existing and new analysis techniques. These techniques are briefly summarized in the following paragraphs. Significant techniques are amplified in Section VI of this document. Amplifications are included for spectrometric analysis and ferrographic analysis.

a. Analysis Specimen. During the Oil Analysis Program several specimen formats were utilized with respect to particle analysis. These formats were subjected to one or more analysis techniques. Specimen formats included Millipore patch, ferrogram, and direct lubricant. Direct lubricant analysis refers to analysis of debris while still suspended in a lubricant sample. This specimen format is obvious and will not be further explained. Both the Millipore patch and ferrogram specimen formats, on the other hand, involve separation of debris from the fluid sample. These approaches are discussed in the following paragraphs.

(1) Millipore Patch. This specimen format is created by passing a lubricant sample through a filter patch. Contained particulates are thus filtered from the fluid sample and deposited on the patch filter matrix. Filter sizes can be selected according to user requirements. Lubricant flow is induced through the filter patch by a vacuum technique. Following flushing and drying the filter patch, the resulting debris deposit can be utilized under various analysis techniques.

(2) Ferrogram. This specimen format is created by passing a lubricant sample over a glass substrate which is suspended in a variable strength high gradient magnetic field. Contained particulates are those precipitated from the fluid sample by magnetic attraction. These particles in turn are deposited on the glass substrate. The variable field high gradient magnet serves to classify the debris with respect to size/mass over the length of the substrate. Following flushing and fixing, the resulting substrate debris deposit can be utilized under various analysis techniques. A more detailed description of the ferrogram is provided under Section VI of this document.

b. Analysis Techniques. The above outlined wear particle specimen formats were subjected to various analysis techniques in order to characterize the respective debris. These analysis techniques include the Millipore Particle Measurement Computer, the Ferroscope, the Scanning Electron Microscope, the Royco Particle Counter, and the Spectrometer. A brief description of each is provided in the following paragraphs.

(1) Millipore Particle Measurement Computer (πMC). The πMC system utilizes a chemically treated transparent Millipore patch specimen. This technique operates on the light blockage principal. When light passes through the transparent patch, a photo detector registers the light blocked by a particle. The computer analyzes this blockage to determine the major dimension of the particle. Typically, five fields on the patch are analyzed for particle sizes relative to seven thresholds (1μm, 3μm, 5μm, 7μm, 10μm, 15μm, and 40μm). The particle counts in these five fields are normalized to 100 ml of sample volume to yield the particle size distribution and total particle count. This data is useful for trending total particle count versus equipment operating time and also trending the ratio of large-to-small particle counts versus equipment operating time.

(2) Ferroscope. The Ferroscope or optical microscope is capable of utilizing both the Millipore patch and ferrogram specimen formats. However, as the name implies, the ferrogram format is specifically tailored to Ferroscopic analysis. Analysis yields data concerning particle morphology, gross composition, height of entry deposit, gross indications of particle quantity, and ratio of large-to-small particles. Particles can be categorized with respect to:

Shape
Surface
Size (length, width, and height)
Color (via polarizer/analyzer combinations)
Composition (via red/green filter combinations)
Quantity
Size Distribution.

(a) Densitometer. Ferroscope utility can be enhanced by the utilization of an integrated densitometer. This accessory is primarily utilized for ferrogram specimen characterization. The densitometer indicates, by digital readout, the light blockage of a given microscopic field of view on a ferrogram. By taking several measurements along the length of the ferrogram, one can quantitatively assess both debris quantity as well as size distribution.

(3) Scanning Electron Microscope (SEM). SEM analysis is capable of utilizing both specially coated Millipore patch and ferrogram specimen formats. The electron microscope is capable of higher magnification than the optical microscope. In this microscope an electron beam excites the specimen. The specimen image can then be formed from the transmitted electrons, reflected electrons, absorbed electrons, or the secondary electrons. Typically, the secondary electron image is used to study the particle morphology in great detail. With the addition of an X-ray detector to the microscope, particle composition may be studied qualitatively. Qualitative information suggests the possible source of that particle. The Millipore patch or ferrogram specimen is prepared by coating the specimen with carbon or gold, by means of evaporation, before introduction to the SEM.

(4) Royco Particle Counter. Royco Counter analysis characterizes debris directly in the lubricant sample. The Royco Counter operates on the principal of light blockage. A light source passes light through a small critical volume of sample liquid. The reduction in light intensity (blockage), due to particles passing one at a time through the critical volume, is monitored by a photodiode. The particle is counted and its major dimension is determined in this manner. These quantities and dimensions are integrated, or categorized, into five selected size ranges (i.e. 2-5 μm, 5-7 μm, 7-15 μm, 15-25 μm, 25-100 μm) thus yielding data concerning particle size distribution and total particle count. The total count and size distribution versus equipment operating time may be considered for developing equipment trending.

(5) Spectrometer (Baird Atomic FAS-2). Spectrometric analysis, as in the case of the Royco, characterizes debris directly in the lubricant sample. The spectrometer is the unit currently used throughout the military system (i.e. SOAP program, NOAP program, and ASOAP program) for oil analysis. The atomic emission type spectrometer burns the oil sample in an arc between two carbon electrodes. A diffraction grating analyzes the emitted light spectrum into distinct spectral patterns for each of 12 elements. (Twenty different elements may be analyzed simultaneously.) The spectrum intensity indicates the concentration of the spectrum identified element in parts per million (PPM) by weight. The concentrations of the 12 elements are monitored with respect to equipment life, in order to assess changes of the wear state.

c. Wear Particle Analysis

(1) Technique Summary. In order to clarify the above discussions of wear particle analysis techniques, a summary of devices and their respective specimen format is presented in the following table:

TABLE 5. ANALYSIS TECHNIQUE SUMMARY

	SPECIMEN FORMAT		
DEVICE	Millipore Patch	Ferrogram	Oil Suspension
π MC	X		
Ferroscope	X	X	
Densitometer		X	
SEM	X	X	
Royco Counter			X
Spectrometer			X

(2) Based on program performance, a list of analysis techniques and their respective major advantages and disadvantages are summarized in Table 6.

TABLE 6. ANALYTICAL TECHNIQUES, ADVANTAGES, AND DISADVANTAGES

TECHNIQUE	DATA	ADVANTAGES	DISADVANTAGES
Millipore Particle Measurement Computer (π MC)	Determines particle counts in seven ranges: 1-3 μm, 3-5 μm, 5-7 μm, 7-10 μm, 10-15 μm, 15-40 μm, >40 μm	Water is filtered from sample. Gas bubbles present no problem.	- Provides no composition data or morphology data. - Timely specimen preparation. - Timely analysis procedure
Spectrometer (FAS-2)	PPM by weight for 12 elements.	- Gives composition of sample debris. - No special sample preparation. - Rapid analysis.	- Provides PPM of elements irrespective of compounds. - Provides no morphology data. - Particle sizes are limited. - Concentrations reflect everything in sample.
Royco Particle Counter	Determines particle counts in five ranges: 2-5 μm, 5-7 μm, 7-15 μm, 15-25 μm, 25-100 μm	- Rapid analysis. - Limited sample preparation in most cases.	- Subject to vibration. - Coincidence of particles, gas bubbles, and water influences count. - Counts all debris regardless of source. - Provides no composition or morphology data. - Counts 5K to 30K particles per 10 ml (dilution of samples may be needed to avoid saturation).
Ferroscope	Determines particle dimensions: length, width, height. Provides gross composition, particle morphology, and density readings (gross particle number and gross size distribution).	- Allows for analysis by color. - Capable of recording images with camera (color). - Indicates morphology.	- Low magnification and small depth of focus. - Provides limited particle composition analysis. - Magnetic debris limited. - Time consuming. - High cost. - Special specimen preparation. - Quantitative.
Densitometer	Determines percent of area covered. Provides gross particle quantity and gross size distribution.	- Indicates quantity and size distribution. - Quantitative.	- Timely specimen preparation.
Scanning Electron Microscope (With X-ray Spectrometer)	Determines particle morphology and composition.	- Determines composition of a particle and detailed morphology. - Allows great depth of focus.	- Loses optical characteristics. - Costly. - Time consuming. - Timely specimen preparation.

C. BENCH TESTING AND ANALYSIS

1. GENERAL

a. Bench testing was performed on ball bearings, roller bearings, gears, and pistons/cylinders. Each component was run to failure under operating conditions approximating component field operating conditions. Independent closed-loop lubrication systems were used for each component in order to eliminate sources of contamination other than that produced by the component itself. Surface wear of each component was monitored throughout each test sequence. Periodic oil samples were systematically extracted from the lubricant system for utilization in the wear particle categorization effort. Surface analysis results were then correlated with wear particle analysis results.

b. The following paragraphs will deal with each component on an individual basis. Each section will include a discussion of test procedure, surface monitoring, and wear debris analysis.

2. BALL BEARING BENCH TESTING. Ball bearing bench testing was performed by SKF Industries, Inc. Bearing tests were divided between uninterrupted and interrupted sequences. Details of this test effort and respective analysis effort are provided in the following paragraphs.

a. Ball Bearing Test Procedure

(1) The test program consisted of endurance and bench testing of ball bearings in closed-loop lubrication systems. The deep groove ball bearings were made of through-hardening grade AISI 52100 steel and were tested under radial load. Component steel was carbon vacuum deoxidized (CVD) bearing quality steel. A schematic drawing of the type of test ball bearing is shown in Figure 1.

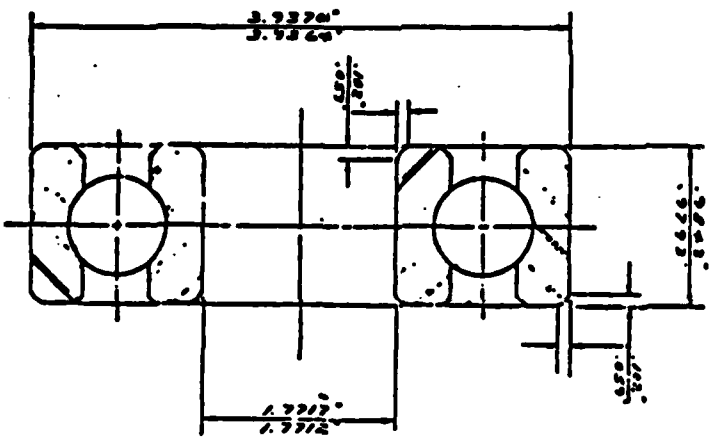


FIGURE 1
SCHEMATIC DRAWINGS OF TEST BALL BEARING
(TYPE 6309 DEEP-GROOVE BALL BEARING)

(2) The bearing tests were conducted on standard SKF type R-2 machines. A line diagram of the standard machine setup is shown in Figure 2. In the present series of tests, the existing lubrication system on the machine was disconnected and a separate, closed-loop lubrication system, shown schematically in Figure 3, was installed for each test bearing. The oil was recirculated by a magnetically coupled centrifugal pump. An assembly drawing of the pumping chamber of the pump is shown in Figure 4. Teflon tubing was used in these isolated lubrication systems to prevent complication in ferrogram analysis due to chemical interactions between the tubing and the ester base MIL-L-23699 oil.

(3) The test parameters for the ball bearing tests are listed in Table 7. Under the test conditions used, the theroetical L_{10} life (life by which 10% of the bearings are expected to fail) for the ball bearing type is 10 million revolutions (m.r.) (Appendix A). The theoretical L_{50} life is computed for a Weibull slope of 1 and is 5 times the L_{10} life as shown in the table. The number of stress cycles on the inner ring (f_i) for one revolution of the inner ring is given by:

$$f_i = 0.5\ Z\ (1 + Dw/dm\ \cos\alpha),$$

where

	Ball Bearing
Z = No. of rolling elements	8
Dw = diameter of rolling elements (mm)	17.5
dm = pitch diameter (mm)	72.5
α = contact angle (degrees)	0
f_1 = No. of stress cycles/rev. of inner ring	5

(4) A computer monitoring system was set to abort a test when the bearing operating temperature rises above 125°C. A Robertshaw vibraswitch was also set to terminate the test when bearing spalling failure occurred, by reacting to an increase in vibration level of the test head.

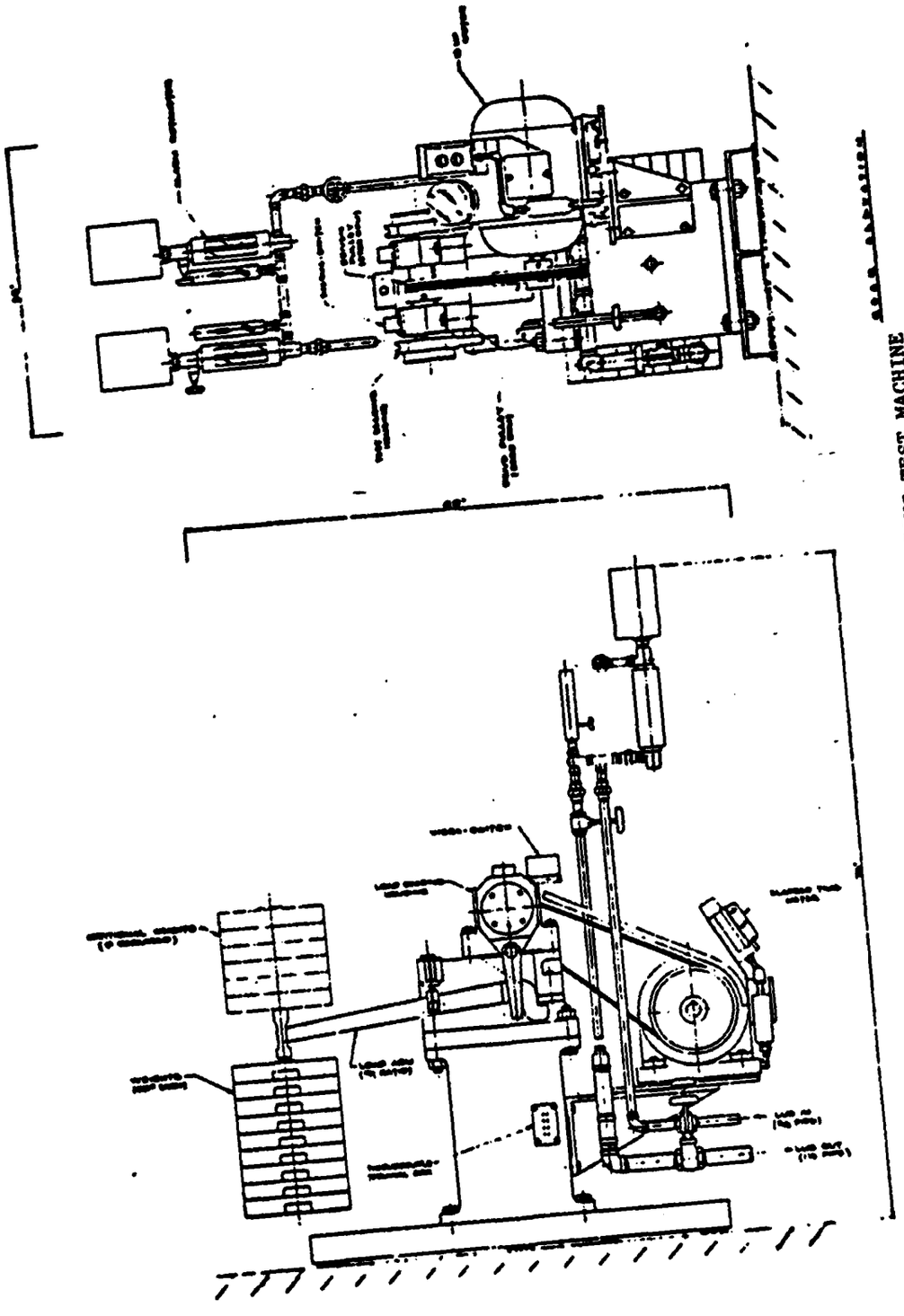


FIGURE 2. SKF TYPE R2 BEARING TEST MACHINE

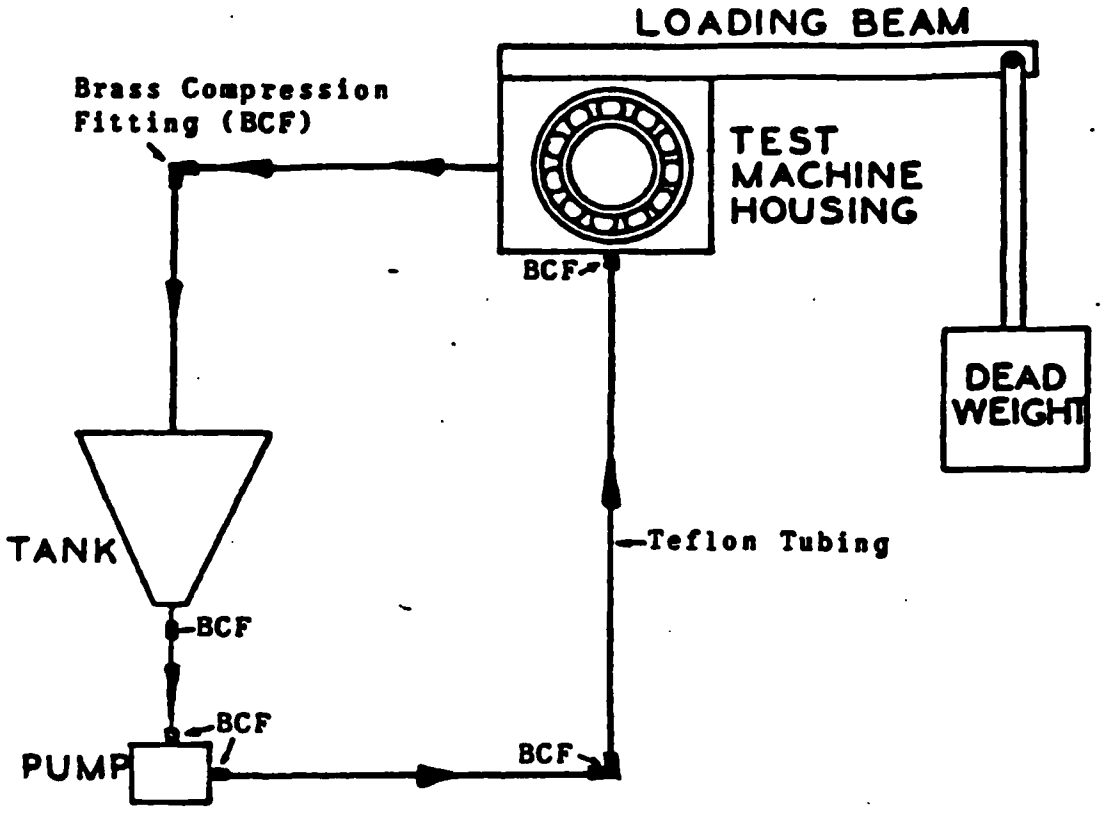
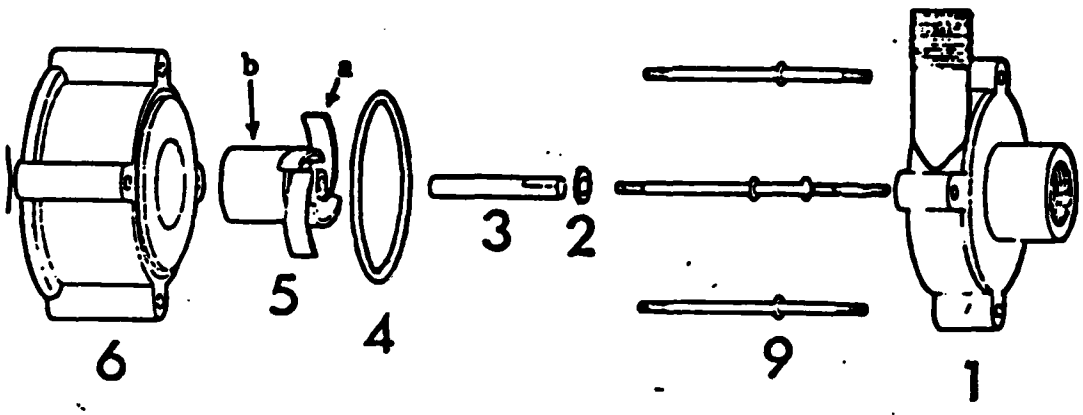


FIGURE 3
SCHEMATIC DIAGRAM OF CLOSED-LOOP LUBRICATION
SYSTEM FOR OIL ANALYSIS PROGRAM



NO.	OIL WETTED PART	MATERIAL
1	Front	Polypropylene
2	Washer	Titanium
3	Shaft	Titanium
4	O-Ring	Buna-N
5a	Impeller	Polypropylene
5b	Magnet	Epoxy (Black)
6	Magnet Housing	Polypropylene

FIGURE 4

OIL WETTED COMPONENTS OF THE RECIRCULATING PUMP

TABLE 7. BALL BEARING TEST PARAMETERS

	6309 Deep-Groove Ball Bearing
1. Bore diameter (D, mm)	45
2. Speed (N, rpm)	9,700
3. DN x 10^{-6}	0.44
4. Lube	MIL-L-23699
5. Lube viscosity at 38/100°C (cs)	25/5.1
6. Radial load (kN)	18.8
7. Axial load (kN)	0
8. Bearing capacity (kN)	40.5
9. Theoretical L_{10} Life:	
10^6 inner ring revolutions	10
10^6 stress cycles	50
10. Theoretical L_{50} Life:	
10^6 inner ring revolutions	50
10^6 stress cycles	250
11. Operating temperature (C)	90
12. Lube film parameter	1.8

(5) In order to accelerate bearing failure, the inner ring surfaces of the test bearings were initially dented with a Vickers pyramidal indenter using a 10 kg load. The indentor has an apex angle of 136° giving a diagonal-to-depth ratio of approximately 4.3. On a bearing surface having a hardness of R_c60, the length of the diagonal of the dent is approximately 160 μm.

(6) Fourteen ball bearings were tested. Ten bearings were subjected to endurance testing and four were subjected to interrupted test sequences. Respective designations for these bearings are given in Table 8. As can be observed from this table, two designation systems, SKF and Navy, were utilized under the test program. These designations will be used interchangeably throughout this report.

(7) Three R-2 machines each having two test heads were set up to test the bearings. Endurance testing of ten bearings was first completed in order to establish the time intervals at which the remaining tests should be interrupted for visual and scanning electron microscopic examination of the surface of the inner ring. The following approximate schedule of observations was chosen based on the endurance test results:

Ball bearings: 5, 75 and 150 x 10^6 revs.

(8) All ball bearing tests were conducted utilizing ester base MIL-L-23699 lubricant. This lubricant was provided to SKF by the Navy.

(9) In order to minimize liquid borne debris and thus simplify the debris analysis process, the as-received oil was filtered through a 3μm Millipore filter before being used for the tests. About two gallons of oil were used to fill each tank at the start of the test. The amount was not allowed to decrease below 1.5 gallons. This was achieved by adding new oil to each tank at recorded intervals.

TABLE 8. BALL BEARING OIL SAMPLES

Bearing I.D.		Bearing Running Time at Which Consecutive Oil Samples Were Taken (million revs.)*																			
Navy	SKF	1	2	3	4	5	6	7	8	9	10	11	12	13	14	15	16	17	18	19	20
ENDURANCE TESTS																					
BQ	001	.06	12.8	27.9	57	91	131	161	109	229	242	-	-	-	-	-	-	-	-	-	-
BR	002	.06	12.8	27.9	57	91	131	161	109	229	242	268	295	338	364	394	400	-	-	-	-
BS	007	.05	39.6	66	97	151	194	211	239	263	302	320	369	396	423	468	489	495	545	560	573
BT	010	.05	39.6	66	98	151	194	211	-	-	-	-	-	-	-	-	-	-	-	-	-
BU	012	.06	13.4	-	-	-	-	-	-	-	-	-	-	-	-	-	-	-	-	-	-
BV	017	.06	14.2	21.5	28.5	68	86	114	153	172	200	216	259	287	314	358	385	398	415	468	484
BW	019	15	54	72	100	139	153	160	-	-	-	-	-	-	-	-	-	-	-	-	-
BX	020	27	52	91	109	158	185	212	256	267	-	-	-	-	-	-	-	-	-	-	-
BY	021	25.6	52.9	95	122	151	166	193	199	210.1	227	268.3	285.7	318.1	345.7	375.3	417.1	431.6	-	-	-
BZ	024	27	43	86	113	141	185	212	241	294	310	-	-	-	-	-	-	-	-	-	-
BENCH TESTS																					
BA	025	15.7	22.1	72	86.7	100	123.3	137.9	182.7	209.5	222.9	224.7	-	-	-	-	-	-	-	-	-
BB	026	1.7	16.3	57.6	75	80.6	-	-	-	-	-	-	-	-	-	-	-	-	-	-	-
BC	028	14.5	59.3	86.1	99.5	120.9	162.7	176.3	190.6	195.3	260.2	288	308	-	-	-	-	-	-	-	-
BD	029	5.2	19.6	61.4	75	89.4	131	159	107	207	-	-	-	-	-	-	-	-	-	-	-

* Underlined sample running times indicate periodic surface examinations of bearing inner ring tracks.

(10) Oil samples were collected three times a week from all the tests. The samples were withdrawn by a 0.25-inch glass tube fitted with a suction bulb. A separate sampler was maintained for each tank. To inhibit chemistry changes in the lubricant, the samples were kept cold until they were subjected to analysis. The time table for oil sample withdrawal for ball bearings is given in Table 8. The times at which interrupted test bearings were examined are underlined. When a given bearing failed, an analysis of the oil samples in the reverse order revealed the time in the life of the bearing at which a noticeable change in the characteristics of the oil borne debris occurred.

(11) The bearings were modified to facilitate their assembly and disassembly for periodic examination of the inner-ring surfaces during bench test. The modified 6309 ball bearings used a snap cage as in standard SKF endurance tests instead of the riveted ribbon cage used in most field applications. Sixteen ball bearings were modified for use in this program; of these, 14 ball bearings were tested.

b. Ball Bearing Surface Monitoring

(1) The average dimension of the diagonal of the two dents on each of the test bearings, the corresponding Rockwell hardness (R_c) values, and the fatigue lives of the ball bearings are listed in Table 9. It is seen from the table that of the 14 ball bearings tested, 7 failed at the dent, 5 did not fail at the dent, and 2 tests were suspended without failure.

(2) The results of Weibull analysis of the fatigue life data for the ball bearings are presented in Table 10. The table shows that the L_{10} life of the 6309 bearing is approximately 7 times greater than its theoretical life.

(3) The character of a rolling contact surface is described by surface roughness given in μm AA and the RMS slope angle of the asperities. The slope angle is measured with reference to the horizontal so that the flatter the surface the lower the slope angle. These parameters were measured on selected

TABLE 9. SUMMARY OF BALL BEARING TEST RESULTS

Type Test	Bearing ID Navy	Bearing ID SKF	Indent Size (um)	Rockwell Hardness (R_c)	No. of Oil Samples	Life (m.r.)	Element Failed
Endurance	BQ	001	162	60.4	10	243	IR(a)
"	BR	002	161	60.8	16	408	IR(b)
"	BS	007	163	60.0	20	596	IR(a)
"	BT	010	163	60.0	7	211	IR(a)
"	BU	012	163	60.0	2	13.4	IR(a)
"	BV	017	161	60.8	20	484	T*
"	BW	019	162	60.4	7	160	IR(a)
"	BX	020	162	60.4	9	267	IR(a)
"	BY	021	162	60.4	17	375	IR(b)
"	BZ	024	161	60.8	10	310	IR(b)
Bench	BA	025	163	60.0	11	225	IR(b)
"	BB	026	162	60.4	5	80.6	IR(b)
"	BC	028	160	61.0	12	288	T
"	BD	029	161	60.8	9	167	IR(a)

* T = Terminated without failure
(a) = Failed at Vickers indentation
(b) = Did not fail at Vickers indentation

TABLE 10. WEIBULL ANALYSIS OF BALL BEARING FATIGUE LIFE RESULTS

	Ball Bearing 6309
1. Median Bias Corrected L_{10}	
10^6 revolutions	70.4
10^6 stress cycles	352.0
2. 90% Confidence Interval for L_{10}	
10^6 revolutions	25.5 - 123.6
10^6 stress cycles	127.5 - 615.0
3. Weibull Slope	1.58
4. Improvement Over Theoretical Life of 10 m.r.	7.04X
5. Median Bias Corrected L_{50}	
10^6 revolutions	255.8
10^6 stress cycles	1279.0
6. 90% Confidence Interval for L_{50}	
10^6 revolutions	171.3 - 374.5
10^6 stress cycles	856.5 - 1872.5

endurance test bearings in the unrun and failed states. On the interrupted test bearings, BC and BD, these values were also measured when the bearings were disassembled for intermittent examinations. These measurements, listed in Table 11, indicate that rolling contact causes surface roughening and an increase in the asperity slope angle. Intuitively it would appear that the flattening of the asperities during rolling contact should give lower slope angle and surface roughness values. This apparent contradiction is explained by the presence of a large number of debris dents on the rolling surface. The sharp edges of the dents and their large peak-to-valley heights leads to the higher slope angle and surface roughness values measured on the failed bearings. This is clearly illustrated in Figure 5 which shows the cross groove profiles taken on bench test bearing BC in the unrun and run conditions. To appreciate the significance of the tracings, it is necessary to understand how they are made. These traces are made in such a way that if the radius of the groove was perfect, the trace would be a straight line except for the trailing ends. In the cross groove tracing of the unrun bearing BC-028, a small deviation is observed. The maximum deviation from perfect radius is approximately 1μm and is not significant to the normal performance of the bearings.

(4) Surface examination was also conducted with the help of optical and scanning electron microscopes. The type of surface defects present on the as-finished bearing consisted of the artificially induced Vickers indentation and grinding furrows. These are illustrated in Figure 6. During the formation of the Vickers indentation, a raised shoulder of metal is formed around the dent. For a material of hardness R_c50 the maximum height of the shoulder is approximately 1.6μm, Figure 7. The height is 1μm for an R_c60 material. Such a shoulder is also present on the sides of a grinding furrow although to a much lesser extent since it is formed in a metal removal process. The presence of such a shoulder and elastic deformations around such defects during rolling contact, subjects the surrounding material to significantly higher stresses.

(5) Due to these higher stresses the material suffers plastic deformation resulting in glazing and microspalling, Figure 8. Surface dents may also be formed due to debris present in the lubricant. One such dent, presently called a multifragmented dent, due to its multifaceted appearance, with its

TABLE 11. BALL BEARING SURFACE MEASUREMENT DATA AS A FUNCTION OF MILLION REVOLUTIONS

Bearing ID (Navy-SKF)	Million Revolutions	Surface Roughness (μmAA)	Slope Angle (Deg)
BQ-001	Unrun	0.036	1.27
	242	0.09	2.3
BR-002	Unrun	0.042	1.33
	408	0.05	2.1
BU-012	Unrun	0.036	1.57
	13.4	0.044	1.7
BC-028	Unrun	0.025	1.23
	14.5	0.045	1.38
	59.3	0.06	1.65
	162.7	0.074	2.27
BD-029	Unrun	0.025	1.15
	5.2	0.041	1.30
	75	0.063	2.03

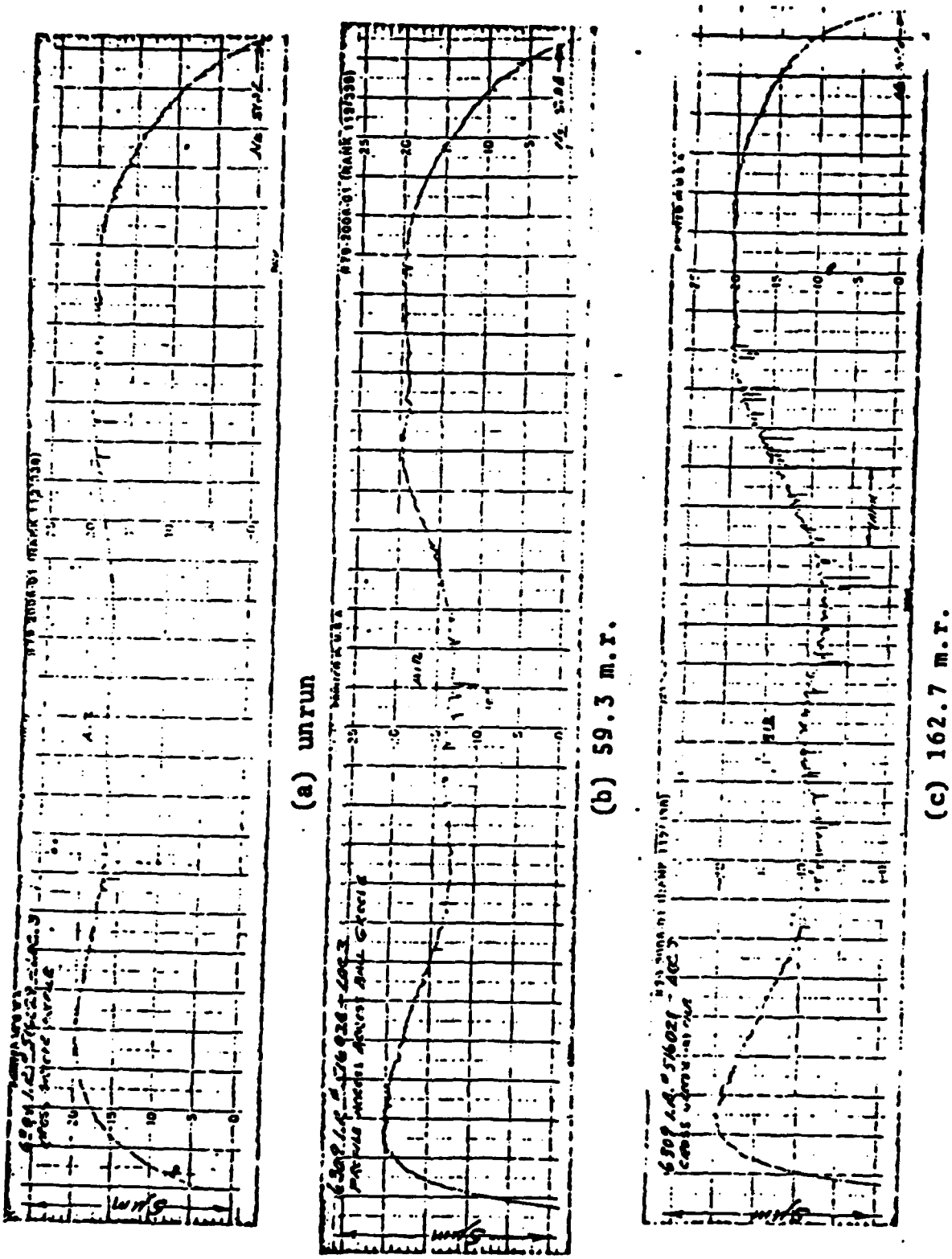
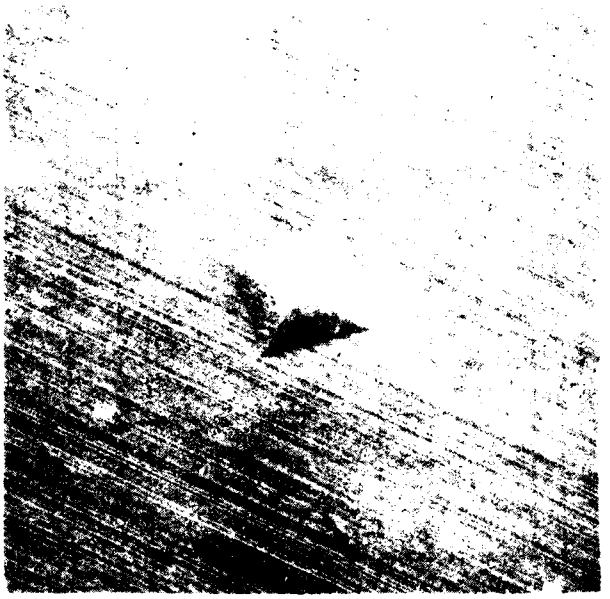


FIGURE 5
CHANGES IN PROFILE AND SURFACE TEXTURE OF BEARING NO. BC-028
INNER RING RACEWAY WITH ROLLING CONTACT RUNNING TIME



3629 125X

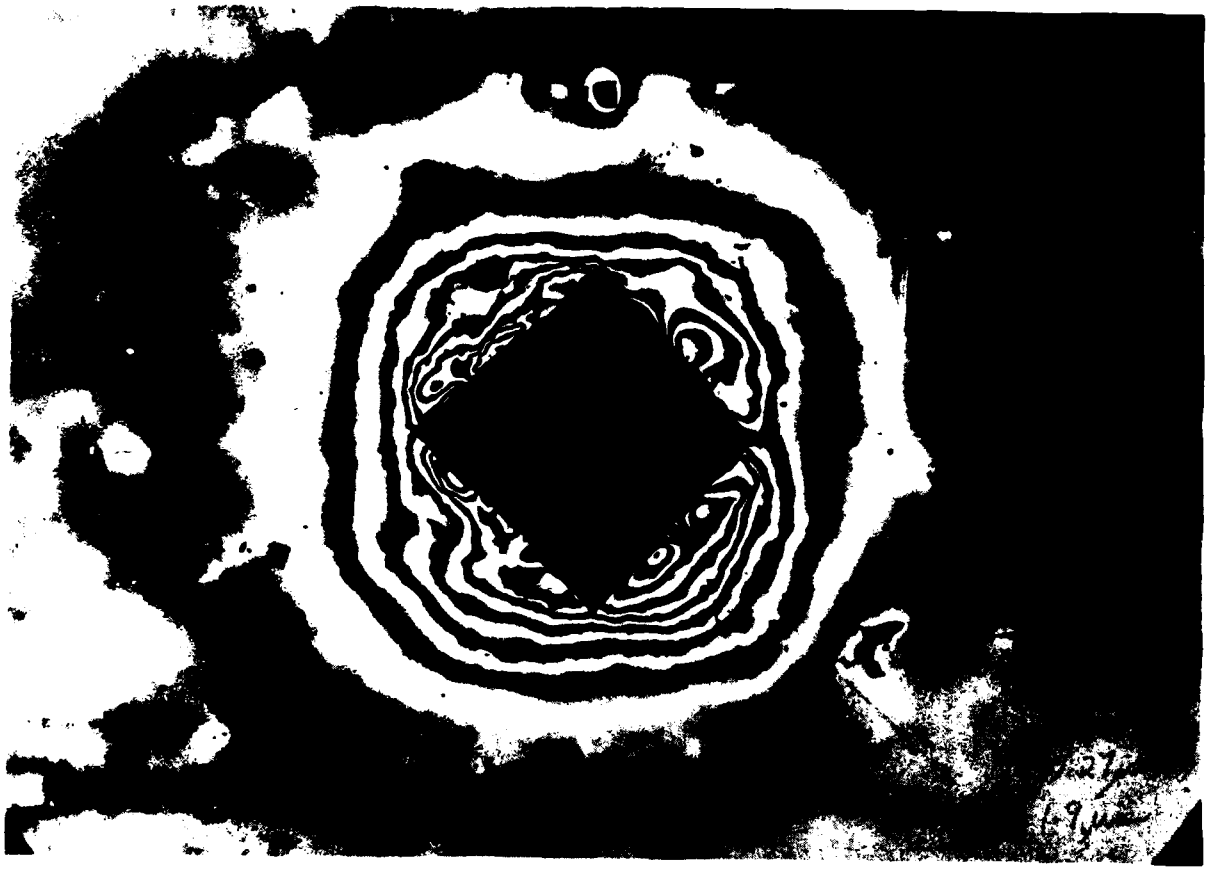
A. ARTIFICALLY INDUCED VICKERS HARDNESS INDENT



3632 125X

B. FURROW GENERATING DURING MANUFACTURING

FIGURE 6. SURFACE DAMAGE ON RACEWAY OF AN AS-FINISHED BALL BEARING (NO. BA-025)



220X

FIGURE 7. INTERFERENCE MICROGRAPH OF A VICKERS INDENTATION ON A Rc50 HARDNESS STEEL SUBSTRATE. (COURTESY OF DR. A. W. RUFF, NATIONAL BUREAU OF STANDARDS)



3707 86.7 m.r. 250X

A. SURFACE DISTRESS - A - AND MICRO-SPALLING - B - AT DENT IN FIGURE



3735 86.7 m.r. 100X

B. SURFACE DISTRESS AT FURROW SHOWN IN FIGURE



Rolling Direction

3738 137.9 m.r. 250X

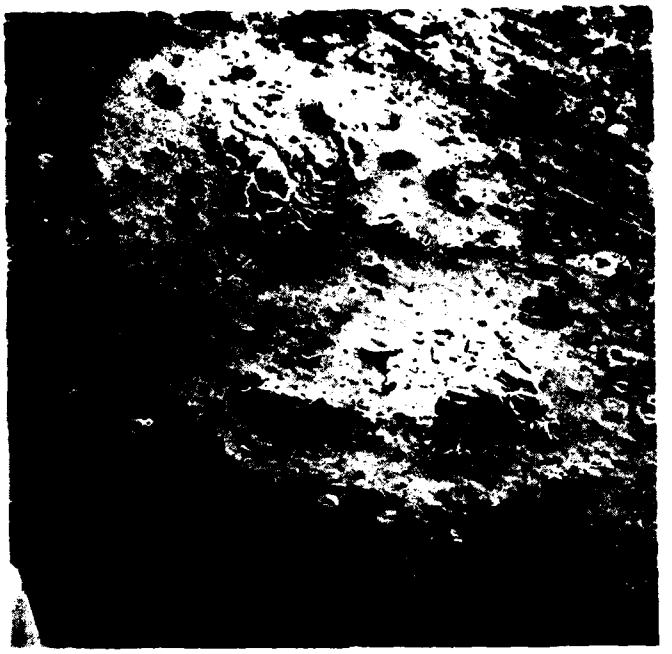
C. ROLLING CONTACT INDUCED MULTIFRAGMENT DENT

FIGURE 8. ROLLING CONTACT INDUCED DAMAGE ON BALL BEARING RACEWAY

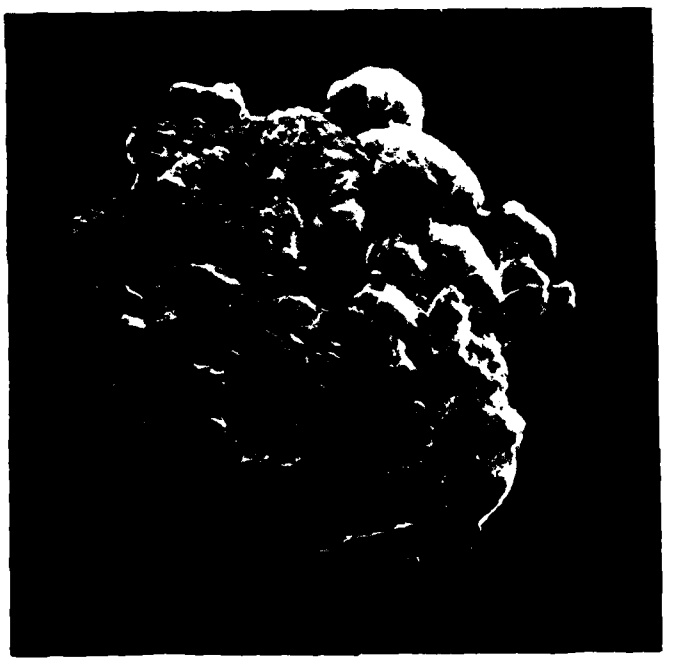
associated glazed area, is also shown in Figure 8C. The glazed area in this case is predominantly on the lagging end of the dent. This is due to the fact that the wear debris was pushed into the inner ring surface, creating a shoulder ahead of the ball. These higher stressed areas undergo a higher fatigue rate than the rest of the surface and therefore become preferential failure initiation sites.

(6) Subsurface defects, such as inclusion stringers, can also act as stress raisers causing the surrounding material to fatigue at a higher rate. It is difficult to follow the progression of failure at such areas since they are not noticeable until the spall breaks out. For example, in the case of bearing BA-025, a new surface defect was detected at 182 m.r. This defect was not detected during the previous intermittent examination at 138 m.r. Spalling at this defect occurred at 225 m.r. The appearance of the defect at 182 m.r. and that of the spall formed at 225 m.r. are shown in Figure 9. In general, the time between the break out of the spall to the surface to the formation of the spall size at which the machine is shut off by the vibraswitch is about 8 to 12 m.r. under the accelerated test conditions used. Although under normal load conditions the progression to failure would take considerably longer, it would still be difficult to detect a subsurface-initiated spall at the early stages of its inception, by techniques that examine surfaces or the wear particles generated therefrom.

(7) The kinematics of the bearing is also important to the way failure progresses around a surface defect. In the case of ball bearings there are only two points across the groove at which pure rolling occurs, Figure 10. Between these two points the rolling elements slide in a direction opposite to their direction of rolling (negative slip). Outside the bands the slip is positive. The effect of negative slip on failure progression at the Vickers indentation is clearly evident in the series of micrographs shown in Figure 11 taken from bearing BD-029. During the early stages, the trailing edges of the dent are curved in. Once the material around the dent grows sufficiently weak due to fatigue or the presence of cracks, it deforms in the direction of sliding (into



3932 182.7 m.r. 1500X
BA-025



3999 224.7 m.r. 10X
BA-025

FIGURE 9. APPEARANCE OF SPALL INITIATION SITE AND SPALL ON BEARING NO. BA-025

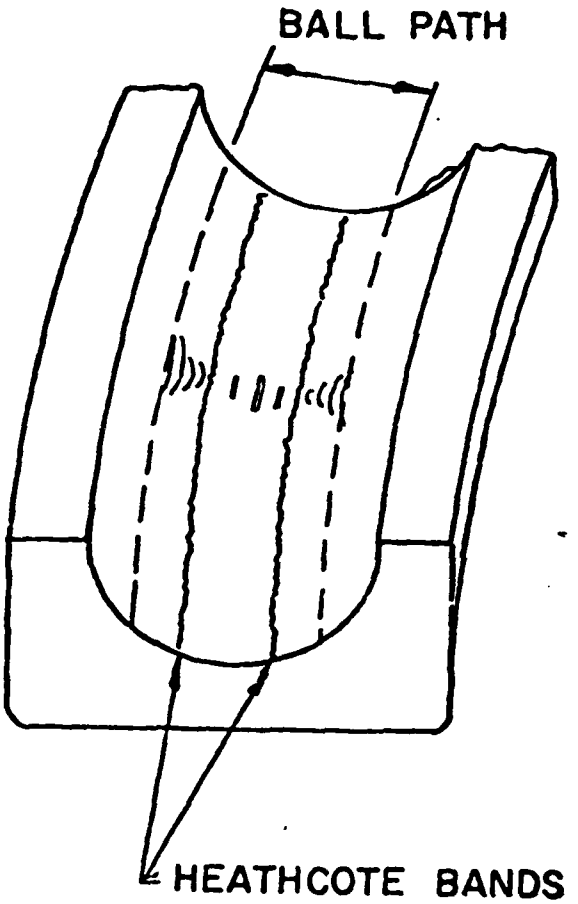
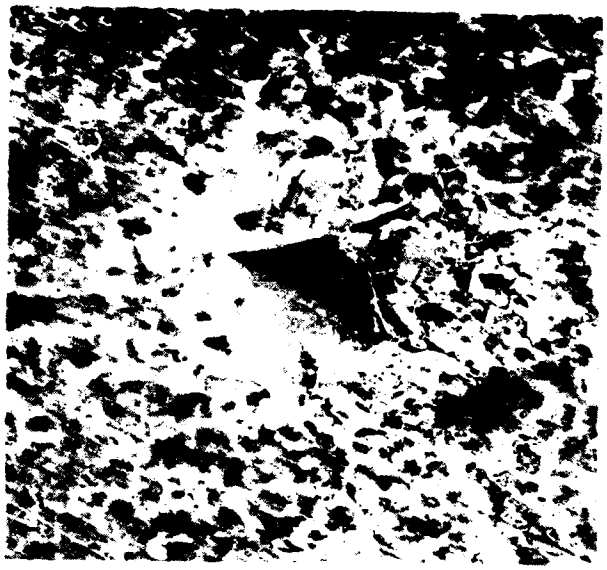


FIGURE 10. SKETCH OF INNER RING BALL GROOVE SHOWING THE LOCATION OF PURE ROLLING (HEATHCOTE) AND SLIDING REGIONS.



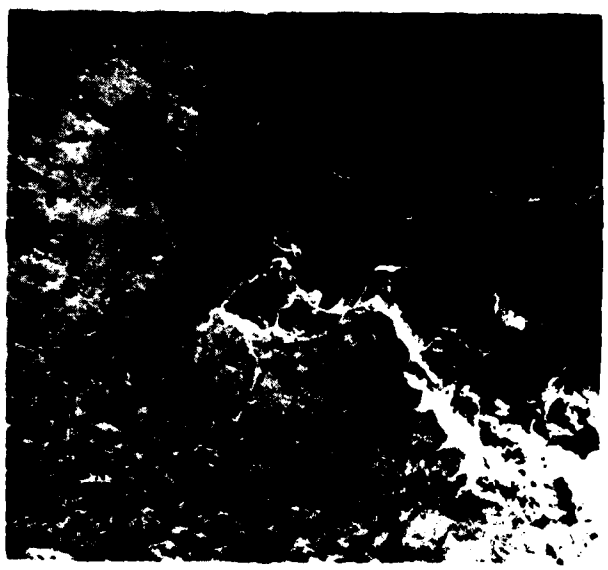
4089 5.2 m.r. 250X



4249 75 m.r. 250X



4342 207 m.r. 10X



4344 207 m.r. 250X

FIGURE 11. PROGRESSION OF FAILURE AT THE 0° VICKERS INDENTATION ON BEARING NO. BD-029.

the dent). Further testing leads to spalling. In the case of bearing BD-029, gross deformation of the material at the trailing end of the dent was observed at 75 m.r. The bearing failed at 207 m.r. The second dent on the same bearing had suffered apparently the same level of damage at 75 m.r. but was not spalled at 207 m.r., Figure 12.

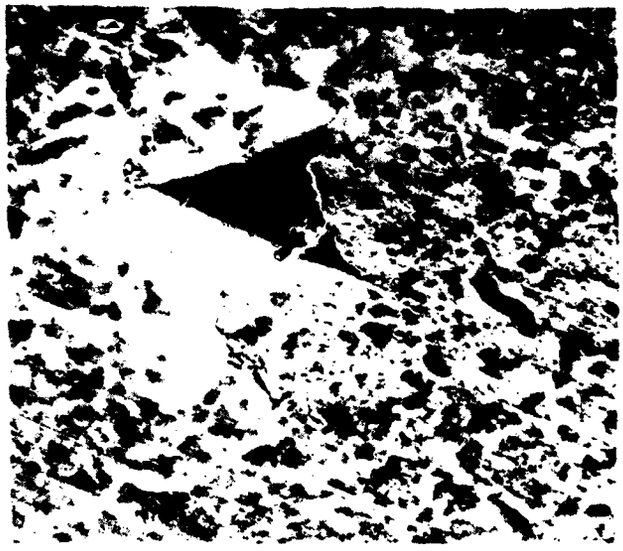
(8) Bearing kinematics and the way the stress wave travels over a point also affects the appearance of the material at the leading and the lagging ends, Figure 13. The leading end material contains a few large cracks curved in the direction of rolling, Figure 13A. The appearance of the surface is smooth as in a glazed region. The lagging end of the spall contains a multitude of fine cracks curved opposite to the direction of rolling, Figure 13B.

c. Ball Bearing Wear Particle Analysis

(1) Wear debris analysis was performed on respective ball bearing bench test lubricant samples by SKF Industries, Foxboro Analytical, and Naval Air Engineering Center (NAVAIRENGCEN). As previously described, lubricant samples were withdrawn periodically from the ball bearing test apparatus. These lubricant samples served as the host media for fluid-borne debris analysis. Table 8 summarizes the sample number and respective operating times for each ball bearing series.

(2) Analysis has verified that component life normally can be classified into three distinct phases: wear-in/break-in, normal wear, and wear-out/abnormal wear. It is not true, however, that all components transition through all three phases. A detailed discussion of this wear process is presented in Section VI.

(3) Each ball bearing wear life phase will be evaluated with respect to wear debris characteristics that present themselves during the respective phase. Particle characteristics such as quantity, size distribution, composition, and morphology will be correlated to surface wear condition/life during the ball bearing bench test sequence.

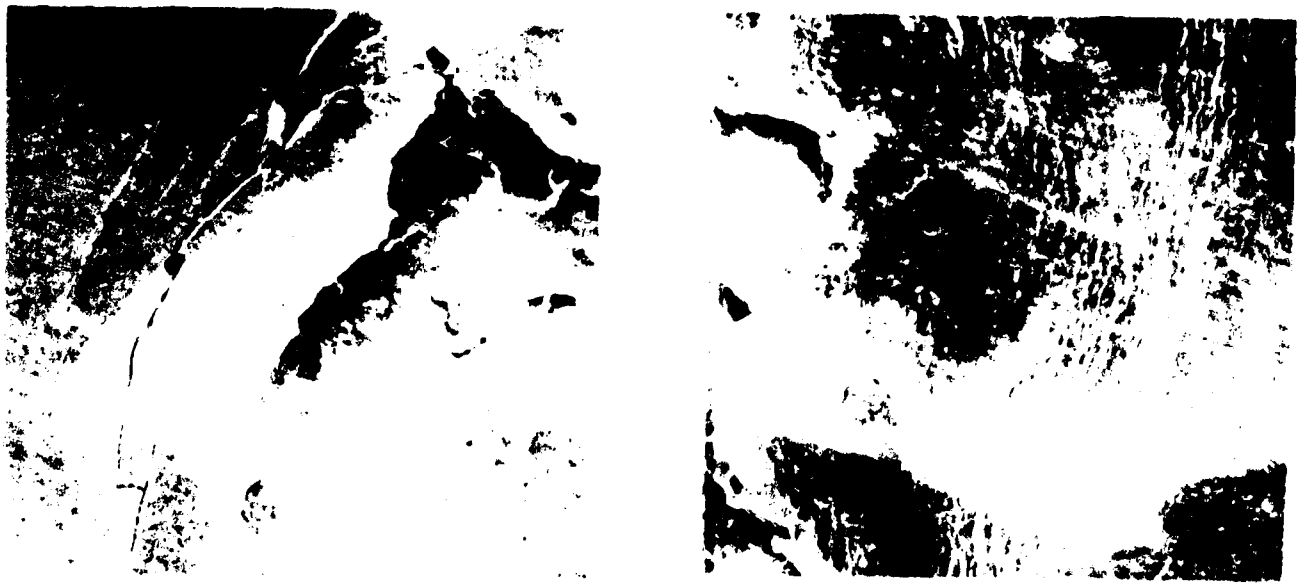


4259 75 m.r. 250X



4347 207 m.r. 250X

FIGURE 12. DAMAGE AT THE 180° VICKERS INDENTATION ON BEARING NO. BD-029.



4002 LEADING EDGE 50X 4000 LAGGING EDGE 100X

FIGURE 13. APPEARANCE OF THE LEADING AND LAGGING EDGES OF A SPALL ON BEARING NO. BA-025 AFTER 224.7 M.R.

(a) Particle Quantity

1. The quantity of wear debris contained in lubricant samples taken during ball bearing testing was primarily monitored utilizing ferrographic analysis techniques. Particle counting technique results were discounted as a result of the presence of nonmagnetic lubricant pump debris found in the respective oil samples. Ferrographic magnetic precipitation techniques served to minimize the complicating effects of this nonmagnetic debris. Spectrometric analysis concentration readings were also discounted with respect to particle quantity monitoring as a result of their inherent size sensitivity limitation. This limitation is discussed in detail in Section VI.

2. Lubricant-borne particle quantity/concentration levels basically followed a bathtub curve plot over the wear life of the ball bearings. Figure 14 represent plots for two of the ball bearings sequences, BQ and BX. Figures 15 and 16 represent series of ferrography entry deposit micrographs of these sequences, which can be directly related to sample debris concentration levels. These micrographs provide graphic evidence of the bathtub plot.

3. Each sequence can be divided into three wear regimes: wear-in, normal wear, and wear-out/abnormal wear, as shown in Figure 17. Initial wear-in of the ball bearings results in a high wear rate, thus a high level of debris concentration. The second regime, normal wear, results in a much lower wear rate thus a much lower level of debris concentration. Abnormal wear, the final regime, results in an accelerated wear rate and thus an ever increasing level of debris. This increase was typical of all ball bearing test failures.

4. It is to be noted that these lubricant systems were not equipped with a filter. As a consequence, decreases in debris concentration must have resulted from a combination of natural filtration (that is, plating

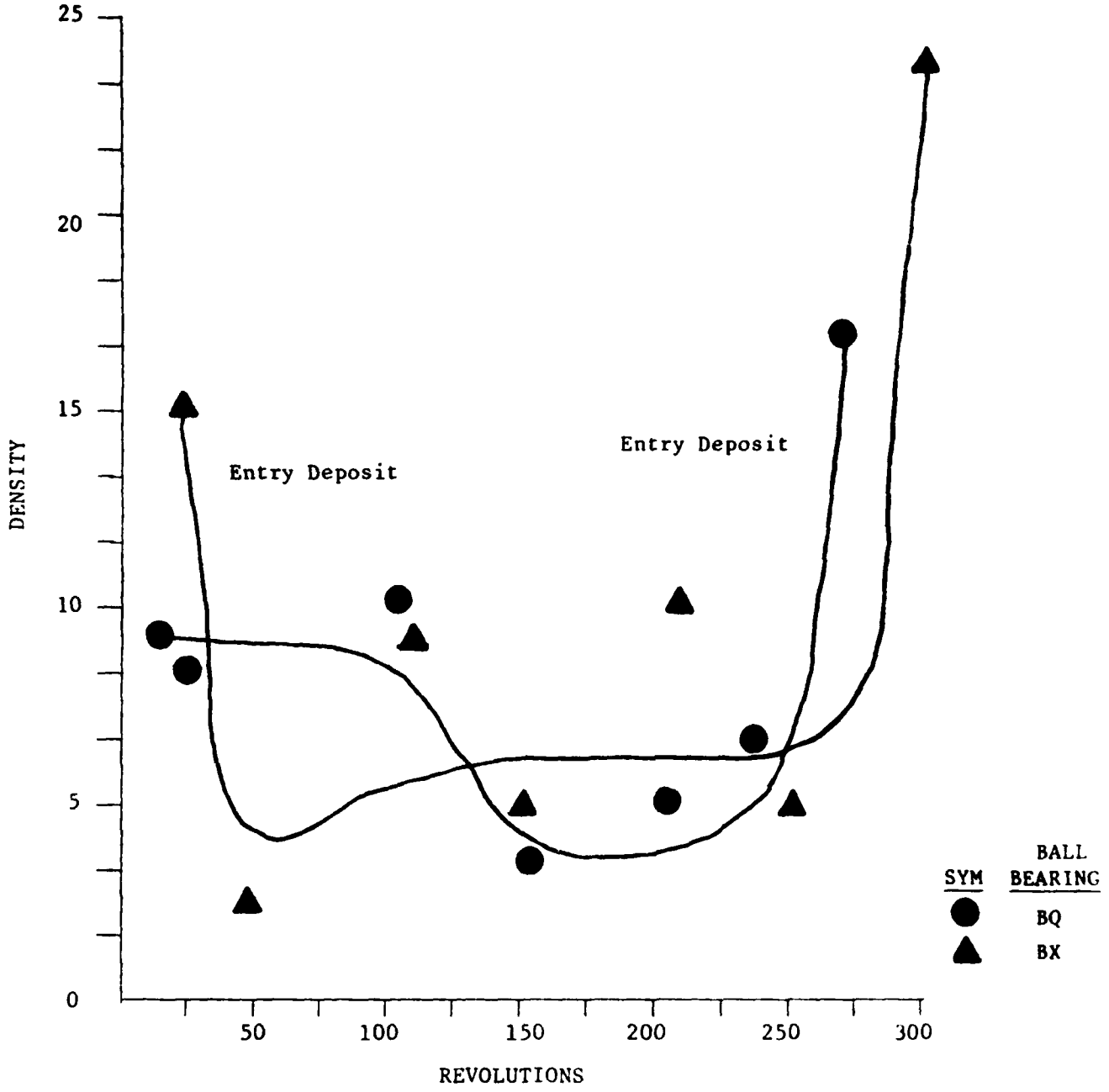
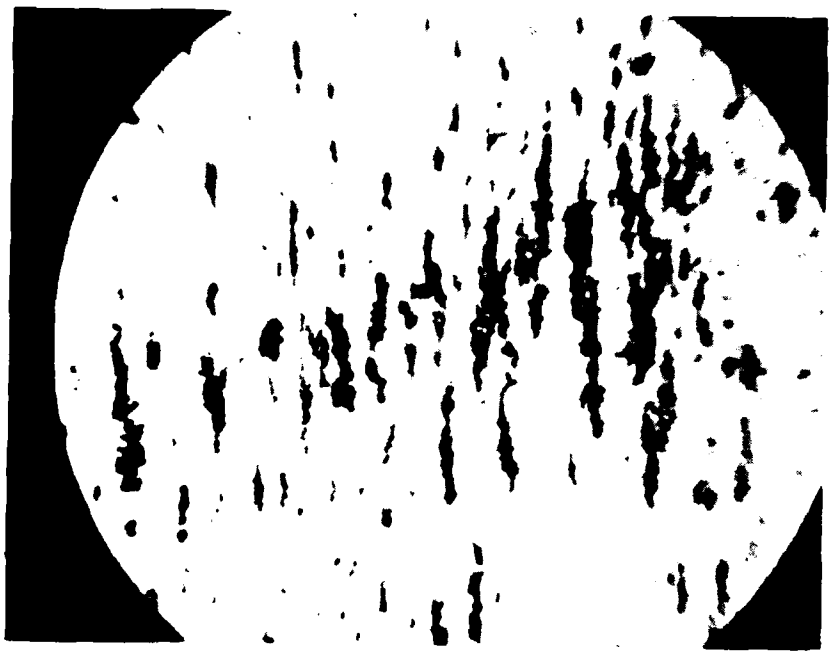


FIGURE 14
BALL BEARING TEST SEQUENCES BQ AND BX
FERROGRAPH DENSITY DATA

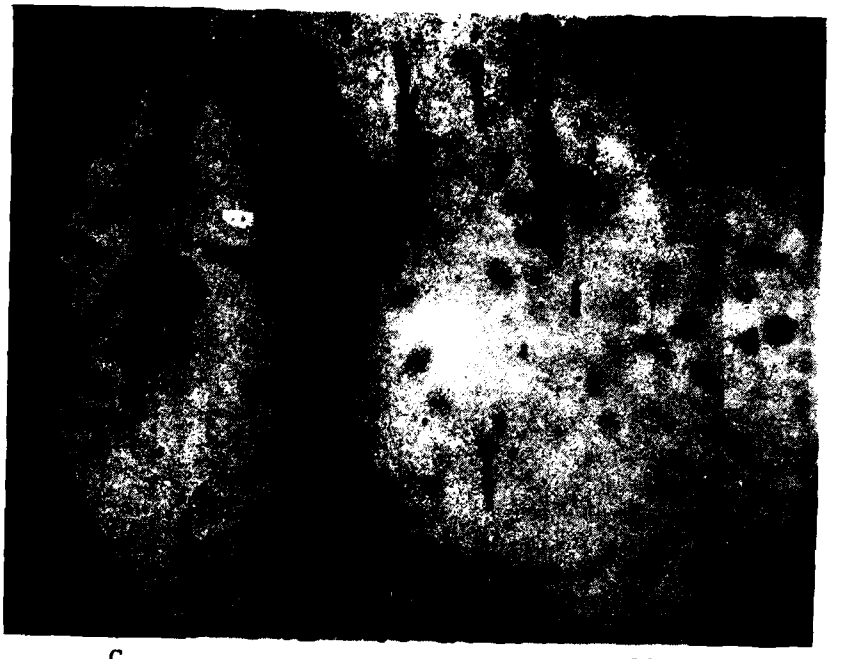


A. 12.8 m.r.

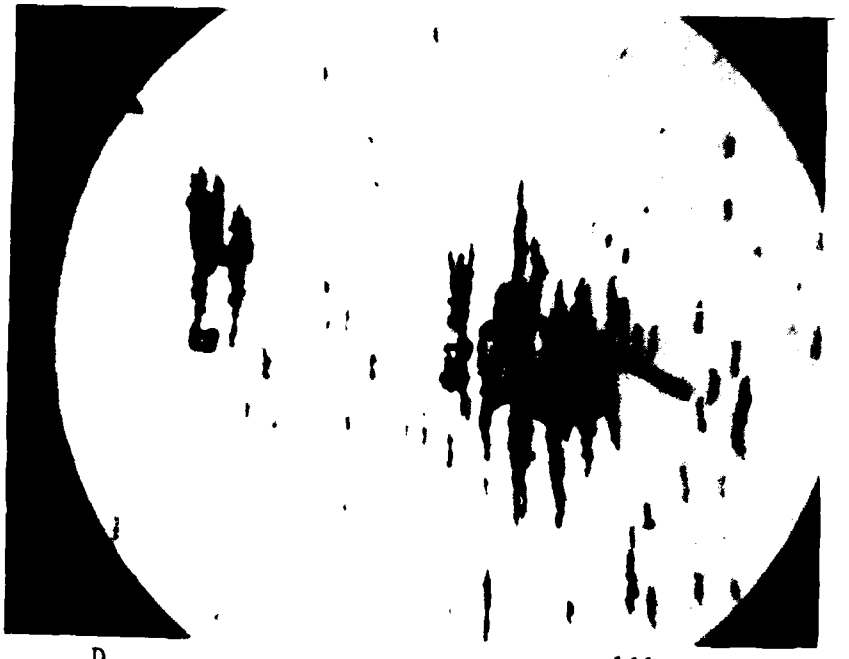


B. 27.9 m.r.

FIGURE 15
BALL BEARING TEST SEQUENCE BQ
ENTRY DEPOSIT
LOW MAGNIFICATION
(Sheet 1 of 4)

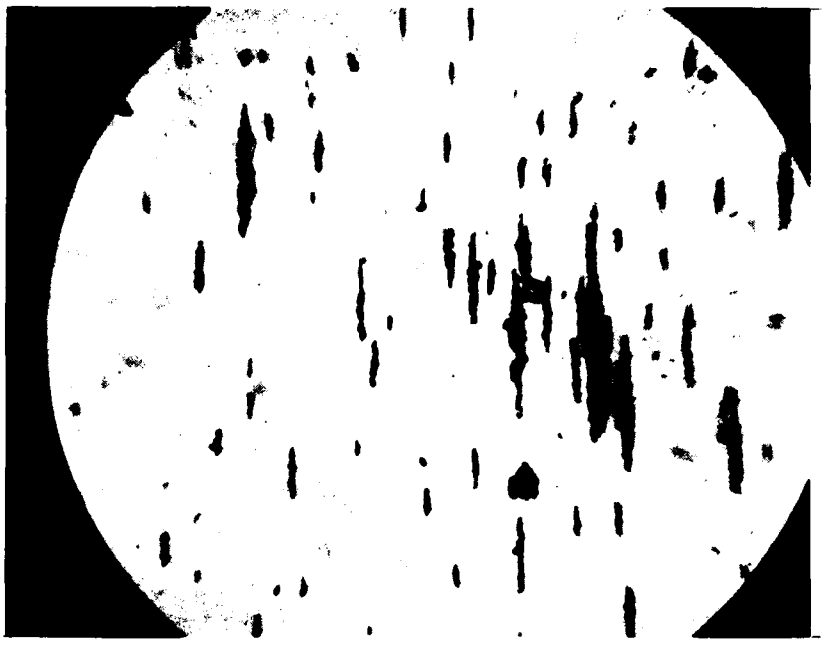


C. 91 m.r.

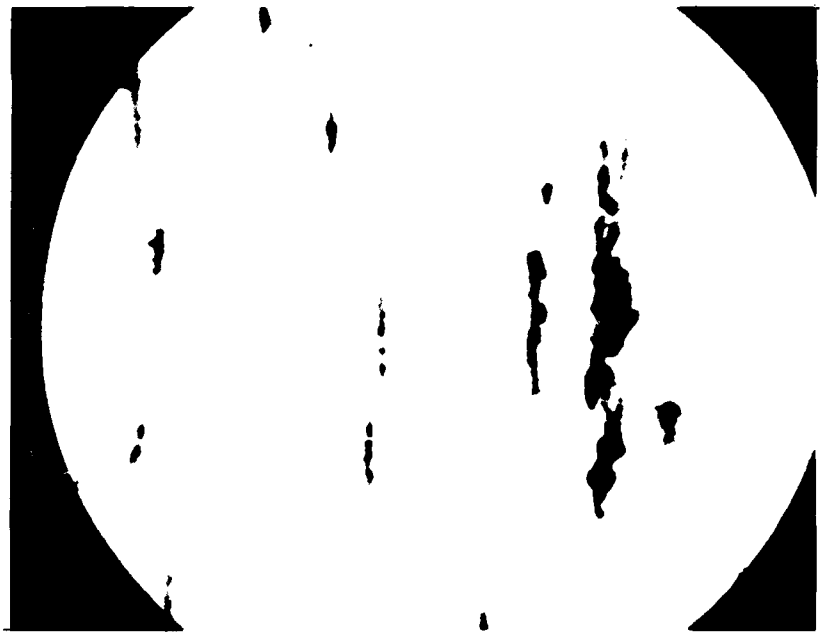


D. 161 m.r.

FIGURE 15
BALL BEARING TEST SEQUENCE BQ
ENTRY DEPOSIT
LOW MAGNIFICATION
(Sheet 2 of 4)



E. 189 m.r.



F. 229 m.r.

FIGURE 15

BALL BEARING TEST SEQUENCE BQ

ENTRY DEPOSIT

LOW MAGNIFICATION

(Sheet 3 of 4)



G. 242 m.r.

FIGURE 15

BALL BEARING TEST SEQUENCE BQ

ENTRY DEPOSIT

LOW MAGNIFICATION

(Sheet 4 of 4)



A. 27 m.r.

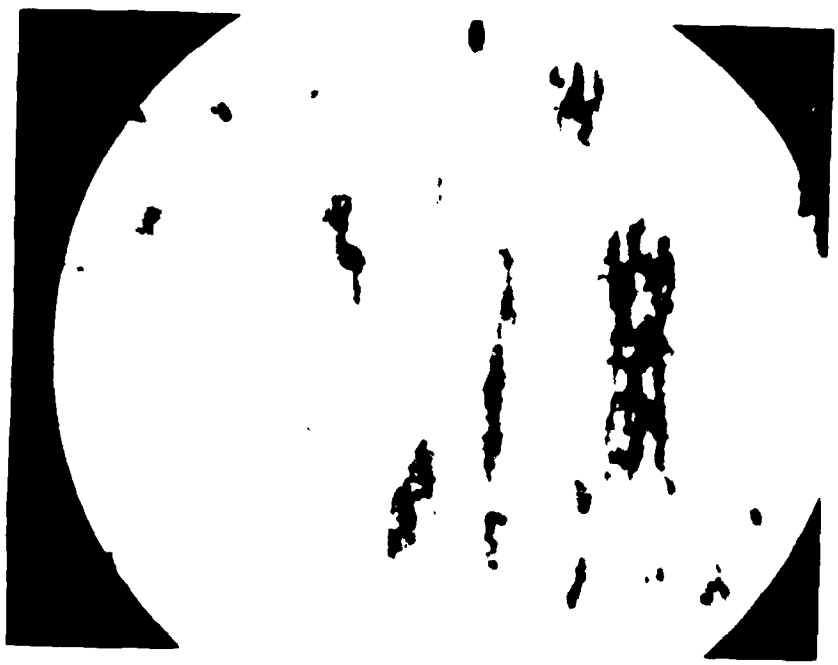


B. 52 m.r.

FIGURE 16
BALL BEARING TEST SEQUENCE BX
ENTRY DEPOSIT
LOW MAGNIFICATION
(Sheet 1 of 4)



C. 91 m.r.

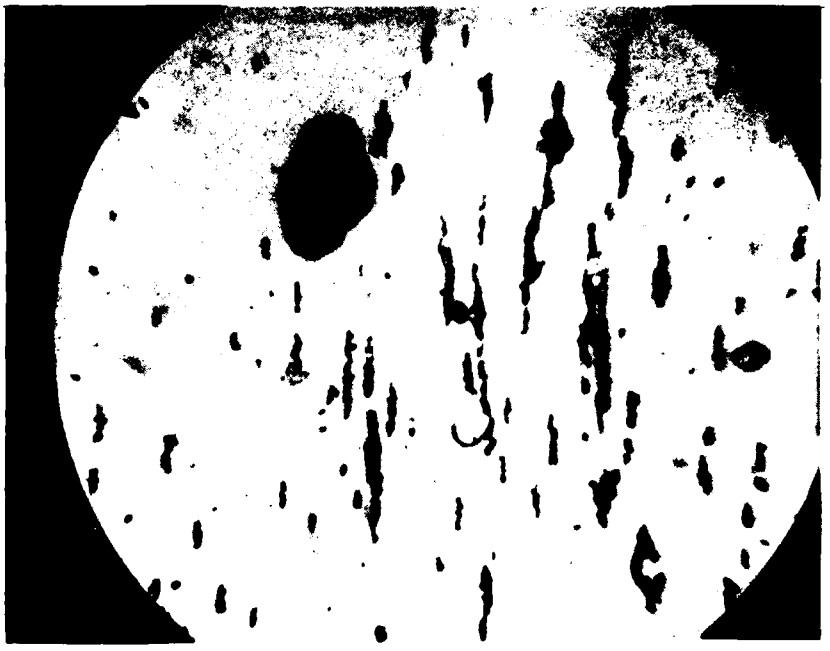


D. 158 m.r.

FIGURE 16
BALL BEARING TEST SEQUENCE BX
ENTRY DEPOSIT
LOW MAGNIFICATION
(Sheet 2 of 4)



E. 212 m.r.



F. 256 m.r.

FIGURE 16

BALL BEARING TEST SEQUENCE BX

ENTRY DEPOSIT

LOW MAGNIFICATION

(Sheet 3 of 4)



G. 267 m.r.

FIGURE 16
BALL BEARING TEST SEQUENCE BX
ENTRY DEPOSIT
LOW MAGNIFICATION
(Sheet 4 of 4)

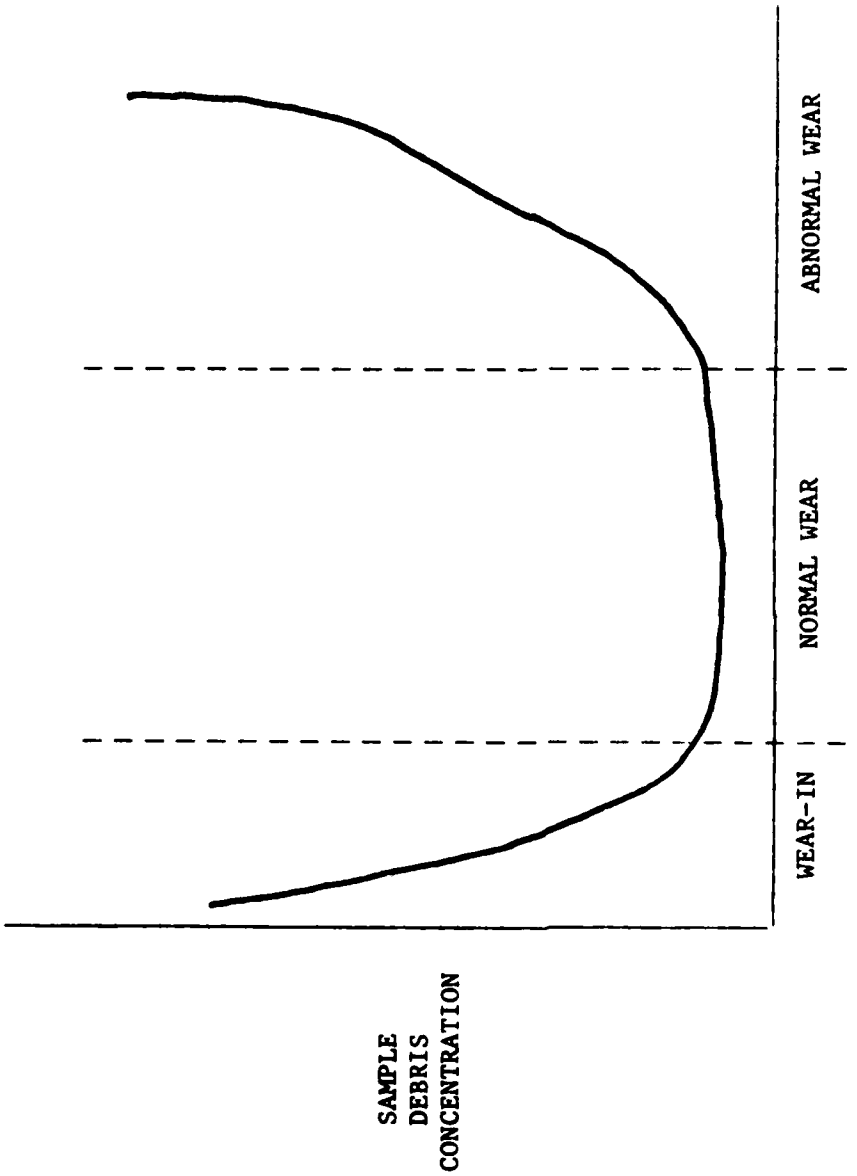


FIGURE 17

TYPICAL BALL BEARING TEST SEQUENCE
DEBRIS CONCENTRATION VERSUS WEAR LIFE

out, settling effects, etc.) and a particle grinding process which causes particle breakup. This grinding process will eventually reduce debris size to a level below the monitoring technique sensitivity level. Grinding effects are further discussed in Section VI.

5. Figure 18 represents a debris deposit plot for ball bearing test sequence BA. Figure 19 presents the respective series of ferrography entry deposit micrographs from this sequence. This bearing was one of the four ball bearing test sequences that were periodically interrupted for wear surface analysis. As can be seen from this plot, a "bathtub" trend is not apparent. It is concluded that the periodic disassembly/reassembly of the bearing resulted in reoccurrences of a wear-in process and thus an erratic plot of sample debris concentration. This effect is detailed in Section VI. As a result of this wear-in reoccurrence in the inspected ball bearing sequences, debris analysis results from these series are suspect.

6. Tables 12 and 13 represent spectrometric readings from sequences BA and BX. As can be seen from the iron (Fe) concentration readings there is little indication of wear debris concentration variation. These results are typical of spectrometric analysis of ball bearing sequence oil samples. A detailed discussion of this effect is presented in Section VI.

7. Table 14 represents particle counting data from bearings BQ, BX, and BA. As can be seen, this data is erratic and does not follow the wear debris trends as indicated by the ferrographic analysis. These variations are typical of the ball bearing test sequences and are concluded to be a result of oil pump wear. It appears that the utilized test oil pump resulted in the generation of wear debris consisting of epoxy and titanium. The presence of this debris has been verified optically and in some cases picked by spectrometric analysis as indicated in Table 12. Particle count data from bear- ing BA was further complicated by the reoccurrence of the wear-in process as previously discussed.

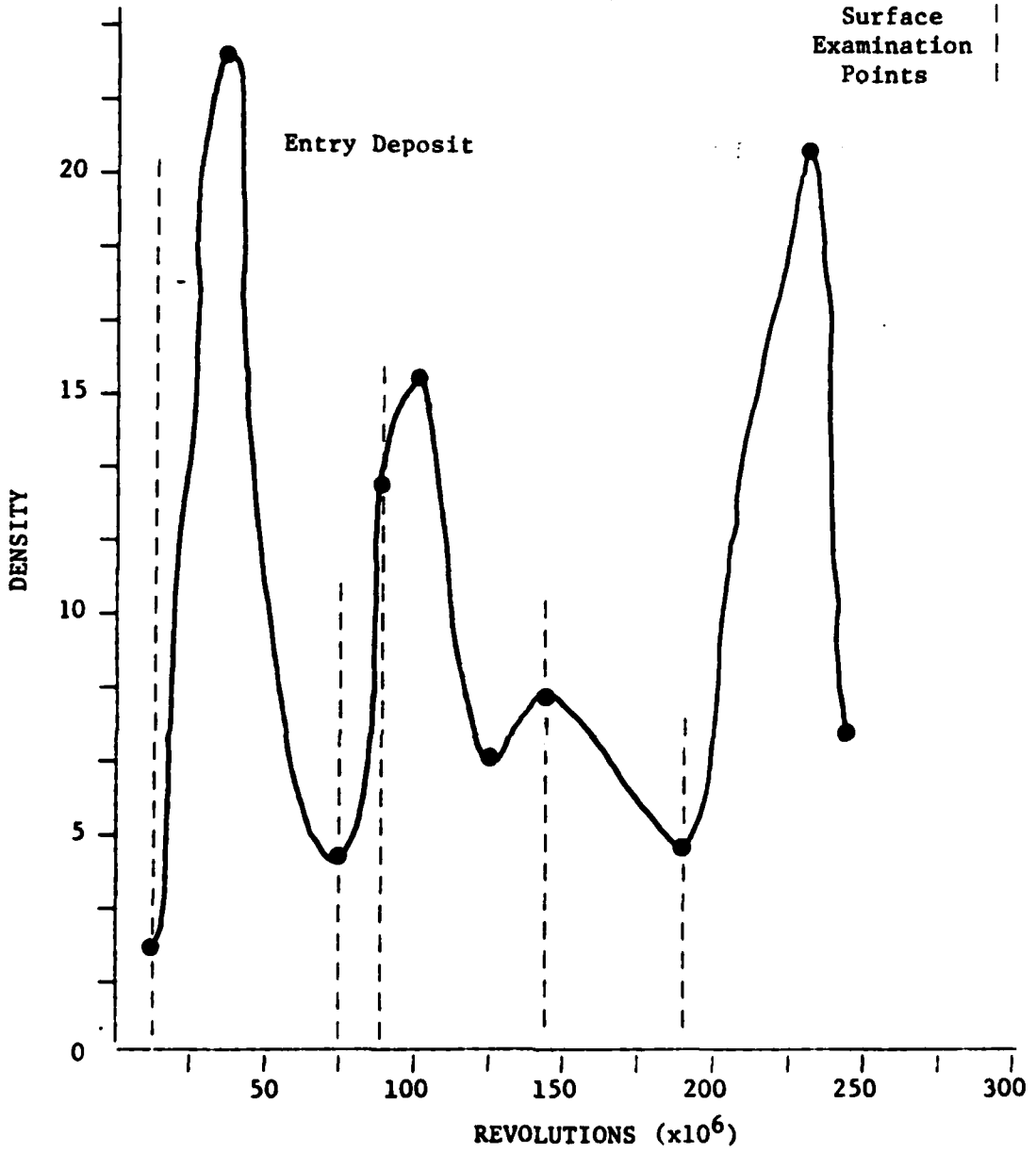
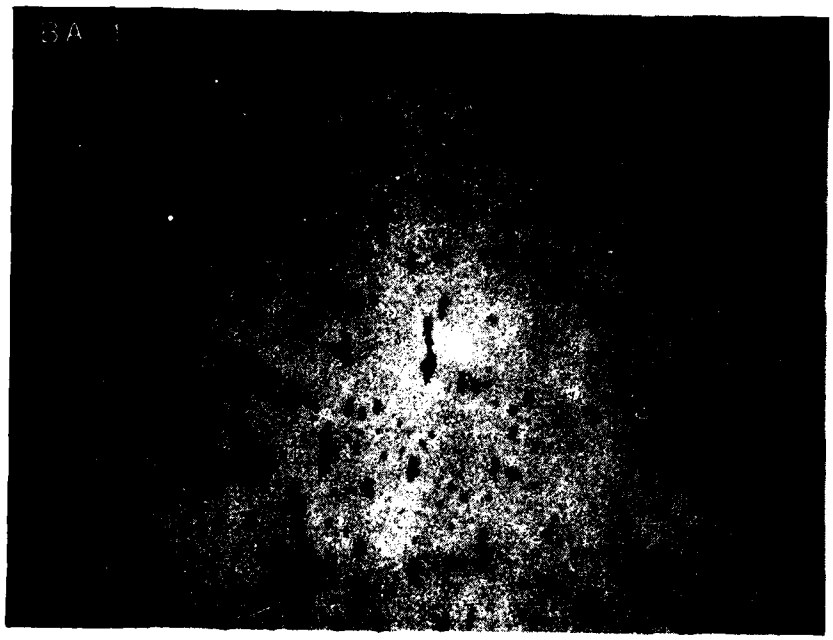


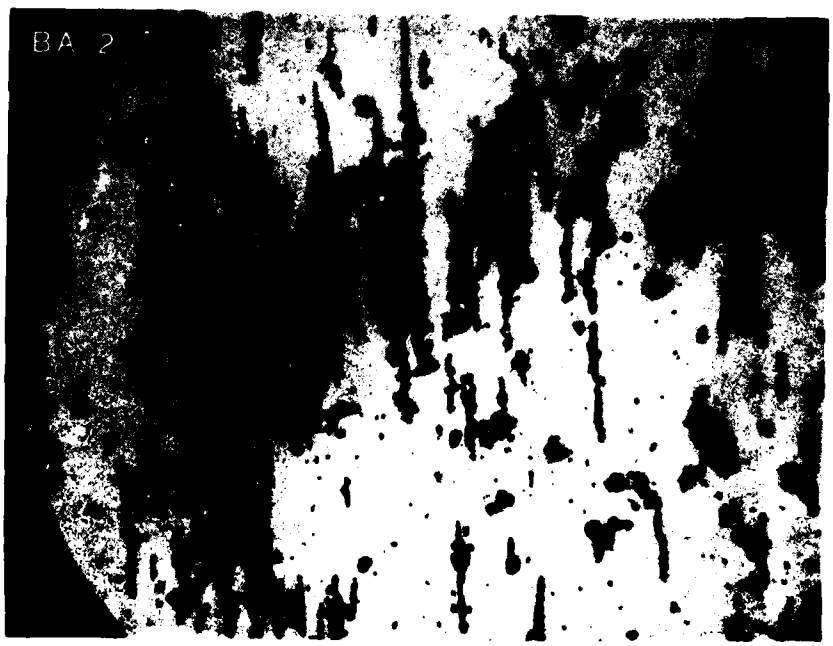
FIGURE 18

BALL BEARING TEST SEQUENCE BA

FERROGRAPH DENSITY DATA

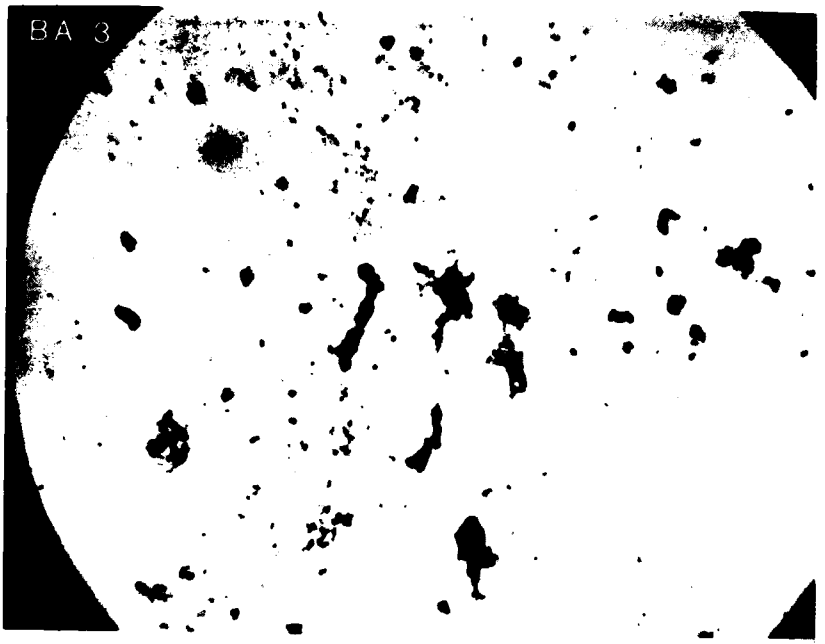


A. 15.7 m.r.

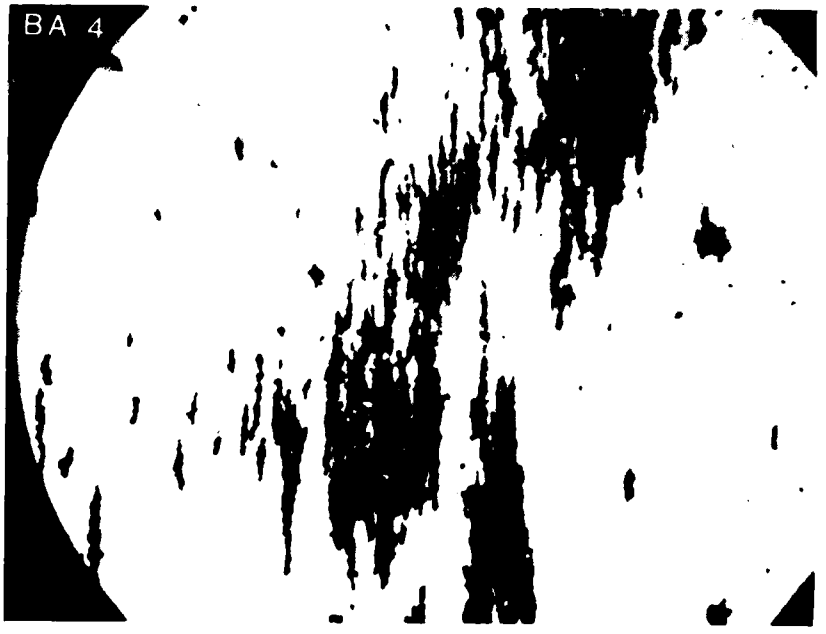


B. 22.1 m.r.

FIGURE 19
BALL BEARING TEST SEQUENCE BA
ENTRY DEPOSIT
LOW MAGNIFICATION
(Sheet 1 of 6)

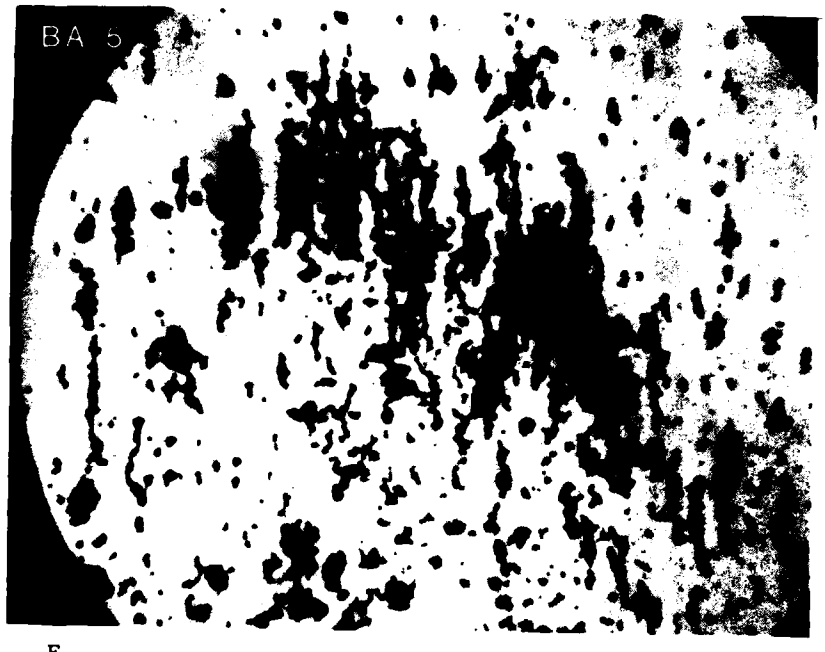


C. 72 m.r.



D. 86.7 m.r.

FIGURE 19
BALL BEARING TEST SEQUENCE BA
ENTRY DEPOSIT
LOW MAGNIFICATION
(Sheet 2 of 6)

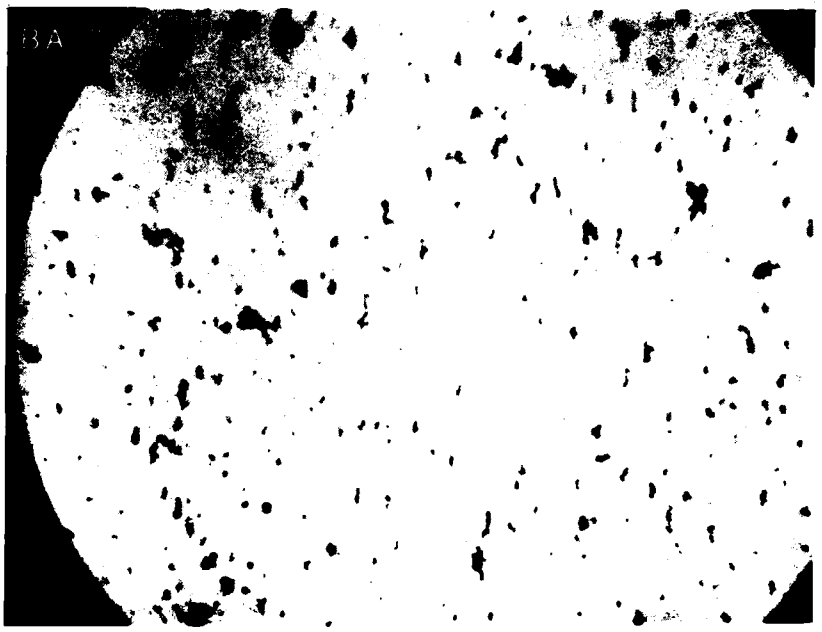


E. 100 m.r.

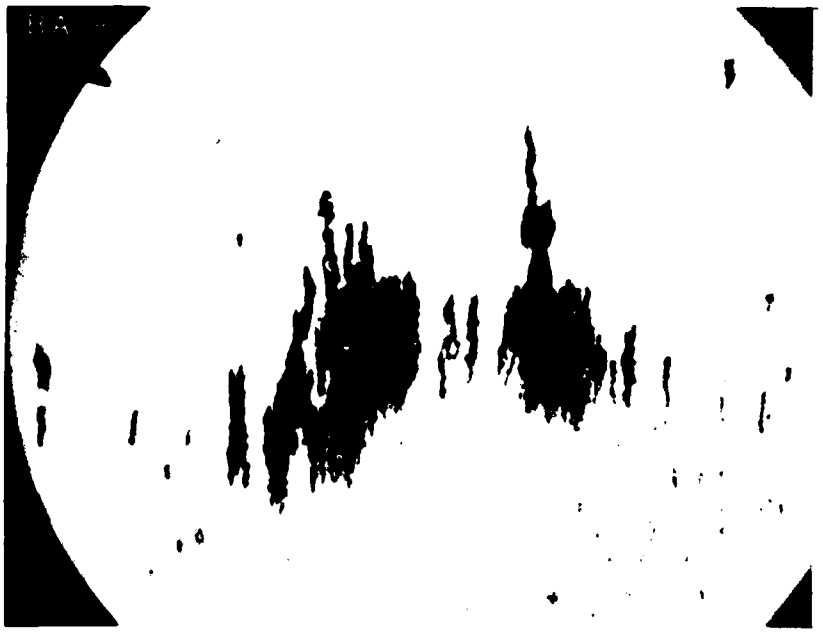


F. 123.3 m.r.

FIGURE 19
BALL BEARING TEST SEQUENCE BA
ENTRY DEPOSIT
LOW MAGNIFICATION
(Sheet 3 of 6)



G. 137.9 m.r.



H. 182.7 m.r.

FIGURE 19
BALL BEARING TEST SEQUENCE BA
ENTRY DEPOSIT
LOW MAGNIFICATION
(Sheet 4 of 6)

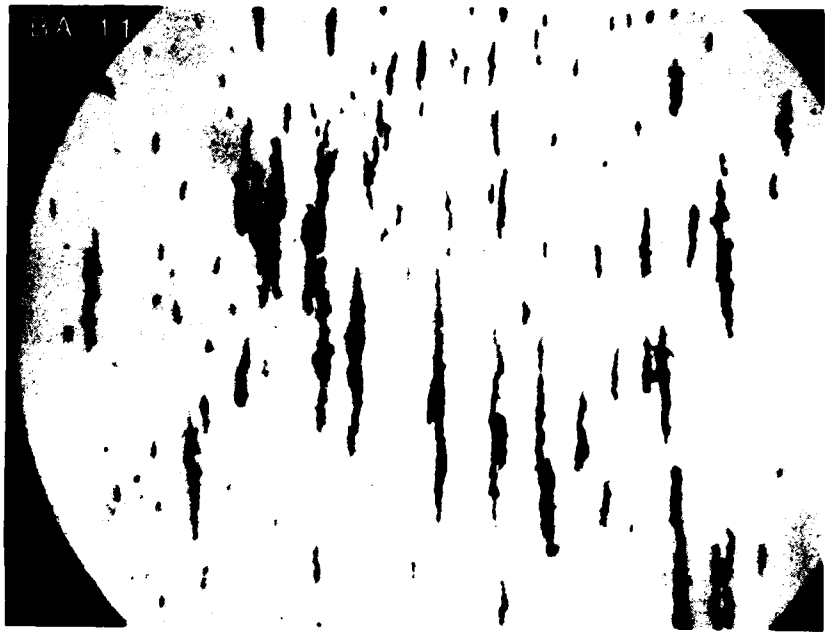


I. 209.5 m.r.



J. 222.9 m.r.

FIGURE 19
BALL BEARING TEST SEQUENCE BA
ENTRY DEPOSIT
LOW MAGNIFICATION
(Sheet 5 of 6)



K. 224.7 m.r.

FIGURE 19
BALL BEARING TEST SEQUENCE BA
ENTRY DEPOSIT
LOW MAGNIFICATION
(Sheet 6 of 6)

TABLE 12. SPECTROMETRIC READING, BEARING BA-025

EVENT	TIME (MIL REVS)	PERCENT TIME	FE (IRON)	SI (SILICON)	SN (TIN)	TI (TITANIUM)	MO (MOLYBDENUM)
1	15.7	6	2	2	12	2	1
2	22.1	9	2	2	11	2	1
3	72.0	32	2	2	10	3	1
4	86.7	38	2	2	12	3	1
5	100.0	44	2	2	14	17	1
6	123.3	54	2	2	13	19	3
7	137.9	61	2	2	13	16	2
8	182.7	81	3	2	12	17	3
9	209.5	93	3	2	13	15	2
10	222.9	99	3	2	14	15	3
11C	224.7	100	2	26	14	6	3

TABLE 13. SPECTROMETRIC READING, BEARING BX-020

EVENT	TIME (MIL REVS)	PERCENT TIME	FE (IRON)	SI (SILICON)	SN (TIN)	TI (TITANIUM)	MO (MOLYBDENUM)
1	27.0	10	1	0	4	3	1
2	52.0	19	1	0	5	2	2
3	91.0	34	1	0	6	2	1
4	109.0	40	1	0	5	2	1
5	158.0	59	1	0	4	2	0
6	185.0	69	1	5	6	2	1
7	212.0	79	1	6	7	2	2
8	256.0	95	0	5	5	1	0
9	267.0	100	1	2	5	1	2

TABLE 14. PARTICLE COUNTS

BEARING ID	SERIES	MIL REVS.	% TIME	TOTAL	ADJUSTED COUNTS (COUNTS/100 CC) (N X 10^4)					PERCENT OF TOTAL COUNTS (N X 10^4)				
					2-5	5-7	7-15	15-25	25+	2-5	5-7	7-15	15-25	25+
BQ-001	1	0.1	0.04	415.3	276.5	77.7	45.6	10.6	4.9	66.58	18.71	10.98	2.55	1.18
	2	12.8	5.29	231.6	153.2	37.0	30.2	8.2	3.0	66.15	15.98	13.04	3.54	1.30
	3	27.9	11.53	1489.9	1024.2	259.3	169.8	27.9	8.7	68.74	17.40	11.40	1.87	0.58
	4	57.0	23.55	436.7	329.0	51.0	40.1	11.1	5.5	75.34	11.68	9.18	2.54	1.26
	5	91.0	37.60	653.7	499.5	97.5	46.0	8.0	2.7	76.41	14.92	7.04	1.22	0.41
	6	131.0	54.13	305.1	248.3	33.0	19.1	3.1	1.6	81.38	10.82	6.26	1.02	0.52
	7	161.0	66.53	622.3	459.7	89.1	57.6	11.8	4.1	73.87	14.32	9.26	1.90	0.66
	8	189.0	78.10	137.0	116.1	13.8	5.9	1.1	0.1	84.74	10.07	4.31	0.80	0.07
	9	229.0	94.63	2256.4	1689.7	324.5	193.2	36.0	13.0	74.88	14.38	8.56	1.60	0.58
	10	242.0	100.00	292.4	259.6	20.8	8.2	2.5	1.3	88.78	7.11	2.80	0.85	0.44
BX-020	1	27.0	10.11	2194.1	2040.4	123.5	26.9	1.0	2.3	92.99	5.63	1.23	0.05	0.10
	2	52.0	19.48	163.3	107.2	29.5	20.1	3.8	2.7	65.65	18.06	12.31	2.33	1.65
	3	91.0	34.08	1406.5	1384.6	20.1	1.0	0.7	0.1	98.44	1.43	0.07	0.05	0.01
	4	109.0	40.82	90.2	58.7	13.1	13.2	3.5	1.7	65.08	14.52	14.63	3.88	1.88
	6	185.0	69.29	35.0	32.0	1.0	1.2	0.1	0.7	91.43	2.86	3.43	0.29	2.00
	7	212.0	79.40	3626.0	3468.0	144.8	12.5	0.7	0.0	95.64	3.99	0.34	0.02	0.0
	9	267.0	100.00	181.4	141.0	23.0	15.0	0.2	2.2	77.78	12.68	8.27	0.11	1.21
BA-025	1	15.7	6.99	234.4	177.1	30.1	21.1	5.0	1.1	75.55	12.84	9.00	2.13	0.47
	2	22.1	9.84	347.7	258.9	48.7	31.4	6.9	1.8	74.46	14.01	9.03	1.98	0.52
	3	72.0	32.04	368.0	255.7	63.9	37.6	8.1	2.7	69.48	17.36	10.22	2.20	0.73
	4	86.7	38.58	249.5	154.6	69.5	20.0	4.5	0.9	61.96	27.86	8.02	1.80	0.36
	5	100.0	44.50	4742.5	3332.2	894.7	404.8	82.4	28.4	70.26	18.87	8.54	1.74	0.60
	6	123.3	54.87	3588.7	3479.0	24.5	72.6	10.6	2.0	96.94	0.68	2.02	0.30	0.06
	7	137.9	61.37	7136.5	6222.4	805.4	99.9	6.9	1.9	87.19	11.29	1.40	0.10	0.03
	8	182.7	81.31	4712.0	4430.1	226.4	48.1	6.1	1.3	94.02	4.80	1.02	0.13	0.03
	9	209.0	93.01	1520.0	1430.0	58.0	26.0	5.0	1.0	94.08	3.82	1.71	0.33	0.07
	10	222.0	99.20	3437.7	3246.1	150.3	34.5	5.6	1.2	94.43	4.37	1.00	0.16	0.03
	11	224.7	100.00	1048.8	938.7	82.7	22.6	3.7	1.1	89.50	7.89	2.15	0.35	0.10

8. Although these particle counts are suspect, it can be noted that wear debris concentration levels for these ball bearing test sequences are of the magnitude of 10^6 per 100 ml oil ($>2\mu m$), in a two-gallon lubrication system.

(b) Particle Size Distribution

1. The size distribution of wear debris contained in lubricant samples taken during ball bearing testing, as with particle quantity, was primarily monitored by ferrograhic analysis techniques. As discussed previously, implemented particle counting technique results were suspect.

2. Figures 20 and 21 present plots of ferrographic density readings at two different locations on the ferrogram for ball bearings BQ and BX test sequences. These locations represent different size ranges of debris as discussed in Section VI. The entry deposit plot represents debris of a relatively large size ($>5\mu m$), while the 50 mm deposit plot represents debris of a relatively small size ($2-5\mu m$). By comparing the relationship of these curves over the bearing life, one can assess the trends in debris size distribution.

3. As can be seen from these plots, a relatively high ratio of large-to-small debris particles is present during both the wear-in and abnormal wear regime as compared to the normal wear regime. This indicates that a significant portion of the debris generated during wear-in and abnormal wear is greater than $5\mu m$ in major dimension. Figures 22 and 23 represent high magnification micrographs of debris deposits for sequences BQ and BX. These micrographs verify that the increase in debris concentration during wear-in and abnormal wear can mainly be attributed to the generation of large debris.

4. It can also be noted that the ratio of large-to-small particles for the abnormal wear regime is significantly higher than that exhibited by the wear-in regime.

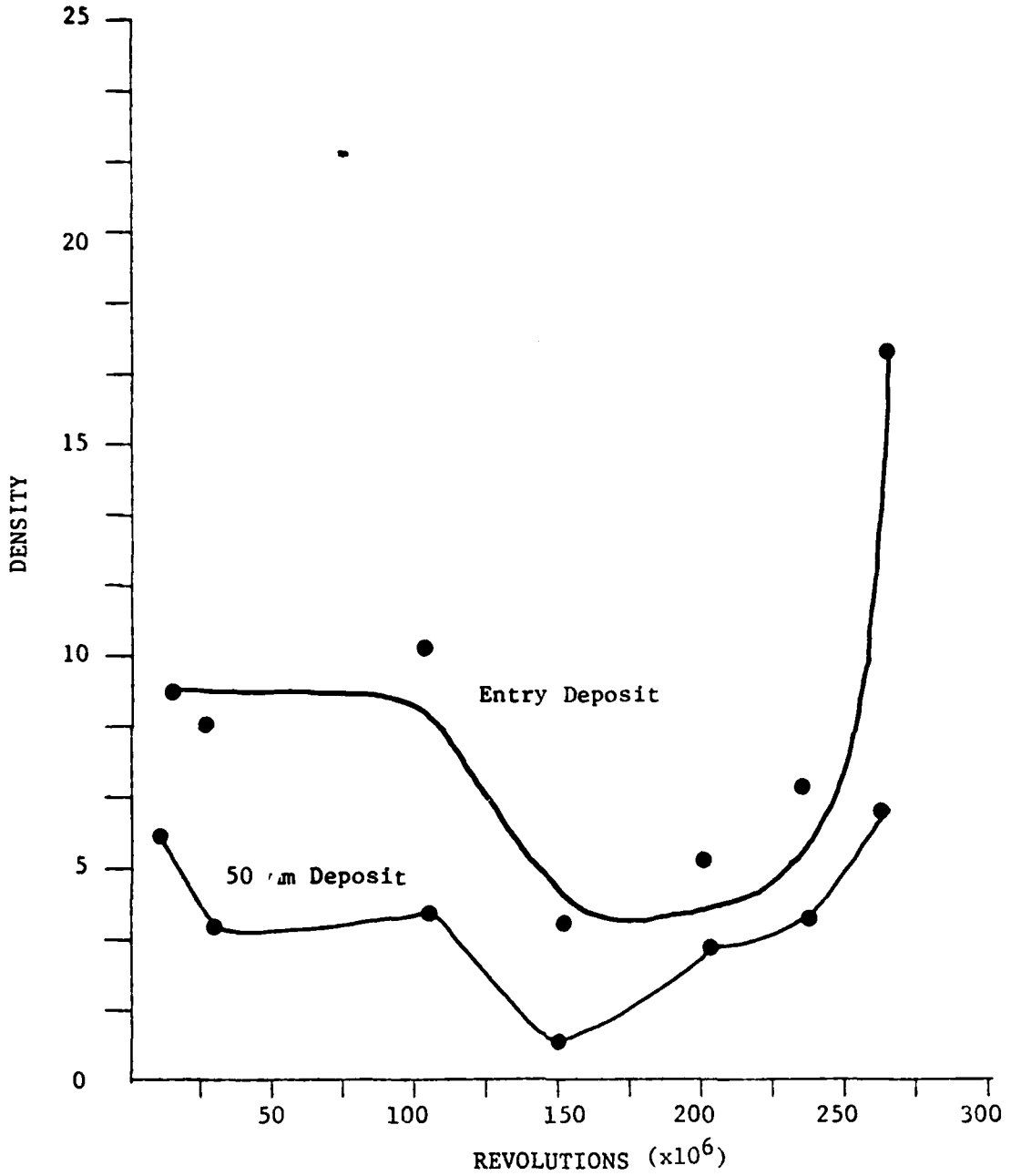


FIGURE 20

BALL BEARING TEST SEQUENCE BQ

FERROGRAPH DENSITY DATA

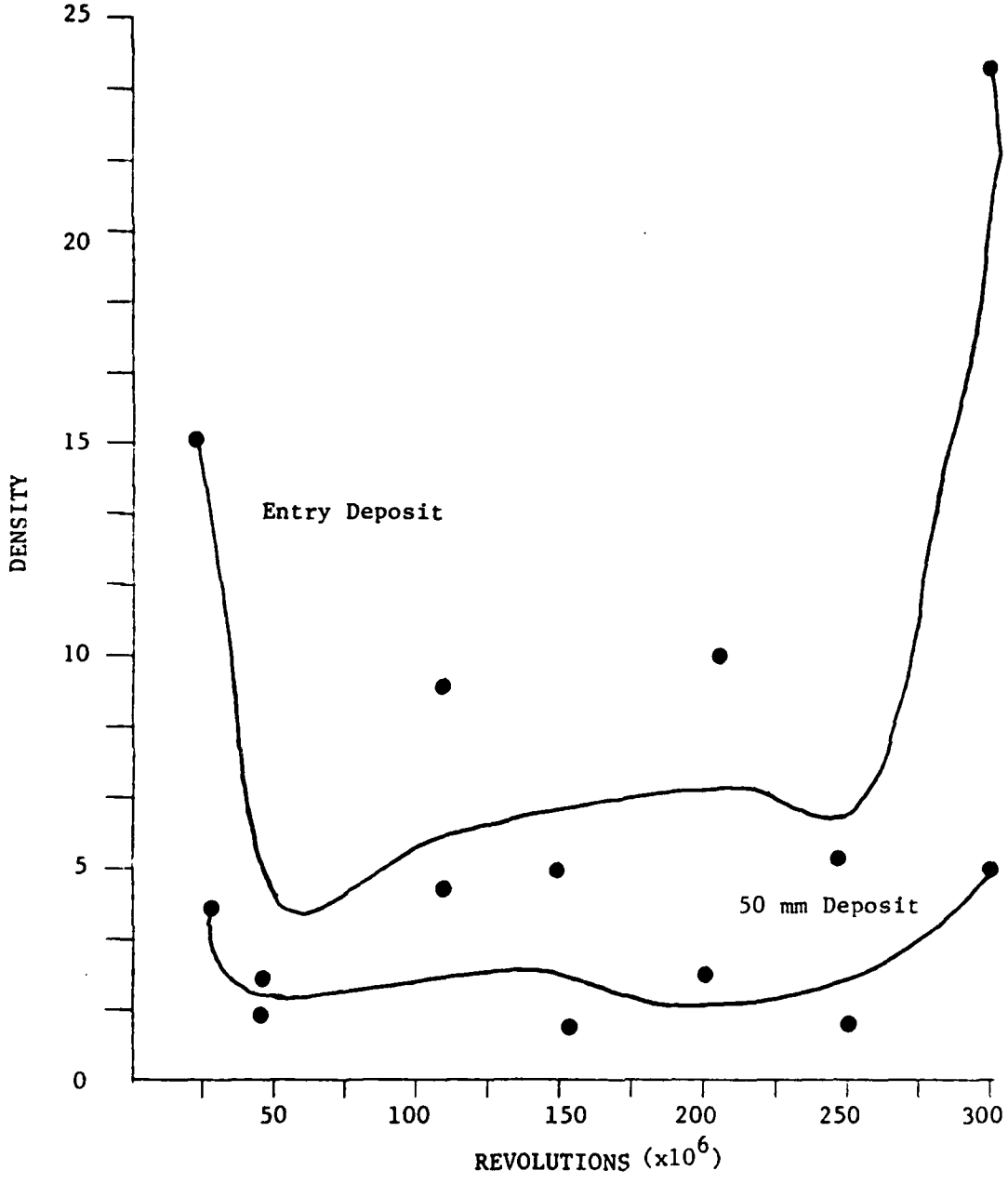


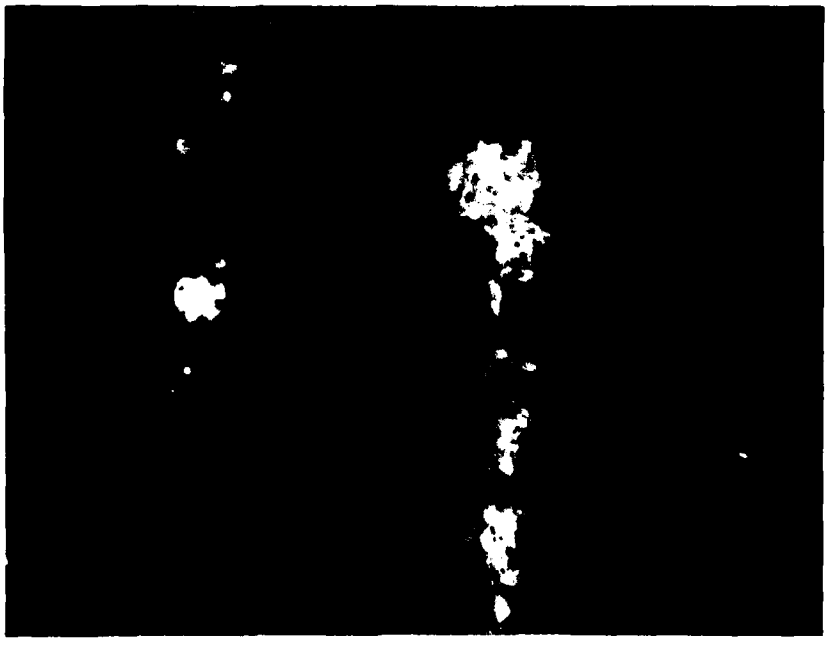
FIGURE 21

BALL BEARING TEST SEQUENCE BX

FERROGRAPH DENSITY DATA



A. 12.8 m.r.



B. 2.9 m.r.

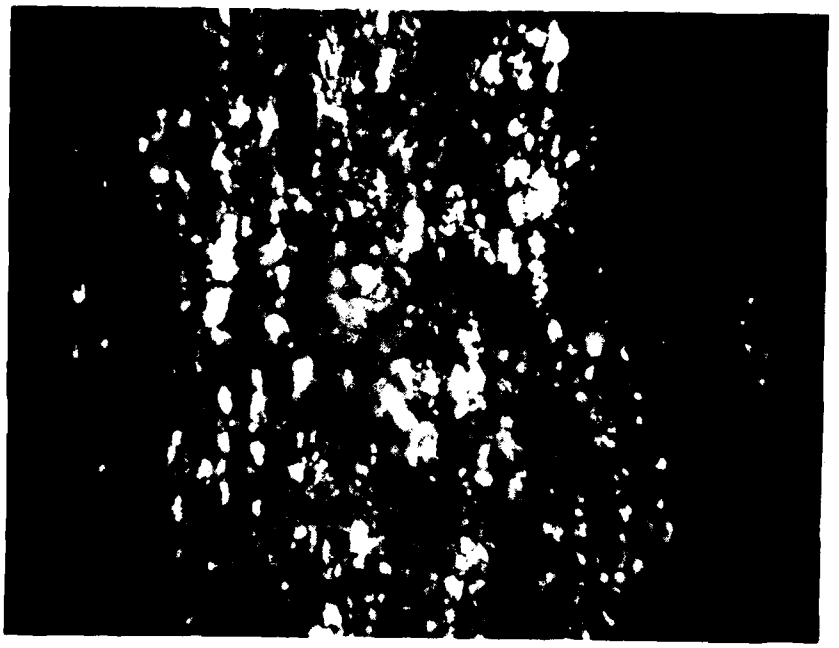
FIGURE 22

BALL BEARING TEST SEQUENCE BQ

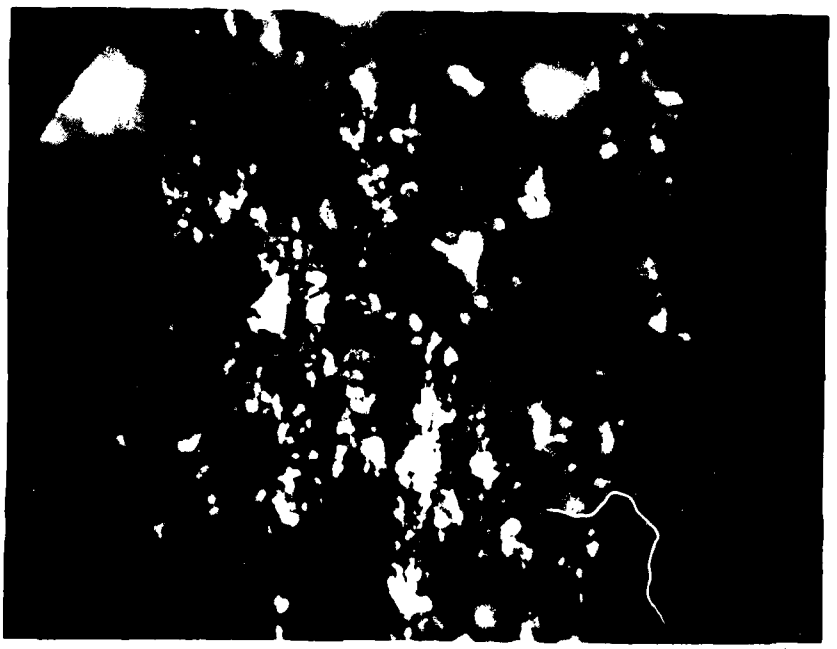
ENTRY DEPOSIT

HIGH MAGNIFICATION

(Sheet 1 of 4)



C. 91 m.r.



D. 161 m.r.

FIGURE 22

BALL BEARING TEST SEQUENCE BQ

ENTRY DEPOSIT

HIGH MAGNIFICATION

(Sheet 2 of 4)



E. 189 m.r.



F. 229 m.r.

FIGURE 22

BALL BEARING TEST SEQUENCE BQ

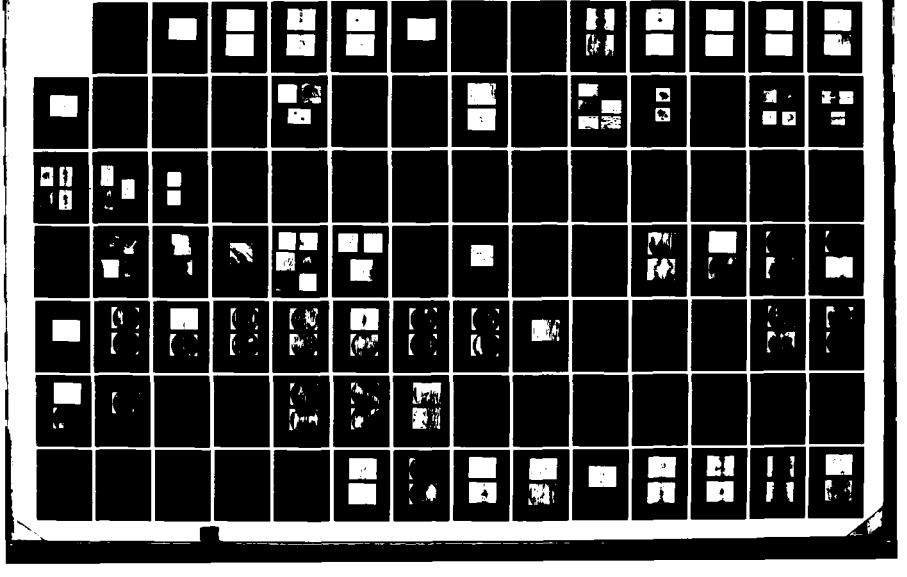
ENTRY DEPOSIT

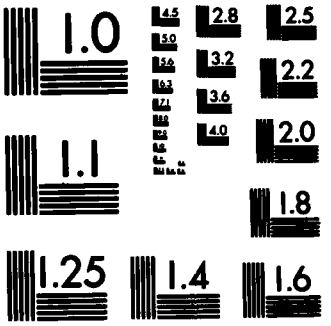
HIGH MAGNIFICATION

(Sheet 3 of 3)

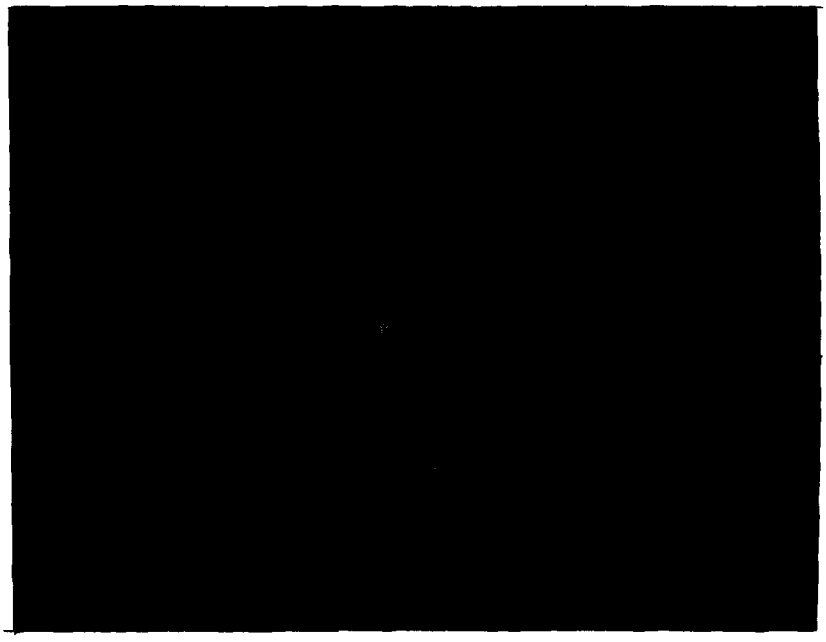
AD-A122 156 OIL ANALYSIS(U) NAVAL AIR ENGINEERING CENTER LAKEHURST NJ SUPPORT EQUIPMENT ENGINEERING DEPT P B SENHOLZI 23 AUG 82 NAEC-92-153 2/6

UNCLASSIFIED F/G 11/8 NL



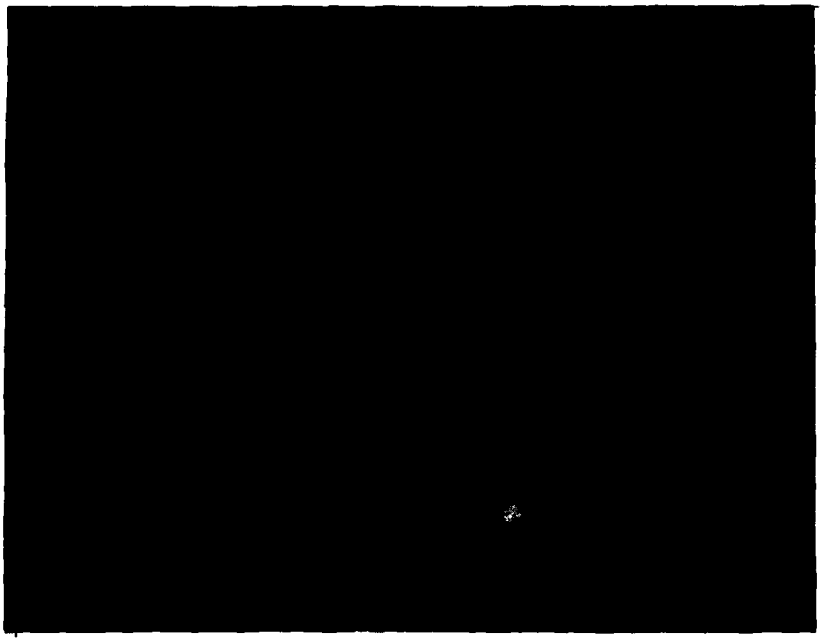


MICROCOPY RESOLUTION TEST CHART
NATIONAL BUREAU OF STANDARDS-1963-A



G. 242 m.r.

FIGURE 22
BALL BEARING TEST SEQUENCE BQ
ENTRY DEPOSIT
HIGH MAGNIFICATION
(Sheet 4 of 4)

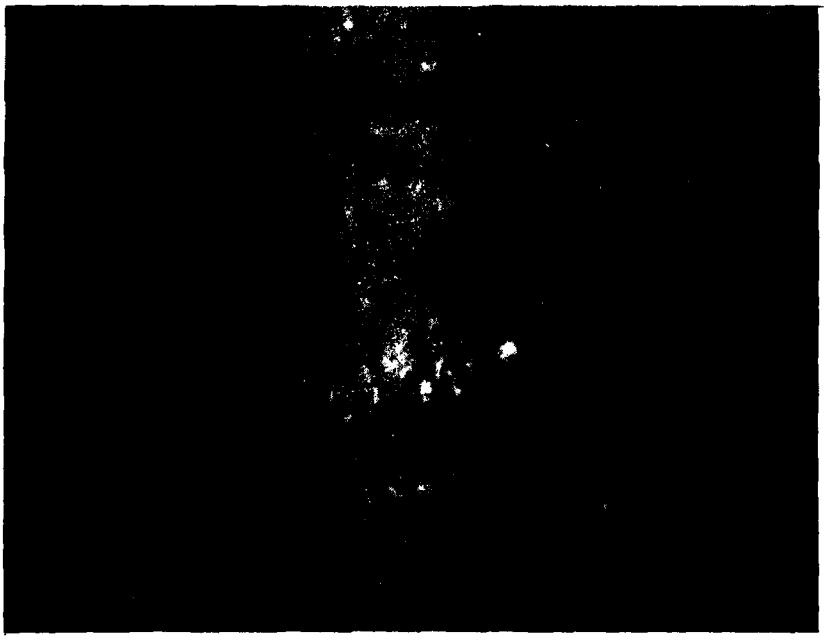


A. 27 m.r.

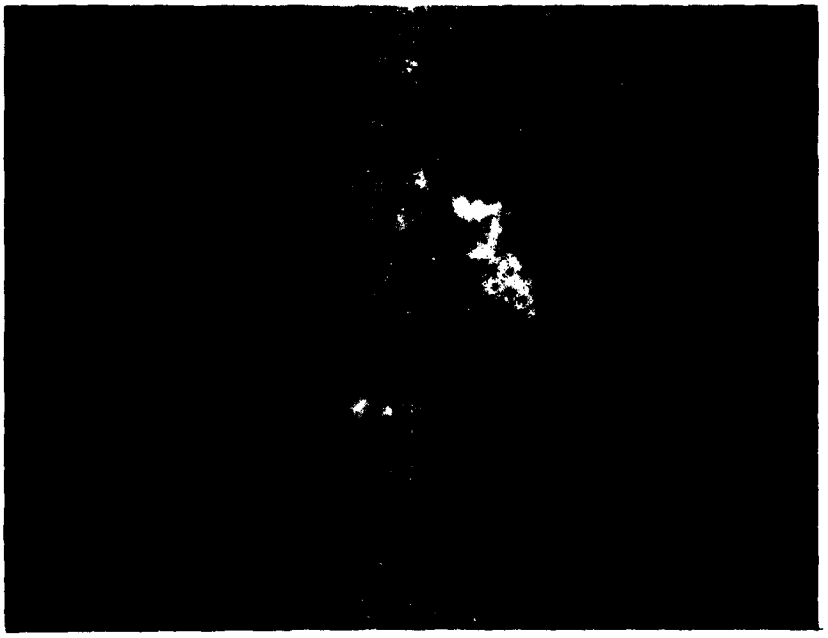


B. 52 m.r.

FIGURE 23
BALL BEARING TEST SEQUENCE BX
ENTRY DEPOSIT
HIGH MAGNIFICATION
(Sheet 1 of 4)



C. 91 m.r.



D. 158 m.r.

FIGURE [illegible]

BALL BEARING TEST SEQUENCE BX

ENTRY DEPOSIT

HIGH MAGNIFICATION

(Sheet [illegible])



E. 212 m.r.



F. 256 m.r.

FIGURE 23
BALL BEARING TEST SEQUENCE BX
ENTRY DEPOSIT
HIGH MAGNIFICATION
(Sheet 3 of 4)



G. 267 m.r.

FIGURE 23
BALL BEARING TEST SEQUENCE BX
ENTRY DEPOSIT
HIGH MAGNIFICATION
(Sheet 4 of 4)

5. Figure 24 represents dual density plots for sequence BA. Figure 25 provides high magnification micrographs of the respective sequence ferrographic deposits. Although this sequence is distorted due to the reoccurrence of a wear-in phenomena, the shift in size distribution observed in sequences BQ and BX is still valid (that is, wear-in and abnormal wear result in the generation of large debris).

6. The above distribution observations were valid for all the ball bearing test sequences. Figure 26 represents a simplistic presentation of this shift in particle size distribution.

(c) Particle Composition

1. Ball bearing testing was designed in such a way as to have each test component operating in an independent lubrication system. This design was implemented in order to limit lubricant borne debris to that being produced by the component and thus simplify the wear debris analysis process. As a result debris composition should not play an important role in this correlation effort since all debris should be the same material as the parent component.

2. However, during the early part of the endurance test phase, some of the oil samples gathered from some of the endurance tests were found to be unduly dark in color. To determine the source of the dark coloration, a sample of the dark oil from bearing BR-002 was taken at 146 m.r. This was filtered through a 0.45 μm Millipore filter which made the oil sample clear again. SEM examination could detect only steel particles. An X-ray diffraction pattern made on the filtered residue showed martensite peaks only. A sample of oil was then subjected to ferrographic and spectrometric analysis. The results of these analyses are shown in Table 15. A value of percent area covered of 31.2% at the 54 mm location is significantly higher than the approximately 8% values measured during the test sequence. The change-over from inverted polyethylene bottles to conical steel tanks for the endurance test oil systems, therefore, proved to be effective in keeping the wear particles in circulation.

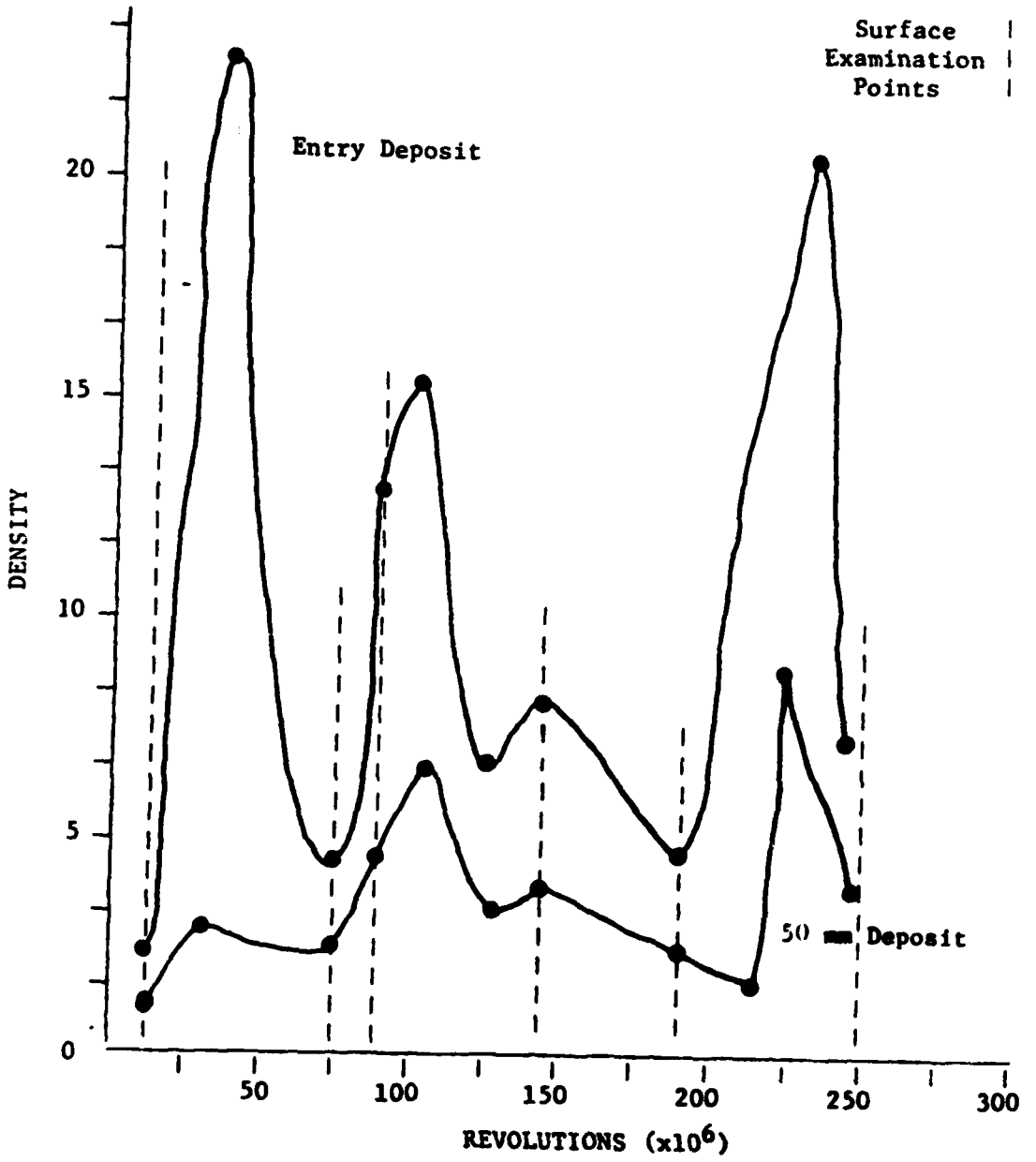


FIGURE 24

BALL BEARING TEST SEQUENCE BA

FERROGRAPH DENSITY DATA



A. 15.7 m.r.



B. 22.1 m.r.

FIGURE 25

BALL BEARING TEST SEQUENCE BA

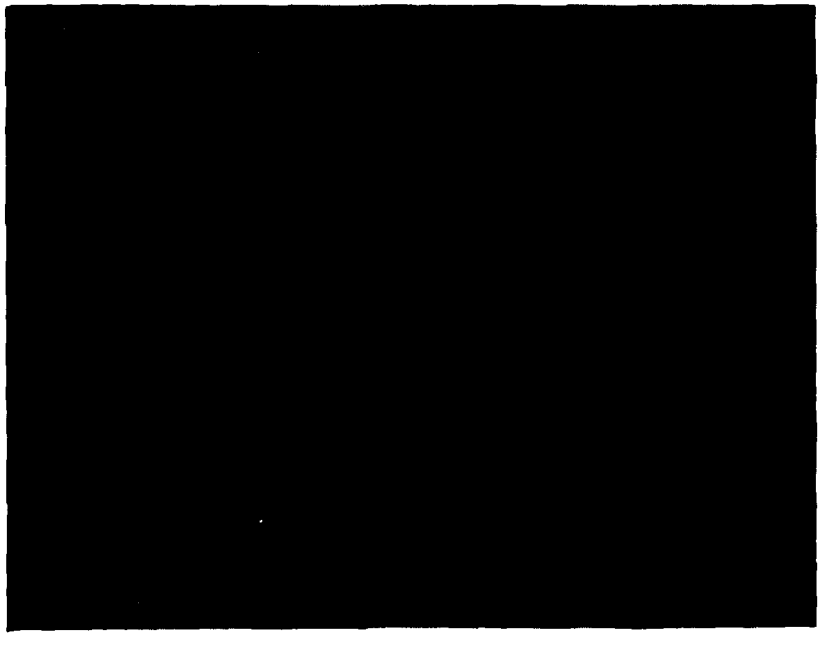
ENTRY DEPOSIT

HIGH MAGNIFICATION

(Sheet 1 of 2)



C. 72 m.r.



D. 86.7 m.r.

FIGURE 25

BALL BEARING TEST SEQUENCE BA

ENTRY DEPOSIT

HIGH MAGNIFICATION

(Sheet 2 of 6)



E. 100 m.r.



F. 123.3 m.r.

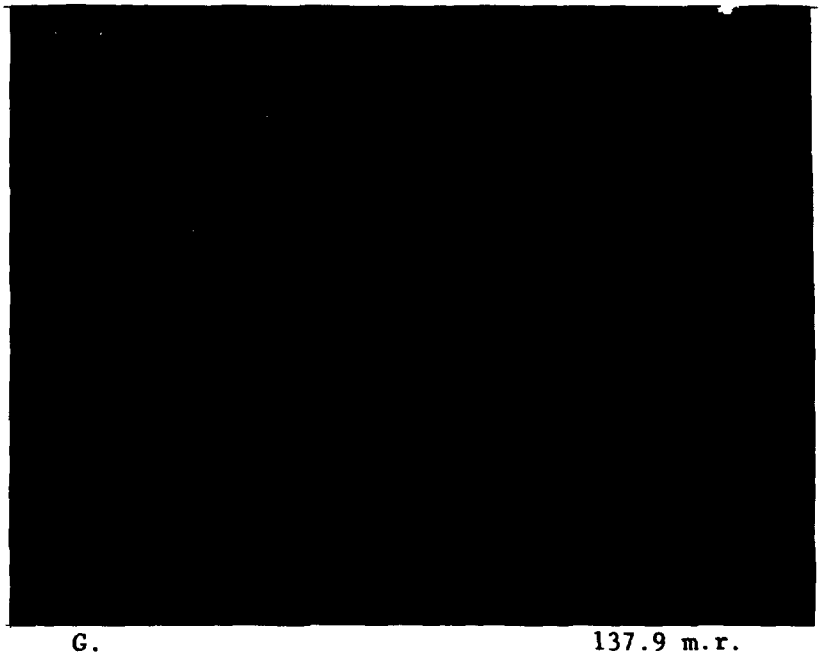
FIGURE 25

BALL BEARING TEST SEQUENCE BA

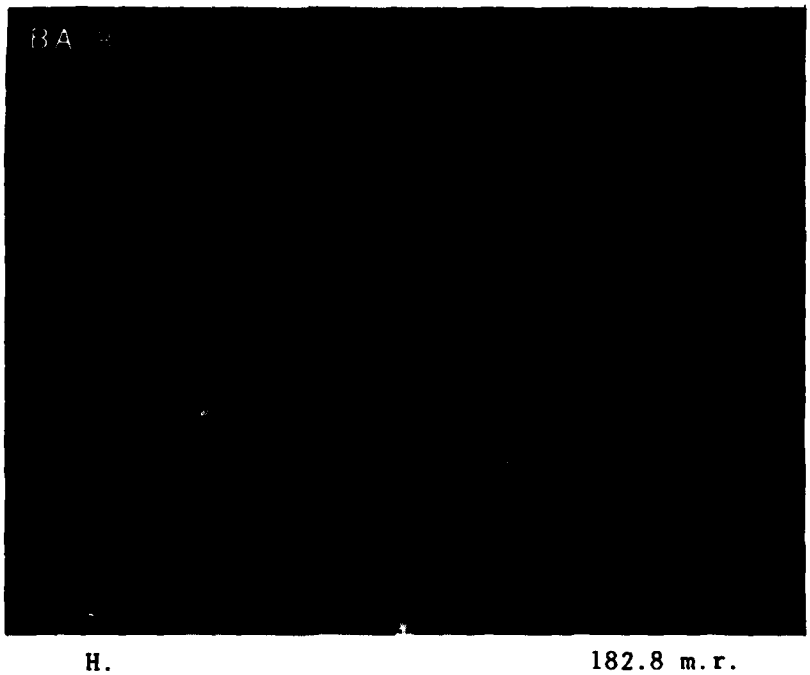
F TRY DEPOSIT

GH MAGNIFICATION

(Sheet 3 of 6)



G. 137.9 m.r.



H. 182.8 m.r.

FIGURE 25

BALL BEARING TEST SEQUENCE BA

ENTRY DEPOSIT

HIGH MAGNIFICATION

(Sheet 4 of 6)



I. 209.5 m.r.



J. 222.9 m.r.

FIGURE 25

BALL BEARING TEST SEQUENCE BA

ENTRY DEPOSIT

HIGH MAGNIFICATION

(Sheet 5 of 6)



K. 224.7 m.r.

FIGURE 25

BALL BEARING TEST SEQUENCE BA

ENTRY DEPOSIT

HIGH MAGNIFICATION

(Sheet 6 of 6)

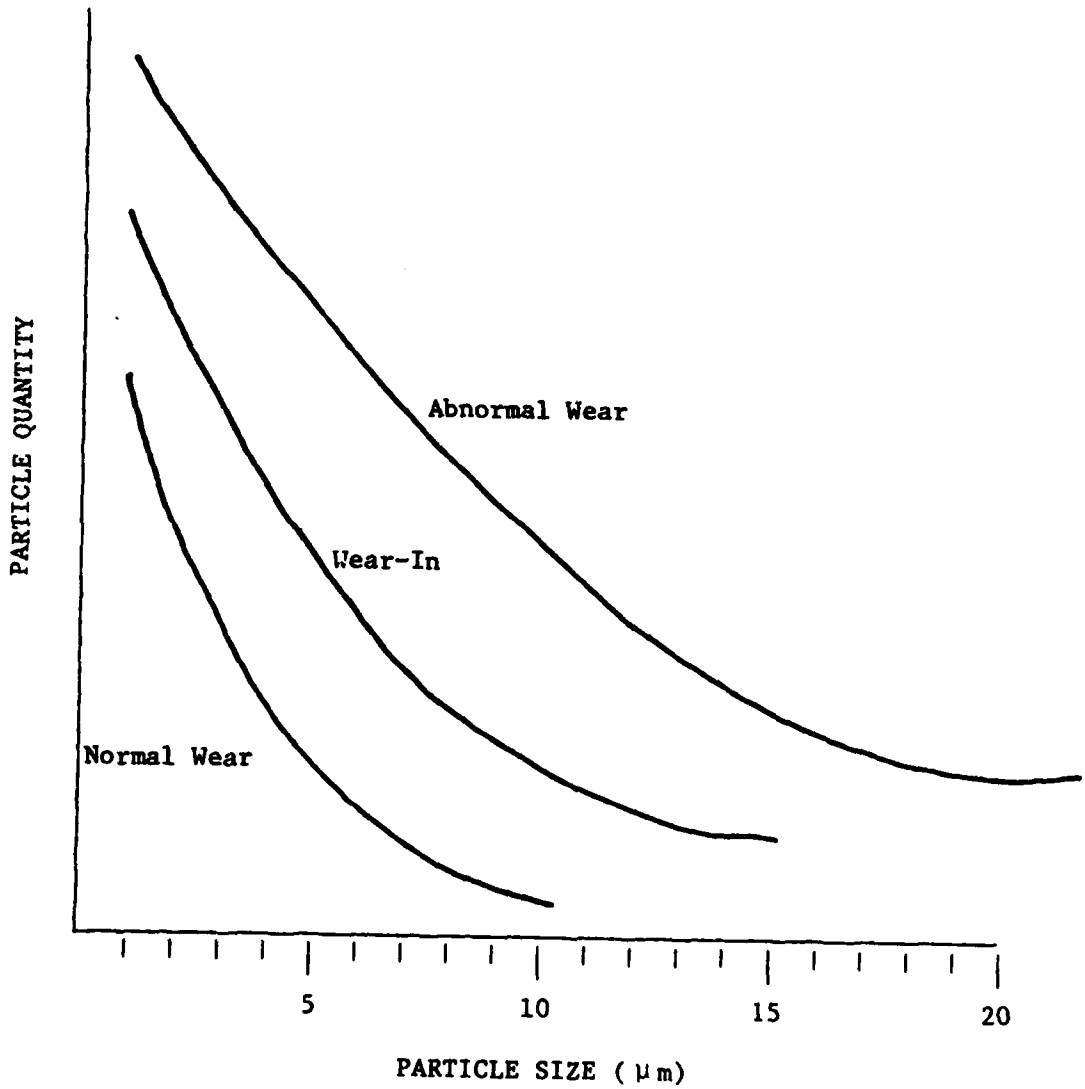


FIGURE 26
PARTICLE SIZE DISTRIBUTION VERSUS WEAR REGIME

TABLE 15. FERROGRAM ANALYSIS REPORT

Ferrogram No.: 3180 Date: 9/16/74

Organization SKF Industries, Inc. Sample No.: 3

Equip. Type: Brg. Test Rig Serial No.: Brg. BR-002 Operating Time: 146 m. rev.

Sample Date: _____ Oil Type: HD #16 Time on Oil: _____

Replenishment Data: _____

Volume of Sample passed along Ferrogram 2.0 cc	Entry	54 mm	50 mm	10 mm
Ferrogram Reading (% area covered)	42.5	31.2	25.6	8.3

Volume of Entry 13.7×10^5 um^3 Height of Entry Deposit 9.0 um

Types of Particles	None	Few	Moderate	Heavy
Normal Rubbing Wear				
Fatigue Chunks (Typical gear surface fatigue)	X			
Spheres (fatigue cracks in rolling bearings)	X			
Laminar Particles (gears or rolling beawrngs)	X			
Severe Wear Particles		X	X	
Cutting Wear Particles (high unit pressure)		X		
Corrosive Wear Particles	X			
Oxides Particles (includes rust)		X		
Dark Metallo-oxide Particles (typical hard steels)	X			
Non-ferrous Metallic		X		
Non-metallic, Crystalline		X		
Non-metallic, Amorphous (i.e. friction polymer)	X			

Considered Judgement of Wear Situation

	Very Low		Normal	X	Caution		Very High (Red Alert)

Emission Spectrometer	Al	Fe	Cr	Ag	Cu	Sn	Mg	Ti	Ni	Si
Test #1 PPM	3	11	0	3	1	11	0	15	3	2
Test #2	4	9	0	3	1	13	1	15	3	2

Comments: Ferrogram contains mostly rubbing wear. However, the wear rate is higher than previous samples. Ferrogram contains severe wear some of which exhibits yellow/brown color (unchanged by heating to 625° for 90 sec.) and are magnetic. Bronze colored non-magnetic severe wear particles are also present. There are some monocrystalline particles which appear to be similar to the hematite produced by fretting.

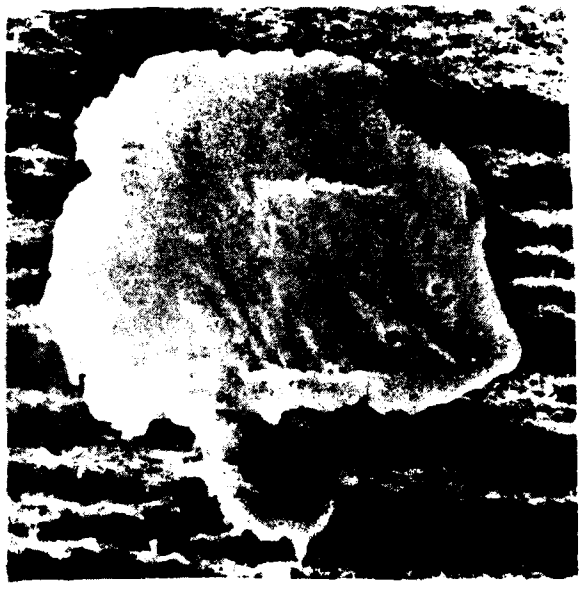
Spectrometric analysis, Table 15, showed the presence of 15 ppm titanium compared to 11 ppm of iron in the same oil sample. SEM examination of the entry deposit on the ferrogram revealed the presence of the titanium particles shown in Figure 27. Results of spectrometric analysis of a number of oil samples taken during the course of the endurance testing are given in Table 16 show a strong correlation between titanium content and the darkness of the sample.

3. A complete re-examination of the oil wetted components in the closed lubrication loop revealed that the center pin and the bushings used to support the plastic-coated magnetic pump impeller are made of corrosion-resistant titanium. This was known to be the case during initial system design. Due to the light load these components were subjected to, the possibility of their wearing was discarded. However, during the re-examination the bushings were noted to be inadequately seated in their pockets. Their sliding against the plastic impeller surface in the presence of wear debris from the bearing, leads to wear of the bushing surfaces. The magnetic impeller is coated with a black epoxy. The surfaces of the impeller and the two titanium bushings were worn in systems from which dark oil samples were obtained. It is therefore clear that under certain conditions in the pump, wear of the titanium bushings and black epoxy coating on the impeller occurs simultaneously. Hence, the correlation between high titanium level and the darkness of the oil. The center pin did not suffer much wear.

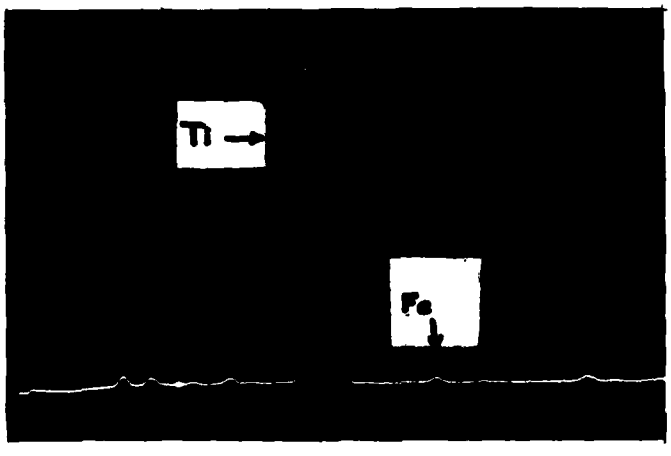
4. To eliminate titanium from the system the titanium bushings were replaced by teflon bushings of the same thickness. These, however, could not withstand the operating conditions in the pump and wore away very rapidly. The wear chips produced would enter the lubrication loop and block one of the orifices in the loop. This slowed down the oil flow causing the bearings to run hotter than normal. Due to the computer temperature monitoring system, the test was aborted in such an event to prevent damage to the bearings. The use of titanium bushings was therefore resumed.



3541 100X
A. THREE Ti PARTICLES DETECTED (MARKED "1", "2", AND "3")



3542 1000X
B. APPEARANCE OF A SINGLE PARTICLE (#1)



3542
C. ENERGY DISPERSIVE SPECTRA FROM PARTICLE IN B.

FIGURE 27

TITANIUM PARTICLES DETECTED IN THE ENTRY DEPOSIT OF A FERROGRAM MADE FROM AN OIL SAMPLE FROM BEARING TEST NO. BR-002 TAKEN AT 146 m.r.

TABLE 16. SPECTROMETRIC ANALYSIS OF OIL SAMPLES FROM BALL BEARING ENDURANCE TESTS

Bearing No.	Mil. Revs.	Fe	Ag	Al	Cr	Cu	Mg	Ni	Pb	Si	Sn	Ti	Mo	Appearance of Sample
BQ-001	242	12.9	0	0	2.1	1.7	2.6	0.1	1.5	0	4.2	1.4	0	Slightly dark
BR-002	0.06	0	0	0	0.1	0	1.0	0.1	1.2	0.9	10.9	1.1	0.7	Clear
BR-002	12.8	0.3	0	0	0.2	1.7	2.4	0	0	3.2	10.0	1.9	0	Clear
BR-002	27.9	4.7	0	0	1.1	0	0.9	0	0	1.2	12.2	28.8	0.7	Dark
BR-002	57.0	9.4	0	0	0.4	0.1	0.8	0.1	0.1	0.5	11.8	28.3	0.1	Dark
BR-002	242	6.2	0	0	1.0	0.2	1.7	0.3	0.3	0.7	12.2	12.6	0.3	Dark
BR-002	408	12.8	0	0	0.9	0.6	2.1	0.1	0.1	1.7	10.4	7.3	0.1	Dark
BS-007	194.4	2.2	0	0	0.5	0	1.0	0.1	0.1	0.2	12.2	18.3	0.5	Dark
BS-007	320	1.2	0	0	0	0	0.8	0.2	0.2	5.7	4.7	17.1	0	Dark
BT-010	194.4	3.4	0	0	0.7	0	0.9	1.0	1.0	0.2	11.4	3.4	0.2	Clear
BV-017	171.6	10.3	0	0	0.4	0	0.8	0	0	0	11.8	20.5	0	Dark
BV-017	415	6.6	0	0	0.4	0	1.0	0.1	0.1	0.3	11.6	8.0	0.3	Dark
BW-109	160	0.4	0	0	0	0	1.0	0.1	0.1	3.6	4.0	1.9	0	Clear
BX-020	158	0.6	0	0	0.6	0.1	0.13	0.3	0.3	2.6	4.9	1.3	0	Clear
Fresh Oil		0	0	0	0	0	0.8	0.1	0	5.3	4.4	0.4	0	

5. Attempts were made to minimize wear of the titanium bushings. Firstly, care was taken to see that they were properly seated in their pocket. Secondly, the pumps were aligned more critically so that there was no bending moment on the spout at which oil enters the pump from the tank. These measures did considerably reduce the wear on the titanium. Most of the subsequent oil samples were clear.

6. This sample pump contamination problem serves to compromise particle counting analysis during the test sequences. However, Ferrographic analysis was only minimally effected by this contamination as a result of its magnetic precipitation operating principle.

(d) Particle Morphology

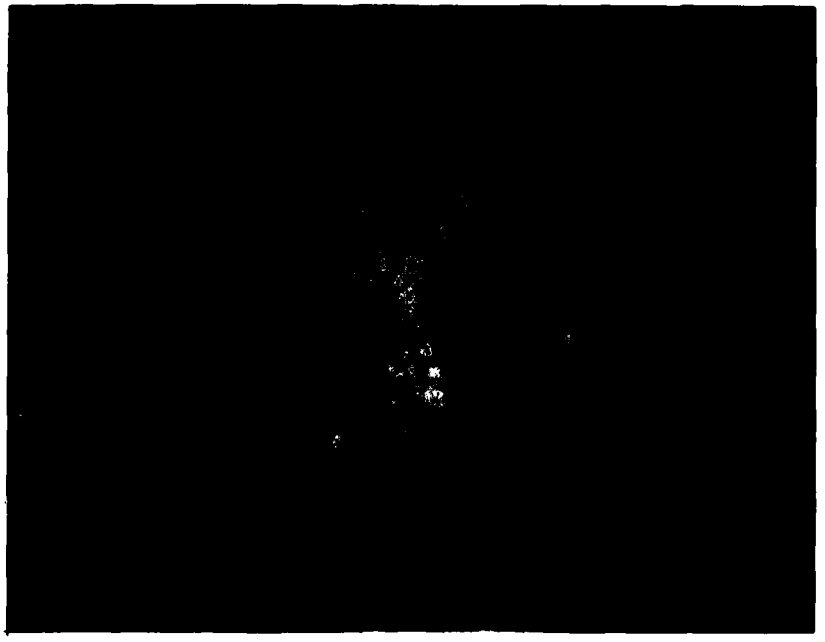
1. The last factor to be considered under ball bearing wear particle analysis is particle morphology or shape. This factor is probably the most unique of the four debris characteristics presented in this discussion.

2. Ball bearing wear-in resulted in the generation of both free metal particles and oxides. Free metal particles consisted primarily of rubbing wear and wear-in particles, the most significant of these being the wear-in particles. These particles result from the finished bearing surface. Typically, during the wear-in period, ridges on the virgin wear surface are flattened and form cornice along the ridge peaks. These cornices subsequently break away in the form of elongated, flat particles. Wear-in ball bearing particles exhibited a length to width ratio of 3:1 and a major dimension to thickness ratio of 4:1. These particles can range in size up to 50μm in major dimension. Figure 28 presents micrographs of the first sample from ball bearing sequence BZ. A wear-in particle is highlighted in these micrographs. Wear-in particles can also be noted in initial micrographs of sequences BQ, BX, and BA presented in Figures 22, 23, and 25 respectively.

3. Oxide particles generated during ball bearing wear-in are generally black oxide, Fe_3O_4. These oxide particles are normally equiaxial and can range up to 30μm in major dimensions.



A. X



B. X

FIGURE 28

BALL BEARING SEQUENCE BZ

WEAR-IN DEBRIS (27 MILLION REV.)

4. Ball bearing normal wear particles are dominated by free metal platelets. These platelets consist of both rubbing wear and laminar particles. Rubbing wear particles exhibit a length to width ratio of 3:1 and a major dimension to thickness ratio of approximately 10:1. Normal wear particles can range in size up to 15μm, however, the majority are less than 2μm in major dimension. Figure 29 presents a series of micrographs depicting typical normal wear debris.

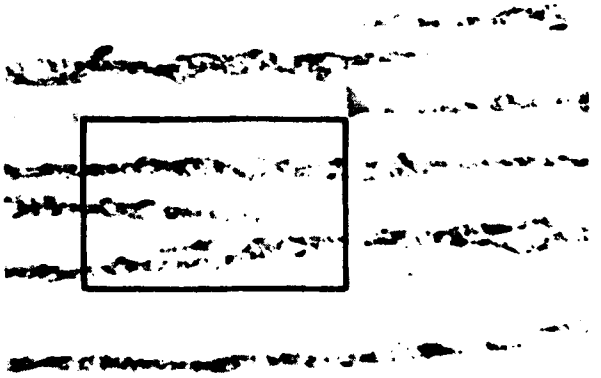
5. Laminar particles are the second type of normal ball bearing wear debris types. This type is greatly outnumbered by the normal rubbing wear particles. It exhibits a length to width ratio of 1:1 and a major dimension to thickness ratio of approximately 20:1. Laminar particles range in size from 10-30μm in major dimension and average 1μm in thickness. It is hypothesized that laminar particles are formed by the passage of a wear particle through a rolling contact zone. Frequent occurrence of holes in these particles serves to support this hypothesis.

6. The predominent abnormal wear mode occurring during ball bearing testing was surface fatigue. Three distinct particles have been associated with rolling contact fatigue: laminar particles, spherical particles, and fatigue spall particles. Laminar particles have been briefly discussed above. During rolling fatigue large laminar particles are produced. Characteristically they range in size between 20-50μm in major dimension. Laminar particles can be present throughout the life of a bearing but increase in both size and quantity at the onset of fatigue spalling. Figure 30 represents micrographs of typical laminar particles.

7. Spherical particles represent the most contraversial particle associated with rolling contact fatigue. These spheres as the name implies, are free metal spherical particles. The spheres are usually less than 2μm in diameter but may reach a diameter of up to 10μm. The exact mechanism of production of these particles has not been totally agreed upon, however, it



A. 225X



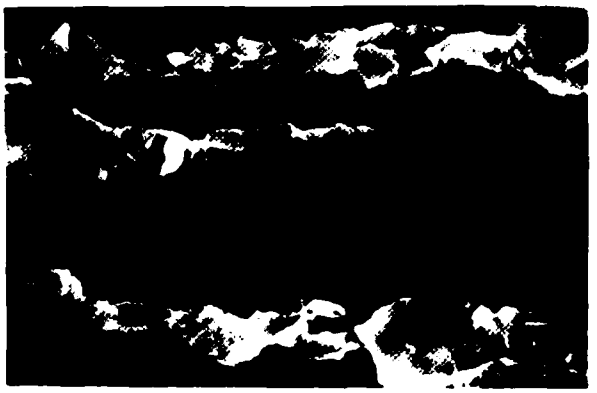
B. 450X



C. 1000X



D. SEM 1000X



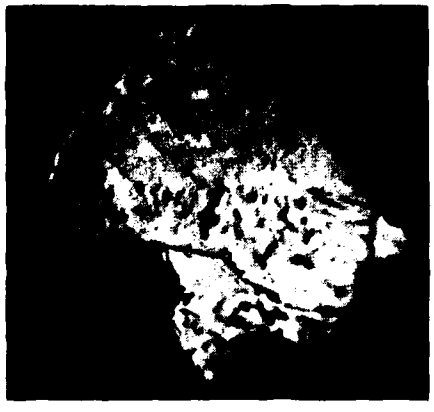
E. SEM 2500X



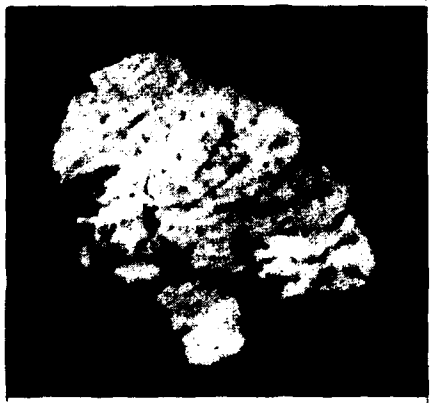
F. SEM 2500X

FIGURE 29

TYPICAL NORMAL RUBBING WEAR PARTICLES



A. 1000X



B. 1000X

FIGURE 30

BALL BEARING ROLLING CONTACT FATIGUE

LAMINAR PARTICLES

has been hypothesized that they are formed in bearing surface fatigue cracks. Figure 31 represents micrographs of typical spherical particles. It has been noted from field equipment monitoring that fatiguing bearings have been estimated to generate several million spheres in the course of a failure. Fatigue failures occurring under this program did not produce spherical particles in any significant quantities. This reason for these limited quantities is thought to result from the accelerated nature of the ball bearing test sequences.

8. Fatigue spall particles are irregularly shaped particles resulting from actual material removal as a pit or spall occurs. These particles exhibit smooth surfaces and can range in size up to 150μm in major dimension. The majority of these particles, however, fall within the 15-25μm size range. Figure 32 represents micrographs of typical fatigue spall particles.

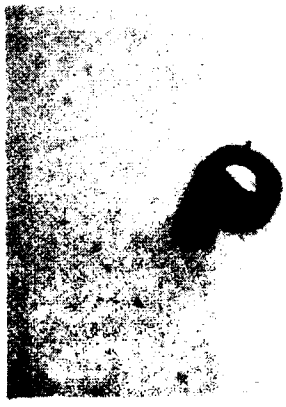
9. The particle morphology summary presented above is typical for the ball bearing sequences conducted under this program.

10. Figure 33 represents debris from ball bearing sequence BC. This debris is somewhat unique under this test program in that some of these particles are polymeric in nature. Several of these particles that appear metallic, upon closer examination, can be associated with an unknown quantity of friction (wear) polymer. The exact nature of this occurrence is unknown; however, this polymer was detected in several bearing sequences.

3. ROLLER BEARING BENCH TESTING. Roller bearing bench testing (as was ball bearing) was performed by SKF Industries, Inc. Bearing tests were again divided between uninterrupted and interrupted sequences. Details of this test sequence are very similar to those described under ball bearing testing; however, for the sake of continuity they will again be described in the following paragraphs.



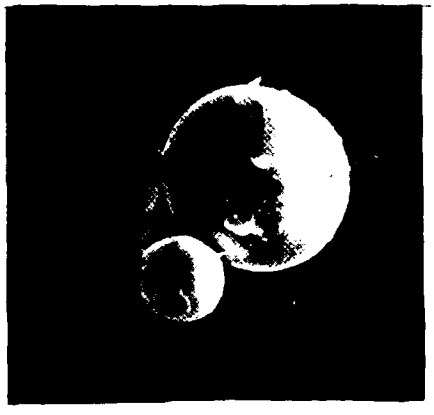
A. 1000X



B. 1000X



C. SEM 1000X



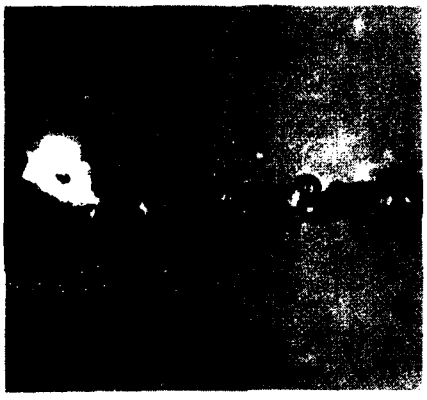
D. SEM 3000X

FIGURE 31

BALL BEARING ROLLING CONTACT FATIGUE

SPHERICAL PARTICLES

(Sheet 1 of 2)



E. SEM 1000X



F. SEM 1000X



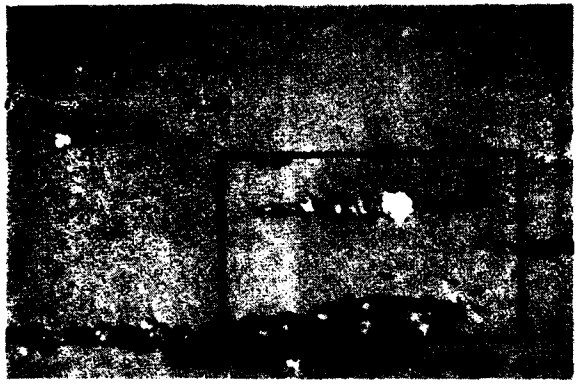
G. SEM 2500X

FIGURE 31

BALL BEARING ROLLING CONTACT FATIGUE

SPHERICAL PARTICLES

(Sheet 2 of 2)



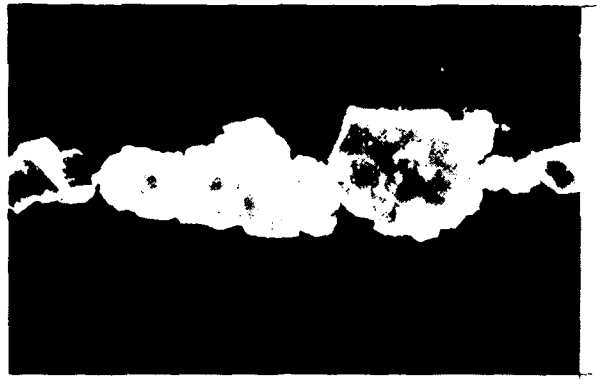
A. 225X



B. 450X



C. 1000X

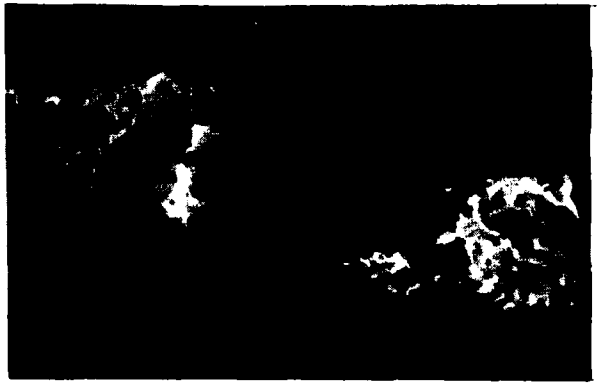


D. SEM 1000X

FIGURE 32
BALL BEARING ROLLING CONTACT
FATIGUE SPALL PARTICLES
(Sheet 1 of 3)



E. 225X

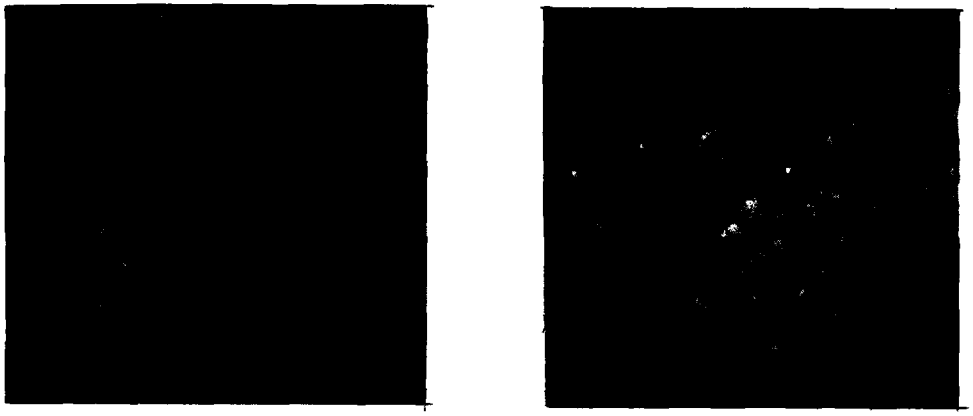


F. 450X



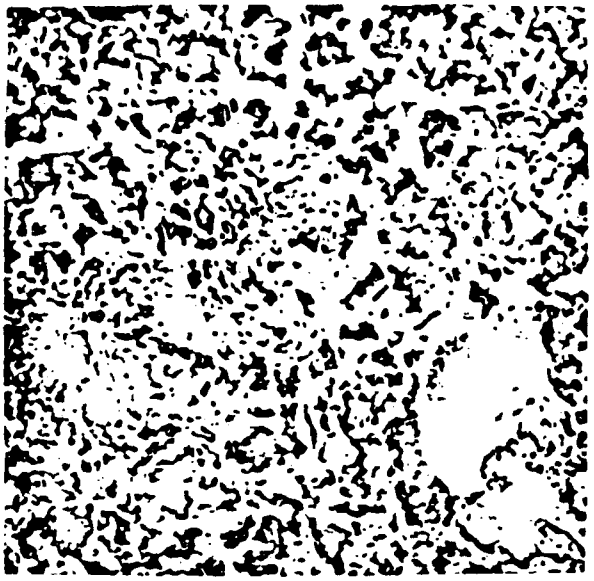
G. 1000X

FIGURE 32
BALL BEARING ROLLING CONTACT
FATIGUE SPALL PARTICLES
(Sheet 2 of 3)



H. 450X I. 1000X

FIGURE 32
BALL BEARING ROLLING CONTACT
FATIGUE SPALL PARTICLES
(Sheet 3 of 3)



4509 1000X



4512 2500X



4510 2500X



4511 5000X

FIGURE 33

BALL BEARING TEST SEQUENCE BC

(162 MILLION REV.)

FRICTION POLYMER

a. Roller Bearing Test Procedure

(1) The test program consisted of endurance and bench testing of tapered roller bearings in a closed-loop lubrication system. The tapered-roller bearings were made of carburizing grade, AISI 4118 steel and were tested under combined radial and thrust loads. Component steel was carbon vacuum deoxidized (CVD) bearing quality steel. A schematic drawing of the type of test bearing is shown in Figure 34.

(2) The bearing tests were conducted on standard SKF type R-2 machines. A line diagram of the standard machine setup is shown in Figure 2. In the present series of tests the existing lubrication system on the machine was disconnected and a separate closed-loop lubrication system, shown schematically in Figure 3 was installed for each test bearing. The oil was recirculated by a magnetically coupled centrifugal pump. An assembly drawing of the pumping chamber of the pump is shown in Figure 4. Teflon tubing was used in these isolated lubrication systems to prevent complication in Ferrogram Analysis due to chemical interactions between the tubing and the ester base MIL-L-23699 oil.

(3) The test parameters for the roller bearing tests are listed in Table 17. Under the test conditions used, the theoretical L_{10} life (life by which 10% of the bearings are expected to fail) for the roller bearing type is 10 million revolutions (m.r.) (Appendix A). The theoretical L_{50} life is computed for a Weibull slope f_i and is 5 times the L_{10} life as shown in the table. The number of stress cycles on the inner ring (f_i) for one revolution of the inner ring is given by:

$$f_i = 0.5\ Z\ (1 + Dw/dm\ \cos\alpha),$$

where

	Roller Bearing
Z = No. of rolling elements	23
Dw = diameter of rolling elements (mm)	7.5
dm = pitch diameter (mm)	58
α = contact angle (degrees)	11.5
f_i = No. of stress cycles/rev. of inner ring	13

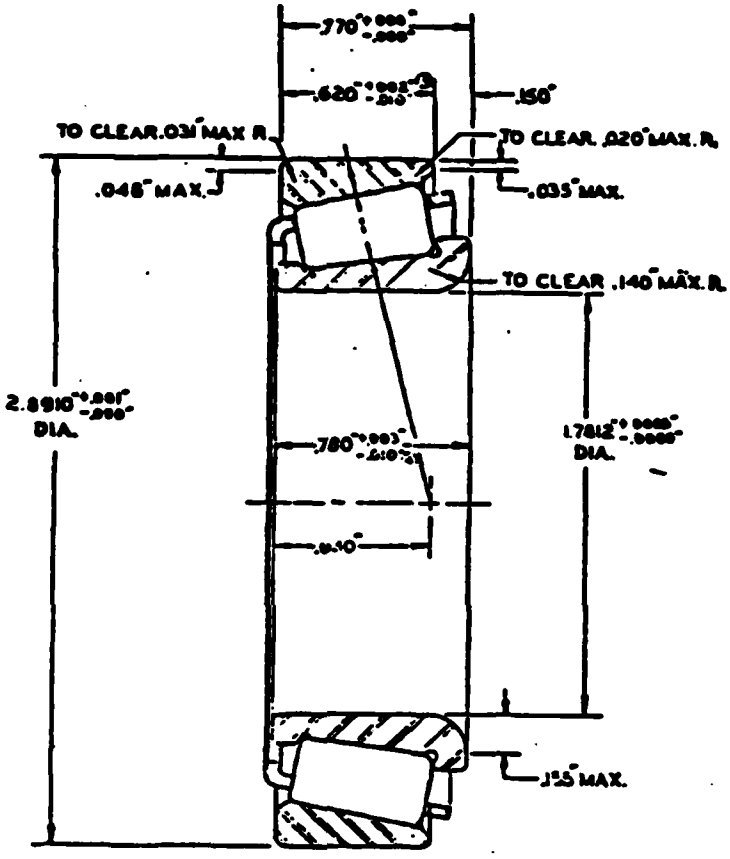


FIGURE 34

SCHEMATIC DRAWINGS OF TEST ROLLER BEARINGS

LM102949/LM102910 TAPERED ROLLER BEARINGS

TABLE 17. ROLLING BEARING TEST PARAMETERS

		LM102949/LM102910 Tapered-Roller Brg.
1.	Bore diameter (D, mm)	45.2
2.	Speed (N, rpm)	2,900
3.	DN x 10^{-6}	0.13
4.	Lube	MIL-L-23699
5.	Lube viscosity at 38/100°C (cs)	25/5.1
6.	Radial load (kN)	19
7.	Axial load (kN)	5.7
8.	Bearing capacity (kN)	46
9.	Theoretical L_{10} Life:	
	10^6 inner ring revolutions	10
	10^6 stress cycles	130
10.	Theoretical L_{50} Life:	
	10^6 inner ring revolutions	50
	10^6 stress cycles	650
11.	Operating temperature (C)	65
12.	Lube film parameter	1.1

(4) A computer monitoring system was set to abort a test when the bearing operating temperature rises above 125°C. A Robertshaw vibraswitch was also set to terminate the test when bearing spalling failure occurred, by reacting to an increase in vibration level of the test head.

(5) In order to accelerate bearing failure, the inner ring surfaces of the test bearings were initially dented with a Vickers pyramidal indenter using a 10 kg load. The indentor has an apex angle of 136° giving a diagonal-to-depth ratio of approximately 4.3. On a bearing surface having a hardness of R_c60, the length of the diagonal of the dent is approximately 160 μm.

(6) A total of 15 roller bearings were tested. Ten bearings were subjected to endurance testing and five were subjected to interrupted test sequences. Respective designations for these bearings are given in Table 18. As with the ball bearings, two designation systems, SKF and Navy, were utilized under the test program. These designations will be used interchangeably throughout this report.

(7) Three R-2 machines each having two test heads were set up to test the bearings. Endurance testing of ten bearings of each type was first completed in order to establish the time intervals at which the remaining tests should be interrupted for visual and scanning electron microscopic examination of the surface of the inner ring. The following approximate schedule of observations was chosen based on the endurance test results:

tapered roller bearings: 5, 25, 50, and 100 x 10^6 revs.

(8) All roller bearing tests were conducted utilizing ester base MIL-L-23699 lubricant. This lubricant was provided to SKF by the Navy.

(9) In order to minimize liquid borne debris and thus simplify the debris analysis process, the as-received oil was filtered through a 3 μm Millipore filter before being used for the tests. About two gallons of oil was used

TABLE 18. ROLLER BEARING OIL SAMPLES

BEARING I.D.		BEARING RUNNING TIMES AT WHICH CONSECUTIVE OIL SAMPLES WERE TAKEN (MILLION REVS.)*																			
Navy	SKF	1	2	3	4	5	6	7	8	9	10	11	12	13	14	15	16	17	18	19	20
ENDURANCE TESTS																					
RQ	101	.05	12.8	21.0	25.5	-	38.1	46.4	59.5	67.5	71.3	-	-	-	-	-	-	-	-	-	-
RR	102	.05	12.8	21.0	25.5	38.1	-	-	-	-	-	-	-	-	-	-	-	-	-	-	-
RS	105	5.0	12.4	-	-	-	-	-	-	-	-	-	-	-	-	-	-	-	-	-	-
RT	106	1.1	8.3	21.6	29.6	37.2	45	53	66.5	72	87.7	99.8	102	-	-	-	-	-	-	-	-
RU	107	1.1	13.6	29.2	42.3	55	60	66	73	77	81.0	-	-	-	-	-	-	-	-	-	-
RV	108	1.1	13.6	29.2	42.3	55	60	66	73	-	-	-	-	-	-	-	-	-	-	-	-
RW	109	4.0	11.7	24.5	31.3	33	37	-	-	-	-	-	-	-	-	-	-	-	-	-	-
RX	110	5	9.4	15.1	-	-	-	-	-	-	-	-	-	-	-	-	-	-	-	-	-
RY	115	0.3	4.1	15.6	22.9	31.3	45.6	53.7	57.2	-	-	-	-	-	-	-	-	-	-	-	-
RZ	116	0.3	4.1	15.6	22.9	31.3	45.6	53.7	62.3	69.6	74	79	85	96.6	109	118	126	138	-	-	-
BENCH TESTS																					
RA	103	0.18	4.7	9.2	16.7	28.8	34.2	42.2	50.5	62	70.4	78.8	91.3	98.2	105.4	117.8	-	-	-	-	-
RB	104	0.35	4.0	-	-	-	-	-	-	-	-	-	-	-	-	-	-	-	-	-	-
RC	111	0.18	4.7	9.2	16.7	28.2	34.2	42.2	50.5	62	70.4	78.8	91.3	98.2	105.4	117.8	-	-	-	-	-
RD	112	0.35	4.0	8.7	-	-	-	-	-	-	-	-	-	-	-	-	-	-	-	-	-
RE	113	0.18	4.7	0.21	16.7	30.0	34.2	46.9	50.9	63.6	71	79.4	91.9	98.8	-	-	-	-	-	-	-

* Underlined sample running times indicate periodic surface examinations of bearing inner ring tracks.

to fill each tank at the start of the test. The amount was not allowed to decrease below 1.5 gallons. This was achieved by adding new oil to each tank at recorded intervals.

(10) Oil samples were collected three times a week from all the tests. The samples were withdrawn by a 0.25 in. glass tube fitted with a suction bulb. A separate sampler was maintained for each tank. To inhibit chemistry changes in the lubricant, the samples were kept cold until they were subjected to analysis. The time table for oil sample withdrawal for roller bearings is given in Table 18. The times at which interrupted test bearings were examined are underlined. When a given bearing failed, an analysis of the oil samples in the reverse order revealed the time in the life of the bearing at which a noticeable change in the characteristics of the oil debris occurred.

(11) The bearings were modified to facilitate their assembly and disassembly for periodic examination of the inner-ring surfaces during bench testing. The land at the smaller end of the cone (inner ring) of the tapered roller bearing was removed. A total of 16 tapered roller bearings were modified for use in this program. Of these, 15 tapered roller bearings were tested. An additional tapered roller bearing was tested due to failure of one of the bench test bearings at 4 m.r. This life was not adequate to obtain a sufficient number of oil samples for wear particle characteristic studies. It was also insufficient to determine the rate of surface damage or failure progression.

b. Roller Bearing Surface Monitoring.

(1) The average dimension of the diagonal of the two dents on each of the tapered roller bearings, the corresponding R_c values and the fatigue lives are listed in Table 19. Of the 15 bearings tested there were 8 cone failures, 2 cup failures, 3 roller failures, 1 combination cup and roller failure, and 1 test was suspended. None of the cone failures occurred at the Vickers indent.

(2) The results of Weibull analysis of the fatigue life data for the roller bearings are presented in Table 20. Previously it was shown that the L_{10} life of the 6309 ball bearing was approximately 7 times greater than its theoretical life. On the other hand, practically no improvement is observed for the tapered roller bearings. It is interesting to note that although the L_{10} life of the tapered roller bearings is approximately 10% that of the ball bearings in terms of the number of revolutions; it is nearly 50% in terms of the number of stress cycles.

(3) Since rolling contact fatigue failures occur due to the presence of cyclic stresses, it seems appropriate that bearing lives be reported in number of stress cycles rather than number of revolutions. This would make it easier and more meaningful to compare fatigue life data from different bearing types and test methods. The difference in life then would reflect only the differences in bearing design, material, or other test parameters. Number of revolutions is only meaningful in reference to a given bearing type. Besides, all other fatigue data is reported in terms of number of stress cycles.

(4) The progression of surface damage and failure on tapered roller bearings was, as with the ball bearings, followed with the help of surface roughness and RMS slope angle measurements and visual and scanning electron microscopic examination of the cone (inner ring), roller end, and flange surfaces of bench test bearing. Particles have a greater probability of staying in the contact.

(5) In the case of tapered roller bearings the initial surface roughness and RMS slope angle of the asperities are greater than those in a ball bearing. With running, the surface roughness and RMS slope angles decrease in the case of tapered roller bearings as shown in Table 21. This is contrary to the behavior of the ball bearings. The changes in surface topography between the unrun and run states are not as clearly evident for the tapered roller bearings as in the case of the ball bearings, Figure 35.

TABLE 19. SUMMARY OF TAPERED ROLLER BEARING TEST RESULTS

Type Test	Bearing ID Navy	Bearing ID SKF	Indent Size (μm)	Rockwell Hardness (R_c)	No. of Oil Samples	Life (m.r.)	Element Failed*
Endurance	RQ	101	153	63.7	10	71.3	Cup
"	RR	102	153	63.7	5	38.1	Cone (b)
"	RS	105	153	63.7	2	12.4	Roller
"	RT	106	153	63.7	12	102.0	Roller
"	RU	107	151	64.4	10	81.0	Cone (b)
"	RV	108	152	64.1	8	72.7	Cone (b)
"	RW	109	152	64.1	6	37.0	Cup and Roller
"	RX	110	153	63.7	3	15.1	Cup
"	RY	115	153	63.7	8	57.2	Cone (b)
"	RZ	116	151	64.4	17	85.0	Cone (b)
Bench	RA	103	152	64.1	15	117.8	T
"	RB	104	154	63.4	2	4.0	Cone (b)
"	RC	111	150	64.7	15	117.8	Cone (b)
"	RD	112	151	64.4	3	8.7	Roller (seam)
"	RE	113	152	64.1	13	98.8	Cone (b)

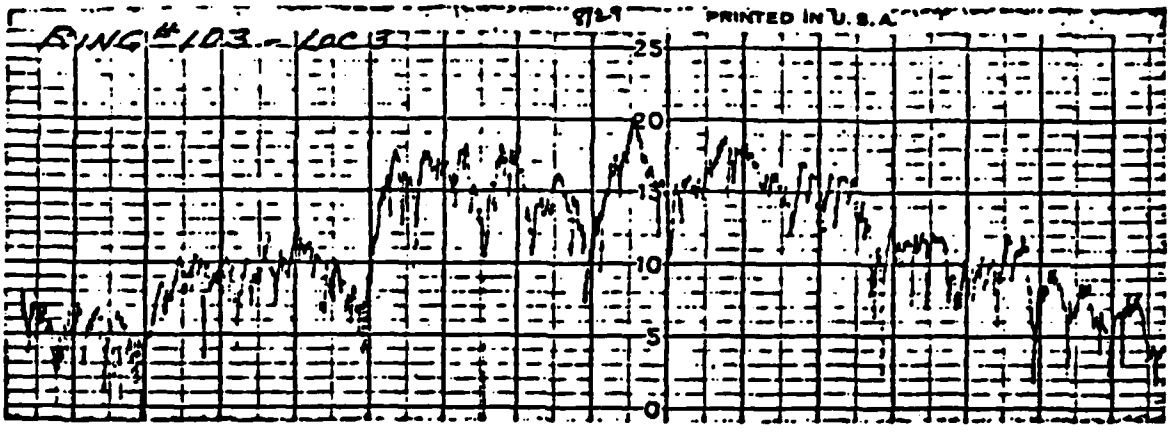
* T = Terminated without failure
(b) = Did not fail at Vickers indentation

TABLE 20. WEIBULL ANALYSIS OF ROLLER BEARING FATIGUE LIFE RESULTS

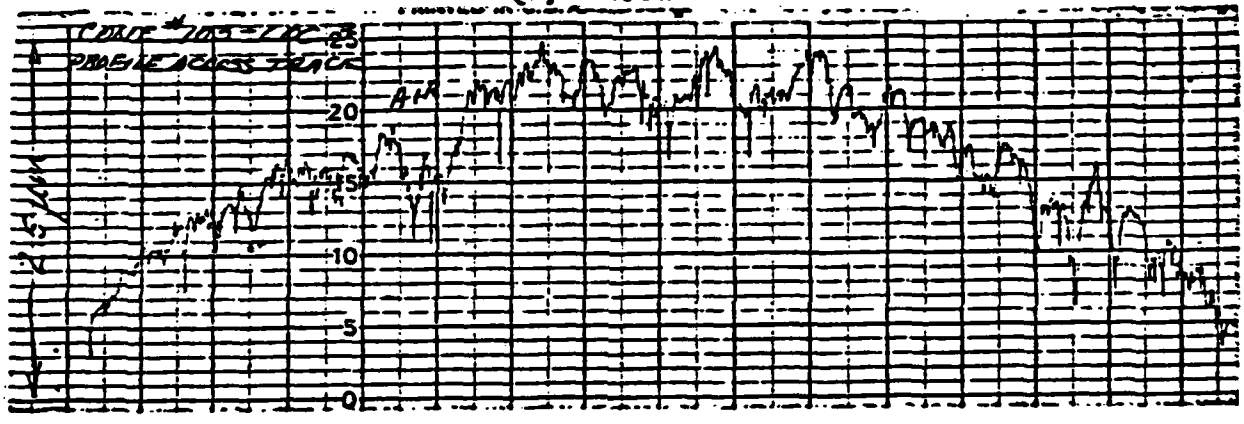
	Tapered Roller Bearing (LM102949/LM102901)
1. Median Bias Corrected L_{10}	
10^6 revolutions	11.36
10^6 stress cycles	147.68
2. 90% Confidence Interval for L_{10}	
10^6 revolutions	3.82-21.67
10^6 stress cycles	49.66-281.71
3. Weibull Slope	1.33
4. Improvement Over Theoretical Life of 10 m.r.	1.14X
5. Median Bias Corrected L_{50}	
10^6 revolutions	51.34
10^6 stress cycles	667.42
6. 90% Confidence Interval for L_{50}	
10^6 revolutions	32.60-76.32
10^6 stress cycles	432.90-992.16

TABLE 21. ROLLER BEARING SURFACE MEASUREMENT DATA AS A FUNCTION OF MILLION REVOLUTIONS

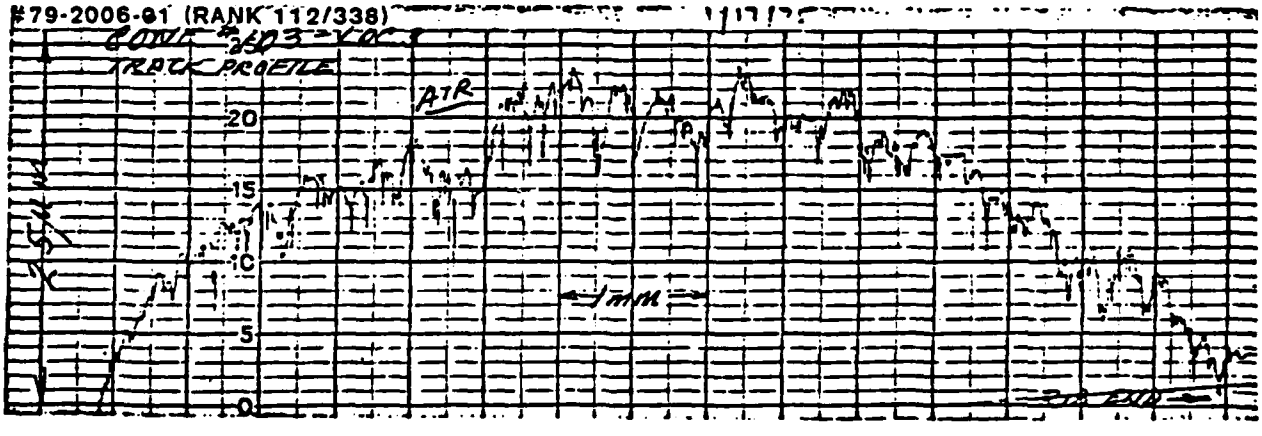
Bearing ID (Navy-SKF)	Million Revolutions	Surface Roughness (μmAA)	Slope Angle (Deg)
RQ-101	Unrun	0.17	2.32
	71.3	0.1	1.32
RR-102	Unrun	0.16	2.18
	38.1	0.14	1.65
RA-103	Unrun	0.143	1.93
	34.2	0.11	1.45
	98.2	0.09	1.42
	117.8	0.10	1.52
RB-104	Unrun	0.10	1.83
	4.0	0.09	1.38



(a) unrun



(b) 34.2 m.r.



(c) 98.2 m.r.

FIGURE 35

CHANGES IN SURFACE TEXTURE OF BEARING NO. RA-103 CONE SURFACE WITH ROLLING CONTACT

(6) A representative series of defects observed on as-finished tapered roller bearings are shown in Figure 36. The cone rface also contained two Vickers indentations, 180° apart as in the case of the ball bearings.

(7) The surfaces that undergo a major change in topography during the early part of the bearing life are the roller ends and flange surfaces, Figure 37. The wear on these surfaces occurs due to sliding and should contribute to a large fraction of the lamellar (rubbing wear) particles observed in the oil samples. The presence of high sliding in the roller end-flange contact is evident in Figure 38. The topography of these surfaces stabilizes within the first few hours of the bearing's life and does not change significantly with further running under the same conditions.

(8) Metal shoulders around dents and furrows on tapered roller bearing surfaces suffer glazing and microspalling as in the case of the ball bearings, Figure 39. However, none of the cone failures occurred at the artificially induced Vickers indentations.

(9) In the case of roller bearings the load is evenly distributed across the contact width. The level of stress at a defect is therefore dependent only on its stress raising ability. The fact that none of the cone failures occurred at the Vickers indentation signifies that the as-finished bearing contains defects that are more severe in their stress raising ability than a dent 150-153 μm in size.

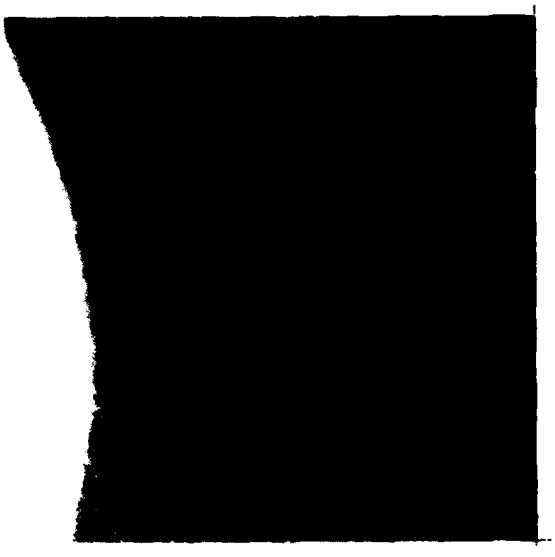
(10) As stated earlier the tapered roller bearings are made of CVD type AISI 4118 steel which contains nominal 0.18% C by weight. The lower carbon content of these steels leads to a higher melting temperature ($\sim$1550°C) compared to the through-hardening grades which contain 0.8-1.0% C ($\sim$1450°C). Due to this increase in the melting temperature at these already high temperatures, the furnace refractories wear to a greater extent. These steels therefore contain a larger amount of slag and inclusion particles. Most of the cone spalls initiated at inclusion stringers, Figures 40A and 40B. The spall in Figure 40B is very close to a Vickers indent but was not initiated by it as judged from the



3701 2500X
A. INCLUSION STRINGER ON CONE SURFACE



3702 125X
B. DENT ON CONE SURFACE

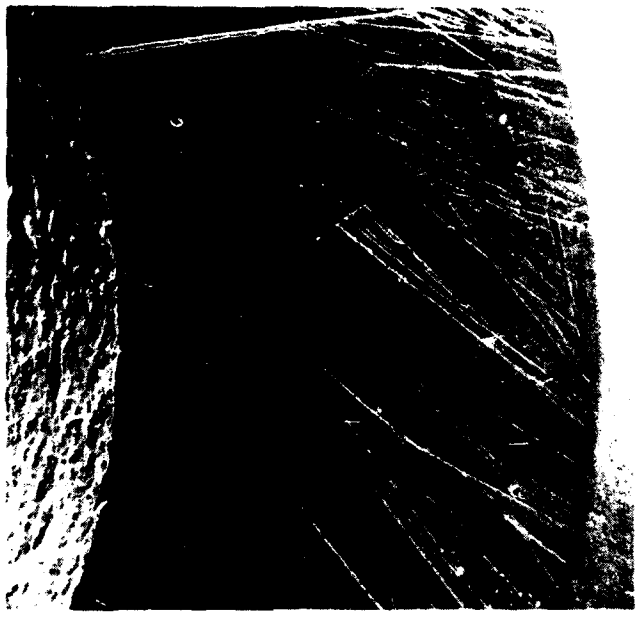


3657 50X
C. GRINDING SCRATCHES ON ROLLER END

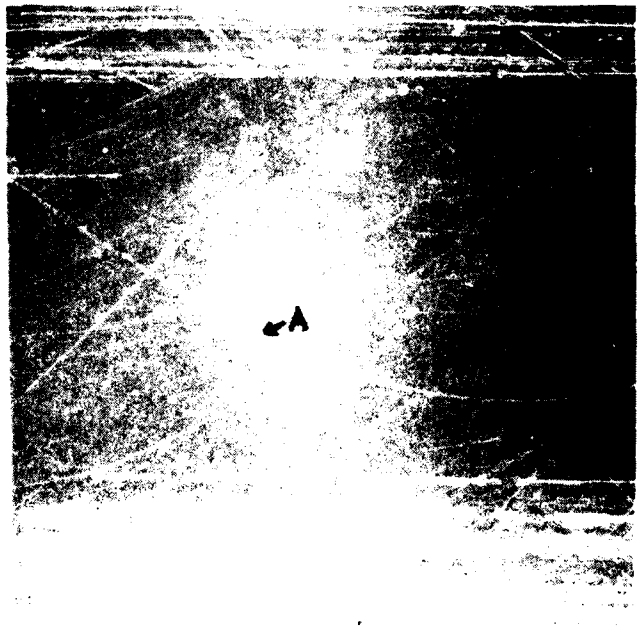


3681 100X
D. GRINDING SURFACES ON FLANGE SURFACE

FIGURE 36. SURFACE DEFECTS ON COMPONENTS OF AS-FINISHED NO. RA-103 TAPERED ROLLER BEARING



3852 7.8 m.r. 50X



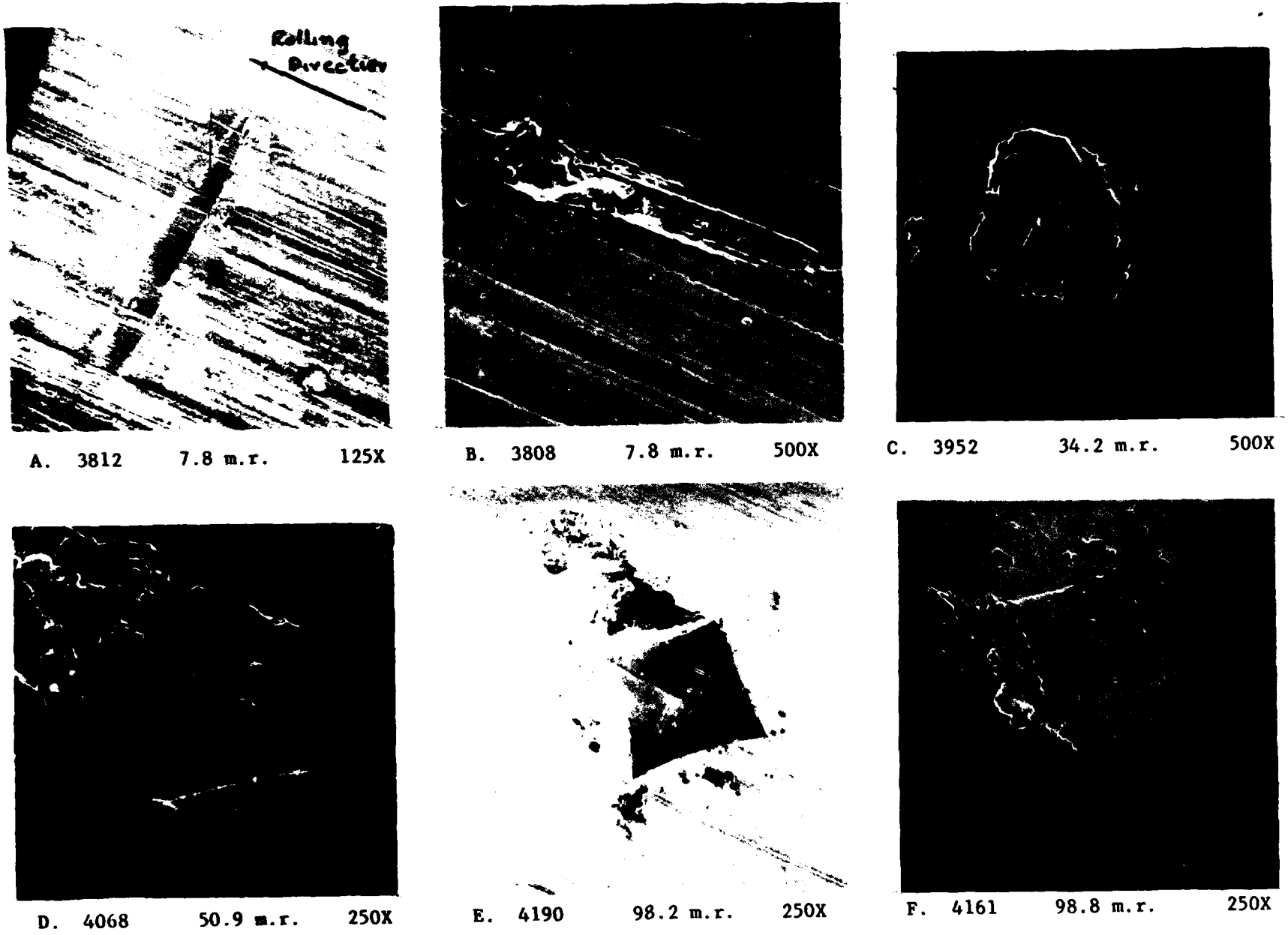
3825 7.8 m.r. 100X

FIGURE 37. WEAR ON ROLLER END AND FLANGE SURFACES DURING ROLLING CONTACT



3769 4 m.r. 1000X

FIGURE 38. EFFECT OF SLIDING IN ROLLER END FLANGE CONTACT ON ROLLER END SURFACE



A. 3812 7.8 m.r. 125X

B. 3808 7.8 m.r. 500X

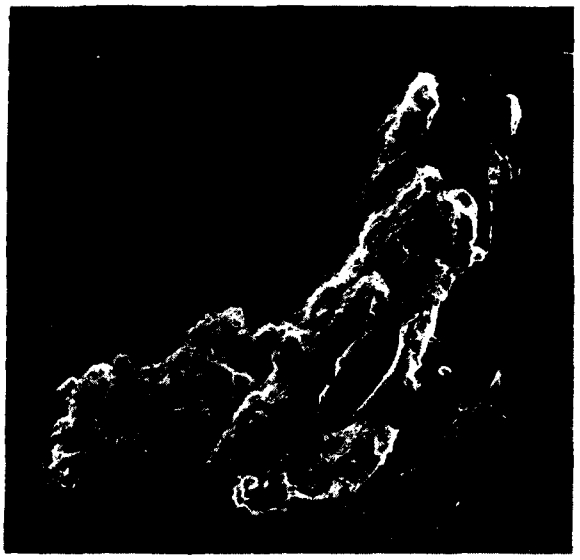
C. 3952 34.2 m.r. 500X

D. 4068 50.9 m.r. 250X

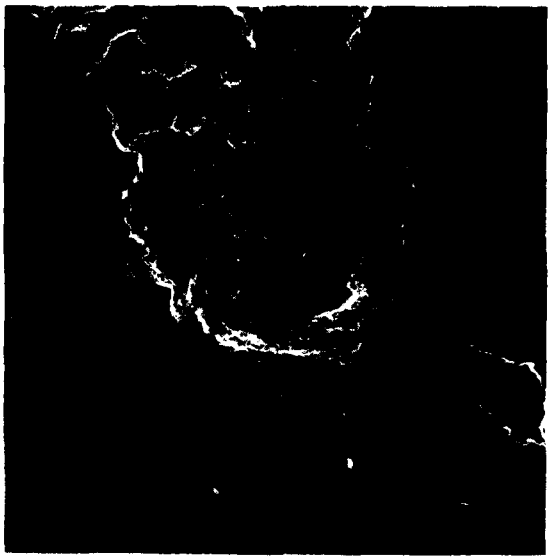
E. 4190 98.2 m.r. 250X

F. 4161 98.8 m.r. 250X

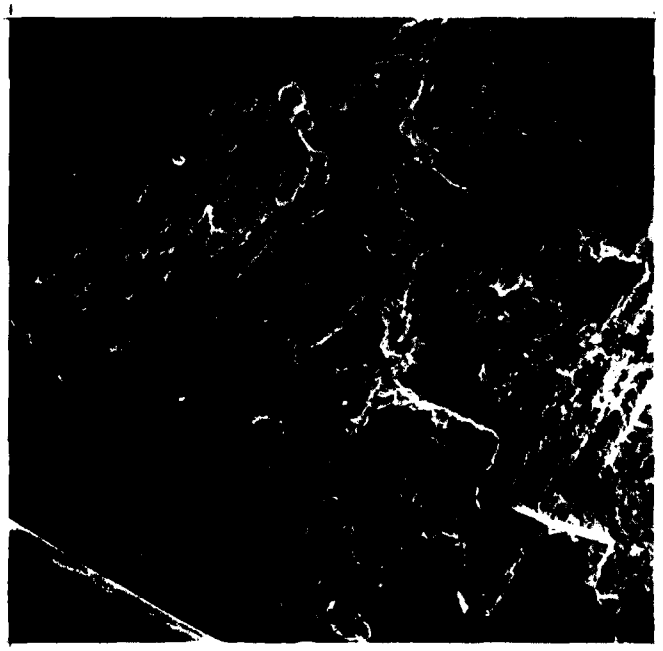
FIGURE 39. SURFACE DAMAGE PRODUCED ON TAPERED ROLLER BEARING CONE SURFACE DURING ROLLING CONTACT



3786 4 m.r. 20X
A. FB-104: INCLUSION STRINGER INITIATED



4170 98.8 m.r. 100X
B. RE-113: ASSOCIATED WITH BUT NOT INITIATED AT VICKERS DENT



3662 38.1 m.r. 10X
C. RR-102: FURROW INITIATED

FIGURE 40. MORPHOLOGIES OF SPALLS ON TAPERED ROLLER BEARING CONE SURFACES

rolling direction. Some spalls were initiated at furrows, Figure 40C. It should be reiterated that the site at which spall initiates is dependent on the stress level and the strength of the material at that point. A close examination of the edge (A) in Figure 40C reveals subsurface cracks that have emerged to the surface, Figure 41.

(11) In the case of tapered roller bearings, it is important that the actual profiles of rollers and raceways meet design specifications as closely as possible. Errors in the profiles can lead to edge loading and excessive sliding in the contact. This causes further damage to the bearing life over and above that caused by the higher inclusion content. The absence of excessive sliding is evident from the retention of the sharp edge of the Vickers dent on a tested cone surface, Figure 39.

c. Roller Bearing Wear Particle Analysis

(1) Wear debris analysis was performed on respective roller bearing bench test lubricant samples by SKF Industries, Foxboro Analytical, and NAVAIRENGCEN. As previously discussed, lubricant samples were withdrawn periodically from the roller bearing test apparatus. These lubricant samples served as the host media for fluid borne debris analysis. Table 18 summarizes the number and respective operating times for each roller bearing series.

(2) As can be expected, there is substantial similarity between particle analysis results of ball and roller bearings. For the sake of brevity similarities under this section will be briefly discussed and the pertinent ball bearing section referenced for a more detailed discussion.

(3) As in the case of ball bearings, the three wear regimes; wear-in, normal wear, and wear-out/abnormal wear will be discussed with respect to the roller bearing wear debris characteristics; quantity, size distribution, composition, and morphology.



3665 38.1 m.r. 100X

FIGURE 41. EMERGENCE OF SUBSURFACE CRACKS ON SPALL SURFACE SHOWN IN FIGURE 40C.

(a) Particle Quantity

1. The quantity of wear debris contained in lubricant samples taken during roller bearing testing was primarily monitored utilizing ferrographic analysis techniques. As in the ball bearing testing, particle counting technique results were discounted as a result of the presence of nonmagnetic lubricant pump debris found in the respective oil samples. Ferrographic magnetic precipitation technique served to minimize the complicating effects of this non-magnetic debris. Spectrometric analysis concentration readings were also discounted with respect to particle quantity monitoring as a result of their inherent size sensitivity limitation. This limitation is discussed in detail in Section VI.

2. As in the case of ball bearing, lubricant borne particle quantity/concentration basically followed a "bathtub" curve plot over the wear life of the roller bearings. Figure 42 represents plots for three of the roller bearing sequences, RT, RU, and RY. Figures 43, 44, and 45 represent series of ferrography entry deposit micrographs of these sequences which can be directly related to sample debris concentration levels. These micrographs provide graphic evidence of the "bathtub" plot.

3. Each roller bearing test sequence, as with ball bearings, can be divided into three wear regimes; wear-in, normal wear, and wear-out/abnormal wear.

4. Initial wear-in of the roller bearings results in a high wear rate thus a high level of debris concentration. The second regime, normal wear, results in a much lower wear rate thus a much lower sample debris concentration. Abnormal wear, the final regime, results in an accelerated wear rate and thus an ever increasing level of debris. This increase was typical of all roller bearing test failures.

5. Comparing the wear quantity characteristics of roller bearings with those of the ball bearings test sequences the following observations can be made:

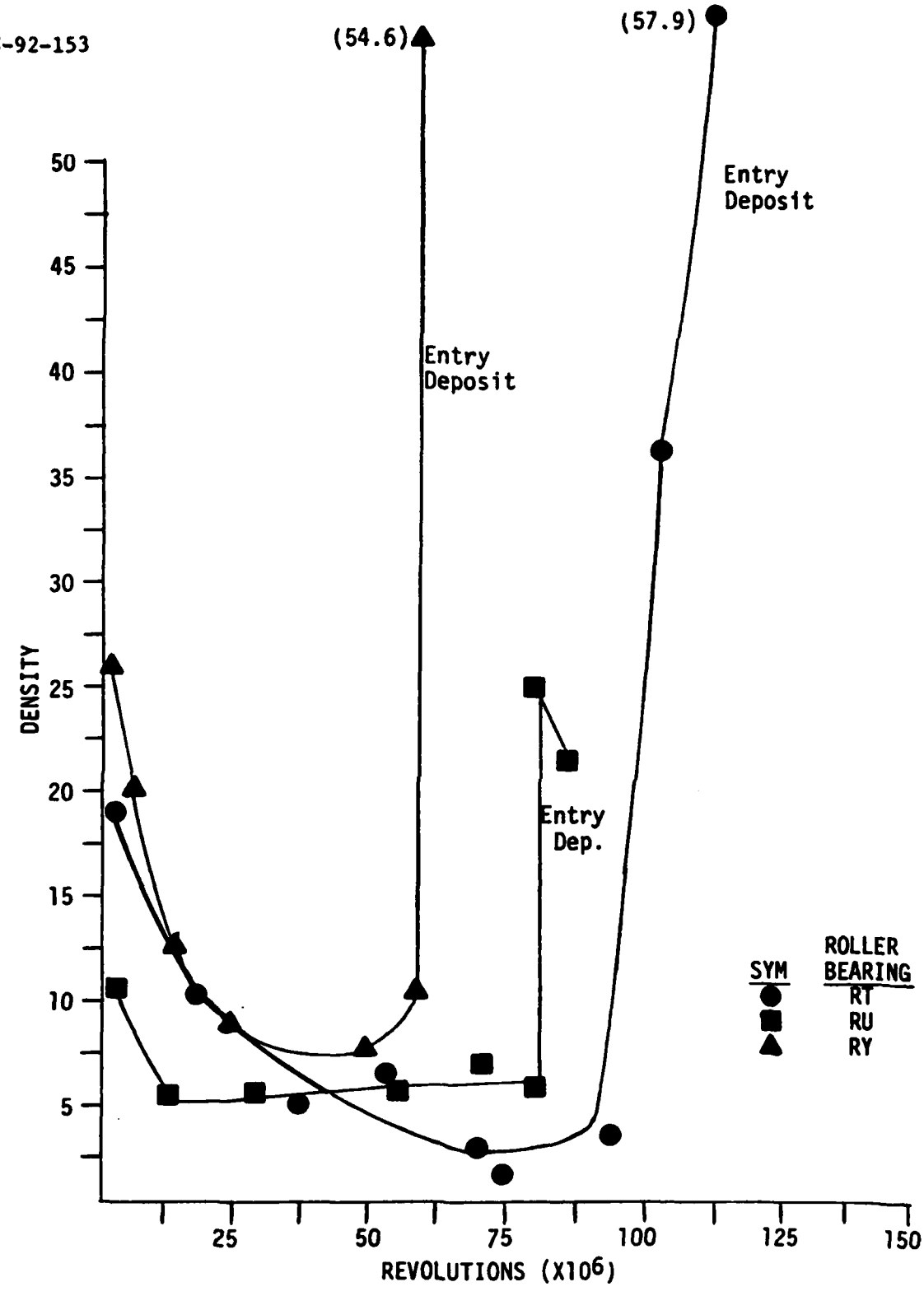
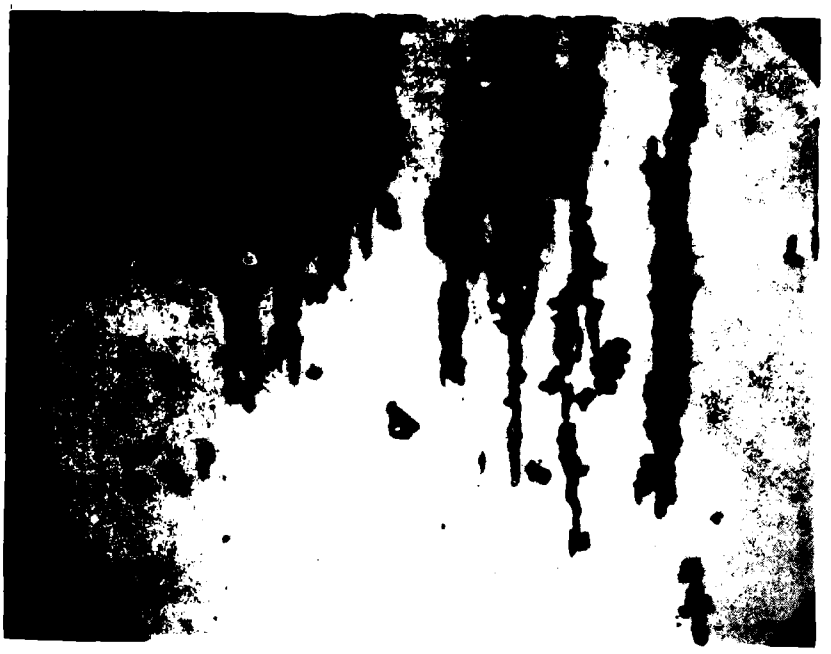


FIGURE 42. ROLLER BEARING TEST SEQUENCES
FERROGRAPH DENSITY DATA



A. 1.1 m.r.



B. 21.6 m.r.

FIGURE 43

ROLLER BEARING TEST SEQUENCE RT

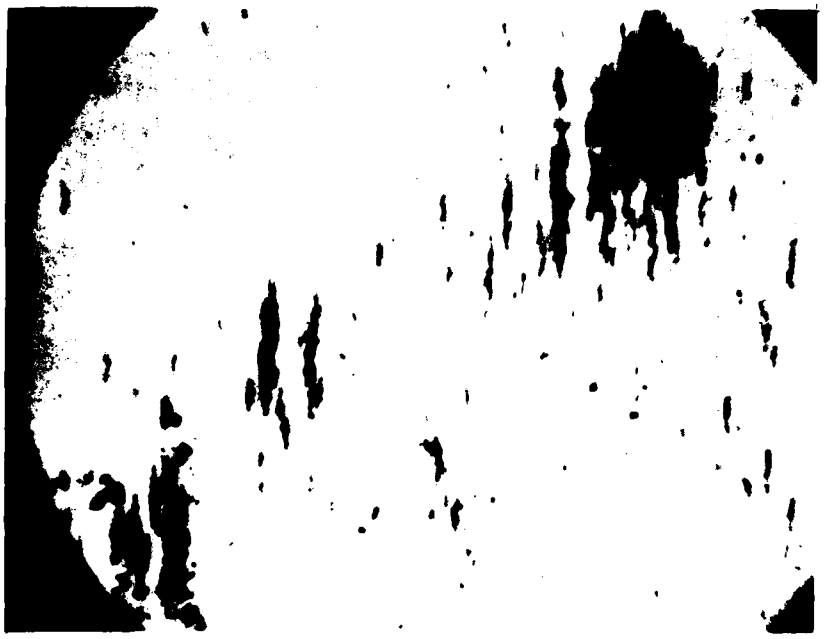
ENTRY DEPOSIT

LOW MAGNIFICATION

(Sheet 1 of 5)

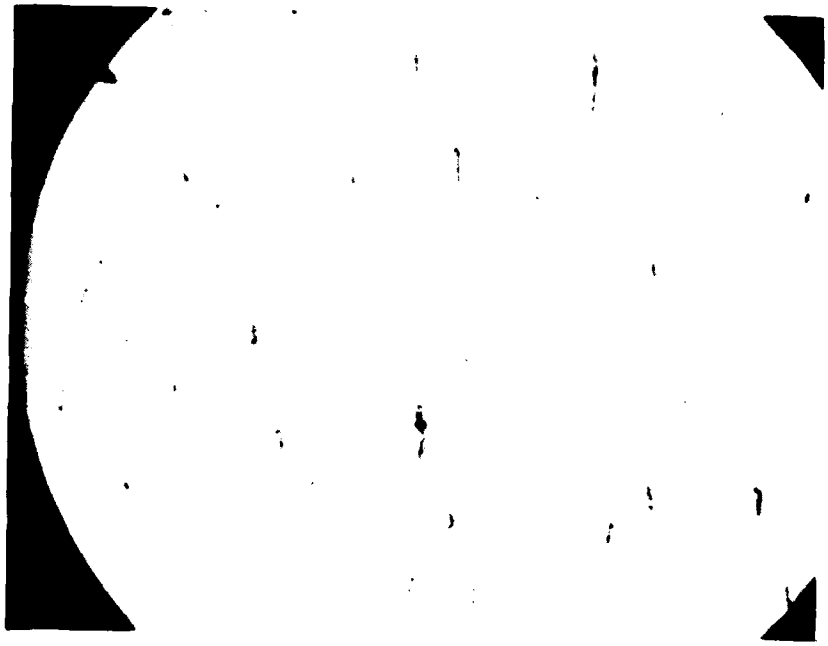


C. 37.2 m.r.



D. 53 m.r.

FIGURE 43
ROLLER BEARING TEST SEQUENCE RT
ENTRY DEPOSIT
LOW MAGNIFICATION
(Sheet 2 of 5)

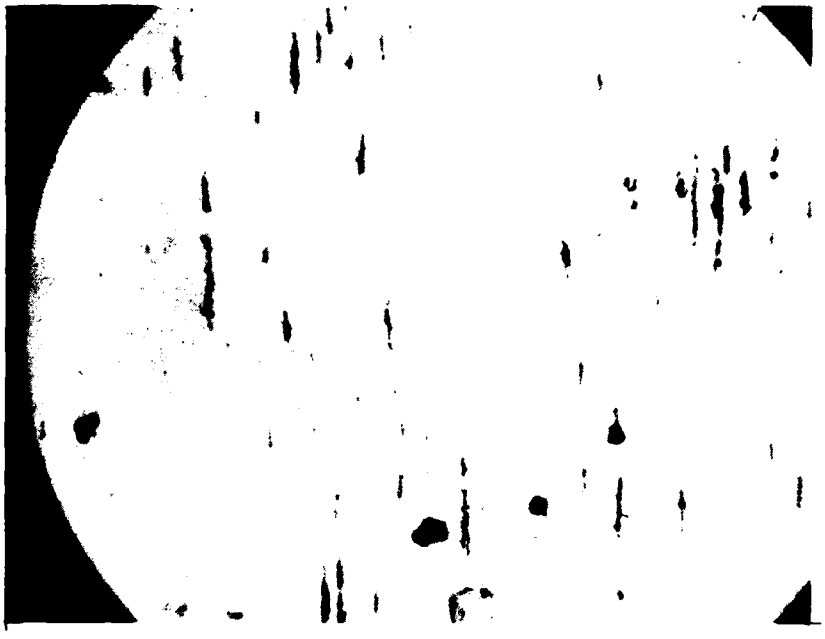


E. 66.5 m.r.



F. 72 m.r.

FIGURE 43
ROLLER BEARING TEST SEQUENCE RT
ENTRY DEPOSIT
LOW MAGNIFICATION
(Sheet 3 of 5)



G. 87.7 m.r.



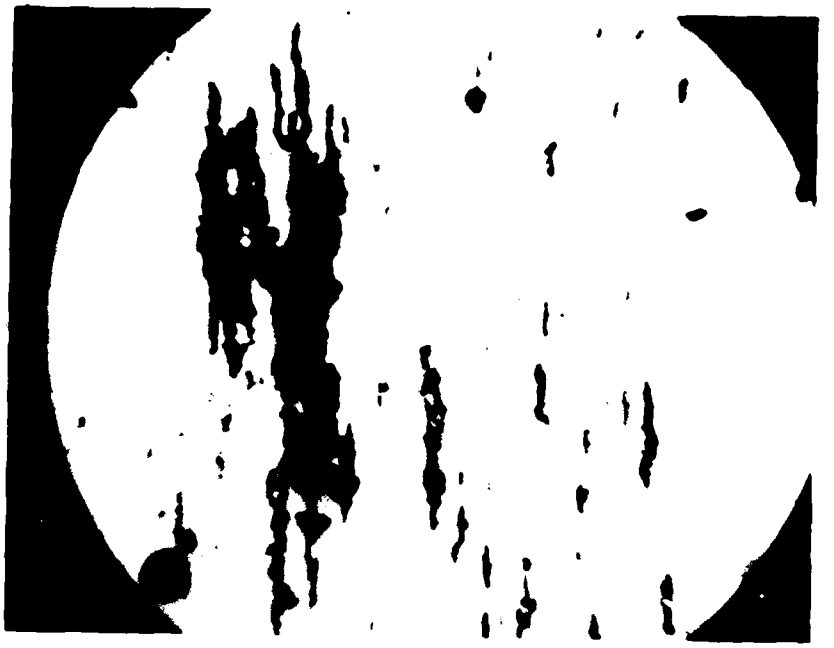
H. 99.8 m.r.

FIGURE 43
ROLLER BEARING TEST SEQUENCE RT
ENTRY DEPOSIT
LOW MAGNIFICATION
(Sheet 4 of 5)

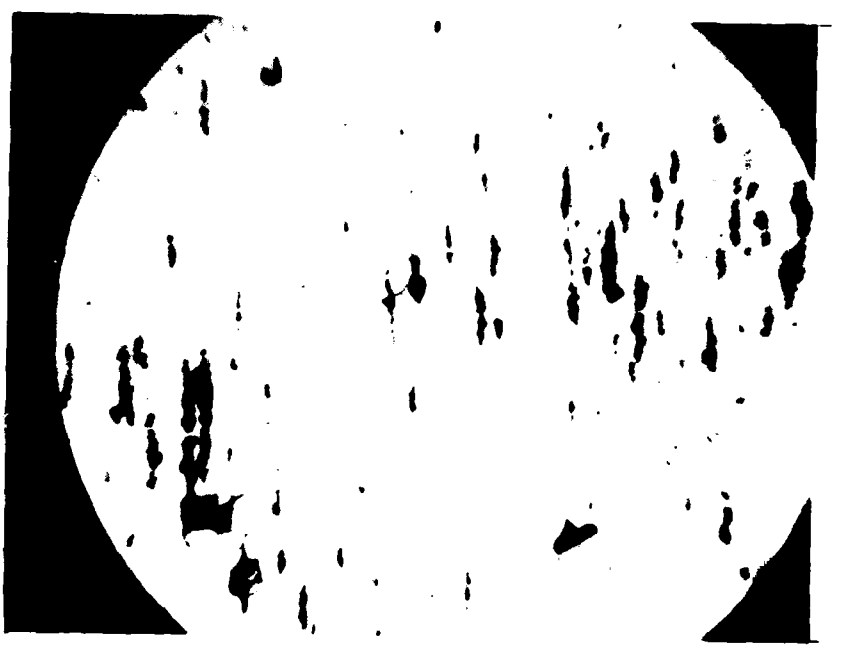


I. 102 m.r.

FIGURE 43
ROLLER BEARING TEST SEQUENCE RT
ENTRY DEPOSIT
LOW MAGNIFICATION
(Sheet 5 of 5)



A. 1.1 m.r.

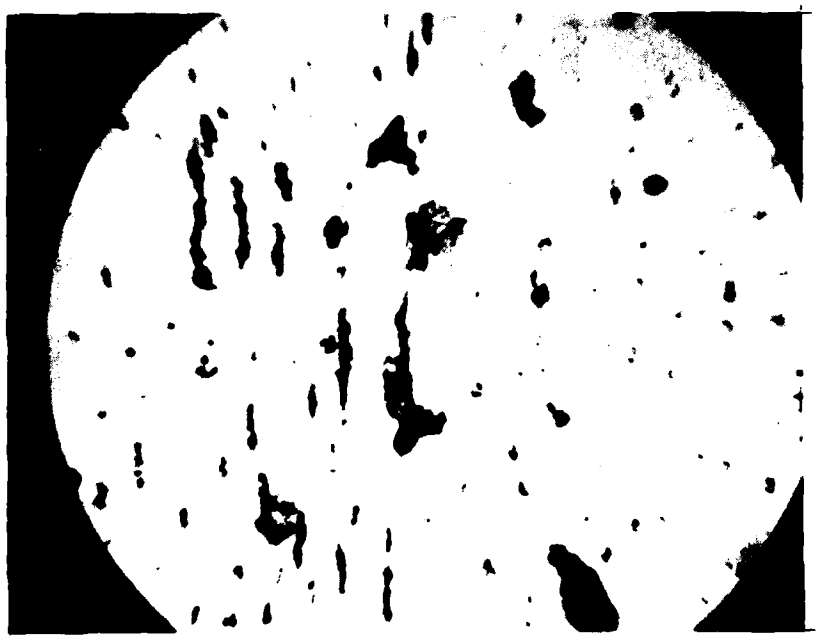


B. 13.6 m.r.

FIGURE 44
ROLLER BEARING TEST SEQUENCE RU
ENTRY DEPOSIT
LOW MAGNIFICATION
(Sheet 1 of 4)



C. 29.2 m.r.

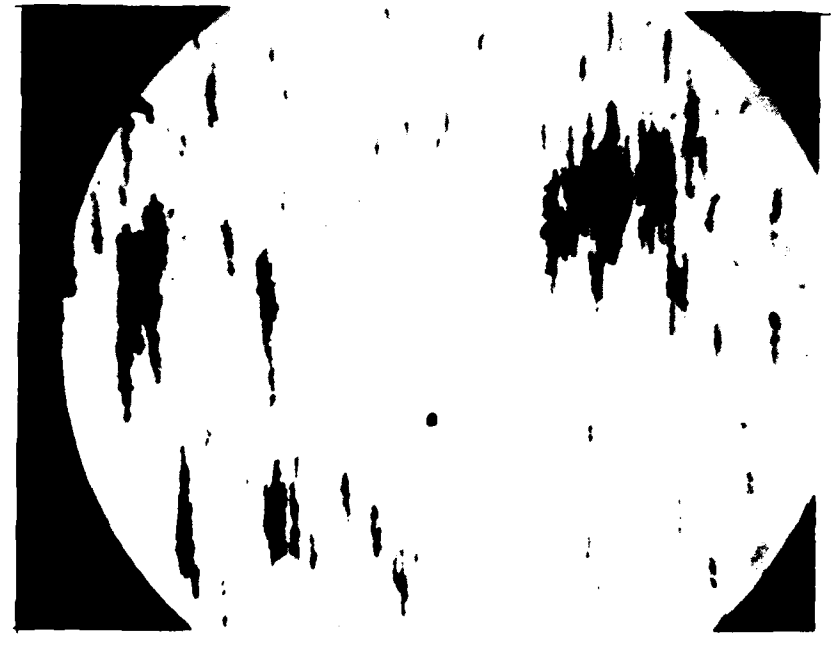


D. 55 m.r.

FIGURE 44
ROLLER BEARING TEST SEQUENCE RU
ENTRY DEPOSIT
LOW MAGNIFICATION
(Sheet 2 of 4)

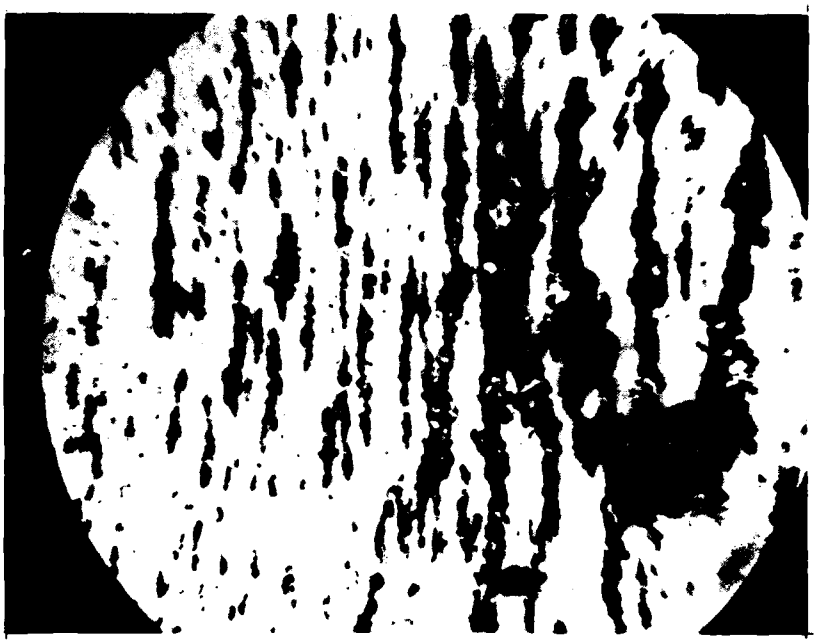


E. 66 m.r.

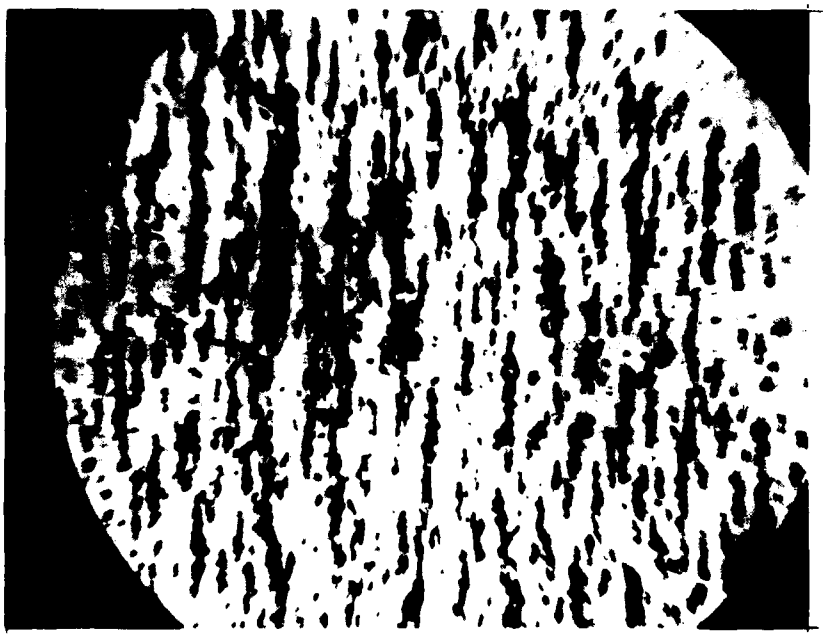


F. 73 m.r.

FIGURE 44
ROLLER BEARING TEST SEQUENCE RU
ENTRY DEPOSIT
LOW MAGNIFICATION
(Sheet 3 of 4)

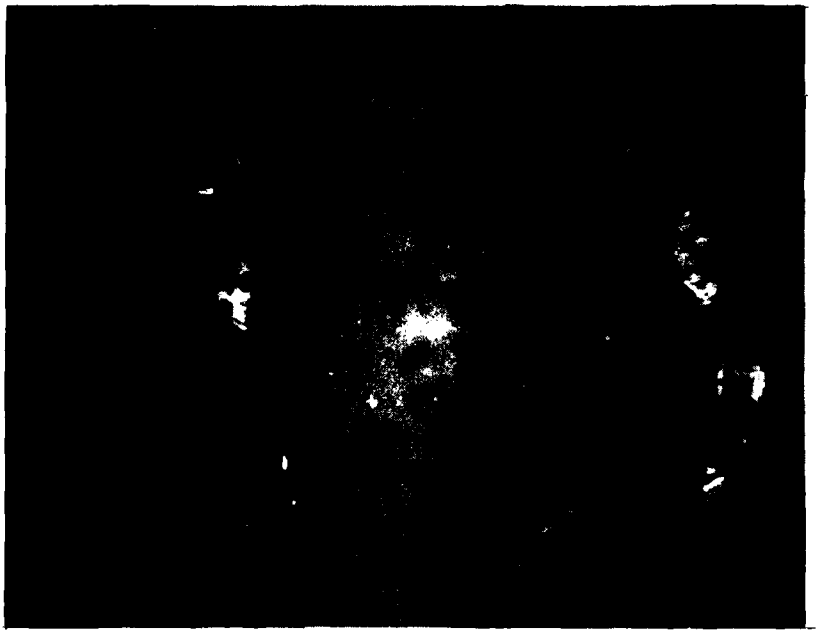


G. 77 m.r.



H. 81 m.r.

FIGURE 44
ROLLER BEARING TEST SEQUENCE RU
ENTRY DEPOSIT
LOW MAGNIFICATION
(Sheet 4 of 4)

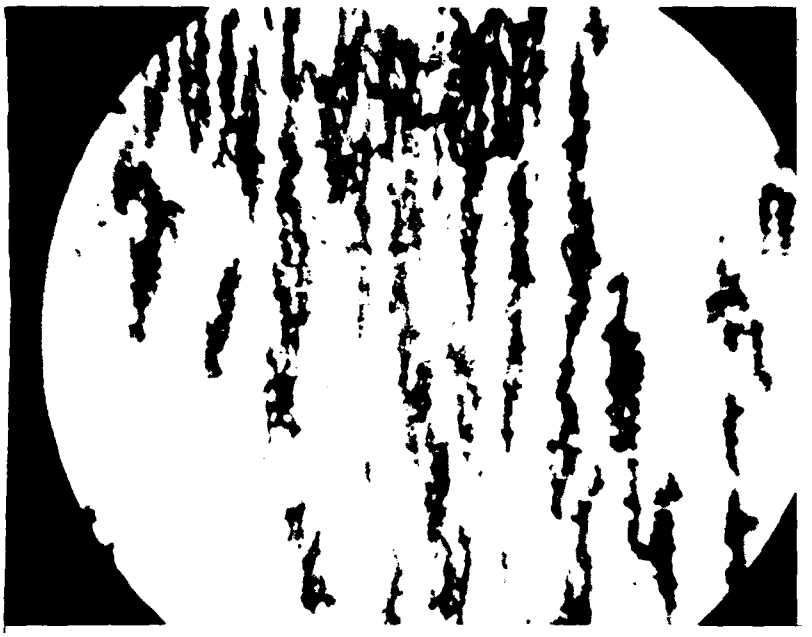


A. 0.3 m.r.

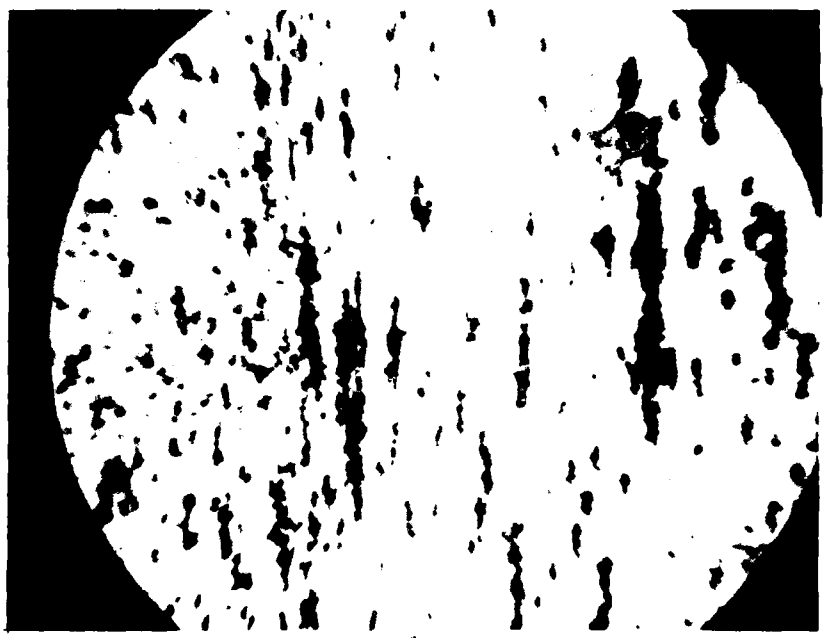


B. 4.1 m.r.

FIGURE 45
ROLLER BEARING TEST SEQUENCE RY
ENTRY DEPOSIT
LOW MAGNIFICATION
(Sheet 1 of 4)



C. 15.6 m.r.



D. 22.9 m.r.

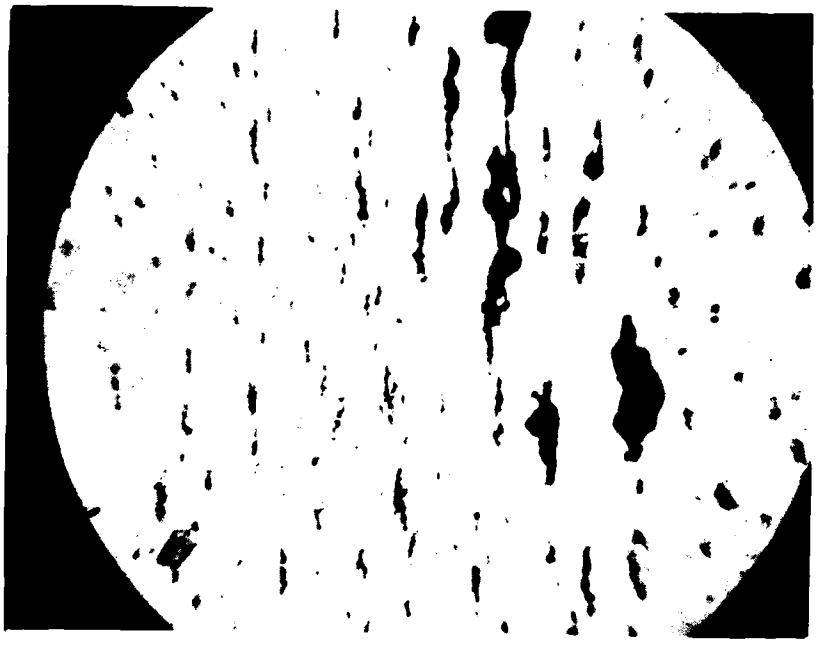
FIGURE 45

ROLLER BEARING TEST SEQUENCE RY

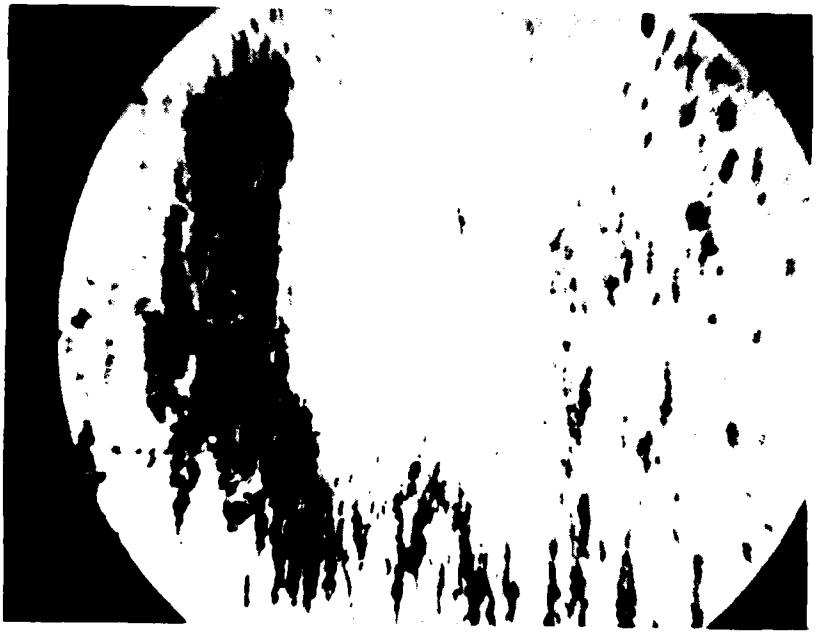
ENTRY DEPOSIT

LOW MAGNIFICATION

(Sheet 2 of 4)



E. 45.6 m.r.



F. 53.7 m.r.

FIGURE 45
ROLLER BEARING TEST SEQUENCE RY
ENTRY DEPOSIT
LOW MAGNIFICATION
(Sheet 3 of 4)



G. 57.2 m.r.

FIGURE 45

ROLLER BEARING TEST SEQUENCE RY

ENTRY DEPOSIT

LOW MAGNIFICATION

(Sheet 4 of 4)

a. Normal wear debris quantity/concentration levels are approximately the same for the two bearing types with roller bearings exhibiting only a slightly higher normal wear concentration level. This factor indicates that the two bearing types exhibit similar normal wear rates under the respective test conditions.

b. Wear-in debris concentration levels for the roller bearing tests were significantly higher than those of the ball bearing tests. This factor indicates that the test roller bearings experience a more severe wear-in process than the test ball bearings under the respective test conditions.

c. Abnormal wear debris concentration levels for the roller bearing tests were almost double the levels experienced under the ball bearing tests. Part of this difference could have resulted from differences in failure criteria, however, it does tend to indicate that roller bearings generate greater quantities of debris during an abnormal wear regime than ball bearings.

6. Figure 46 represents a generalized plot of roller bearing and ball bearing debris concentration versus life. The wear life scale on this figure has been normalized to a percentage in order to eliminate the effects of bearing life differentials as previously discussed.

7. It is to be noted that the roller bearing lubricant systems were not equipped with a filter. As a consequence, decreases in debris concentration must have resulted from a combination of natural filtration (i.e. plating out, settling effects, etc.) and a particle grinding process which causes particle breakup as in the case of the ball bearing test sequences.

8. Figure 47 represents a debris deposit plot for roller bearing sequence RA. Figure 48 presents the respective series of ferrography entry deposit micrographs from this sequence. This bearing was one of the five

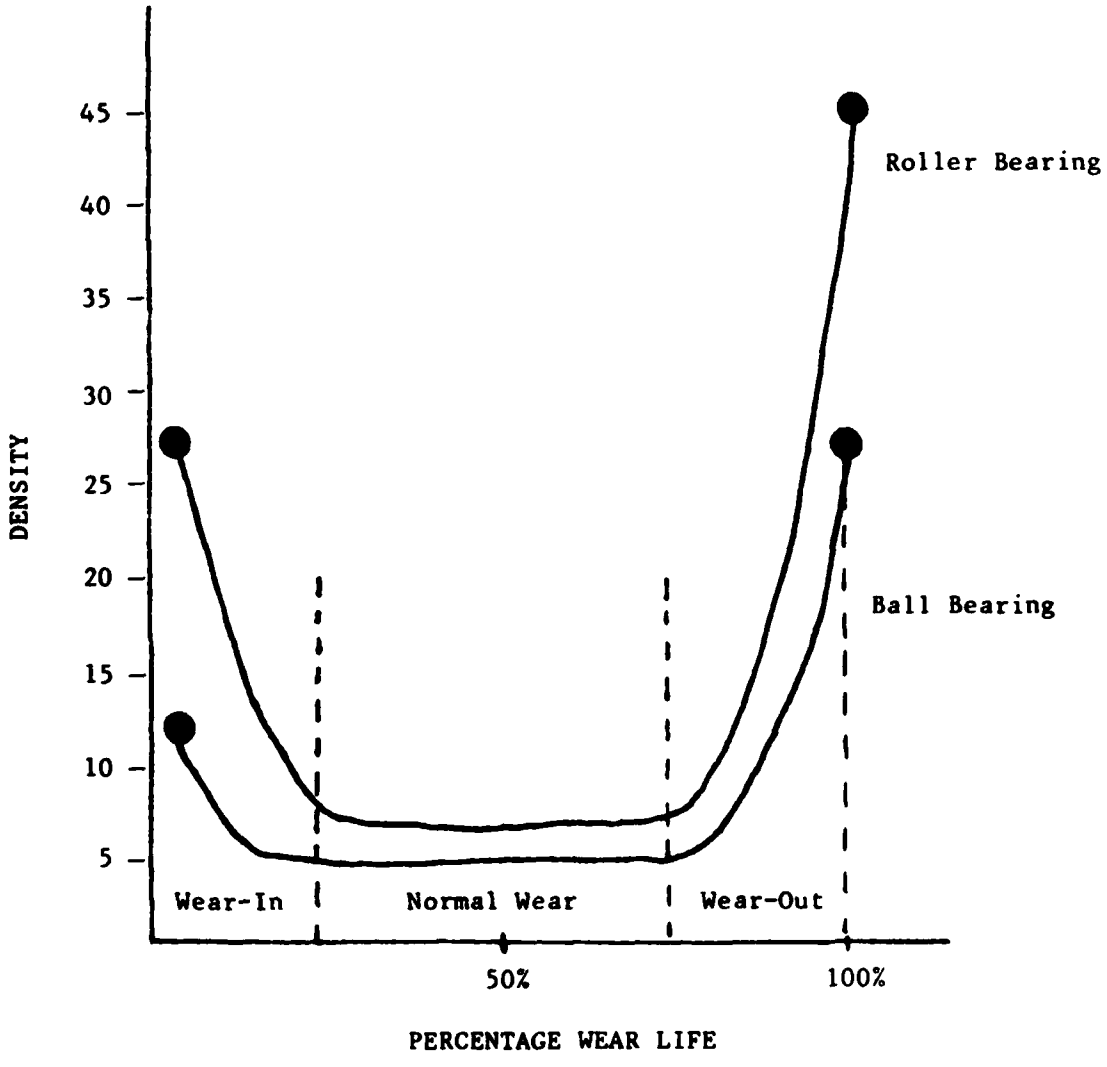


FIGURE 46
GENERALIZED BEARING DEBRIS CONCENTRATION
LEVEL COMPARISON

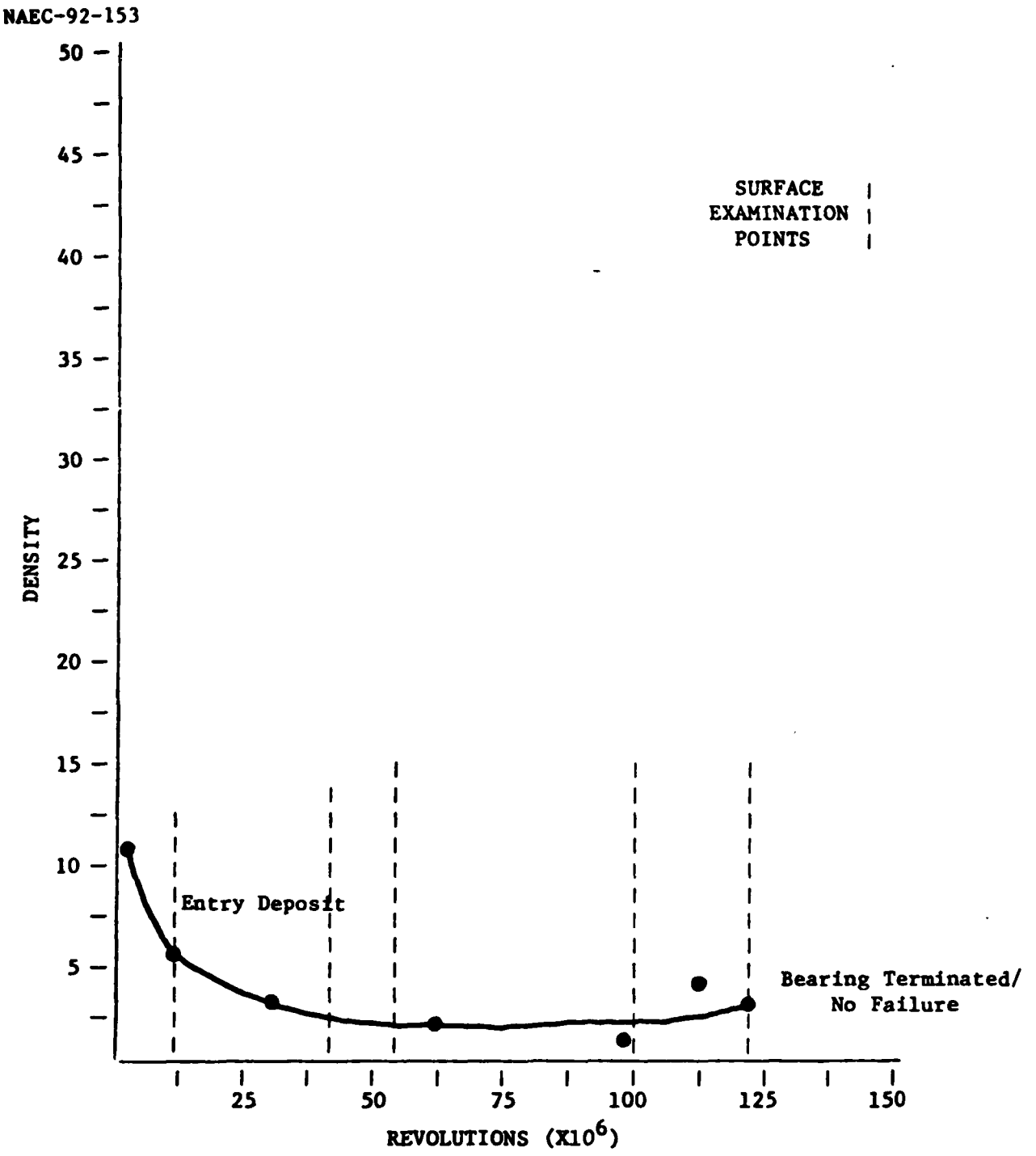
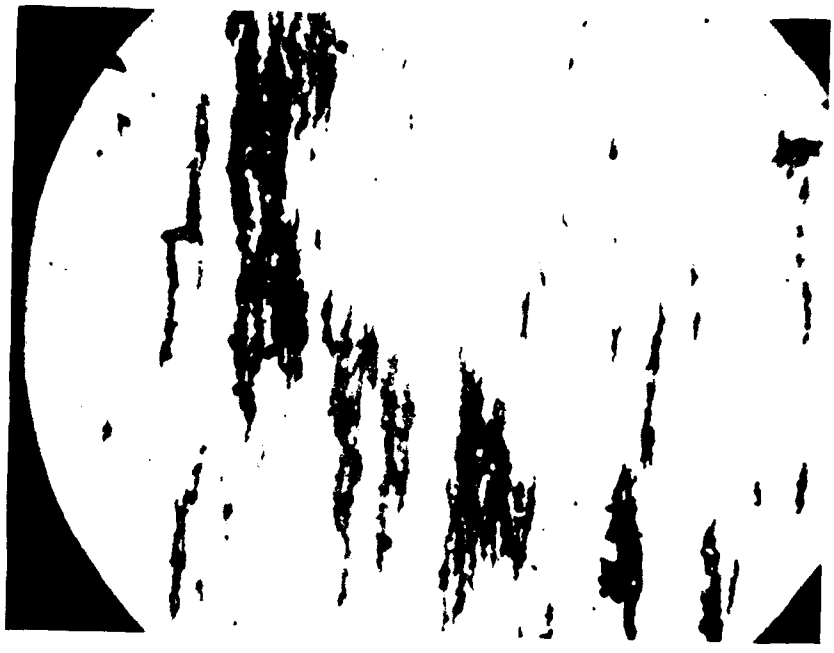


FIGURE 47

ROLLER BEARING TEST SEQUENCE RA

FERROGRAPH DENSITY DATA



A. 0.18 m.r.



B. 9.2 m.r.

FIGURE 48

ROLLER BEARING TEST SEQUENCE RA

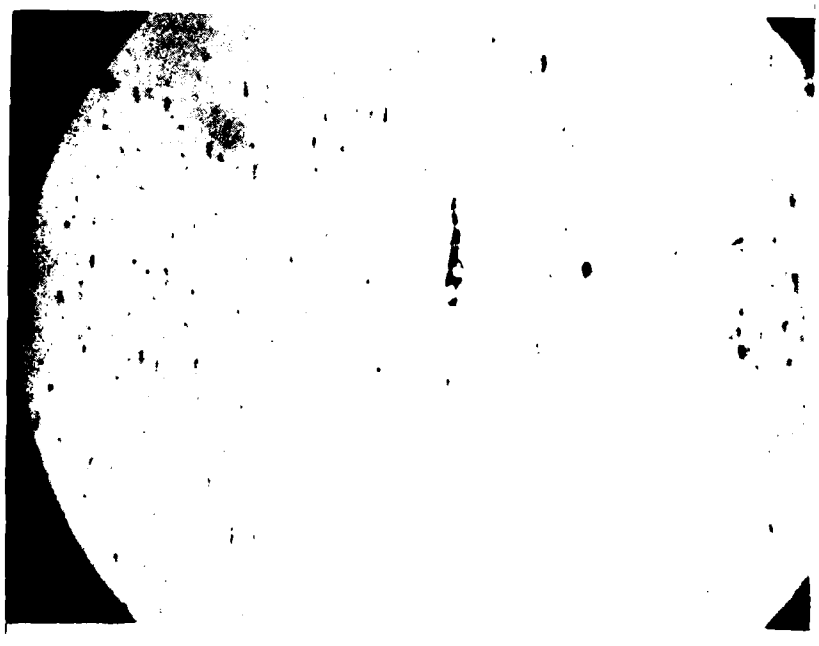
ENTRY DEPOSIT

LOW MAGNIFICATION

(Sheet 1 of 4)



C. 28.8 m.r.

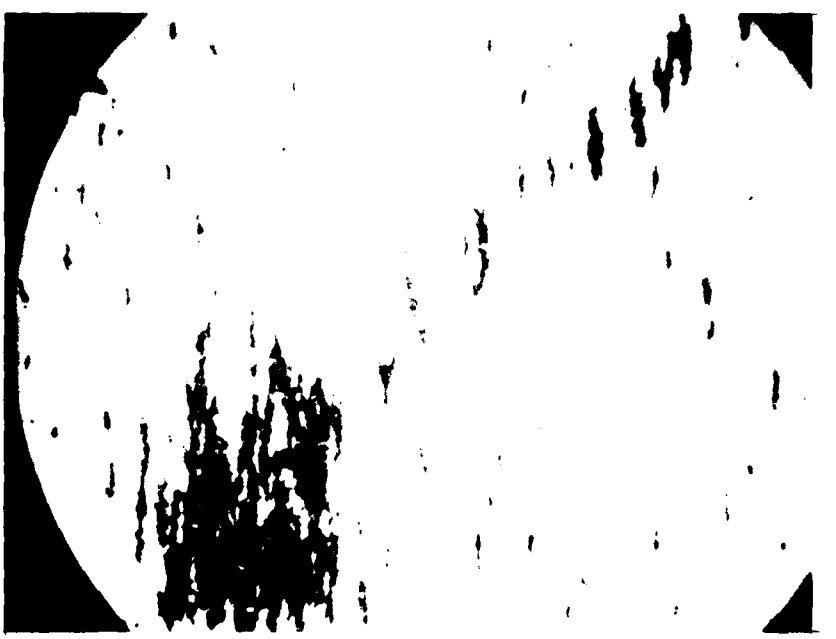


D. 62 m.r.

FIGURE 48
ROLLER BEARING TEST SEQUENCE RA
ENTRY DEPOSIT
LOW MAGNIFICATION
(Sheet 2 of 4)



E. 98.2 m.r.



F. 105.4 m.r.

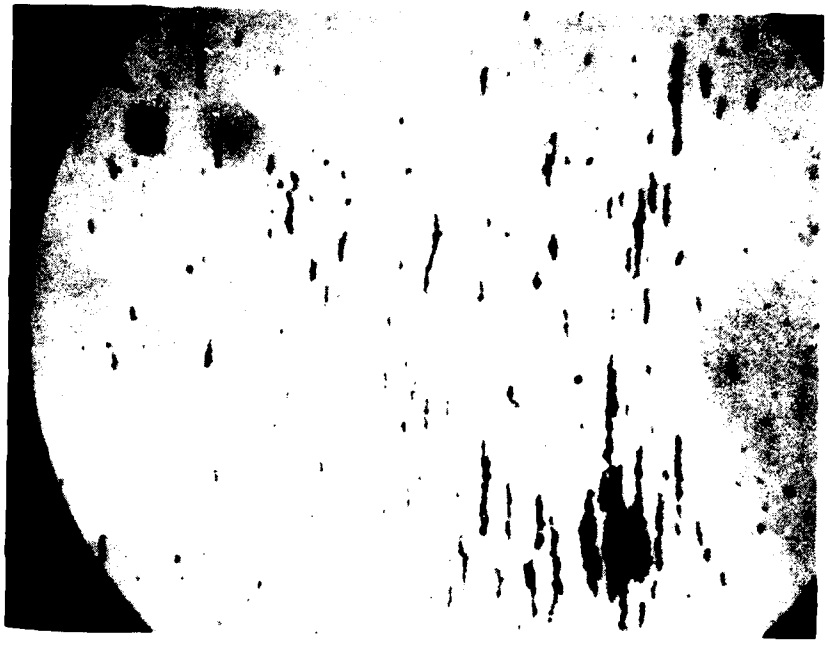
FIGURE 48

ROLLER BEARING TEST SEQUENCE RA

ENTRY DEPOSIT

LOW MAGNIFICATION

(Sheet 3 of 4)



G. 117.8 m.r.

FIGURE 48

ROLLER BEARING TEST SEQUENCE RA

ENTRY DEPOSIT

LOW MAGNIFICATION

(Sheet 4 of 4)

roller bearing tests sequences that were periodically interrupted for wear surface analysis. Contrary to what was experienced during ball bearing inspection, roller bearing disassembly/reassembly appears to have minimal effect on the respective wear rate of the bearing. The reoccurrence of a wear-in process upon reassembly, as experienced during ball bearing testing, does not occur during roller bearing testing. Initial indications are that roller bearings are far less effected by disassembly/reassembly than ball bearings. However, the different disassembly/reassembly procedures utilized on the two bearing types could have contributed to this difference in wear characteristics.

9. The plot presented in Figure 47 for bearing RA is also significant from a second aspect. This particular rolling bearing did not experience a failure and thus the test sequence was terminated as a result of time constraints. As can be observed from the figure, no apparent abnormal wear regime is present. This observation would be expected from a normally running bearing. Also noted on this RA test sequence plot is the relatively mild wear-in and normal wear process experienced by this bearing. Debris levels for this test during wear-in and normal wear were less than those experienced by the remaining roller bearing test sequences. A mild wear-in and relatively low normal wear rate could be indicative of a long life bearing as presented in this test. Figure 49, on the other hand, represents a debris plot of roller bearing test sequence RW. Figure 50 presents the respective series of micrographs for this test sequence. This bearing experienced a relatively short test life, 37 million revolutions. As can be observed from the plot, this bearing experienced a severe/abnormal wear-in process which never subsided during the bearing life. The relatively short life of this bearing could have resulted from either a latent defect in the new bearing or a result of a severe wear-in process. In any case, the wear-in process appears to be a significant factor with respect to bearing life, the exact correlation of which desires further investigation.

10. Tables 22, 23, 24, and 25 represent spectrometric readings from sequences RT, RU, RY, and RW. As can be seen from the iron (Fe) concentration readings, there is little indication of wear debris concentration

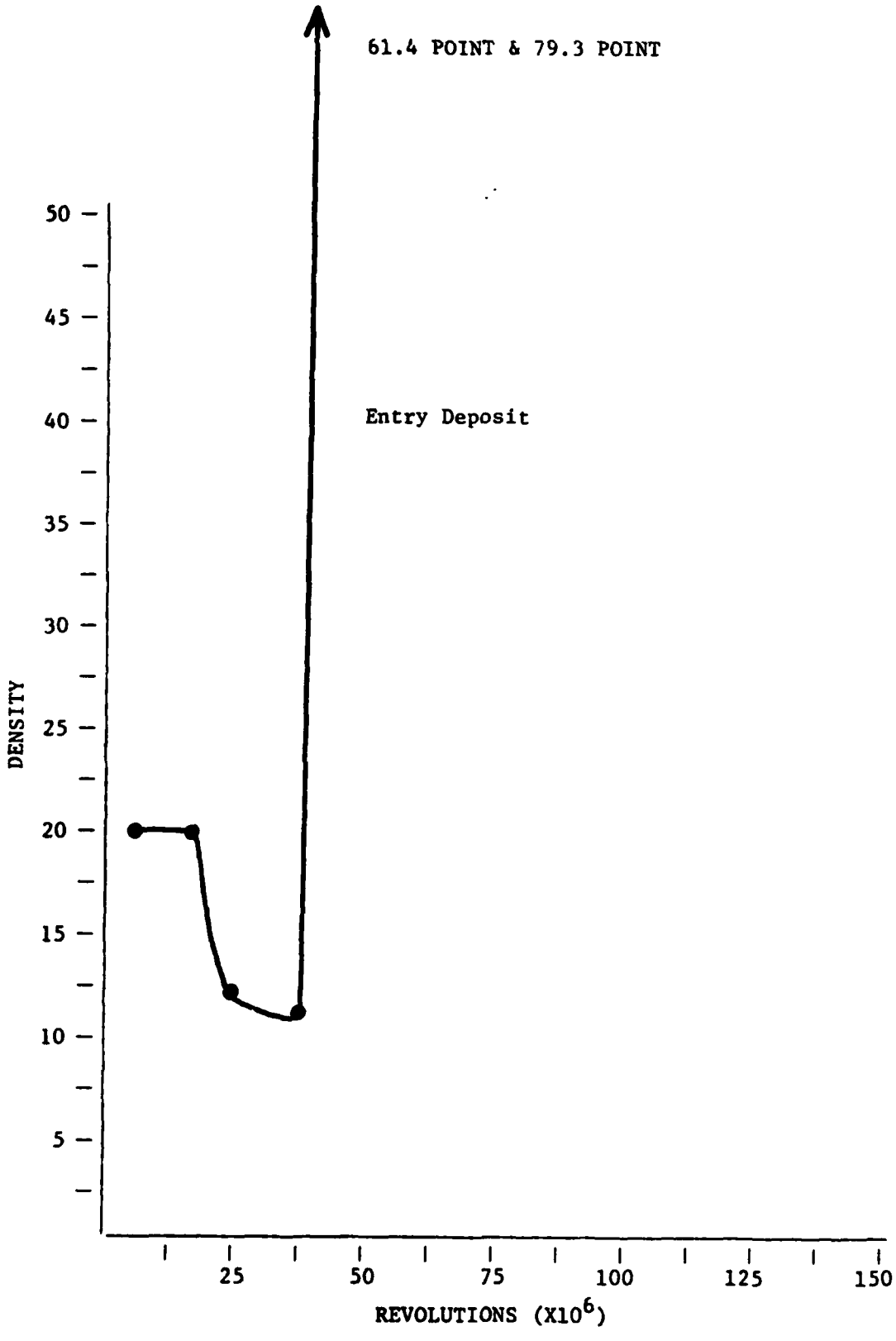
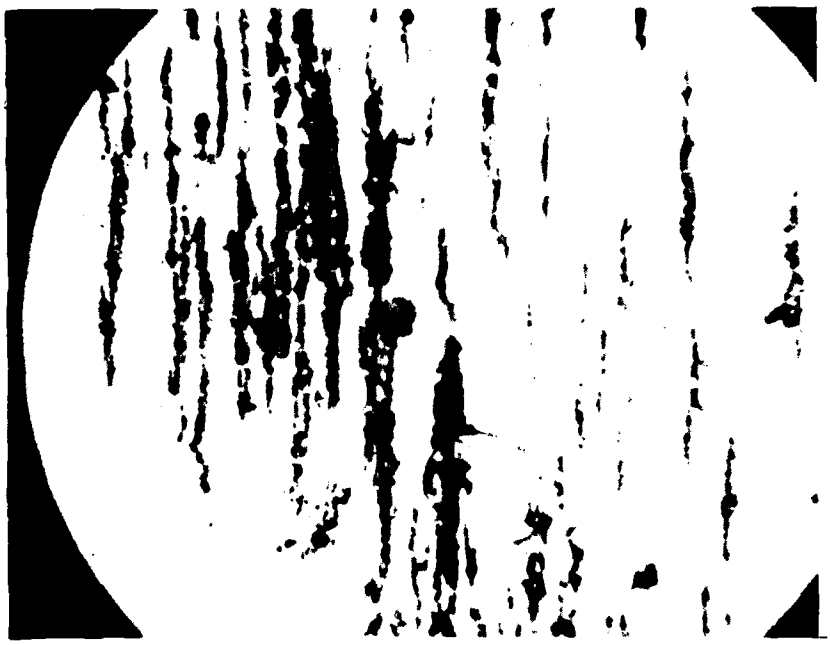
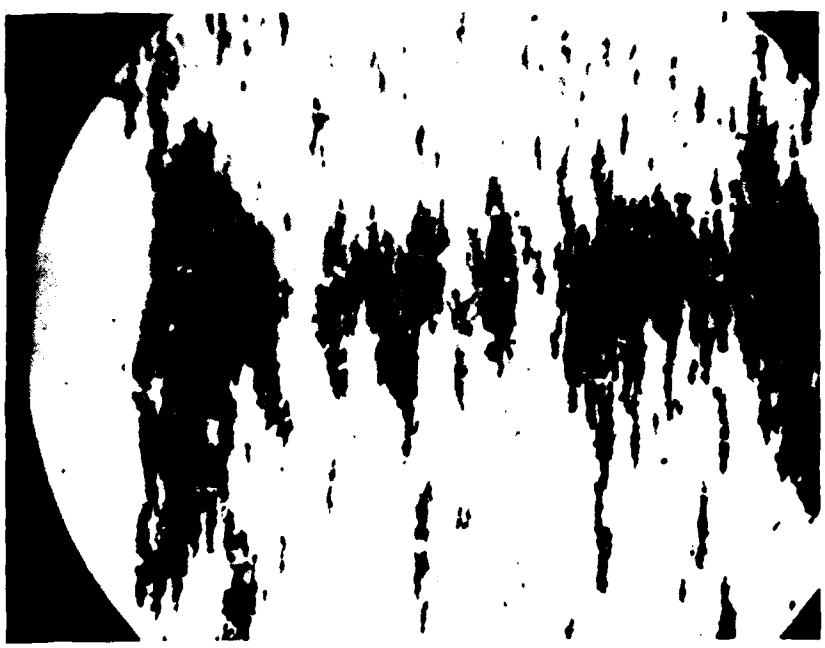


FIGURE 49
ROLLER BEARING TEST SEQUENCE RW
FERROGRAPH DENSITY DATA



A. 4.0 m.r.



B. 11.7 m.r.

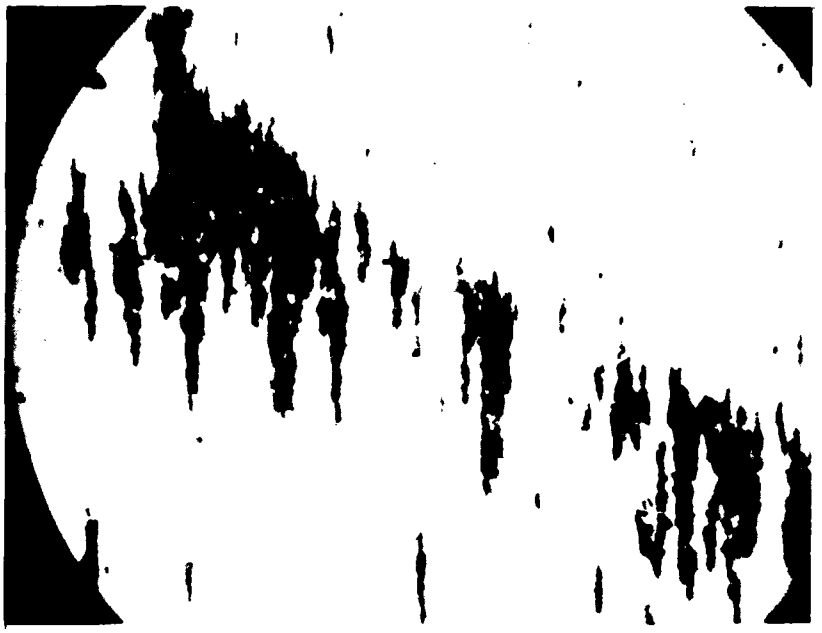
FIGURE 50

ROLLER BEARING TEST SEQUENCE RW

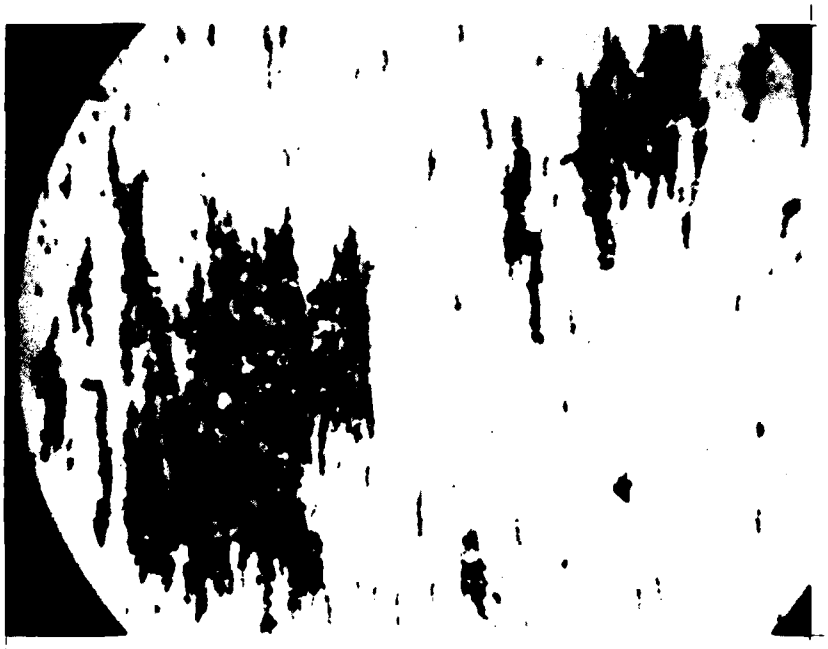
ENTRY DEPOSIT

LOW MAGNIFICATION

(Sheet 1 of 3)



C. 24.5 m.r.



D. 31.3 m.r.

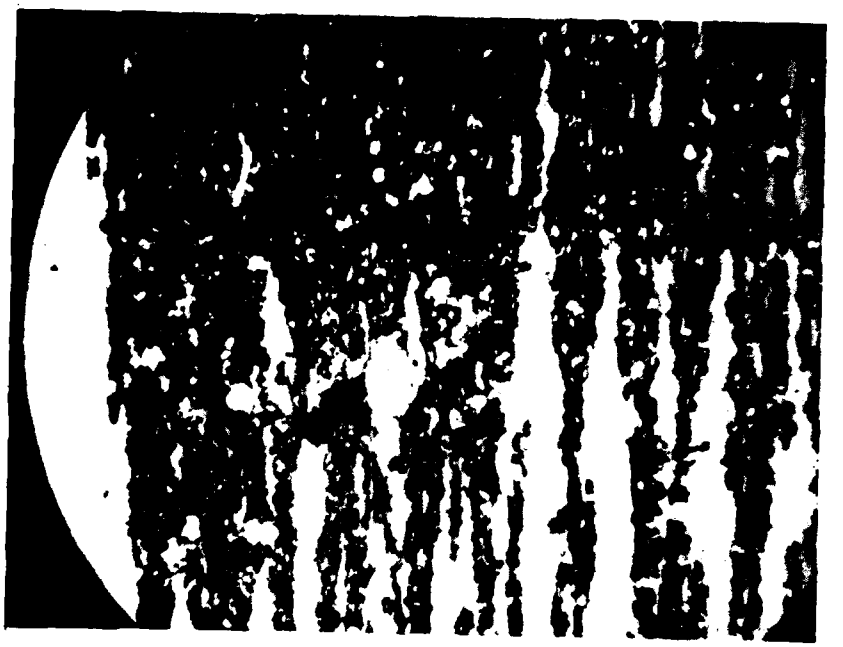
FIGURE 50

ROLLER BEARING TEST SEQUENCE RW

ENTRY DEPOSIT

LOW MAGNIFICATION

(Sheet 2 of 3)



E. 33 m.r.



F. 37 m.r.

FIGURE 50
ROLLER BEARING TEST SEQUENCE RW
ENTRY DEPOSIT
LOW MAGNIFICATION
(Sheet 3 of 3)

TABLE 22. SPECTROMETRIC READING, BEARING RT-106

EVENT	TIME (MIL REVS)	PERCENT TIME	FE (IRON)	SI (SILICON)	SN (TIN)	TI (TITANIUM)	MO (MOLYBDENUM)
1	1.1	1	2	2	10	2	2
3	21.6	21	2	2	10	3	2
4	29.6	29	3	4	11	3	3
5	37.2	36	3	3	12	4	3
6	45.0	44	2	3	12	3	2
7	53.0	51	3	2	12	4	2
8	66.5	65	2	2	12	3	2
9	72.0	70	2	2	11	4	2
10	87.7	85	2	2	12	4	2
11	99.8	97	3	3	14	5	2
12	102.0	100	5	1	11	5	2

TABLE 23. SPECTROMETRIC READING, BEARING RU-107

EVENT	TIME (MIL REVS)	PERCENT TIME	FE (IRON)	SI (SILICON)	SN (TIN)	TI (TITANIUM)	MO (MOLYBDENUM)
1	1.1	1	2	13	12	2	3
2	13.6	16	1	4	10	2	3
3	29.2	36	1	1	9	1	2
4	42.3	52	1	2	10	1	2
5	55.0	67	2	1	12	2	3
6	60.0	74	1	2	10	2	2
7	66.0	81	2	1	11	15	3
8	73.0	90	2	1	5	10	3
9	77.0	95	3	1	10	10	3
10	81.0	100	4	0	10	16	3

TABLE 24. SPECTROMETRIC READING, BEARING RY-115

EVENT	TIME (MIL REVS)	PERCENT TIME	FE (IRON)	SI (SILICON)	SN (TIN)	TI (TITANIUM)	MO (MOLYBDENUM)
1	0.3	0	1	19	11	1	2
2	4.1	7	2	13	10	3	2
3	15.6	27	2	5	12	5	3
4	22.9	40	3	6	14	5	2
5	31.3	54	3	2	13	5	2
6	45.6	79	3	11	12	7	3
7	53.7	93	3	13	1	1	3
8	57.2	100	6	1	13	19	3

TABLE 25. SPECTROMETRIC READING, BEARING RW-109

EVENT	TIME (MIL REVS)	PERCENT TIME	FE (IRON)	SI (SILICON)	SN (TIN)	TI (TITANIUM)	MO (MOLYBDENUM)
1	4.0	10	2	1	9	3	0
2	11.7	31	2	0	9	1	2
3	24.5	66	2	1	9	6	0
4	31.3	84	2	1	9	8	2
5	33.0	89	3	0	8	10	1
6	37.0	100	6	0	9	15	1

variation. These results are typical of spectrometric analysis of roller bearing sequence oil samples. A detailed discussion of this effect is presented in Section VI.

11. Tables 26, 27, 28, and 29 represent particle counting data from sequences RT, RU, RY, and RW. As can be seen, this data is erradic and does not follow the wear debris trends as indicated by the ferrographic analysis. These variations are typical of the roller bearing tests sequences and as in the case of ball bearings, are concluded to be a result of oil pump wear, as explained previously.

12. Although test particle counts are suspect, it can be noted that wear debris concentration levels for these roller bearing test sequences are of the magnitude of 10^6 per 100 ml oil ($> 2\,\mu m$) in a two gallon lubrication system.

(b) Particle Size Distribution

1. The size distribution of wear debris contained in lubricant samples taken during roller bearing testing, as with particle quantity, was primarily monitored by ferrographic analysis techniques as discussed previously. Implemented particle counting technique results were suspect.

2. Figures 51, 52, 53, and 54 present plots of ferrographic density readings at two different locations on the ferrogram for roller bearing test sequences RT, RU, RY, and RW. These locations represent different size ranges of debris as discussed in Section VB. The entry deposit plot represents debris of a relatively large size; $>5\,\mu m$ while the 50 mm deposit plot represents debris of a relatively small size; 2-5 μm. By comparing the relationship of these curves over the bearing life one can assess the trends in debris size distribution.

TABLE 26. PARTICLE COUNTS

SERIES	TIME	% TIME	ADJUSTED COUNTS (COUNTS/100 CC) TOTAL	BEARING NO. RT (SERIES 106) (N X 10^4) 2-5	5-7	7-15	15-25	25+	PERCENT OF TOTAL COUNTS 2-5	5-7	7-15	15-25	25+
1	1.1	1.08	50.2	40.1	4.7	3.2	1.0	1.2	79.88	9.36	6.37	1.99	2.39
3	21.6	21.18	29.5	15.0	3.5	5.7	2.1	3.2	50.85	11.86	19.32	7.12	10.85
4	29.6	29.02	54.5	26.0	9.4	11.0	3.5	4.6	47.71	17.25	20.18	6.42	8.44
5	37.2	36.47	122.6	99.6	10.0	8.3	2.1	2.6	81.24	8.16	6.77	1.71	2.12
6	45.0	44.12	55.4	42.9	4.3	4.9	1.7	1.6	77.44	7.76	8.84	3.07	2.89
8	66.5	65.20	51.0	38.4	5.6	4.6	1.0	1.4	75.29	10.98	9.02	1.96	2.75
9	72.0	70.59	83.1	67.2	7.0	5.2	1.7	2.0	80.87	8.42	6.26	2.05	2.41
10	87.7	85.98	63.9	37.5	8.5	10.6	5.3	2.0	58.69	13.30	16.59	8.29	3.13
11	99.8	97.84	70.0	48.6	7.5	8.3	3.0	2.6	69.43	10.71	11.86	4.29	3.71
12	102.0	100.00	564.2	492.3	46.1	17.4	4.6	3.8	87.26	8.17	3.08	0.82	0.67

TABLE 27. PARTICLE COUNTS

			ADJUSTED COUNTS (COUNTS/100 CC)					PERCENT OF TOTAL COUNTS				
				BEARING NO. RU (SERIES 107) (N X 10^4)									
SERIES	TIME	% TIME	TOTAL	2-5	5-7	7-15	15-25	25+	2-5	5-7	7-15	15-25	25+
1	1.1	1.36	535.9	407.7	67.8	41.5	12.6	6.3	76.08	12.65	7.74	2.35	1.18
2	13.6	16.79	159.3	101.9	25.1	22.0	6.0	4.3	63.97	15.76	13.81	3.77	2.70
3	29.2	36.05	75.5	37.9	14.1	14.3	4.9	4.3	50.20	18.69	18.94	6.49	5.70
4	42.3	52.22	124.9	67.8	22.1	22.2	7.3	5.5	54.28	17.69	17.77	5.84	4.40
5	55.0	67.90	137.7	95.8	16.6	17.6	5.6	2.1	69.57	12.06	12.78	4.07	1.53
6	60.0	74.07	122.7	87.0	16.5	13.0	4.1	2.1	70.90	13.45	10.59	3.34	1.71
7	66.0	81.48	390.1	334.8	29.1	17.7	5.2	3.3	85.82	7.46	4.54	1.33	0.85
8	73.0	90.12	437.3	379.2	33.0	17.1	5.0	3.0	86.71	7.55	3.91	1.14	0.69
9	77.0	95.06	2475.0	2196.0	200.2	60.4	11.8	6.6	88.73	8.09	2.44	0.48	0.27
10	81.0	100.00	2738.2	2508.0	172.2	45.7	7.1	5.2	91.59	6.29	1.67	0.26	0.19

TABLE 28. PARTICLE COUNTS

SERIES	TIME	% TIME	ADJUSTED COUNTS (COUNTS/100 CC) TOTAL	2-5	5-7	7-15	15-25	25+	PERCENT OF TOTAL COUNTS				
			BEARING NO. RY (SERIES 115)						($N \times 10^4$)				
				2-5	5-7	7-15	15-25	25+	2-5	5-7	7-15	15-25	25+
1	0.3	0.52	426.3	391.5	17.8	7.1	4.5	5.4	91.84	4.18	1.67	1.06	1.27
3	15.6	27.27	783.5	718.1	36.6	15.2	4.7	4.9	91.65	4.67	2.45	0.60	0.63
4	22.9	40.03	1182.4	1093.4	66.0	19.9	1.6	1.5	92.47	5.58	1.68	0.14	0.13
6	45.6	79.72	824.3	626.6	80.3	77.6	22.7	17.1	76.02	9.74	9.41	2.75	2.07
7	53.7	93.88	93.1	70.5	8.5	6.2	2.4	5.5	75.73	9.13	6.66	2.58	5.91
8	57.2	100.00	3779.1	3551.6	117.6	67.1	13.2	29.6	93.98	3.11	1.78	0.35	0.78

TABLE 29. PARTICLE COUNTS

			ADJUSTED COUNTS (COUNTS/100 CC)						PERCENT OF TOTAL COUNTS				
				BEARING NO. RW (SERIES 109)					(N X 10^4)				
SERIES	TIME	% TIME	TOTAL	2-5	5-7	7-15	15-25	25+	2-5	5-7	7-15	15-25	25+
2	11.7	31.62	1472.1	1400.0	45.5	21.9	2.7	2.0	95.10	3.09	1.49	0.18	0.14
3	24.5	66.22	1333.4	1239.0	58.1	31.1	4.1	1.1	92.92	4.36	2.33	0.31	0.08
4	31.3	84.59	2704.0	2460.0	161.7	72.0	7.7	2.6	90.98	5.98	2.66	0.28	0.10
5	33.0	89.19	2212.9	2053.7	126.1	28.9	3.1	1.1	92.81	5.70	1.31	0.14	0.05
6	37.0	100.00	5177.4	4436.5	563.0	155.2	17.5	5.2	85.69	10.87	3.00	0.34	0.10

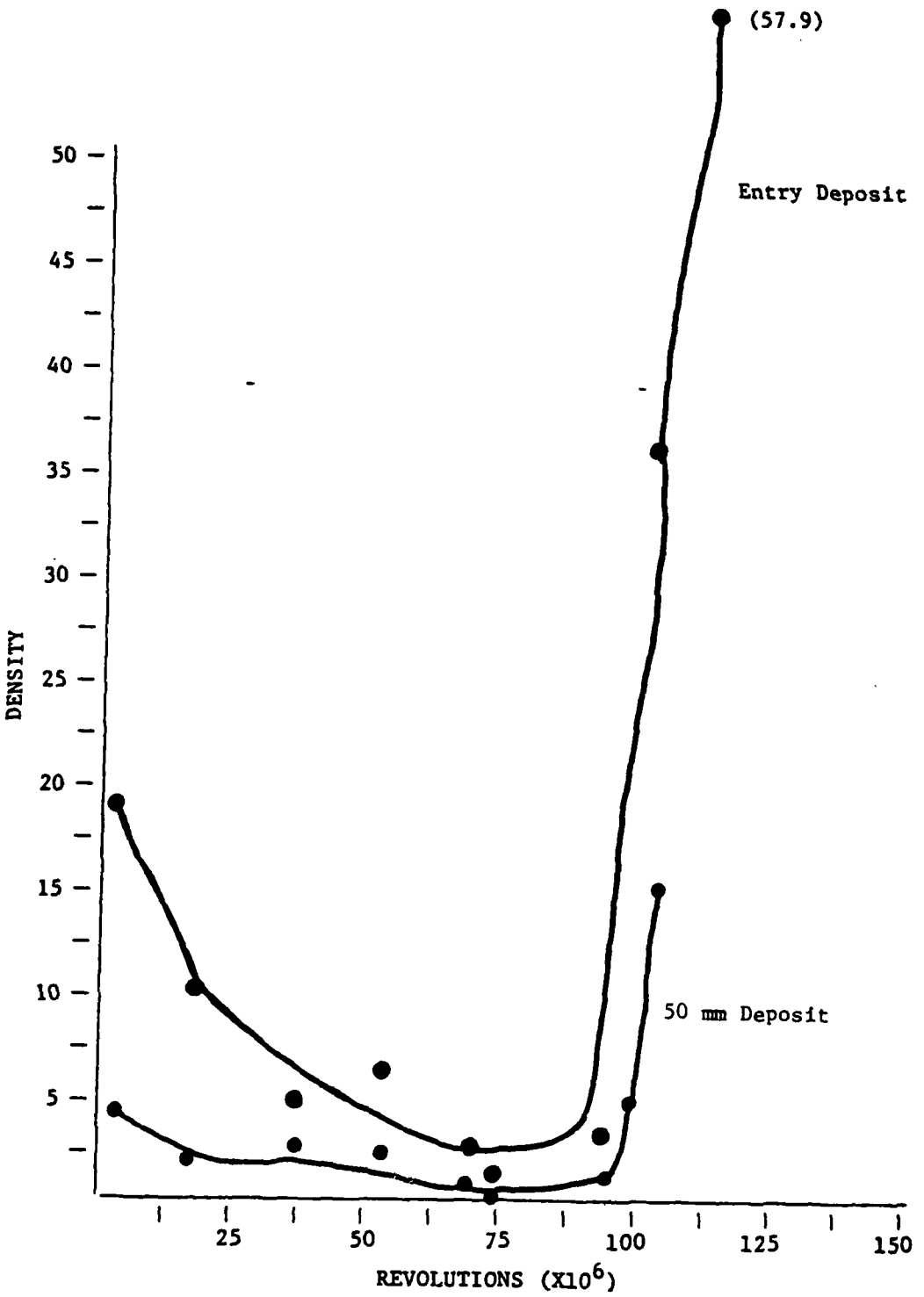


FIGURE 51
ROLLER BEARING TEST SEQUENCE RT
FERROGRAPH DENSITY DATA

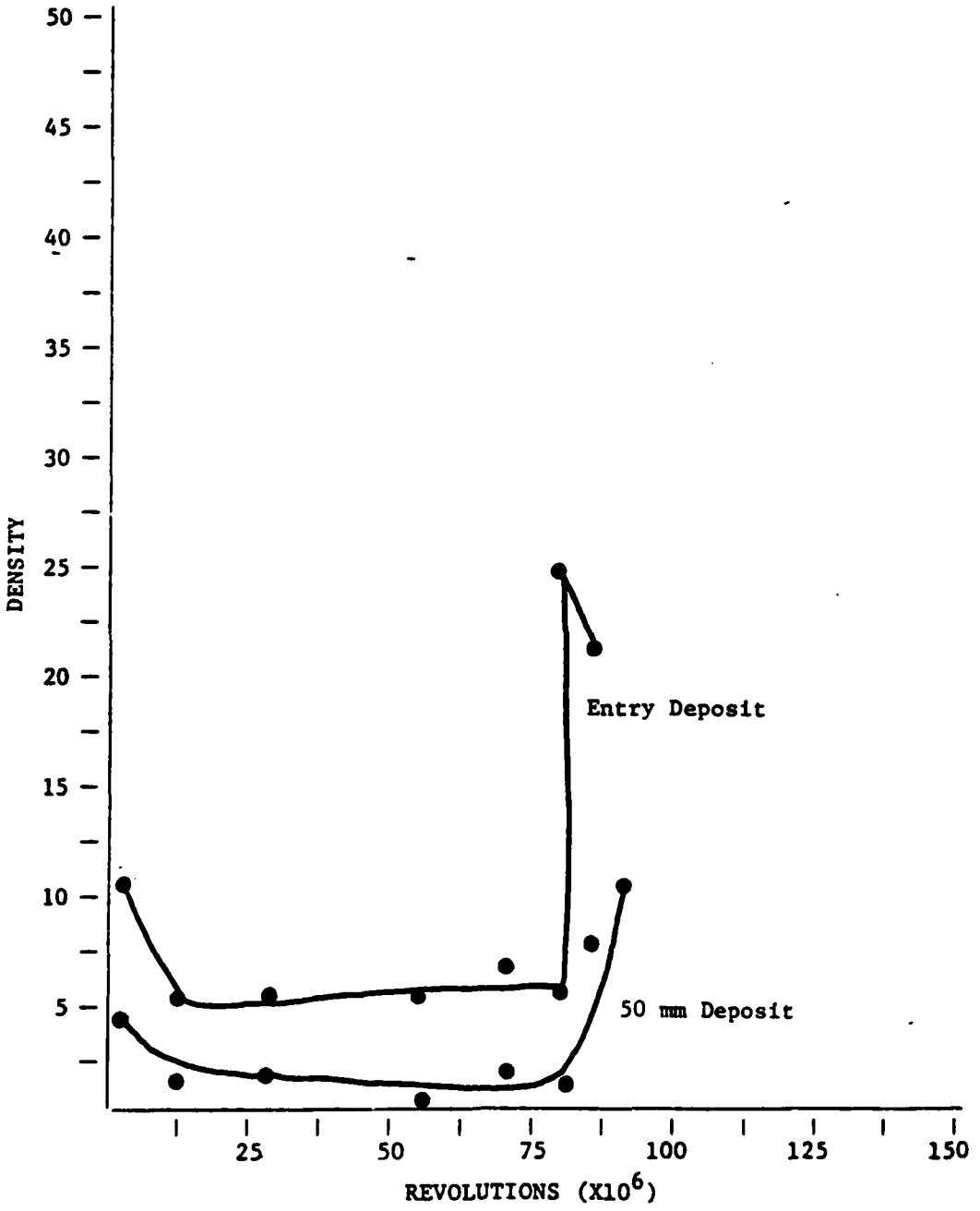


FIGURE 52

ROLLER BEARING TEST SEQUENCE RU

FERROGRAPH DENSITY DATA

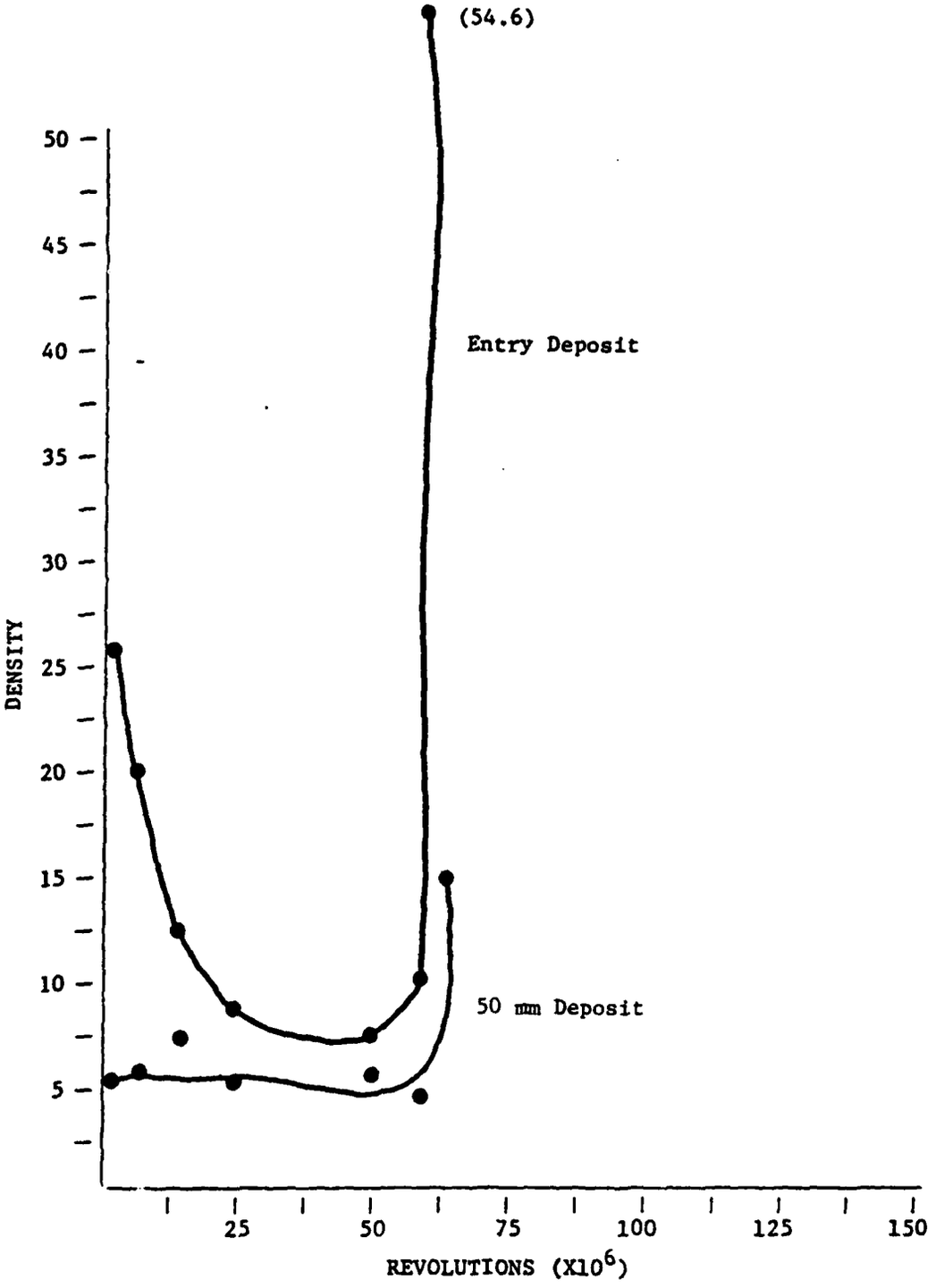


FIGURE 53
ROLLER BEARING TEST SEQUENCE RY
FERROGRAPH DENSITY DATA

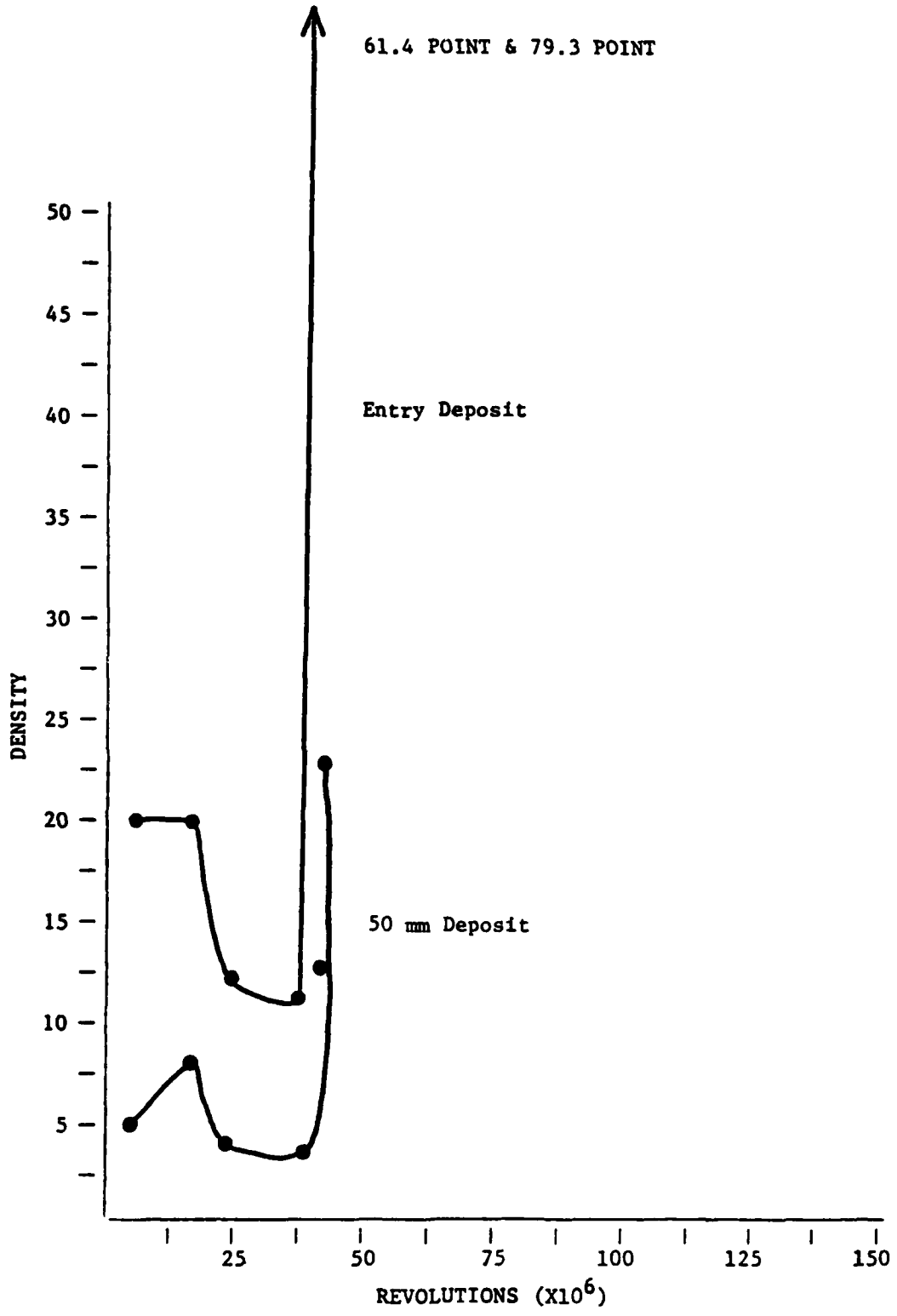


FIGURE 54

ROLLER BEARING TEST SEQUENCE RW

FERROGRAPH DENSITY DATA

3. As can be seen from these plots, there is present a relatively high ratio of large to small debris particles during both the wear-in and abnormal wear regimes as compared to the normal wear regime. This indicates, as in the case of the ball bearings, that a significant portion of the debris generated during wear-in and abnormal wear is greater than 5μm in major dimension. Figures 55, 56, 57, and 58 represent high magnification micrographs of debris deposits for sequences RT, RU, RY, and RW. These micrographs verify that increases in debris concentration during wear-in and abnormal wear can mainly be attributed to the generation of large debris.

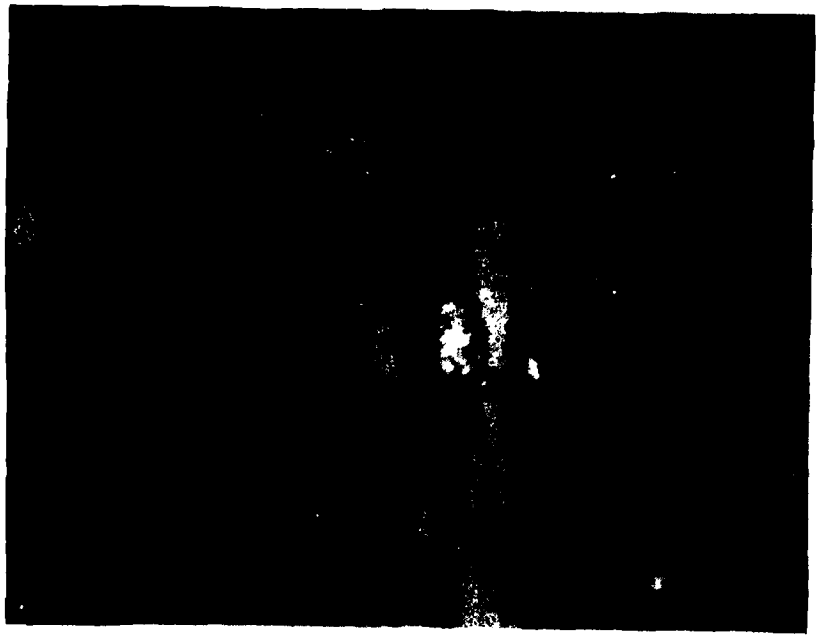
4. It can also be noted that the ratio of large to small particles for the abnormal wear regime is significantly higher than that exhibited by the wear-in regime.

5. In comparing ball bearing and roller bearing debris distributions, the following observations are presented:

a. Normal wear debris size distributions are approximately the same for the two bearing types with roller bearings exhibiting only a slightly higher ratio of large to small particles.

b. Wear-in debris size distributions for the roller bearings indicate a significantly higher ratio of large to small particles as compared to the ball bearing debris distributions. This factor confirms the aforementioned observation that the test roller bearings experience a more severe wear-in process than the test ball bearings under the respective test conditions.

c. Abnormal wear debris size distributions for the roller bearing tests indicate a much higher ratio of large to small debris particles as compared to the ball bearing debris distributions. This factor confirms the aforementioned observation that the test roller bearings generate greater quantities of large debris particles during the abnormal wear regime than do the ball bearings.

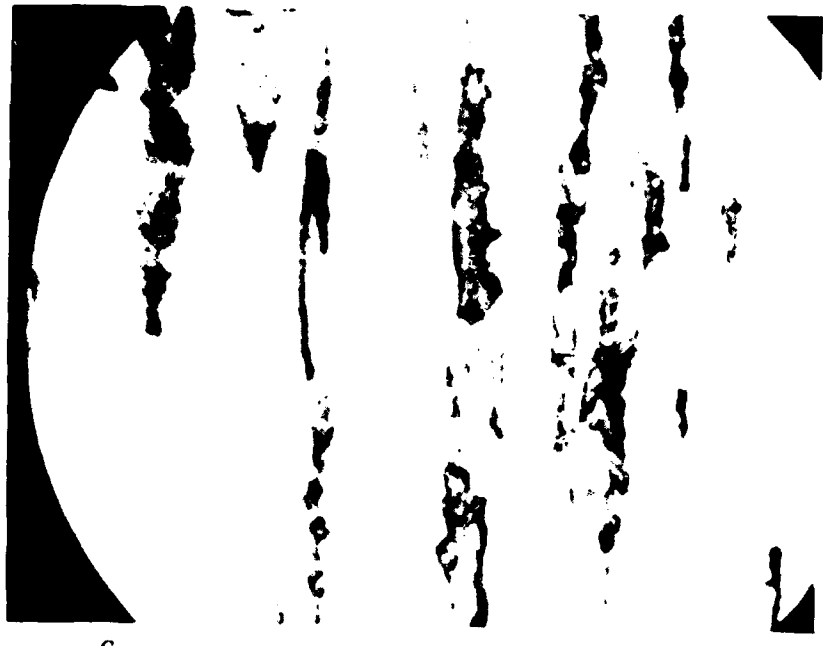


A. 1.1 m.r.

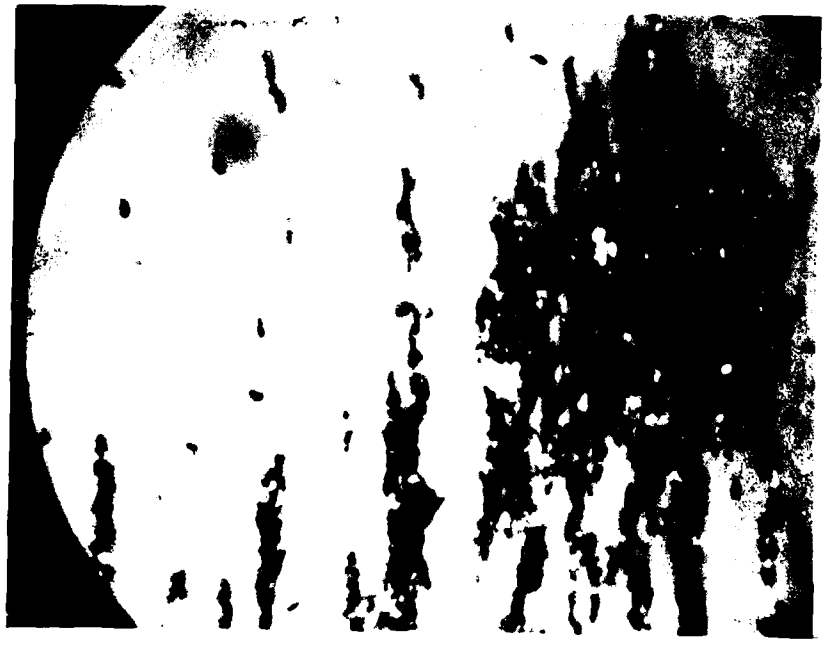


B. 21.6 m.r.

FIGURE 55
ROLLER BEARING TEST SEQUENCE RT
ENTRY DEPOSIT
HIGH MAGNIFICATION
(Sheet 1 of 5)



C. 37.2 m.r.



D. 53 m.r.

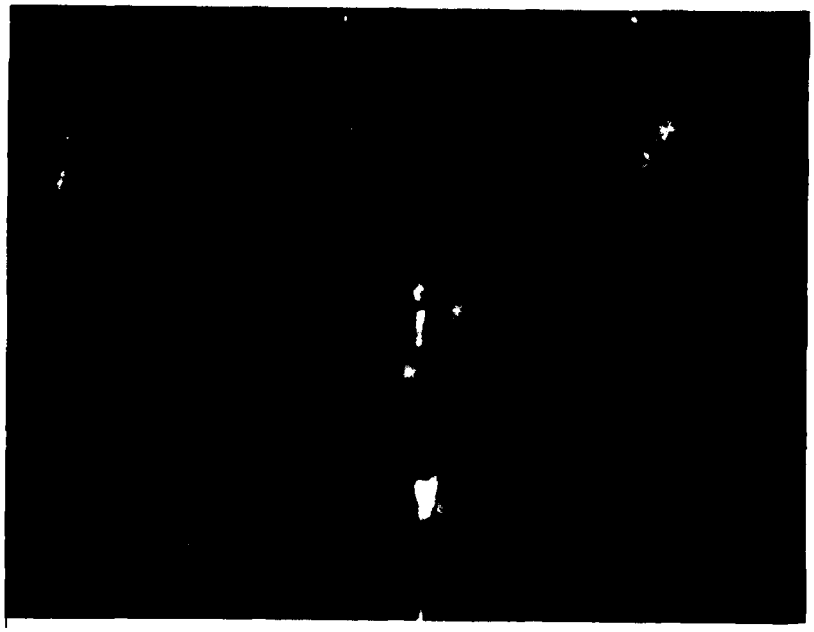
FIGURE 53

ROLLER BEARING TEST SEQUENCE RT

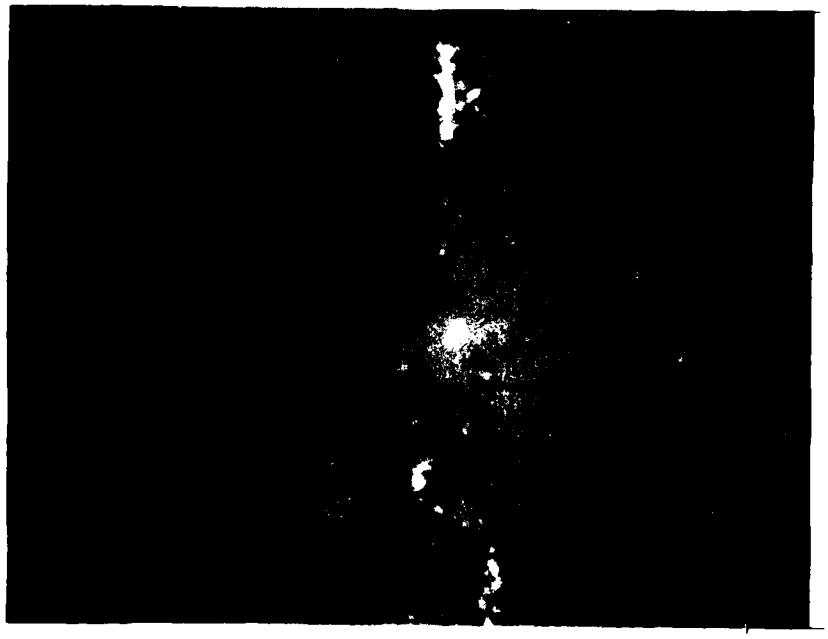
ENTRY DEPOSIT

HIGH MAGNIFICATION

(Sheet 2 of 5)



E. 66.5 m.r.



F. 72 m.r.

FIGURE 55
ROLLER BEARING TEST SEQUENCE RT
ENTRY DEPOSIT
HIGH MAGNIFICATION
(Sheet 3 of 5)

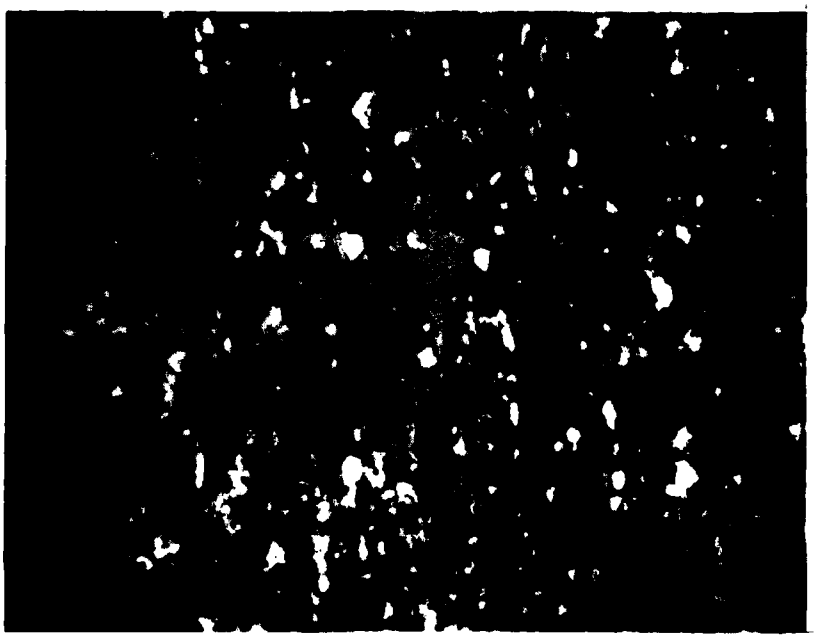


G. 87.7 m.r.



H. 99.8 m.r.

FIGURE 55
ROLLER BEARING TEST SEQUENCE RT
ENTRY DEPOSIT
HIGH MAGNIFICATION
(Sheet 4 of 5)



I. 102 m.r.

FIGURE 55

ROLLER BEARING TEST SEQUENCE RT

ENTRY DEPOSIT

HIGH MAGNIFICATION

(Sheet 5 of 5)



A. 1.1 m.r.



B. 13.6 m.r.

ROLLER BEARING TEST SEQUENCE RU

ENTRY DEPOSIT

HIGH MAG [illegible] CATION

(Sheet [illegible])



C. 29.2 m.r.



D. 55 m.r.

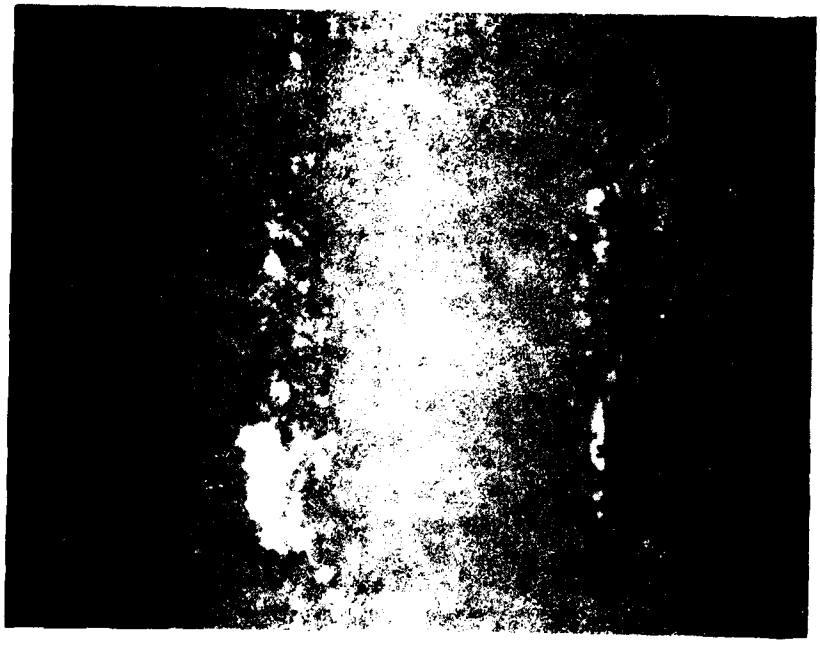
FIGURE 56

ROLLER BEARING TEST SEQUENCE RU

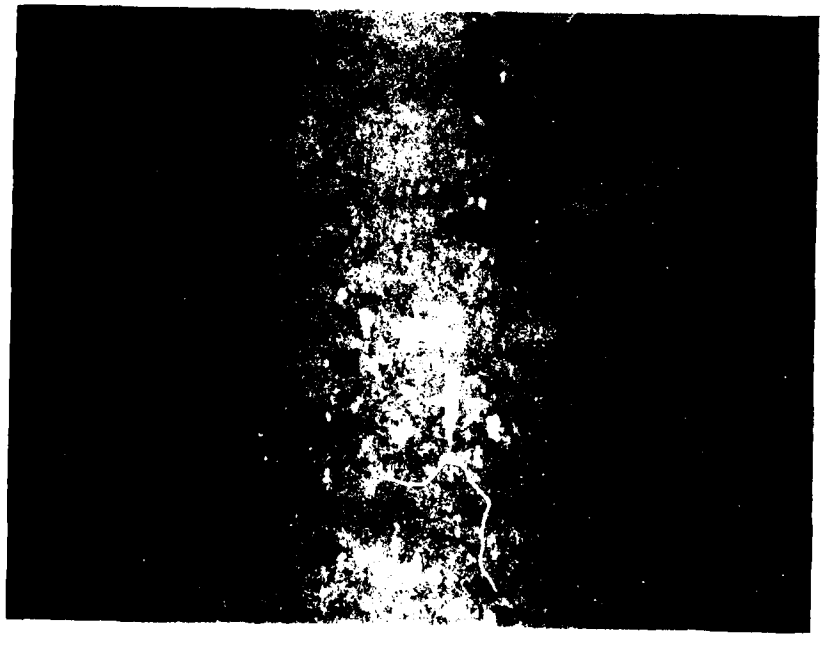
ENTRY [illegible]

HIGH MACH [illegible]

(Sheet [illegible])



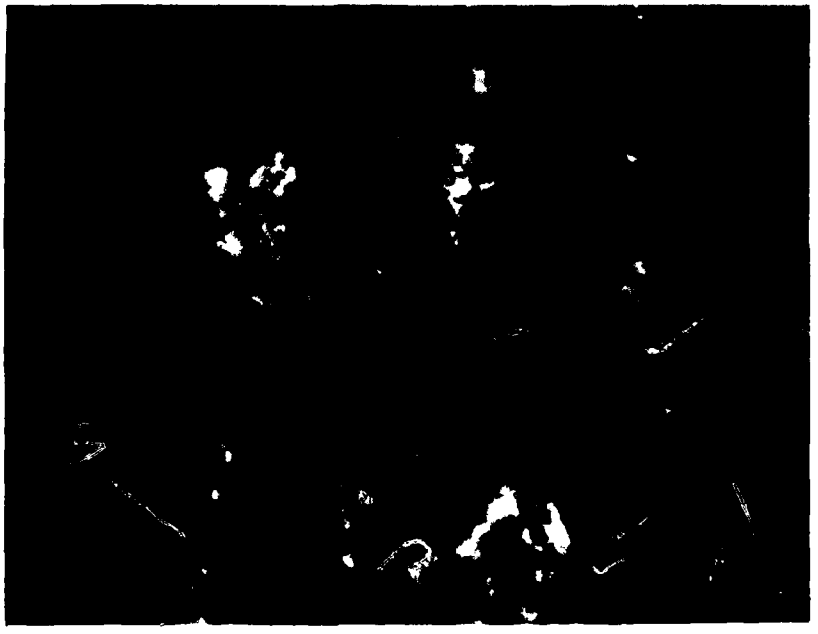
E. 66 m.r.



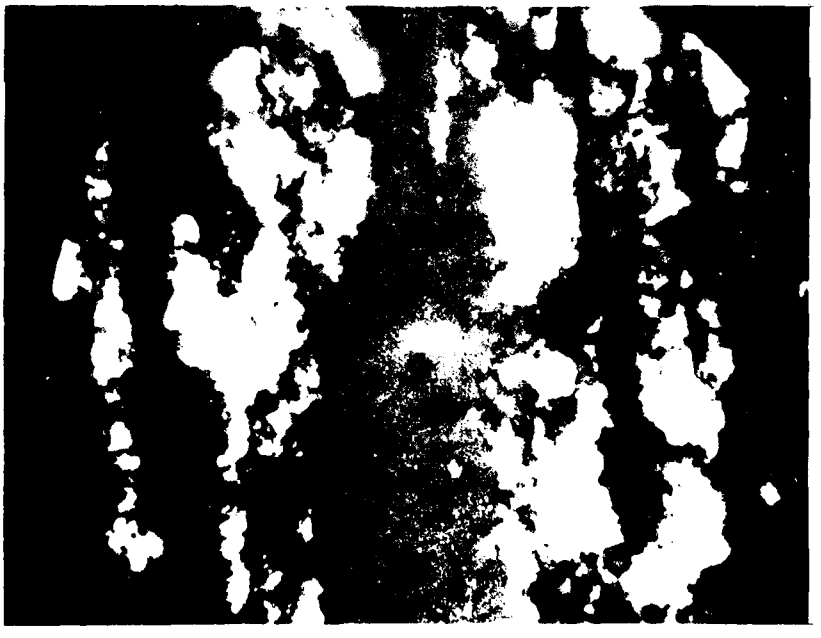
F. 3 m.r.

ROLLER [illegible] OPTICAL RD

[illegible]



G. 77 m.r.

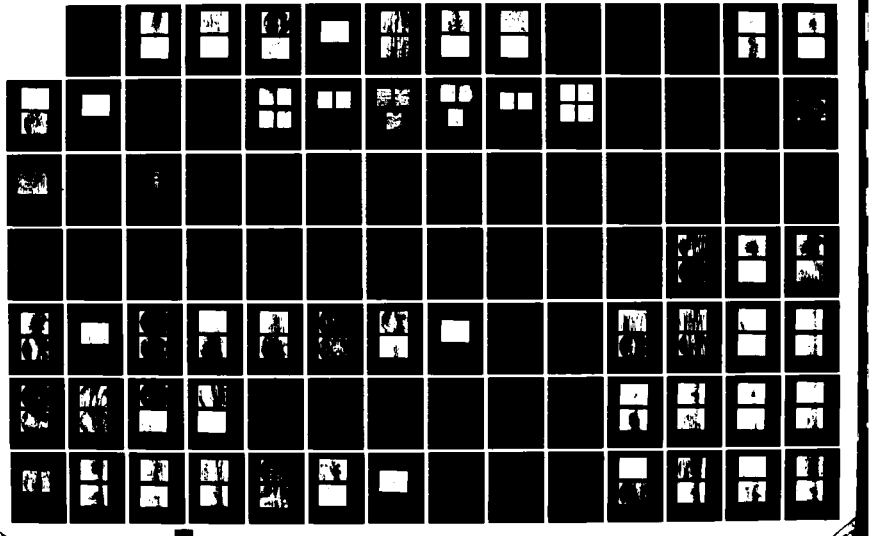


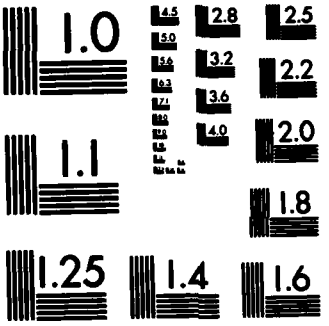
H. 81 m.r.

FIGURE 56
ROLLER BEARING TEST SEQUENCE RU
ENTRY DEPOSIT
HIGH MAGNIFICATION
(Sheet 4 of 4)

AD-A122 156 OIL ANALYSIS(U) NAVAL AIR ENGINEERING CENTER LAKEHURST 3/6
NJ SUPPORT EQUIPMENT ENGINEERING DEPT P B SENHOLZI
23 AUG 82 NAEC-92-153

UNCLASSIFIED F/G 11/8 NL





MICROCOPY RESOLUTION TEST CHART
NATIONAL BUREAU OF STANDARDS-1963-A



A. 0.3 m.r.



B. 4.1 m.r.

FIGURE 57

ROLLER BEARING TEST SEQUENCE RY

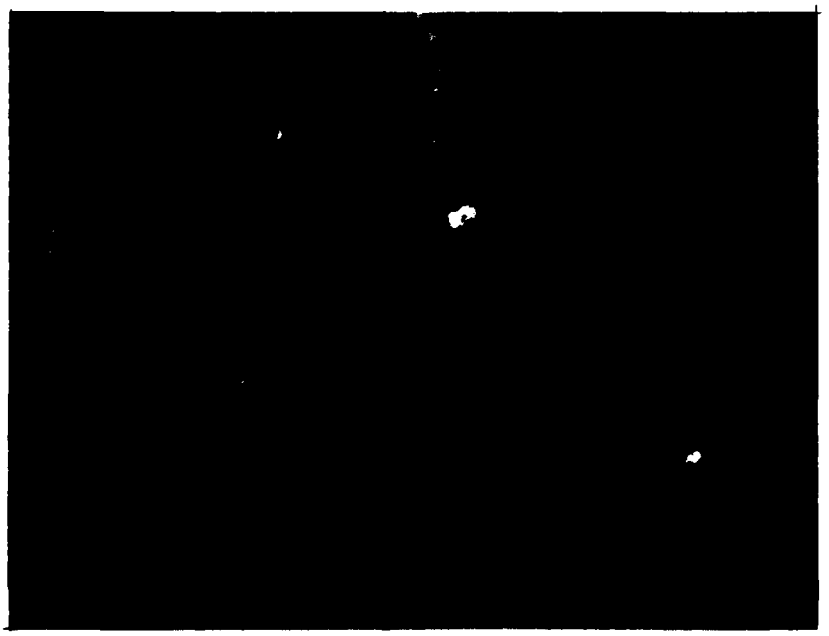
ENTRY DEPOSIT

HIGH MAGNIFICATION

(Sheet 1 of 4)

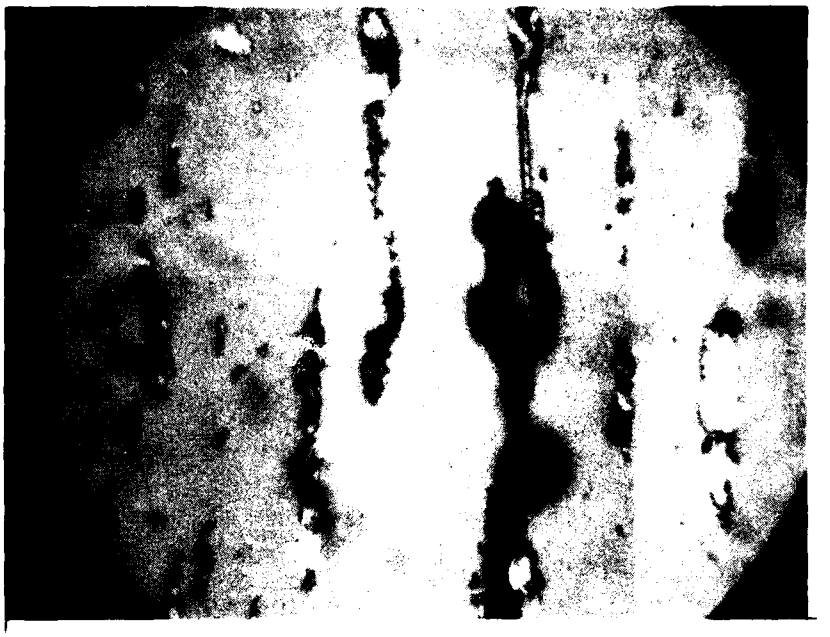


C. 15.6 m.r.



D. 22.9 m.r.

FIGURE 57
ROLLER BEARING TEST SEQUENCE RY
ENTRY DEPOSIT
HIGH MAGNIFICATION
(Sheet 2 of 4)



E. 45.6 m.r.



F. 53.7 m.r.

FIGURE 57

ROLLER BEARING TEST SEQUENCE RY

ENTRY DEPOSIT

HIGH MAGNIFICATION

(Sheet 3 of 4)



G. 57.2 m.r.

FIGURE 57
ROLLER BEARING TEST SEQUENCE RY
ENTRY DEPOSIT
HIGH MAGNIFICATION
(Sheet 4 of 4)



A. 4.0 m.r.



B. 11.7 m.r.

FIGURE 58

ROLLER BEARING TEST SEQUENCE RW

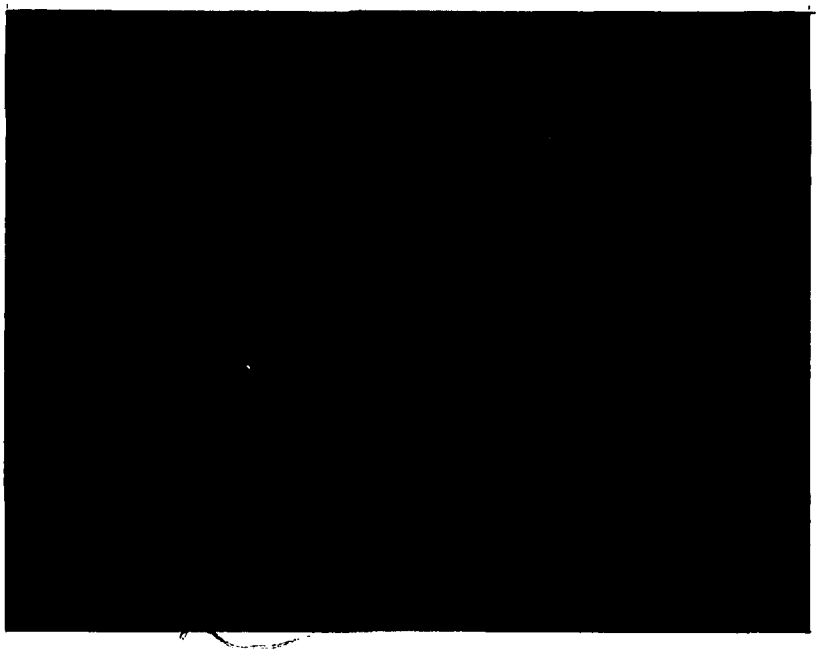
ENTRY DEPOSIT

HIGH MAGNIFICATION

(Sheet 1 of 3)



C. 24.5 m.r.



D. 31.3 m.r.

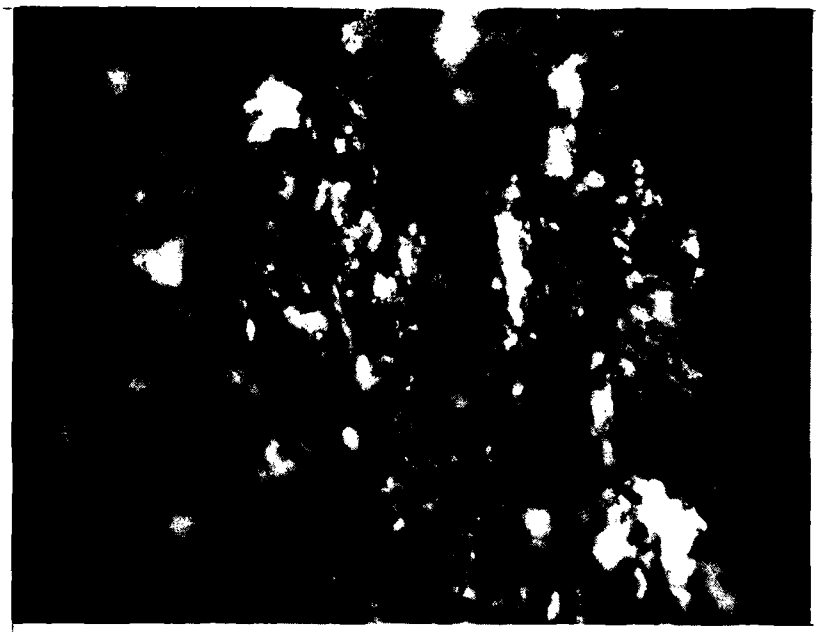
FIGURE 58

ROLLER BEARING TEST SEQUENCE RW

ENTRY DEPOSIT

HIGH MAGNIFICATION

(Sheet 2 of 3)



E. 33 m.r.



F. 37 m.r.

FIGURE 58
ROLLER BEARING TEST SEQUENCE RW
ENTRY DEPOSIT
HIGH MAGNIFICATION
(Sheet 3 of 3)

6. Figure 59 represents a generalized plot of roller bearing and ball bearing debris size distributions for the three wear regimes.

7. Figure 60 represents dual density plots for sequence RA. Figure 61 provides high magnification micrographs of the respective test sequence ferrographic deposits. It can be observed from this sequence that after the wear-in regime the ratio of large to small debris particles remained constant through the test sequence. Since this bearing did not experience a failure and was stopped as a result of time constraints, the constant ratio of large to small debris and thus particle size distribution is expected.

8. The above discussed particle size distribution observations were valid for all the roller bearing test sequences.

(c) Particle Composition

1. Roller bearing testing was designed in such a way as to have each test component operating in an independent lubrication system, as in the case of ball bearings. This design was implemented in order to limit lubricant borne debris to that being produced by the component and thus simplify the wear debris analysis process. As a result, debris composition should not play an important role in this correlation effort since all debris should be the same material as the parent component.

2. However, debris contamination problems were experienced during roller bearing testing as the case with ball bearings. A discussion of this contamination problem is presented under the ball bearing section.

(d) Particle Morphology

1. The last factor to be considered under roller bearing wear particle analysis is morphology or shape. Morphological analysis for roller bearings is very similar to that analysis presented previously for ball

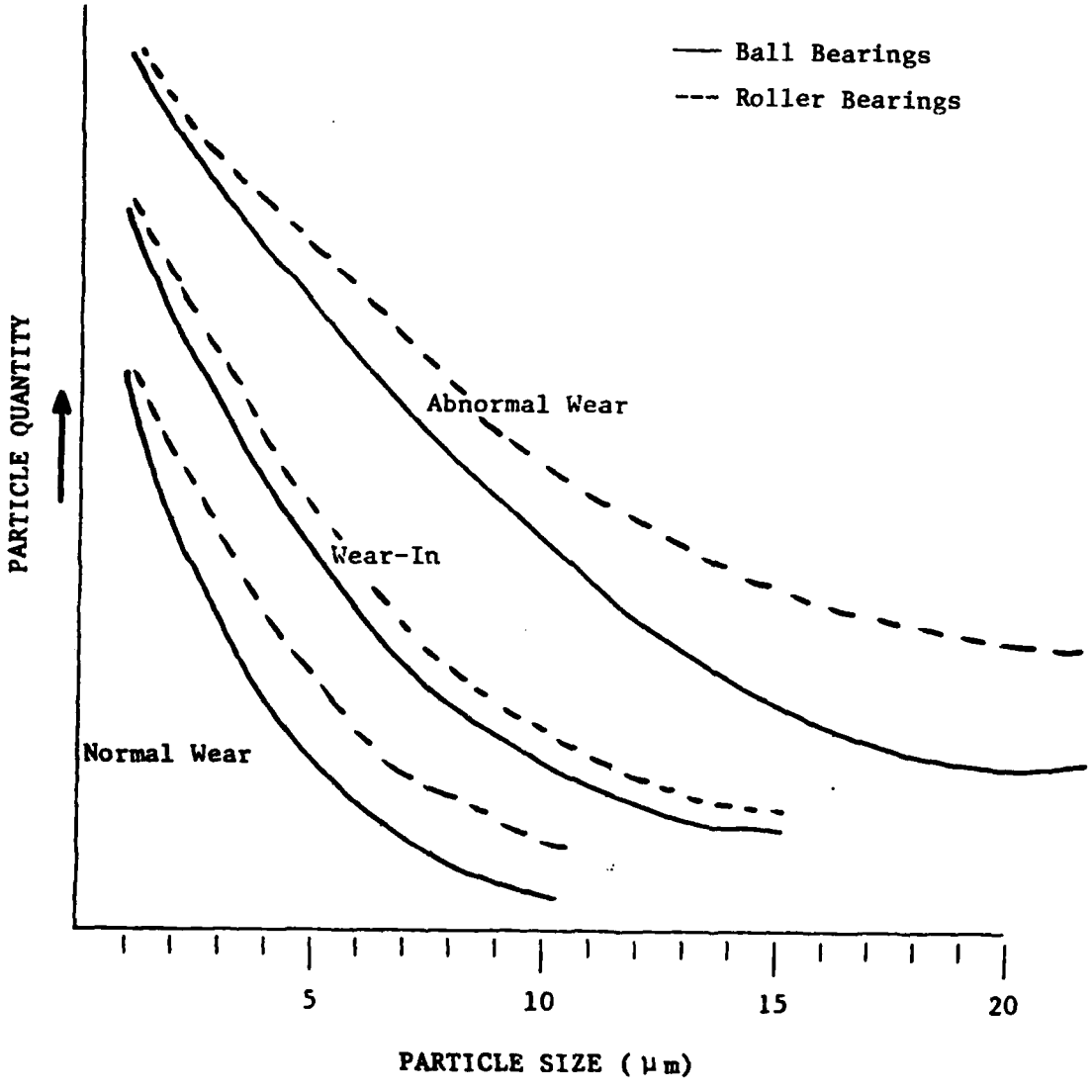


FIGURE 59
GENERALIZED BEARING
PARTICLE SIZE DISTRIBUTION VERSUS WEAR REGIME

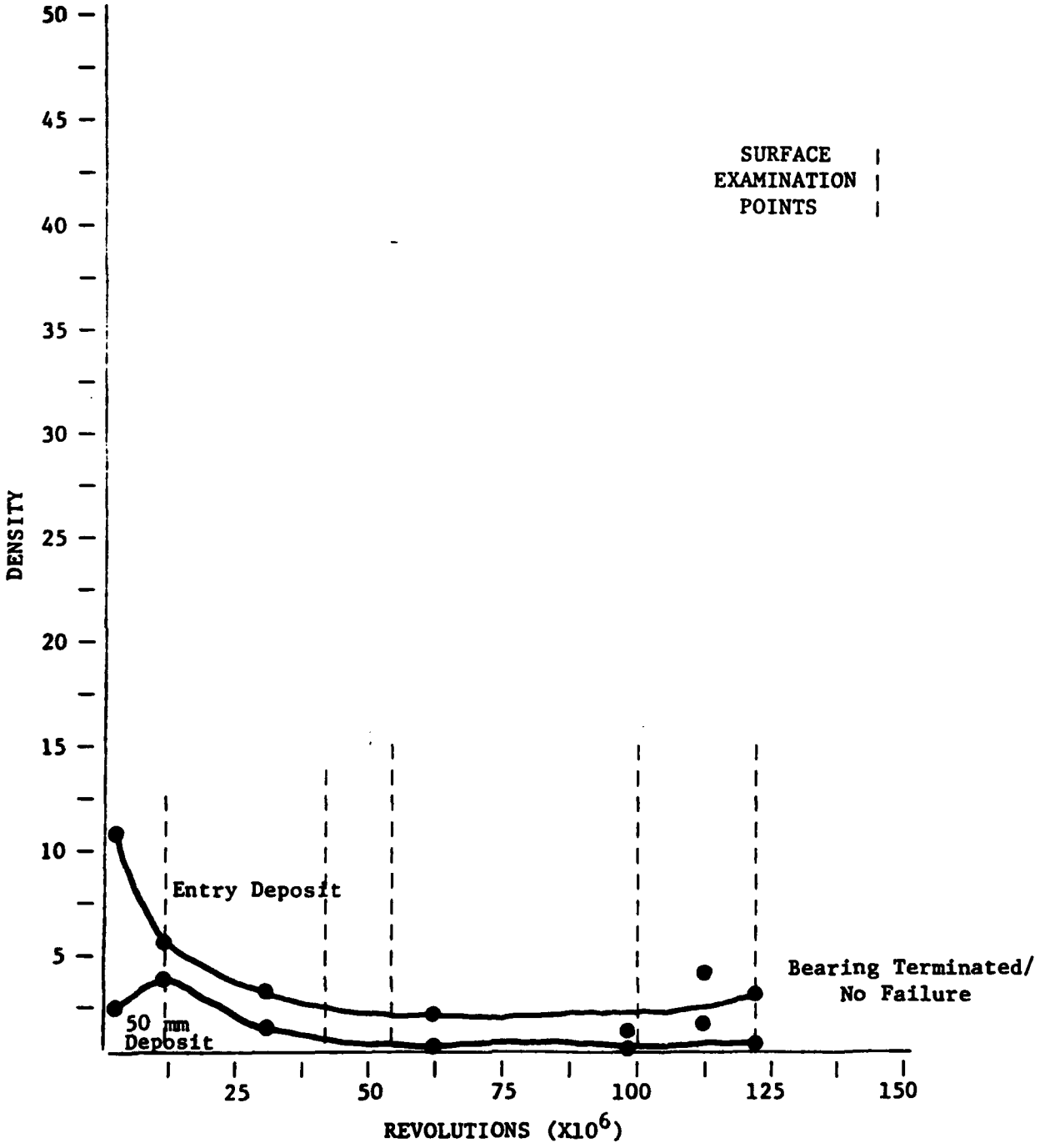
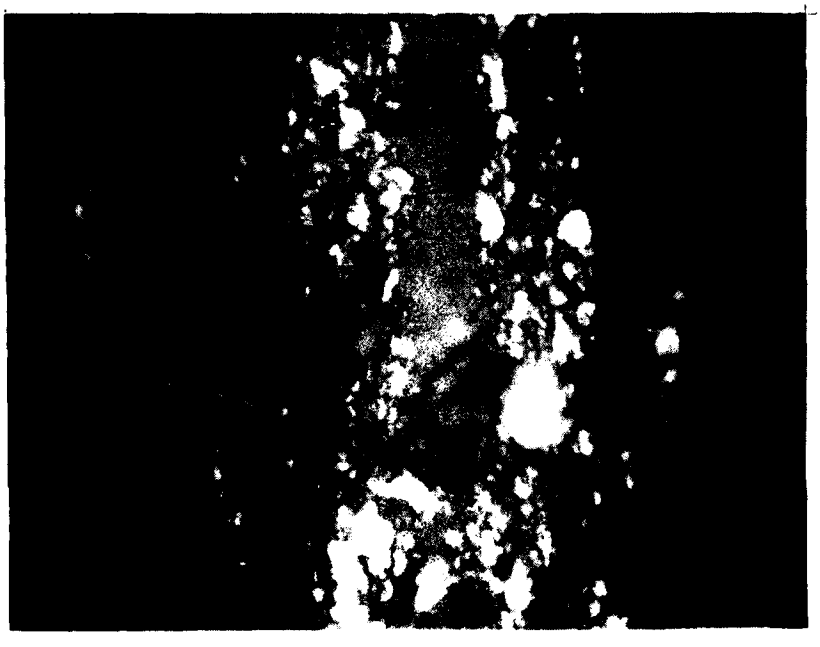


FIGURE 60
ROLLER BEARING TEST SEQUENCE RA
FERROGRAPH DENSITY DATA



A. 0.18 m.r.



B. 9.2 m.r.

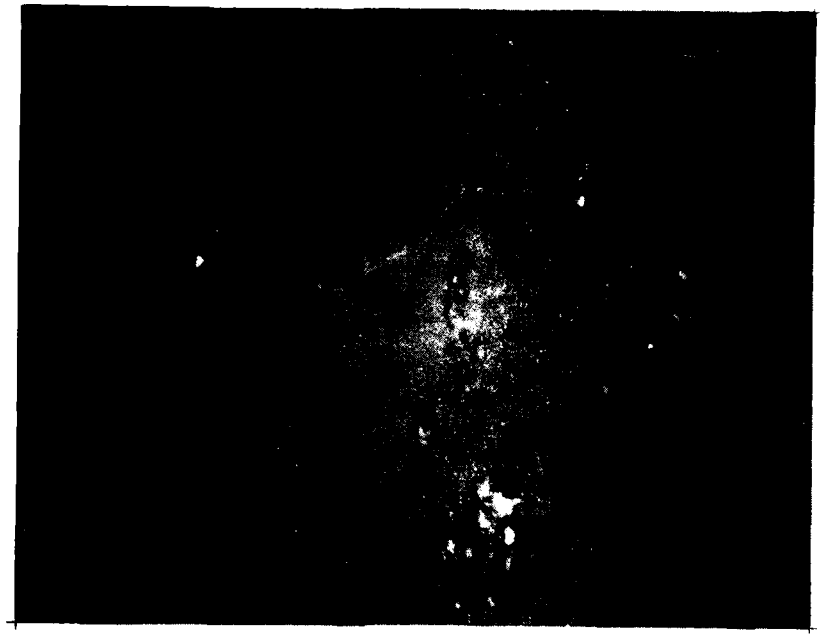
FIGURE 61

ROLLER BEARING TEST SEQUENCE RA

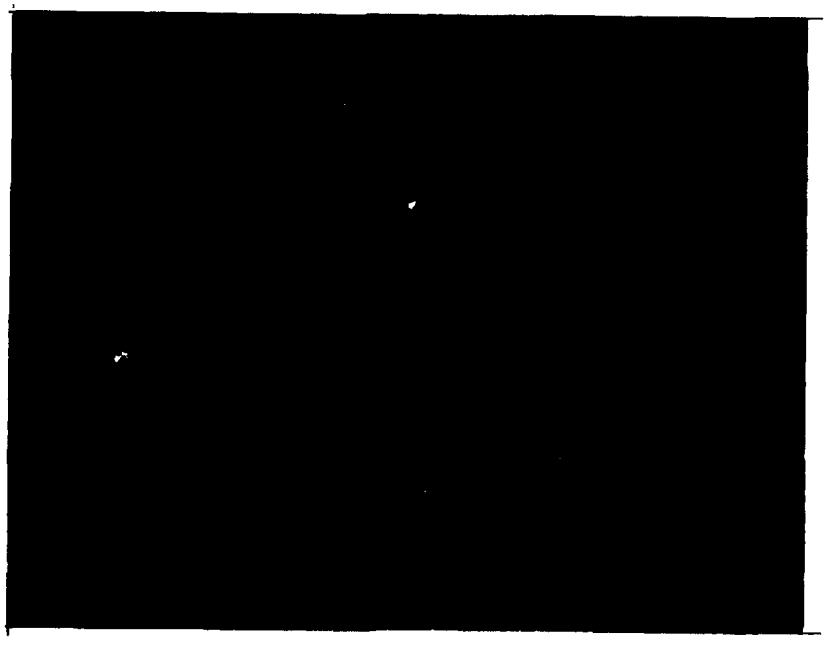
ENTRY DEPOSIT

HIGH MAGNIFICATION

(Sheet 1 of 4)

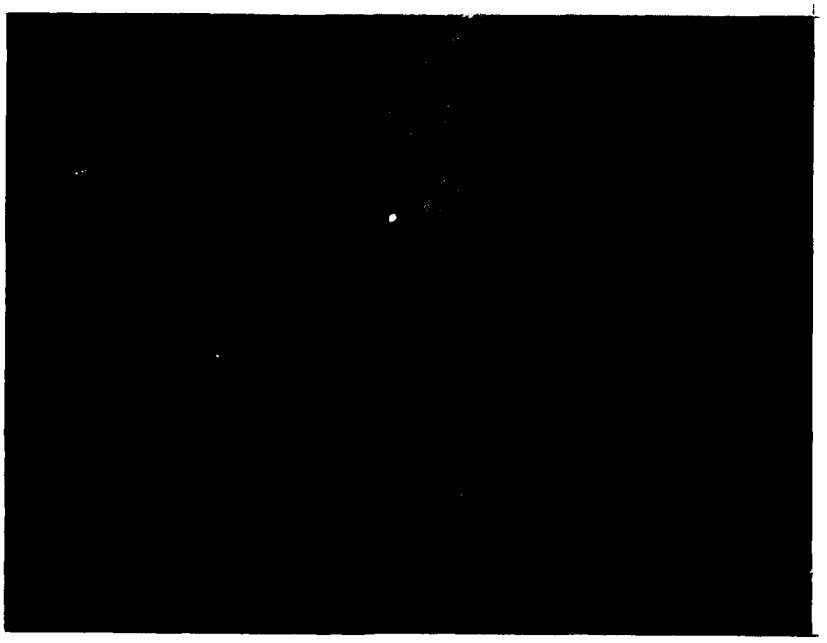


C. 28.8 m.r.



D. 62 m.r.

FIGURE 61
ROLLER BEARING TEST SEQUENCE RA
ENTRY DEPOSIT
HIGH MAGNIFICATION
(Sheet 2 of 4)

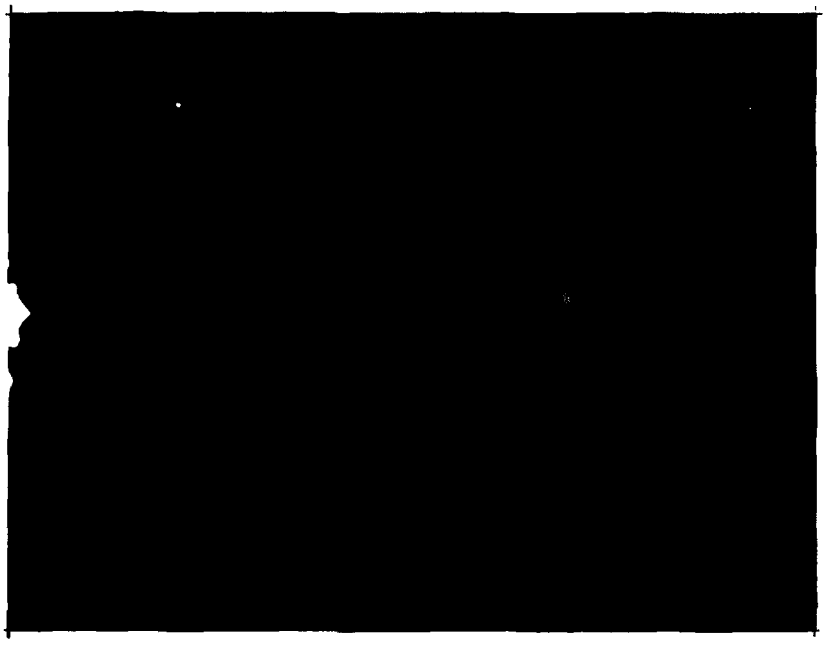


E. 98.2 m.r.



F. 105.4 m.r.

FIGURE 61
ROLLER BEARING TEST SEQUENCE RA
ENTRY DEPOSIT
HIGH MAGNIFICATION
(Sheet 3 of 4)



G. 117.8 m.r.

FIGURE 61
ROLLER BEARING TEST SEQUENCE RA
ENTRY DEPOSIT
HIGH MAGNIFICATION
(Sheet 4 of 4)

bearings. Analysis similarities will be presented under this discussion, however, pertinent ball bearing sections will be referenced for detailed treatments.

2. Roller bearing wear-in debris particle morphology profile is very similar to the debris profile generated during the wear-in of ball bearings. The description of ball bearing wear-in debris morphology, previously presented, is thus applicable to roller bearing wear-in particulates. Roller bearing wear-in particles are highlighted in the initial micrographs of test sequences RT, RU, RY, and RA presented in Figures 55, 56, 57, and 60 respectively.

3. Roller bearing normal wear particulates are dominated by free metal platelets. These platelets consist of rubbing wear, laminar particles, and spiral shaped particles. The presence of both rubbing wear and laminar particles is identical to that observed in the ball bearing test sequences. As a result the discussion of these particle types previously presented is applicable to roller bearing particle morphology.

4. Spiral particles appear to be characteristic of roller bearings and are not observed under normal conditions in ball bearing testing. These particles are small ($\lesssim 5\ \mu m$) and are likely to be produced by roller end-flange contact. The appearance of these particle is very similar to cutting particles produced in an abrasive wear regime or a normal grinding process. Figure 62 presents a micrograph of roller bearing spiral debris as well as grinding process debris particles. Figure 63 and 64 presents a series of micrographs depicting cutting wear debris generated as a result of one surface penetrating another. The effect is the generation of particles much as a lathe tool creates machining swarf; except on a microscopic scale. This effect can be caused by such situations as component misalignment or the presence of abrasive contaminants.



4517 5000X

A. TAPERED ROLLER BEARING



3982 250X

B. BEARING GRINDING OPERATION IN MANUFACTURING

FIGURE 62

SIMILARITY OF APPEARANCE OF CUTTING WEAR PARTICLES

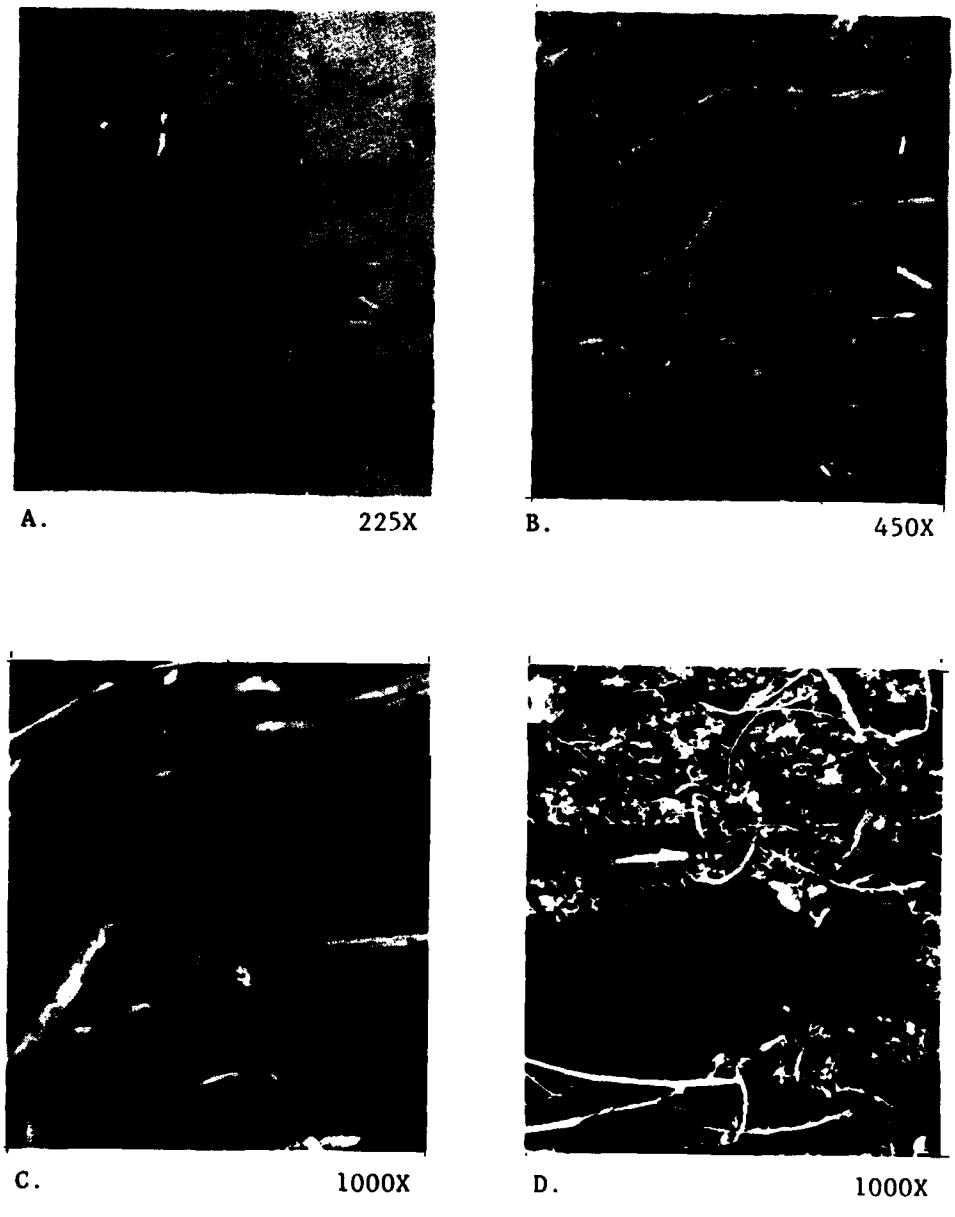


FIGURE 63

ABRASIVE WEAR PARTICLES

(Sheet 1 of 3)



E. 225X



F. SEM 225X

FIGURE 63
ABRASIVE WEAR PARTICLES
(Sheet 2 of 3)



G. SEM 225X



H. SEM 225X



I. SEM 1000X

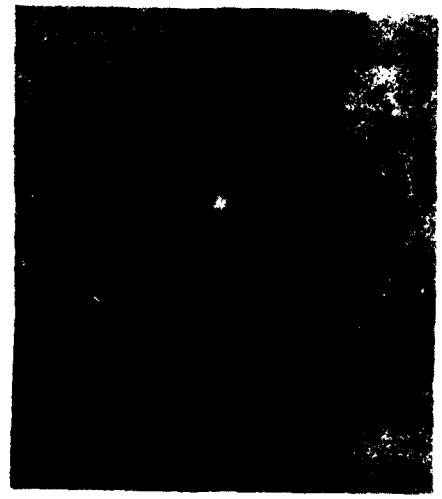
FIG 2

ABRASIVE [illegible] PARTICLES

(Sheet [illegible])



A. 1000X

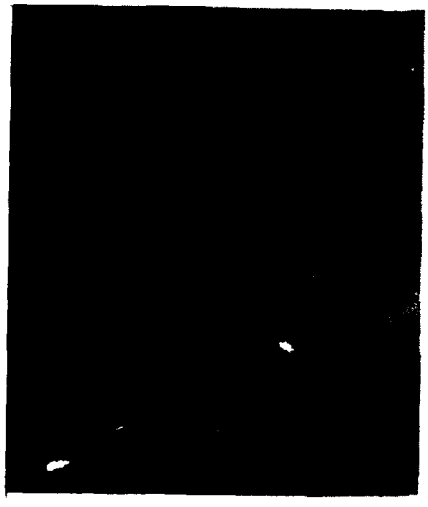


B. 1000X



C. SEM 1000X

FIGURE 64
ABRASIVE WEAR PARTICLES
(Sheet 1 of 3)



D. 450X

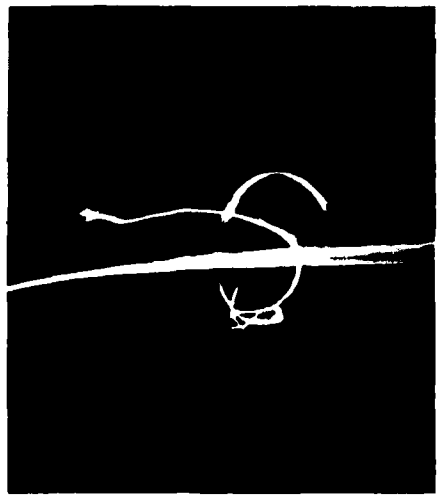


E. SEM 450X

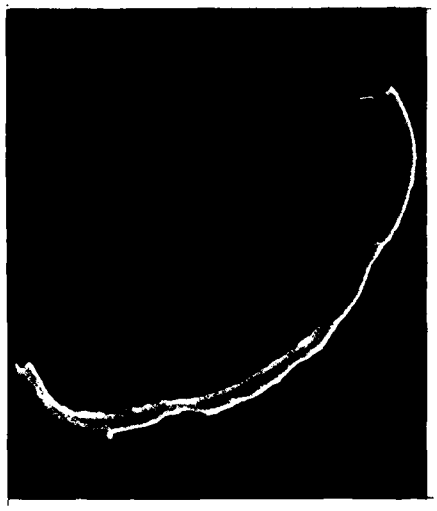
FIGURE 64
ABRASIVE WEAR PARTICLES
(Sheet 2 of 3)



F. SEM 1000X



G. SEM 1000X



H. SEM 1000X



I. SEM 100X

FIGURE 64

ABRASIVE WEAR PARTICLES

(Sheet 3 of 3)

5. As in ball bearing testing, the predominant abnormal wear mode occurring during roller bearing testing was surface fatigue. Three distinct particles have been associated with rolling contact fatigue; laminar particles, spherical particles, and fatigue spall particles. These particle types are the same for both ball and roller bearing test sequences. As a result the discussion previously presented under the ball bearing section is applicable to roller bearings. Roller bearing abnormal wear debris particles are highlighted in the later micrographs of test sequences RT, RU, RY, and RA presented in Figures 55, 56, 57, and 61 respectively.

6. In comparing ball bearing and roller bearing debris morphology the following observations are presented:

a. Wear-in debris particle types are similar for both ball bearing and roller bearing test sequences under the respective test conditions.

b. The normal wear debris particle types of rubbing wear and laminar particles are typical of both bearing types. Roller bearings generate spiral debris during the normal wear regime. The spiral debris is absent during ball bearing testing.

c. Abnormal wear debris particles are similar for both bearing types under the respective test conditions.

d. Roller bearing debris particle types are on the average larger and appear in greater numbers than the ball bearing debris particle types.

7. The particle morphology summary presented above is typical for the roller bearing sequences conducted under this program.

4. GEAR BENCH TESTING. Gear bench testing was performed by the Naval Air Propulsion Center (NAVAIRPROPCEN). Details of this test effort and respective analysis effort is provided in the following paragraphs.

a. Gear Test Procedure

(1) Basically, by definition, a gear has failed when it can no longer efficiently function in the job for which it was designed. The cause of failure may range from excessive wear to catastrophic breakage as defined below.

(a) Wear: A surface phenomenon in which layers of metal are removed, or "worn away", fairly uniformly from the contacting surfaces of gear teeth.

(b) Pitting/Spalling: Surface fatigue failure which occurs when the material endurance limit is exceeded and is directly related to surface contact stress and number of stress cycles. Spalls are irregular shaped large pits.

(c) Scuffing/Scoring: Rapid wear (by alternate welding and tearing) of tooth surfaces resulting from a failure of the oil film due to overheating of the mesh, thus permitting metal-to-metal contact.

(d) Plastic Flow: A surface deformation from the yielding of surface and subsurface material (cold working) which is usually associated with softer gear materials, but which can occur in heavily loaded cases of through hardened gears.

(e) Fracture: Failure caused by breakage of a whole tooth due to excessive tooth loading.

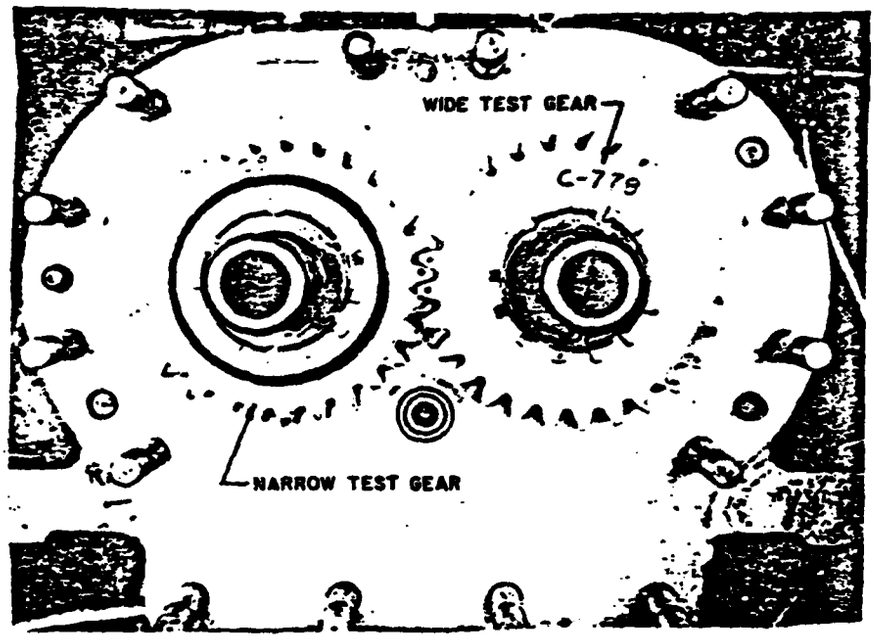
(2) The gear bench test program at NAVAIRPROPCEN was conducted to determine the feasibility of identifying, by used oil analysis, three of the five failure modes discussed above, i.e., wear, pitting, and scuffing/scoring when such failures are simulated on the Ryder Gear Machine. These failure modes were selected, to the exclusion of the others, because of metal particle generation which normally occurs in a progressive manner.

(3) The test program consisted of bench testing of gear sets in a closed-loop lubricant system. Test gears consisted of AISI 9310 aircraft quality steel, case hardened spur gears with 28 teeth at 22.5-degree pressure angle and 8 diametral pitch. Mating (load) gears were the same configuration except for tooth width, and operated at a 1:1 gear ratio. The gear set met both the metallurgical and dimensional specifications as set forth in Test Method D-1947 of the American Society for Testing and Materials (ASTM). A representation of the test gear set configuration is presented in Figure 65.

(4) Gear testing was conducted on a standard Ryder Gear Machine. A picture of a typical Ryder Machine utilizing an Erdco Universal Tester is present in Figure 66. The Ryder test method is normally utilized to determine the load-carrying capacity of petroleum oil and synthetic gear lubricants under ASTM test method D1947-77. An advanced high speed/high temperature model, the Ryder Research Gear Machine, Figure 67, was used in this program. The gear machine operates on the four-square principle in that two parallel shafts are connected by two sets of gears; one set is the replaceable test spur gears and the other is a set of helical gears which are integral with the shafts, Figure 68. Load is applied hydraulically to the test gears by the axial movement of one shaft relative to the other. Gear tooth load, then, is a function of helix angle, shaft cross-sectional area (system constants), hydraulic pressure and gear tooth width. The gear machine has also been used in surface fatigue (pitting) studies because system operating parameters can be readily controlled and imposed on the test gears. Some of these main parameters are:

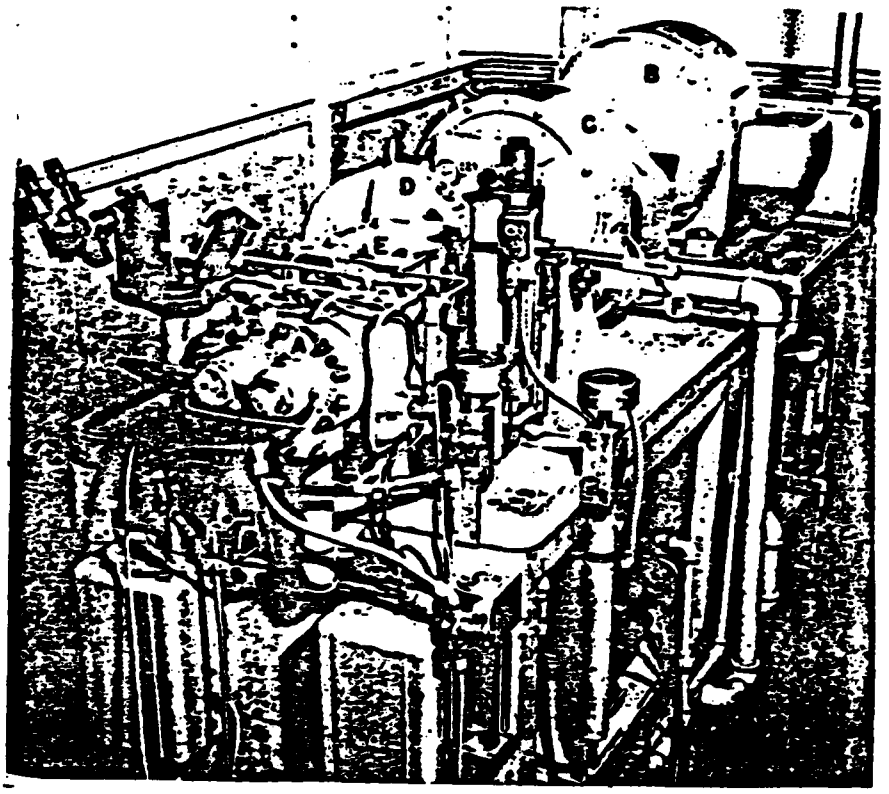
(a) Speed - Sliding velocities/Slide roll ratio

(b) Load - Tooth load/Hertz stress



D-1947

FIGURE 65
GEAR TEST SET CONFIGURATION

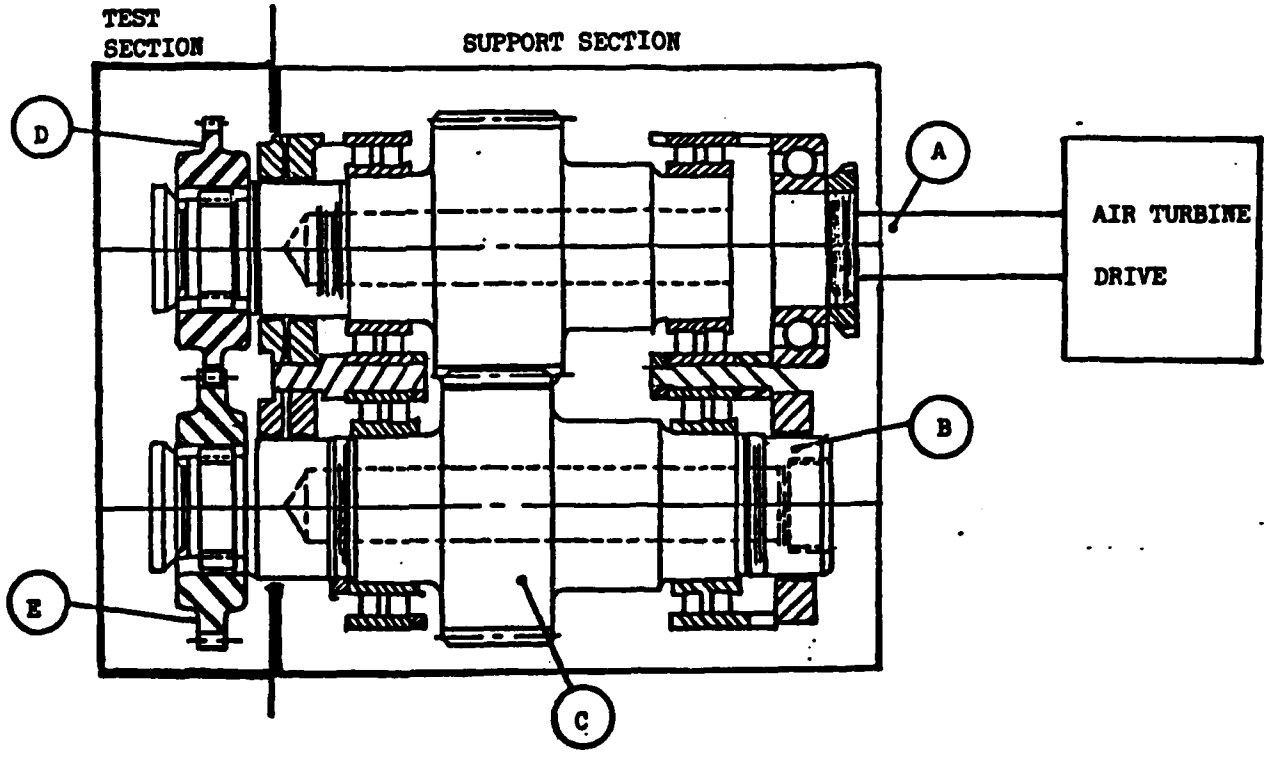


D-1947

A. RYDER GEAR MACHINE
B. DRIVE MOTOR
C. DYNAMATIC COUPLING
D. STEP-UP GEARBOX
E. ADAPTOR
F. INDEXING RATCHET

FIGURE 66

ERDCO UNIVERSAL TESTER



A. DRIVE SHAFT
B. DRIVEN (LOAD) SHAFT
C. HELICAL "SLAVE" GEARS
D. TEST GEAR
E. LOAD GEAR

FIGURE 67

CROSS-SECTION OF RYDER RESEARCH GEAR MACHINE TEST HEAD

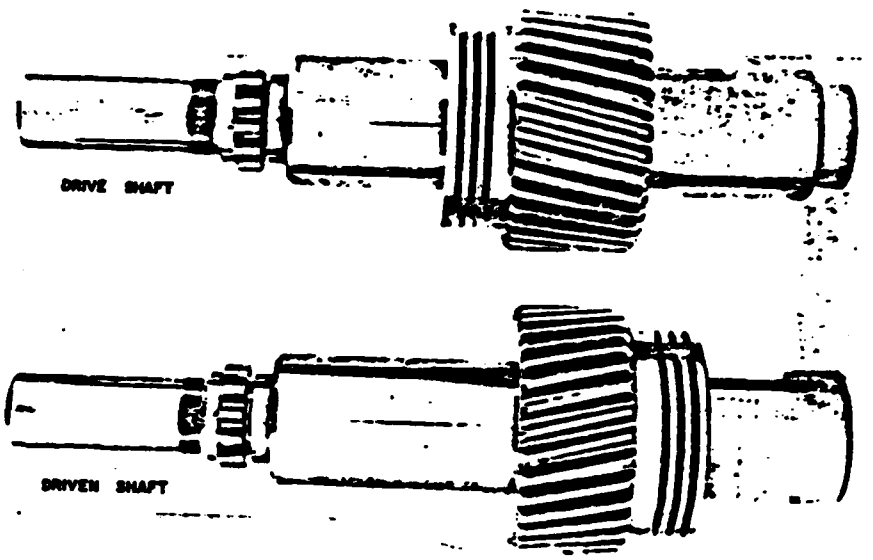


FIGURE 68

SHAFTS WITH INTEGRAL SLAVE GEARS

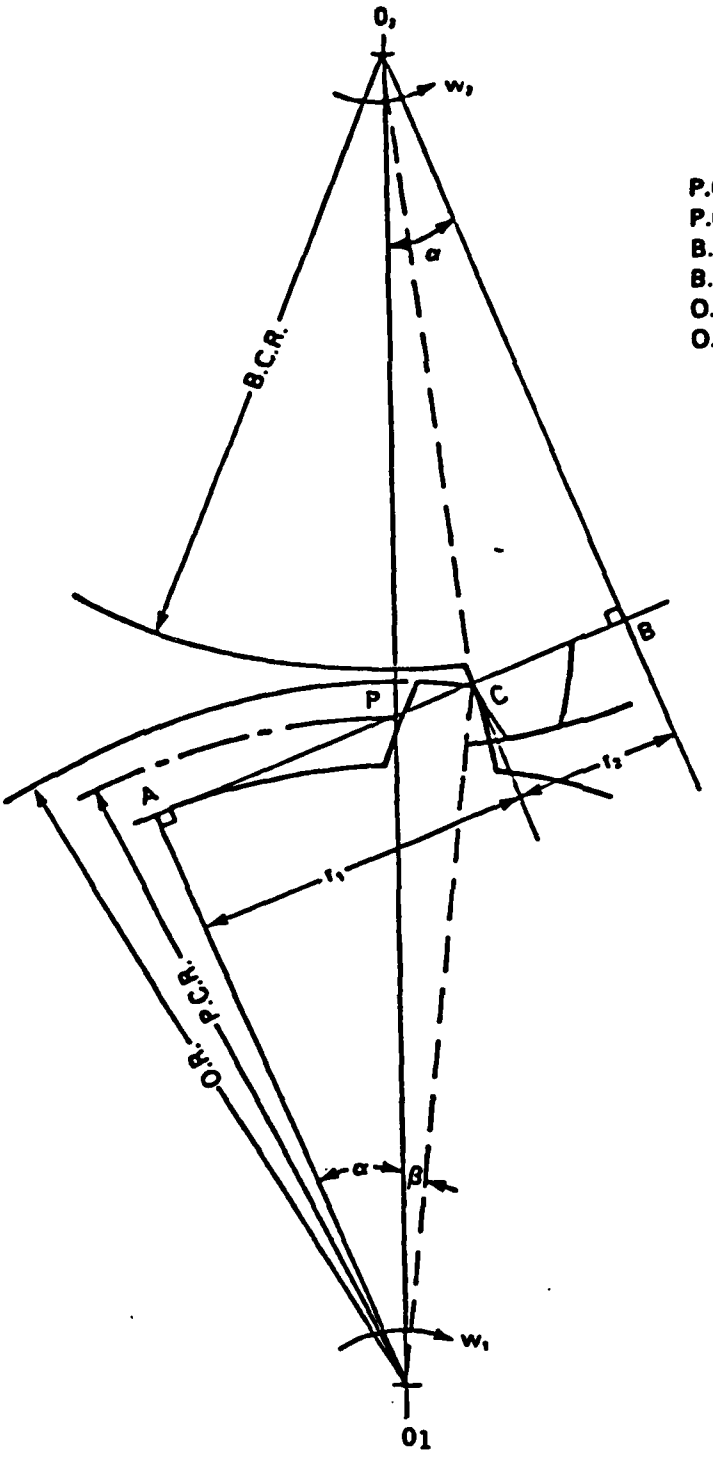
(c) Temperature - Range of oil temperatures to 426.7°C (800°F)

(d) Test oil flow rates

(5) Ryder gear-mesh configuration results in a combination of sliding and rolling contact. The path of contact lies on the common tangent to the base circles and the length of the contact path is limited by the outside diameter of the gears. The tooth action results in a combination of rolling and sliding between engaging profiles. Pure rolling occurs only at the pitch point and maximum sliding velocity at the tip of a tooth, point C, indicated in Figure 69.

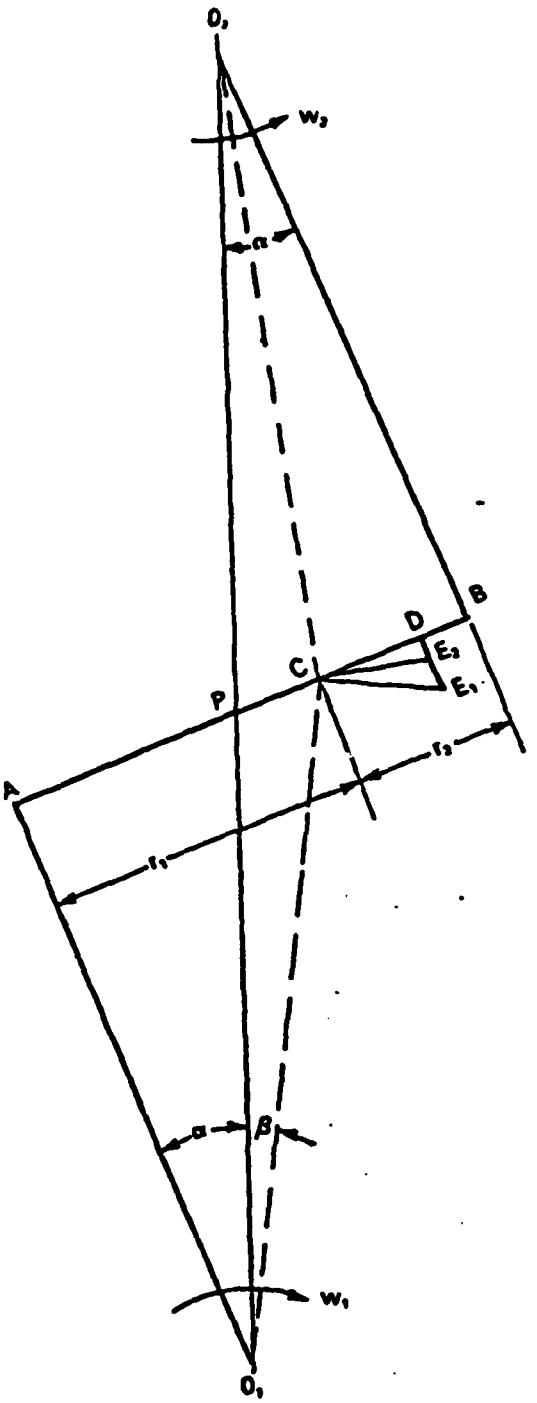
(6) The point of contact travels along the common tangent to the base circles and the common tangent is normal to the tooth profiles at the point of contact. Each of the contact points on mating flanks has a tangential velocity. The velocity vector diagram for the maximum sliding velocity at point C has been indicated in Figure 70. The maximum sliding velocity (V_s) across the line of action is the difference of the velocity components for point C (gear tip) across the line of action. The slide/roll ratio for point C is the ratio of sliding and rolling velocities at point C. At the point of contact, each tooth flank may be considered to be part of a cylinder, and therefore can be represented by two cylinders.

(7) The basic Ryder test oil system is a closed-loop, recirculating system as shown schematically in Figure 71. The system is completely isolated from the support oil system, Figure 72, which avoids the introduction of wear debris from all other sources except for the test oil pump. The 100 mesh (149 μm) filter was left in the system since its size (filtration) would not interfere with metal particles carried by the oil for subsequent analyses. The original test oil system was later replaced by a second oil system which was used in SKF Industries, Inc., bearing bench tests previously discussed. The change was made late in the gear bench tests (last two fatigue tests) when it was suspected that metal particle retention or contamination of the first system from one test to the next. A schematic diagram of the second test oil system is shown in Figure 73.



P.C.D. = 3.5 in. (pitch circle dia.)
P.C.R. = 1.75 in.
B.C.D. = 3.2336 (base circle dia.)
B.C.R. = 1.6168 in.
O.D. = 3.72 in. (Outer Dia.)
O.R. = 1.86 in.
u = pressure angle = 22½°
$w_1 = w_2 = 10{,}000$ r.p.m.

FIGURE 69
RYDER GEAR-MESH GEOMETRY DIAGRAM



U_1 = $\overline{CE_1}$ = Velocity vector for point C from driving gear.

U_2 = $\overline{CE_2}$ = Velocity vector for point C from driven gear.

$\overline{CD}$ = Velocity component of U_1, U_2 along line of action.

V_1 = $\overline{DE_1}$ = Velocity component of U_1 across line of action

V_2 = $\overline{DE_2}$ = Velocity component of U_2 across line of action

V_s = Sliding velocity across line of action (Max) = $V_1 - V_2$

V_s = $\overline{DE_1} - \overline{DE_2}$

Slide/roll ratio (Max) = $V_s/(V_1 + V_2)$

FIGURE 70

RYDER GEAR-MESH, VELOCITY VECTOR DIAGRAM

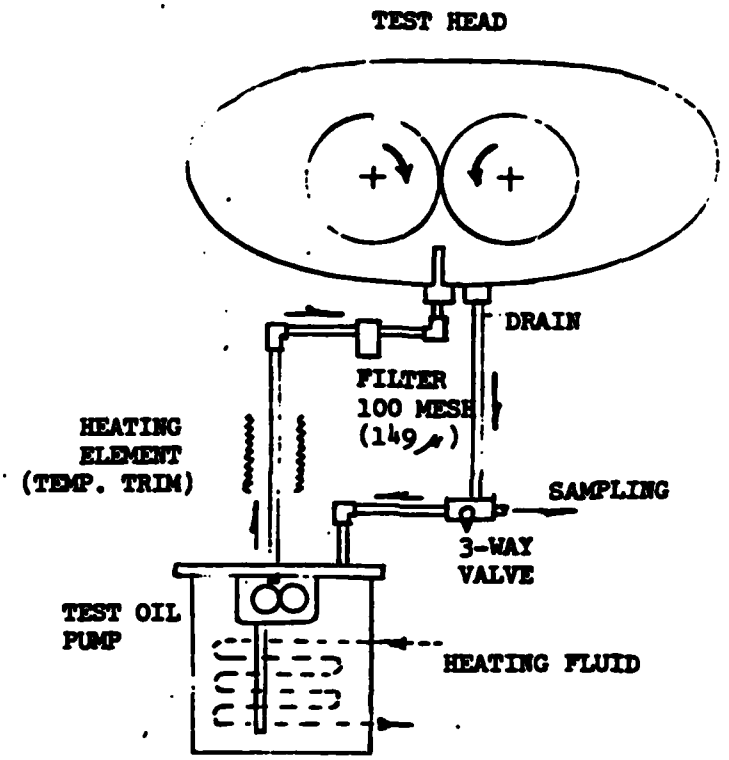
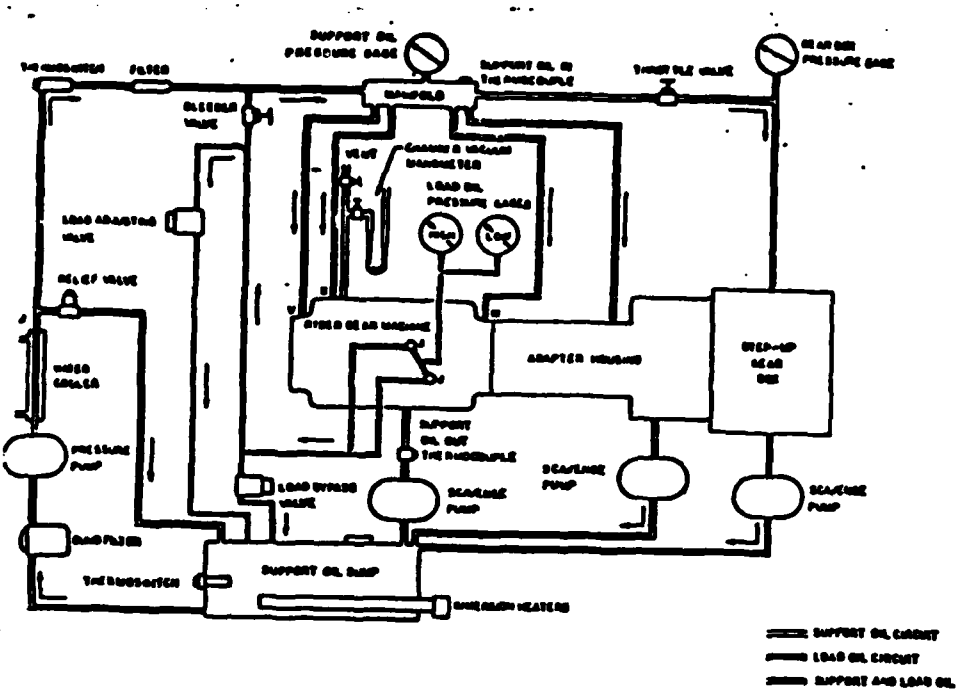


FIGURE 71

SCHEMATIC DIAGRAM OF STANDARD CLOSED-LOOP
GEAR LUBRICATION SYSTEM



ASTM D-1947

FIGURE 72

SCHEMATIC DIAGRAM OF SUPPORT AND
LOAD OIL SYSTEM FOR RYDER GEAR MACHINE

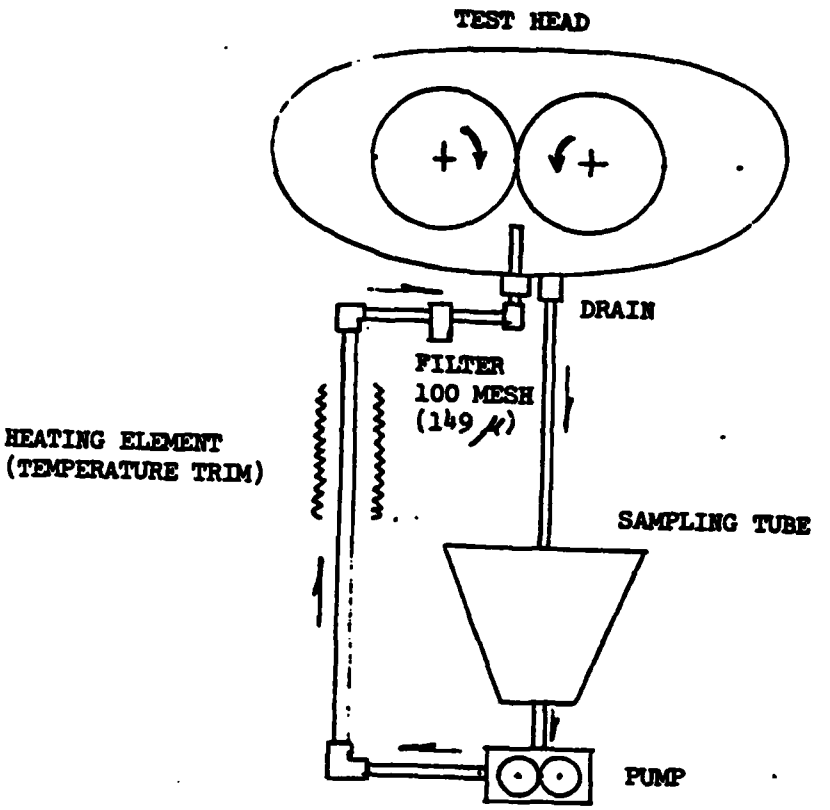


FIGURE 73

SCHEMATIC DIAGRAM OF SKF "CLEAN" CLOSED-LOOP
GEAR LUBRICATION SYSTEM

(8) A qualified Military Specification MIL-L-23699 oil was used in the test oil system throughout the program.

(9) In general, the gear bench test program was designed to provide three types of surface failures common to gear systems. The combinations of operating conditions for the program, were selected to produce scuffing/scoring and fatigue failure modes with normal wear considered as the extended operation prior to any pitting fatigue failures. A total of 420 hours of machine time was scheduled for the program. The condition of gear tooth surfaces was monitored by a closed circuit television system and photographically documented at prescribed sampling intervals. The planned test procedures for the specific failure modes sought are outlined below:

(a) Scuffing/Scoring Failure Mode

1. Pre-Test

   a. Photographs of typical unused tooth surface (minimum of two sets of prints).

   b. Circulate test oil until 73.9°C (165°F) operating temperature is attained.

   c. Take oil samples for background reading (two sample bottles).

2. Test - Conduct standard scuff tests at 10,000 rpm with following modifications:

   a. Use 40,300 N/m (230 PPI) load increments.

   b. Break-in run at 40,300 N/m (230 PPI) load for ten minutes.

   c. Take oil samples.

d. Evaluate scuff and record.

e. Photographs of average (typical) tooth surface.

f. Increase load in 40,300 N/m (230 PPI) increments and run ten minutes at each load until 5 percent average scuff is obtained and record.

g. Photographs of highest, average, and lowest scuffed tooth surfaces.

h. Continue test at constant load for one additional hour.

i. Take oil samples.

j. Re-evaluate scuff and record.

k. Photographs of the same tooth surfaces taken in (g) above.

Repeat (f) through (k) for approximate values of 10 percent, 20 percent, 30 percent, etc., to 90 percent average scuffed tooth surfaces. Subsequent photographs at 10 percent, 20 percent, etc., are again highest, average, and lowest scuffed surfaces and not necessarily the same teeth as 5 percent condition.

(b) Normal Wear and Fatigue Failure Modes

Note: Normal wear is assumed during test operation until fatigue pitting occurs.

1. Test Conditions: 10,000 rpm, ambient test oil temperature.

2. Pre-Test:

   a. Photographs of typical (unused) tooth surface (minimum of two sets of prints).

   b. Circulate oil for 10 minutes.

   c. Take oil samples for background reading (two sample bottles each) before and after the oil is circulated.

3. Test:

   a. Run-in for 10 minutes at each 40,300 N/m (230 PPI) load increment up to 362,500 N/m (2070 PPI) load. Read and record scuff after each load increment.

   b. Take oil samples at 201,400 N/m (1150 PPI) and 362,500 N/m (2070 PPI) loads.

   c. Take photographs of typical tooth surfaces only at 362,500 N/m (2070 PPI).

   d. If average scuff is less than 10 percent, continue test at constant 362,500 N/m (2070 PPI) load.

   e. Take photographs and oil samples every 5 hours up to 30 hours and every 10 hours thereafter until pitting occurs.

(10) A total of nine gears were tested. Five gears were subjected to scuffing/scoring test parameters. One of these test sequences was aborted however, as a result of the inadvertent use of a wrong lubricant. The remaining four gears were subjected to normal wear/fatigue test parameters. Respective designations for these test sequences are given in Table 30.

(11) As mentioned previously all gear testing was conducted utilizing ester base MIL-L-23699 lubricant. In order to minimize liquid borne debris and thus simplify the debris analysis process, the test oil was filtered through a 3 μm Millipore filter prior to gear testing.

(12) Oil samples collected throughout the program were appropriately identified and subjected to spectrometric and ferrographic analyses. These analyses were directed at determining significant changes in metal content, particle size, shape or distribution which can be associated with the type failure modes.

b. Gear Surface Monitoring

(1) A summary of the entire gear bench test program is presented in Table 30. The table identifies the type test performed and all related oil samples, test times, and gear tooth surface evaluations which are necessary for the projected analyses. In addition, the last column attempts to give pertinent information which describes procedures and/or operations applicable to the oil samples. The individual tests performed and relatable results are discussed below.

(a) Scuffing/Scoring Test (GA) - This initial test was conducted in accordance with the procedures outlined in previous paragraphs. The pre-test and early load schedule were appropriately followed and gave the desired results, i.e., 5 percent scuff was attained and continued operation for one hour at constant load produced an insignificant increase in scuff to 7 percent. The next

TABLE 30. OIL ANALYSIS PROGRAM SUMMARY OF GEAR BENCH TESTS

(Sheet 1 of 7)

TYPE TEST	TEST IDENT.	SAMPLE NO.	TOTAL TIME (HRS)	TOTAL REV. ($X10^6$)	TOOTH LOAD N/m X 10^3	TOOTH LOAD (PPI)	FAILURE AVG. SCUFF (PERCENT)	WOAP Fe (PPM)	REMARKS
SCUFFING	GA-								
TEST GEAR SET NARROW M-1425 WIDE L-1637 "A" SIDE		GA-0505-1	0	0	0	(0)	0	2	Circulated new oil
		GA-0505-2	0.17	0.1	40.3	(230)	0	3	Initial 10 min. run
		GA-0505-3	2.67	1.6	402.8	(2300)	7	7	Load increased in 40,300 N/m (230 PPI) increments (10 min. each) to 5% scuff. Then, run 1 hour at 402,800 N/m (2300 PPI).
		GA-0525-4	3.58	2.15	483.4	(2760)	80	175	Increased load to 483,400 N/m (2760 PPI) and obtained 15% scuff. Then, ran at constant load (35 min.). Scuff increased to 80%.
SCUFFING	GC-								
TEST GEAR SET NARROW M-1484 WIDE L-1597 "B" SIDE		GC-0625-1	0	0	0	(0)	0	2	Circulated new oil
		GC-0625-2	0.17	0.1	40.3	(230)	0	5	Initial 10 min. run
		GC-0635-3	2.67	1.6	402.8	(2300)	9.8	15	Load increased in 40,300 N/m (230 PPI) increments (10 min. each) to 5% scuff. Then, run 1 hour at 402,800 N/m (2300 PPI).
		GC-0655-4	3.43	2.06	523.6	(2990)	63	197	Increased load to 523,600 N/m (2990 PPI) and obtained 28% scuff. Then, ran at constant load (16 min.). Scuff increased to 63%.

TABLE 30. OIL ANALYSIS PROGRAM SUMMARY OF GEAR BENCH TESTS

(Sheet 2 of 7)

TYPE TEST	TEST IDENT.	SAMPLE NO.	TOTAL TIME (HRS)	TOTAL REV. ($X10^6$)	TOOTH LOAD N/m X 10^3	TOOTH LOAD (PPI)	FAILURE AVG. SCUFF (PERCENT)	NOAP Fe (PPM)	REMARKS
SCUFFING	GD-								
TEST GEAR SET NARROW M-1396 WIDE L-1745 "A" SIDE		GD-0665-1	0	0	0	(0)	0	3	Circulated new oil
		GD-0665-2	0.17	0.1	40.3	(230)	0	4	Initial 10 min. run
		GD-0665-3	0.33	0.2	80.6	(460)	0	6	Increased load in 40,300 N/m (230 PPI) increments, run for 10 min. at each load.
		GD-0665-4	0.50	0.3	120.8	(690)	0	9	
		GD-0665-5	0.67	0.4	161.1	(920)	0	7	
		GD-0665-6	0.83	0.5	201.4	(1150)	1	7	
		GD-0665-7	1.0	0.6	241.7	(1380)	2.5	7	
		GD-0665-8	1.17	0.7	282.0	(1610)	5.7	8	
		GD-0665-9	1.33	0.8	322.2	(1840)	7.3	10	
		GD-0665-10	1.50	0.9	362.5	(2070)	10.4	13	
		GD-0665-11	1.67	1.0	402.8	(2300)	12.4	18	
		GD-0665-12	1.83	1.1	443.1	(2530)	20.8	34	
		GD-0665-13	2.0	1.2	483.4	(2760)	23.8	32	
		GD-0665-14	2.17	1.3	523.6	(2990)	28.9	43	
		GD-0665-15	2.33	1.4	563.9	(3220)	50.0	144	

TABLE 30. OIL ANALYSIS PROGRAM SUMMARY OF GEAR BENCH TESTS

(Sheet 3 of 7)

TYPE TEST	TEST IDENT.	SAMPLE NO.	TOTAL TIME (HRS)	TOTAL REV. ($\times 10^6$)	TOOTH LOAD N/m X 10^3	TOOTH LOAD (PPI)	FAILURE AVG. SCUFF (PERCENT)	NOAP Fe (PPM)	REMARKS
SCUFFING	GE-								
TEST GEAR SET NARROW M-1396 WIDE L-1745 "B" SIDE		GE-0715-1	0	0	0	(0)	0	2	Circulated new oil
		GE-0715-2	0.17	0.1	40.3	(230)	0	4	Initial load run
		GE-0715-3	0.33	0.2	80.6	(460)	0	5	Increased load in 40,300 N/m (230 PPI) increments, run for 10 min. at each load.
		GE-0715-4	0.50	0.3	120.8	(690)	0	5	
		GE-0715-5	0.67	0.4	161.1	(920)	0	5	
		GE-0715-6	0.83	0.5	201.4	(1150)	0	8	
		GE-0715-7	1.0	0.6	241.7	(1380)	0	6	
		GE-0715-8	1.17	0.7	282.0	(1610)	1.0	6	
		GE-0715-9	1.33	0.8	322.2	(1840)	1.8	7	
		GE-0715-10	1.50	0.9	362.5	(2070)	2.0	6	
		GE-0715-11	1.67	1.0	402.8	(2300)	3.4	8	
		GE-0715-12	1.83	1.1	443.1	(2530)	6.1	9	
		GE-0715-13	2.00	1.2	483.4	(2760)	12.2	9	
		GE-0715-14	2.17	1.3	523.6	(2990)	16.2	19	
		GE-0715-15	2.33	1.4	563.9	(3220)	23.0	21	
		GE-0715-16	2.50	1.5	604.2	(3450)	69.6	177	

TABLE 30. OIL ANALYSIS PROGRAM SUMMARY OF GEAR BENCH TESTS

(Sheet 4 of 7)

TYPE TEST	TEST IDENT.	SAMPLE NO.	TOTAL TIME (HRS)	TOTAL REV. ($\times 10^6$)	TOOTH LOAD N/m $\times 10^3$	TOOTH LOAD (PPI)	FAILURE PITS	FAILURE AVG. SCUFF (PERCENT)	WOAP Fe (PPM)	REMARKS
FATIGUE	GF-									
TEST GEAR SET HARROW M-1485 WIDE L-1659 "A" SIDE		GF-0765-1	0	0	0	(0)	NONE	0	3	Circulated new oil
		GF-0765-2	0.83	0.5	201.4	(1150)		0	8	Load increased from 40,300 to 201,400 N/m (230 to 1150 PPI) in 40,300 N/m (230 PPI) increments (10 min. each).
		GF-0775-3	1.50	0.9	362.5	(2070)		1.7	8	Load increased from 201,400 to 362,500 N/m (1150 to 2070 PPI) in 40,300 N/m (230 PPI) increments (10 min. each).
		GF-0775-4	2.5	1.5	362.5	(2070)		3.5	9	Constant load for 1 hour
		GF-0775-5	3.5	2.1	362.5	(2070)		4.1	9	
		GF-0785-6	4.5	2.7	362.5	(2070)		4.3	10	
		GF-0785-7	5.5	3.3	362.5	(2070)		4.6	9	
		GF-0785-8	6.5	3.9	362.5	(2070)		4.6	9	
		GF-0795-9	11.5	6.9	362.5	(2070)		5.5	10	Constant load for 5 hours
		GF-0805-10	16.5	9.9	362.5	(2070)		6.3	11	
		GF-0835-11	21.5	12.9	362.5	(2070)		6.7	11	
		GF-0845-12	26.5	15.9	362.5	(2070)		7.0	10	
		GF-0855-13	31.5	18.9	362.5	(2070)		7.2	11	
		GF-0865-14	41.5	24.9	362.5	(2070)		8.1	11	Constant load for 10 hours
		GF-0875-15	51.5	30.9	362.5	(2070)		8.2	11	
		GF-0905-16	61.5	36.9	362.5	(2070)		8.2	13	
		GF-0915-17	71.5	42.9	362.5	(2070)		10	14	
		GF-0925-18	81.5	48.9	362.5	(2070)		13	17	
		GF-0935-19	91.5	54.9	362.5	(2070)		15	17	
		GF-0945-20	101.5	60.9	402.8	(2300)		18	21	Increased load to 402,800 N/m (2300 PPI) constant load for 10 hours.
		GF-0975-21	111.5	66.9	402.8	(2300)		24.2	24	Constant load for 10 hours
		ABORT TEST: NO PITTING FAILURES								

TABLE 30. OIL ANALYSIS PROGRAM SUMMARY OF GEAR BENCH TESTS

(Sheet 5 of 7)

TYPE TEST	TEST IDENT.	SAMPLE NO.	TOTAL TIME (HRS)	TOTAL REV. ($\times 10^6$)	TOOTH LOAD N/m $\times 10^3$	TOOTH LOAD (PPI)	FAILURE PITS	FAILURE AVG. SCUFF (PERCENT)	WOAP Fe (PPM)	REMARKS
FATIGUE	GG-									
TEST GEAR SET HARROW M-1485 WIDE L-1659 "B" SIDE		GG-0995-1	0	0	0	(0)	-	0	4	Circulated new oil
		GG-0995-2	0.83	0.5	201.4	(1150)	NONE	0	4	Load increased from 40,300 to 201,400 N/m (230 to 1150 PPI) in 40,300 N/m (230 PPI) increments (10 min. each).
		GG-1005-3	1.83	1.1	443.1	(2530)		9	11	Load increased from 201,400 to 443,100 N/m (1150 to 2530 PPI) in 40,300 N/m (230 PPI) increments (10 min. each).
		GG-1005-4	2.83	1.7	443.1	(2530)		9.8	11	Constant load for 1 hour
		GG-1045-5	3.83	2.3	443.1	(2530)		11.4	13	
		GG-1045-6	4.83	2.9	443.1	(2530)		11.9	13	
		GG-1055-7	5.83	3.5	443.1	(2530)		12.5	14	
		GG-1055-8	6.83	4.1	443.1	(2530)		13	13	
		GG-1065-9	11.83	7.1	443.1	(2530)		13.5	10	Constant load for 5 hours
		GG-1065-10	16.83	10.1	443.1	(2530)		13.8	9	
		GG-1075-11	21.83	13.1	443.1	(2530)		14.7	12	
		GG-1075-12	26.83	16.1	443.1	(2530)		15.2	11	
		GG-1085-13	31.83	19.1	443.1	(2530)		15.6	11	
		GG-1115-14	41.83	25.1	443.1	(2530)	SPALL 2 TEETH	16.7	12	Constant load for 10 hours
		GG-1125-15	51.83	31.1	443.1	(2530)	SAME	17.4	11	
		GG-1135-16	61.83	37.1	443.1	(2530)	3 TEETH	18	10	
		GG-1145-17	71.83	43.1	443.1	(2530)	4 TEETH	22	17	
		GG-1155-18	81.83	49.1	443.1	(2530)	SAME	24.5	19	
		GG-1185-19	91.83	55.1	443.1	(2530)	SAME	33.4	25	
		ABORT TEST: SPALLS ON 4 TEETH								

TABLE 30. OIL ANALYSIS PROGRAM SUMMARY OF GEAR BENCH TESTS

(Sheet 6 of 7)

TYPE TEST	TEST IDENT.	SAMPLE NO.	TOTAL TIME (HRS)	TOTAL REV. ($X10^6$)	TOOTH LOAD N/m X 10^3	TOOTH LOAD (PPI)	FAILURE PITS	FAILURE AVG. SCUFF (PERCENT)	WOAP Fe (PPM)	REMARKS
FATIGUE	GH-									
TEST GEAR SET HARROW M-1997 WIDE M-1750 "A" SIDE		GH-2255-1	0	0	0	(0)	-	0	1	New oil
		GH-2255-2	0	0	0	(0)	-	0	1	Circulated new oil
		GH-2255-3	0.83	0.5	201.4	(1150)	NONE	0	4	Load increased from 40,300 to 201,400 N/m (230 to 1150 PPI) in 40,300 N/m (230 PPI) increments (10 min. each).
		GH-2255-4	1.83	1.1	443.1	(2530)	NONE	2.8	5	Load increased from 201,400 to 443,100 N/m (1150 to 2530 PPI) in 40,300 N/m (230 PPI) increments (10 min. each).
		GH-2265-5	6.83	4.1	443.1	(2530)	MILD-12 TEETH	4	4	Constant load for 5 hours
		GH-2275-6	11.83	7.1	443.1	(2530)	NO CHANGE	5.4	5	
		GH-2305-7	16.83	10.1	443.1	(2530)		6.5	6	
		GH-2305-8	21.83	13.1	443.1	(2530)		6.7	6	
		GH-2315-9	26.83	16.1	443.1	(2530)		7.6	7	
		GH-2315-10	31.83	19.1	443.1	(2530)		8.1	7	
		GH-2325-11	36.83	22.1	443.1	(2530)		8.4	7	
		GH-2325-12	41.83	25.1	443.1	(2530)		9.0	8	
		GH-2335-13	51.83	31.1	443.1	(2530)		10.0	9	Constant load for 10 hours (oil added)
		GH-2345-14	61.83	37.1	443.1	(2530)		10.3	4	
		GH-2305-15	71.83	43.1	443.1	(2530)		10.8	5	
		GH-2395-16	81.83	49.1	443.1	(2530)		11	6	
		GH-2405-17	91.83	55.1	443.1	(2530)		11.3	10	
		GH-2415-18	98.83	59.3	483.4	(2760)		11.4	15	Load increased to 483,400 N/m (2760 PPI) constant load for 7 hours

ABORT TEST: NO SIGNIFICANT INCREASE IN FATIGUE PITTING

TABLE 30. OIL ANALYSIS PROGRAM SUMMARY OF GEAR BENCH TESTS

(Sheet 7 of 7)

TYPE TEST	TEST IDENT.	SAMPLE NO.	TOTAL TIME (HRS)	TOTAL REV. ($\times 10^6$)	TOOTH LOAD N/m X 10^3	TOOTH LOAD (PPI)	FAILURE PITS	FAILURE AVG. SCUFF (PERCENT)	NOAP Fe (PPM)	REMARKS
FATIGUE										
	GI-									
TEST GEAR SET NARROW N-1997 WIDE N-1750 "b" SIDE		GI-2455-1	0	0	0	(0)	-	0	1	New oil
		GI-2455-2	0	0	0	(0)	-	0	1	Circulated new oil
		GI-2455-3	1.0	0.6	241.8	(1380)	-	0	1	Load increased from 40,300 to 241,800 N/m (230 to 1380 PPI) in 40,300 N/m (230 PPI) increments (10 min. each).
		GI-2465-4	2.0	1.2	483.4	(2760)	MILD 2 TEETH	1.6	2	Load increased from 241,800 to 483,400 N/m (1380 to 2760 PPI) in 40,300 N/m (230 PPI) increments (10 min. each).
		GI-2475-5	7.0	4.2	483.4	(2760)	MILD 3 TEETH	2	2	Constant load for 5 hours
		GI-2475-6	12.0	7.2	483.4	(2760)	NO CHANGE	2.6	2	
		GI-2485-7	17.0	10.2	483.4	(2760)		3	2	
		GI-2485-8	22.0	13.2	483.4	(2760)		3.7	2	
		GI-2515-9	27.0	16.2	483.4	(2760)		4	2	
		GI-2515-10	32.0	19.2	483.4	(2760)		4.4	2	
		GI-2525-11	42.0	25.2	483.4	(2760)		4.8	2	Constant load for 10 hours
		GI-2535-12	52.0	31.2	483.4	(2760)		5	2	
		GI-2545-13	62.0	37.2	483.4	(2760)		5	3	
		GI-2555-14	72.0	43.2	483.4	(2760)		5.3	2	
		GI-2585-15	82.0	49.2	523.6	(2990)		5.6	3	Load increased to 523,600 N/m (2990 PPI) constant load for 10 hours.
		GI-2595-16	92.0	55.2	523.6	(2990)	4TH TOOTH LARGE SPALL	6.3	3	
		GI-2605-17	102.0	61.2	563.9	(3220)		7	4	Load increased to 563,900 N/m (3220 PPI) constant load for 10 hours
		GI-2615-18	112.0	67.2	563.9	(3220)		7.3	3	

ABORT TEST: NO SIGNIFICANT INCREASE IN FATIGUE PITTING

scuff level attained was 15 percent instead of the 10 percent as directed, but the test was continued at constant load for one hour. After 35 minutes at load, a sudden increase in scuff level was indicated by changes in specific operating parameters. Upon visual inspection by closed circuit television the average scuff level had increased to 80 percent and the test was terminated.

(b) Scuffing/Scoring Test (GB) - This test was aborted and all information discarded when it was determined that the wrong oil was inadvertently used in the test oil system.

(c) Scuffing/Scoring Test (GC) - The first test procedure was repeated in this test with some "controlled" changes in test oil flow which were intended to promote (a) the onset of scuffing at low tooth load (reduced oil flow), and (b) the retardation of scuffing at the high tooth loads (increased oil flow). However, the imposed test oil flow changes proved ineffective in controlling the scuff phenomenon. Consequently, scuffing again increased significantly during the attempted one hour at constant load and the test was terminated. At this point, it was determined that standard scuffing test procedures may be a better method to provide samples of scuffing at 5, 10, 20, 30, etc., percent levels and the next two tests were conducted in this manner.

(d) Scuffing/Scoring (GD) - This test was performed in accordance with standard ASTM scuffing test procedures, i.e., test operation for ten minutes at each load increment and evaluation of the average percent scuff. The procedure provided various scuffing values from 1 to 50 percent and oil samples for appropriate analyses.

(e) Scuffing/Scoring Test (GE) - A second test was conducted following the procedures used in the above (GD) test. Again, scuff values were obtained which varied from 1 to 70 percent. The random nature of the scuffing phenomenon precludes exact and/or repeatable scuffing values even at the same load setting, i.e. in tests GD and GE at the same load of 483,350 N/m (2760 PPI), the scuffing values were 23.8 and 12.2 percent, respectively. This variability is not uncommon in the scuffing failure mode for the Ryder Gear Machine.

(f) Normal Wear/Fatigue Test (GF) - This initial test for the normal wear/fatigue failure modes was conducted in accordance with the procedures outlined under previous paragraphs. As specified, following "run-in" of the gears, the test was conducted at a constant load of 362,500 N/m (2070 PPI) for 91.5 hours without fatigue (pitting) failure. The test was continued at an increased tooth load of 402,790 N/m (2300 PPI) without fatigue failure and finally aborted at 111.5 hours (approximately 6.7×10^7 cycles). In this test, oil samples and surface conditions prior to fatigue (pitting) failure, were considered to be representative of normal wear. However, the amount of scuffing incurred generated a quantity of metal particles which would mask any normal wear particles and would preclude meaningful analysis.

(g) Normal Wear/Fatigue Test (GG) - A second fatigue test was conducted following the established procedures, but with increased test oil flow (to restrict scuffing) and at higher constant tooth load (443,000 N/m or 2530 PPI). At this load, two teeth exhibited fatigue spalls after approximately 42 hours of operation. Although a third and fourth tooth spalled at approximately 62 and 72 hours respectively, continued operation indicated no further change and the test was aborted at approximately 92 hours.

(2) With approximately 50 percent of the scheduled 420 test hours completed, the program was reviewed. It was concluded that two additional normal wear/fatigue tests would be conducted with efforts directed to reducing scuffing/scoring as well as improving cleanliness in the test oil system. To meet these requirements, NAVAIRPROPCEN installed a second test oil jet and the "clean" test oil system used in SKF Industries, Inc. bearing tests. The additional test oil jet provided more test oil to the gear mesh and a resultant decrease in the amount of scuffing/scoring (subsequently shown in tests GH and GI). The effectiveness of the "clean" oil system can only be determined by ferrographic analysis of initial samples in the final two test sequences. With the Ryder Gear Machine modified as described, the final two sequences were conducted and are discussed below.

(a) Normal Wear/Fatigue Test (GH) - This test was essentially a repeat of test GG, i.e. constant tooth load of 443,000 N/m (2530 PPI) except that test oil flow was significantly increased with the two oil jets. The increased flow resulted in much lower average tooth scuffing throughout the entire test. At approximately 7 hours, mild pitting was evident on 12 of the 28 teeth. The test was continued at constant load to 91.8 hours with no significant increase in either number or size of pits. An additional 7 hours was completed at increased tooth load without significant change and the test was aborted at 98.8 hours total time.

(b) Normal Wear/Fatigue Test (GI) - This test was essentially a repeat of the previous test except that tooth load was increased to 483,350 N/m (2760 PPI) in an attempt to induce larger size pits and/or spalls. Mild pitting was observed on two teeth after 2 hours of operation with a third tooth pitting after 7 hours. The test was continued for 72 hours (total) with no significant change in number or size of pits. The load was then increased to 523,630 N/m (2990 PPI) and after 20 hours (total 92 hours), a fourth tooth developed a medium size spall. Since the average percent scuff was still relatively low, the load was again increased to 563,900 N/m (3220 PPI). However, the pits/or spalls did not change and the test was aborted at 112 hours.

(3) The gear bench tests in the Ryder Gear Machine have successfully produced gear failure modes typically found in gears and/or gear systems. The condition of gear tooth surfaces at various degrees of wear or failure was photographically documented throughout the program. The tests provided sequential oil samples taken at specific intervals in each failure mode which were then subjected to extensive analyses.

c. Gear Wear Particle Analysis

(1) Wear debris analysis was performed on respective gear bench test lubricant samples by Foxboro Analytical and NAVAIRENGCEN. As discussed earlier,

lubricant samples were withdrawn periodically from the gear test apparatus. These lubricant samples served as the host media for fluid borne debris analysis. Table 30 summarizes the sample number and respective operating times for each gear test sequence.

(2) As in the case of rolling element bearing analysis, gear tests sequences will be evaluated with respect to the three wear regimes/phases: wear-in, normal wear, and wear-out/abnormal wear. Each gear wear life regime will be evaluated with respect to wear debris characteristics that present themselves during the respective regime. Particle characteristics (i.e. quantity, size distribution, composition, and morphology) will be correlated to surface wear condition/life during the gear bench test sequences.

(a) Particle Quantity

1. The quantity of wear debris contained in lubricant samples taken during gear testing was primarily monitored utilizing ferrographic analysis techniques. Particle counting technique results were discounted as a result of contaminants found in the respective oil samples. Ferrographic magnetic precipitation techniques served to minimize the complicating effects of this undesirable contaminant. Spectrometric analysis concentration readings were also discounted with respect to particle quantity monitoring as a result of their inherent size sensitivity limitations, as discussed in Section VI.

2. Gear test sequence lubricant borne particle quantity/concentration plots basically fall into two generalized groups. Figures 74 and 75 represent plots for gear sequences GG and GH. Figures 76 and 77 represent series of ferrography entry deposit micrographs of the respective sequences. As can be observed from the plots and verified by the micrographs, sequence debris concentration generally follow the expected bathtub curve. Sequences GG and GH, as previously discussed, fall within the gear test sequence group directed at normal wear and fatigue failure. Although these tests are accelerated in nature, this test group is more representative of a field operating gear wear life than the scuffing sequence test group to be discussed later in this section.

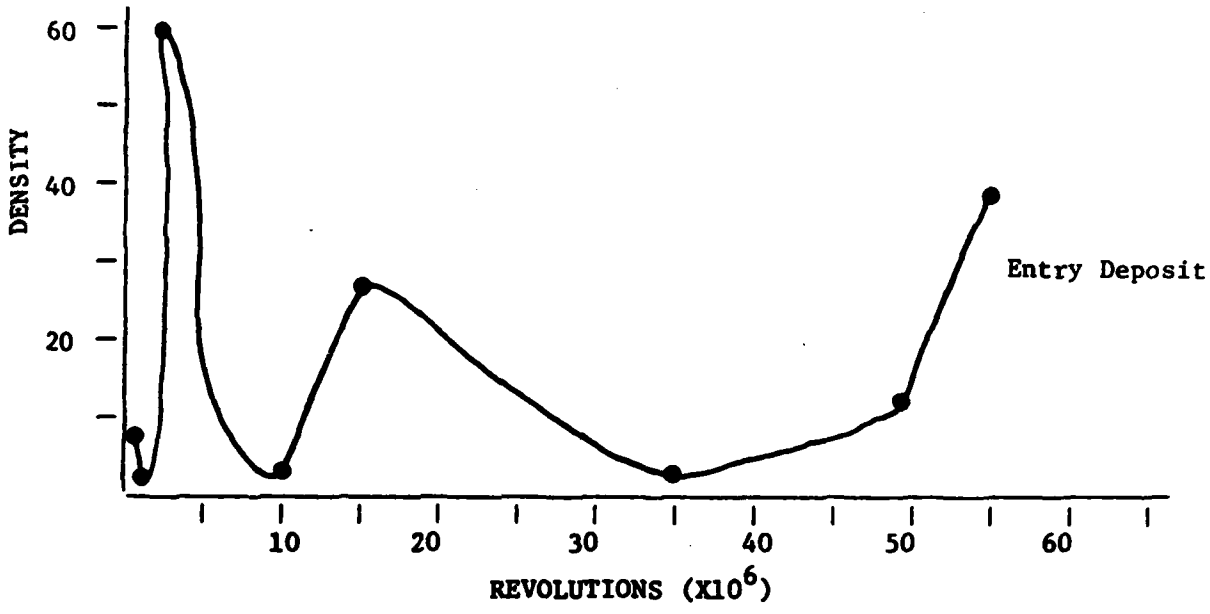


FIGURE 74

GEAR TEST SEQUENCE GG
FERROGRAPH DENSITY DATA

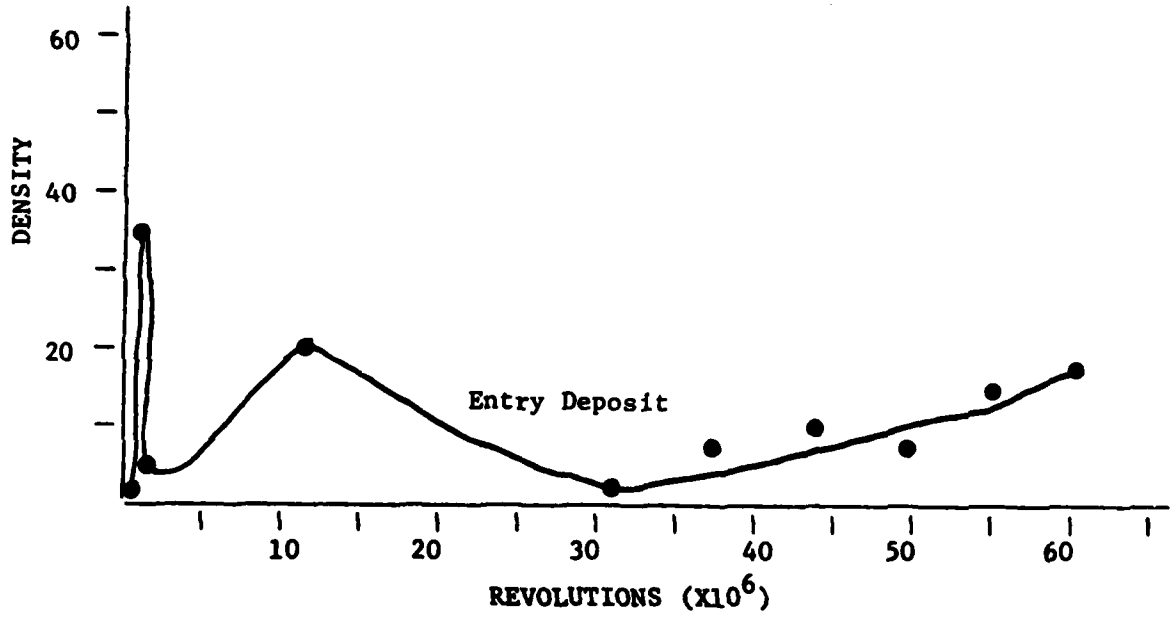


FIGURE 75

GEAR TEST SEQUENCE GH
FERROGRAPH DENSITY DATA



FIGURE A 0 m.r.

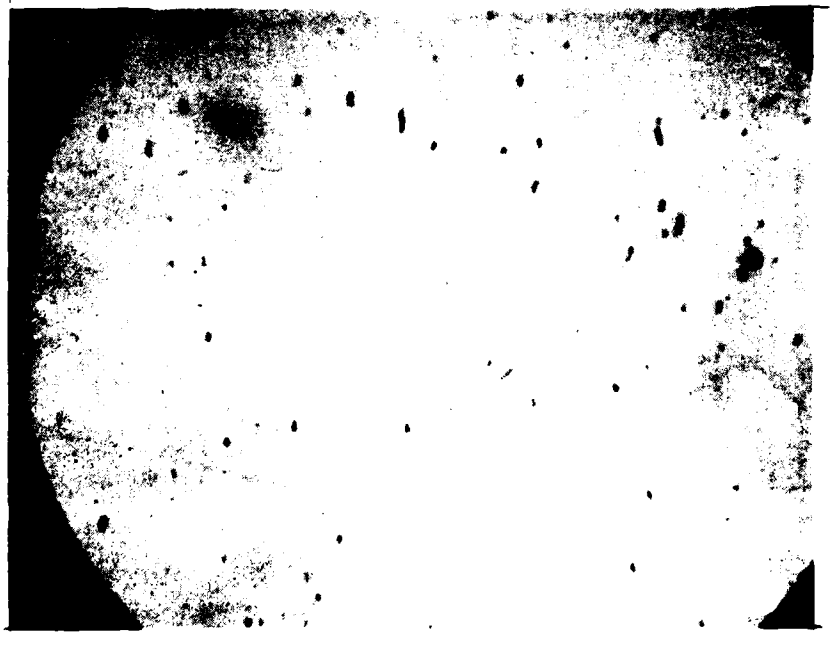


FIGURE B 0.5 m.r.

FIGURE 76

GEAR TEST SEQUENCE GG

ENTRY DEPOSIT

LOW MAGNIFICATION

(Sheet 1 of 5)



FIGURE C 1.1 m.r.

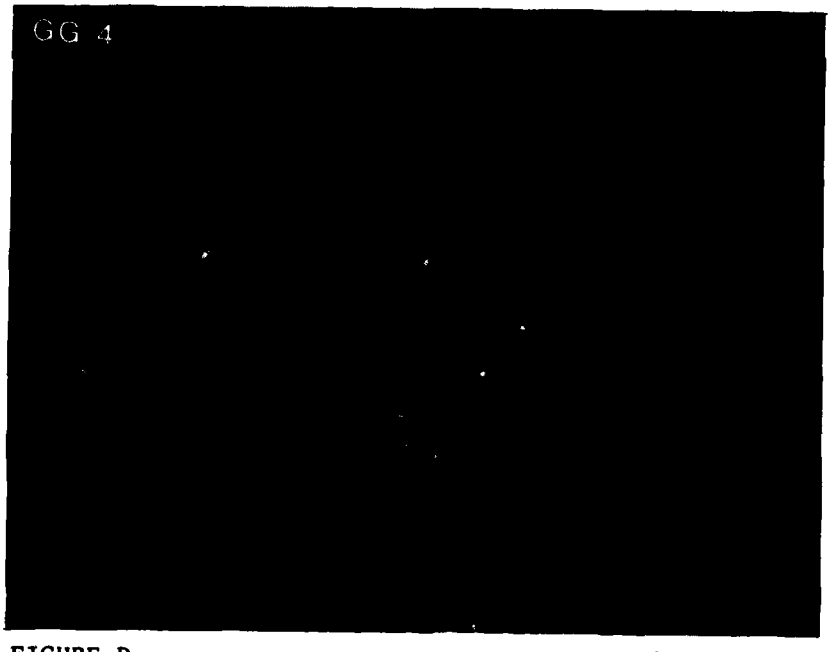


FIGURE D 1.7 m.r.

FIGURE 76

GEAR TEST SEQUENCE GG

ENTRY DEPOSIT

LOW MAGNIFICATION

(Sheet 2 of 5)

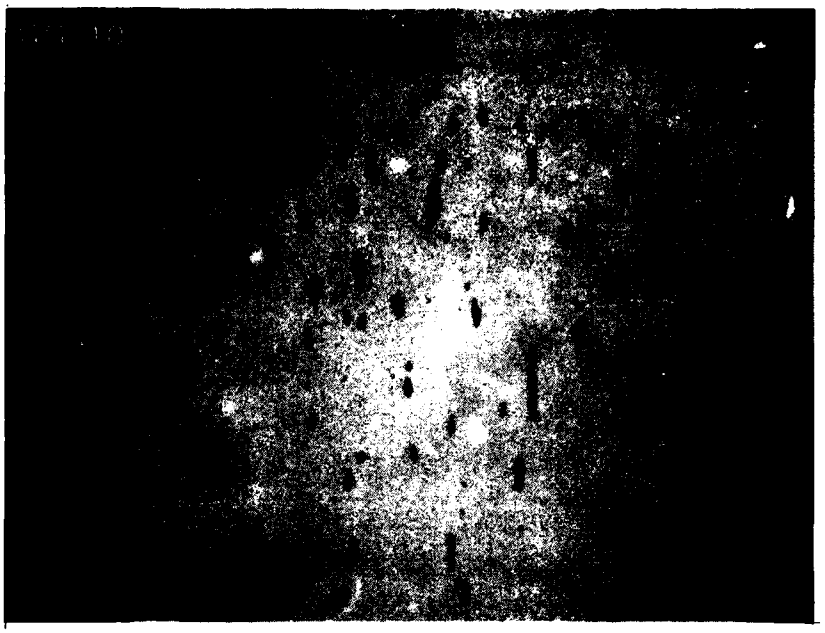


FIGURE E 10.0 m.r.



FIGURE F 16.1 m.r.

FIGURE 76

GEAR TEST SEQUENCE GG

ENTRY DEPOSIT

LOW MAGNIFICATION

(Sheet 3 of 5)

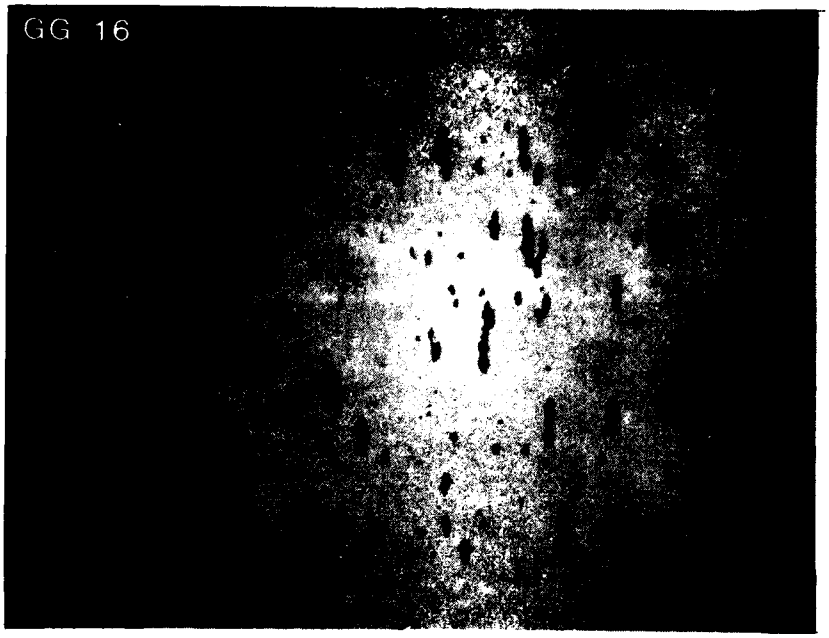


FIGURE G 37.1 m.r.

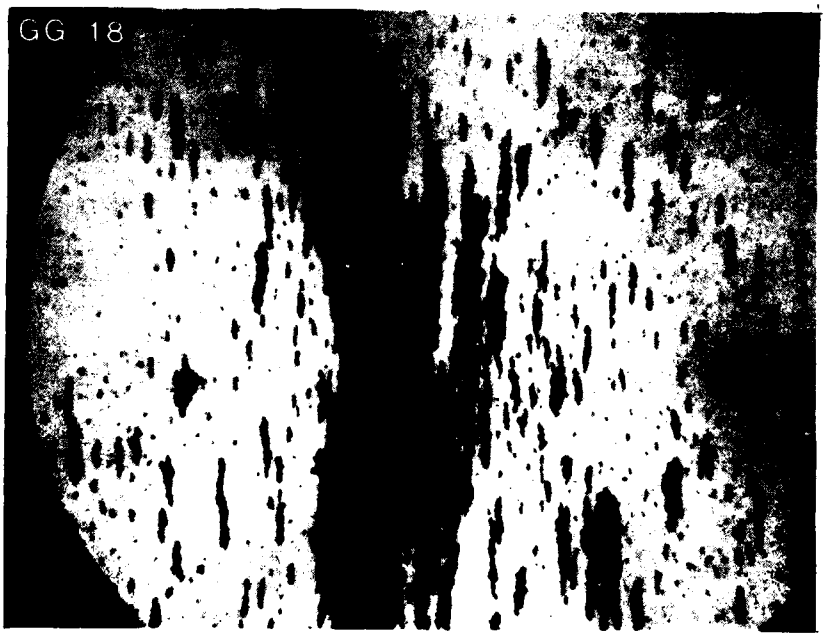


FIGURE H 49.1 m.r.

FIGURE 76
GEAR TEST SEQUENCE GG
ENTRY DEPOSIT
LOW MAGNIFICATION
(Sheet 4 of 5)



FIGURE I 55.1 m.r.

FIGURE 76
GEAR TEST SEQUENCE GG
ENTRY DEPOSIT
LOW MAGNIFICATION
(Sheet 5 of 5)

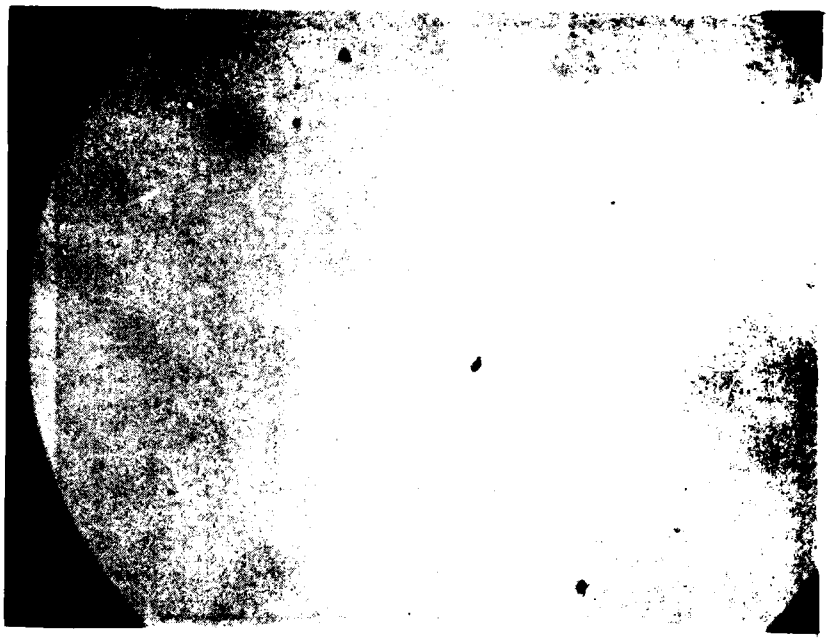


FIGURE A 0 m.r.



FIGURE B 0 m.r.

FIGURE 77
GEAR TEST SEQUENCE GH
ENTRY DEPOSIT
LOW MAGNIFICATION
(Sheet 1 of 6)



FIGURE C 0.5 m.r.

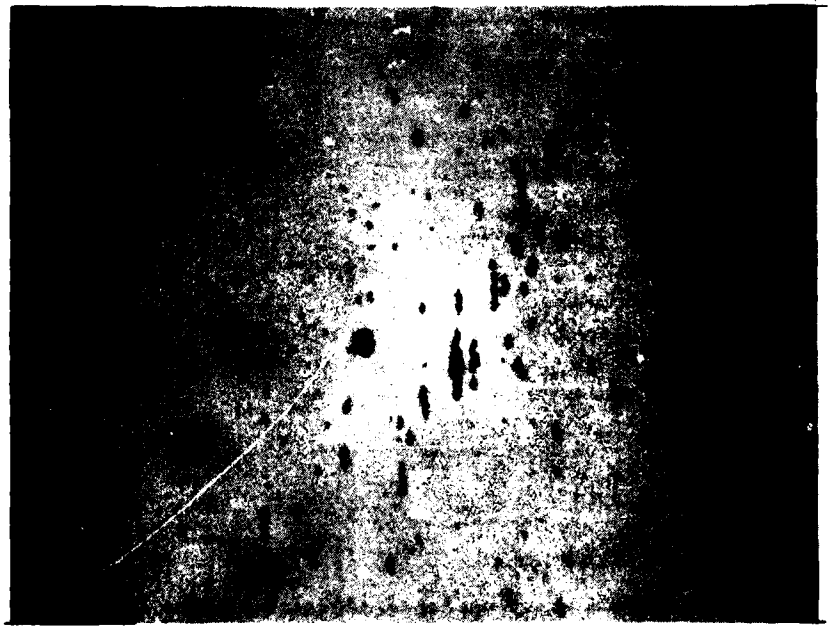


FIGURE D 1.1 m.r.

FIGURE 77
GEAR TEST SEQUENCE GH
ENTRY DEPOSIT
LOW MAGNIFICATION
(Sheet 2 of 6)

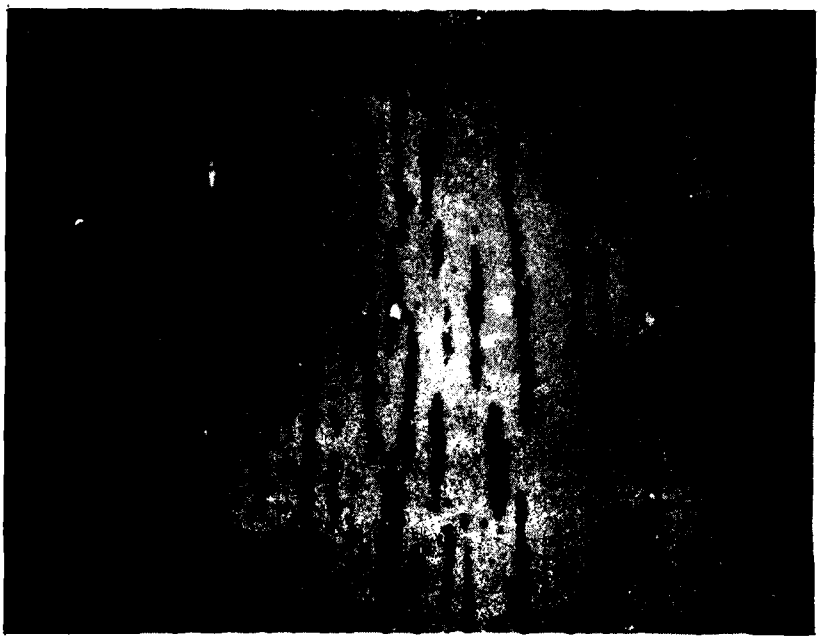


FIGURE E 13.1 m.r.



FIGURE F 31.1 m.r.

FIGURE 77
GEAR TEST SEQUENCE GH
ENTRY DEPOSIT
LOW MAGNIFICATION
(Sheet 3 of 6)

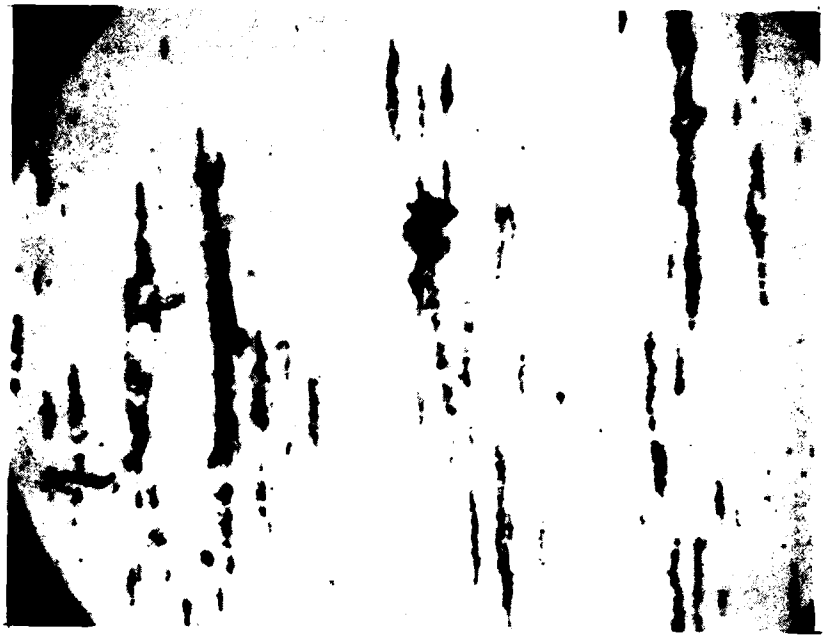


FIGURE G

37.1 m.r.

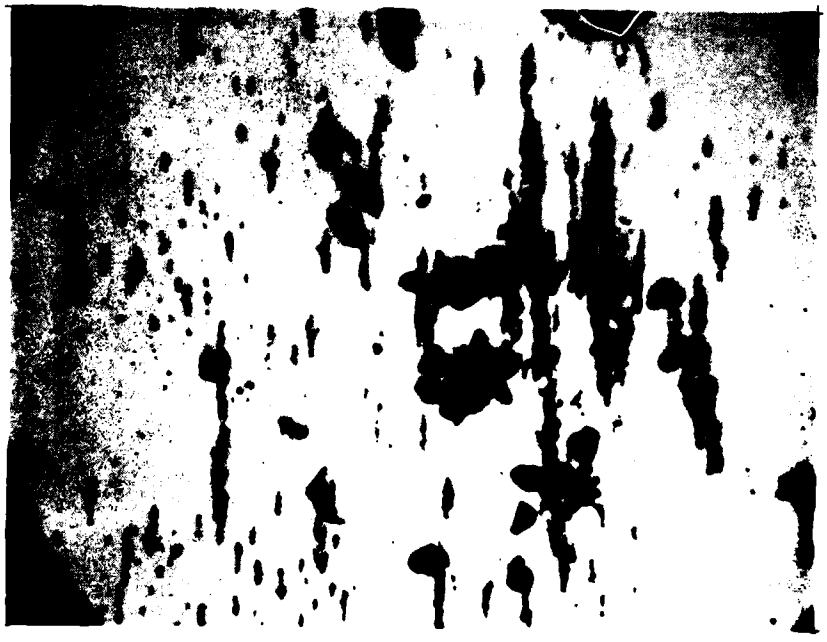


FIGURE H

43.1 m.r.

FIGURE 77
GEAR TEST SEQUENCE GH
ENTRY DEPOSIT
LOW MAGNIFICATION
(Sheet 4 of 6)



FIGURE I 49.1 m.r.



FIGURE J 55.1 m.r.

FIGURE 77
GEAR TEST SEQUENCE GH
ENTRY DEPOSIT
LOW MAGNIFICATION
(Sheet 5 of 6)

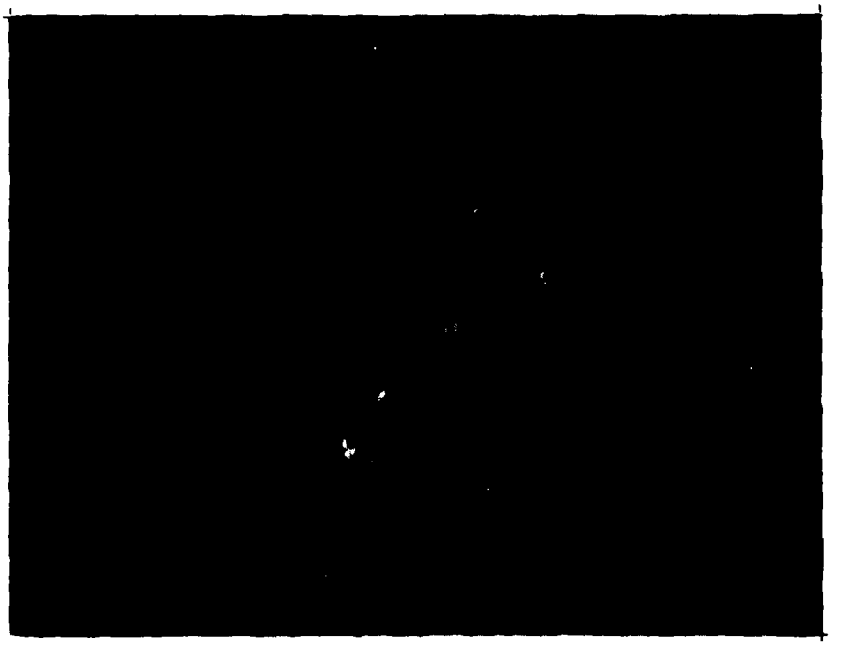


FIGURE K 59.3 m.r.

FIGURE 77
GEAR TEST SEQUENCE GH
ENTRY DEPOSIT
LOW MAGNIFICATION
(Sheet 6 of 6)

3. Normal wear/fatigue gear test sequences can thus be discussed from the aspect of wear-in, normal wear, and wear-out/abnormal wear. As seen in Figures 74 and 75, wear-in of the test gears results in a high wear rate thus a high level of debris concentration. This regime, as compared with rolling element bearings, appears rather short lived. The difference between the bearing and gear wear-in process timing is significant, however, relative stress levels may be a contributing factor in this difference.

4. The second regime, normal wear, results in a much lower wear rate thus a much lower sample debris concentration level. Abnormal wear, the final regime, results in an accelerated wear rate and thus an ever increasing level of debris. This description was typical of all normal wear/fatigue group gear test sequences.

5. It can be noted that during test sequence GH, mild fatigue pitting was noted about 5 million revolutions into the test sequence. This pitting correlates with the increased debris level noted at this test period as indicated in Figure 75. Also during this sequence, GH, oil was added to the system at about 30 million revolutions into the test. This oil addition correlates with the decrease in debris level at this point as indicated in Figure 75. Finally, sequence GH did not result in a severe wear failure and was terminated due to time constraints.

6. The previously mentioned fatigue present at 5 million revolutions did not progress during the remainder of the sequence. Test gear scuffing initiated at the 1 million revolution point and progressed almost linearly to the 11% level at test termination, 60 million revolutions. This lack of severe wear situation accounts for the mild buildup of debris during this sequence.

7. It can be noted that during test sequence GG, a fatigue spall was noted at the 25 million revolution test point. This spall would correlate with the increased debris level at this point as depicted in Figure 74.

The accelerated scuff level, as well as progressing fatigue level, from the 40 million revolution point directly correlates to the increasing debris level from this point as depicted in Figure 74. The increased severity of this abnormality as compared to sequence GH resulted in an increased debris over the level exhibited under GH.

8. The second gear sequence group is depicted in Figures 78 and 79 representing plots for gear sequences GD and GE. Figures 78 and 79 represent series of ferrography entry deposit micrographs of the respective sequences. As can be observed from the plots and verified by the micrograph sequences, debris concentration levels progressively increase during the testing format and do not follow a bathtub curve. Sequence GD and GE, as previously discussed, fall within the gear test group directed at scuffing simulation. This group of test sequences is highly accelerated testing and as such, does not exhibit a traditional wear-in and normal wear regime as expected. As a result, an abnormal wear regime, scuffing, is apparent throughout each test sequence.

9. As can be noted from the plots in Figure 80, scuffing results in a rapid buildup of debris under the test conditions utilized. Resulting debris levels were significantly higher than the levels exhibited by the fatigue testing under sequence GH. These results are typical of the scuffing gear test sequences monitored under this effort.

10. It can be noted that the lubricant systems utilized in the gear test sequences were equipped with only a coarse filter, 149 μm. As a result, decreases in debris concentration levels must have resulted from a combination of natural filtration and a grinding process. This phenomenon was also observed during bearing testing as previously presented.

11. Tables 31, 32, and 33 represent particle counting data from sequences GD, GH, and GG respectively. As can be seen, this data is erradic and does not follow the wear debris trends as indicated by the ferrographic analysis. These variations are typical of the gear test sequences and



FIGURE A 0 m.r.



FIGURE B 0.1 m.r.

FIGURE 78
GEAR TEST SEQUENCE GD
ENTRY DEPOSIT
LOW MAGNIFICATION
(Sheet 1 of 4)



FIGURE C

0.2 m.r.

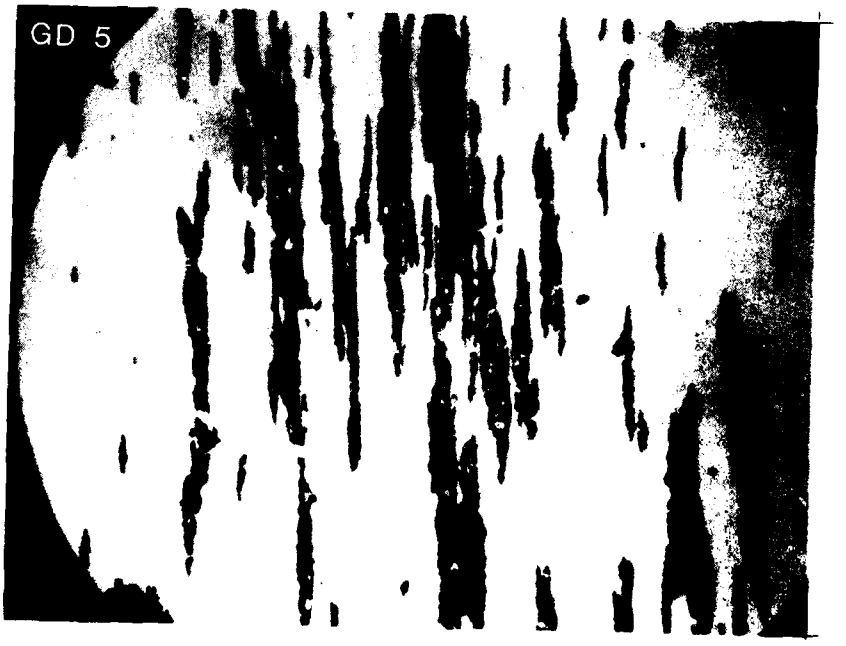


FIGURE D

0.4 m.r.

FIGURE 78

GEAR TEST SEQUENCE GD

ENTRY DEPOSIT

LOW MAGNIFICATION

(Sheet 2 of 4)



FIGURE E 0.7 m.r.



FIGURE F 1.0 m.r.

FIGURE 78
GEAR TEST SEQUENCE GD
ENTRY DEPOSIT
LOW MAGNIFICATION
(Sheet 3 of 4)

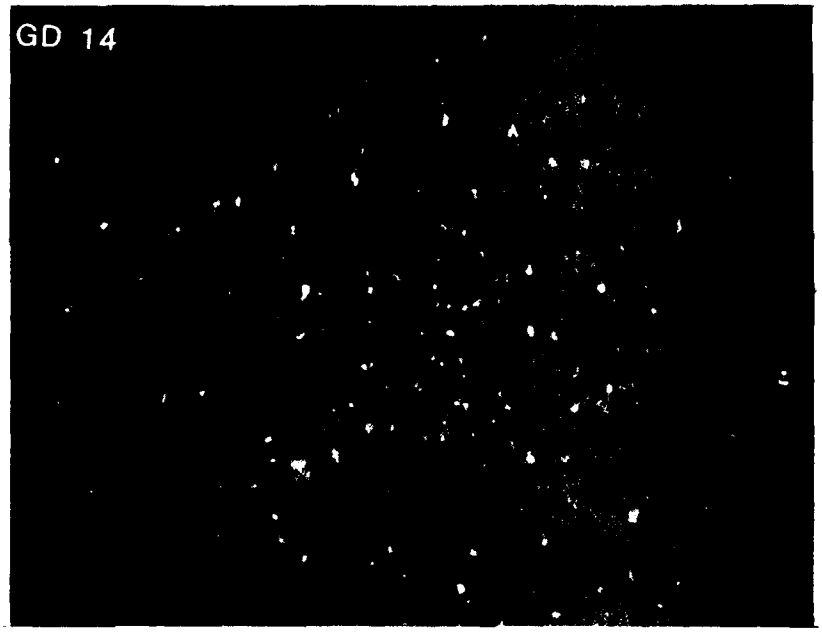


FIGURE G 1.3 m.r.

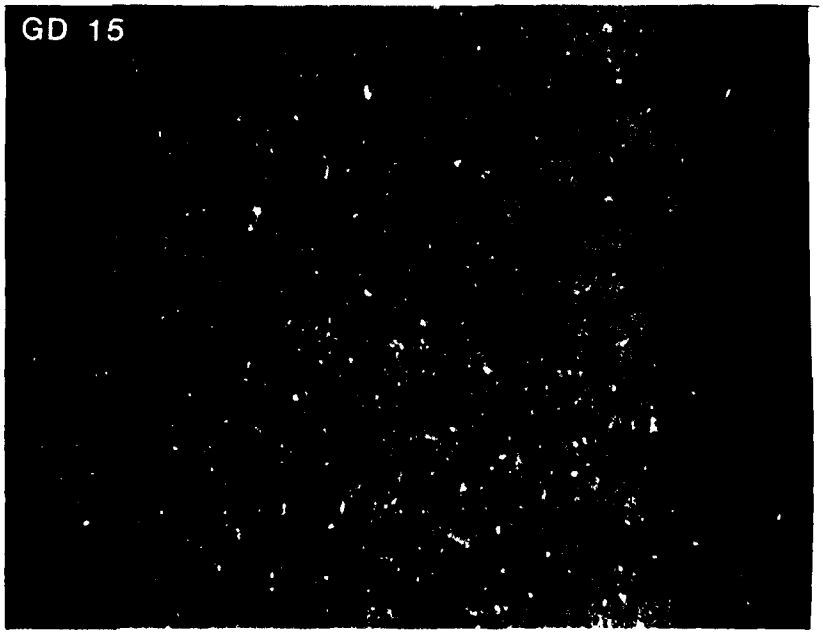


FIGURE H [illegible] m.r.

[illegible]

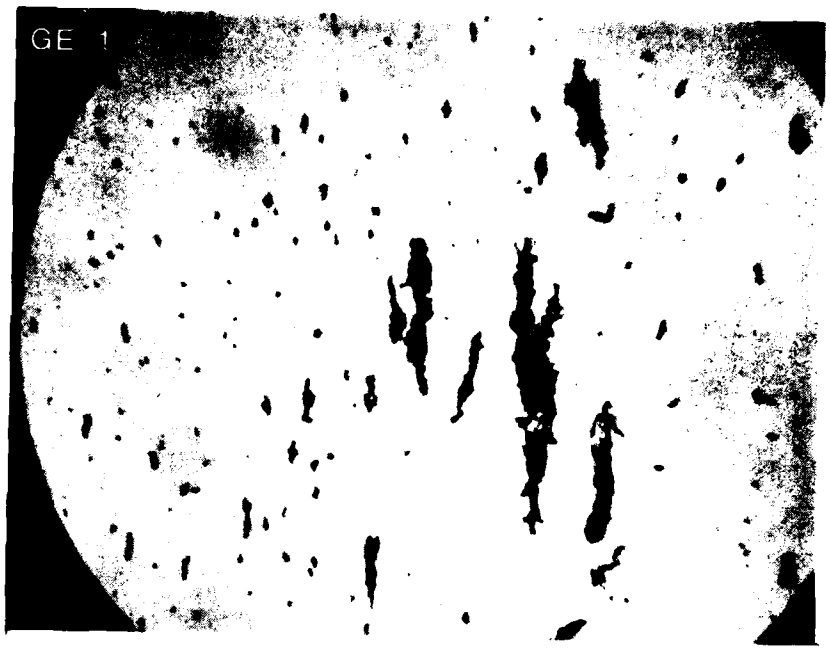


FIGURE A

0 m.r.

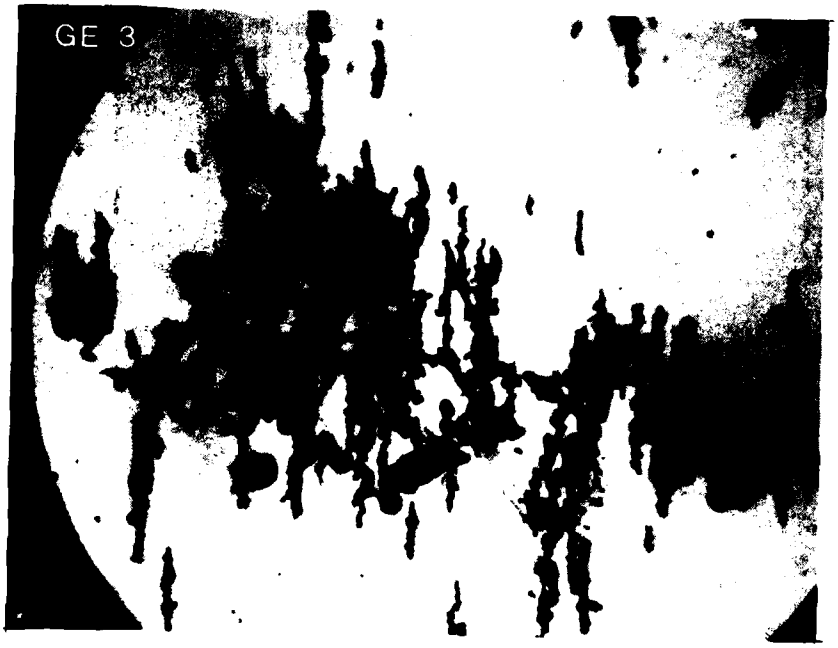


FIGURE B

0.2 m.r.

FIGURE 79
GEAR TEST SEQUENCE GE
ENTRY DEPOSIT
LOW MAGNIFICATION
(Sheet 1 of 4)



FIGURE C 0.3 m.r.



FIGURE D 0.4 m.r.

FIGURE 79
GEAR TEST SEQUENCE GE
ENTRY DEPOSIT
LOW MAGNIFICATION
(Sheet 2 of 4)

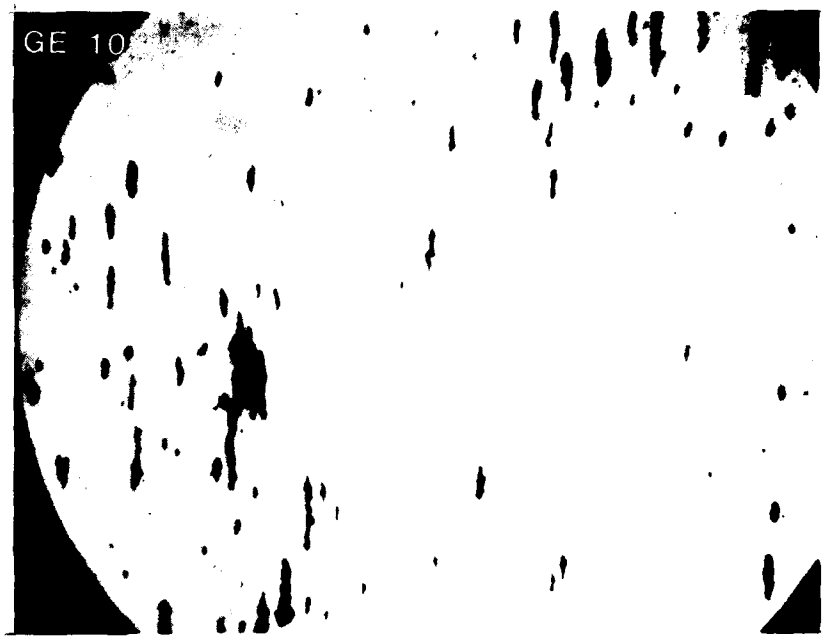


FIGURE E 0.9 m.r.

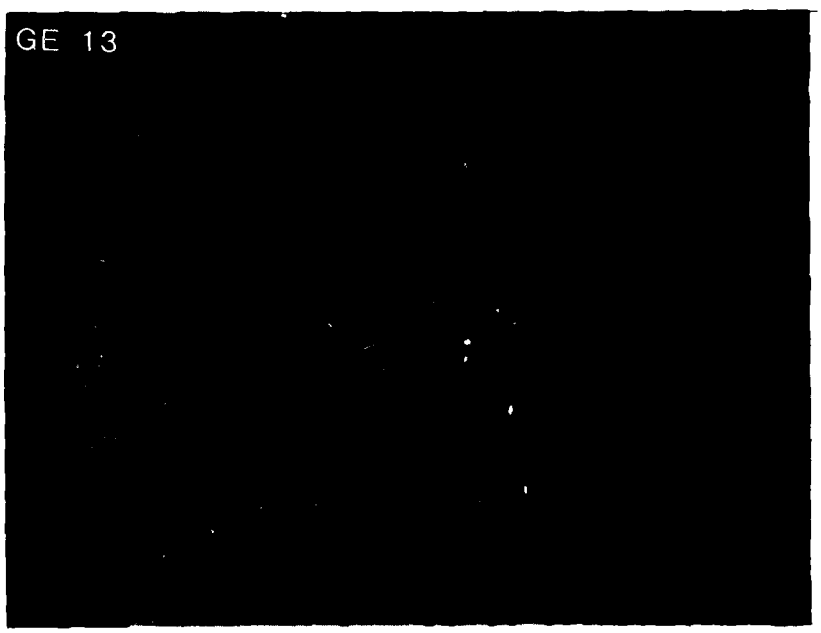


FIGURE F 1.2 m.r.

FIGURE 79
GEAR TEST SEQUENCE GE
ENTRY DEPOSIT
LOW MAGNIFICATION
(Sheet 3 of 4)



FIGURE G 1.4 m.r.



FIGURE H 1.5 m.r.

FIGURE 79
GEAR TEST SEQUENCE GE
ENTRY DEPOSIT
LOW MAGNIFICATION
(Sheet 4 of 4)

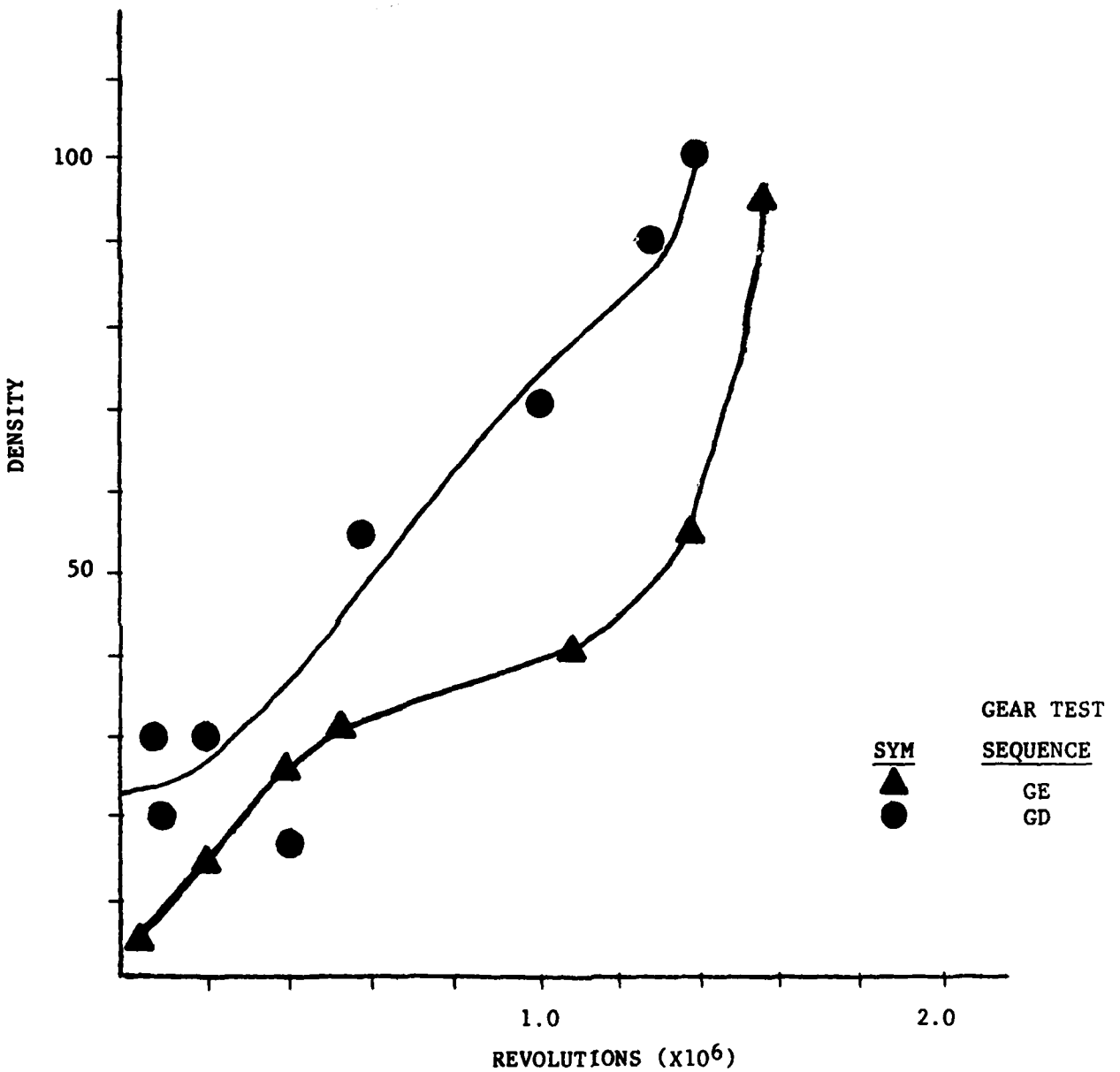


FIGURE 80
GEAR TEST SEQUENCES GD AND GE
FERROGRAPH DENSITY DATA

TABLE 31. PARTICLE COUNTS

SERIES	TIME	% TIME	ADJUSTED COUNTS (COUNTS/100 CC) TOTAL	GEAR NO. GD 2-5	5-7	7-15	15-25	25+	PERCENT OF TOTAL COUNTS ($N \times 10^4$) 2-5	5-7	7-15	15-25	25+
1	0.0	0.0	136.3	103.8	14.2	11.4	4.7	4.2	75.05	10.27	8.24	3.40	3.04
2	0.1	7.14	442.4	369.6	36.6	19.6	8.6	8.0	83.54	8.27	4.43	1.94	1.81
3	0.2	14.29	1359.1	1472.0	267.0	95.7	17.3	7.1	79.18	14.36	5.15	0.93	0.38
5	0.4	29.57	1346.8	1188.0	105.9	35.5	8.6	8.8	88.21	7.86	2.64	0.64	0.65
6	0.5	35.71	1213.0	1060.0	105.0	31.6	10.1	6.3	87.39	8.66	2.61	0.83	0.52
7	0.6	42.86	1139.4	1017.0	88.2	22.5	6.0	5.7	89.26	7.74	1.97	0.53	0.50
8	0.7	50.00	1423.0	1208.0	146.9	46.3	14.7	12.1	84.54	10.32	3.25	1.03	0.85
9	0.8	57.14	2023.5	1699.0	246.2	59.0	11.3	7.0	83.91	12.27	2.92	0.56	0.35
10	0.9	64.29	2954.8	2441.0	310.5	165.9	25.8	11.6	82.61	10.51	5.61	0.87	0.39
11	1.0	71.43	3495.3	2683.0	628.1	163.7	15.8	4.7	76.76	17.97	4.68	0.45	0.13
12	1.1	78.57	4609.1	3727.0	707.3	144.4	21.3	9.1	80.86	15.35	3.13	0.46	0.20
14	1.3	92.86	928.0	795.5	88.3	33.6	7.0	3.4	85.72	9.52	3.64	0.75	0.37

TABLE 32. PARTICLE COUNTS

SERIES	TIME	% TIME	ADJUSTED COUNTS (COUNTS/100 CC) TOTAL	GEAR NO. GH 2-5	5-7	7-15	15-25	25+	PERCENT OF TOTAL COUNTS ($N \times 10^4$) 2-5	5-7	7-15	15-25	25+
4	1.1	1.85	5524.7	4098.0	1181.0	211.4	13.6	20.7	74.18	21.38	3.83	0.25	0.37
5	4.1	6.91	6103.7	5091.0	914.0	88.7	7.8	2.2	83.41	14.97	1.45	0.13	0.04
6	7.1	11.97	6409.0	5268.0	1022.0	99.5	12.9	6.6	82.20	15.95	1.55	0.20	0.10
7	10.1	17.03	5995.1	3283.0	2254.0	444.5	10.4	3.2	54.76	37.60	7.41	0.17	0.05
10	19.1	32.21	6511.5	6127.0	360.5	16.4	5.7	1.9	94.10	5.54	0.25	0.09	0.03
11	22.1	37.27	6862.7	5729.0	1011.0	108.5	10.6	3.6	83.48	14.73	1.58	0.15	0.05
12	25.1	42.33	6237.2	4308.0	1646.0	252.9	21.9	8.4	69.07	26.39	4.05	0.35	0.13
13	31.1	52.45	6823.3	5687.0	1001.0	117.0	13.8	4.5	83.35	14.67	1.71	0.20	0.07
14	37.1	62.56	2243.1	2146.0	60.4	26.3	6.8	3.6	95.67	2.69	1.17	0.30	0.16
15	43.1	72.68	2304.5	2455.0	114.4	26.6	3.7	1.6	94.38	4.39	1.03	0.14	0.06
16	49.1	82.80	1951.6	1831.0	86.7	26.5	5.3	2.1	93.82	4.44	1.36	0.27	0.11
17	55.1	92.92	2372.8	2226.0	104.6	31.2	6.8	4.0	93.81	4.42	1.31	0.29	0.17
18	59.3	100.00	2082.3	1957.0	86.1	30.5	6.4	2.3	93.98	4.13	1.46	0.31	0.11

TABLE 33. PARTICLE COUNTS

SERIES	TIME	% TIME	ADJUSTED COUNTS (COUNTS/100 CC) GEAR NO. GG					PERCENT OF TOTAL COUNTS (N X 10)				
			TOTAL	2-5	5-7	7-15	15-25	25+	2-5	5-7	7-15	15-25	25+
1	0.0	0.0	582.4	472.9	67.3	32.4	6.9	3.0	81.20	11.56	5.56	1.18	0.50
2	0.5	0.91	395.6	329.5	39.4	21.6	5.5	2.6	82.53	9.96	5.46	1.39	0.66
3	1.1	2.00	778.4	233.7	390.7	80.6	9.9	5.6	37.73	50.19	10.35	1.26	0.46
7	3.5	6.35	369.2	228.3	131.4	6.7	1.8	1.0	61.84	35.59	1.81	0.49	0.27
8	4.1	7.44	703.3	586.6	79.7	27.8	6.1	3.1	83.41	11.33	3.95	0.87	0.44
10	10.1	18.33	408.4	353.2	37.2	12.5	3.1	2.4	86.48	9.11	3.06	0.76	0.59
11	12.1	22.77	389.6	652.3	88.0	27.9	8.1	4.3	83.24	11.14	3.53	1.03	1.05
12	16.1	29.22	4441.6	3477.6	724.8	202.3	26.3	10.6	78.30	16.32	4.55	0.59	0.24
13	19.1	34.66	304.7	247.0	30.2	19.8	5.5	2.2	81.06	9.91	6.50	1.81	0.72
18	49.1	89.11	1083.2	945.3	110.7	30.4	5.0	1.8	86.47	10.13	2.78	0.46	0.16
19	55.1	100.00	2473.7	2155.5	255.7	55.3	5.3	1.9	87.14	10.34	2.24	0.21	0.08

are concluded to be a result of extraneous contamination, the nature of which will be discussed under Particle Composition, subsection (c).

12. Although these particle counts are suspect, it can be noted that wear debris concentration levels for these gear test sequences are of the magnitude of 10^7 per 100 ml oil ($> 2\ \mu m$). This level is higher than the debris concentration levels experienced under the bearing test sequences; 10^6 per 100 ml oil.

(b) Particle Size Distribution

1. The size distribution of wear debris contained in lubricant samples taken during gear testing as with particle quantity, was primarily monitored by ferrographic analysis techniques. As described previously, implemented particle counting technique results were suspect.

2. Figures 81 and 82 present plots of ferrographic density readings at two different locations on the ferrogram for gear sequences GG and GH. The entry deposit plot represents debris of a relatively large size, $> 5\ \mu m$ while the 50 mm deposit plot represents debris of a relatively small size, 2-5 μm. By comparing the relationship of these curves over the gear life, one can assess the trends in debris size distribution.

3. As can be observed from these plots, a relatively high ratio of large-to-small debris particles is present during both the wear-in and fatigue wear regimes, as compared to the normal wear regime. This indicates that a significant portion of the debris generated during wear-in and the fatigue wear regime is greater than $5\ \mu m$ in major dimension. Figures 83 and 84 represent high magnification micrographs of debris deposits for sequences GG and GH respectively. These micrographs verify that increases in debris concentration during wear-in and fatigue wear can mainly be attributed to the generation of large debris.

NAEC-92-153



FIGURE 81
GEAR TEST SEQUENCE GG
FERROGRAPH DENSITY DATA

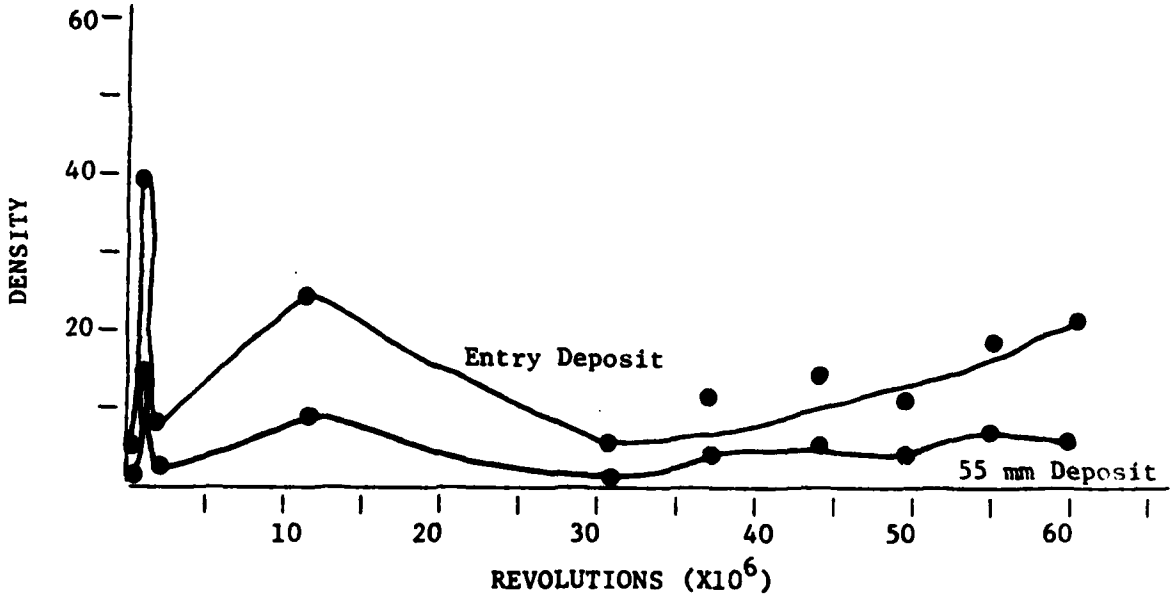


FIGURE 82
GEAR TEST SEQUENCE GH
FERROGRAPH DENSITY DATA



A. 0 m.r.

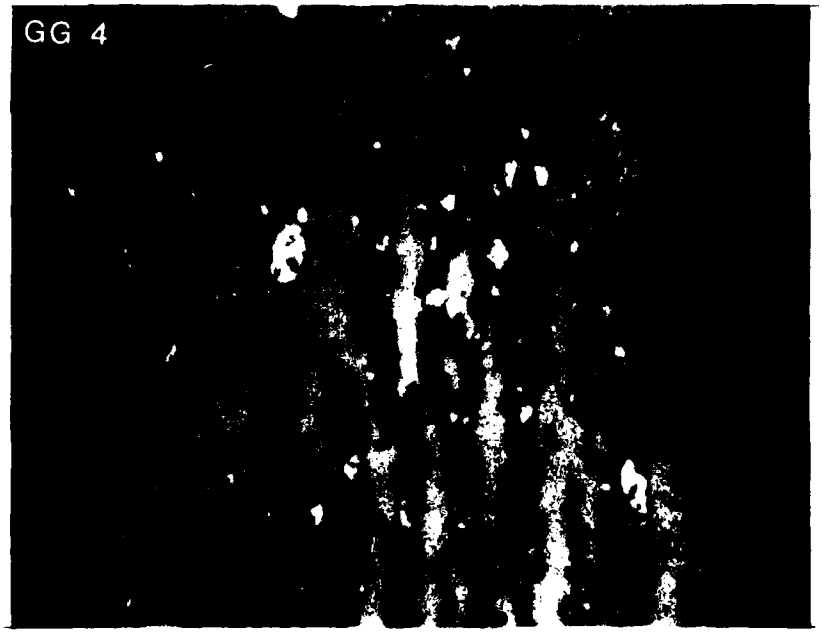


B. 0.5 m.r.

FIGURE 83
GEAR TEST SEQUENCE GG
ENTRY DEPOSIT
HIGH MAGNIFICATION
(Sheet 1 of 5)

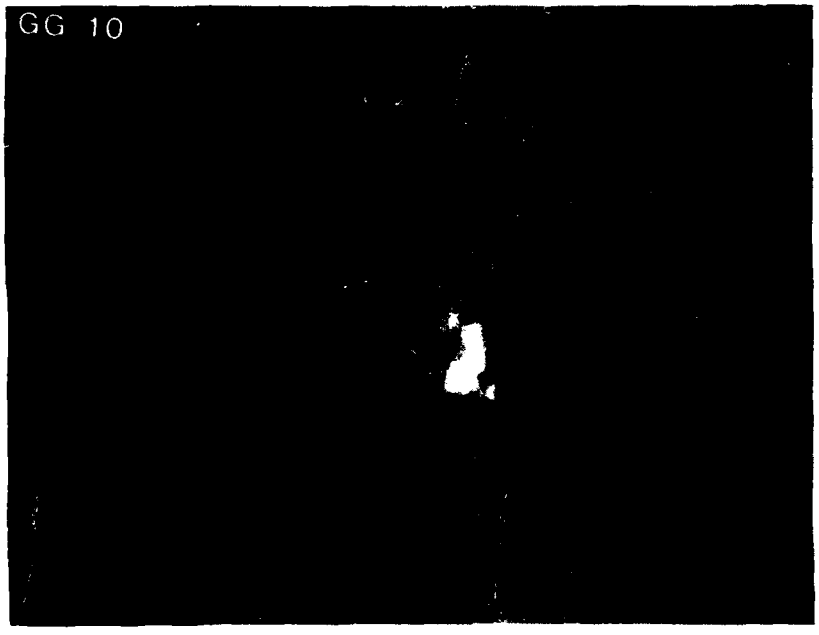


C. 1.1 m.r.



D. 1.7 m.r.

FIGURE 83
GEAR TEST SEQUENCE GG
ENTRY DEPOSIT
HIGH MAGNIFICATION
(Sheet 2 of 5)



E. 10.1 m.r.



F. 16.1 m.r.

FIGURE 83
GEAR TEST SEQUENCE GG
ENTRY DEPOSIT
HIGH MAGNIFICATION
(Sheet 3 of 5)



G. 37.1 m.r.



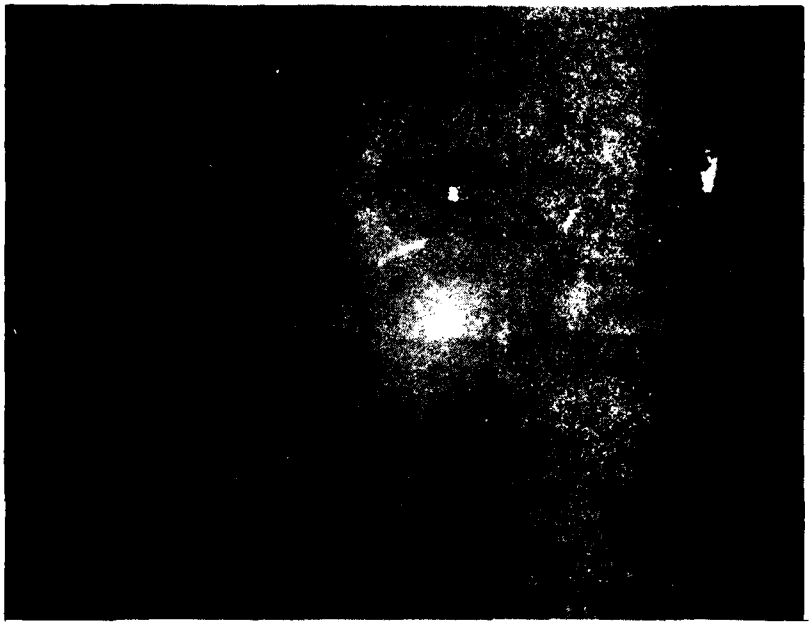
H. 49.1 m.r.

FIGURE S3
GEAR TEST SEQUENCE GG
ENTRY DEPOSIT
HIGH MAGNIFICATION
(Sheet 4 of 5)



I. 55.1 m.r.

FIGURE 83
GEAR TEST SEQUENCE GG
ENTRY DEPOSIT
HIGH MAGNIFICATION
(Sheet 5 of 5)

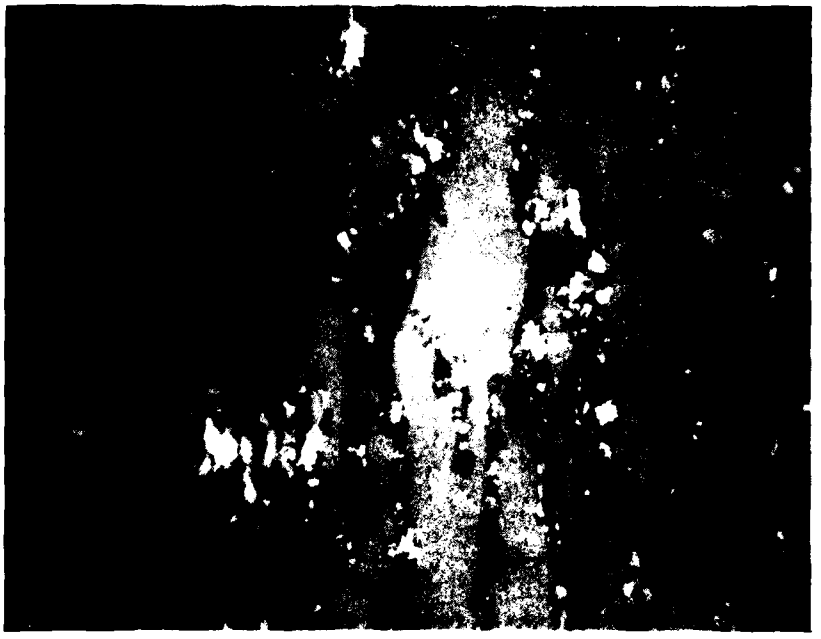


A. 0 m.r.



B. 0 m.r.

FIGURE 84
GEAR TEST SEQUENCE CH
ENTRY DEPOSIT
HIGH MAGNIFICATION
(Sheet 1 of 6)

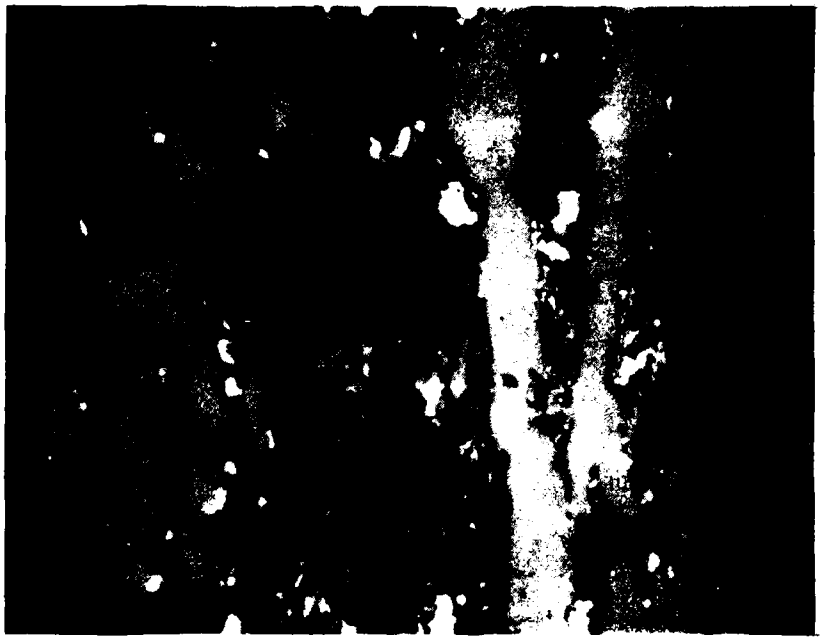


C. 0.5 m.r.



D. 1.1 m.r.

FIGURE 54
GEAR TEST SEQUENCE GH
ENTRY DEPOSIT
HIGH MAGNIFICATION
(Sheet 2 of 2)

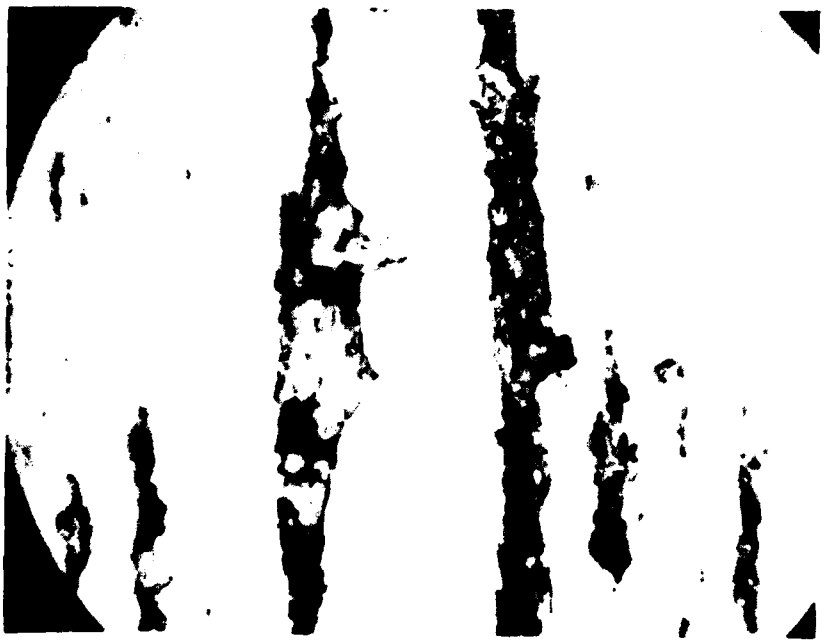


E. 13.1 m.r.



F. 31.1 m.r.

FIGURE 85
GEAR TEST SEQUENCE GH
ENTRY DEPOSIT
HIGH MAGNIFICATION
(Sheet 5 of 6)



G. 37.1 m.r.



H. 43.1 m.r.

FIGURE 84
GEAR TEST SEQUENCE GH
ENTRY DEPOSIT
HIGH MAGNIFICATION
(Sheet 4 of 6)

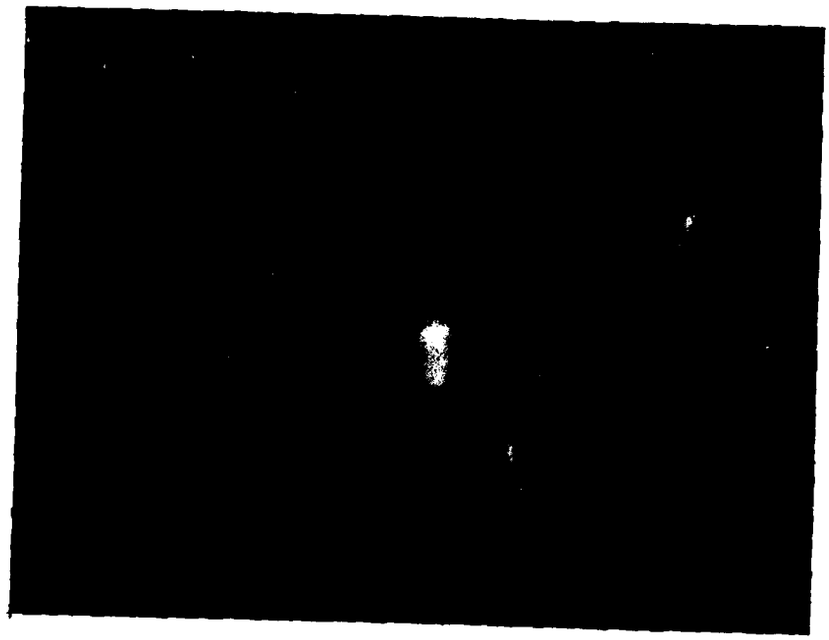


I. 49.1 m.r.



J. 55.1 m.r.

FIGURE 84
GEAR TEST SEQUENCE GH
ENTRY DEPOSIT
HIGH MAGNIFICATION
(Sheet 5 of 6)



K. 59.3 m.r.

FIGURE 84
GEAR TEST SEQUENCE GH
ENTRY DEPOSIT
HIGH MAGNIFICATION
(Sheet 6 of 6)

4. It can also be noted that the ratio of large-to-small particles for the fatigue wear regime is significantly higher than the ratio exhibited for the wear-in regime.

5. Figures 85 and 86 present plots of ferrographic density readings at two different locations on the ferrogram for gear sequences GD and GE respectively. By comparing the relationship of these curves over the gear life one can assess the trends in debris size distribution.

6. As previously mentioned test sequences GD and GE fall within the scuffing gear test group. These sequences were subjected to a highly accelerated test and as such did not experience a traditional wear-in and normal wear pattern. The severity of the test resulted in the progression of scuffing throughout the test. Contrary to previously cited abnormal wear modes, it can be noted from these plots that there exists a relatively high proportion of small debris as compared to large debris. This indicates that a significant portion of the debris generated during a scuffing wear regime is small debris, less than 5 μm in major dimension. Scuffing is the first abnormal wear regime identified under this program, that has resulted in a shift in the debris size distribution toward the small debris region. Figures 87 and 88 represent high magnification micrographs of debris deposits for sequences GD and GE. These micrographs verify that increases in debris concentration during gear scuffing can mainly be attributed to the generation of small debris.

7. Figures 89 and 90 represent plots of average scuffing for test sequences GD and GE. It can be noted from these plots that they can be directly correlated with the 50 mm deposit density plots presented in Figures 85 and 86.

8. Figure 91 represents a plot of the average scuffing for gear test sequence GH. Although the scuffing level is relatively low during this test, the trend directly correlates with the 50 mm deposit density plot

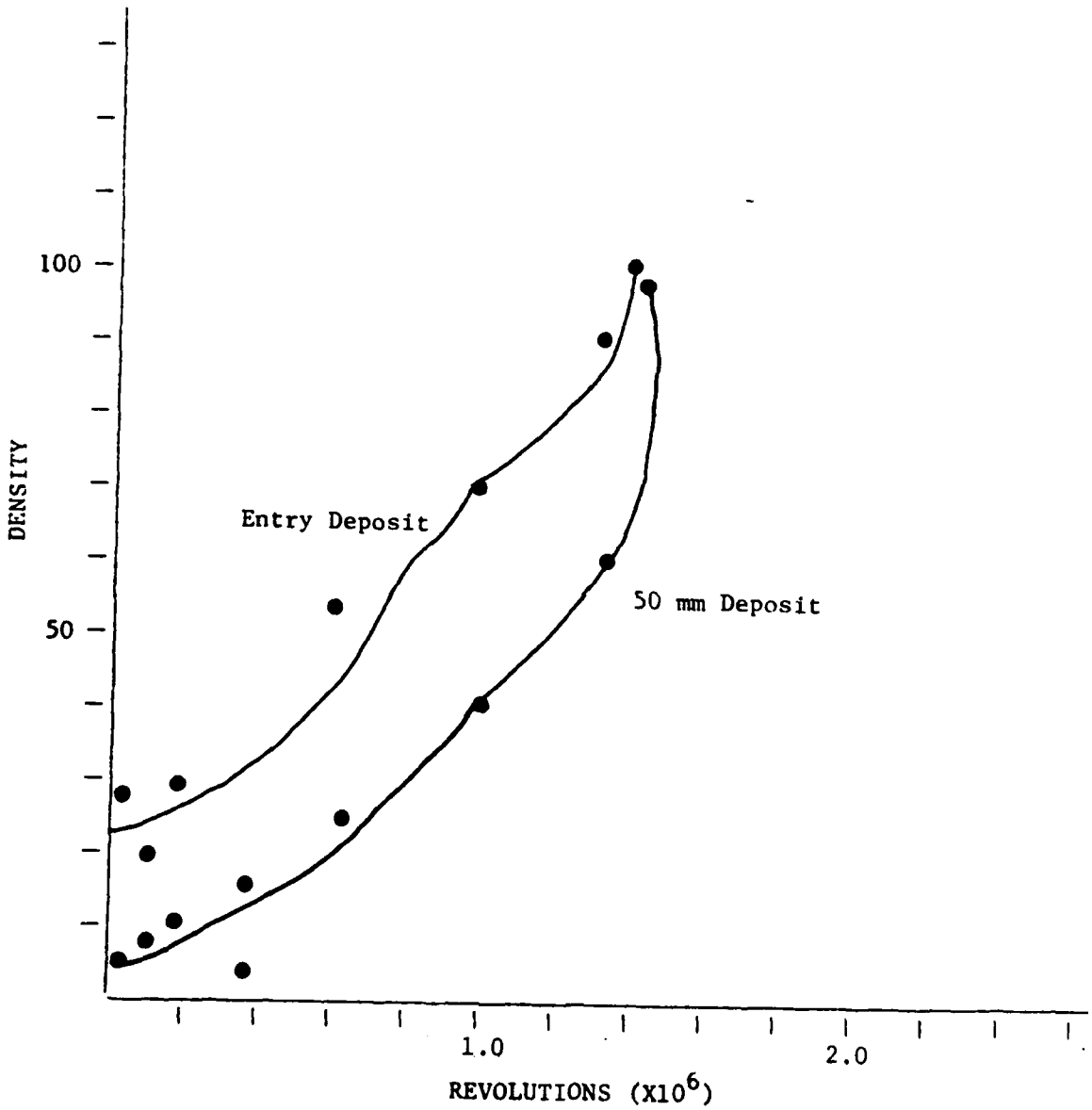


FIGURE 85
GEAR TEST SEQUENCE GD
FERROGRAPH DENSITY DATA

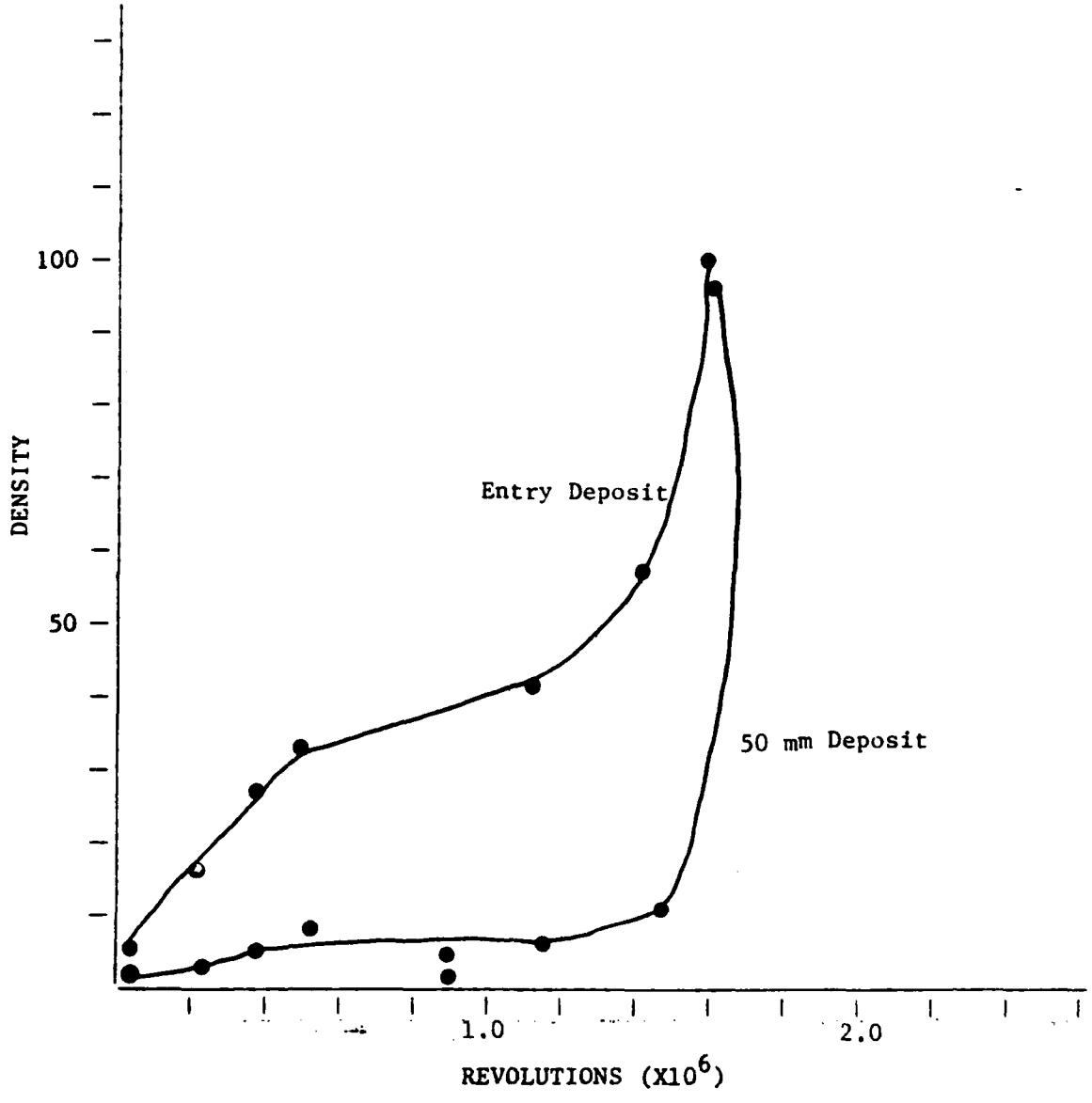


FIGURE 86
GEAR TEST SEQUENCE GE
FERROGRAPH DENSITY DATA



A. 0 m.r.



B. 0.1 m.r.

FIGURE 87
GEAR TEST SEQUENCE GD
ENTRY DEPOSIT
HIGH MAGNIFICATION
(Sheet 1 of 4)

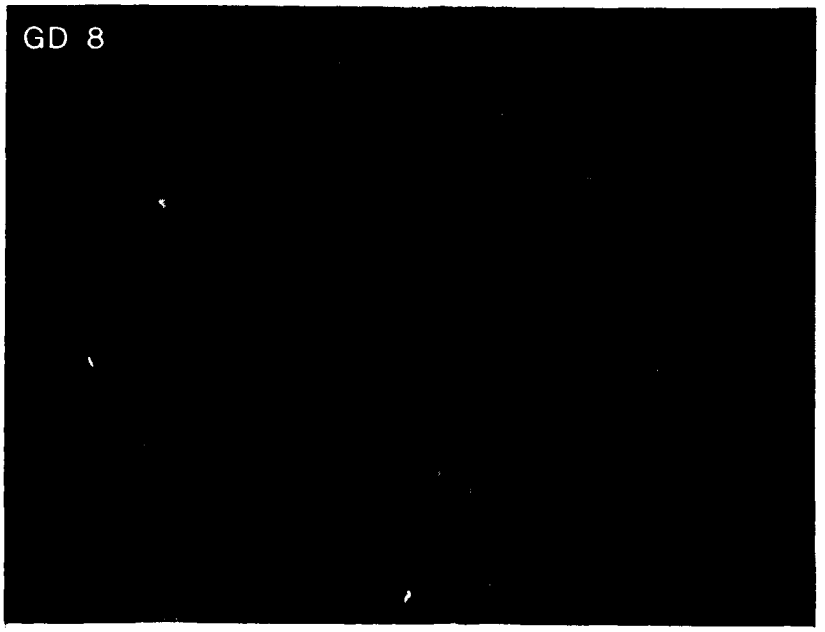


C. 0.2 m.r.



D. m.r.

FIGURE
GEAR TEST SEQ
ENTRY
HIGH MACH
(Sh



E. 0.7 m.r.



F. 1.0 m.r.

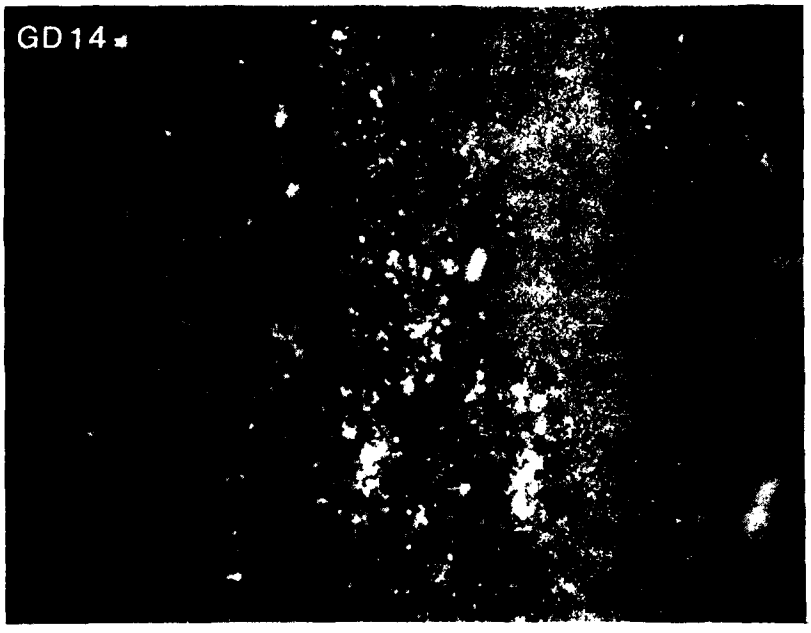
FIGURE 87

GEAR TEST SEQUENCE GD

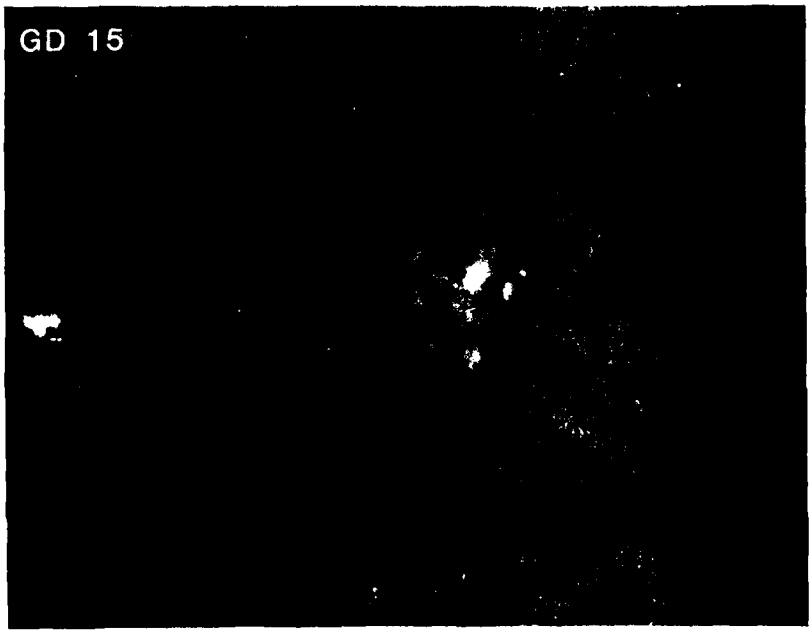
ENTRY DEPOSIT

HIGH MAGNIFICATION

(Sheet 3 of 4)



G. 1.3 m.r.



H. 1.4 m.r.

FIGURE 3-7

GEAR TEST SEQUENCE

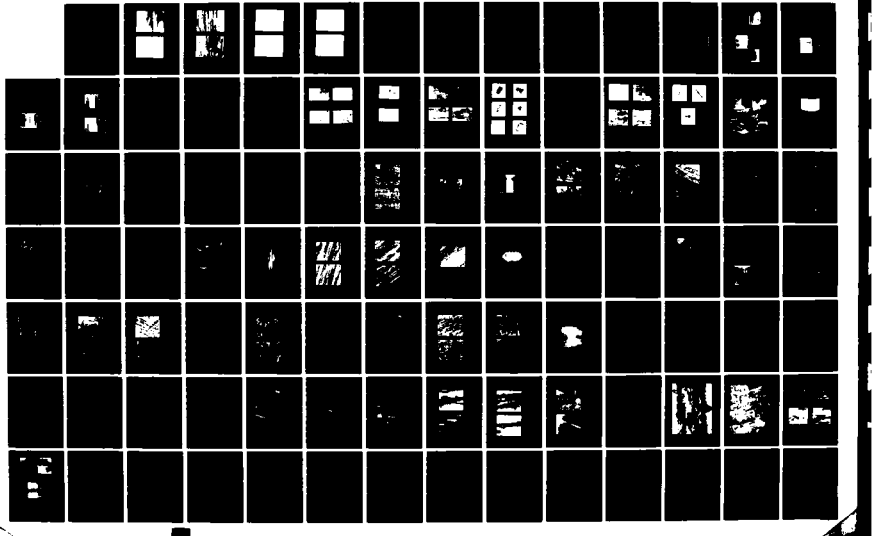
ENTRY DEPOSIT

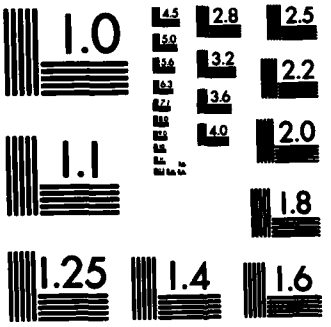
HIGH MAGNIFICATION

(Sheet 4)

AD-A122 156 OIL ANALYSIS(U) NAVAL AIR ENGINEERING CENTER LAKEHURST 4/6
NJ SUPPORT EQUIPMENT ENGINEERING DEPT P B SENHOLZI
23 AUG 82 NAEC-92-153

UNCLASSIFIED F/G 11/8 NL

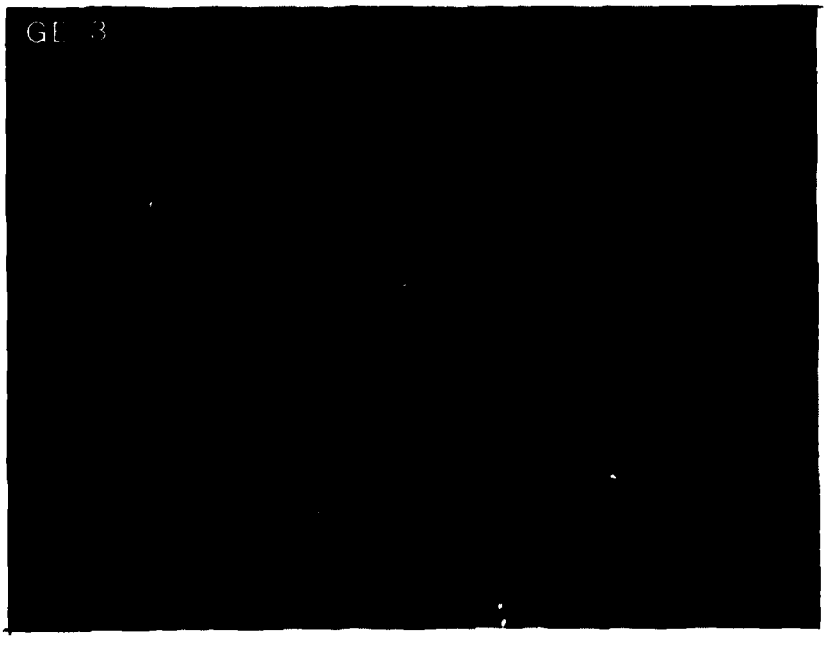




MICROCOPY RESOLUTION TEST CHART
NATIONAL BUREAU OF STANDARDS-1963-A



A. 0 m.r.



B. 0.2 m.r.

FIGURE 88
GEAR TEST SEQUENCE GE
ENTRY DEPOSIT
HIGH MAGNIFICATION
(Sheet 1 of 4)



C. 0.3 m.r.

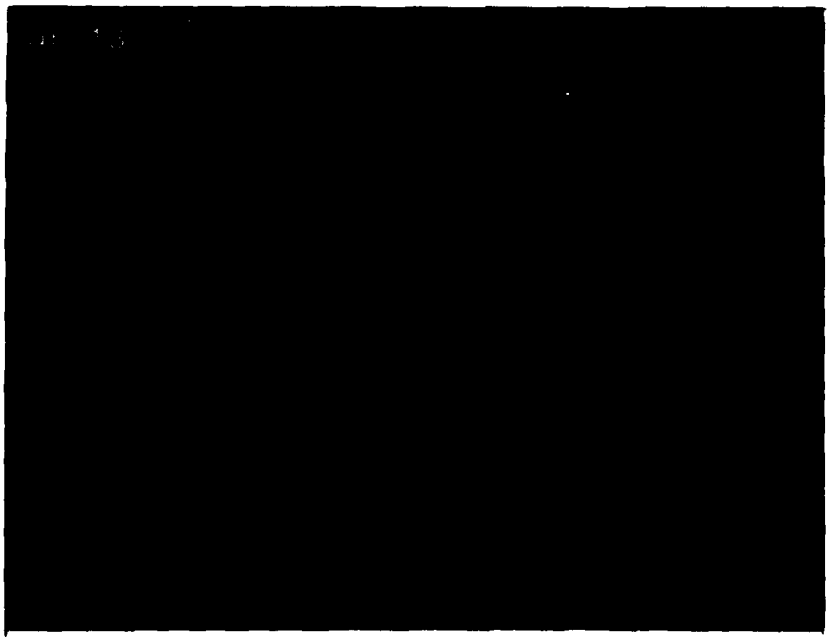


D. 0.4 m.r.

FIGURE 88
GEAR TEST SEQUENCE GE
ENTRY DEPOSIT
HIGH MAGNIFICATION
(Sheet 2 of 4)



E. 0.9 m.r.



F. 1.2 m.r.

FIGURE 88
GEAR TEST SEQUENCE GE
ENTRY DEPOSIT
HIGH MAGNIFICATION
(Sheet 3 of 4)



G. 1.4 m.r.



H. 1.5 m.r.

FIGURE 88
GEAR TEST SEQUENCE GE
ENTRY DEPOSIT
HIGH MAGNIFICATION
(Sheet 4 of 4)

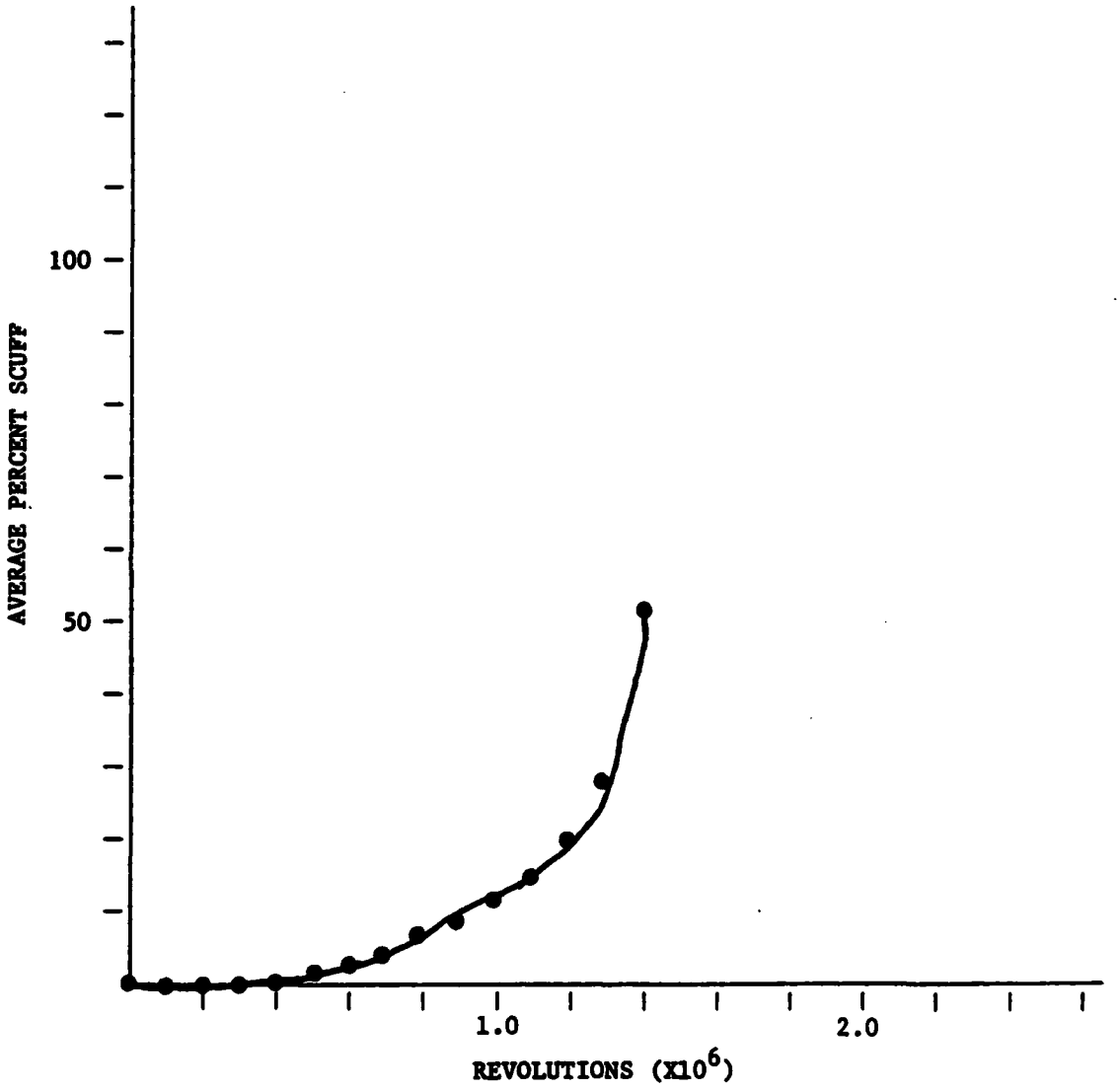


FIGURE 89
GEAR TEST SEQUENCE GD
SCUFF VERSUS RUNNING TIME

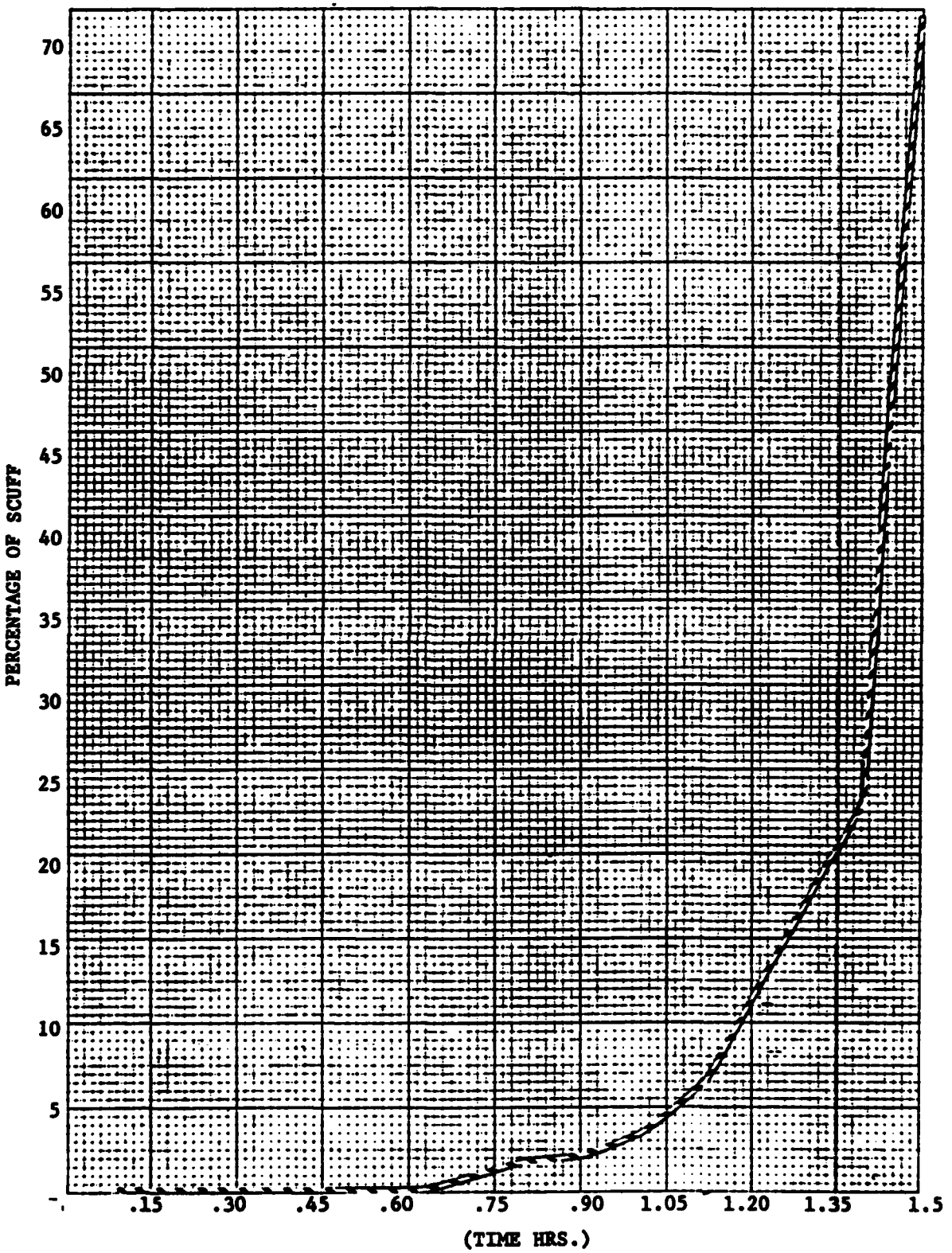


FIGURE 90

GEAR TEST SEQUENCE GE AVERAGE PERCENT SCUFF VERSUS WEAR LIFE

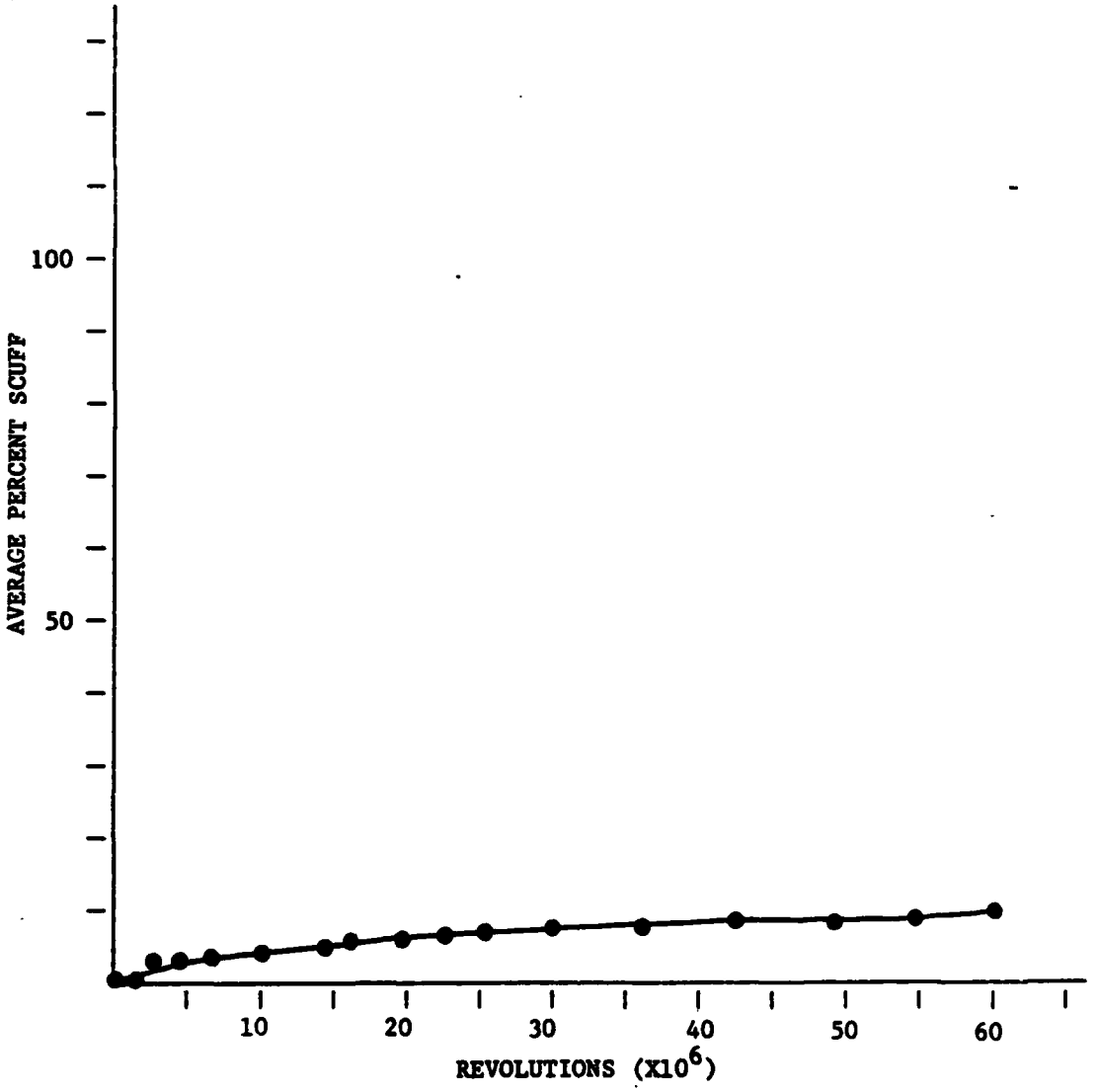


FIGURE 91

GEAR TEST SEQUENCE GH

AVERAGE PERCENT SCUFF VERSUS RUNNING TIME

presented in Figure 82. [With the exception of the plot anomalies caused by the fatigue pit (15 MR) and the oil addition (30 MR).] This correlation further reinforces the generation of small debris during the scuffing wear regime.

9. The above distribution observations were valid for all testing under both groups of the gear test sequences. Figure 92 represents a simplistic presentation of this shift in particle size distribution.

10. Figures 93, 94, 95, 96, and 97 represent spectrometric iron (Fe) concentration plots for gear test sequences GA, GC, GD, GE, GF, GG, GH, and GI. It is apparent from these plots that spectrometric oil analysis is very effective in monitoring gear scuffing and ineffective in monitoring gear pitting. This behavior is consistent with the argument that spectrometric analysis is insensitive to large debris particles. Fatigue pitting has been shown to generate large debris and thus falls outside the spectrometers upper sensitivity limit. Scuffing has been shown to generate small debris and thus falls within the spectrometers sensitivity limits. A detailed description of this effect is presented in Section VI.

(c) Particle Composition

1. Gear testing was designed in such a way as to minimize lubricant borne debris other than that contributed by the test gear set. As a result, debris composition should not play an important role in this debris analysis effort.

2. However, due to the utilization of the ryder gear test machine as the gear test platform, extraneous contamination control was difficult. Tables 34, 35, 36, and 37 represent summaries of spectrometric analysis reading from gear sequences GD, GE, GG, and GH. As can be observed from these tables, the test systems exhibited significant levels of both silicon and titanium. These contaminants, although having minimal effect on the ferrographic analysis, significantly effected sample particle counting techniques.

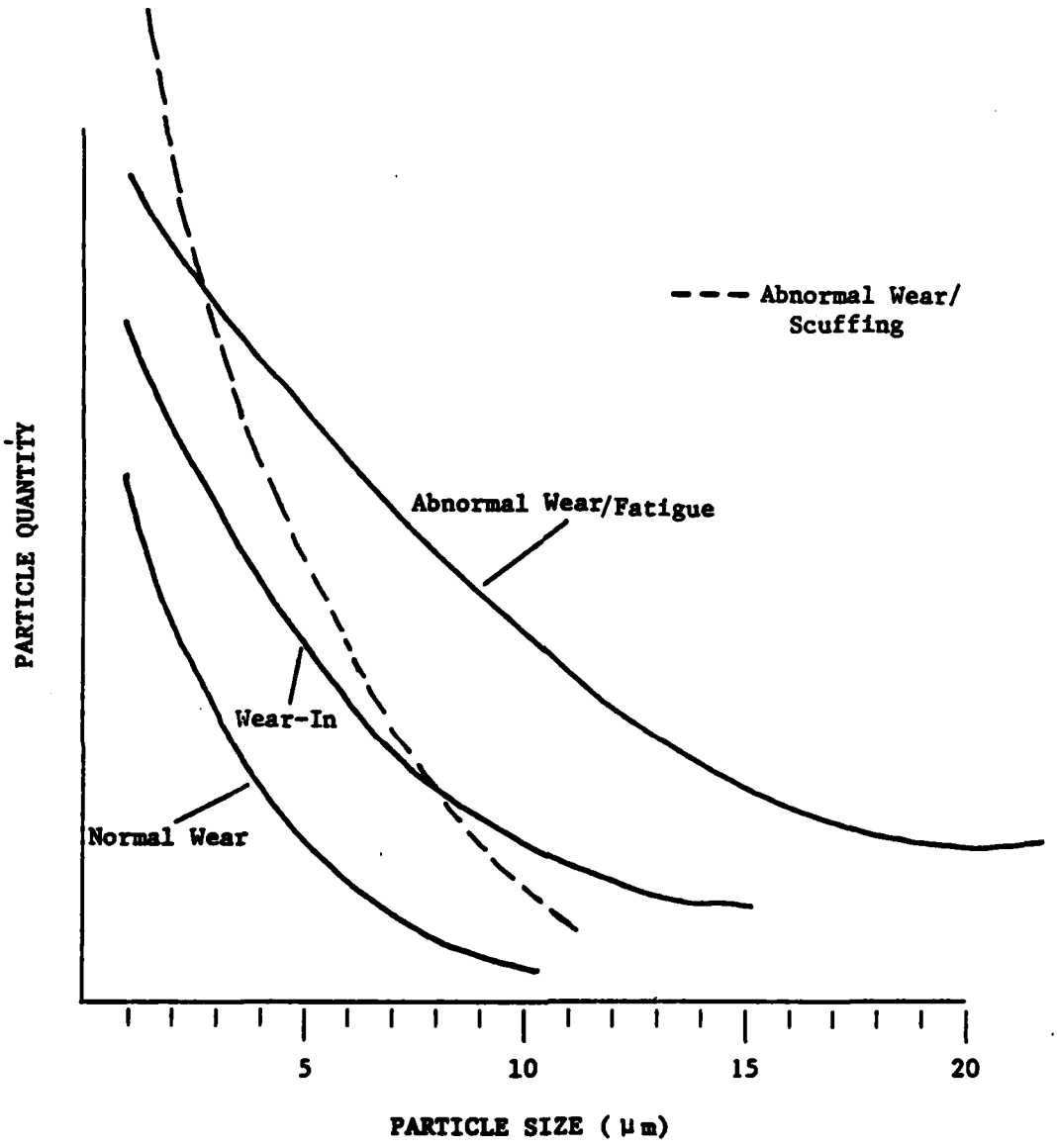


FIGURE 92
PARTICLE SIZE DISTRIBUTION VERSUS WEAR REGIME
GEAR TEST SEQUENCES

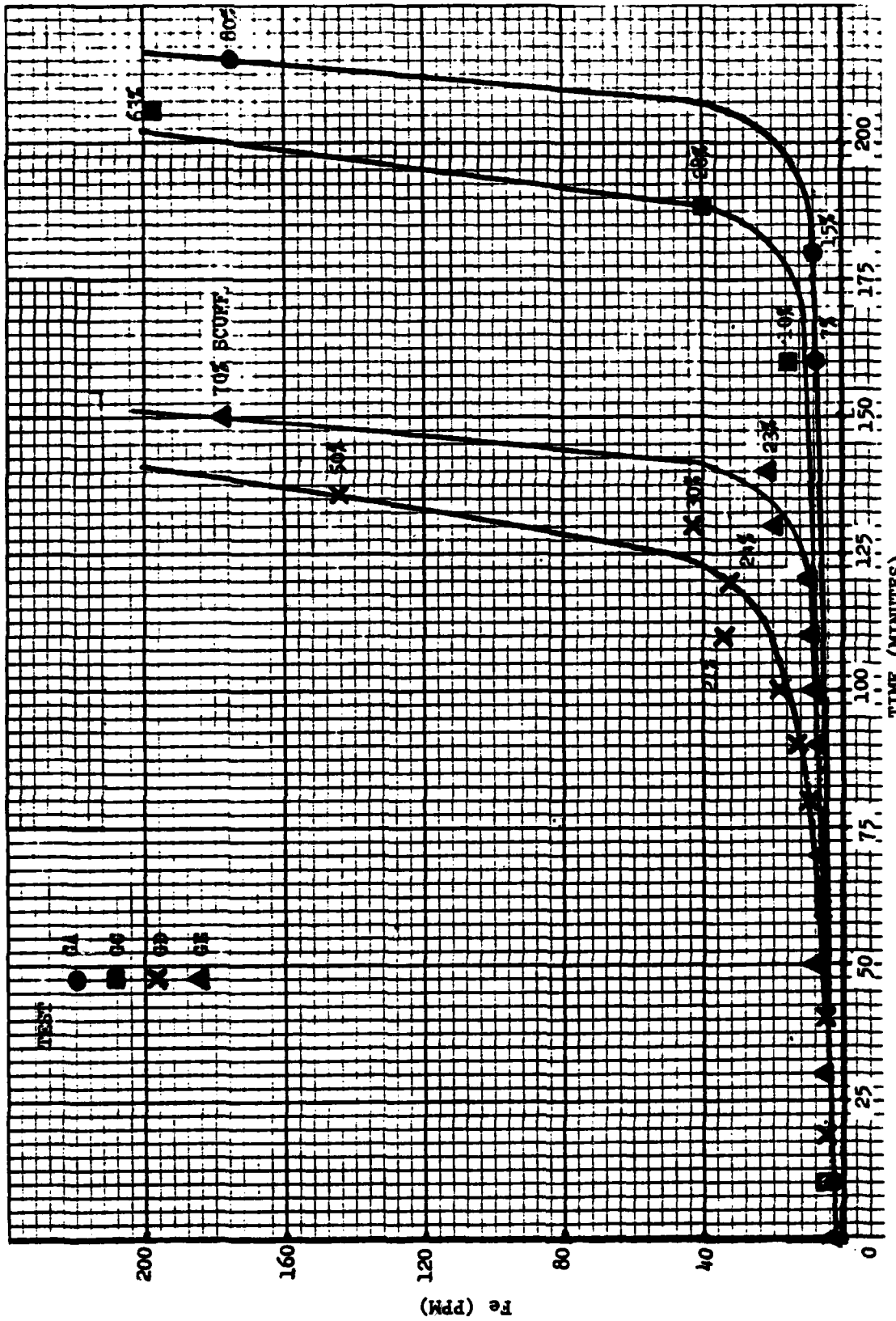


FIGURE 93. OIL ANALYSIS PROGRAM GEAR SCUFFING TESTS

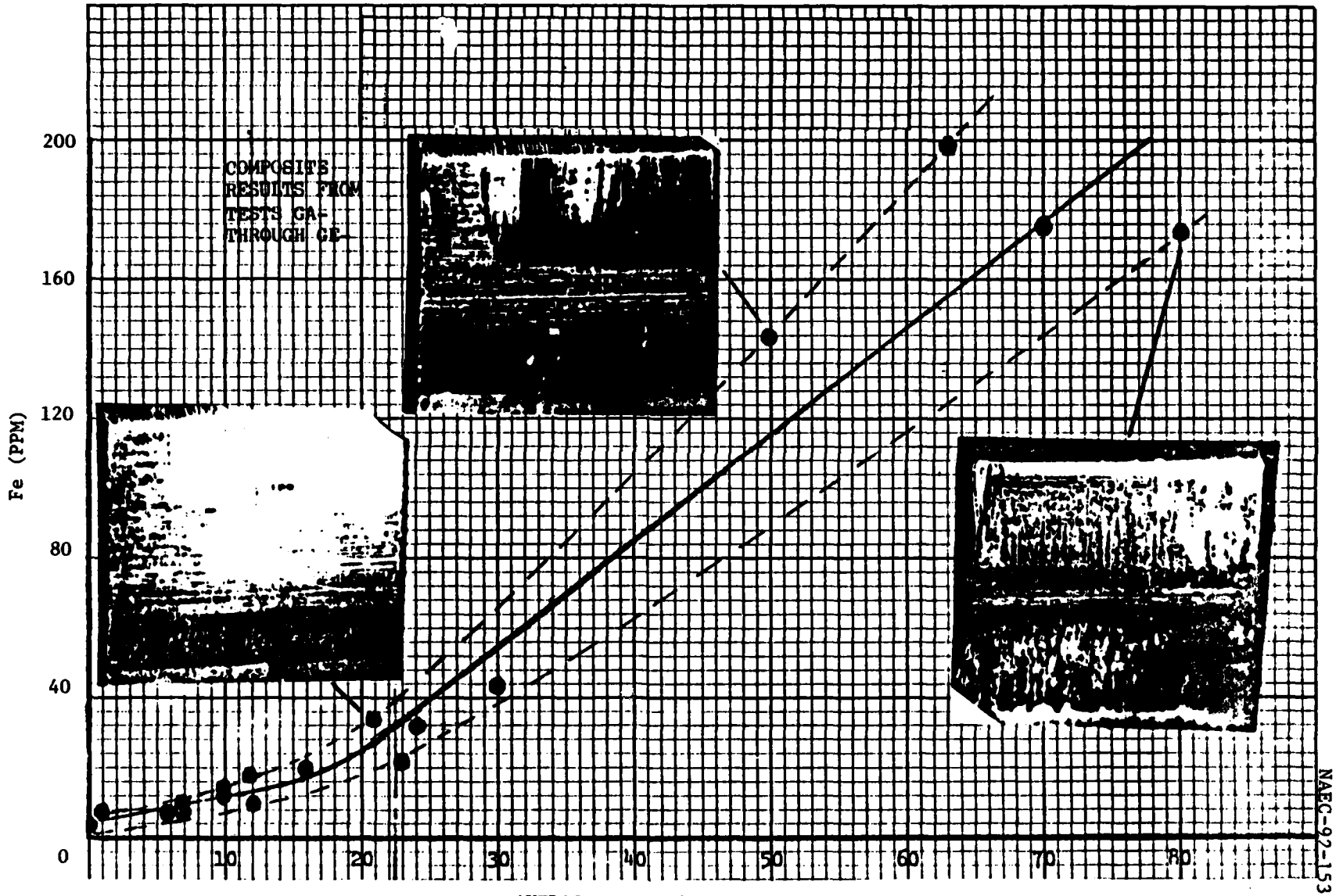


FIGURE 94. OIL ANALYSIS PROGRAM GEAR SCUFFING TESTS

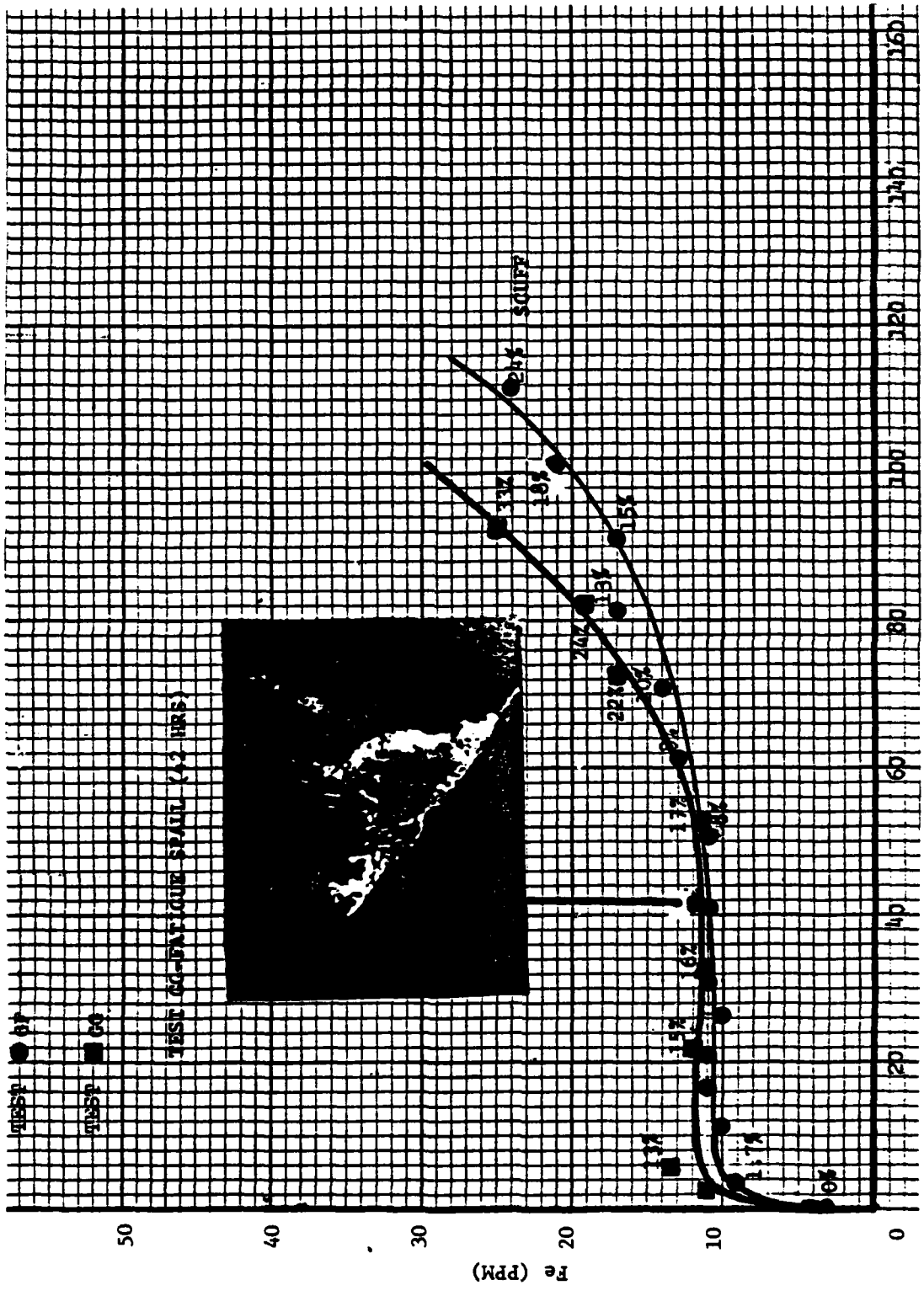


FIGURE 95. OIL ANALYSIS PROGRAM GEAR NORMAL WEAR/FATIGUE TESTS

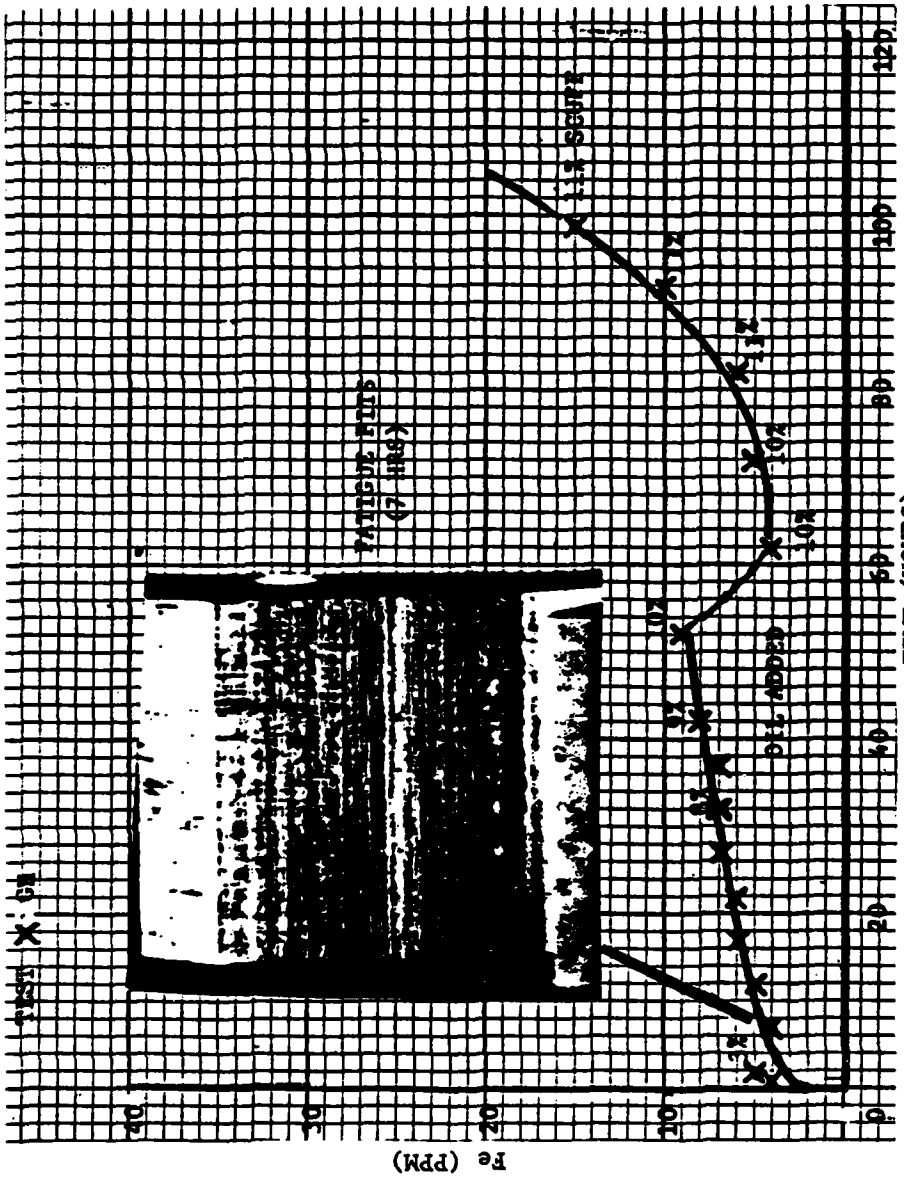


FIGURE 96. OIL ANALYSIS PROGRAM GEAR NORMAL WEAR/FATIGUE TESTS

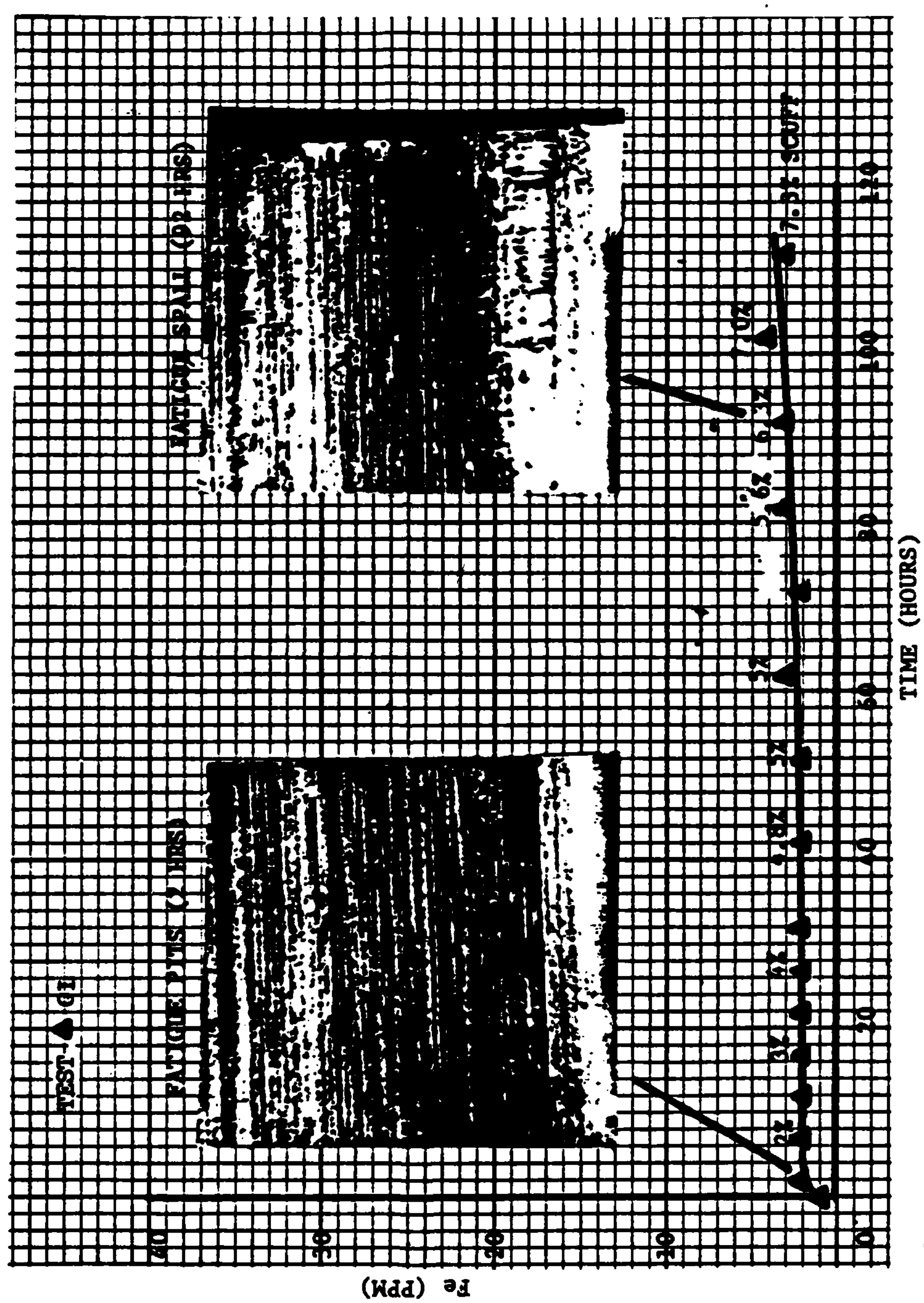


FIGURE 97. OIL ANALYSIS PROGRAM GEAR NORMAL/WEAR FATIGUE TESTS

TABLE 34. SPECTROMETRIC READING, GEAR GD

EVENT	TIME (MIL REVS)	PERCENT TIME	FE (IRON)	SI (SILICON)	SN (TIN)	TI (TITANIUM)	MO (MOLYBDENUM)
1	0.0	0	3	14	16	2	2
2	0.1	7	4	6	15	2	2
3	0.2	14	6	15	14	2	2
4	0.3	21	9	11	14	1	2
5	0.4	28	7	9	15	2	2
6	0.5	35	7	16	17	2	2
7	0.6	42	7	8	16	2	2
8	0.7	50	8	8	15	2	2
9	0.8	57	10	11	16	2	2
10	0.9	64	13	12	17	2	2
11	1.0	71	18	13	15	2	2
12	1.1	78	34	21	19	2	2
13	1.2	85	32	23	15	2	2
14	1.3	92	43	26	15	2	2
15	1.4	100	44	29	15	2	2

TABLE 35. SPECTROMETRIC READING, GEAR GE

EVENT	TIME (MIL REVS)	PERCENT TIME	FE (IRON)	SI (SILICON)	SN (TIN)	TI (TITANIUM)	MO (MOLYBDENUM)
1	0.0	0	2	8	6	2	0
2	0.1	6	4	5	9	2	0
3	0.2	13	5	7	5	2	0
4	0.3	20	5	11	7	2	0
5	0.4	26	5	7	9	2	1
6	0.5	33	8	10	6	2	2
7	0.6	40	6	9	11	3	1
8	0.7	46	6	13	7	2	1
9	0.8	53	7	13	6	2	1
10	0.9	60	6	13	7	3	1
11	1.0	66	8	15	7	2	0
12	1.1	73	9	15	10	3	1
13	1.2	80	9	23	7	2	1
14	1.3	86	19	20	7	2	1
15	1.4	93	21	24	7	2	0
16	1.5	100	177	30	8	3	0

TABLE 36. SPECTROMETRIC READING, GEAR GG

EVENT	TIME (MIL REVS)	PERCENT TIME	FE (IRON)	SI (SILICON)	SN (TIN)	TI (TITANIUM)	MO (MOLYBDENUM)
1	0.0	0	4	6	13	1	2
2	0.5	0	4	5	13	1	3
3	1.1	1	11	8	14	2	2
4	1.7	3	11	9	14	1	2
5	2.3	4	13	12	13	1	3
6	2.9	5	13	13	14	2	3
7	3.5	6	14	18	15	1	3
8	4.1	7	13	19	13	2	3
9	7.1	12	10	21	13	2	3
10	10.1	18	9	30	12	1	3
11	13.1	23	12	32	11	2	3
12	16.1	29	11	29	10	2	3
13	19.1	34	11	40	11	2	3
14	25.1	45	12	43	12	2	4
15	31.1	56	11	36	14	2	4
16	37.1	67	10	34	15	2	4
17	43.1	78	17	39	13	1	3
18	49.1	89	19	35	12	2	3
19	55.1	100	25	37	15	2	3

TABLE 37. SPECTROMETRIC READING, GEAR GH

EVENT	TIME (MIL REVS)	PERCENT TIME	FE (IRON)	SI (SILICON)	SN (TIN)	TI (TITANIUM)	MO (MOLYBDENUM)
1	0.0	0	1	0	16	2	1
2	0.0	0	1	0	11	5	1
3	0.5	0	4	0	15	28	2
4	1.1	1	5	0	13	45	1
5	4.1	6	4	0	13	63	2
6	7.1	11	5	0	18	85	1
7	10.1	17	6	0	13	97	2
8	13.1	22	6	0	13	100	1
9	16.1	27	7	0	14	99	1
10	19.1	32	7	0	13	98	1
11	22.1	37	7	0	13	99	1
12	25.1	42	8	0	15	104	1
13	31.1	52	9	0	13	66	1
14	37.1	62	4	0	16	23	2
15	43.1	72	5	0	12	23	1
16	49.1	82	6	0	13	23	2
17	55.1	92	10	0	12	22	2
18	59.3	100	15	0	14	25	2

(d) Particle Morphology

1. The last factor to be considered under gear testing wear particle analysis is particle morphology.

2. Gear wear-in resulted in the generation of free metal particles. These particles consisted primarily of rubbing wear and wear-in particles. The description of rubbing wear particles, as presented under the ball bearing section, is applicable to this case, and as a result will not be repeated here. Gear wear-in debris results from the presence of machined surface finishes. The break-in of these grooved surfaces creates elongated free metal particles. They generally exhibit a length to width ratio of 5:1. Their actual size and thickness is dependent on groove geometry, however, they generally fall within the 5-50μm range in major dimension. Typical gear wear-in debris paricles are presented in Figure 98.

3. Gear normal wear particulates are dominated by free metal platelets. These platelets are mainly composed of rubbing wear particles. This particulate generally exhibits a length to width ratio of 2:1 and a major dimension to thickness ratio of 10:1. Particle size, ranges up to 15μm in major dimension, however, the majority of the particles are less than 2μm in major dimension. The description of rubbing wear presented previously, is applicable to this case and can be referred to for a more detailed treatment.

4. Abnormal gear wear particulates will be covered from both the aspects of fatigue/pitting and scuffing. Gear fatigue spall particles are smooth surface free metal particles. They exhibit a length-to-width ratio of 4:1 and a major dimension to thicksness ratio of approximately 5:1. Particle size ranges up to 150μm in major dimension; however, the majority fall within the 15-25 μm range.

5. Figure 99 presents micrographs of typical gear fatigue particles.



A. 225X



B. 450X



C. 1000X



D. SEM 1000X

FIGURE 98
GEAR WEAR-IN PARTICLES
(Sheet 1 of 2)



E. 1000X



F. 1000X

FIGURE 98
GEAR WEAR-IN PARTICLES
(Sheet 2 of 2)



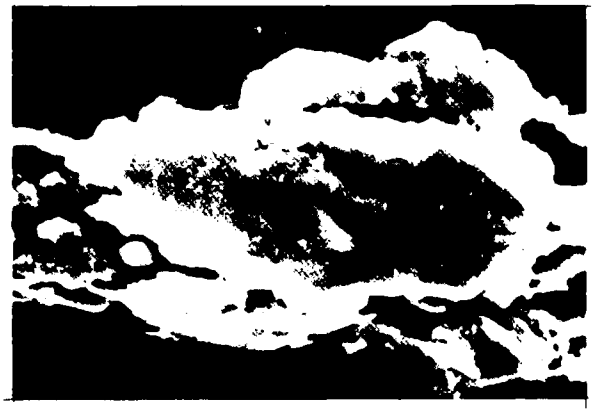
A. 225X



B. 450X



C. SEM 1000X



D. SEM 3000X

FIGURE 99
GEAR FATIGUE PARTICLES
(Sheet 1 of 2)

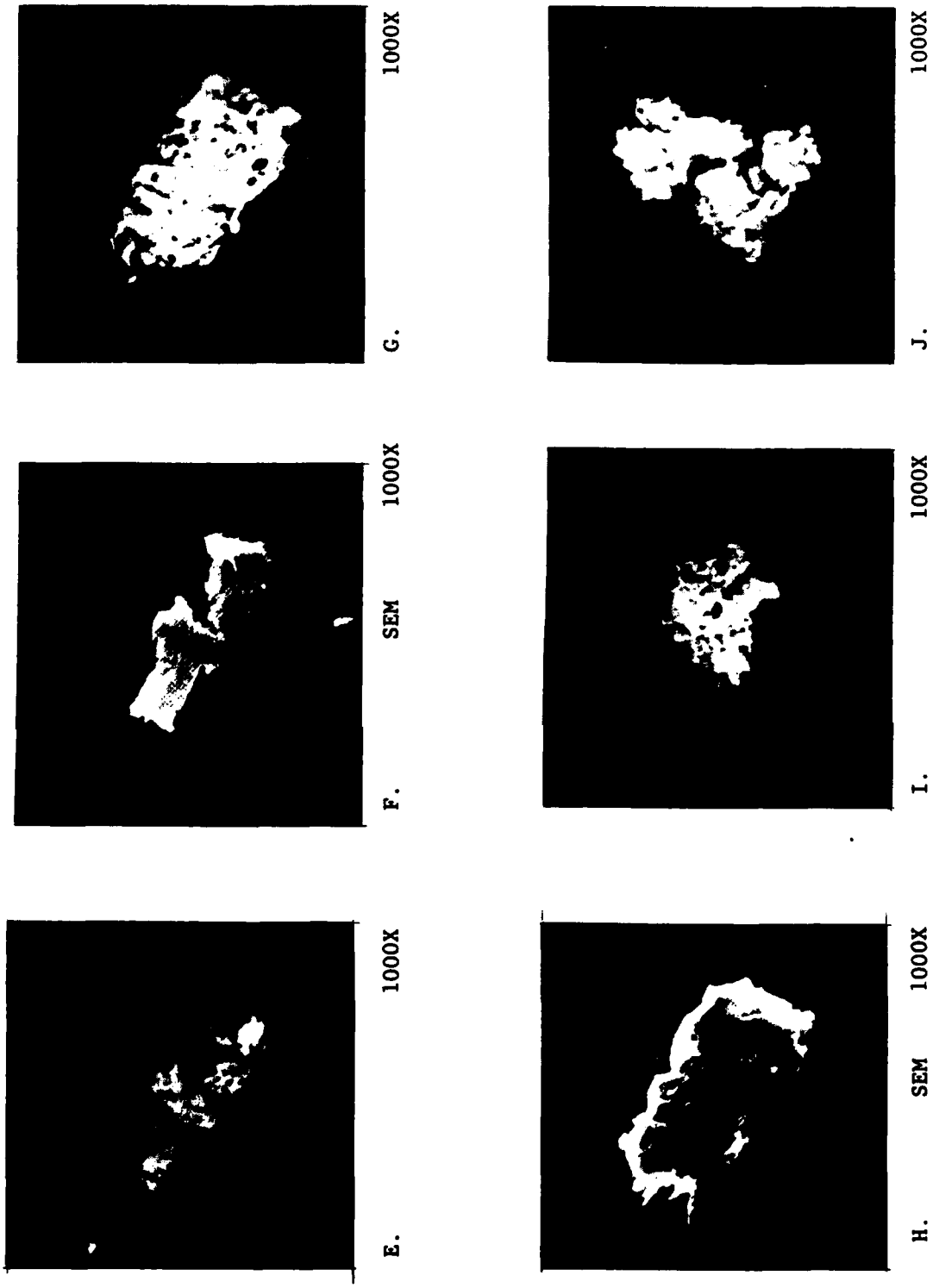


FIGURE 99

GEAR FATIGUE PARTICLES

(Sheet 2 of 2)

6. Gear scuffing particles are free metal platelets with some indications of surface oxidation. They exhibit a major dimension to width ratio of about 3:1 and a major dimension to thickness ratio of approximately 10:1. Scuffing particles range in size up to 150μm in major dimension, however, the majority is less than 5μm in major dimension. As a result of the thermal nature of gear scuffing, quantities of oxide may be present in the respective debris as well as the presence of partial particle surface oxidation. Figure 100 represents micrographs of typical gear scuffing particles.

7. The particle morphology summary presented above is typical for the gear test sequences conducted under this program. Particle type frequency data is presented for gear sequences GD, GE, GG, and GH under Appendices J, K, L, and M respectively.

5. SLIDING BENCH TESTING. Sliding contact bench testing was performed by the Franklin Institute Research Laboratories (FIRL). Details of this test effort and respective analysis effort is provided in the following paragraphs.

a. Sliding Contact Test Procedure

(1) The fourth and last wear mechanism to be considered under this program is piston/sylinder sliding contact. Exact component configuration is not as straight-forward a selection process as with the previous mechanisms. After considerable investigation it was decided that an evaluation of sliding contact could best be achieved by running an engine under controlled laboratory conditions. Selection considerations included (1) high temperature, (2) type of lubrication, (3) effect of corrosion products from both combustion and lubricant breakdown, and (4) blowby effects in distributing particles produced by the wear process as well as contaminants.

(2) The test engine, a Petter stationary diesel, Figure 101, is a 4-cycle, air-cooled, vertical, one-cylinder unit. The cylinder, Figure 102, is one



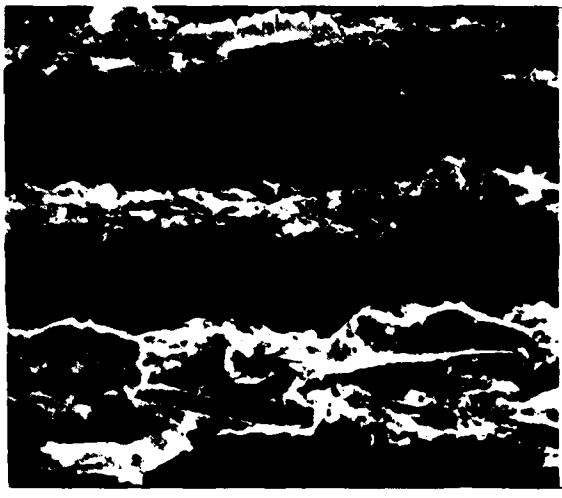
A. 225X



B. 450X



C. 1000X



D. SEM 1000X

FIGURE 100

GEAR SCUFFING PARTICLES

(Sheet 1 of 2)



E. 1000X



F. 1000X



G. 1000X

FIGURE 100
GEAR SCUFFING PARTICLES
(Sheet 2 of 2)

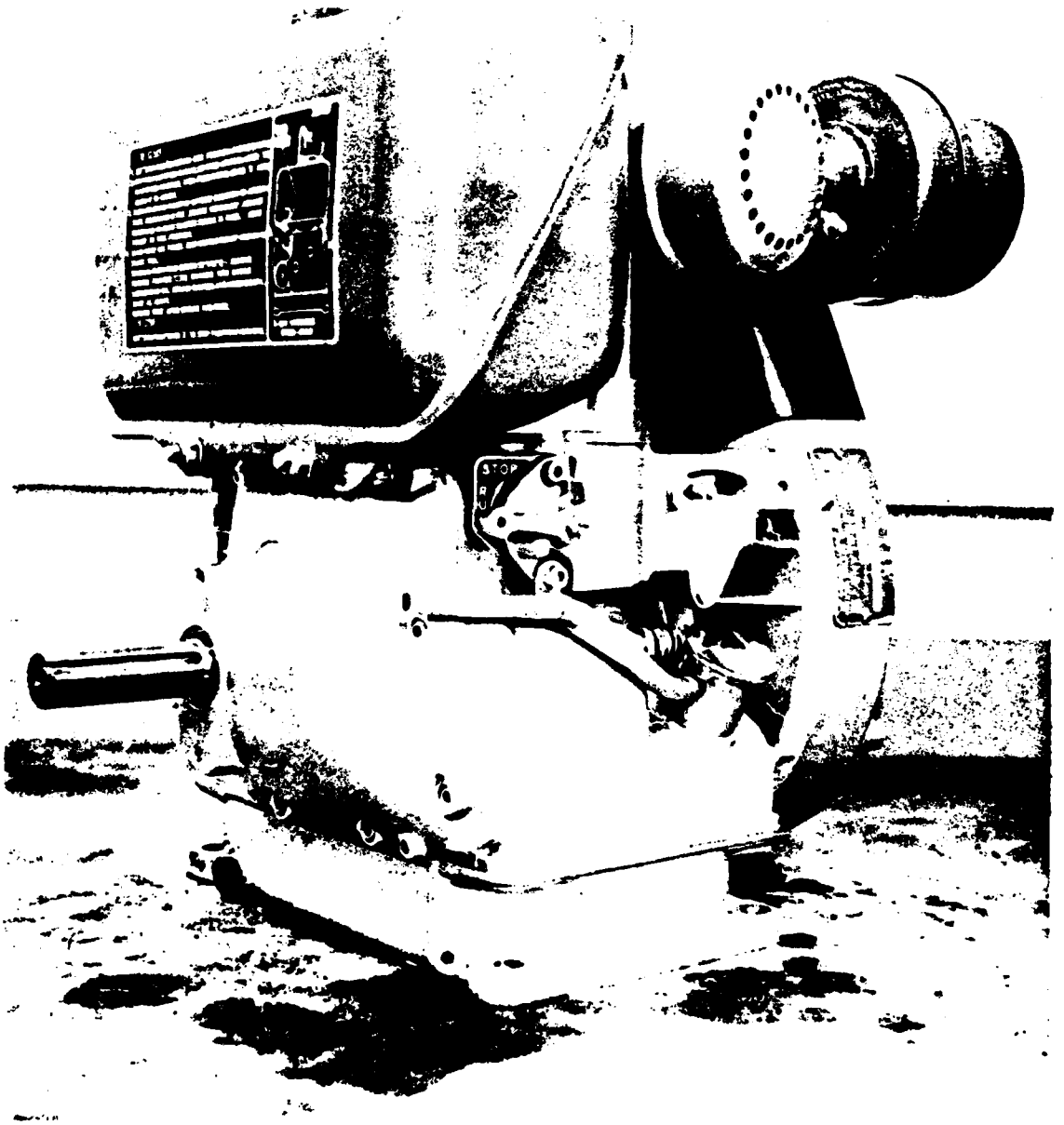


FIGURE 101
SINGLE-CYLINDER TEST ENGINE

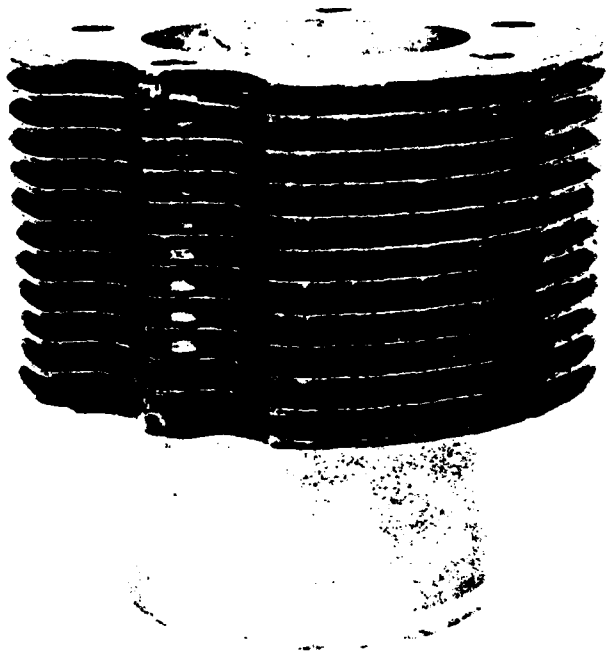


FIGURE 102
CYLINDER

piece, cast iron with fins and is separable which makes for easy assembly and disassembly. The piston, Figure 103, is made of aluminum with two compression rings, the top one being chrome plated, and one oil control ring at the bottom of the piston skirt. Crankshaft bearings are aluminum-tin with steel backing. The small end connecting rod bearing is bronze on a steel backing. Other components in the oil wetted system are the rocker arm assembly and the cam shaft gearing. The engine has a variable speed control governor. Bore size in 3 in. and stroke is 2.25 in. with a displacement of 15.9 cubic inches. The engine has a 5 horsepower rating at 3600 rpm. An oil temperature gage was inserted in the bottom of the oil sump for purposes of this test sequence.

(3) A hydraulic system consisting of a pump, a restrictor valve, and a reservoir was used to load the engine. Load was changed by adjusting the restrictor valve and a pressure gage reading is used to calculate horsepower. The pump is directly coupled to the engine and operates at engine output speed which was obtained from an extension shaft mounted on the cam shaft.

(4) The engine was operated at constant speed and load for this program. It was estimated that the pump required 1.5 HP from the engine operating at 1800 rpm to maintain a constant oil gage pressure of 200 psi. NAVAIRENGCEN supplied the oil which was specified as MIL-L-2104 diesel engine lubricating oil.

(5) Immediately at the end of each run, an oil sample was taken from the middle of the sump to avoid sludge from the bottom by means of a large hypodermic needle fastened to a fixed length of copper tubing. The temperature of oil in the sump was also recorded at the same time. Some oil was added periodically to maintain the required level in the engine. However, the amounts were not sufficient to have caused significant dilution effects. The samples obtained were immediately sealed in bottles and the data recorded.

(6) Sample numbers were recorded using a 6 digit numbering system. The first two digits are letters; the first being S and the second representing the build, in this case A is the first build and B the second. The next four



FIGURE 103
PISTON WITH COMPRESSION RINGS AND WRIST PIN IN PLACE.

digits are numbers representing the Julian date. The time at the start of a run, the time of engine shutdown and the time the oil sample was taken were also recorded.

(7) In this test sequence, two techniques for analyzing the oil were employed. Standard spectrometric oil analysis program procedures were applied to part of each sample, while a Ferrogram slide was prepared from another portion of each sample. The particulate matter on the slides was analyzed at FIRL and NAVAIRENGCEN in conjunction with SEM studies of the worn surfaces.

(a) First Build-SA

1. The engine was run for 54 hours 10 minutes and this included 4 short runs and 6 long runs in excess of 7 hours each. Oil samples were taken after each of these runs. A standard commercial grade oil filter (about 40 μm) was used in the lubrication system.

2. Increasingly heavy blowby was observed throughout the testing of this build, and oil contamination particle concentrations increased with each successive spectrometric analysis. The combination of these indicated that considerable wear was sustained by the engine. Upon disassembly, it was determined that the cylinder bore was worn considerably and there was a carbon buildup at the upper end. The piston rings exhibited pronounced wear bands. The most damaging wear had occurred on the wrist pin bearing.

(b) Second Build-SB

1. A new cylinder, piston, piston rings, and connecting rod bearings were used in the second build. The cylinder bore was measured before assembly onto the engine. The whole engine was thoroughly cleaned to remove contaminants, debris, and sludge from the first build. Two flushing runs with fresh oil were made to trap and remove particles from the system. The oil was then changed and the oil filter removed.

2. The engine ran for 103 hours 50 minutes under constant conditions. Fifteen oil samples were taken. As the testing progressed, there was a steady increase in blowby and also in oil leakage from the bottom of the cylinder. There was an increased concentration of impurities reflected in the spectrometric analysis data; however, less wear was indicated than in the first build.

3. Upon disassembly, a crack in the bottom (oil control) piston ring was noted and some wear was evident on the cylinder bore. The cylinder bore was remeasured and Table 38 contains the readings before and after running. The measurements were taken by rotating the cylinder when mounted on a lathe. A dial gauge set at various axial locations inside the cylinder, measured deviations from a preset nominal value. Analysis of this cylinder bore wear data, indicates that on the average, the bore diameter increased by .0024" due to wear after 103 hours and 50 minutes of constant speed and load operation. The table shows the deviation from nominal both before and after running. The locations denoted in inches from the cylinder head surface, encompass those portions of the bore surface worn by the piston rings. The wear is well below the 0.010" level, which the engine manufacturer considers unacceptable wear. The variation in readings between the two planes, indicates some distortion of the cylinder in terms of end squareness, out-of-round and taper. This does have an influence on wear, but in this case did not appear to have a drastic effect.

b. Sliding Contact Surface Monitoring. The major wearing components in the engine were characterized with regard to chemical composition and surface finish in the scanning electron microscope (SEM) in the unrun condition. After the two runs were completed, surface conditions were again analyzed and the results for each of the components are discussed in the following paragraphs. The qualitative chemical analysis findings are summarized in Table 39.

(1) Cylinder Wall

(a) New Cylinder. The as-finished, unrun cylinder wall was relatively rough with three prominent sets of finishing lines. One set of lines

TABLE 38. MEASUREMENT OF WEAR IN CYLINDER BORE DIAMETRAL CHANGE IN TWO PERPENDICULAR PLANES (MEASURED IN .0001")

(SECOND RUN)

DISTANCE FROM HEAD END OF CYLINDER (inches)	FIRST PLANE			SECOND PLANE		
	Before	After	Net	Before	After	Net
1/2	-7	+17	+24	-1	+25	26
3/4	-3	+21	+24	-1	+24	26
1	-1	+23	+24	-2	21	23
1-1/2	-1	+25	+27	-3	20	23
2	-1	+25	+27	-2	20	22
2-1/2	0	_24	_24	-2	18	20
3	0	_33	_33	-2	17	19

TABLE 39. WEAR COMPONENTS

COMPONENT	X-RAY FLUORESCENCE	
	Major Elements	Minor
Cylinder Wall	Fe	Si
Piston Rings	Fe	Cr, Mn, Si
Bottom Ring	Fe	Cr, Mn, Si
Middle Ring	Fe	Cr, Mn, Si
Top Ring	Cr	
Wrist Pin	Fe + Cr	Mn, Si
Wrist Pin Bearing	Cu + Sn	Pt
Large End Connecting Rod Bearing	Al + Sn	

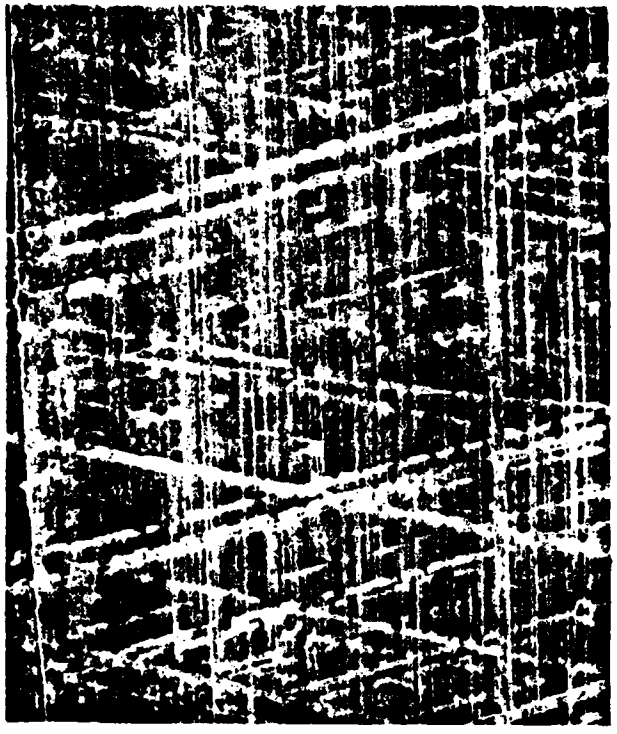
runs axially along the wall while the other two sets cut across each other with each making an angle of about 70° with the axial lines, as shown in Figure 104. The cross-hatch lines are more widely spaced and much coarser in nature and they have tongues of smeared metal associated with them.

(b) After Testing. Following running, the regions at the top and bottom of the piston's stroke (actually the limit of the rings' motion) had the most pronounced wear in the form of shiny circumferential bands around the cylinder wall, Figures 105 and 106. The area between these limits experienced less severe wear with the cross-hatch finishing lines being smoothed over and the tongues of metal either worn off or deformed into the low areas of the surface, Figure 107. The general nature of the wear was the same on both runs, but based upon the extent of the shiny areas, the total amount of wear appeared greater in the cylinder from the first run. Measurements of the cylinder's bore taken before and after running in the second run were given in Table 38.

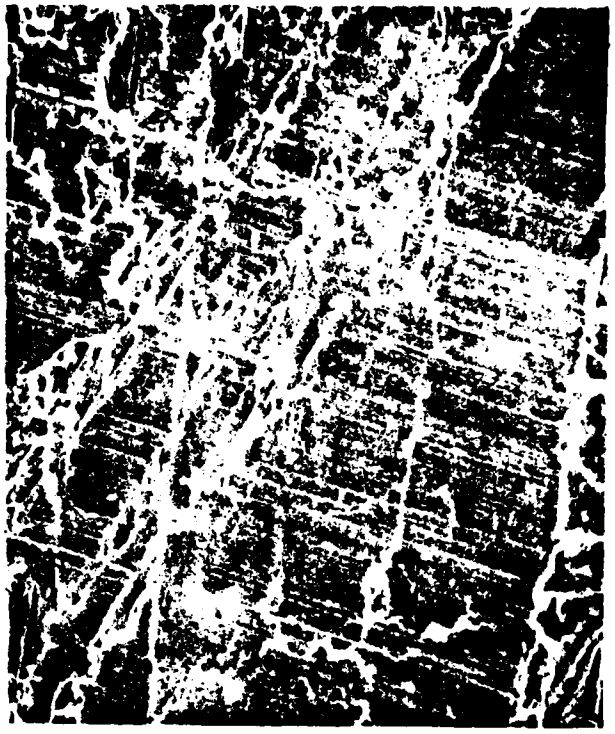
(2) *Piston Rings.* Two of the three cast iron piston rings were unplated while the top compression ring had a chrome plating. All rings were analyzed in the SEM at the conclusion of each completed run.

(a) Top Ring. Figure 108 shows a ring in the unused condition. The circumferential finishing lines are assumed to have been on the ring before plating and it can be seen that the plating followed but did not cover over or fill in the lines. After running, the top circumference of the outside diameter of the ring was worn smoother than the remainder of the ring. This is shown in the SEM micrographs of Figure 109. As determined by x-ray fluorescent analysis in the SEM, in neither location was all the plating worn away. The top ring from the second run appeared essentially the same as that from the first run.

(b) Middle Ring. A new middle ring has a much coarser finish than an unrun top ring, as is illustrated by comparing Figure 108 with Figure 110. However, after the first run, the running wear pattern was similar to that



A. 50X



B. 300X

NAEC-92-153

FIGURE 104

SEM MICROGRAPHS OF THE UNRUN SURFACE OF A CYLINDER WALL

(Sheet 1 of 2)

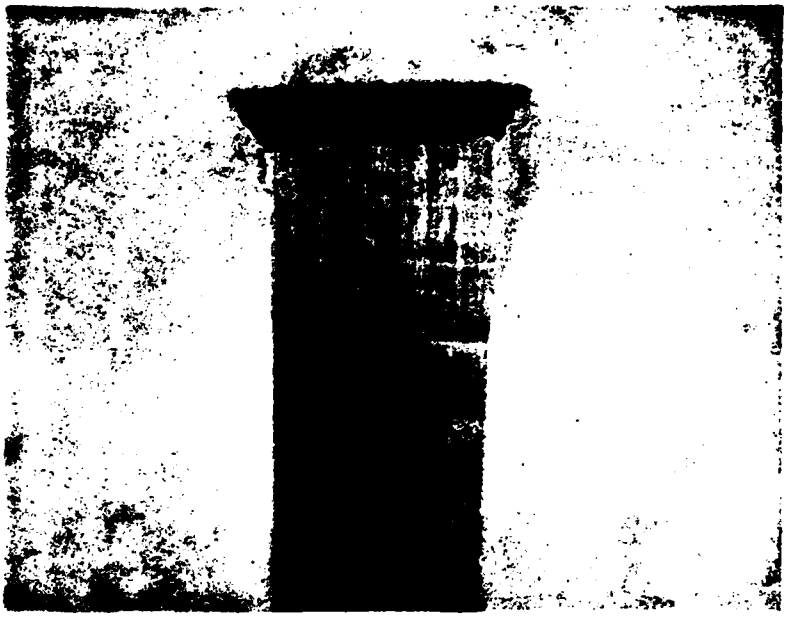


C. 1000X

FIGURE 104

SEM MICROGRAPHS OF THE UNRUN SURFACE OF A CYLINDER WALL

(Sheet 2 of 2)



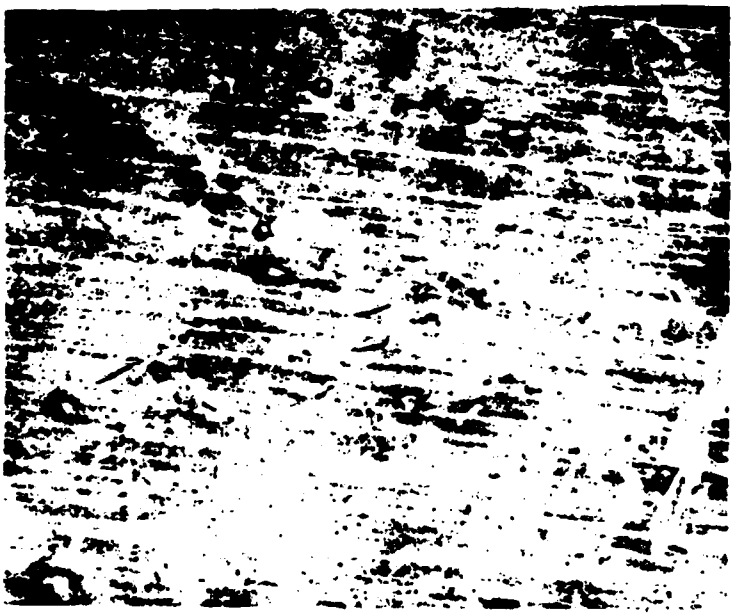
2.5X

FIGURE 105

SEGMENT OF THE CYLINDER WALL FROM THE FIRST RUN



B. 1000X



A. 300X

FIGURE 106

SEM MICROGRAPHS OF A SHINY REGION ON THE CYLINDER WALL



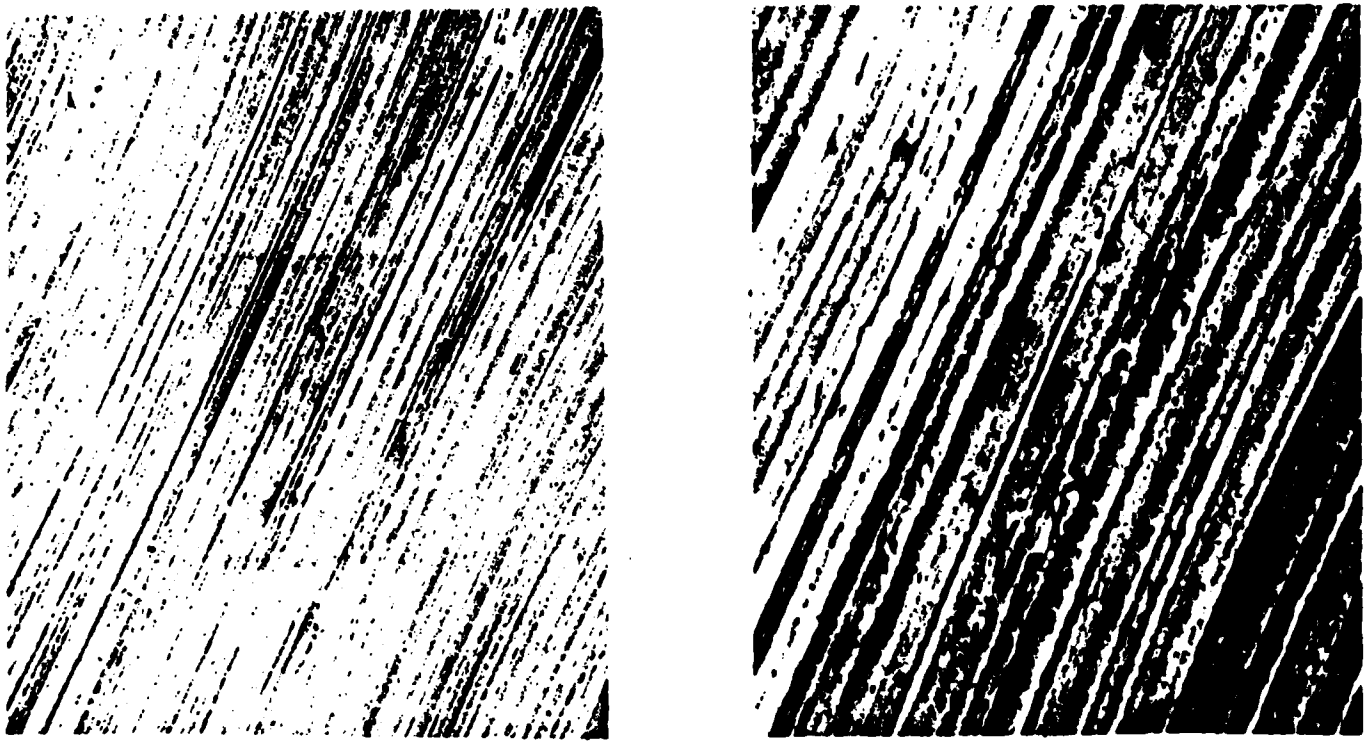
A. 300X



B. 1000X

FIGURE 107

SEM MICROGRAPHS OF A MODERATELY WORN AREA ON THE SURFACE OF THE CYLINDER WALL AT THE CONCLUSION OF THE FIRST TESTING RUN

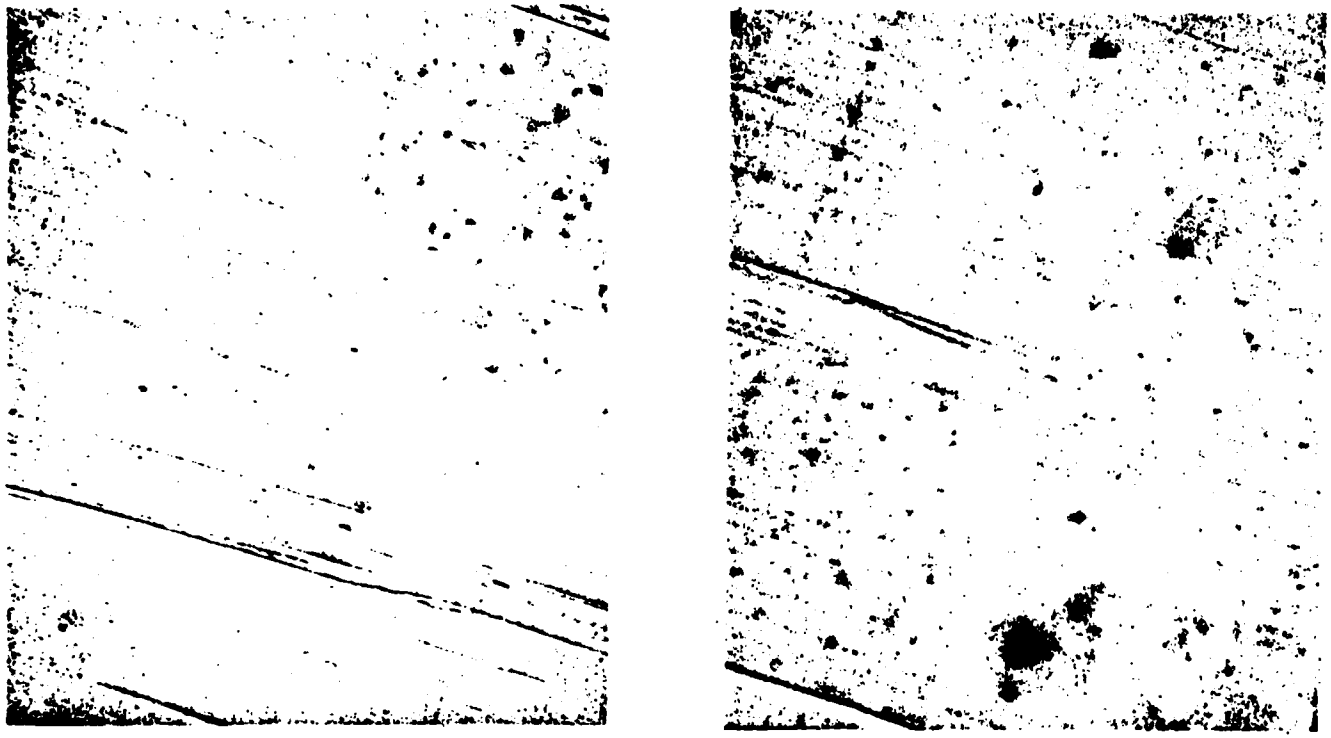


A. 300X

B. 1000X

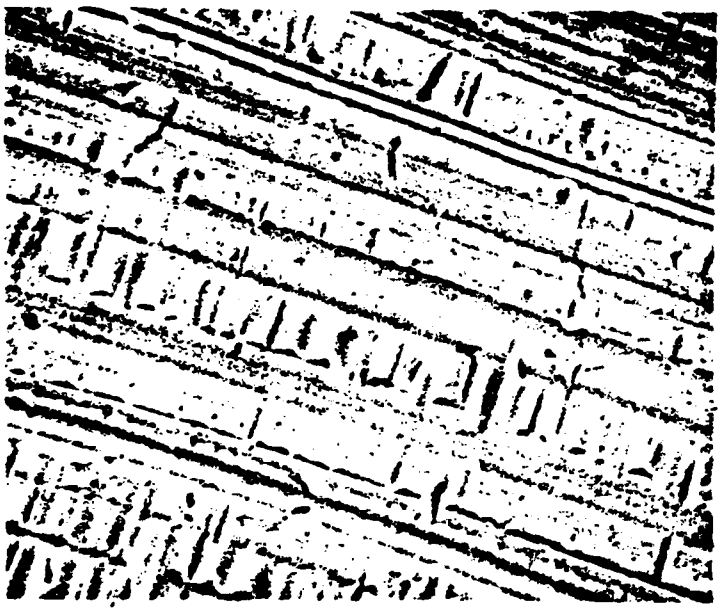
FIGURE 108

SEM MICROGRAPHS OF THE UNRUN CHROME PLATED TOP PISTON RING

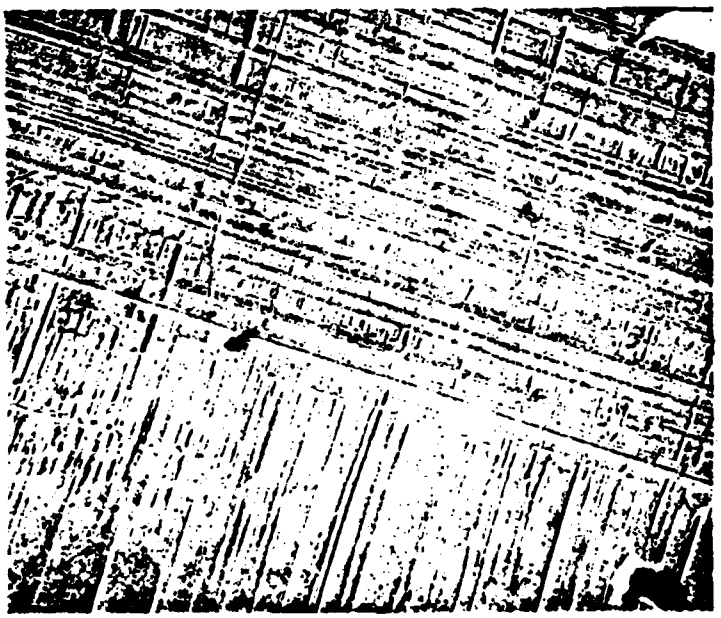


A. 300X B. 1000X

FIGURE 109
SEM MICROGRAPHS OF WEAR SURFACE OF THE TOP RING AFTER FIRST RUN
(Sheet 1 of 2)



D. 1000X

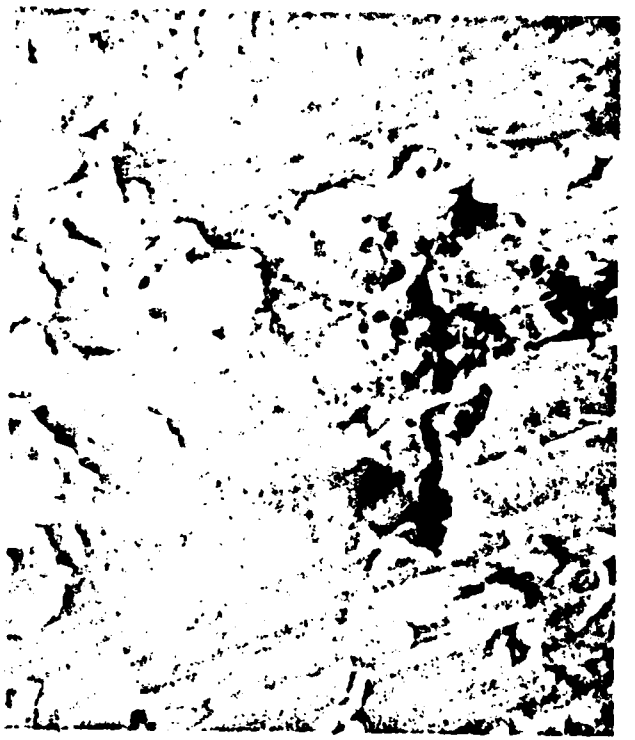


C. 300X

FIGURE 109
SEM MICROGRAPHS OF WEAR SURFACE OF THE TOP RING AFTER FIRST RUN
(Sheet 2 of 2)



A. 300X



B. 1000X

FIGURE 110

SEM MICROGRAPHS OF THE SURFACE OF A NEW CENTER PISTON RING

on the top ring, in that the wear was more pronounced on the upper circumference of the outside diameter, as shown in Figure 111. The depth of the coarse finishing grooves was accentuated by the wear, and the features in the deeper grooves in Figure 111C and 111D appear the same as in an unrun ring, Figure 110. After the second run the wear on the middle ring was somewhat less than in the first run, but, except for the degree of wear, the characteristics of the surfaces were similar, including the greater degree of wear at the top circumference.

(c) Bottom (Oil Control) Ring

1. This ring, as shown in Figure 112, has two separate wear surfaces with identical surface finish, Figure 113A and 113B. After running the surfaces on both these segments were similar, Figure 114. The effects of runs 1 and 2 were essentially the same. Also, a comparison between Figures 114 111C shows that the wear on the bottom ring was similar to that on the bottom of the middle ring.

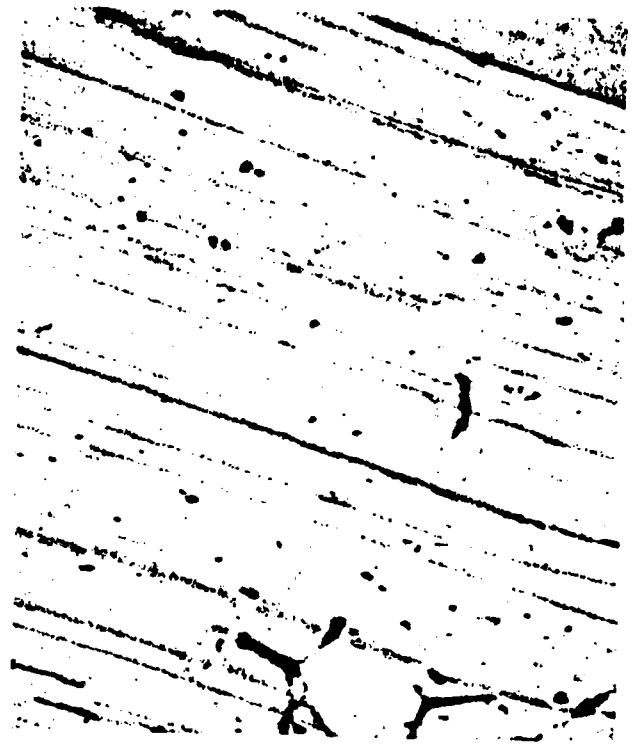
2. When the engine was disassembled after the termination of the second run, a crack was found on the bottom piston ring, Figure 115. Although it could not be ascertained whether the damage occurred during disassembly it seems reasonable that the oil leakage problem and the apparent increase in blowby were a consequence of this failure.

(3) Steel Wrist Pin

(a) New. After the first run, the steel wrist pin appeared as in Figure 116. The region in contact with the wrist pin bearing is between the two forward circumferential bands while the ends outside these bands, were in contact with the piston. The bands themselves did not contact any surface during running and thus represent the as-finished surface. The dark coloration is a surface deposit, in part, the result of lubricant degradation. Fine circumferential finishing lines are present on this unrun surface, Figure 117.



A. 300X



B. 1000X

FIGURE 111

SEM MICROGRAPHS OF THE TOP AND BOTTOM OF THE CONTACT CIRCUMFERENCE OF THE MIDDLE PISTON RING

(Sheet 1 of 2)

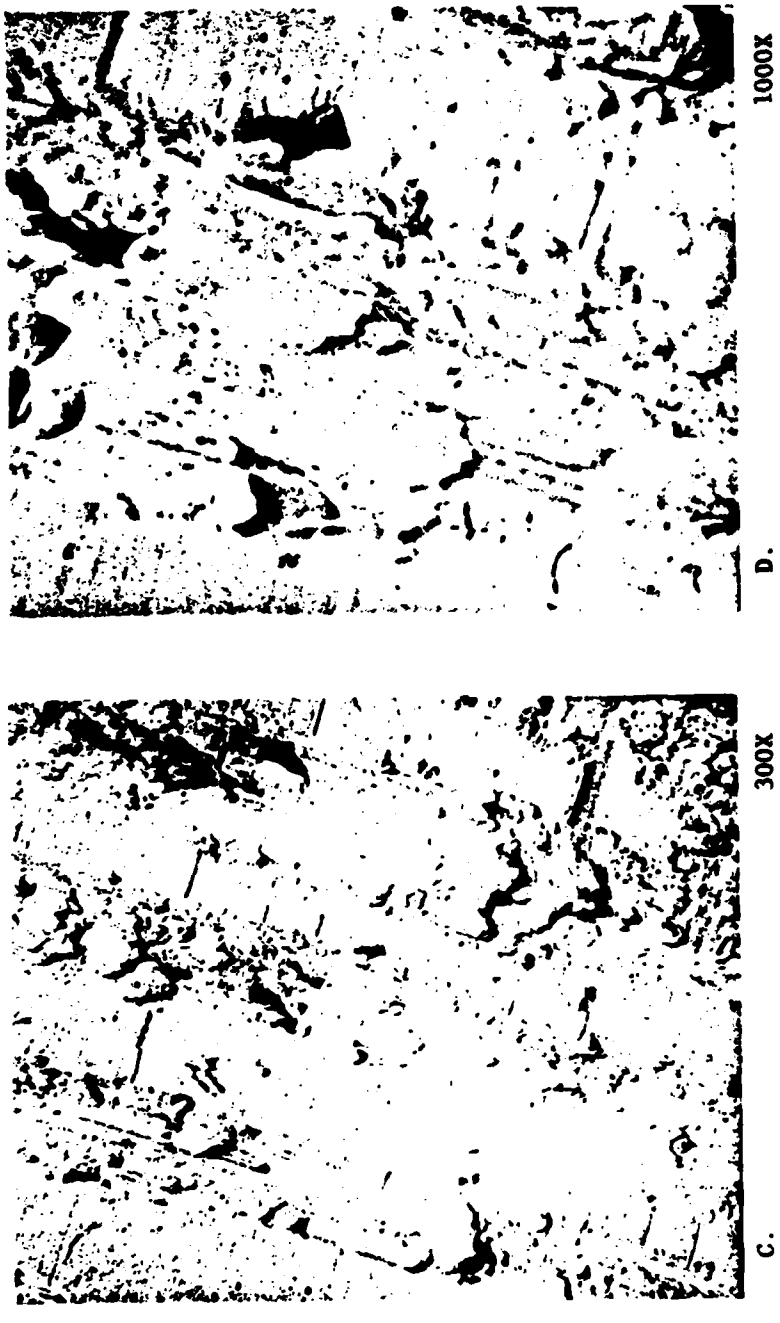


FIGURE 111
SEM MICROGRAPHS OF THE TOP AND BOTTOM OF THE CONTACT
CIRCUMFERENCE OF THE MIDDLE PISTON RING
(Sheet 2 of 2)



A. 4X

FIGURE 112
MACROGRAPH OF AN UNRUN BOTTOM PISTON RING

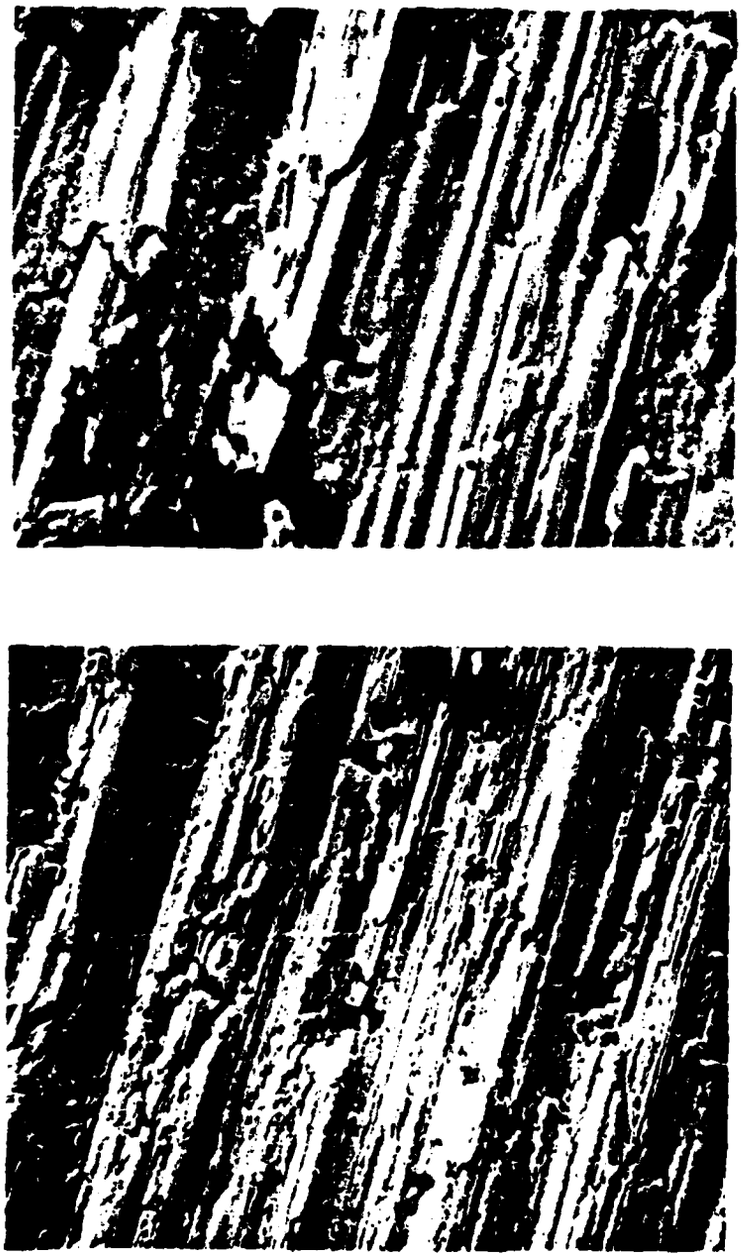
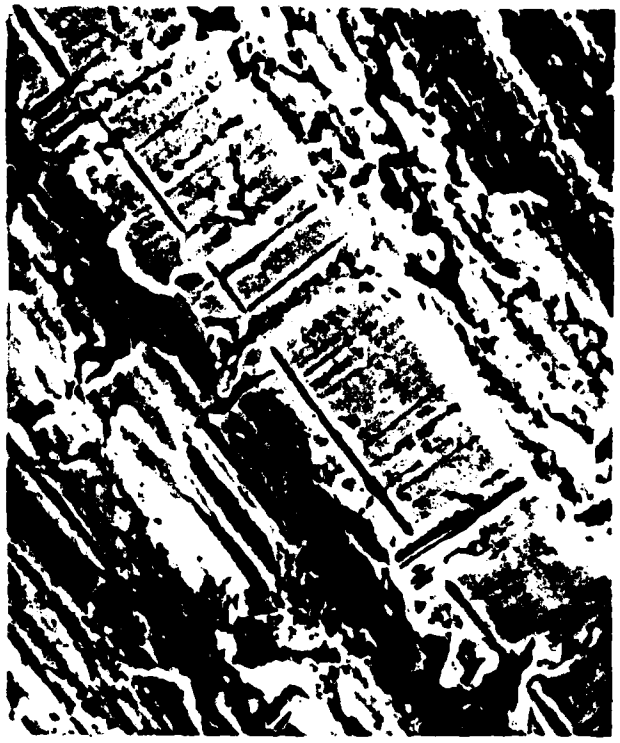


FIGURE 113
SEM MICROGRAPHS OF AN UNRUN BOTTOM PISTON RING



A. 300X



B. 1000X

NAEC-92-153

FIGURE 114

SEM MICROGRAPHS OF THE SURFACE OF THE BOTTOM RING

AFTER THE COMPLETION OF THE SECOND TESTING RUN

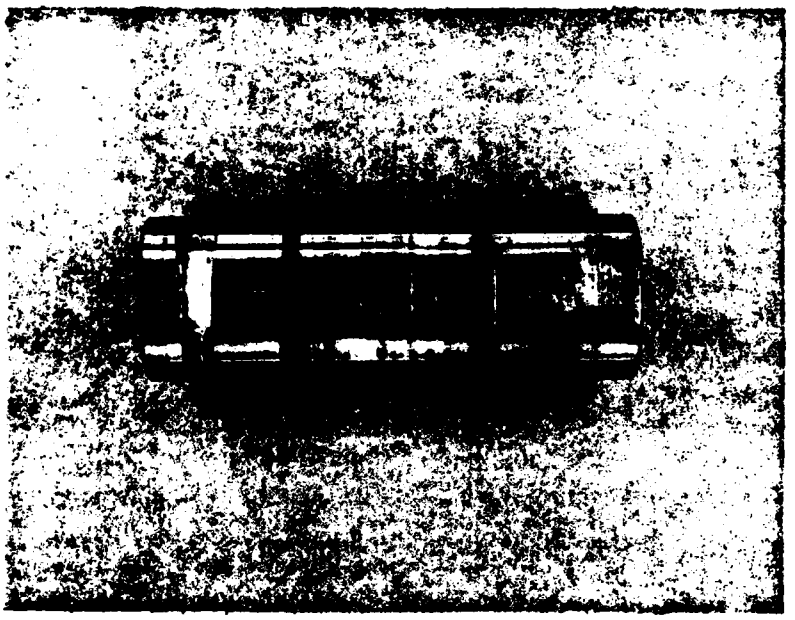


100X

FIGURE 115

SEM MICROGRAPH OF A CRACK ON THE WEAR SURFACE

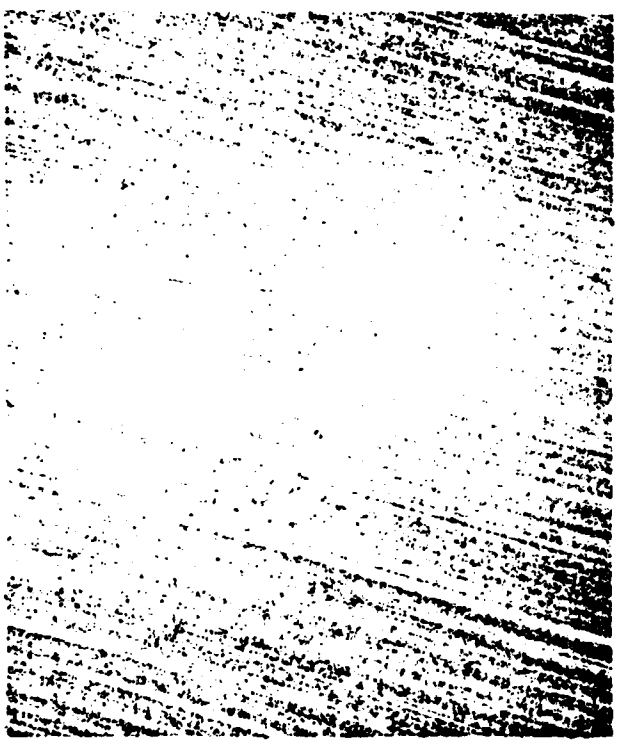
OF THE BOTTOM RING FROM THE SECOND RUN



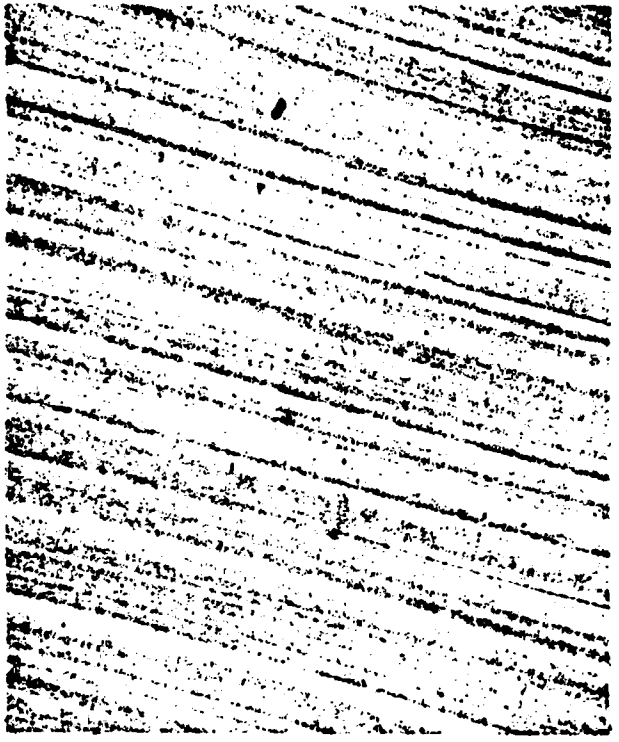
1X

FIGURE 116

MACROGRAPH OF WRIST PIN REMOVED FOLLOWING COMPLETION OF FIRST TEST SEQUENCE



A. 300X



B. 1000X

FIGURE 117

SEM MICROGRAPHS OF AN UNWORN REGION ON THE SURFACE
OF THE WRIST PIN OF THE PREVIOUS FIGURE

(b) Run A

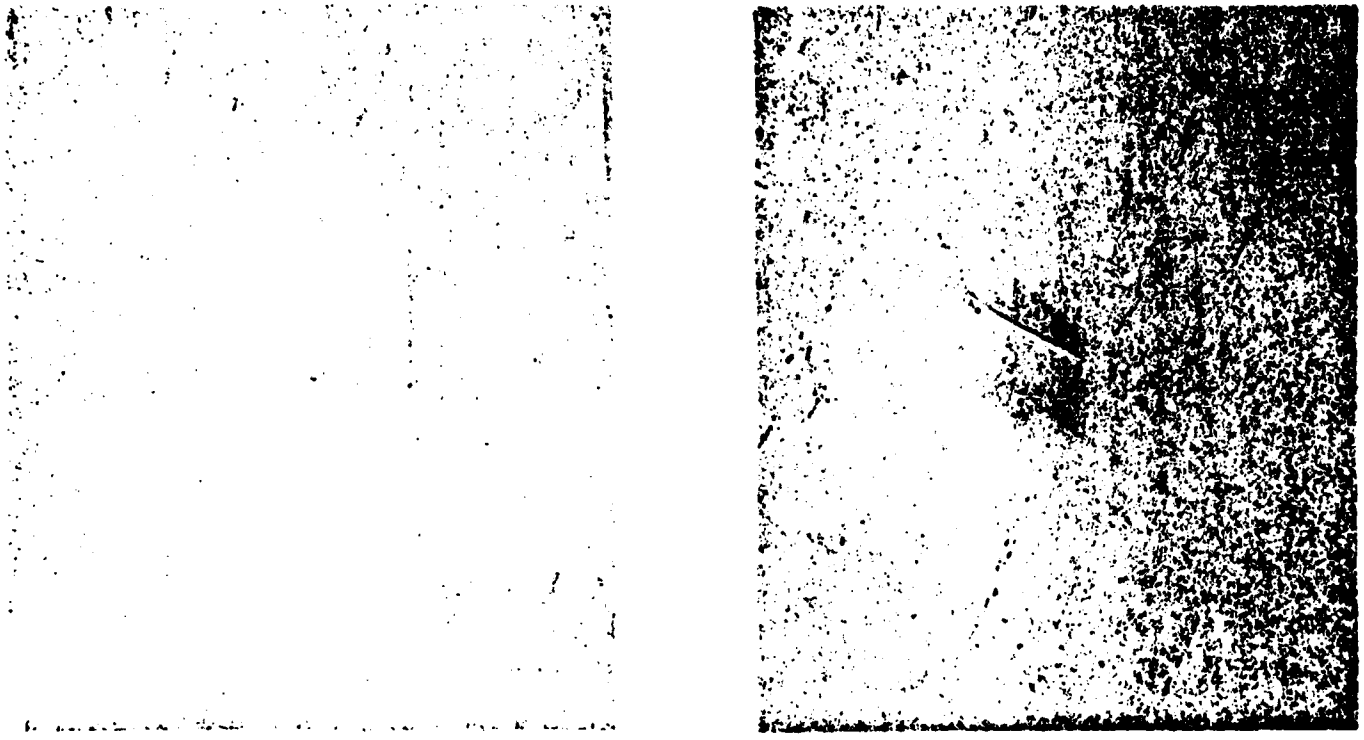
1. The bearing contact surface showed varying degrees of wear, consistent with the wear on the wrist pin bearing to be discussed in the next section. In some locations the surface had been worn uniformly smooth, Figure 118 while in other areas, Figure 119 strings of small pits indicated some corrosion had occurred. The nature of this corrosion is characteristic of the effects of condensation and acidity build up in the lubricant, between mating surfaces during shut down periods.

2. There were several patches or circumferential streaks of dark build up material on the bearing contact surface. These were visible to the eye or under a low power light microscope. In the SEM they appeared as in Figure 120. X-ray fluorescent analysis in the SEM, showed these regions to be rich in copper and sulfur, indicating they were formed from wear products of the wrist pin bearing in conjunction with the sulfur in the oil.

(c) Run B. The wrist pin and also the wrist pin bearing from the second test series showed less wear than the components from the first test. As can be seen in Figure 121, what appear to be finishing lines remain on the bearing contact surfaces.

(4) Wrist Pin Bearing (Small End Connecting Rod Bearing)

(a) The contact surface of this bearing, which is a copper-tin-lead alloy, is illustrated in the as-finished unrun condition in Figure 122. During the first run, the spectrometric data showed the Cu content in the oil was increasing, and thus this component was assumed to be the one that was experiencing degradation. Examination after completion of the test revealed that extensive damage had occurred, Figures 123 and 125. In fact, a major portion of the original surface had been worn away and the worn areas were black, indicating an adherence or incorporation of lubricant degradation products and the



A. 300X B. 1000X

FIGURE 118

SEM MICROGRAPHS OF THE BEARING CONTACT SURFACE OF THE WRIST PIN FROM TEST 1 SHOWING A REGION WHICH HAD BEEN WORN SMOOTH



A. 300X



B. 1000X

FIGURE 119

SEM MICROGRAPHS OF THE BEARING CONTACT SURFACE

OF THE WRIST PIN FROM TEST 1



A. 50X

FIGURE 120

SEM MICROGRAPHS OF A REGION OF BUILT UP MATTER ON THE BEARING CONTACT SURFACE OF THE WRIST PIN OF FIGURE 119

(Sheet 1 of 2)



B. 300X

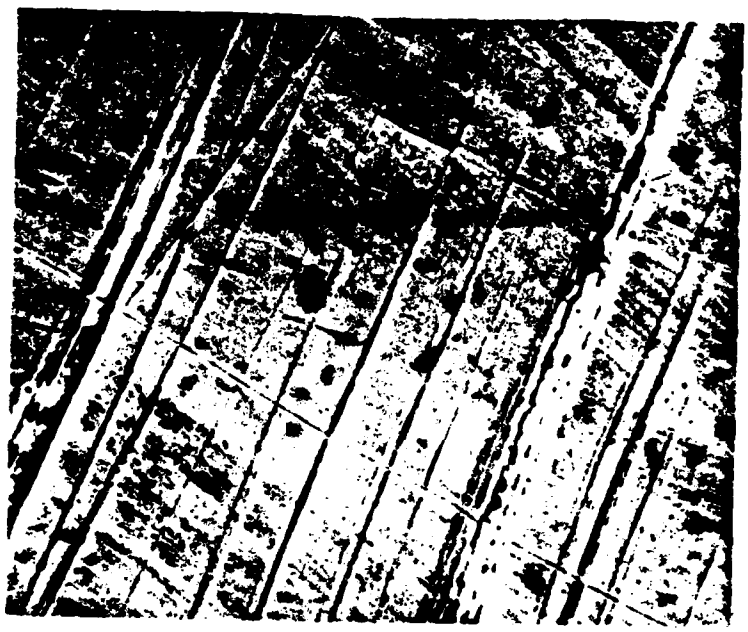


C. 1000X

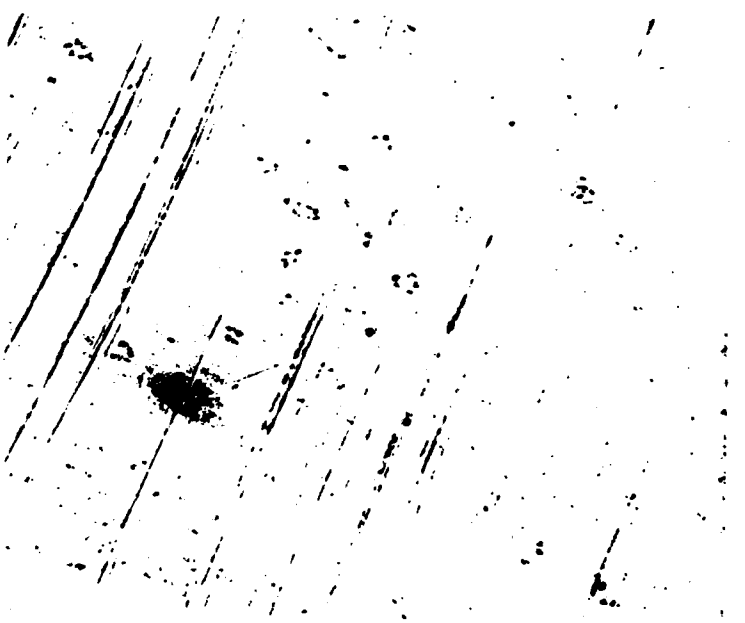
FIGURE 120

SEM MICROGRAPHS OF A REGION OF BUILT UP MATTER ON THE BEARING CONTACT SURFACE OF THE WRIST PIN OF FIGURE 119

(Sheet 2 of 2)



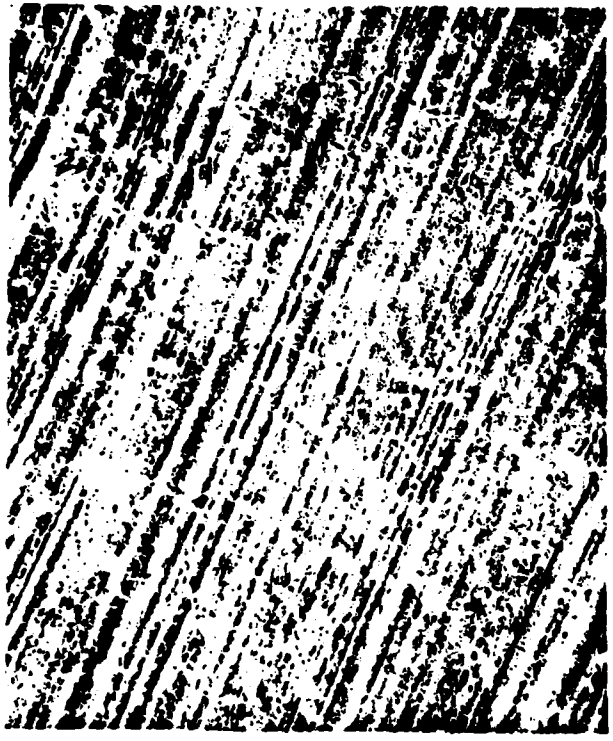
B. 1000X



A. 300X

FIGURE 121

SEM MICROGRAPHS OF THE BEARING CONTACT SURFACE OF THE WRIST PIN FROM RUN 2



A. 300X



B. 1000X

NAEC-92-153

FIGURE 122

SEM MICROGRAPHS OF THE SURFACE OF AN UNRUN WRIST PIN BEARING



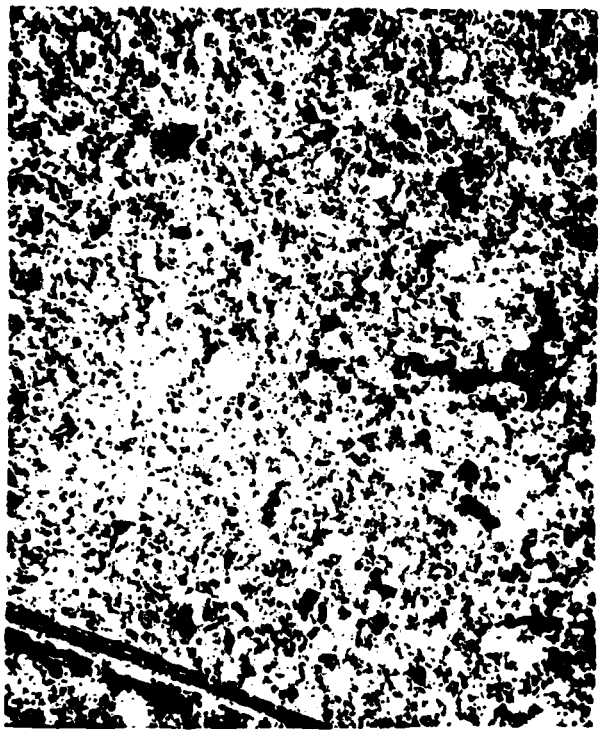
FIGURE 123 1X

PHOTOGRAPH OF THE WRIST PIN BEARING AFTER SECTIONING
FOLLOWING COMPLETION OF THE FIRST RUN

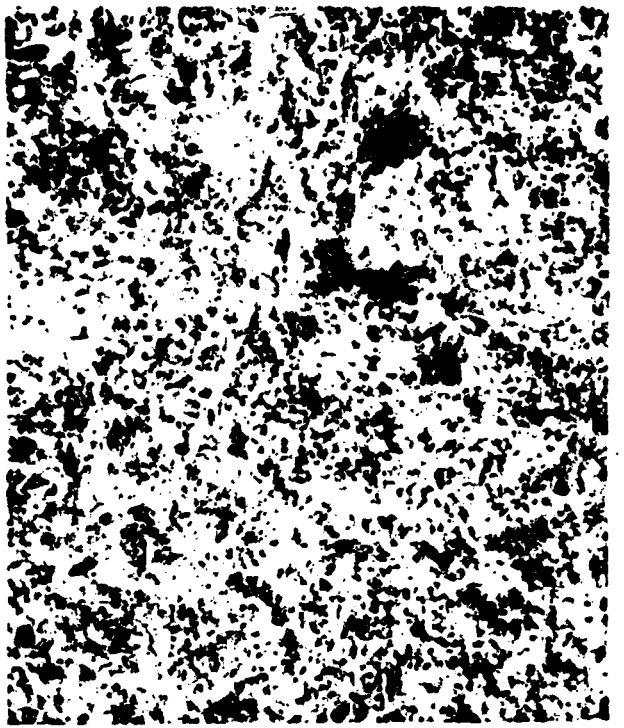


FIGURE 124 1X

PHOTOGRAPH OF THE WRIST PIN BEARING AFTER SECTIONING
FOLLOWING COMPLETION OF THE SECOND RUN



A. 300X



B. 1000X

FIGURE 125

SEM MICROGRAPHS OF THE WORN SURFACE OF THE WRIST PIN BEARING

AFTER COMPLETION OF THE FIRST RUN

formation of copper-sulfur compounds. As noted above, in the discussion of the wear surface of the wrist pin from the first run, black streaks or bands rich in copper and sulfur were present. This appears to have been picked up from the bearing, based upon the similar nature of the surfaces in Figures 125A and 125B.

(b) Relatively little damage was incurred on the bearing from the second test run, Figures 124 and 126.

(5) Crankshaft Bearing. The contact surface of this bearing is an aluminum-tin alloy which, in the unrun condition, has fine details as shown in Figure 127. The wear on this bearing was limited in both runs, Figure 128, being primarily in the form of a smearing out or flattening of the tongues of metal produced by the finishing operation. Relatively deep scoring marks were present on the segments of the crankshaft bearing from the second run, Figure 129. Since the lines are present completely around both segments they appear to be the result of some debris that may have become lodged in the shaft.

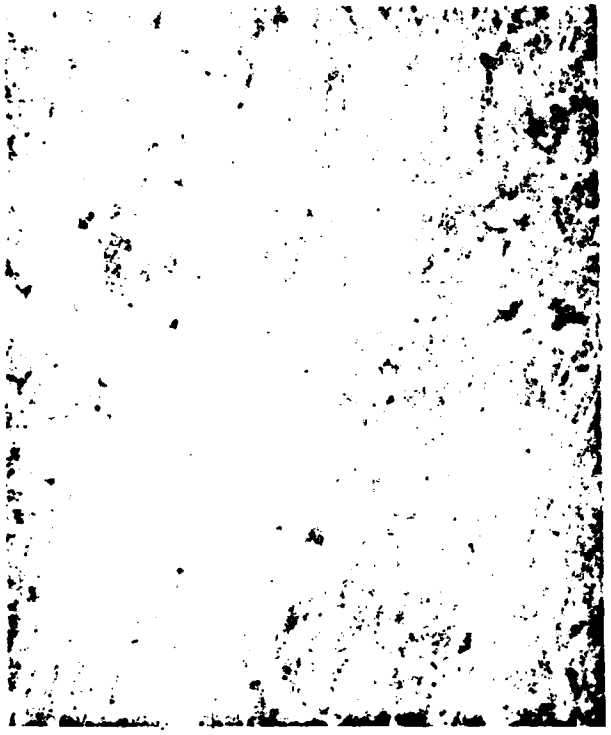
c. Sliding Contact Wear Particle Analysis

(1) Wear debris analysis was performed on respective sliding contact bench test samples by FIRL, Foxboro Analytical, and the NAVAIRENGCEN. As previously discussed, lubricant samples were withdrawn periodically from the sliding contact test engine. These lubricant samples served as the host media for fluid borne debris analysis. Table 40 summarizes the sample number and respective operating times for each sliding contact test sequence.

(2) As in the previous three analysis sections, wear life phases will be evaluated with respect to wear debris characteristics. However, a relevant sliding failure was not experienced during the test sequences.

(a) Particle Quantity

1. As in the previous cases, the quantity of wear debris contained in lubricant samples taken during sliding contact testing, was primarily monitored utilizing ferrographic analysis techniques. Particle counting



A. 300X

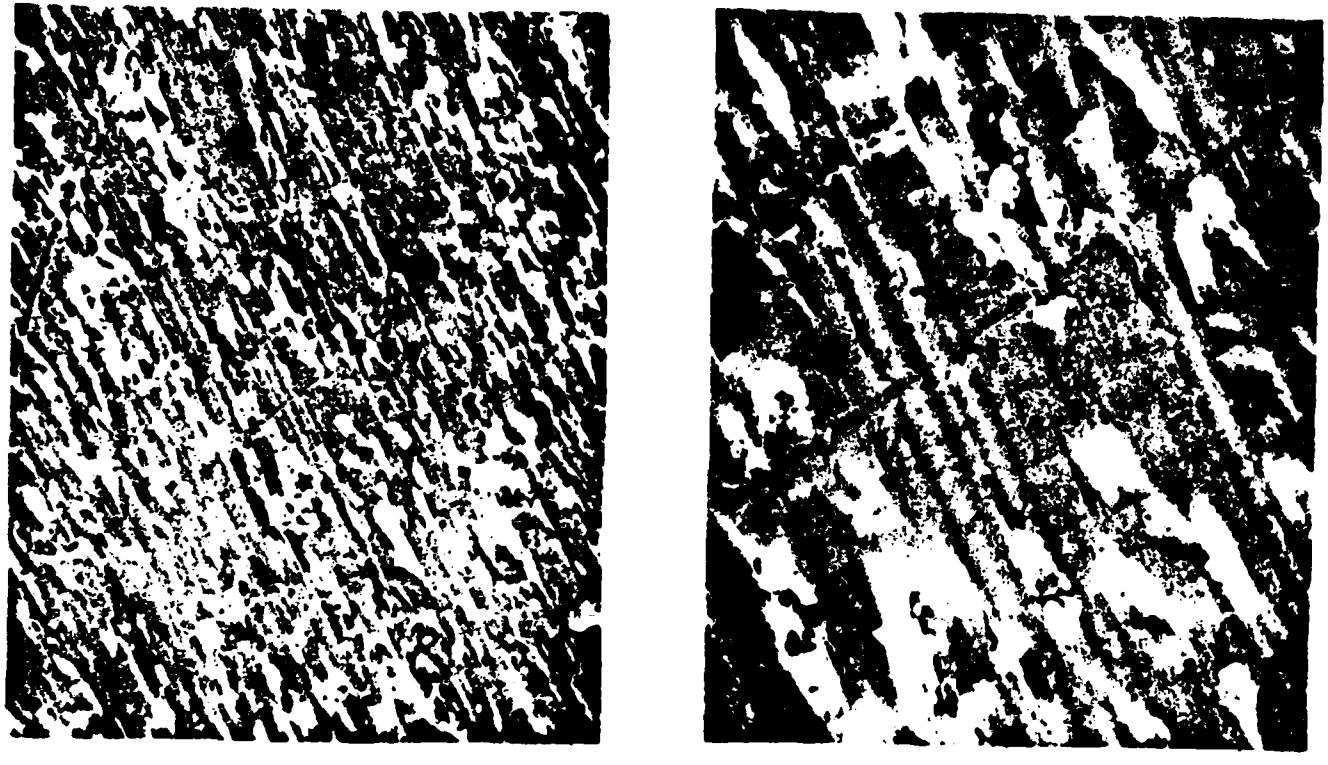


B. 1000X

FIGURE 126

SEM MICROGRAPHS OF THE SURFACE OF THE WRIST PIN BEARING

AFTER COMPLETION OF THE SECOND RUN



A. 300X B. 1000X

FIGURE 127

SEM MICROGRAPHS OF THE UNRUN SURFACE OF THE ALUMINUM-TIN CRANKSHAFT BEARING



A. 300X



B. 1000X

NAEC-92-153

FIGURE 128

SEM MICROGRAPHS OF A TYPICAL REGION ON THE CRANKSHAFT BEARING

AT THE COMPLETION OF THE FIRST RUN

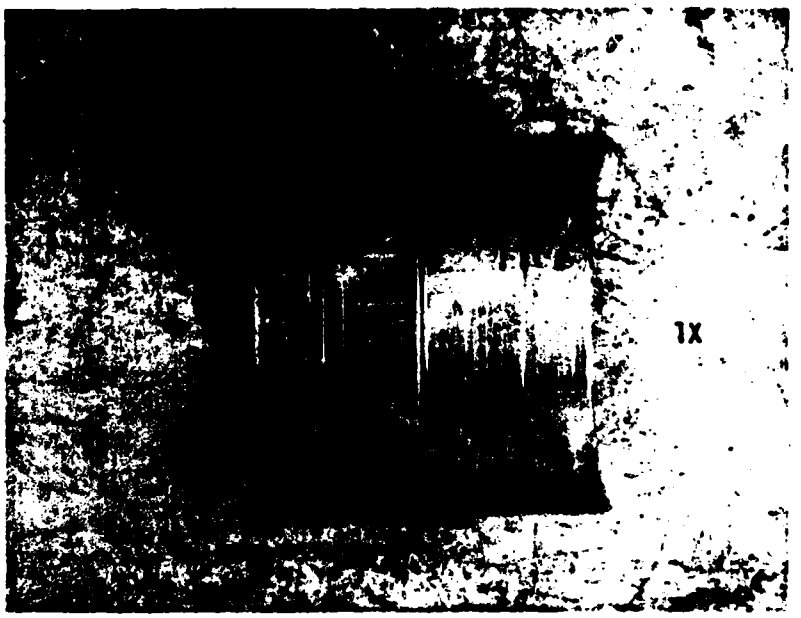


FIGURE 129
TWO SEGMENTS OF THE CRANKSHAFT BEARING
AT THE CONCLUSION OF THE SECOND RUN

TABLE 40

SLIDING CONTACT TEST SEQUENCE SUMMARY

FIRL Code	NAEC Ferrogram Number	Running Time	Cumulative Running Time	Spectrometric Results (parts per million) Fe	Al	Cr	Cu	Pb	Sn
		FIRST RUN							
Base Stock	96, 4740*			3	3	1	1	14	0
4253		1hr, 0Min.	1hr, 0 Min.						
4268	71, 4844	2 45	3 45	45	16	5	75	30	2
4269		7 35	11 20	58	17	7	122	36	7
4270		2 10	13 30	60	16	6	130	34	10
4273	67	7 10	20 40	80	18	6	185	29	10
4274		7 50	28 30	92	20	8	139	22	9
4275		7 15	35 45	118	21	7	136	21	9
4276		7 55	43 40	123	25	8	127	24	14
4277	89, 4443	7 35	51 15	145	35	8	132	31	20
4280		2 55	54 10						
		SECOND RUN							
4304	4760	4hr.	Run in (New Oil)	12	12	2	7	8	0
4305		4hr.	Run in (New Oil)	14	12	1	26	9	0
4308		1 50	1 50 (New Oil)	18	13	2	29	8	0
4318		7 45	9 35	34	16	5	41	15	0
4319		8	17 35	42	15	7	43	15	0
4322		7 55	25 30	57	21	10	43	15	0
4323		7 55	33 25	45	20	10	32	12	0
4324		7 45	41 10	65	24	12	40	14	0
4325		7 15	48 25	63	24	13	37	13	0
4326	4673*	7 15	55 40	76	26	14	42	13	0
4329	38, 4759	8 15	63 55	77	25	14	39	14	0
4330	55	8 20	72 15	65	22	11	32	10	0
4331	119	8 50	81 5	99	26	15	43	14	0
4336	43	6 30	87 35	91	25	10	40	11	0
4337	23, 4750X	8 15	95 50	64	21	7	26	8	0

*Four digit numbered Ferrograms were prepared at an oil dilution of 125:1 while Ferrograms with two and three digit numbers were at 10:1 dilution.

+ 10:1 Dilution

X An accidental oil spill at the end of 4336 necessitated the addition of some fresh oil at the start of this run.

technique results were discounted as a result of the presence of non-wear contaminants. Spectrometric analysis concentration readings were also discounted with respect to particle quantity monitoring as a result of the previously discussed size sensitivity limitations, described in Section VI.

2. Figure 130 represent ferrography entry deposit density plots for both sliding contact test sequences, SA and SB respectively. As observed from sequence SA, a progressive buildup of debris was present throughout the test sequence. The absence of an indication of wear-in during the SA sequence is unexplained. Sequence SB, reflects a fluctuating debris level. This sequence was run-in prior to this test; however, a wear-in process is still apparent in the initial operating period. Total debris levels for these sliding sequences are greater than the levels experienced in the bearing and gear sequences.

3. Progressive increases in debris levels probably resulted from high wear rates as verified during disassembly inspection.

4. As noted earlier, a relevant wear failure did not occur (not including copper bearing) during these sequences thus limiting the discussion of debris quantity.

(b) Particle Size Distribution

1. The size distribution of wear debris contained in the lubricant samples, taken during sliding contact testing, as with particle quantity, was primarily monitored by ferrographic analysis techniques.

2. Figures 131 and 132 present ferrographic density plots at two different locations for sequences SA and SB respectively. A comparison of these two density location curves reflects the size distribution trends exhibited during the sequences. The entry deposit plot represents debris of a relatively large size, $>5\,\mu m$; while the 50 mm deposit plot represents debris of a relatively small size, $2\text{-}5\,\mu m$.

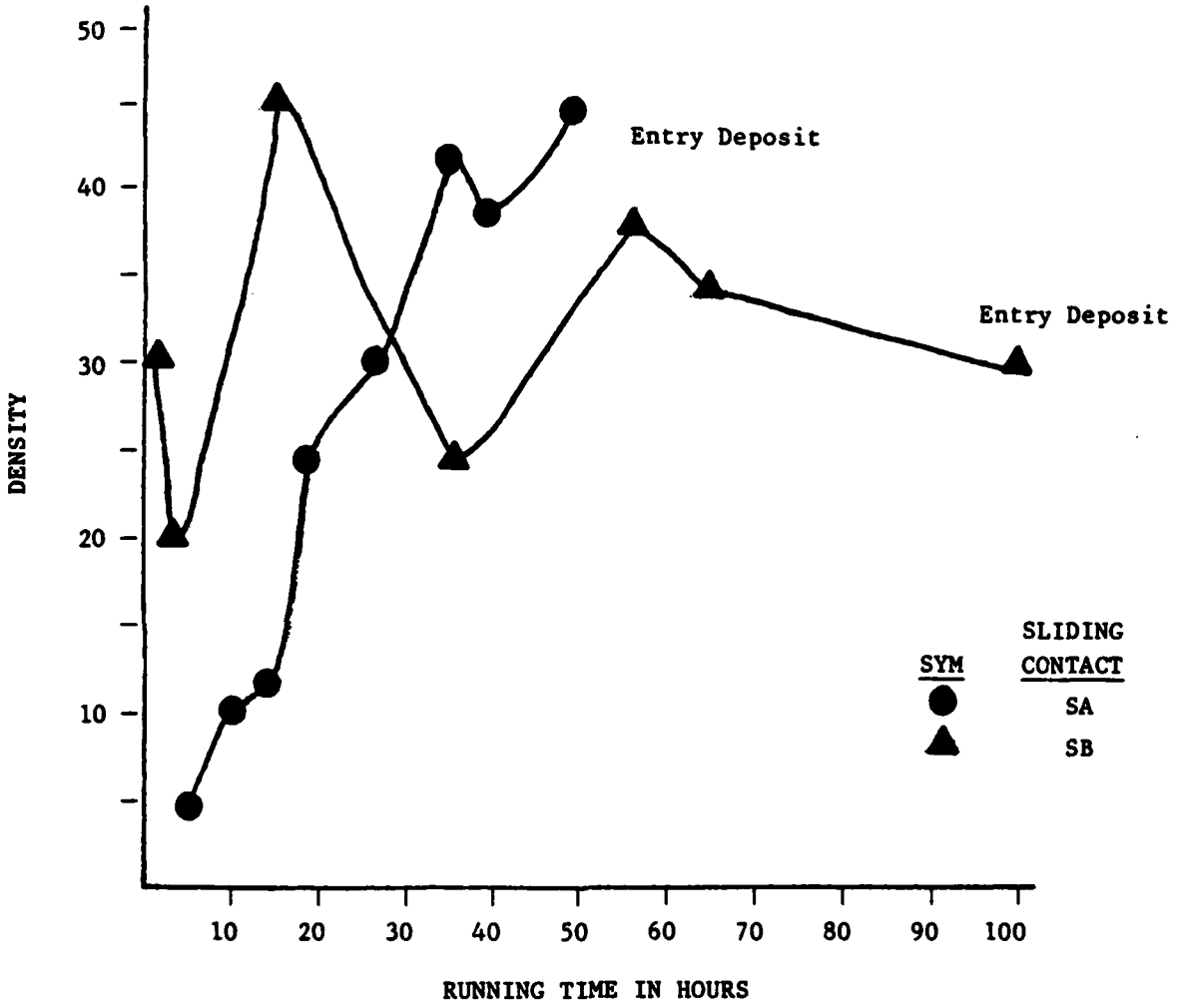


FIGURE 130

SLIDING CONTACT TEST SEQUENCES SA AND SB

FERROGRAPH DENSITY DATA

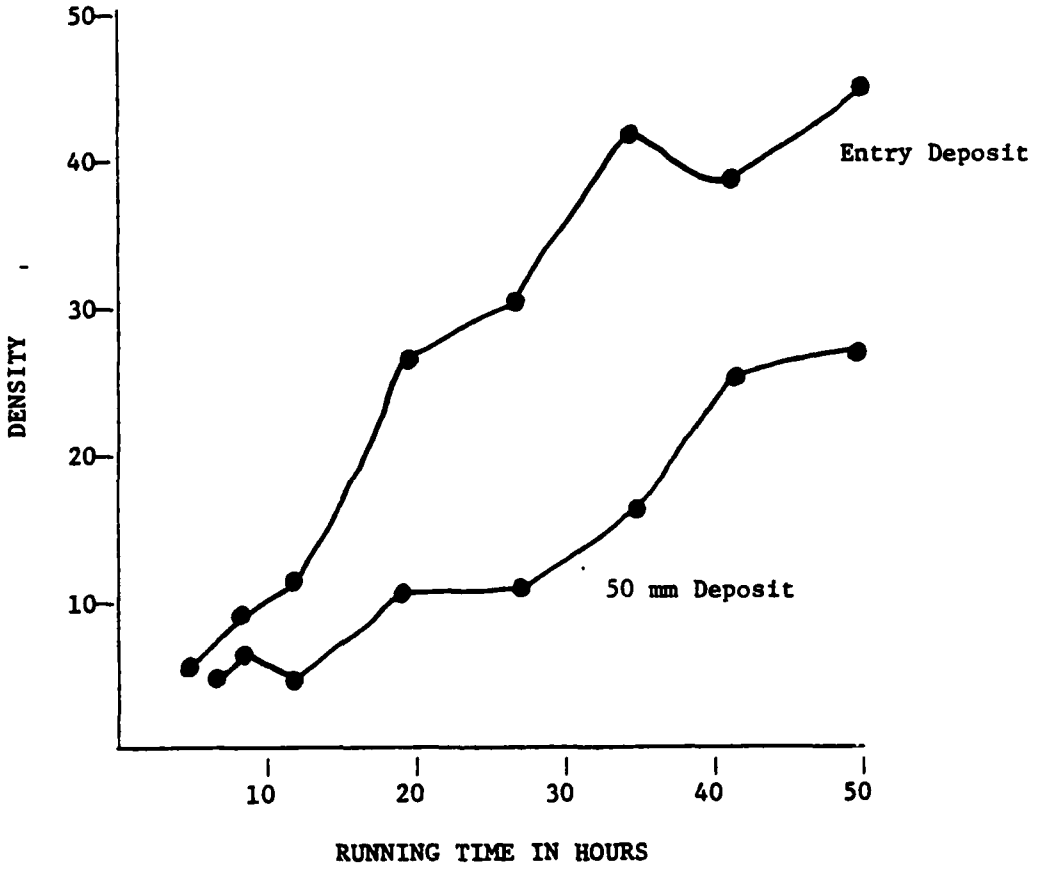


FIGURE 131
SLIDING CONTACT TEST SEQUENCE SA
FERROGRAPH DENSITY DATA

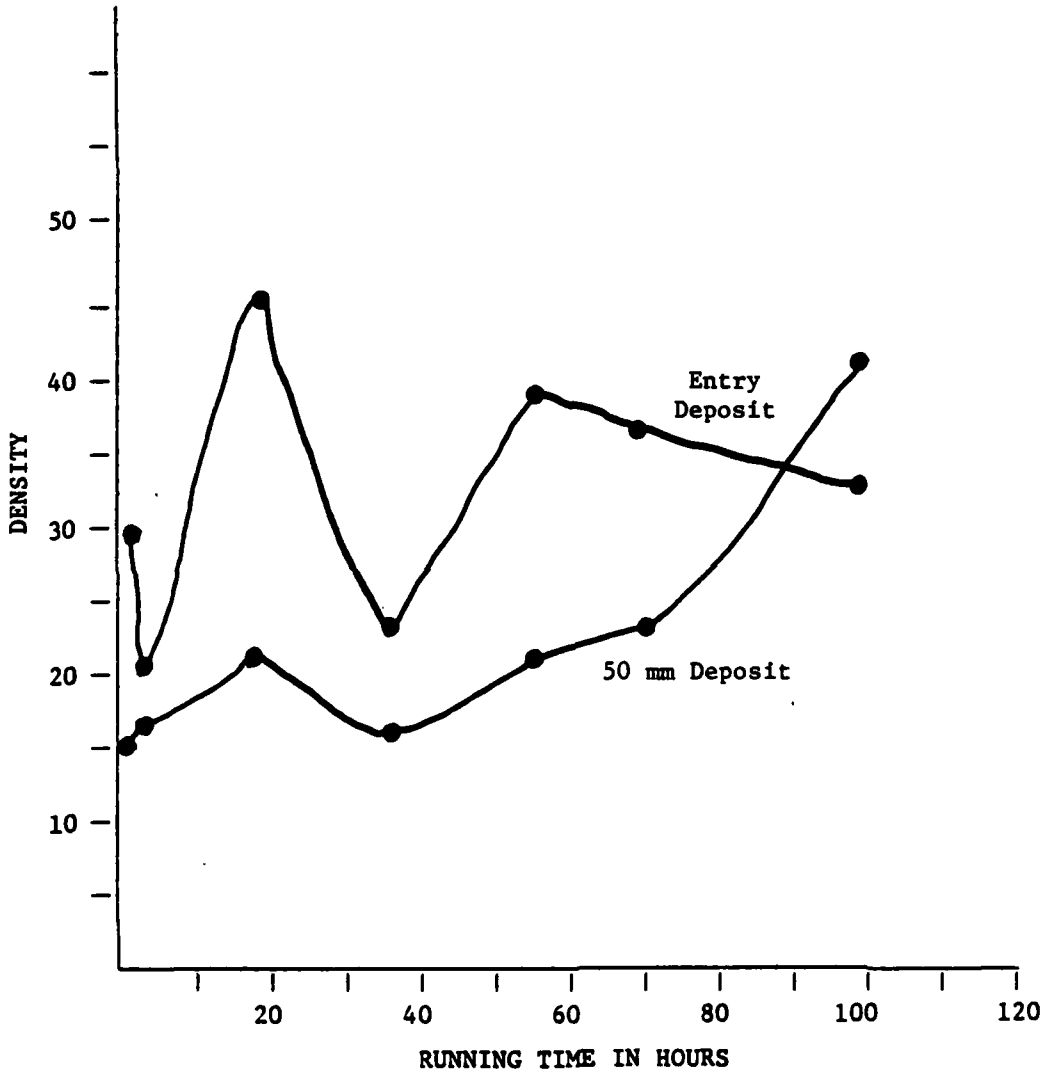


FIGURE 132

SLIDING CONTACT TEST SEQUENCE SB

FERROGRAPH DENSITY DATA

3. As can be observed from both these plots, sliding contact exhibits a relatively low ratio of large to small debris particles. This ratio indicates that a significant portion of the debris generated during sliding contact is small debris.

4. It is also interesting to note that on Figure 132, sequence SB, the curve for the small debris is less erratic than for the large debris. Also on this plot, the small debris curve actually intersects the large debris curve, again, indicating the large amount of small debris being generated. The wear-in portion of this plot reflects a relatively high ratio of large to small debris, as indicated throughout this testing program.

5. Figure 133 represents spectrometric analysis plots for sequences SA and SB. The presented plots represent the concentration level of iron (Fe) over the test sequences. These plots can be correlated to the small debris, 50 mm deposit, trends previously presented. This correlation reinforces the previously discussed size sensitivity exhibited by the spectrometer.

6. Sliding contact ferrographic analysis resulted in codeposition phenomena along the ferrogram slide. This phenomena complicated, but did not jeopardize, the dual plot assessment presented herein. The codeposition phenomena is described in the following paragraphs.

a. During first run SEM analysis, it was difficult to determine specific differences between ferrograms from any given running period. This was due in part, to the limited field examined at any one location, when viewing at a high enough magnification to resolve details and also in part to the codeposition of particles with a range of sizes at all positions along the slide. Large ferromagnetic particles did tend to be at or near the 55 mm position (the entrance end of the slide where the particles which are most attracted by the magnetic field deposit) but smaller particles occurred at all locations.

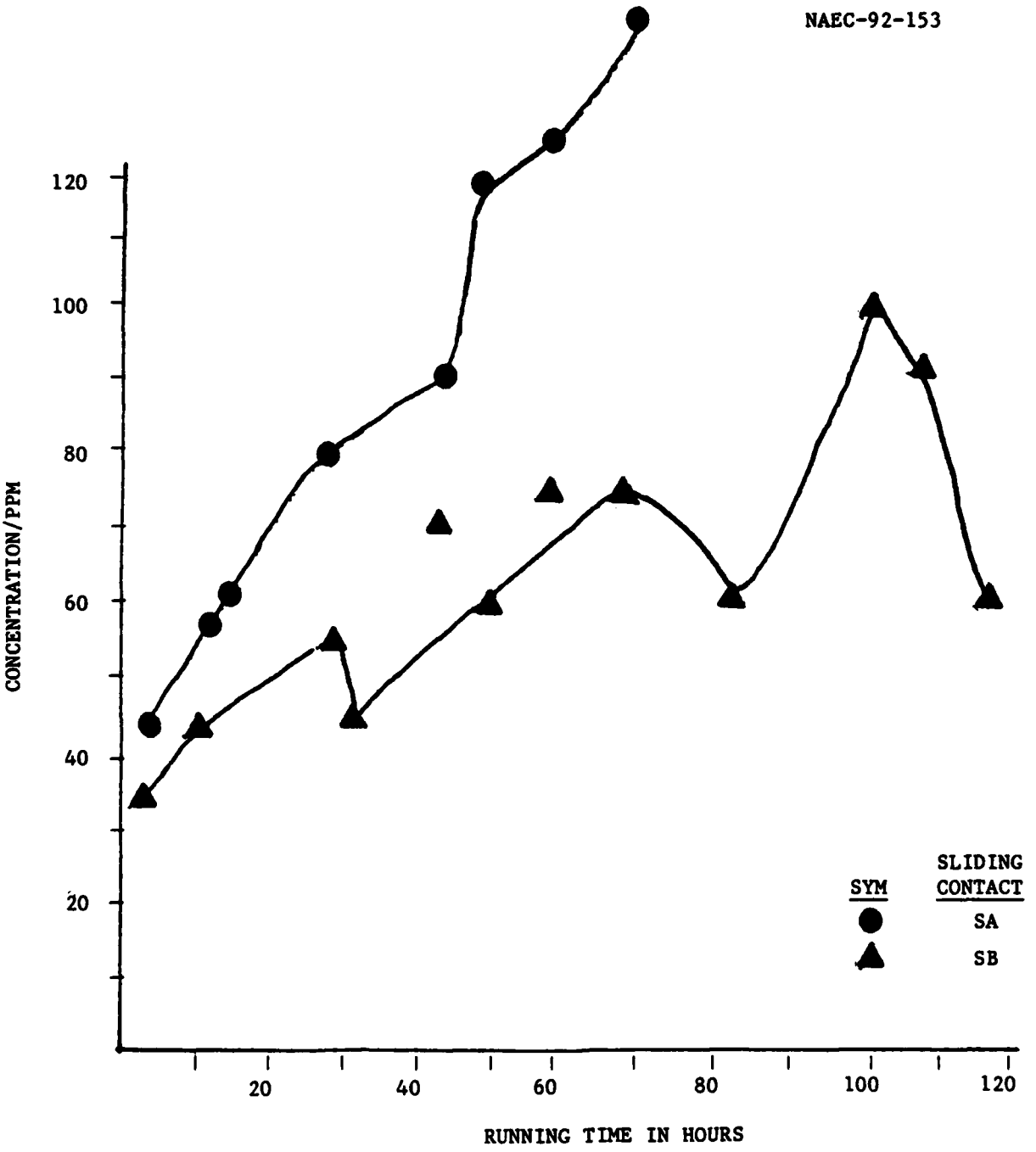


FIGURE 133

SLIDING CONTACT TEST SEQUENCES SA AND SB

SPECTROMETRIC OIL ANALYSIS

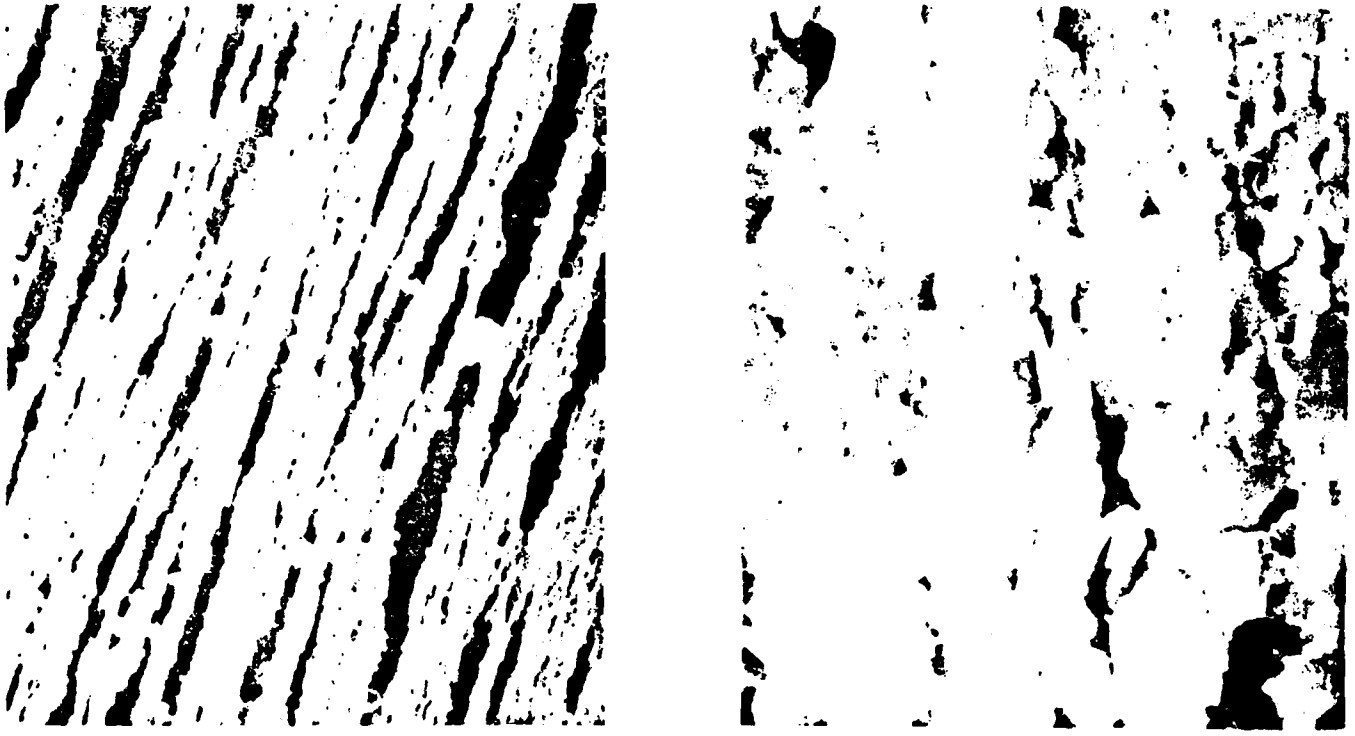
Since similar findings were made in the analysis of ferrograms from the second run and since there was less oil degradation to hamper the resolution of individual particles on these ferrograms, SEM micrographs from the second run ferrograms are presented to illustrate this phenomenon. In the micrographs of Figures 134, 135, and 136 of ferrogram 4673 (4326) (prepared at an oil dilution of 10:1), there appears to be essentially the same distribution of small particles at all positions. Dilution of the oil to 125:1 reduced the total number of particles on a slide, but did not effect a separation of particles according to size. Findings were similar to those on the 10:1 dilution slide. An example of this on ferrogram 4759 (4329) is presented in Figure 137.

(c) Particle Composition. As a result of the numerous oil wetted wearing components in the test engine, debris composition holds more significance in this test sequence than it has in previous component testing. Table 40 summarizes spectrometric analysis data for sequences SA and SB. It can be noted, that besides the element of prime concern, Fe, there exists in the lubricant system significant concentration levels of Al, Cr, Cu, and Sn. Debris made up of these elements was generated by various wearing components within the test engine. The copper (Cu) for instance, in sequence SA, resulted from the degrading copper wrist pin bearing. Copper particles also were detected on the ferrogram slides analyzed under this series, Figure 138.

(d) Particle Morphology

1. The final factor to be considered under the sliding contact wear particle analysis is particle morphology.

2. Sliding surface wear-in, like gear wear-in, results from the presence of machined surface finishes. The general description of wear-in particles previously discussed is applicable to sliding contact and can be referred to for a detailed description.



A. 1000X B. 10,000X

FIGURE 134

SEM MICROGRAPHS OF FERROGRAM 4637 (4326) AT ABOUT THE 50 mm POSITION

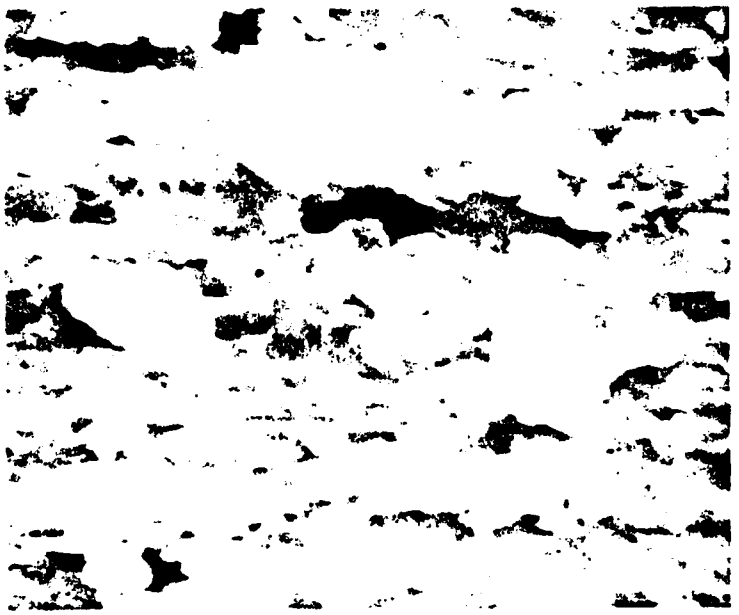


FIGURE 135
SEM MICROGRAPHS AT 10,000X OF FERROGRAM 4673 (4326)
(Sheet 1 of 2)



B. 35 mm



C. 25 mm

FIGURE 135
SEM MICROGRAPHS AT 10,000X OF FERROGRAM 4673 (4326)
(Sheet 2 of 2)

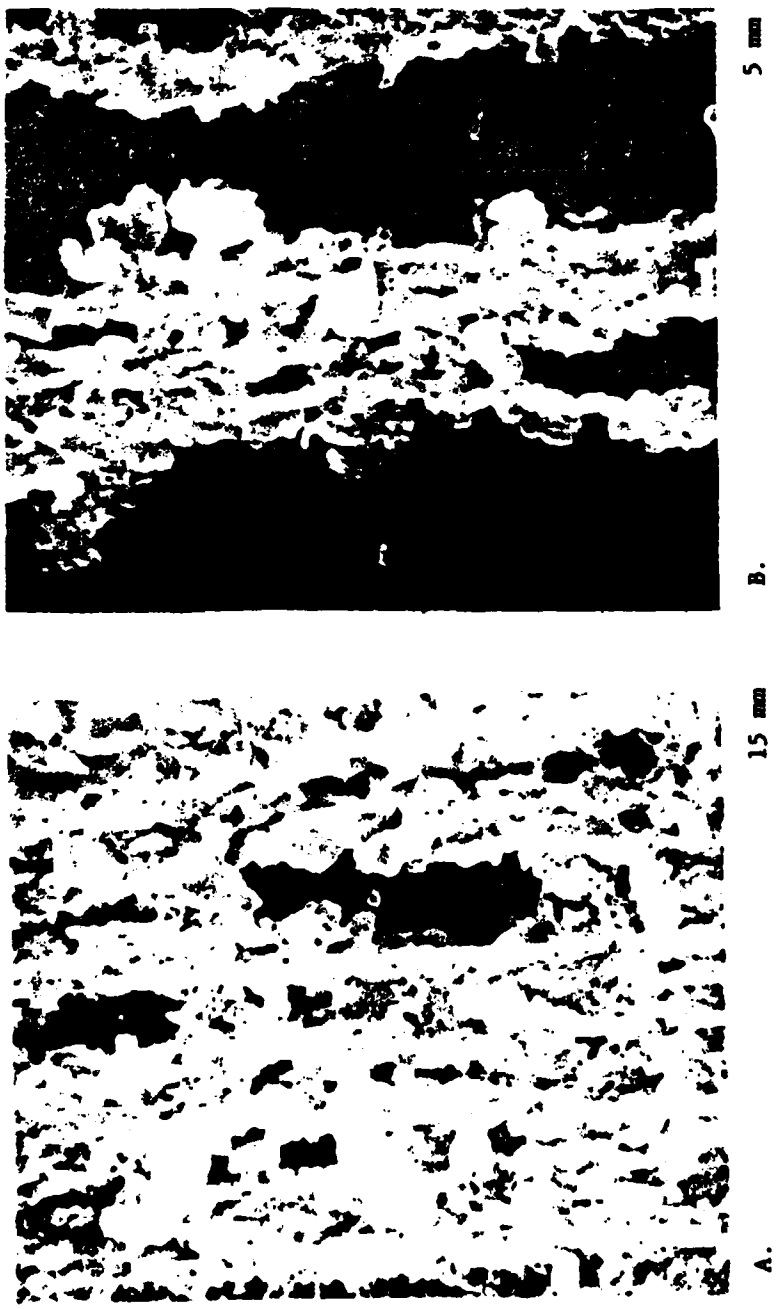
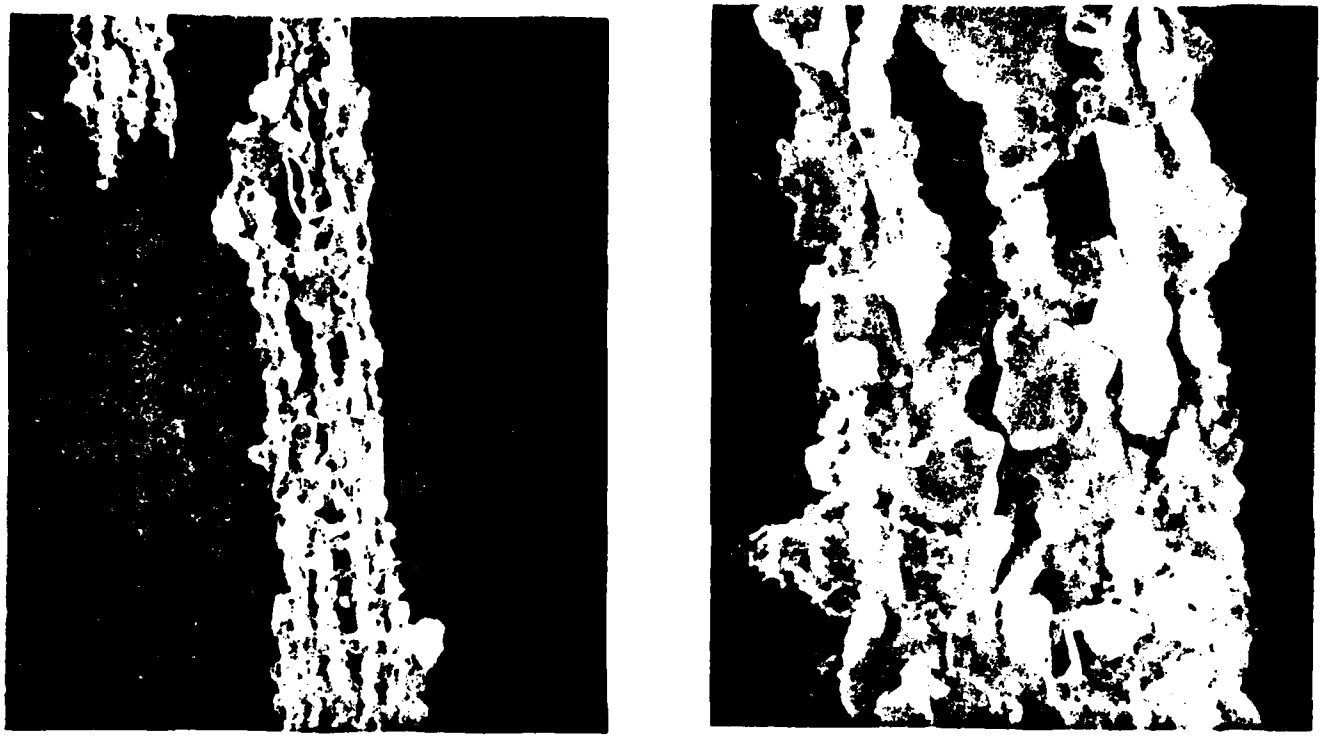


FIGURE 136
SEM MICROGRAPHS AT 10,000X OF FERROGRAM 4673 (4326)



A. 3000X B. 10,000X

FIGURE 137

SEM MICROGRAPHS OF FERROGRAM 4759 (4329) AT THE 50 mm POSITION



A. 300X



B. 1000x

FIGURE 138

SEM MICROGRAPHS OF FERROGRAM 89 (4277) AT THE 55 mm POSITION. A. HEAVY AGGLOMERATION OF LARGE PARTICLES IS EVIDENT AS IS A FORMLESS SUBSTANCE COVERING MANY OF THE PARTICLES. OTHER THAN S NO SPECIFIC ELEMENTS WERE FOUND IN NONPARTICULATE MATTER, INDICATING IT TO BE SOME FORM OF OIL DEGRADATION PRODUCT (ELEMENTS LOWER IN ATOMIC NUMBER THAN Na CANNOT BE ANALYZED FOR). THE BLOCKY PARTICLES WERE RICH IN Cu AND SOME AL AND Pb WAS ALSO PRESENT.

3. Normal wear of a sliding contact results in the generation of substantial amounts of rubbing wear particles. The description of rubbing wear particles previously presented is thus applicable and will not be repeated. Figure 139 presents a micrograph from test sequence SA, which represents the normal rubbing wear particles generated. This debris is correlated to the "new" (prerun) surface of the center piston ring from the test engine presented in Figure 140.

4. An abnormal sliding wear regime did not present itself during the test sequence; however, the following description is presented based on sliding contact monitoring of field equipments.

5. Severe sliding wear commences when the wear surface stresses become excessive due to load and/or speed. The shear mix layer then becomes unstable and large particles break away, causing an increase in the wear rate. If the stresses applied to the surface are increased further, a second transition point is reached when the complete surface breaks down and a catastrophic wear rate ensues.

6. Severe sliding wear particles range in size from 20 μm up in major dimension. Some of these particles have surface striations as a result of sliding. They frequently have straight edges and their major dimension to thickness ratio is approximately 10:1. As the wear becomes more severe within this wear mode, the striations and straight edges on the particles become more prominent.

7. Figure 141 presents micrographs of typical severe sliding contact wear particles.

D. WEAR PARTICLE ANALYSIS SUMMARY

1. In order to logically present this rather lengthy wear particle analysis effort the following summary is presented.



SA 10000X

FIGURE 139

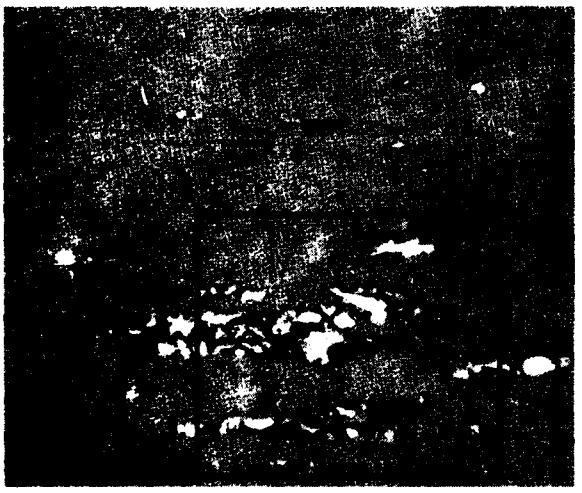
SLIDING CONTACT RUBBING WEAR DEBRIS



SA 1000X

FIGURE 140

PRERUN PISTON RING SURFACE



A. 225X



B. 450X



C. 1000X



D. SEM 1000X

FIGURE 141

TYPICAL SEVERE SLIDING CONTACT

WEAR PARTICLES

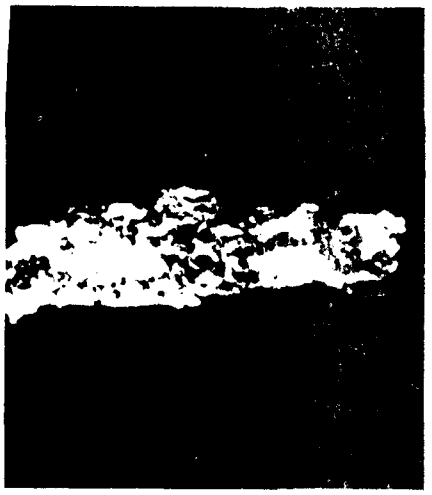
(Sheet 1 of 2)



E. 450X



F. 1000X



G. 1000X

FIGURE 7-7

TYPICAL SEVERE ROLLING CONTACT

WEAR PARTICLES

(Sheet 2 of 2)

2. Ball bearings, roller bearings, gears, and piston/cylinder components generate distinct wear particles which are a function of component life phase and when applicable, respective wear mode. Such particle characteristics as size, size distribution, quantity, composition, and morphology serve to create this unique component signature. The following text describes wear particle characteristic classifications based on program bench test results. Each component will be described with respect to wear-in, normal wear, and the classical abnormal wear modes of overspeed, overload, and fatigue. A general discussion of the wear modes of abrasive contamination and oxidative or corrosive environment will follow the component classifications.

a. Ball Bearings

(1) Wear In: New ball bearings produce free metal particles and oxides. These particles are usually platelets but random shapes are also produced. A length to width ratio of 3:1 and a major dimension to thickness ratio of 4:1 is exhibited by the free metal particles. Oxide particles, generally black oxide, are more equiaxial. The particles range in size up to 50 μm in major dimension. As compared to normal bearing wear, a high ratio of large to small particles exists. The quantity of particles present, is significantly higher than the amount present in a normal wear situation.

(2) Normal Wear: The majority of normal wear ball bearing wear particles are a combination of rubbing wear platelets and laminar particles. The platelets exhibit a length to width ratio of 3:1 and a major dimension to thickness ratio of approximately 10:1. Platelets range in size up to 15 μm in major dimension but the majority are less than 2 μm. Laminar particles exhibit a length to width ratio of 1:1 and a major dimension to thickness ratio of approximately 20:1. The laminar particles range in size from 10-30 μm in major dimension and average 1 μm in thickness. Ball bearing bench tests exhibited total particle counts ($\succ$2 μm) on the magnitude of 10^6 per 100 cc in a two gallon lubrication system.

(3) Fatigue: Fatigue presents itself as the dominant ball bearing failure/wear mode. Prior to fatigue pitting, ball bearings produce unique free metal spherical particles. The exact mechanism of production of these spheres has not, as yet, been totally agreed upon, however, their presence has been correlated to rolling contact fatigue. These spheres are usually less than 2 μm in diameter but may reach a diameter of up to 10 μm. Usually large laminar particles accompany the spherical particles. Once the ball bearing initiates a fatigue spall, it produces free metal platelets. These particles exhibit smooth surfaces with a length to width ratio of 2:1 and a major dimension to thickness ratio of approximately 4:1. Particle major dimension can vary up to 150 μm. The majority of the large particles, however, fall with the 15-25 μm range. The average ratio of large to small particles for a fatigue spall is high. The total quantity of particles present is drastically increased over the normal level.

(4) Excessive Load: This wear mode was not considered under this program.

(5) Excessive Speed: This wear mode was not considered under this program.

b. Tapered Roller Bearings. As a direct result of similar wear mechanisms present in ball and roller bearings, wear particles produced by each component are very similar.

(1) Wear-In: Roller bearing wear-in is very similar to ball bearing wear-in. The general description of wear-in particulates presented under the ball bearing section of this section is thus applicable to roller bearing wear in particulates.

(2) Normal Wear: Normal wear roller bearing wear particulates are a combination of rubbing wear platelets, laminar particles, and spiral shaped

particles. The platelets produced by roller bearings are similar to those produced by ball bearings. They exhibit a length to width ratio of 2:1 and a major dimension to thickness ratio of approximately 10:1. These platelets range in size up to 15μm in major dimension, but the majority is less than 2μm. Relatively very few platelets are produced by the bearing. Laminar particles produced exhibit a length to width ratio of 1:1 and a major dimension to thickness ratio
of approximately 20:1. These particles range in size up to 50μm in major dimension with a majority falling between 5-50μm. Their thickness is approximately 1μm. Spiral particles appear to be characteristic of roller bearings and are not observed under normal conditions in ball bearing testing. These particles are small and are likely to be produced by roller-end-flange contact. The appearance of the particle is very similar to cutting particles produced in a normal grinding process, but on a micro scale. The overall ratio of large to small particles exhibited by roller bearings under normal conditions is slightly higher than the ball bearing ratio. Roller bearing bench tests exhibited total particle counts ($>2\mu$m) on the magnitude of 10^6 per 100 cc in a two gallon lubrication system.

(3) Fatigue: Roller bearing fatigue is very similar to ball bearing fatigue. The general description of fatigue particulates, presented under the ball bearing section of this summary, is thus applicable to roller bearing fatigue particles.

(4) Excessive Load: This wear mode was not considered under this program.

(5) Excessive Speed: This wear mode was not considered under this program.

c. Gears

(1) Wear-In: Gear wear-in results from the presence of machined surface finishes. The break-in of these grooved surfaces creates elongated free metal particles. Wear-in particles generally exhibit a length to width ratio of

5:1. Their actual size and thickness is dependent on groove geometry, however, as compared to normal wear, they exhibit a relativly high ratio of large to small particles. The quantity of particles present is higher than the amount present during normal wear.

(2) Normal Wear: The majority of normal wear gear wear particles are rubbing wear platelets of free metal. They generally exhibit a length to width ratio of 2:1 and a major dimension to thickness ratio of 10:1. Particle size ranges up to 15μm in major dimension, however, the majority of particles are less than 2μm. Gear bench tests exhibited total particle counts ($>2\mu$m) on the magnitude of 10^7 per 100 cc.

(3) Fatigue/Pitting: Gear fatigue spall particles are smooth surfaced free metal platelets. They exhibit a length to width ratio of 4:1 and a major dimension to thickness ratio of approximately 5:1. Particle size ranges up to 150μm in major dimension. The majority of large particles, however, fall into the 15-25μm range. The ratio of large particles to small particles is very high. The total quantity of particles present is drastically increased over the normal wear level.

(4) Scuffing: Excessive speed or load results in gear tooth scuffing or scoring. The wear particles produced are free metal platelets with some indications of surface oxidation. The major dimension to thickness ratio is about 3:1. Particles range in size from 150μm down, however, the majority is less than 5μm in major dimension. The ratio of large to small particles is low. The total quantity of wear particles is significantly greater than in the normal wear case.

d. Piston/Cylinder. Sliding contact results in wear particles very similar to those produced under the gear bench testing. This similarity is due to similar wear mechanisms present in each component.

(1) Wear-In: Sliding surface wear-in, like gear wear-in, results from the presence of machined surface finishes. The general description of wear-in particulates presented under the gear section of this summary is thus applicable to sliding surface wear-in particulates.

(2) Normal Wear: Again, based on similar wear mechanisms, the description of normal gear wear particles is applicable as a description of normal sliding wear particulates.

(3) Fatigue: Fatigue is not a major abnormal wear mode with respect to sliding contact and thus will not be considered in this discussion.

(4) Excessive Load and Speed: Excessive load and speed, with respect to sliding contact, produces wear particles composed mainly of platelets of free metal. Their major dimension to thickness ratio is about 10:1. Particle size ranges up to 1 mm in major dimension, depending on the degree of excess load and speed. The ratio of large to small particles increases with stress level. Total quantity of wear particles greatly increases over the normal wear level. Particle may show signs of surface oxidation or "temper" blueing in the case of speed and surface striations present in an overload situation.

e. Contaminant and Corrosive Wear Mode. In order to complete the discussion of wear particle/wear mode correlations, several wear situations need to be described above and beyond those presented above. These wear situations are very prevalent and can be classified as oxidation or corrosive environment and abrasive contamination. A general discussion of these situations is as follows:

(1) Oxidative or Corrosive Environment: The susceptibility of the wear surfaces to oxidation can increase as a result of several factors. Included are:

Inadequate lubricant supply
Temperature increase
Deterioration of the lubricant
Presence of water contamination

In terms of wear debris, oxidation can show itself in three forms:

a. Temper colors and particle oxidative attack. Temper colors are an optical effect caused by oxidation to depths of about 50 nanometers. The colors vary from straw brown through blue depending on the exact depth of oxidation. When environmental conditions become oxidative, the edges of particles and any cracks in their surfaces are initially visible as distinct black lines that emphasize the particle outline and morphology. Particles generated by scuffing or scoring of gears always display these effects. Particles displaying the above colors or dark edges are almost invariably caused by overheating of the wear surfaces. The particle size also increases.

b. Red Oxide. These particles are composed of Hematite, Fe_2O_3. They usually appear as red translucent polycrystalline particles to a maximum size of 150 μm. The majority of particles, however, are 20 μm or less.

c. Black Oxide. These particles are composed of Fe_3O_4 and free iron. Particles with any free metal content being totally opaque. They appear as black polycrystalline particles or as grey platelets. It is hypothesized that oxidation of the polycrystalline particles, occurs at the surface while the platelets are oxidized subsequent to formation. As in the case of red oxide, the size variation is to a maximum of 150 μm with the majority being less than 20 μm.

1. The generation of red oxide rather than black signifies a milder wear mode. If red oxide is the primary type of debris generated by the system, the possibility of general rusting must be considered.

2. Other corrosive wear modes may operate. For instance, lubricant from refrigerant pumps has been analyzed where the wear debris is primarily the halides of iron.

(2) Abrasive Contamination: Abrasive contamination may be defined in simple terms as solid particles that are harder than the wearing surfaces, i.e., road dust. These particles can cause abnormal wear in one of two ways:

(a) Cutting Wear. This type of wear occurs when one wear surface is significantly harder than the other, i.e., journal bearings. The hard contaminant particles are pressed by the wear contact into the softer surface. The soft surface then holds the abrasive particle in such a way that it behaves very much like a lathe tool and cuts away the harder wear surface. The generated cutting wear particles themselves look exactly like miniature pieces of lathe swarf, their length and thickness being determined by the size of contaminant particles and the wear surfaces materials.

1. This type of wear may also be seen in the final stages of machine failure without the presence of abrasive particles. If a hard wear surface has roughened for any reason, i.e., fatigue pitting, then the resulting hard sharp edges may generate cutting debris, i.e. a fractured element in a rolling contact bearing may generate cutting wear from the softer separator.

2. Dramaticaly Increased "Normal Wear": When the two wear surfaces are of comparable hardness, abrasive contaminants may increase the normal rubbing wear. The abrasive particles roll between the two surfaces causing high local stresses that generate large quantities of normal rubbing wear. Components that may be affected in this way are cylinder walls and pistons in reciprocating machines, mating gear teeth, and cams and their followers. Although this wear mode is not identifiable by the morphology of an individual wear particle, the dramatically increased quantities of wear debris and the presence of the abrasive particles is sufficient warning. The wear rate can increase by a factor of ten or more.

3. The particles described in all the above correlations are confined to iron based alloys. Other engineering alloys will generally produce particles of similar morphology for comparative wear modes. The obvious exception being the effects of oxidative and corrosive environments.

4. Results and conclusions generated through component bench testing (Laboratory Program Phase) are now being verified by application of analysis techniques to field equipment lubricant samples (System Application Phase). Twenty thousand of these field samples have been collected from such equipment as turbine engines, helicopter gearboxes, tank engines, and ship equipment. Application of analysis techniques to these samples, will serve to verify wear particle analysis diagnostic capability. Results of the System Application Phase will be published at a future date.

VI. TEST RAMIFICATIONS

A. GENERAL. During the conductance of the laboratory study several significant test ramifications were identified. These ramifications, although alluded to in the previous section, warrant further discussion. Ramifications include the following:

- Fluid Sampling
  - Wear Process
  - Contamination/Filtration
  - Lubricant Antiwear Properties
  - Spectrometric Oil Analysis
  - Analytical Ferrography
  - Interrupted Testing
  - Improved Oil Analysis

B. FLUID SAMPLING

1. In order to establish the operating conditions and health of machines by analysis of the particulate matter in their lubricating fluid, it is essential that the lubricant sample contain a representative selection of particles. Since the particulate matter exists as a separate phase in the fluid, it cannot be assumed that a uniform distribution exists throughout the oil at all times and locations. Consequently, careful attention must be given to the method of lubricant sampling.

2. There are basically two types of lubricant sampling approaches: in-line and extracted. The in-line technique involves real time analysis of the oil during its circulation through the lubricant system. Currently, the in-line technique development is still in its infancy. Such areas as location, flow, pressure, sensitivity, and vibration are critical with respect to in-line applications.

3. The second type of sampling technique is that of extraction which involves obtaining a representative volume of oil from the system for analysis at a remote location. This type of sampling is presently the predominent technique and will thus receive major emphasis in the following text.

4. During normal operation of lubrication and hydraulic systems, the wear particle concentration in the fluid approaches/achieves an equilibrium level for each given set of operational parameters. Since wear debris is continually generated in any operational mechanical system, the achievement of an equilibrium level implies that particles are removed from the fluid at the same rate as they are generated. Known and suspected particle loss mechanisms include:

a. Filtration
b. Settling
c. Adhering to solid surfaces
d. Breakdown during repeated passage through wear contacts
e. Oxidation
f. Chemical attack
g. Oil loss

5. Having established that both particle generation and loss mechanisms affect the particle equilibrium level in fluids, the following guidelines should be used when specifying sampling procedures:

a. Samples should be taken from a single representative location in a system. The different parts of any one system may have different particle concentrations, e.g., before and after a filter.

b. The lubricant sample should be taken during equipment operation (after a "warm-up" period) or shortly after shutdown. A sample should never be taken more than one hour after shutdown because of the possibility of losing large particles. These measures serve to minimize the settling effect of particles in the lubricant.

c. If samples are to be taken while a system is operating, it is desirable to do so during specific operating conditions. It has been observed that the particle concentration in the lubricating oil of gas turbines for example, varies significantly between high and low power settings.

d. If samples are to be taken after machine shutdown, the effect of particle settling rates and the location of the sampling point must be considered.

e. A further consideration is the effects of an oil change. Since a complete lubricant change removes the majority of particles from the system, the operational period necessary to return to normal equilibrium must be considered. Following a lubricant change, the quantity of wear debris in the oil will increase with operating time until an equilibrium level is reached. Each machine will have a characteristic operating time necessary to return to its normal equilibrium level.

f. Lubricant samples are withdrawn from a system by one of four basic techniques: filler sampling, drain sampling, valve sampling, and pipe sampling. For the sake of continuity, samples should be withdrawn utilizing the same technique and location throughout an equipment monitoring effort. The sample volume should never exceed 80% of the total sample container volume.

(1) Filler Sampling - This technique involves inserting a sampling tube into the lubricant from the top of the sump. The tube should be extended into the lubricant a distance of at least half of the sump lubricant depth, but no more than one inch from the sump bottom. This location insures a representative sample, and eliminates sampling sludge from the sump bottom. Once inserted,

the lower end of the tube should be allowed to fill with lubricant. Upon filling, the upper tube end should be closed in order to hold the lubricant, and the tube withdrawn. The resulting trapped lubricant can then be drained into the sample bottle. This procedure should be repeated until a desired sample volume is collected. Plastic or glass sampling tubes can be used according to the application. Sampling tube cleanliness is essential and should be checked before each sample is taken. If visually contaminated, the sampling tube should be flushed with filtered freon until the contamination is removed. Cap the sample bottle immediately after sampling.

(2) Drain Sampling - This technique involves obtaining a sample from the bottom of the lubricant sump. When the sample is removed from the bottom of a sump there is the probability of obtaining a high particulate volume as a result of sedimentation. The drain outlet in the sump should be opened and the lubricant should be allowed to flow out (approximately 1/2 pint) in order to wash out any accumulated sediment. Once this wash out procedure has been accomplished, a sample bottle can be filled from the drain flow. Upon filling the bottle, the drain should be reclosed. Cap the sample bottle immediately after sampling.

(3) Valve Sampling - This technique involves the utilization of a permanently installed sampling valve. When using this technique, enough lubricant must be drained from the valve before sampling to thoroughly flush the sampling line. This flush volume will vary with respect to the sampling port design. As a general guide the dead volume of lubricant in the sample system should be estimated, and approximately twice that volume extracted before the actual sample is taken. Upon completion of the sampling process, immediately close the sampling valve and cap the sample bottle.

(4) Pipe Sampling - The sampling technique which gives the most representative sample is one in which the sample is taken from an oil carrying pipe, scavenged from the wearing parts and prior to filtering. Clearly, it is necessary for the machine to be operational to do this. Care must also be taken

that the sample is representative of the complete system, i.e., that the scavenged oil has passed through all the wearing parts. If the pipe is large and the flow velocity is low, sampling from the bottom of the pipe should be avoided.

g. The top of each sample bottle should be securely tightened and sealed with teflon tape to prevent loosening and leakage. Bottles should be plainly labeled for correlation with respective data sheets. Care should be taken in bottle packaging in order to prevent breakage during shipment to the analysis facility. Data sheets should be shipped with samples in a waterproof pouch to protect them from possible lubricant spills and leakage.

h. Required sample volume will vary as a function of desired analysis techniques. In order to perform a thorough analysis using existing techniques, a volume of 100 ml should be withdrawn from the system. For a truncated analysis, less of a volume is required, however, the volume should never be less than 15 ml. The withdrawn sample volume should be immediately replaced by an equal volume of clean compatible lubricant when it depletes the total system volume below specified safe limits.

6. SAMPLING CONTAINERS

a. If the oil samples are to be analyzed for particle content, the use of plastic bottles should be avoided. Plastic materials in contact with oils, particularly the polyester oils, may contribute particles of plastic, gels, and corrosive liquids. For example, the plasticizer in polyvinyl chloride tubing may leach out and cause corrosion of metal wear particles. Further, a gel-like compound is generated which gathers in wear particles to create agglomerates which float in the oil. The most prevelant difficulty with plastic bottles is that they may become sticky and hold the wear particles on their inner surface so that the oil sample is no longer representative after storage in the bottle. Metal containers can be used but there is danger that particles from the can, particularly particles of metal plating, may be confused with wear particles. It is best to use glass.

b. It is recommended that the sample bottle hold at least 15 ml and be made of clear glass with flat sides. The advantage of clear glass and flat sides is that the sample may be visually examined. Visual examination can yield important information concerning:

(1) Color - Oxidation due to overheating, or lubricant degradation generally darkens an oil.

(2) Sludge - The degree of sludge formation after sample storage.

(3) Severe Wear - Very severe wear cases frequently result in large individual wear particles that may be seen in the oil.

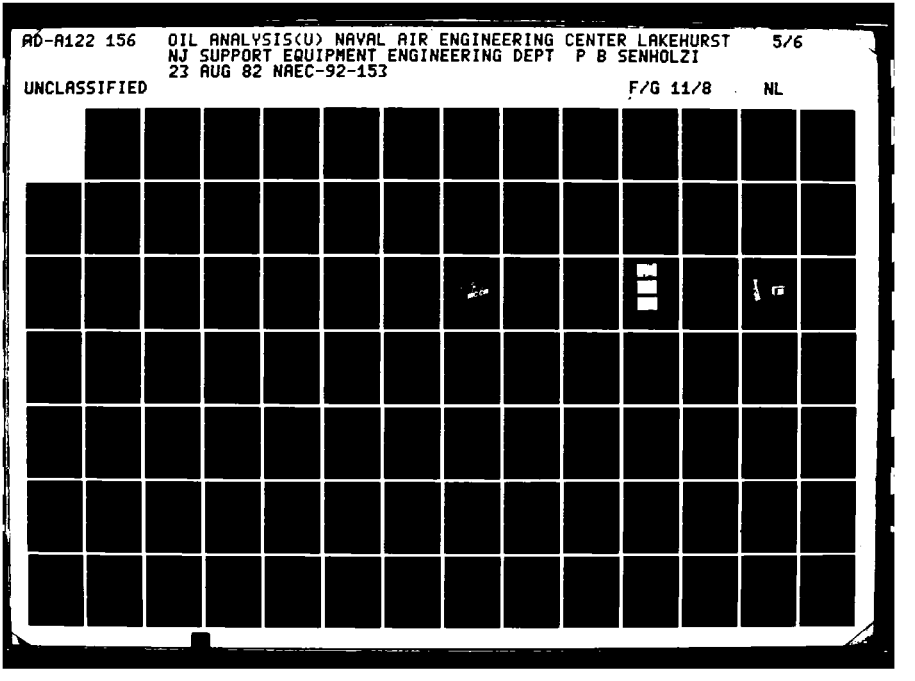
(4) Foreign Liquids - The detection of foreign liquids in the oil. For example, in one case a large fraction of the liquid was found to be a detergent that was heavier than the oil.

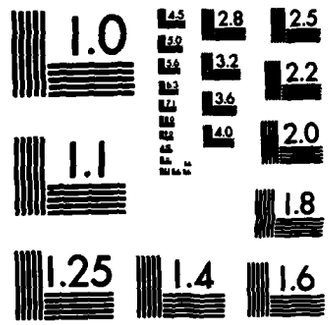
These conditions may be missed if the bottles are cylindrical and made of dark glass.

c. Glass bottles are often fitted with plastic screw-on caps. These caps have liners which are designed to provide a sealing surface against the lip of the bottle. Many cap designs employ fibrous backing material with a thin plastic coating on the surface. The polyester oils will often attack the coating and release sticky material and fibrous particles into the oil samples. Also, the papers used contain clay particles which may contaminate the sample. Although such particles are easily distinguished from wear particles, they may distort information on the solid contamination level of the oil sample.

d. Teflon cap liners have solved these problems. Teflon, however, creep under the compressive stress of the seal and the cap may loosen quently, if the sample is to be shipped or stored, it is advisable cap using shrink sleeving or teflon tape .

AD-A122 156 OIL ANALYSIS(U) NAVAL AIR ENGINEERING CENTER LAKEHURST 5/6
NJ SUPPORT EQUIPMENT ENGINEERING DEPT P B SENHOLZI
23 AUG 82 NAEC-92-153
UNCLASSIFIED F/G 11/8 NL





MICROCOPY RESOLUTION TEST CHART
NATIONAL BUREAU OF STANDARDS-1963-A

e. A standard SOAP sampling bottle is recommended for use as a suitable container. If a cleaned bottle is not available, bottle cleaning can be accomplished by the following steps: wash, rinse, wash, dry, and cap (i.e., SOAP bottle with acceptable cap seal.)

7. SAMPLE STORAGE. In order to insure viable Oil Analysis Program test results, representative oil specimens must be analyzed from respective test systems. These samples, when subjected to analytical techniques, after various storage periods, must remain representative of the test system lubricant. Under the Oil Analysis Program, a study was initiated to investigate the storage characteristics of oil samples. The following findings, some still not fully explained, were uncovered:

a. Different lubricants exhibit significantly different abilities to retain particles in suspension. Although lubricants exhibit similar viscosities, they do not necessarily exhibit similar settling rates as illustrated in Figure 142. The 54 mm labelled plots on this graph represent sinking rates of particles in the 5-7 μm size range, while the plots labelled 50 mm represent sinking rates of particles in the 2-5 μm range. The lubricants reflected in Figure 142 have identical viscosities.

b. The particle agglomeration characteristics of different lubricants exhibit substantial variation.

c. The longer an oil specimen is stored, the more difficult it is to redisperse the contained particles.

d. If a sample is to be stored for an extended period (more than one week), proper storage procedures must be followed. The sample should be stored in a cold environment (approximately -20°F). Low temperatures will serve to retard any chemical reactions that may occur in the lubricant sample.

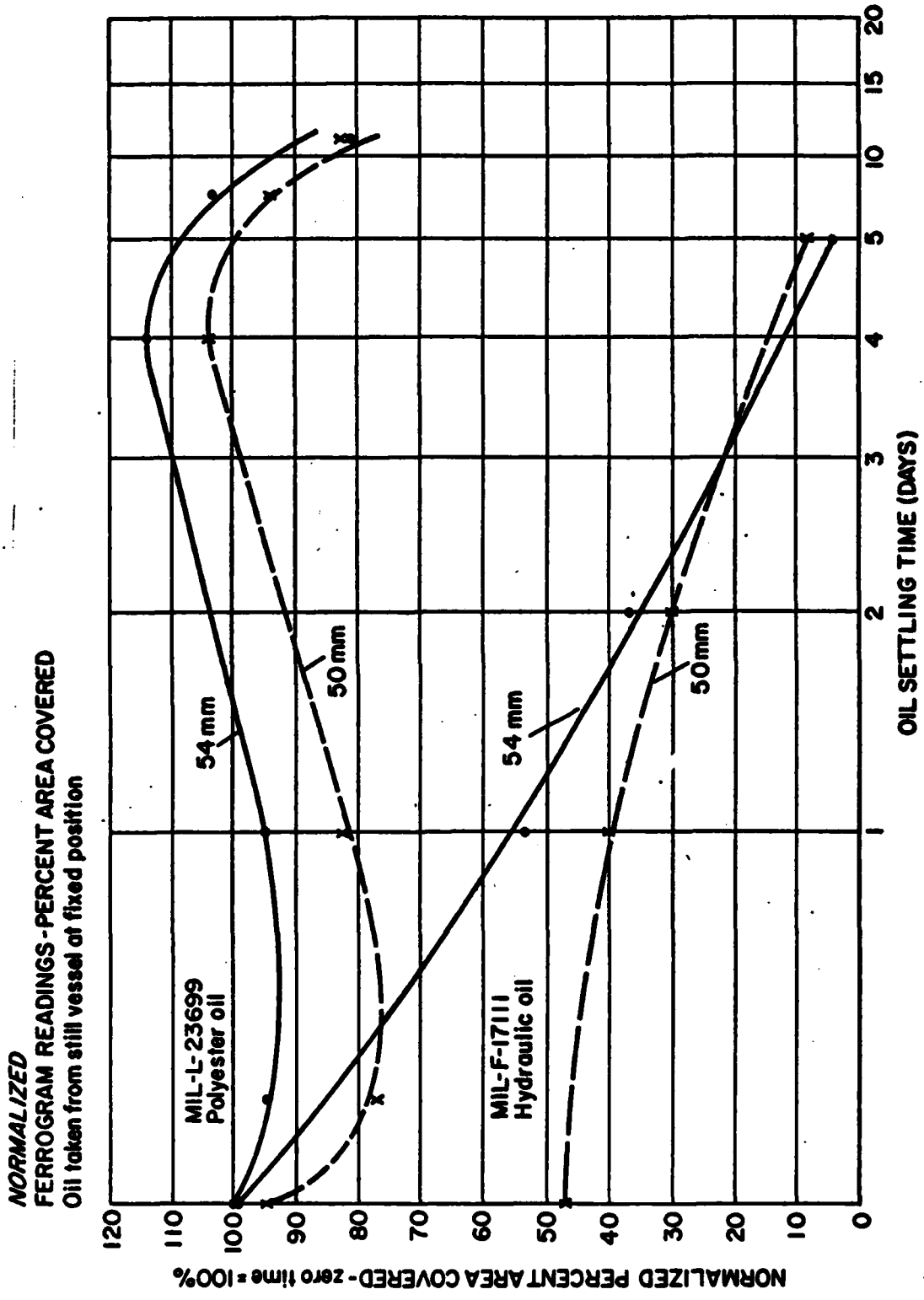


FIGURE 142. OIL SETTLING RATES

8. SAMPLE DISPERSION

a. Very little difficulty is experienced with the handling and storage of oil samples, providing the sample bottle is well designed. However, it is important that the particles be totally dispersed before any of the oil from the sample bottle is analyzed. Otherwise, the withdrawn oil will not have the same particle distribution as when it is subjected to analysis.

b. Particles tend to stick to the bottom and sides of the sample bottle if the oil is stored for more than one or two days. It has been found that heating the bottle of oil to 65°C (150°F) followed by vigorous shaking by hand, disperses the particles adequately. Severe machine shaking at room temperature is not as effective. It is hypothesized that waxes and gels are formed on the bottle's surfaces and that the particles become entrapped. Sample heating tends to disperse these waxes and gels.

9. SAMPLING INTERVAL

a. The sampling interval will be a function of monitored equipment type, respective operating parameters, and how important early warning is to the user. These factors should be analyzed in each monitoring case and an applicable sample interval be defined.

b. Experience has shown that in a large percentage of failures, evidence of an abnormality existed at or close to the inception of the machine's running. In other words, the machine was defective from the start. The reasons for this are obvious. Many failures are the result of improper assembly, poor design, a defective part or defective material. Such difficulties exist at the inception and usually give evidence of their presence.

c. The exceptions are mishandling of the machine such as overtemperature, speed or load, shock, etc., and contamination, such as the failure of an air filter. However, many of these events are detectable directly by the user or by the oil analysis; for example, sand in the oil.

d. Fatigue phenomena, the loosening of fasteners, etc., may not reveal itself at the inception.

e. If a system is new or has just been overhauled, it is desirable to sample the system every few hours to ensure a normal break-in and to detect an inherent problem.

f. Once a normal break-in has been established, depending upon the degree of reliability of failure prediction required, the sampling interval can be extended. The following sampling periods are suggested as a guideline for various systems.

	HOURS
Aircraft Gas Turbine	10 - 200
Airborne Hydraulic Systems	20 - 200
Diesel Engines	100 - 500
Heavy Transmissions	100 - 500
Surface Hydraulic Systems	50 - 500

10. EXTRANEOUS CONTAMINATION. Two main sources of possible contamination not previously mentioned, are lubricant contamination and residual contamination. Each of these sources can seriously affect wear particle analysis and as such, their effect must be minimized.

a. Lubricant Contamination. This type of contamination is introduced into a system by the lubricant itself. Samples submitted should be accompanied by an unused lubricant sample, obtained from the same lubricant batch as that used in the equipment. This sample will be utilized to establish a baseline level of contamination contributed by the lubricant. This baseline should be taken into consideration during the analysis process.

b. Residual Contamination. This type of contamination is introduced into the system by initial assembly of the equipment or by maintenance actions performed on the equipment. In the case of program test equipment, residual/

cross-contamination could carry over from previous test runs. This residual contamination effect can be minimized by proper flushing of the lubrication system before initial startup, after pertinent maintenance actions, and between selective test runs. Three flushes using clean lubricant, or a combination of appropriate solvents and clean lubricant are normally sufficient to purge a lubricant system of the major portion of residual contamination.

11. FACTORS INFLUENCING OPERATIONAL TIME TO EQUILIBRIUM

a. Since an individual particle life expectancy does not vary greatly with the actual particle concentration (agglomeration and its subsequent effects on settling and filtration efficiency being a possible exception), it follows that the particle loss rate is the primary dictator of the time required to reach a debris equilibrium level, while the combination of particle generation rate and particle life expectancy dictates the actual particle concentration level achieved at equilibrium.

b. Factors which influence the operational time to equilibrium are:

(1) Filtration - A prime factor is the number of times a particle of a given size and material may, on the average, pass through the filter. The better the filter the shorter the time to equilibrium.

(2) The Oil Pumping Rate - The oil cycle pumping rate is expressed in volume per unit time divided by the volume of lubricant in the system. On some systems the volume of oil is circulated as much as five times per minute while on others rates of once per hour or longer may be normal. This factor applies to losses in the filter, and to breakdown of the particles during repeated passage through the wear contacts.

(3) Dispersive Qualities of the Lubricant - In systems where the fluid contains detergent additives, these additives prevent agglormeration of the particles and also discourage their adhering to surfaces, thus increasing

their life expectancy. Diesel engine lubricants usually contain such additives to prevent the deposits on cylinder walls.

(4) Locations of Slow Moving Oil - If there are locations within a system where the oil moves slowly, the particles may settle out or adhere to the localized surfaces. The bottom of sumps, oil tanks, etc., are examples of these locations.

(5) Other Factors - Other factors which affect time to equilibrium are oxidation of particles, chemical attack on particles, and system oil loss.

12. SAMPLE DATA. In order to thoroughly and effectively perform an analysis on a lubricant sample, a comprehensive set of background information must be submitted with the sample. The following information is required:

a. Activity

Name
Address
Code
Contact Personnel (Responsible Party, Sampler, Phone Number)

b. Equipment

Type (component)
Model
End Item
Serial Number
Operating Parameters
Operating Environment
Wear Components (lubricated)
Wear Materials (versus wear components)
Time on Equipment (mileage)
Time Since Overhaul
Recent Maintenance Actions

c. Lubricant

Type
Specification
Capacity
Additives
Time Since Filter Change
Time Since Lubricant Change
Lubricant Added Since Change/Time
Filter Size (Normal Rating and Absolute Rating)
Filter Type

d. Sample

Date/Time
Number
Technique
Location with Respect to Filter
Sample Frequency
Time After Shutdown

e. Observations/Comments.

A detailed approach to lubricant sampling is included as Appendix O of this report.

C. WEAR PROCESS.

1. GENERAL

a. Analysis has verified that component wear life can be classified in three distinct phases: wear-in/break-in, normal wear, and wear out/abnormal wear. However, all components do not necessarily transition through all three phases.

2. WEAR-IN/BREAK-IN

a. The wear-in/break-in phase involves the period of transition of the "as finished" surface to a smooth low wearing surface of a wear component. During this phase the ridges of the original component ground or machined surfaces are flattened and form cornices along the ridge peaks. These cornices subsequently break away. Mechanical work at the wear surface breaks down the crystalline structure of the metal, resulting in a thin layer of short range crystalline order with about a 1μm thickness for steel. During its formation, the layer exhibits super ductility and may flow along the surface a distance several hundred times its thickness. Its ability to flow results in a very smooth wear track.

b. In some cases this wear-in process accelerates and directly enters into an abnormal wear mode (i.e., infant mortality). This phenomenom results from factors such as severe surface damage caused by the manufacturing process, or component handling/installation, as well as severe subsurface defects. Other factors greatly influencing this wear-in phase are design/operating criteria, lubrication, and contamination (see "Contamination/Filtration"). The wear-in process is a critical interaction that greatly influences future component wear rate/life.

3. NORMAL WEAR

a. When a stable wear surface is formed the component enters into the normal wear phase. An equilibrium developes between wear particle removal rate and wear surface regeneration rate. The wear rate in this phase is primarily a function of the degree of intersurface activity.

b. Although this phase is considered normal, over a period of time enough material could be removed from the surface to increase tolerances beyond efficient operating limits, and thus result in the necessity for some form of appropriate maintenance.

c. Excessive quantities of contamination, such as sand in a lubrication system, can substantially increase the wear generation rate without completely removing the wear surface. Although catastrophic failure is unlikely, such systems can wear beyond efficient tolerances quite rapidly.

4. WEAR OUT/ABNORMAL WEAR

a. A component enters an abnormal wear phase when the equilibrium condition of the normal phase is upset. This equilibrium is disrupted by an increase in wear surface removal rate, to a condition where the layer is removed faster than it is generated.

b. There exists several competing wear modes in a system which could drive it individually or collectively into an abnormal wear situation. Predominant wear modes can idealistically be classified as overload, overspeed, and fatigue. A more practical classification considers such prevalent wear modes as misassembly, lubricant starvation, overheating, abrasive contamination, and corrosive contamination. In reality an abnormal wear situation will include two or more of these wear modes. An example of this is a component subjected to lubricant starvation. This component will encounter both surface overload and a more oxidative environment.

c. Abnormal wear situations, in most cases, result in accelerated deterioration of lubricated wear surfaces. If unchecked this deterioration will lead to unacceptable system operation, and in some cases catastrophic failure of the wearing component as well as secondary damage.

d. This abnormal wear process, in some cases, is preventable/reversible if detected at an early stage. A system can be brought back into a normal operating wear phase/state through institution of required preventive maintenance. An example of this, would be the detection of high particulate contamination in a lubricant system. Extensive damage can be avoided by draining the fluid and flushing the system and replacing it with clean lubricant and a clean filter.

5. The above three phases serve to classify the wear states of all lubricated components. It is necessary for any oil analysis technique to be able to determine which wear phase a component is operating in at any particular time. Corrective action would only be required under phase three, abnormal wear, since the wear in and normal wear phases are not detrimental to system operation except as noted.

D. CONTAMINATION/FILTRATION

1. GENERAL

a. The contamination considered in this discussion is limited to particulate contaminants and does not include chemical contamination. Oil filtration regulates the concentration and size of contamination in the system. Better, more efficient filtration is presently being developed which will have a direct effect on an oil analysis program. Contamination is a good indicator of wear but also tends to accelerate the wear process.

b. Fluid contamination is controlled by various methods to provide an acceptable wear service life and reliability for all components in an oil lubricated or hydraulic system. This wear service life is dependent among others on two factors: the contamination level (concentration and size) of the system fluid, and the contaminant tolerance level of the system components. These two factors must be properly balanced to achieve desired life and reliability. This relationship is called the Contamination Control Balance.

2. CONTAMINATION LEVEL. The contamination level can be determined by performing a particle size distribution analysis on a sample of fluid. The parameters which influence the contamination level are:

a. Effective filtration ratio of the filter assembly. The ratio between particle separation performance of the filter element and escape flow paths in the filter element.

b. Flow rate of fluid through the filter assembly. The more frequently the fluid passes through the filter, the cleaner the system lubricant will become.

c. Rate at which contaminant enters the system fluid. The contamination level will increase as more contaminant enters the system.

3. TYPES OF CONTAMINATION. Contamination types can be classified into the following generalized categories.

a. Residual Debris. Particles remaining on mechanical parts as a result of manufacturing and assembly, and picked up by the lubrication system during the break-in period.

b. Generated Debris. Particles produced as a result of prevalent system wear mechanisms. These particles indicate the condition of the mechanical system.

c. Ingested Debris. Particles ingested through breathers, wiper seals, and openings during maintenance operations.

d. Regenerated Debris. Particles which evade or escape capture by the filter.

4. CONTAMINANT TOLERANCE LEVEL. Component contaminant tolerance level is determined by performing a contaminant sensitivity test on critical components. The test consists of sequentially subjecting the lubrication system of equipment to increasing particle size ranges while operating at rated conditions. The introduction of contamination into the lubrication system is related to component damage. The parameters of the system which directly affect the contamination tolerance level are:

a. Design resistance of the component to contaminant wear. The net result of toughness and compatibility of material, magnitude of mechanical and hydrostatic loading on wear surfaces, and configuration of leakage paths and wear surfaces.

b. Antiwear protection offered by the system fluid. Usually in the form of antiwear additivies introduced into the lubricant.

c. Duty cycle or operating conditions imposed on the components or system by the machine application. The level of the operating conditions (pressure, speed, temperature) has a significant influence on the contaminant tolerance level of a component.

5. EFFECT OF CONTAMINATION. Lubricant debris contamination can have a drastic effect on system wear. This effect is discussed as follows:

a. Contamination particles which cause wear, are those large enough to break the lubricant film and small enough to become caught in the contact or wear area. They must also be small enough to be circulated by the lubricant.

b. These contaminant particles will result in surface denting in the contact area, when carried there by the lubricant.

c. This surface denting causes stress risers which creates a nucleus for surface initiated fatigue spalling.

d. Surface denting also causes a localized breakdown in the lubricant film thus resulting in high cyclic stresses or a fatigue prone area.

e. Surface denting, if unchecked, has an accelerating effect. The more denting that occurs, the more secondary particles that are generated which in turn results in increased denting.

f. One of the most significant findings to result from the Oil Analysis Program has been the full realization of what a truely clean lubrication system can mean in terms of extending the life of operating components. Ultra clean lubrication systems, utilized in ball bearing bench tests, have resulted in the extension of bearing operational lives in excess of 40 times their calculated expected lives.

g. The lubricant used in these bearing tests was filtered through a 3 μm Millipore filter before being used for the tests. No in-line filtration was employed. Special system components were utilized to provide an uncontaminated system.

h. In order to induce/accelerate bearing failure, intentional damage was inflicted on the bearing surface by means of indentation.

6. FILTRATION. A prime factor in the control of lubricant contamination is filtration.

a. Filtration controls the effect of contamination. There are two basic types of filter systems, natural and mechanical.

(1) Natural filter effects are caused by particles settling in the oil sump, plating out on the mechanism walls, and collecting in "dead" areas of the system.

(2) Mechanical filtration is provided by installing various types of filters in the system, and passing the oil through them to remove the particles.

b. Higher filtration results in longer wear life.

c. There are two aspects of mechanical oil filtration that are interesting. One is the effect of clean oil on wear component life, and the other is the effect of filtration oil samples.

d. The true realization of contamination control is still in its infancy with respect to lubricant systems, whereas the fluid power industry has placed great emphasis in this area.

e. The institution of contamination control and oil analysis represents somewhat of a dichotomy. Oil analysis relies on the analysis of wear particulates carried in the lubricant, while contamination control tries to eliminate/minimize oil borne particulates. Contamination control will thus necessitate a complete revision of present oil sampling techniques and procedures.

f. As described in Section VIB, "Wear Process," surface initiated fatigue is a predominate competing wear mode in lubricated components. To highlight this affect the following test results are reported:

(1) Bearings were subjected to testing in ultraclean lubricant systems, in order to categorize generated wear particles and relate them to respective bearing wear conditions.

(2) As previously mentioned, these bearings although running at high speed and high load conditions would no fail.

(3) This extended life was a direct result of the "clean" lubrication system.

(4) This "clean" system resulted in a minimization of surface denting. The reduced amount of surface dents limited the potential for surface initiated spalling, thus minimizing one of the predominant competing wear component failure modes.

(5) These tests emphasize the criticality of system cleanliness, and filtration levels with respect to component failure modes.

g. A future trend in oil lubricated systems is the use of better in line particle filtration. This additional filtration will require different techniques to obtain oil samples for analysis.

h. An oil filter can profoundly modify the particle distribution in the machine's lubricant. The filter changes the particle population in two ways:

(1) First, the filter lowers the density of the particles in the oil. The average particle which remains in the oil of a filtered system was generated more recently than in the case of a system with no filter.

(2) Secondly, the filter will remove large particles more effectively than the small ones so that the density of the larger particles is reduced. This may aid or hinder the detection of the onset of severe wear. If the sample is taken before the filter, the presence of quantities of large particles is an indication that their generation rate is high, i.e., they are being produced here and now.

7. CONTAMINANT SENSITIVITY OF ROLLER BEARINGS VERSUS BALL BEARINGS. Test results have shown that the artificially induced Vickers hardness indentation is significantly more effective in initiating a spall in a ball bearing than in a roller bearing. This tends to indicate that ball bearings are more sensitive to contamination than roller bearings. Possible explanation of this effects is as follows:

a. Bearing material for the ball bearing is AISI 52100 steel and the roller bearing is AISI 4118 steel. The roller bearing steel melts at a higher temperature and therefore wears to a greater extent, which neutralizes the effect of the indentation.

b. The heat treatment consisted of thorough hardening for the ball bearings and carburizing for the roller bearings. The softer core of the roller bearings apparently spreads out the stress effect.

c. In the case of roller bearings, the load is evenly distributed across the contact width. The level of stress at a defect is therefore dependent only on its stress raising ability. On the ball bearings, the indentation occurs in a negative slip area which has a more significant effect.

d. Load distribution on the roller bearing is spread over a much larger area than on the ball bearing, which makes the ball bearing susceptible to flaws.

e. There exists greater defects with greater stress raising ability in the as finished bearing than the stress raising ability of the indent of a roller bearing.

E. LUBRICANT ANTIWEAR PROPERTIES

1. In the course of preparing suspensions of wear particles under sample dispersion program investigation and sinking rate testing (see "Fluid Sampling"), wear particles were generated in the laboratory. These particles were generated in a rubbing wear test machine employing several different lubricating and hydraulic fluids. This testing served to quantify relative wear rates (under fixed test conditions) of the respective lubricants.

2. During this testing, six runs were conducted; three with lubricating oil of different base stocks and three with hydraulic fluids commonly used in military systems. Samples containing rubbing wear particles were prepared with the following six oils.

MIL-L-23699 synthetic (ester) lubricating oil
MIL-L-7808G synthetic (ester) lubricating oil
Petroleum base lubricating oil
MIL-H-5606 petroleum base hydraulic fluid
MIL-F-17111 petroleum base hydraulic fluid
MIL-H-83282 synthetic hydrocarbon hydraulic fluid (fire retardant type)

3. Wear particles were generated in each oil with a rubbing wear test machine. The wear machine was adapted to rotate a 4-inch rod of 1/4 inch diameter

1018 steel. A flat 1-inch plate, 1/8 inch thick of 1018 steel was fitted to a movable arm on the machine to bear against the 1/4 inch diameter rod. Selected weights were used to establish the desired contact load. The wear parts operated immersed in 30 ml of oil.

4. The wear machine was run for 30 minutes (break-in period) at a contact load of three pounds. Following wear-in, the load was increased to 10 pounds and the machine operated for an additional 60 minutes. Oil temperatures were recorded initially, at 30 minutes, and at the end of the run. The speed was 20 cm/sec. The 30 ml oil sample containing the wear particles was diluted by adding clean oil for a total volume of 150 ml. Ferrograms were prepared from each oil batch.

5. Figure 143 shows the volume of entry deposit (particles $> 5\,\mu m$) for each of the above six oils. Figure 144 displays the percentage area covered by particles 1.25 mm below the entry deposit (particles $5\text{-}10\,\mu m$) for the selected oils. This information can be correlated to total particle content of the oil.

6. The rubbing wear particle chains generated under MIL-L-23699 oil were similar to those generated with the MIL-L-7808 oil. However, in comparison, the rubbing wear particle chains generated with the petroleum base lubricating oil were finer (in the sense of being narrower) and the entry deposit was substantially smaller, as would be expected from lower wear rates.

7. Petroleum base hydraulic fluids, MIL-F-17111, MIL-H-5606C, and MIL-H-83282 exhibited wear particles in chains similar to the petroleum lubricating oils.

8. In all of the cases the predominant wear particle type was "rubbing wear" from the shear mixed layer.

9. Interestingly, the synthetic hydrocarbon hydraulic fluid, MIL-H-83282 showed the least wear among the oils tested. The volume of wear particles generated by this fluid was 80 times less than the volume of wear particles generated by polyester lubricating oil, MIL-L-23699.

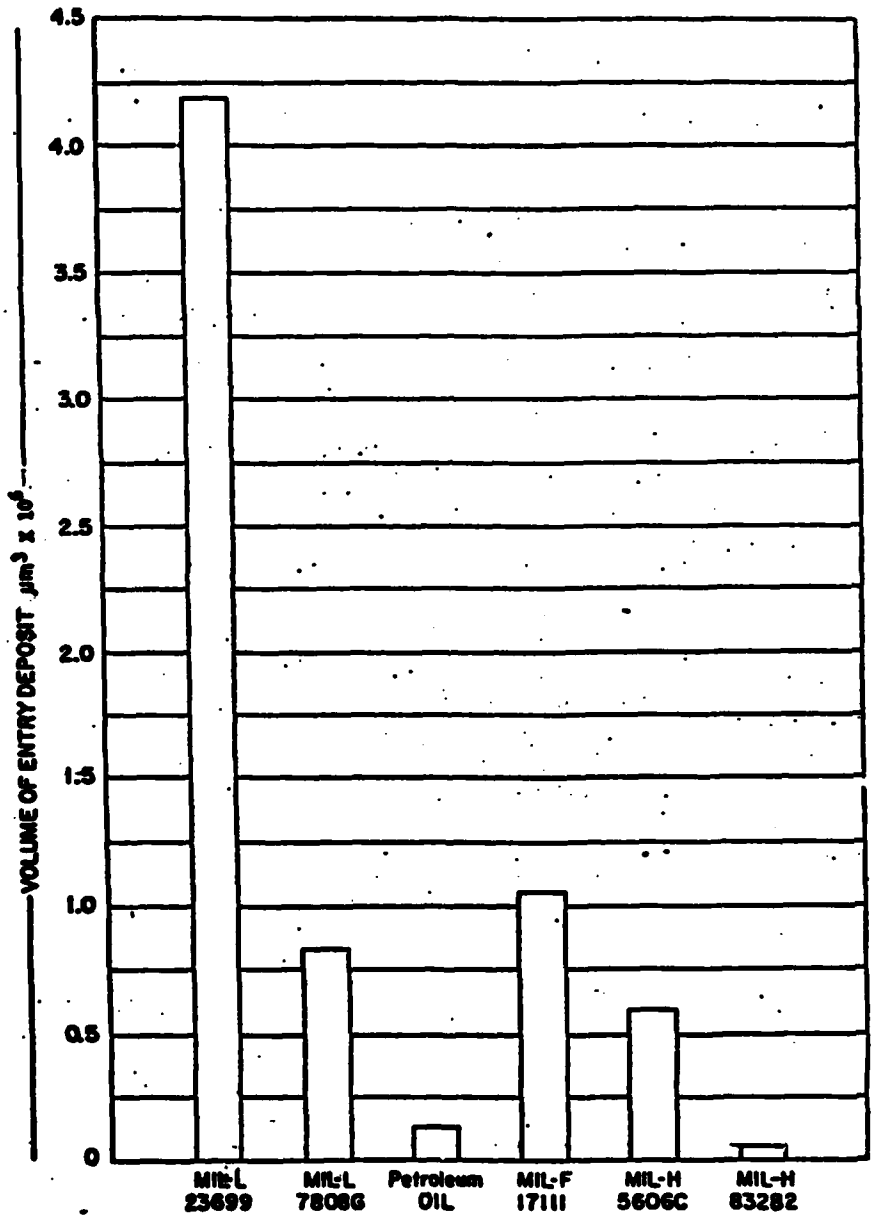


FIGURE 143

ANTIWEAR PROPERTIES

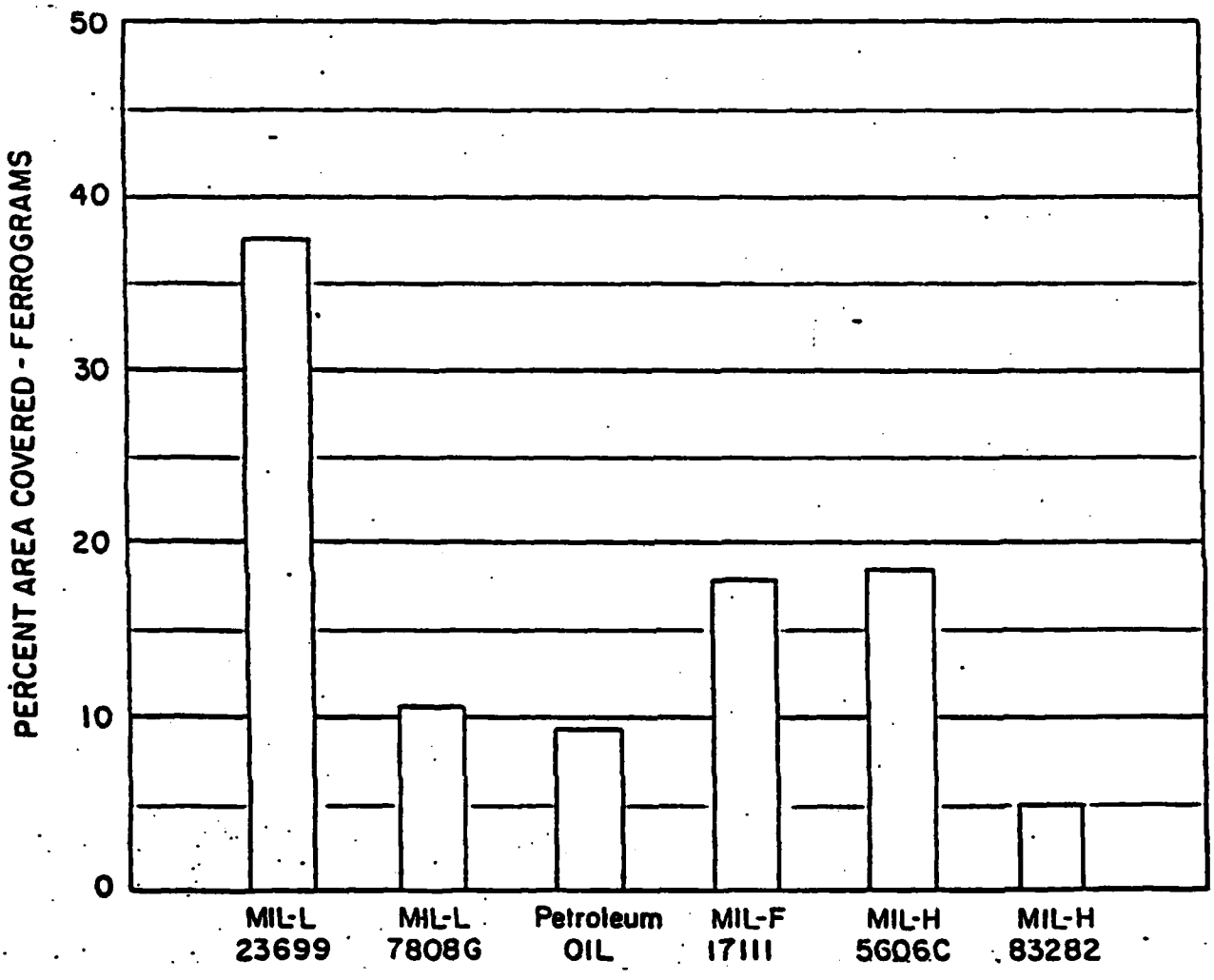


FIGURE 144

ANTIWEAR PROPERTIES

10. The ratio of wear particle volumes observed applies for the conditions of the test, and will not necessarily hold at higher loads, temperatures, or speeds.

11. These tests serve to highlight the significant differences in wear rates exhibited by various lubricants and additives under fixed operating conditions.

F. SPECTROMETRIC OIL ANALYSIS

1. The most prevelant approach to oil analysis is spectrometric oil analysis. This approach has been adapted by the Department of Defense as well as some facets of the industrial community.

2. The technical basis of the spectrometric approach is the determination of lubricant sample contaminant types and respective concentration levels. Utilizing this data, an analysis is performed which draws a comparison with known contaminant baselines established for the engine/component being monitored.

3. The two most commonly used methods of evaluating concentrations in oil are the emission spectrometer and the atomic absorption spectrometer. Of the two, the emission spectrometer is more widely used today because of its ability to analyze samples in the as received state, analyze more than one element at a time, inherit greater adaptability to different operating locations, and because it allows automatic transcription of the results to standard forms and punched cards or tape.

4. All branches of the military presently use an oil analysis program (OAP). The recently consolidated program has been named the Joint Oil Analysis Program (JOAP). Originally the Air Force program was the SOAP; the Army, AOAP; and the Navy, NOAP. The Air Force program is the most extensive. The types of equipment monitored by the various services is as follows.

a. Air Force

(1) Aircraft propulsion (gas turbine engines)
(2) Accessory equipment (transmission, starters, gear boxes, hydraulic systems, etc.)

b. Army

(1) Aircraft propulsion (gas turbine engines) and systems
(2) Ground equipment (tanks, generators, etc.)

c. Navy

(1) Aircraft propulsior (gas turbine and reciprocating engines)
(2) Ship equipment (main propulsion systems, pitch controls, etc.)

(3) Ground equipment

5. Oil Analysis has had a varying record of effectiveness in detecting/predicting impending mechanical malfunction or failures. Where oil analysis has been documented as being responsible for a substantial number of valid engine removals, these removals before failure have resulted in many tangible and intangible benefits, such as maintenance saving due to prevention of secondary engine damage and, more importantly, flight safety.

6. However, during the six-month period ending June 1972, 39% (28) of 72 gas turbine engines removed as a result of NOAP recommendations had negative findings (no discrepancy noted) upon disassembly. Also during this period, 143 gas turbine engines were removed because of metal contamination in the oil systems; 14% (20) of these engines were being monitored by the NOAP but had not been identified by NOAP as discrepant.

7. Naval Safety Center records for a five-year period revealed that 19% of the engine related major accidents resulted from failure of oil wetted components.

8. The above listed statistics indicate the need for improvement of the oil analysis program. Shortcomings of this program involve both administrative and technical elements.

a. Administrative Shortcomings

(1) Transit time from squadron to laboratory of the oil samples for the engines cited in the above discussion averaged 4.4 days. Such excessive transit times delay SOAP analysis and increase the probability of engine/component failure before detection. The time from detection of an abnormal condition to failure is unpredictable and may be as soon as the next flight. The service provided to operating activities culminates in timely recommended maintenance actions by the laboratory based on sample results. Laboratory interviews, control group monitoring, nd the examination of oil analysis records, reflect instances of lack of response and feedback to laboratory recommendations.

(2) Squadron-initiated feedback information as delineated in NAVMATINST 4731.1 is generally not being provided. This instruction requires operators to submit an oil sample and a Maintenance Feedback Form (NAVMAT 4731/1) to a laboratory after completion of maintenance that would affect the oil-wetted system, such as an oil pump change. Laboratory interviews, control group monitoring, and the review of oil analysis records revealed only a modicum of feedback responsiveness.

b. Technical Shortcomings

(1) Sample integrity is of prime importance in any oil analysis technique as covered in Section VIB. Sampling procedures in the SOAP are not strictly adhered to in all cases. Samples with a nonrepresentative debris distribution or samples containing foreign contaminants are prevalent. Detection of erroneous samples is difficult.

(2) A critical technical shortcoming of spectrometric analysis has been identified under this program. This shortcoming involves an inherent insensitivity to large debris/particles. Spectrometric insensitivity limit appears to fall in the range of particle size from 5-7 μm. Above this level, debris is not indicated in the spectrometer reading.

(a) A test result example in order to support this shortcoming, is presented in Figure 145. This dual plot presents the trend of both spectrometric results and ferrographic results plotted over the life of a roller bearing. The spectrometric data plot represents the concentration level (ppm) of iron (Fe) contained in lubricant samples taken during bearing operation. This plot (with a slight exception in the last sample) does not vary over the bearing life. The ferrography plot represents entry deposit density readings of ferrograms made from the above reference series of lubricant samples. This plot shows significant variation during the initial and final stages of bearing life. As indicated in Section V, 1, typical debris size in an entry deposit is $> 5\,\mu m$. Thus, spectrometric analysis is not sensitive to debris in the critical size range.

(b) Figure 145 test results are typical under the Oil Analysis Program. Of the 28 ball and roller bearings tested until failure, spectrometric analysis indicated only three abnormal wear situations.

(c) During gear testing, however, spectrometric analysis was very sensitive with respect to monitoring scuffing wear. Figure 146 represents a plot of the percent scuff versus operating time for gear set GE. Figure 147 represents the spectrometric iron (Fe) readings for lubricant samples taken during the respective test sequence. As can be seen, a very good correlation exists between the data plots. At first glance these results appear contradictory to the above reported bearing results. However, a closer look at scuffing wear indicates that this abnormal wear situation results in the generation of large amounts of relatively small wear debris. This is contrary to the majority of abnormal wear modes which results in the generation of large wear particulates.

(d) Figure 148 represents the plot of debris quantity over the respective gear life. This quantity is divided by particle size ranges. As can be seen, the majority of debris generated during scuffing falls into the 3-5 μm size range. This scuffing falls within the sensitivity limits of the spectrometer and as such does not represent a contradiction to this size limitation.

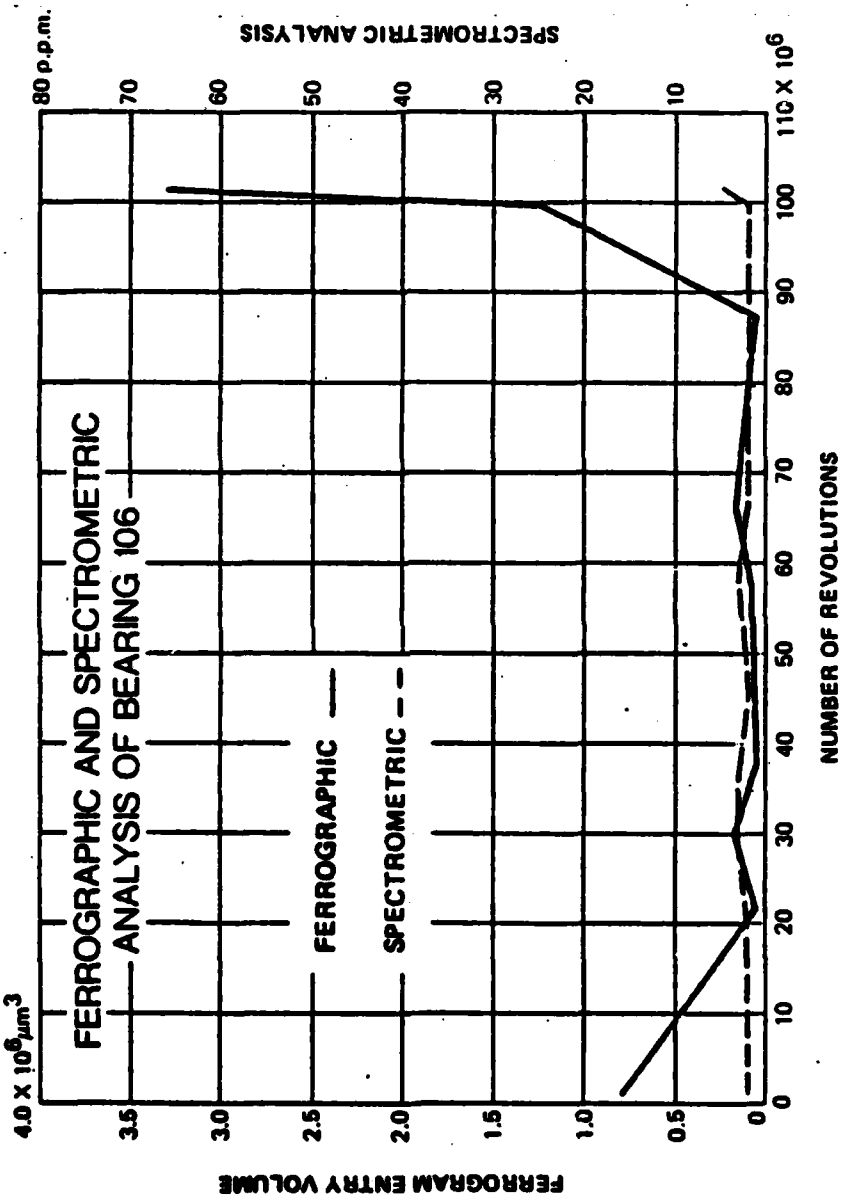


FIGURE 145. ROLLER BEARING TEST SEQUENCE

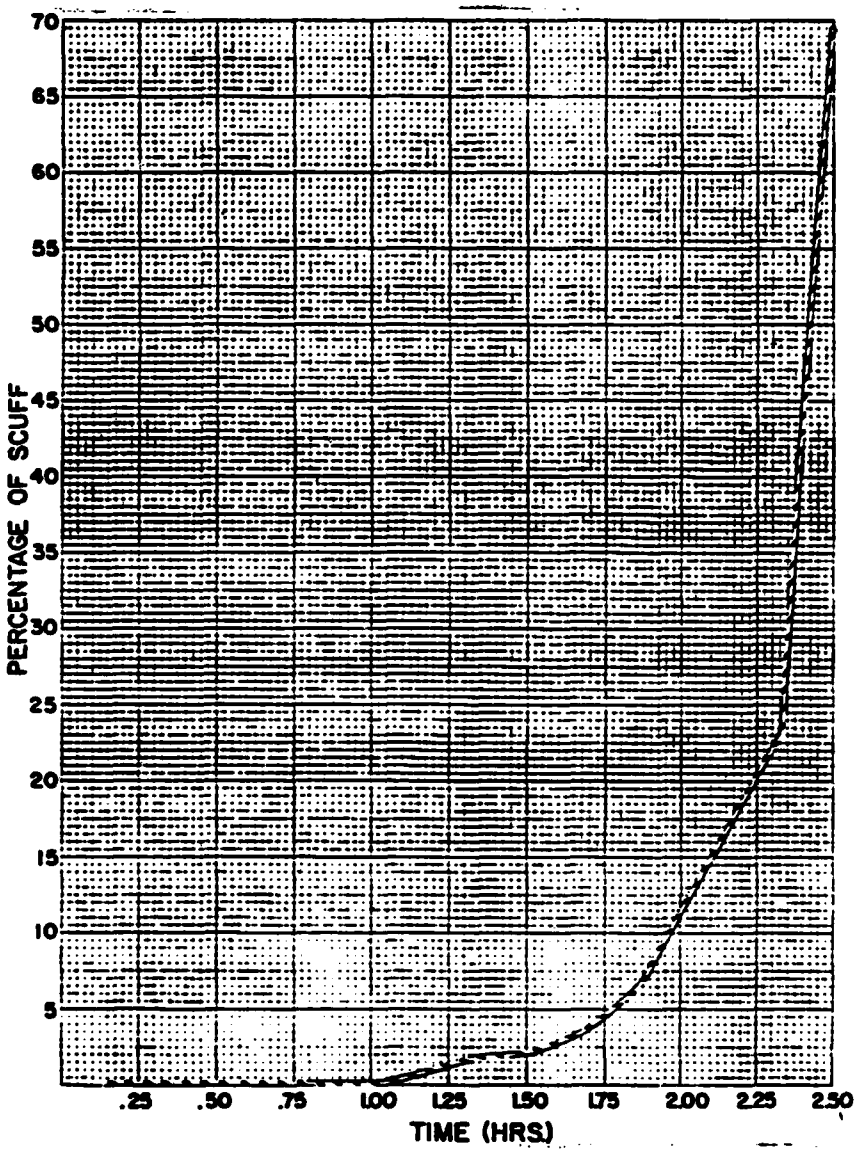


FIGURE 146. GEAR TEST SEQUENCE SCUFFING

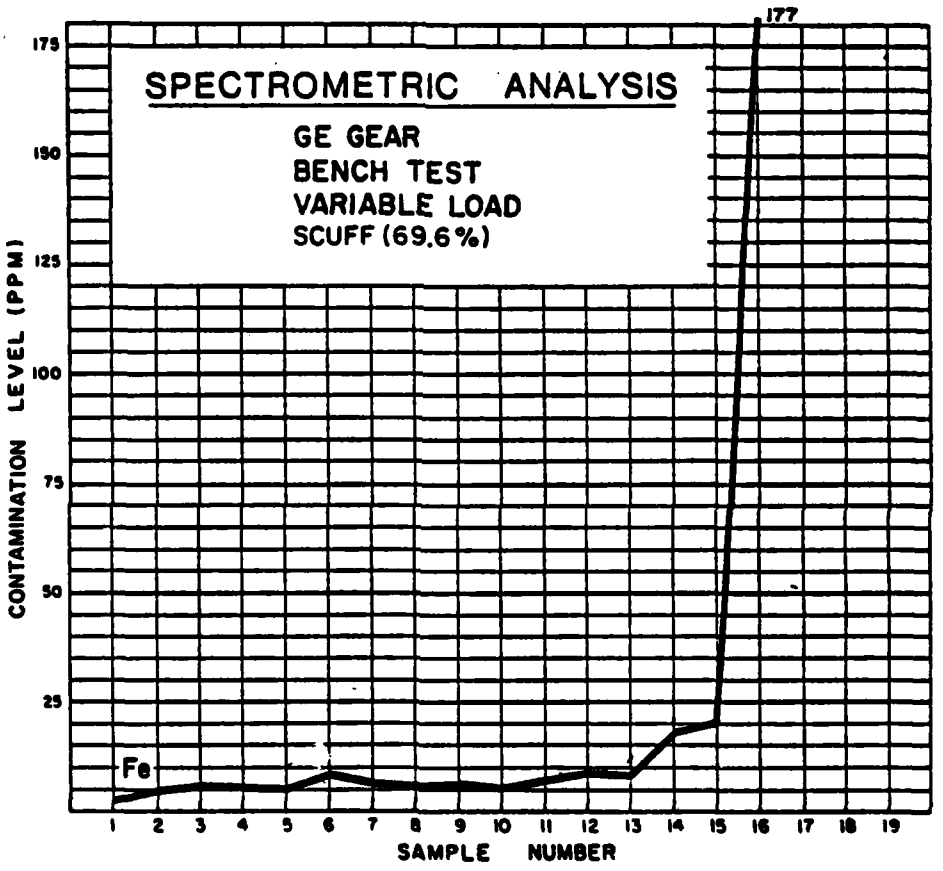


FIGURE 147. SPECTROMETRIC ANALYSIS

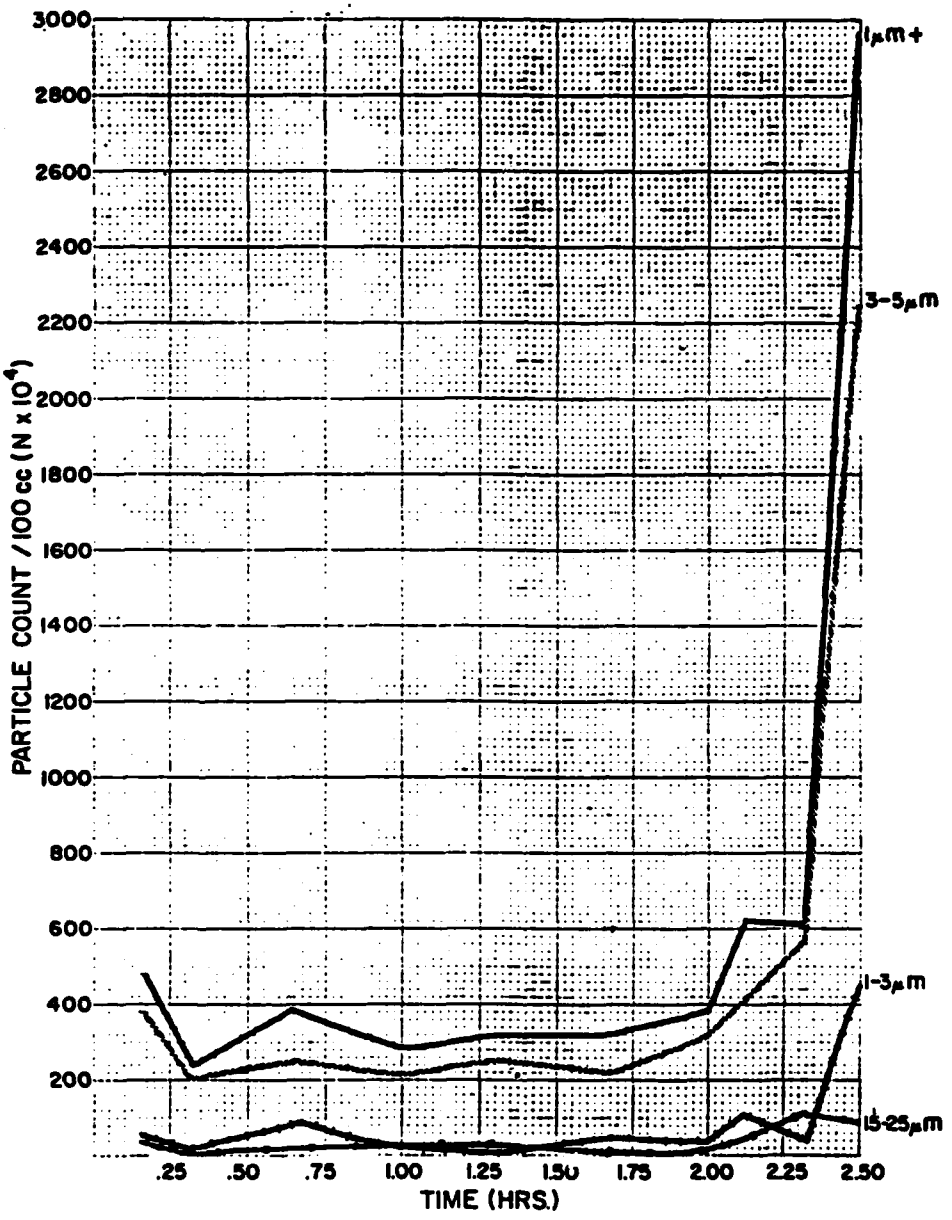


FIGURE 148. PARTICLE COUNTS

(e) According to the above logic, the spectrometer, as a result of size sensitivity, can only reflect/monitor effectively wear modes that generate small debris such as gear scuffing. However, in practice, spectrometric oil analysis has been able to monitor such wear modes as rolling contact fatigue and gear fatigue. An explanation for this situation is proposed as follows. For wear modes that generate large debris, this debris is picked up by the lubricant and circulated throughout the lubricant system. During this process some of the debris is subjected to various system interacting surfaces and are broken down into smaller debris. Small secondary particles are also generated as a result of surface denting of the wear area by the large primary particles. This process is illustrated in Figure 149. Presented test results were conducted by Dr. J. Johnson at Michigan Technological University. The Figure represents the ferrographic percentage density readings with time for data taken during a diesel engine test sequence. As can be seen, an equilibrium wear rate of large particles is established within the first two hours of operation. The locus of maximum readings with time for each Ferrogram location (Section) indicates that a "grinding" mechanism is operative.

(f) It is proposed that it is this grinding process or after effect to the large wear debris generation, that spectrometric analysis monitors. This after effect, however, results in a built-in lag time when detecting an abnormality. This lag can be seen in Figure 150 which in this case is approximately 13×10^6 revolutions.

(g) In the series of bearings that were run to failure under this program, each was heavily stressed in order to conserve test time. Spectrometric analysis was ineffective in detecting failure in these components, because the accelerated progression time to failure of the abnormal wear mode was less than the lag time resulting from the size sensitivity limitations. In the case of lightly stressed components, the spectrometric analysis could be effective in monitoring an abnormality because the progression time to failure of an abnormal wear mode would be greater than the lag time resulting from sensitivity constraints.

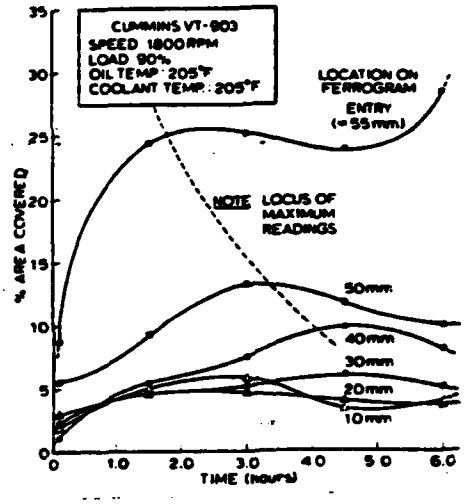


FIGURE 149. PERCENTAGE AREA COVERED AS A FUNCTION OF THE TEST TIME

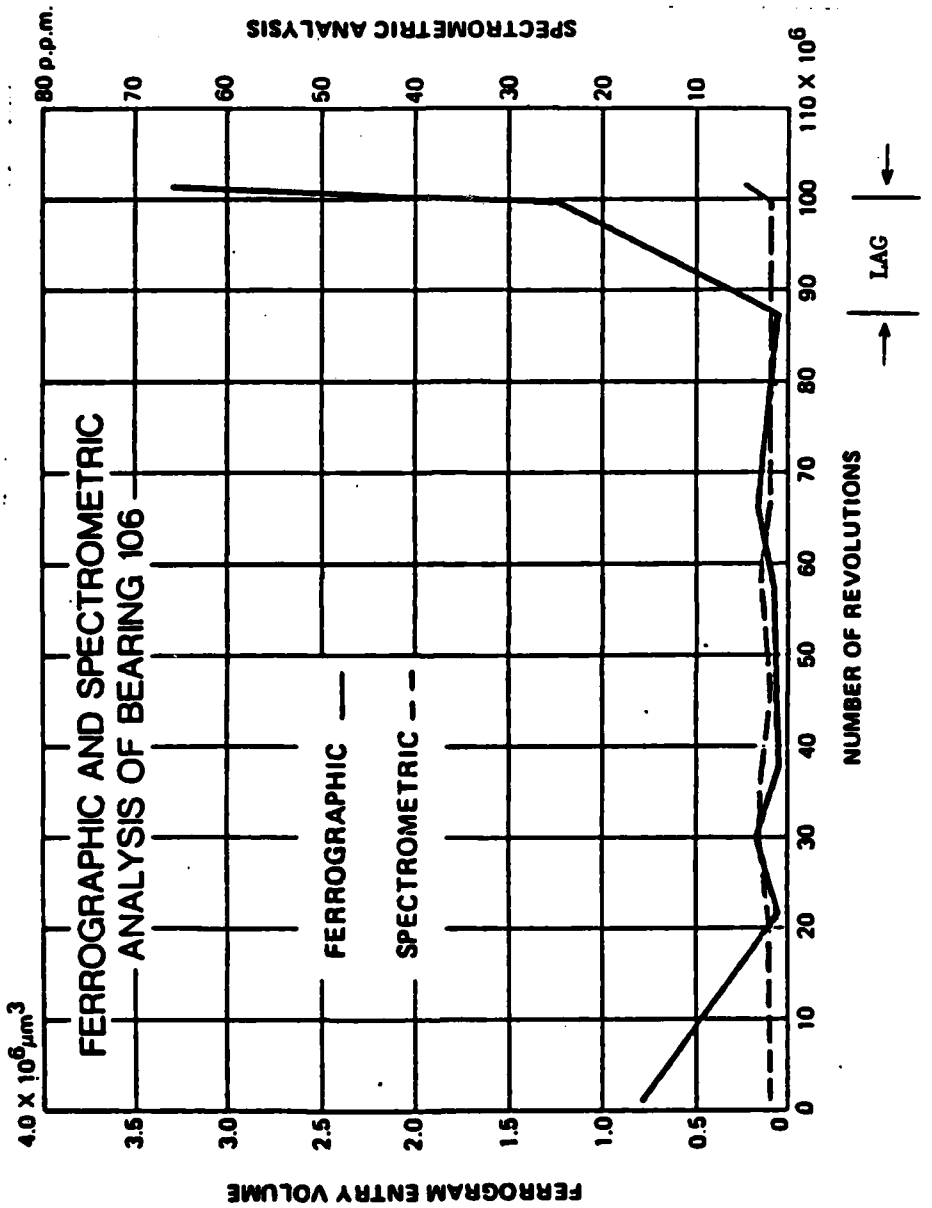


FIGURE 150. SPECTROMETRIC LAG TIME

(3) A third technical shortcoming of spectrometric analysis is that it gives no indication of the size distribution of debris that it is measuring.

(4) Another spectrometric analysis technical limitation is that the spectrometer reports elemental analysis but is blind to chemical form. Therefore, SOAP is unable to differentiate between wear metal particles and the metal's corrosion product.

(5) The inability to determine particle shape is also a technical limitation of SOAP. Recent work in the area of particle shape determination with the use of a scanning electron microscope has revealed specific details of wear particle shape. Particle morphology offers promise in improving equipment heath monitoring techniques.

9. FUTURE. A future trend is toward high filtration lubricant systems. This filtration will remove the large particles from the oil sample, thus eliminating secondary small particle effects that SOAP relies on for detection criteria. This will severely limit the present sampling technique as it exists today.

G. ANALYTICAL FERROGRAPHY

1. One of the most predominant oil debris analysis techniques utilized under this program is Ferrographic Analysis. This analysis technique is a relatively new approach and as such warrants a detailed discussion.

2. There presently exists three types of Ferrography equipment: Analytical Ferrography, Direct Reading Ferrography, and Real Time Ferrography.

a. Analytical Ferrography. The ferrography analyzer flows a lubricating oil sample over an inclined glass substrate (slide) positioned in the field of a high gradient magnet. The high gradient field separates particles from the oil as it flows through the influence of the magnetic field. The particles are chemically affixed to the slide and are thus conveniently displayed for analysis.

b. Direct Reading (DR) Ferrography. The DR ferrography passes an oil sample through a clear glass capillary tube positioned in the field of a high gradient magnet. Two fiber optic light tubes are positioned about the capillary tube; one at a point where large particles are collected on the capillary tube walls and one where small particles are collected on the tube walls. Light blockage at these two points is indicative of the large particle density (gross quantity) and the small particle density (gross quantity). The digital readouts at these two points are also indicative of the relative particle distribution in the sample oil.

c. Real Time Ferrography. The real time ferrograph is a prototype in-line monitor for an oil lubricating system. The system oil flow passes through a capacitive detector. A high gradient magnet collects the wear particles on the capacitive detector, which in turn gives an indication of gross particle quantity and relative size distribution. After the readings are taken the capacitive detector is flushed and ready for the next reading.

3. Discussions under this section will be limited to analytical ferrography which was the technique primarily utilized under the Oil Analysis Program.

4. BACKGROUND

a. Analytical ferrography is based on the magnetic precipitation and subsequent analysis of wear debris from a lubricant sample. The approach utilized involves passing a volume of lubricant over a glass substrate which is supported over a magnetic field. Permanent magnets are arranged in such a way as to create a varying field strength over the length of the substrate. This varying strength results in the precipitation of wear debris (magnetic and ferromagnetic) in a distribution with respect to size/mass over the substrate length (approximately 55 mm). Once rinsed and fixed to the substrate this deposit serves as an excellent media for optical analysis of the wear particulate.

b. Ferrographic substrate deposit analysis involves the characterization of debris quantity, distribution, elemental composition, and morphology. This total analysis effort involves both quantitative and qualitative assessments.

c. Quantitative assessments are derived for quantity and size distribution characterization utilizing a light reflected/light transmitted type densitometer. These assessments are registered by indicating the percentage of blocked area in a particular microscopic field of view. Readings are taken over the length of the substrate in order to characterize relative debris size distribution.

d. Elemental composition and morphological debris assessments are very qualitative in nature. They involve the manual characterization of debris deposits relying on observations conducted primarily through an optical microscope.

e. The analytical ferrography approach consists of three main components: Ferrography Analyzer, Ferrogram, and the Ferroscope.

(1) Ferrography Analyzer

(a) The purpose of a ferrography analyzer is to magnetically precipitate lubricant borne debris onto a glass substrate. The analyzer consists basically of two components; a pump and a magnet. A detailed breakdown of the analyzer is given in Figure 151.

(b) During the respective analyzer procedure, a prepared lubricant sample is pumped over a substrate suspended in a variable magnetic field as explained above.

(2) Ferrogram

(a) As stated above the ferrography analyzer separates debris from a lubricant sample by relying on the magnetic susceptability of the debris. The debris is precipitated and fixed onto a glass substrate or Ferrogram.

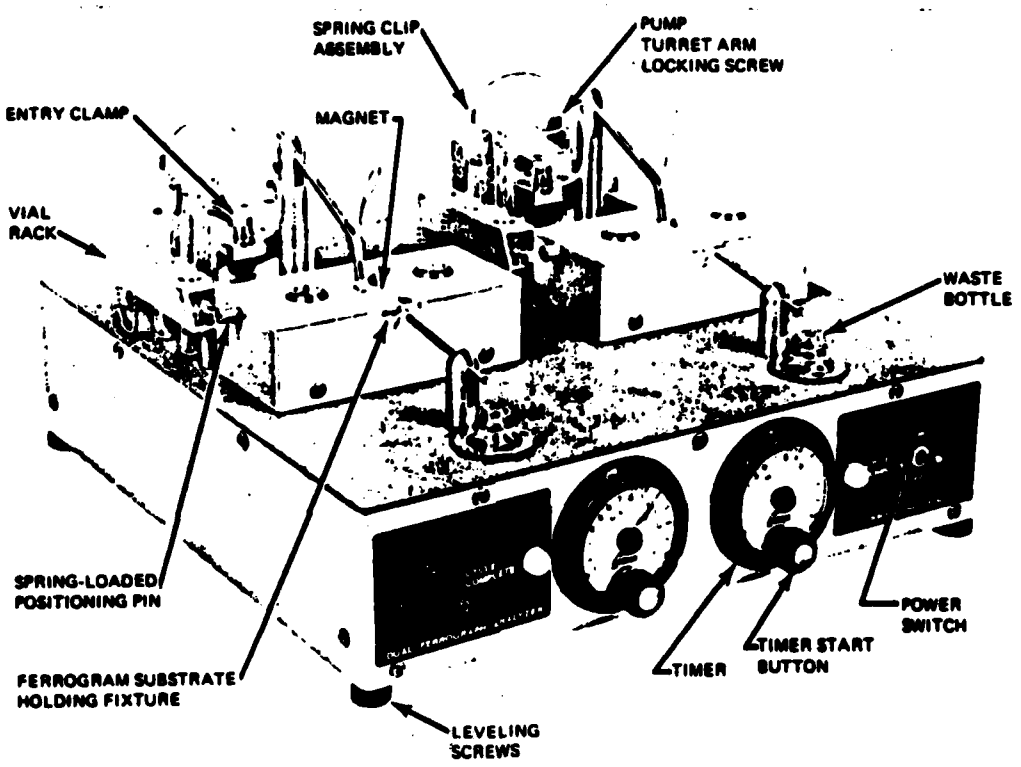


FIGURE 151. FERROGRAPH ANALYZER

(b) The ferrogram is a transparent glass slide (25 mm x 60 mm) which contains a u-shaped nonwetting agent barrier on its surface. This barrier serves to channel the sample flow although the length of the slide. The foot of the barrier serves as the point of sample introduction (entry deposit) and the open end of the barrier serves as the sample exit point (exit deposit), Figure 152.

(c) Magnetic and ferromagnetic particles are deposited along the length of the slide with respect to size/mass. All positions of deposited particles along the Ferrogram are indicated in millimeters from the exit deposit toward the entry deposit. Large magnetic particles in general, are thus deposited between the 54 mm and 55 mm slide position. These particles generally are > 5 μm in major dimension. Small magnetic particles, in general, are deposited at the exit end of the slide. These paticles are submicron in major dimension. An illustration of particle size with respect to ferrogram location is presented in Figure 153.

(d) The ferrogram displays the magnetic particles in strings transverse to the oil flow across the Ferrogram. Some hybrid particles, a combination of magnetic and nonmagnetic materials, also appear on the ferrogram. It should be pointed out that some nonmagnetic materials are important contributors to the wear process and will not be collected in a representative manner. Nonmagnetic abrasives and nonmagnetic wear debris will only be represented as traces on the Ferrogram. Their presence is noted (possibly overlooked) but not easily assessed.

(e) Although the ferrograph separates particles and lubricating oil magnetically, other effects come into play that influence particle separation. In addition to the magnetic effects, gravitational and mechanical net effects are involved. Gravitational effects bring about settling of particles along the Ferrogram. Mechanical net effects refer to the strings of particle transverse to the ferrogram acting as physical dams to particles carried with the lubricating oil along the slide. Forces opposing particle collection are the lubricating oil viscosity and flow effects. The aforementioned trapping

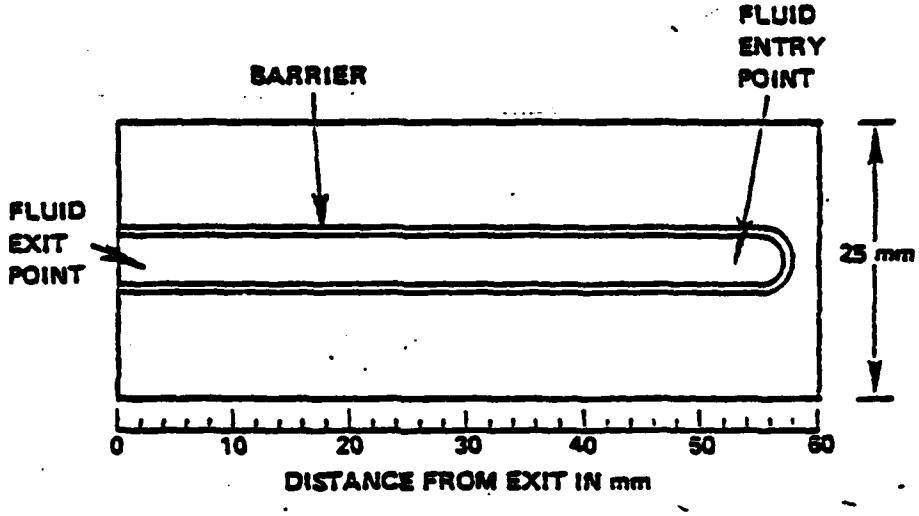
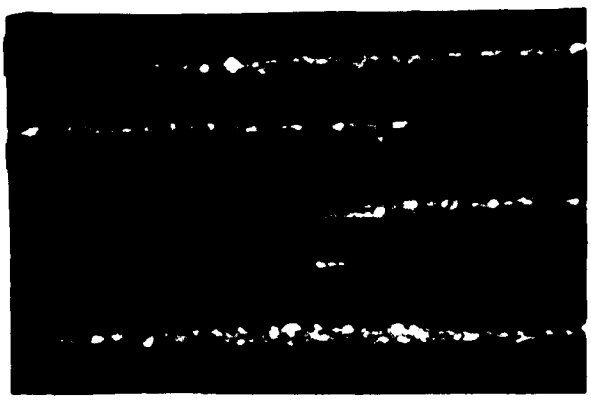


FIGURE 152. FERROGRAM



A. Entry Deposit 1000X



B. 50 mm Deposit 1000X



C. 10 mm Deposit 1000X

FIGURE 153

FERROGRAM PARTICLE SIZE VERSUS LOCATION

mechanisms affect different particles in different ways. Magnetic, ferromagnetic (hybrid), and nonmagnetic particle collection is aided by gravitational effects and mechanical net effects. Obviously, only the magnetic and ferromagnetic particles are influenced by the magnetic collection effects.

(3) Ferroscope

(a) In order to assess the aforementioned ferrogram deposit characteristics of quantity, size distribution, composition, and morphology, an optical microscope technique is employed called the ferroscope. The ferroscope consists of a bichromatic microscope with an integrated densitometer as shown in Figure 154. Particle characterization is accomplished by the analysis of such aspects as transparency, orientation, color, surface texture, and location on slide as well as assessing density readings (percent blockage) along the slide deposit.

(b) A detailed procedure for the preparation and analysis of a ferrogram is presented in NAVAIRENGCEN Report No. NAEC-MISC-92-0458 "Sample Preparation/Ferrogram Procedure/Ferrogram Analysis," reference (ss). As a result of this reference a detailed decision of procedure will not be presented in this discussion.

(4) Above and beyond the equipment described above, supplemental equipment and techniques have been employed in Ferrogram Analysis. Three of these supplemental approaches are included in the following sections. Ferrogram Heating, Scanning Electron Microscope, and Energy Dispersive X-Ray Spectrometer.

5. FERROGRAM HEATING

a. Gross composition of particles on a ferrogram can be determined by heating the ferrogram and observing the induced temper colors. Heating of ferrograms promotes the chemical combination of some wear debris with oxygen. The oxide layers formed and the thickness of the layers when observed with an optical microscope are seen to have characteristic colors. These colors are indicative of particle composition and crystal lattice orientation. However, similar

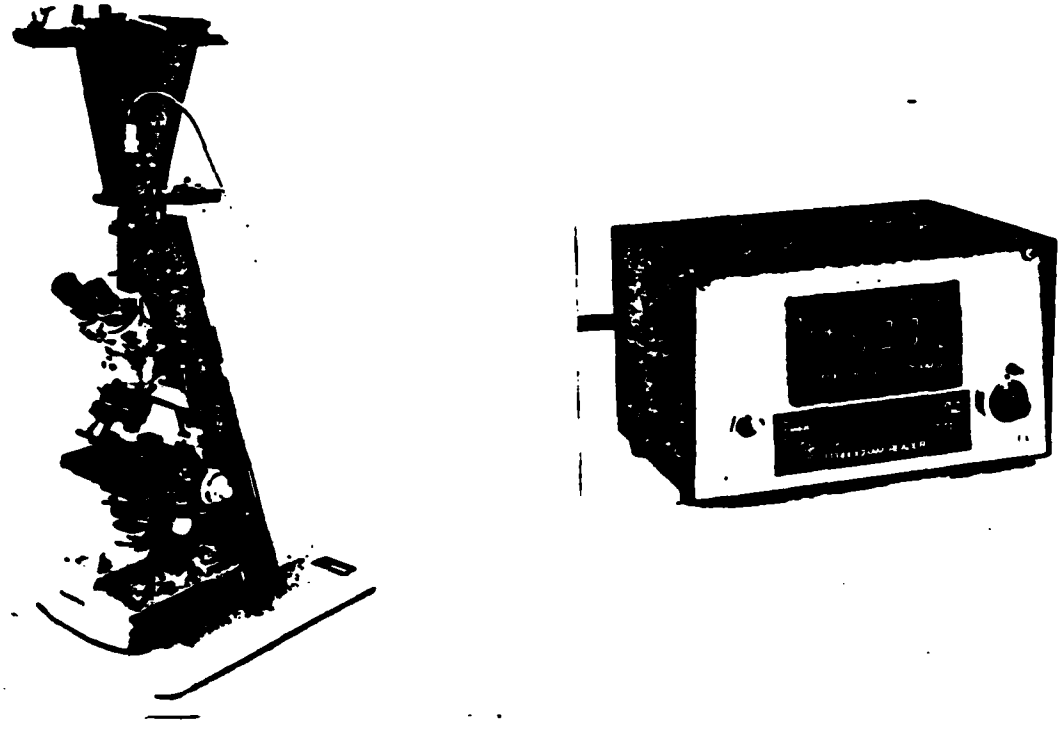


FIGURE 154. FERROSCOPE AND DENSITOMETER

colors can be observed for more than one element or compound. Hence, this is why only gross composition can be determined by induced temper colors.

b. Typically a ferrogram is heated to 650°F (343°C) for 90 seconds. This combination of temperature and time is adequate to turn carbon steels blue. The color change (bright white in unheated state) is readily observed with the optical microscope.

c. Details on heating ferrograms for the observation of temper colors can be found in "The Use of Temper Colors in Ferrography," by Barwell, Bowen and Wescott; Wear, 44 (1977) 163-171, reference (e).

d. Note that the particles on a ferrogram may display temper colors before the initial heating of the ferrogram. This gives an indication of the temperature of the environment that the particles were generated in. This information can be interpreted in terms of lubricant starvation, high speed, or high load through further investigation.

6. SCANNING ELECTRON MICROSCOPE (SEM)

a. Various techniques have been developed to permit electron microscope evaluation of the particles on the ferrogram. Several approaches to ferrogram slide preparation are presented in the following paragraphs.

(1) Conventional Ferrogram

(a) The specimen is a glass slide, 24 mm wide x 60 mm long x 0.3 mm thick. A polymer barrier layer is present around the edge of the slide to contain the oil during preparation. The slide cannot be examined in a scanning electron microscope (SEM) without overcoating with an electrically conductive layer due to severe charging problems that will be encountered associated with the glass substrate.

(b) The ferrogram slide can be broken into smaller sections by scratching (one or two) lines on the side opposite the deposit to avoid generation of glass fragments around the particles. The slide is supported on a block that is recessed in the central region while being scratched. Pressure is then applied to crack the slide along the scratch. The slide segment is then mounted on an SEM specimen stub for conductive coating.

(c) The most satisfactory coating material has proven to be evaporated carbon. The deposit is applied in a vacuum evaporator while the specimen is rotated to obtain uniform deposition. The coating thickness usually lies in the 300-500 A range. The carbon coating appears to be durable, adherent, protective, and presents no interferences for subsequent X-ray analysis. Metal coatings such as evaporated gold could also be employed but have no advantage over carbon and can give rise to overlap lines in the X-ray spectrum.

(2) Uncoated Ferrogram

(a) Two techniques to avoid overcoating the ferrogram after preparation have been used with limited success. In the first the blank ferrogram slides are precoated with evaporated carbon. Only the central portion is coated as the polymer barrier film is rendered ineffective if covered with carbon. The slide can then be used in the ferrograph in the customary fashion. After deposition of the particles the ferrogram can be examined directly in the SEM. Since there is no coating over the particles, they must be resting on the substrate if charging is to be avoided. Problems of insufficient conductivity are noted much more frequently here than with overcoated Ferrograms, particularly near the initial deposit. Particles can also be dislodged from the substrate during handling and examination. The advantage of the method lies in the preservation of topographic detail on the particles and the lack of any X-ray absorbing layer.

(b) The second method employed aluminum alloy plates, 6061-T6 aluminum, in place of the glass ferrogram slide. The aluminum slides were thicker (0.6 mm) than usual but appeared to perform satisfactorily in the ferrograph. The slides containing particle deposits were cut into smaller sections using a metal shear and then examined directly in the SEM. Occasional problems associated with particle charging were noted here also. A more serious problem was associated with the substrate contribution to the X-ray emission spectrum and the obvious interference with any aluminum-containing wear particles.

(3) Extracting Particles from the Ferrogram

(a) It is useful on occasion to be able to examine particles from one limited region of the Ferrogram using other techniques. This could involve electron diffraction studies of an individual particle or group of particles, for example. We have successfully applied a plastic film striping procedure to this problem. A suitably sized piece of the cellulose acetate tape is softened with acetone and pressed and held into contact with the previously carbon coated Ferrogram. After hardening for about 15 minutes the film is carefully peeled off the Ferrogram, carrying with it the deposited wear debris. The film is then coated with carbon in an evaporator, cut into the appropriate size, placed on small support grids (3 mm diameter in our case) and washed carefully in a suitable solvent. This leaves the wear particles sandwiched between two thin carbon films on the support grid. Except for interference from the support grid bars in those areas, the debris can then be examined as before and also in electron and X-ray transmission geometries.

b. The analyst can utilize the great depth of focus and high resolution of the SEM during study of particle morphology in great detail. However, a limitation of the SEM is the inability of the SEM to pick up the optical characteristics of the particles. This merger of optical characteristics and the electron image details requires the coordination of data between the optical microscope and the SEM.

7. ENERGY DISPERSIVE X-RAY (EDX) SPECTROMETER. The EDX spectrometer is an accessory used in conjunction with the SEM. The spectrometer is designed to analyze the energies associated with the X-rays from the wear particles excited by the electron beam of the SEM. These energies (X-rays) are picked up by an X-ray detector scintillator. The scintillation intensity is analogous to the X-ray energy. The spectrometer electronics counts the scintillations and integrates them simultaneously for each energy level. Each energy level is in turn analogous to the frequency of the X-ray. This frequency is characteristic of each element. After the frequency is determined, the element analyzed is determined. Analysis of a compound results in the elements composing that compound. The data derived in this manner is qualitative but may be semi-qualitative with the necessary options for the spectrometer to expand its capabilities.

a. Determination of the composition of wear debris particles in the size range below 100 μm using X-ray emission analysis requires very careful measurements and calibration. The X-ray production from the iron and nickel particles has been calculated as a function of size using Monte Carlo methods. The correction factor needed for the particle size effect has been determined. Experimental measurements have been conducted on an NBS standard reference material (Fe-3Si) that confirm the results of these calculations. Figure 155 shows the calculated results for iron and the measured results for Fe-3Si particles and for Al particles (from other work). Particles of iron larger than about 3 μm (in the smallest dimension) can be analyzed without making size corrections. In iron particles of size less than 1 μm the correction is very significant.

b. Measurements of X-ray emission from strings of identical particles have been made on ferrograms using the SEM X-ray detector system. Electron and X-ray scattering to neighboring particles can interfere with quantitative analysis of unknown particles of interest. The effect of string orientation relative to the X-ray detector is important. The particles labeled in Figure 156 were examined under constant electron beam exposure and geometrical conditions. The Ni-K X-ray line emission was measured in each case using the SEM X-ray detector system.

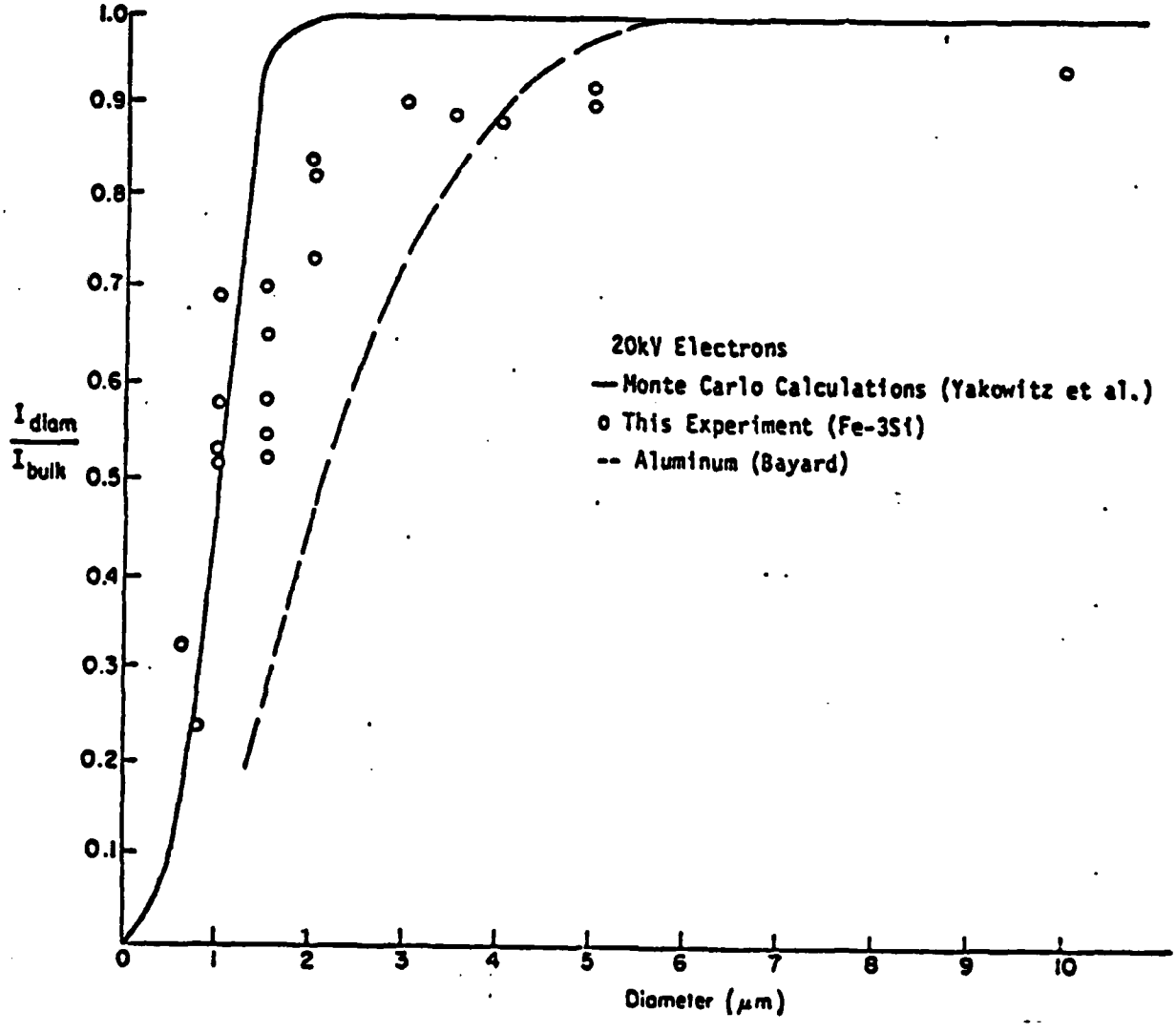
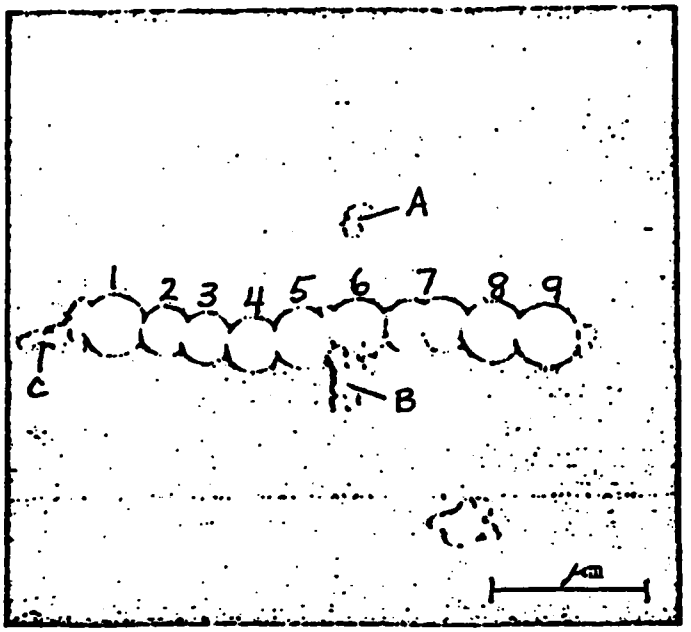


FIGURE 155. X-RAY EMISSION ANALYSIS



String of Ni coated SiO_2 spheres, 0.7 m and 5 m diameter, on a Ferrogram. X-ray analysis results for labeled particles are given below.

Particle	1	2	3	4	5	6	7	8	9
Time for 10^3 counts (sec.)	108	87	79	70	77	104	76	60	58
Particle	A	B	C	1R	9R				
Time for 10^3 counts (sec.)	350	112	360	99	53				

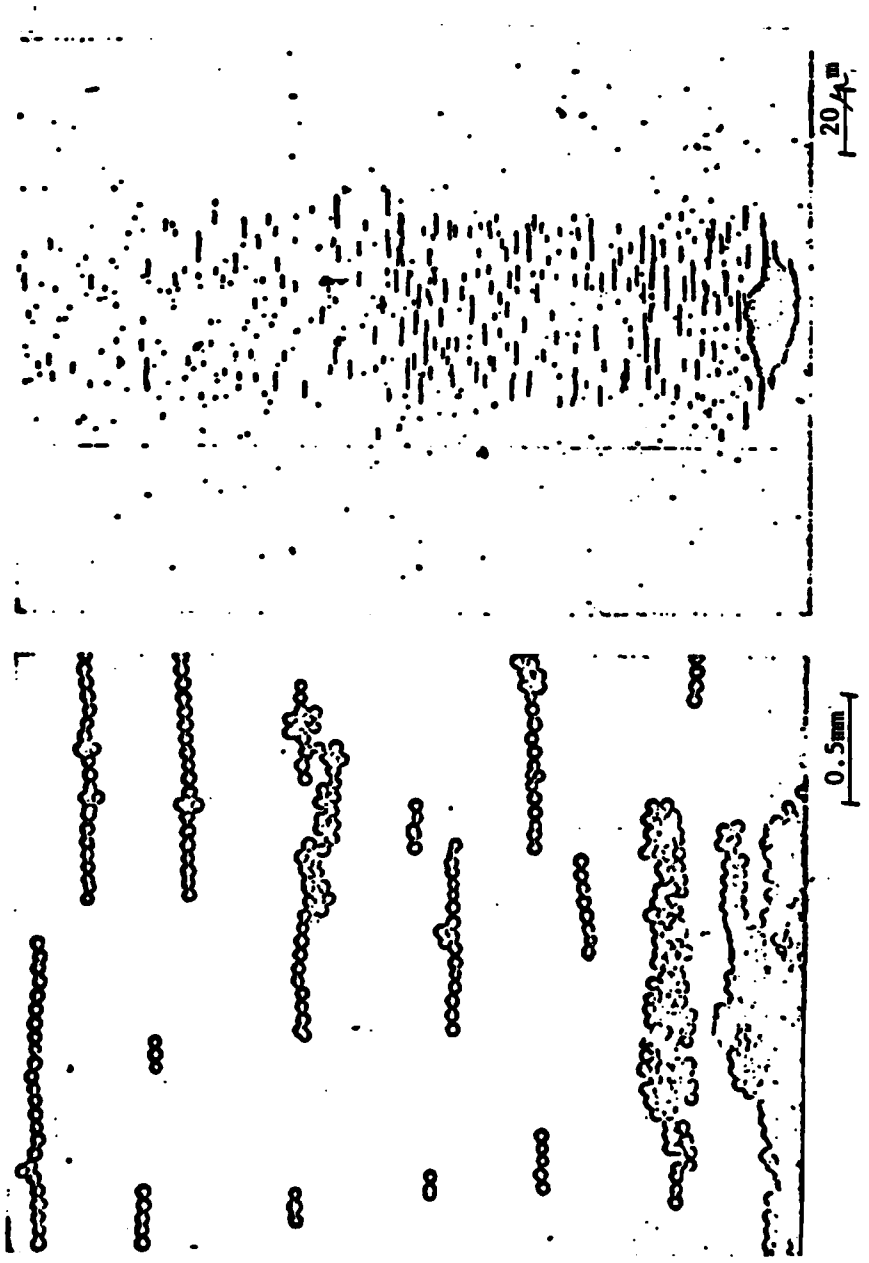
FIGURE 156. X-RAY EMISSION ANALYSIS

c. Particles A, B, C are actually clusters of the smaller spheres. The variation in Ni count rate for the 5μm spheres (particles 1 through 9) is due partially to statistical variations (about 6%) and partially to a real variation in Ni content spheres. The observed average value is 80 $\pm$ 18 sec., a variation of about 25%. The string was rotated 180 degrees in the SEM and the end particles reanalyzed. The values (1R, 9R) are not significantly different than the original values, indicating that electron excitation from adjacent particles is not a significant factor. The Ni emission from the cluster of small spheres B is reasonably close to that from the larger spheres suggesting a similar Ni content. The clusters A and C appear thinner and penetration of the electron beam through the particles is more significant. According to Figure 155 a correction factor of about 0.3 is indicated for correction at 0.7μm particle diameter. Considering particle clusters A and C in Figure 156, the corrected time for 10^3 counts would be (350)(0.3) = 100 sec., which is reasonably consistent with the count period values obtained for the 5μm spheres.

8. SAMPLE DILUTION

a. Lubricant sample dilution is a prime factor under ferrographic analysis. A discussion of this topic is presented below.

b. The effect of sample dilution has been studied by using particles obtained from an oil sample from a jet engine. The purpose was to determine the quantitative capability for sizing particles through the Ferrograph method. After initial evaluation, the Ferrogram was washed carefully, removing and recovering all the particles. They were then placed in fresh oil at a 5:1 dilution relative to the original sample and a second Ferrogram was made. The ratio of initial deposit volume was 6.6 and the percent area coverage ratios at 54 mm and 50 mm were 6.3 and 7.1 respectively. These ratios are to be compared to the dilution ratio 5.0. Porous silica spheres of diameter 5 $\pm$ 1 μm were obtained and impregnated with nickel to serve as ferromagnetic particles of known size, shape, and magnetic moment. Oil samples containing these spheres were prepared at two concentrations having a ration 10:1. Ferrograms prepared from these oil samples, Figure 157, had an initial volume ratio of 11 and a



FERROGRAM OF NICKEL-COATED SILICA SPHERES, 5 μm DIAMETER, 2000:1 DILUTION. F2897

FIGURE 157. SAMPLE DILUTION

percent area coverage ratio of 8.3 at 54 mm. These results, Table 41, suggest that quantitative comparisons of Ferrograph response can be made in some cases to a precision of about 30% (depending on the actual particle distributions involved).

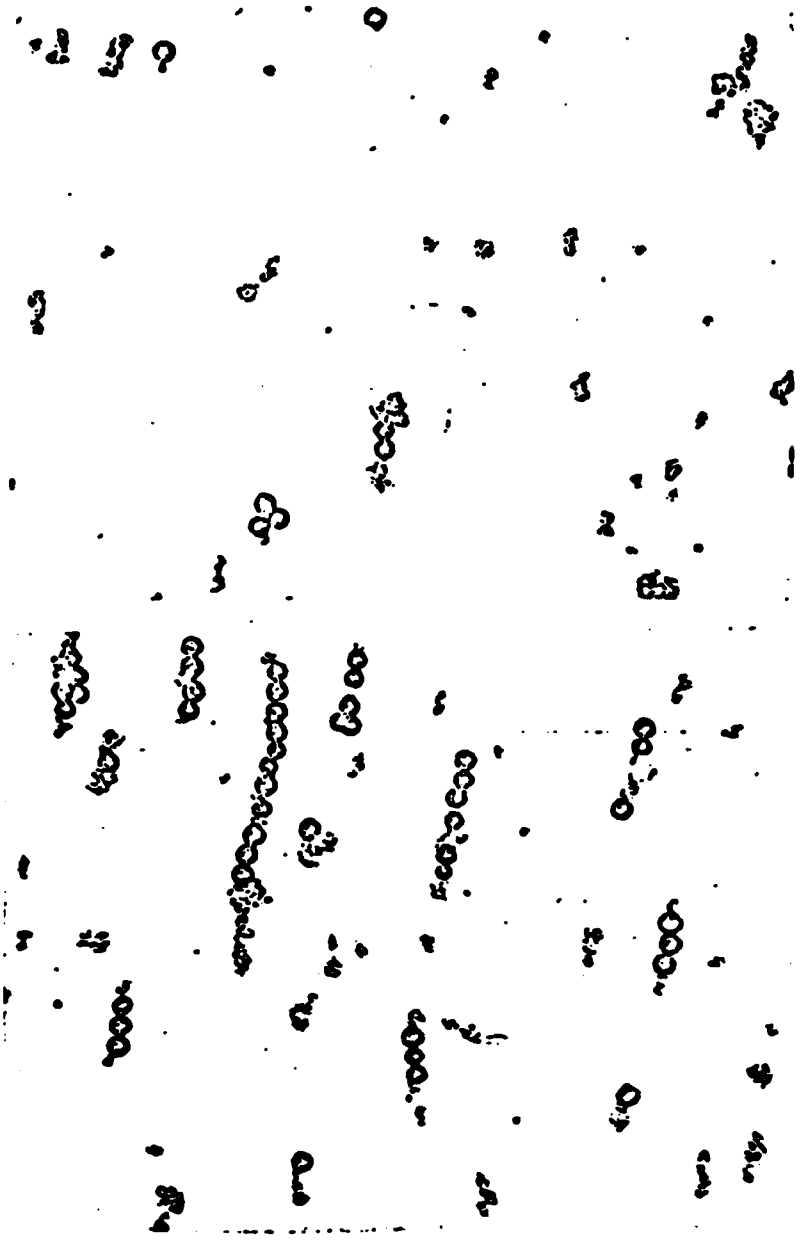
c. Oil samples containing a mixture of 5 μm diameter and 0.7 μm diameter Ni impregnated SiO_2 spheres have been passed through the Ferrograph in order to evaluate the instrument characteristics on a particle mixture containing two principal sizes. Figure 158 shows some details of the particle strings obtained using this mixture. The tendency for small particles ($< 1\,\mu$m) to deposit next to larger particles is shown. Other mixtures including SiO_2 spheres (without nickel) also have been studied in order to examine the Ferrograph response to nonmetallic abrasive particles. It is found that particle size differentiation is good on the Ferrogram; only rarely are the larger particles found below the entry deposit as long as the proper sample dilution is used. However, frequently small particles are present in the entry deposit. The nonmetallic spheres are generally found outside of the strings of metal spheres although some association with metal spheres in the strings has been observed, possibly as a result of aggregation in the oil. The great majority of nonmetallic spheres do not deposit on the Ferrogram.

d. Metal powders of iron, nickel, and stainless steel (size 3 to 40 μm) was obtained in order to extend the Ferrograph evaluation to nonspherical particles and to other metals. A greater tendency for small particles to deposit near the entry region is found when using these irregularly shaped particles than when only employing spherical particles. Figure 159 A and B shows this effect with a mixture of 30 μm Ni and 3 μm Fe particles. A study of these simulated debris samples involving filtration through Nuclepore filters ($< 1\,\mu$m) has confirmed the degree of selection obtained between metallic and nonmetallic particles using the Ferrograph, Figure 159 C and D. Ratios of 1:1 and 40:1 in volume of particles present in these two classes have been used in the samples studied.

TABLE 41. FERROGRAPH EVALUATION - DILUTION EFFECTS

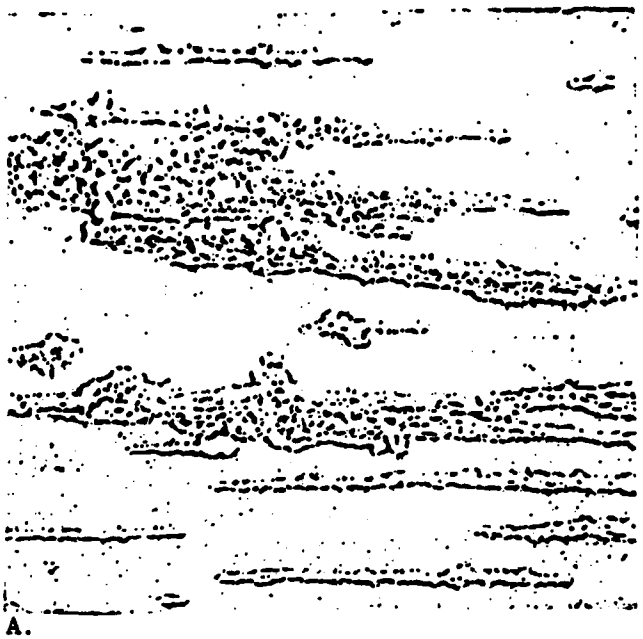
Sample	Initial Deposit		Percent Area Coverage			
	Volume	Height	Initial	54 mm	50 mm	10 mm
K9	6.6×10^6	65 µm	36	14	5	4
1/5:K9*	1.0×10^6	24 µm	11	2.2	0.7	1
ratio	6.6	---	--	6.3	7.1	4
NBS-7	1.2×10^6	23 µm	14	5	0.6	0.5
1/10:NBS-7	0.11×10^6	12 µm	2.5	0.6	---	---
ratio	11	---	--	8.3	---	---

*Particles were washed from original Ferrogram

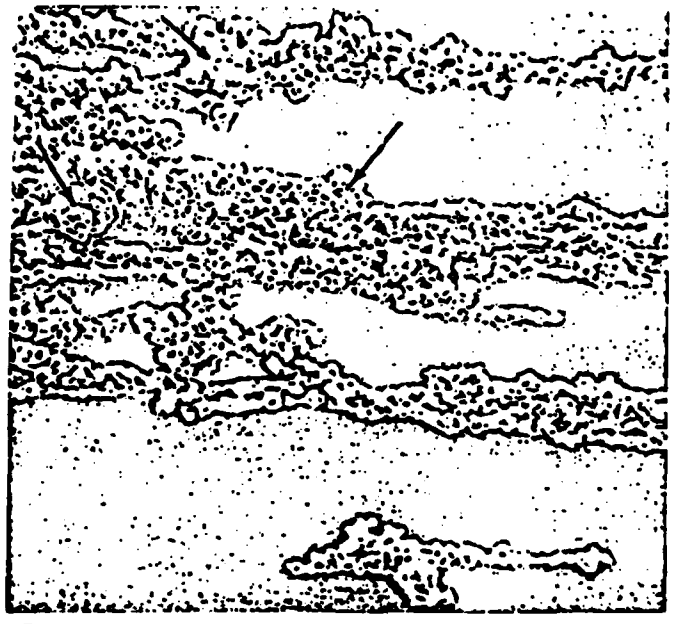


FERROGRAM OF NICKEL-COATED SILICA SPHERES, MIXTURE OF 5 μm 0.8 μm DIAMETER, 2000:1 DILUTION. F2902

FIGURE 158
SIZE DISCRIMINATION



A.
FERROGRAM OF A MIXTURE OF 30μm Ni PARTICLES AND 3μm Fe PARTICLES. ENTRY DEPOSIT REGION CONTAINS ALL LARGE PARTICLES. MANY SMALL PARTICLES ARE ALSO PRESENT.



B.
DETAILS IN ENTRY DEPOSIT. LARGE Ni PARTICLES IDENTIFIED AT ARROWS. SMALL Fe PARTICLES FROM END OF STRING AT BOTTOM.

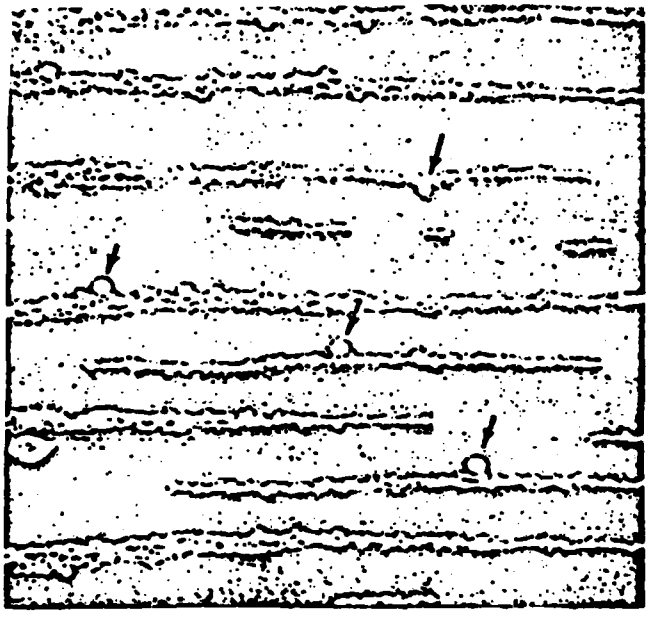
FIGURE 159

SIZE DISCRIMINATION

(Sheet 1 of 2)



C.
OIL SAMPLE CONTAINING EQUAL VOLUME MIXTURE OF 5μm SiO2 SPHERES AND 3μm Fe PARTICLES, FILTERED THROUGH 1μm NUCLEPORE FILTER.



D.
FERROGRAM OF AN EQUAL VOLUME MIXTURE OF 5μm SiO2 SPHERES AND 3μm Fe PARTICLES. FOUR SiO2 SPHERES ARE SEEN IN THIS REGION.

FIGURE 159

SIZE DISCRIMINATION

(Sheet 2 of 2)

9. FERROGRAM STORAGE

a. Ferrogram storage is another element under Ferrographic technology worthy of discussion. A description of storage variables covered under this program is summarized in the following paragraphs.

b. Ferrograms were exposed to ammonia fumes and high relative humidity to determine the influence of a chemical environment on the life of ferrograms and oil samples.

(1) Exposure to ammonia. Duplicate Ferrograms were prepared from a MIL-L-23699 used oil sample. One Ferrogram was stored under normal ambient conditions. The second Ferrogram was exposed at room temperature successively to a hydrous ammonia gas, then strong ammonia fumes from a solution of ammonium hydroxide. Each of these Ferrogram exposures lasted for three days in a special gas-tight chamber. No differences were found in the appearance of the Ferrogram exposed to ammonia and the one stored under normal conditions.

(2) Exposure to high relative humidity conditions. Ferrograms in duplicate were prepared froma MIL-L-23699 used oil samples. The resulting Ferrograms contained a typical distribution of rubbing wear particles (particles from the shear mix layer). One Ferrogram was stored under normal ambient conditions, the other was placed in a humidity chamber at 90% - 95% relative humidity for a period of seven days. No obsrevable difference could be found between this Ferrogram and the one stored under normal conditions for the same preiod of time.

(3) Resistance to oxidation. The resistance of rubbing wear particles to oxidation has been known for several years. However, it is difficult to explain the much greater resistance to oxidation of the particles compared with the steel from which they were generated. The 52100 and 1018 steels from which they were generated oxidize readily in a humidity chamber. Two hypotheses have been put forward to explain the particles resistance to oxidation.

(a) The particles are so small that differences in the material composition over the particle surface is negligible. Electrochemically induced oxidation would, therefore, be suppressed.

(b) The shear mix layer contains organics and oxides as well as the metal. If polymers generated by the oil were folded into the shear mix layer by the shearing motions on the surface (curl >0), protective films would be present on the surface of the particles. The view that an organic protective film plays a part is supported by the fact that heating ferrograms above 330°C on a hot plate, oxidizes the particles.

10. FERROGRAPHY SEVERITY OF WEAR INDEX

a. Wear monitoring of a system or equipment, as stated early, is performed by the trending of analysis data over time. One such trending parameter developed under Ferrography is the severity of wear index.

b. Numerical density readings can be obtained from a Ferrogram by the use of a densitometer in conjunction with a bichromatic microscope. The readings are expressed as the percent area covered by the particles in a field of view normally 1.2 mm in diameter. The recommended locations for taking density readings are at the region of maximum coverage near the entry point (larger than 5μm particle) of the fluid onto the Ferrogram (approximately 55 mm from the exit of the Ferrogram) and at a point 50 mm (corresponding to particles in the 2-5μm range) from the exit of the Ferrogram. These locations correspond to regions representative of two size ranges of particles as described. In this case, the readings have been assigned the terms A_L and A_S respectively.

c. Ferrograph analyzers are designed such that all the large particles of ferromagnetic composition are precipitated at or near the entry point while the majority of 2-5μm particles are precipitated at or before the 50 mm point. Ferrograph analyzers do not prevent the early precipitation of small particles. What the analyzers achieve is the i.. sition of higher sinking velocities on

larger particles. This results in a point on each Ferrogram prior to which all particles of a given size will have precipitated. The larger the particle size the closer to the entry region is the corresponding point for that particle size. These cutoff points are of course subject to variables such as fluid viscosity, local magnetic field variations, particle shape, and particle magnetic susceptibility.

d. The normal wear process, i.e., the wear mode associated with smooth stable surfaces generates particles with a maximum size of 15μm, the majority of which are 2μm or less. Any abnormal wear mode, i.e., any wear mode that significantly reduces the potential life of a wear surface, generates a particle distribution with a maximum size greater than 15μm. The actual maximum size is dependent on the wear mode.

e. In view of the above discussion it is understandable that for a normal wear process, the value at A_L would be similar to A_S. Usually A_L is slightly greater than A_S. However, if a severe wear mode develops, the value of A_L will be significantly larger than A_S. Consequently, the parameter $(A_L - A_S)$ may be used as an indication of abnormality.

f. The onset of an abnormal wear mode usually results in a significant increase in the quantity of wear debris. Consequently, either of the terms A_L or $(A_L + A_S)$ may be used as an indication of this factor.

g. As a single parameter that is sensitive to the onset of severe wear the product of $(A_L + A_S)$ (quantity) and $(A_L - A_S)$ (severity) may be used. This parameter, termed the SEVERITY OF WEAR INDEX, is denoted as S_A based on readings of a Ferrogram.

Now $(A_L + A_S)(A_L - A_S) = A_L^2 - A_S^2$

Therefore, $S_A = A_L^2 - A_S^2$

h. Since different machine lubrication systems exhibit extreme variations in both particle distribution and quantitative level it is not feasible to assign absolute levels to these parameters. The user must establish what the normal running values are for each of the systems that he intends to monitor. To obtain the best sensitivity, the normal running values of A_L should be in the range 10-40. Should the users normal running values be higher than this then the oil sample must be diluted. Conversely, if the readings are too low, a larger volume of sample must be used.

i. It is recommended that two parameters be monitored for each system. $(A_L + A_S)$ as an indicator of the general level of wear and S_A as an indicator of the severity of the wear. $(A_L + A_S)$ is also used to detect certain noncatastrophic wear modes such as excessive rubbing wear and some types of oxidative wear. On the other hand, the index S_A is used to indicate the onset of a severe wear mode that will quickly result in failure.

j. This severity of wear index is quite controversial and its exact numerical representation could vary between laboratories.

11. ELEMENTS OF OIL ANALYSIS VERSUS FERROGRAPHY

a. Oil analysis is based on four elements that a successful analysis must determine. These four elements are:

(1) Quantity or total number of particles
(2) Size distribution of total number of particles
(3) Composition or elemental analysis of particles
(4) Particle morphology

b. Considering these four elements and the Ferrography system, the following observations are noted:

(1) The quantity or total number of particles indicates where the wearing system is in its life. Typically the total number of particles increases rapidly to a high value, then drops and levels off to a relatively constant value, and finally increases rapidly prior to failure. This description

represents wear-in, normal wear, and wear-out, respectively, during the life of a wearing system.

(2) The Ferrography system incorporates a densitometer in the bichromatic microscope. Density readings of large particles (5μm and larger, A_L) and the density of small particles (2μm to 5μm range, A_S) are representative of the quantity of particles present. A_L and A_S may be monitored, separately or combined, throughout the wear system life to determine the first element of oil analysis.

(3) The second element of oil analysis is a determination of the size distribution of the total number of particles. Generally, the ratio of large to small particles assumes a high value during wear-in, decreases to a smaller value during normal wear, and finally increases to a value, greater than during wear-in, during wear out or abnormal wear.

(4) The Ferrography system densitometer gives density readings, A_L and A_S, that are indicative of quantity. Trending of the density readings with respect to time serves to monitor the quantity of large and small particles. The trending of the ratio of large to small particles is directly related to these density readings. This data is sufficient to monitor the trend in size distribution of the total number of particles.

(5) The severity of wear index, S_A, is a second Ferrography indicator of particle size distribution. One half of the equation for severity of wear is an indicator of wear severity in the wearing system. The second half of the equation considers the quantity of particles. Multiplied together, the equation is weighted to consider the distribution of particles.

(6) The third element of oil analysis is composition or elemental analysis of the particles. The Ferrography system offers a number of approaches to this element. First, the optical properties of the particles, observed with

the bichromatic microscope, are an indication of particle composition. Second the use of polarized light with a crossed analyzer, highlights the color of some particles. Also, depolarization of this polarized/analyzed light gives an indication of the crystal structure of some particles which reflects composition. Third, the use of bichromatic light (red reflected light and green transmitted light) is an aid in distinguishing between metallic and nonmetallic particles. Fourth, a Ferrogram can be heated and the resultant temper colors observed with the microscope. The temper colors are indicative of particle composition. Finally, the magnetic separation approach, employed by ferrography serves as a descriminator between magnetic and non-magnetic debris and thus serves as an indicator of composition.

(7) Despite these techniques for determining particle composition, the Ferrography system does not have an exact qualitative capability. However, in many situations the Ferrography system qualitative capability is adequate. The capability can be supplemented with an X-ray analysis system such as an energy dispersive X-ray (EDX) spectrometer.

(8) The fourth element of oil analysis is particle morphology. Particle morphology is important in assessing the wear mode of the wearing component. The Ferroscope, an optical microscope, with a magnification of approximately 100X to 1000X is capable of studying particle morphology.

(9) Should a higher magnification of particles be needed, the scanning electron microscope can be used to supplement the morphological characterization of particles (done with the Ferroscope).

12. FERROGRAPHY OBSERVATIONS. Several different Ferrographic approaches to the study of metal wear particles using microscopy and diffraction techniques have been evaluated under this program. Principal observations are as follows:

a. The Ferrography technique can reliably extract ferromagnetic wear particles from a lubricating oil sample and deposit the particles on a substrate suitable for microscope examination.

b. The particles are deposited so that smaller, lower magnetic moment particles are on the average located further from the entrance end of the Ferrogram. The physical sizes of the particles may deviate by a factor of 5 within one particle string, due to local magnetic field gradients.

c. Nonmagnetic particles are found randomly deposited on the Ferrogram, generally not within the strings of magnetic particles. However, examples have been found of particles containing a small proportional amount of iron located in such strings. The iron content may be transferred magnetic wear metal in some cases.

d. The glass substrate Ferrogram can be examined in the SEM after overcoating with about 200A of carbon. (Carbon precoated glass slides can be used in the Ferrograph and examined without overcoating.) Care must be taken with such preparations or particles may be dislodged during handling.

e. The particle density within the strings is too great for certain analyses. Particle sizing and shape classifying would not be possible. X-ray emission analysis is complicated by excitation or absorption by neighboring particles. Techniques for recovering particles of interest from a Ferrogram after dilution and redeposition of the particles on suitable substrates can probably be developed.

f. X-ray emission analysis of individual particles by electron beam excitation can be conducted. Many precautions are noted that must be considered in such studies. Semi-quantitative analysis requires corrections for substrate and neighboring particle effects.

g. Spheroidal particles have been observed in nearly all oil samples examined, including both gear wear and bearing wear samples. Typically from one to five spheroids may be found on one Ferrogram, i.e., a very small proportion of all wear particles. The surfaces of those particles are relatively smooth in nearly all cases. X-ray analysis has proven that the small ($<5\ \mu m$) spheroids usually produce only an iron emission line. Larger spheroids have been identified

as having significant concentrations of other elements and may be oxides, silicates, etc. Some of the larger (>5 μm) spheroids may be partially composed of organic materials.

13. ADVANTAGES AND DISADVANTAGES OF FERROGRAPHY. Probably the most important aspect of this discussion is the following summary of disadvantages and advantages of Ferrographic Technology based on Oil Analysis Program experience.

a. Disadvantages

(1) Nonmetallic and nonmagnetic particles are randomly placed on the Ferrogram or not picked up at all. Nonmetallic and iron magnetic particles may contribute to the wear progression of a wearing system. However, when the nonmetallic and nonmagnetic particles are not truly represented on a Ferrogram sample, it is difficult to assess the wear situation. A representative presentation of these particle types would help clarify the wear situation.

(2) Limited material identification capability is available. The use of illumination techniques and temper colors allows for gross composition analysis of particles. State-of-the-art techniques for these two methods does not permit precise composition determination.

(3) Considerable time is spent preparing and analyzing samples.

(a) In order to make a Ferrogram that yields density readings in the linear range (density reading versus sample oil volume across slide) it is often necessary to dilute the sample. The required dilution is determined by trial and error. This is time consuming. Also, the quality of the Ferrogram is dependent on the care taken in making it. Lack of care can result in the remaking of a slide.

(b) To analyze a slide requires a technician to assess the particles on a Ferrogram under various illuminations, magnifications, and to take density readings. Morphological characterization of the particles requires the technician to objectively distinguish the particle types present and interpret any other information he may read from the Ferrogram, based on his objective/subjective combination of slide data with supplemental data supplied with the sample.

(c) The Ferrogram analysis requires technician experience, technique, and time to gain useful data.

(4) High relative costs for materials, preparation, and analysis. The considerable time spent preparing and anayzing samples results in considerable corresponding costs. Materials or the sample kit required for the analysis is relatively costly.

(5) Considerable operator training and experience is necessary. In order to effectively use the Ferrograph Analyzer, densitometer, and bichromatic microscope extensive training of the operator is required. After this training, the operator must gain experience in reading a Ferrogram, which is necessary to allow the technician to take the basic mechanics of Ferrography and tailor them to the specific and unique case at hand.

(6) No equipment calibration is available. There is no calibration available to insure the integrity of the entire Ferrography system before usage.

(7) Repeatability of ferrography is questionable. Major shortcomings that were identified with respect to analytical ferrography repeatability are as follows:

(a) The lcc pipettes provided with Ferrogram kits are not calibrated. The 1 cc of fluid delivered is only somewhere in the "ballpark" of 1 cc. This results in substantial variation in volume of sample liquid and fixer when preparing a sample for a Ferrogram. Variation problems can be corrected by using calibrated pipettes. They should be used only once and thoroughly cleaned if to be reused. This problem has since been corrected by the manufacturer.

(b) Ferrography peristaltic pumping rates vary considerably. The varying pump rate is dependent on the inside diameter and outside diameter of the utilized turret tube. It is difficult to precisely control the turret tube inside diameter and the interaction of the tube and the pump itself, noting that sample fluid was run across the Ferrogram according to time. The problem can be corrected by running the entire volume of liquid in the prepared sample bottle across the slide. This action bypasses the problems due to turret tube inside diameter and outside diameter affecting pump rate. This problem has since been partially corrected by changing from a time to volume basis as recommendation and also tightening the specifications on the delivery tubing. However, pump characteristics vary considerably from equipment to equipment with respect to pumping rate.

(c) The linearity of Ferrogram density readings to allow for comparison between Ferrograms was a questionable area. Could the densities of two different Ferrograms be compared to trend results over time associated with each Ferrogram? The problem was addressed by Oklahoma State University. OSU determined that density readings are linear with respect to the volume of liquid pumped across the Ferrogram as long as the density readings do not exceed 40% (above which is the nonlinear range). It is to be noted that there is a minimum acceptable density usually taken to be 10%. This problem has since been minimized by adjusting sample dilution in order to fall within the linear density range.

(d) The shift of the Ferrography entry deposit is another problem area. The shift of the entry deposit depends on the extension of the turret

tube from the turret tube holder and the exact positioning of the Ferrogram on the Ferrography Analyzer. This shift results in high or low density readings being reported for the entry deposit.

(e) No standardized procedure was available for ferrography sample preparation. The problem has been eliminated through the development of a standardized procedure, reference (ss).

b. Advantages

(1) Gross size distribution data is presented. Density readings, A_L and A_S, are typically taken and are representative of the quantity of large and small particles. This data also gives an indication of the size distribution of particles.

(2) Particle morphology can be easily studied. The Ferrograph Analyzer separates the sample oil from the sample debris, flushes any oil adhering to the debris, and chemically affixes the debris to the glass slide or Ferrogram. The debris is conveniently displayed on a glass slide for examination with an optical microscope (Ferroscope). Note that the particle debris has also been classified from large to small from the entry deposit to the exit deposit respectively.

(3) Gross total quantity of debris is easily obtained. Density readings representative of large particles and small particles are indicative of the gross total quantity of debris. These readings can be trended over a series of Ferrograms to assess the status of the wear system.

(4) Metallic and nonmetallic particles can be distinguished. With the bichromatic microscope, a combined illumination of red reflected light and green transmitted light can be used to analyze the Ferrogram. Metallic particles will reflect the red light and appear red. The nonmetallics will transmit the green light in various degrees resulting in a yellow or greenish appearance.

(5) Limited material identification can be made. Use of illumination techniques and temper colors allows for gross composition analysis of particles on the Ferrogram. In this manner, the composition data of the particles can be enhanced by the morphological character of particles. All this data is integrated with information about the wear system (i.e. material survey data).

(6) Ferrography can indicate, although qualitatively, all four prime wear debris characteristics: quantity, size distribution, composition, and morphology.

H. INTERRUPTED TESTING. As discussed in Section V, bearing testing consisted of both interrupted and noninterrupted test sequences. Several bearings of both the roller and ball bearing groups where periodically disassembled in order to monitor surface wear progression. It appears from debris analysis data that dismantling and reassembling a test ball bearing frequently results in the c-currence of a new wear-in/break-in period. Figure 160 represents density readings of large debris over the life of a bearing. This graph indicates high density readings subsequent to some of the periodic bearing examinations. As a result, these tests have shown that from a wear point of view, the dismantling of machinery for visual inspection may be a detrimental technique. Conclusions regarding the influence on the wear lives of the bearings cannot be drawn from this limited test sample. Roller bearing dismantling and reassembly did not result in a significant wear-in reocurrence.

I. IMPROVED OIL ANALYSIS APPROACH

1. GENERAL

a. The following discussion will deal with the development of an improved approach to oil analysis based on program test results.

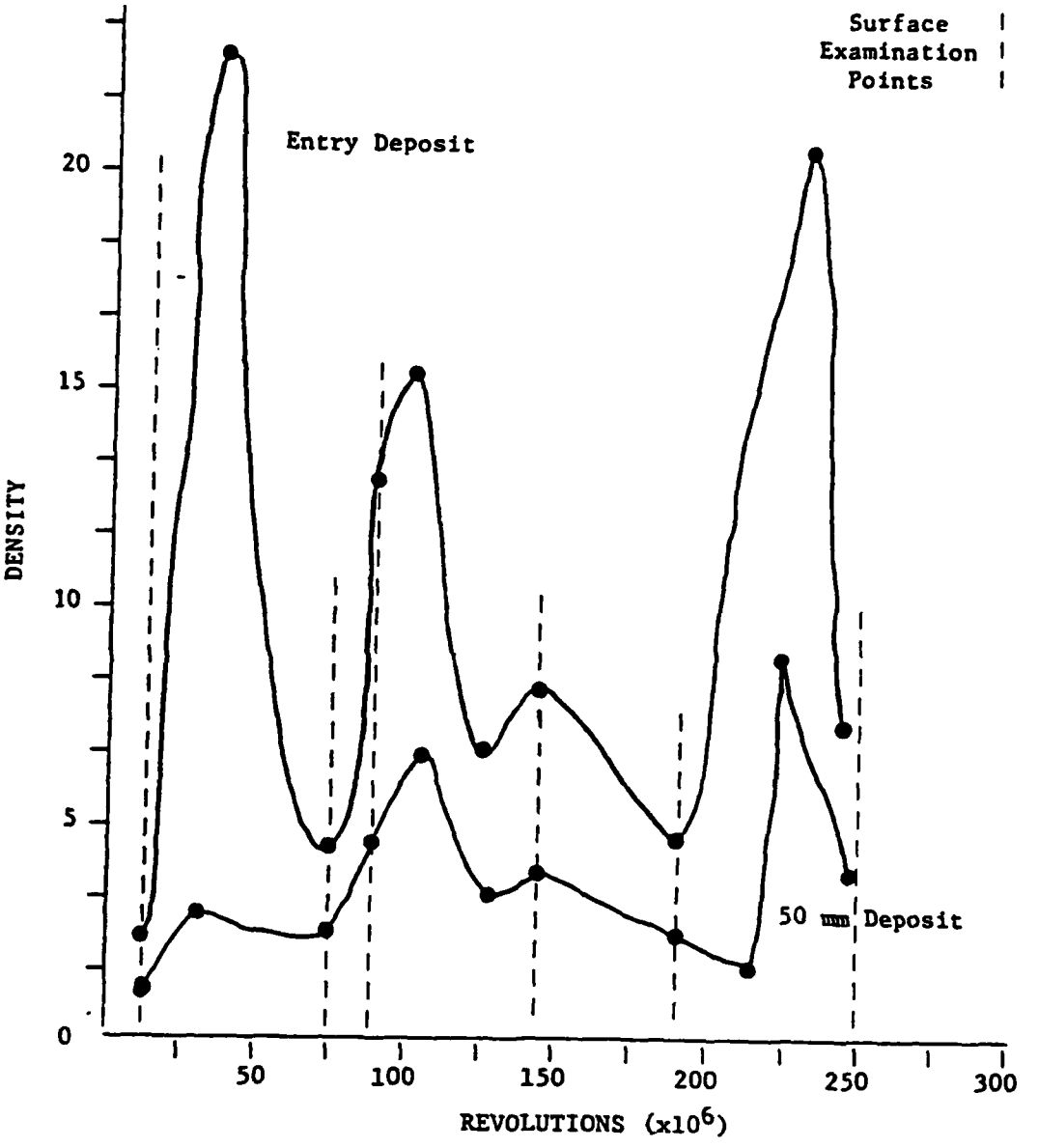


FIGURE 160
BALL BEARING TEST SEQUENCE BA
FERROGRAPH DENSITY DATA

b. As previously mentioned in this document, wear particle analysis technology is based on the premise that debris generated during a wear process can serve to reflect surface conditions present in the respective process. As a result, the analysis of wear debris can be utilized as a nondestructive indicator of system/process surface wear condition. In the case of lubricated components, this debris is picked up and carried by the lubricant thus wear particle analysis is sometimes referred to as oil analysis.

c. Based on tests performed under the Oil Analysis Program, four critical wear debris characteristics have been identified as reflecting surface wear conditions. These characteristics are: debris quantity, size distribution, composition, and morphology.

d. By monitoring the above four parameters, wear particle analysis technology can provide information as to system wear rate, wear severity, wear components, and active wear modes as shown in Figure 161. In the analysis process, it is impossible to assign quantitative assessment criteria for each parameter, for every system. Analysis determinations have to be based on a comparison criteria. Parameter readings must be compared with "normal" readings for a particular system. An effective implementation method is the trending of each parameter. Trending will reflect pertinent shifts in parameter readings, thus reflecting a system wear abnormality.

2. APPLICATIONS

a. A systematic attack on the problem of machinery wear involves both wear prevention and wear control. Wear prevention is implemented by optimizing the wear resistance of an equipment design. This design effect impacts such aspects as materials, lubricants, additives, tolerances, filtration, and surface finish. Wear control is concerned with the minimization of equipment wear rate (i.e., extension of wear life). This control approach is implemented during equipment manufacture, quality assurance, operation, and maintenance.

WEAR PARAMETERS	WEAR RATE	WEAR SEVERITY	WEAR SOURCE	WEAR TYPE
Quantity	X	X		X
Distribution	X	X		X
Composition			X	X
Morphology		X	X	X

FIGURE 161. CRITICAL WEAR PARTICLE ANALYSIS PARAMETERS

b. Wear particle analysis technology exhibits numerous effective applications within this systematic wear attack. The five major applications of wear particle analysis are as: a research tool, a design tool, a quality assurance tool, a troubleshooting tool, and a health monitoring technique.

c. The above five applications can be utilized for oil, hydraulic fluid and grease lubricated systems. In some cases these applications can also be utilized for dry wear. Although these areas represent fertile areas of wear particle analysis utilization, applications are not restricted solely to those mentioned.

d. The following discussion will center on the application of wear particle analysis as a wear control approach or as an equipment health monitoring technique.

3. HEALTH MONITORING DECISION PROCESS. In order to effectively implement any health monitoring technique, a viable decision process must be developed. The following discussion will summarize a projected wear particle analysis decision process.

a. Elements. The projected decision process required for wear particle analysis implementation, consists of four elements: detection, diagnosis, prognosis, and prescription.

(1) Detection. The detection element provides a first cut or preliminary determination as to the health of a machine (i.e., is the machine wearing normally or abnormally?). If no abnormalities are detected, no further analysis is required until the next detection sampling interval. If an abnormality is suspected, the next step of the decision process is pursued.

(2) Diagnosis. The second element of the decision process serves to further clarify the machinery wear abnormality. It provides a determination as to what machine component(s) are wearing and proceeds to define what wear mode(s)

are present. Based on these determinations, the analysis process is transitioned to the next decision element.

(3) Prognosis. The prognosis element of the decision process serves to define the course of the machine wear abnormality. It provides a prediction of residual life (time until failure) based on wear severity, wear component, and respective wear mode.

(4) Prescription. The last element of the analysis process serves to define a course of corrective action. It provides maintenance recommendations based on residual life, wearing component, and respective wear modes.

b. Parameters. Technical feasibility of this decision process relies on the ability of wear particle parameters to reflect wear abnormalities and abnormality ramifications. Based on wear particle analysis research, the following marriage of decision elements and wear particle parameters have been developed.

(1) Detection. As indicated above, the purpose of the detection element is to provide an initial determination as to the health of a machine. Based on technology research, abnormal wear can be effectively detected by monitoring both wear particle quantity and size distribution.

(2) Diagnosis. Once an abnormality has been detected, it is the purpose of the diagnosis element to provide information as to the source and type of the respective wear abnormality. Again, based on pertinent technology research, abnormal wear condition clarification can be accomplished by performing an elemental analysis and a morphology classification of the respective wear debris.

(3) Prognosis. Prognosis determinations are based on the analysis and interpretation of the above monitored parameters. Analysis criteria developed through knowledge, experience, and parameter trending of individual equipment types, serve to drive these determinations.

(4) Prescription. As in the prognosis decision element, prescription determinations are based on the analysis and interpretation of previously mentioned parameters. Analysis criteria developed through individual equipment experience and parameter trending also drive the prescription determinations.

c. Maintenance Level

(1) Implementation of the health monitoring decision process, requires the assignment of monitoring responsibility to pertinent maintenance levels. The detection decision element should be implemented at the first line or organizational level of maintenance. Abnormal wear detection capability will be applied either in-line with respect to the equipment lubrication system, or off-line in the general vicinity of the equipment. Determination as to in-line or off-line applications will be based on equipment cost and criticality considerations. Front line assignment of the detection element serves to provide diagnostic capability to the first line maintenance community, provides real time wear condition monitoring, minimizes existing sampling problems, eliminates a substantial portion of the existing oil sampling workload (i.e., samples are only submitted when an abnormality is detected), and will thus result in a decrease in the number of required centralized oil analysis laboratory facilities.

(2) The diagnosis, prognosis, and prescription decision elements should be implementd at a centralized facility located either at the intermediate or depot maintenance levels. These element implementations require relatively advanced analysis equipment, advanced operator training, and a developed equipment wear expertise. Assignment of these decision elements to a centralized location will serve to promote these requirments as well as optimize facility utilization, and amortize facility costs over numerous supported operating facilities.

(3) The total wear particle health monitoring decision process, as described, is summarized in Figure 162.

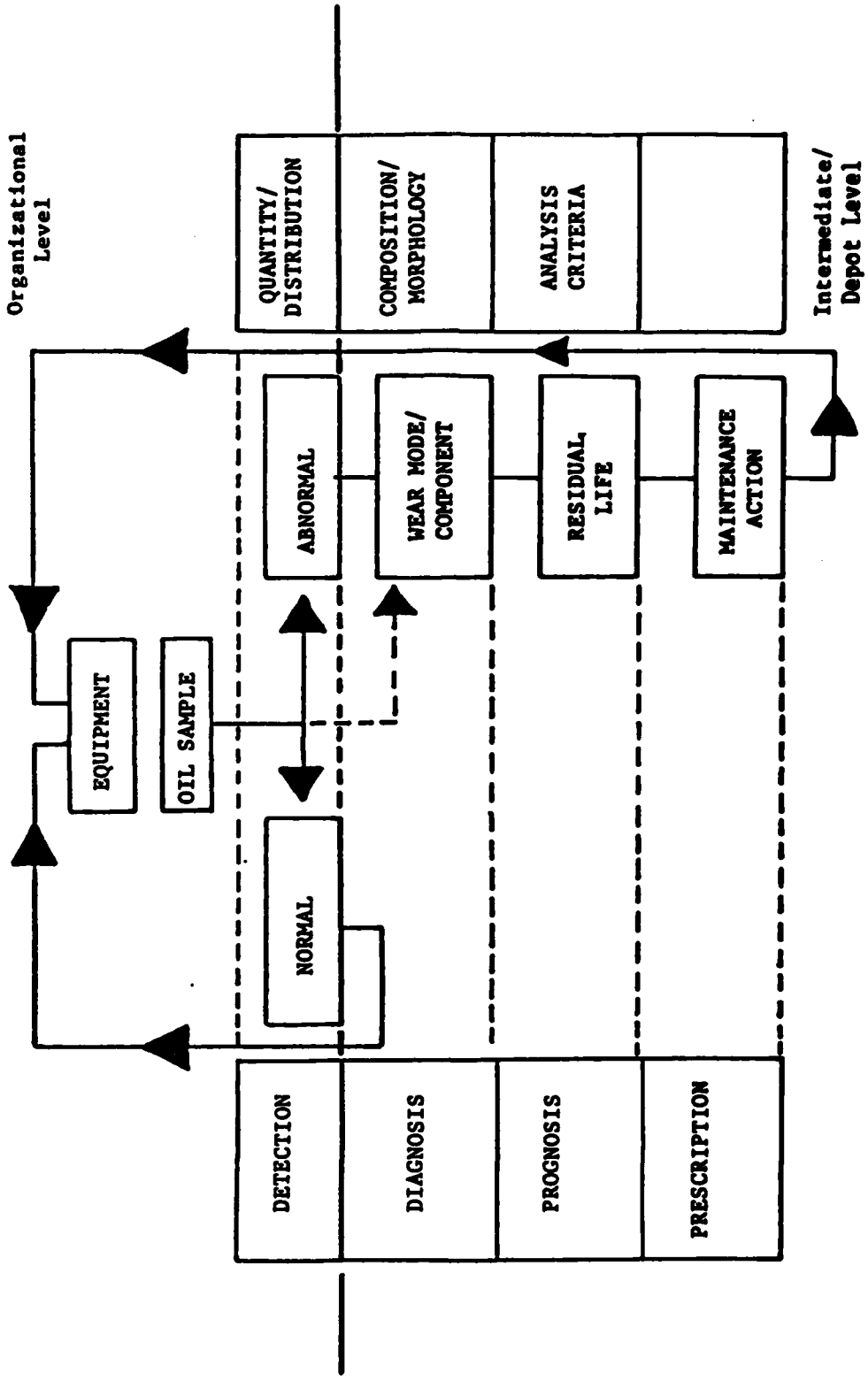


FIGURE 162. WEAR PARTICLE ANALYSIS HEALTH MONITORING DECISION PROCESS

4. PROPOSED HEALTH MONITORING EQUIPMENT. Full implementation of the health monitoring decision process requires identification of specific wear particle analysis equipment capable of effectively monitoring the pertinent parameters at the specified maintenance levels. Since the decision elements of prognosis and prescription involve no required monitoring equipment, this discussion will focus on the elements of detection and diagnosis. A proposed equipment approach for these elements is as follows:

a. Detection. Detection element analysis equipment has to be capable of monitoring wear debris quantity and size distribution at the first-line maintenance level. In the case of high cost and/or critical equipment, this monitoring capability would preferably be performed in-line in the respective equipment lubricant system. A particle counter would serve to meet these requirements. This application is not as simple as it appears, however. No present particle counter has thoroughly demonstrated required operational and sensitivity capability.

b. Diagnosis. Diagnosis element analysis equipment has to be capable of monitoring all wear debris critical parameters; quantity, size distribution, composition, and morphology. This monitoring effort will be implemented at the intermediate or depot maintenance level. No existing analysis technique will provide this total required capability, thus a combination of techniques need to be identified. Three types of analysis equipment, utilized collectively, will provide necessary capability. These equipments are a particle counter, a spectrometer, and a ferrography. This three element approach is, however, only an interim solution. A new analysis technique needs to be developed which will exhibit the required capabilities.

(1) Particle Counter. The particle counter would provide information as to wear debris quantity and size distribution and would be the laboratory equivalent of the detection unit described under the above subparagraph. Laboratory counters are presently available which surpass necessary sensitivity and operational requirements dictated by this application.

(2) Spectrometer. Spectrometric analysis provides data as to the concentration levels of present wear debris elements. This information would obviously apply to the wear debris analysis parameters of quantity and composition. Laboratory spectrometers are presently available which satisfy capability requirements of this application with one exception. Present instruments exhibit an insensitivity to the analysis of large debris particles. This insensitivity, although undesirable, does not present a major shortcoming when the spectrometer is utilized in conjunction with the other two proposed analysis equipments.

(3) Ferrography. The ferrograph is a relatively new wear debris analysis technique. It provides a combination of qualitative and quantitative assessments of wear debris quantity, size distribution, composition, and morphology. This technique, however, is primarily attuned to the analysis of ferrous wear debris. The exhibited atunement is a result of the magnetic separation principles that are employed by ferrography. This technique is presently available for laboratory application.

c. Data generated from the above three equipments is analyzed collectively. Each input serves to reinforce and/or complement the other inputs. Diagnostic decisions will be based on this collective data analysis. A summary of the proposed equipments versus parameter capability is provided in Figure 163.

d. The equipment proposed in this discussion serves to represent one approach to wear particle analysis. It is not meant to infer that these equipments cannot be substituted for, or supplemented by, other types of pertinent analysis equipment. The ultimate capability is to develop an analysis technique that could indicate all four debris characteristics.

5. WEAR DEBRIS SAMPLING

a. As previously discussed, a critical aspect in the wear particle analysis approach is the wear debris sample. Care must be taken to ensure that

PARTICLE PARAMETERS	QUANTITY	DISTRIBUTION	COMPOSITION	MORPHOLOGY
Particle Counter	X	X		
Spectrometer	X		X	
Ferrograph	X	X	X	X

FIGURE 163. WEAR PARTICLE ANALYSIS EQUIPMENT CAPABILITY

the analyzed wear debris sample is representative of the total wear debris being generated in the monitored system.

b. In the case of oil lubricated components, the generated wear debris is picked up by the oil and circulated throughout the lubricant system. Sampling of oil borne wear debris can be accomplished by either an in-line or off-line technique.

c. These two sampling approaches rely heavily on the fact that significant wear debris is picked up by the lubricant and circulated throughout the lubrication system. A prime factor affecting this debris circulation is the lubricant filter. This filter is designed to remove debris from the lubricant. Traditionally, lubricant filtration has been relatively course, thus uneffective in removing significant wear debris from the lubricant. Recently, however, equipment lubrication filtration has been improving. This improvement is being driven by the realization of the deliterious accelerating effects of lubricant borne debris on the system wear rate. Improved filtration will eventually lead to the condition where significant wear debris will no longer be circulating in the system; it will be, for the most part, entrapped in the filter. This condition will tend to nullify the effectiveness of both present in-line and off-line sampling approaches. Drastic modifications of present sampling techniques will have to be developed in order to obtain a representative wear debris sample from a highly filtered system.

6. HEALTH MONITORING EQUIPMENT

a. A second critical aspect in the wear particle analysis approach is the analysis equipment. The equipment proposed under previous sections include an in-line particle counter, a laboratory particle counter, a spectrometer, and a ferrograph.

b. In order to fully implement this proposed equipment approach, several problems have to be overcome. These problems fall into two categories: equipment development and procedural development.

(1) Equipment development problems involve the in-line particle counter and the spectrometer. Lack of a demonstrated in-line particle counter with required application durability and sensitivity, creates a major void in the proposed analysis approach. Spectrometer insensitivity to large wear particles, although a shortcoming, presents itself as less of a severe problem. Both of these problem areas, however, are receiving research emphasis and should be resolved in the near future.

(2) Equipment procedural problems involve analysis equipment repeatability. Necessary standardization and calibration procedures have not been developed for the total equipment package. This situation hinders quantitative wear debris analysis as well as inter-laboratory joint monitoring efforts. Some standardization efforts are presently being implemented; however, the equipment calibration area requires further investigation.

7. WEAR PARTICLE ANALYSIS INTERPRETATION

a. The third and final critical wear particle analysis aspect is analysis interpretation. Assuming a valid sample has been obtained and a pertinent equipment analysis has been performed, one must then proceed to relate generated data to the respective equipment wear condition. This process involves considerable interpretation and is complicated by equipment characteristics, operating parameters, and operating environment.

(1) Equipment characteristics will have a decided effect on the four critical monitored parameters. Such characteristics as number of wearing components, equipment materials, lubricant, lubricant capacity, and filtration level will all tend to complicate wear debris analysis results.

(2) Equipment operating parameters will also affect wear debris parameters, thus wear debris analysis. Parameters such as load, speed, and operating cycle have to be considered in the wear particle interpretation process.

(3) The third factor, operating environment, can affect the wear rate of the respective equipment as well as directly contribute to the oil borne debris circultated by the equipment. These effects will futher tend to distort/ complicate wear debris analysis results.

b. In order to counter these interpretation challenges, one must rely on a combination of trending techniques, equipment knowledge, and monitoring experience.

(1) Trending of monitored parameters will serve to highlight pertinent parameter changes with respect to a particular equipment. Parameter trending as opposed to parameter threshold limits, will tend to minimize the distorting effects of equipment operating parameters and operating environment.

(2) An in-depth technical knowledge of the monitored equipment is very advantageous with respect to wear particle analysis. This knowledge is especially useful in minimizing the complicating effects of equipment characteristics.

(3) Finally, monitoring experience serves to fine tune wear particle analysis interpretation. The experience factor tends to minimize all three of the interpretation distortion elements. This factor is the most critical in any wear particle analysis application.

c. In order to implement the above discussion, and thus complete the wear particle analysis application process, the following approach is proposed. To effectively develop interpretation capability, an in-depth knowledge of the monitored equipment must first be acquired. Once acquired, control groups of respective equipment must be established and monitored on a trial basis. This trial program will serve to establish wear trends and analysis criteria. Once developed, these trends and criteria can be applied to the total inventory of equipments of the respective type.

8. WEAR PARTICLE ANALYSIS HEALTH MONITORING PAYOFF

a. The application of wear particle analysis as a health monitoring technique, exhibits numerous potential advantages over present oil analysis techniques (i.e., spectrometric oil analysis). These advantages are composed of both general and specific elements directed at the operation and maintenance of mechanical equipment. General advantages include: increased availability, decreased maintenance cost, increased life, and increased safety.

b. Specific advantages are an increased monitoring effectiveness with a decreased sample workload. It is projected that monitoring effectiveness can be raised considerably from the present level of 60%. By utilization of the detection approach, laboratory sample analysis workload will be cut down by approximately 75%. This decreased sample workload, although somewhat offset by increased individual sample analysis requirements, will tend to decrease the number of required laboratories.

c. A less obvious payoff of wear particle analysis is the potential expanded application of the technology. Hydraulic and grease lubricated component diagnostics, design assistance, quality assurance, and troubleshooting are a few of the potential expanded areas.

d. These general and specific wear particle analysis payoffs will result in substantial time, cost, manpower, energy, and material savings for both the governmental and industrial communities.

VII. CONCLUSIONS AND RECOMMENDATIONS

A. The Oil Analysis Program, as a result of its broad coverage, has generated numerous conclusions and recommendations. For the sake of clarity, this section will be subdivided into the categories of Oil Analysis, Test Ramifications, and Analysis Techniques.

B. CONCLUSIONS. The following conclusions have resulted from the Oil Analysis Test Program and subsequent analysis.

1. OIL ANALYSIS

a. Present oil analysis techniques are based on assumed critical particle characteristics and have been applied by trial and error with varying effectiveness.

b. Wear debris particles can be classified into 12 main categories: rubbing wear, cutting wear, fatigue chunks, laminar particles, spherical particles, corrosive wear particles, oxide particles, dark metallo-oxide particles, nonferrous metallic particles, hybrid particles, nonmetallic crystalline particles, and amorphous particles.

c. Component wear life can normally be classified into three distinct phases/regimes; wear-in/break-in, normal wear, and wear-out/abnormal wear. It is not true, however, that all components transition through all three phases.

d. Four wear particle characteristics are critical with respect to oil analysis; particle quantity/concentration, particle size distribution, particle composition, and particle morphology.

e. Wear rate and thus lubricant borne particle concentration level usually follows a bathtub curve over the wear life of an oil wetted component. Relatively high generation rates are present during component wear-in and abnormal wear regimes. This concentration level is affected by lubricant addition or deletion.

f. The component wear-in regime results in the generation of large wear particles and thus creates a relatively high ratio of large to small particles in the lubricant when compared to the normal wear regime.

g. Component abnormal wear regimes typically result in the generation of large wear particles and thus create a relatively high ratio of large to small particles in the lubricant when compared to the normal wear regime. One exception to this, is gear scuffing wear which results in the generation of an abundance of small wear particles. This regime thus creates a relatively small ratio of large to small particles in the lubricant when compared to the normal wear regime. This ratio is not affected by lubricant addition or deletion.

h. Particle morphology serves to reflect the surface wear condition of a component. Distinct particle shapes can be associated with individual components, wear regimes, and wear modes.

i. Wear debris quantity serves to reflect wear rate, wear severity, and wear type.

j. Wear debris size distribution serves to reflect wear rate, wear severity, and wear type.

k. Wear debris composition serves to reflect wear source.

l. Wear debris morphology serves to reflect wear severity, wear source, and wear type.

m. Wear debris quantity and size distribution collectively serve as a first indicator of a wear abnormality; i.e. detection. This detection capability, in the case of oil analysis, should be implemented at the organizational level of maintenance. In the case of high cost or critical applications, this detection capability should be in-line with respect to the equipments lubrication system.

n. Wear debris quantity, size distribution, composition, and morphology collectively serve to clarify an abnormal wear situation; i.e. diagnosis, prognosis, and prescription. As a result of operator and equipment requirements this capability, in the case of oil analysis, should be implemented at a central, intermediate, or depot level maintenance facility.

o. Wear particle characteristics should be trended for analysis purposes. This trending analysis will tend to minimize analysis variations resulting from equipment operating profile and operating environment.

p. Improved oil analysis techniques appear cost effective.

2. TEST RAMIFICATIONS

a. Representative debris sampling is a critical and often neglected aspect of any oil analysis technique.

b. High filtration technology is now being implementd on new equipment in order to extend equipment wear life. This high filtration, however, will render current oil analysis fluid sampling techniques obsolete.

c. A "clean" lubricant will result in significant extentions of component wear life. The clean lubricant will minimize debris surface denting and thus potential surface initiated fatigue nucleation sites.

d. Lubricated systems can be broken down into four main wearing components: ball bearings, roller bearings, gears, and sliding contact.

e. A Vicker's indent on the inner race surface of the test ball bearings provided a representative accelerated simulation of surface initiated rolling contact fatigue. Rockwell and Knopp indents were respectively too severe and too benign.

f. Disassembly/reassembly of a ball bearing results in the initiation/reoccurrence of a wear-in process.

g. Vicker's indents on the inner ring surface of a roller bearing did not have an accelerating effect on surface initiated rolling fatigue. This phenomena was a result of the load distribution and material characteristics of roller bearings as compared to ball bearings. As a result, ball bearings appear more sensitive to solid contamination than do roller bearings.

h. Roller bearing disassembly/reassembly did not result in the reoccurrence of a wear-in regime.

i. Circulation of debris results in a grinding process which causes particle breakup. This process is caused by particles being caught in the contact area of the operating component and will result in an accelerated increase in small debris formation.

j. The wear life of a component appears to be an inverse function of severity of the wear-in process of that component. Whether the wear-in process is a controlling life factor, a reflection of latent defects, or a combination of both has not been clarified.

k. Roller bearings appear to experience a more sever wear-in process than ball bearings.

3. ANALYSIS TECHNIQUES

a. Spectrometric oil analysis exhibits both administrative and technical shortcomings.

(1) Spectrometric oil analysis sample transit time averages 4.4 days. This transit time is excessive.

(2) Spectrometric oil analysis feedback is generally not provided.

(3) Spectrometric oil analysis sampling procedures are not strictly adhered to.

(4) The emission spectrometer exhibits an inherent insensitivity to large debris/particles. This insensitivity limit appears to fall in the particle size range from 5-7 μm.

(5) As a result of the presence of a grinding mechanism in a system, previously discussed, spectrometric analysis monitors a secondary effect of large debris generation. This secondary effect results in a spectrometer sensitivity "lag time" when monitoring an abnormal wear regime.

(6) Spectrometric oil analysis gives no indication of wear particle size distribution or morphology.

(7) Spectrometric oil analysis reports debris elemental analysis but is blind to chemical form.

b. Analytical Ferrographic wear particle analysis techniques exhibit both advantages and disadvantages.

(1) Advantages include:

- Ferrography provides indications of wear particle quantity, size distribution, composition, and morphology.

(2) Disadvantages include:

- Sensitivity limited to magnetic debris
- Qualitative material and morphology indications
- Extended analysis time requirements are exhibited
- High relative costs are incurred
- Considerable operator training/experience are required
- Lacks calibration
- Repeatability is questionable between laboratories.

C. RECOMMENDATIONS. The following recommendations have resulted from the oil analysis test program and subsequent analysis.

1. OIL ANALYSIS

a. Verify oil analysis conclusions under field test equipment monitoring program.

b. Develop an in-line wear debris monitor for high cost or critical applications.

c. Enhance current spectrometric oil analysis laboratories with added capability in order to monitor lubricant borne debris quantity, size distribution, and morphology.

d. Develop trending analysis criteria for oil analysis implementation.

e. Oil analysis techniques cover only a portion of potential equipments failures In order to develop a comprehensive diagnostic capability, oil analysis must be integrated with such complementary techniques as vibration monitoring and gas path analysis. This integrated diagnostic approach should be investigated.

2. TEST RAMIFICATIONS

a. Develop a new wear debris sampling technique which is unaffected by high filtration.

b. Investigate the effects of fluid borne solid contaminants on the wear life of components/systems.

c. Investigate the debris "grinding" process exhibited by lubricated components/systems.

d. Investigate the relationship of component/system wear-in severity to respective component system wear life.

3. ANALYSIS TECHNIQUES

a. Reemphasize spectrometric oil analysis program sampling procedures, minimization of sample transit time, and importance of analysis feedback.

b. Investigate the spectrometer's insensitivity to large wear debris particles.

c. Quantify the repeatability of Analytical Ferrography.

d. Develop a standardized procedure for Analytical Ferrography.

e. Develop a calibration standard for Analytical Ferrography/Densitometer.

f. Investigate sample dilution effects on Ferrographic analyses.

g. Develop a comprehensive, fast, low cost, simple, effective, repeatable oil analysis laboratory technique.

VIII. BIBLIOGRAPHY

(a) "Aeronautical Spectrometric Laboratory Manual," Naval Air Systems Command Headquarters, NARFP-P-12, March 1, 1976 (Revised).

(b) Anderson, D.P., Bowen, E.R., Bowen, J.P., "Advances in Wear Particle Analysis," Final Report, ONR-CR-169-007-1F, Foxboro Analytical, February 1979.

(c) Arnel, R.D., Herod, A.P., Teer, D.G., "The Effect of Combined Stresses on the Transition from Mild to Severe Wear," WEAR, 31 (1975) 237-242.

(d) "A Study of Wearing Components in an Oil-Wetted System," Report No. FO C3647, The Franklin Institute Research Laboratories, May 1974.

(e) Barwell, F.T., "The Use of Temper Colors in Ferrography," WEAR, 44 (1977) 163-171.

(f) Beerbower, A., "Mechanical Failure Prognosis Through Oil Debris Monitoring," USAAMRDL-TR-74-100 , 1974.

(g) Begelinger, A., deGee, A.W.J., "Boundary Lubrication of Sliding Concentrated Steel Contact," WEAR, 22 (1972) 337-357.

(h) Begelinger A., deGee, A.W.J., "Thin Film Lubrication of Sliding Point Contacts of AISI 52100 Steel," WEAR, 28 (1974) 103-114.

(i) Bill, R.C., Wisander, D.W., "Surface Recrystallization Theory of the Wear of Copper in Liquid Methane." NASA Technical Note NASA TND-7840. Lewis Research Center and U.S. Army Air Mobility R&D Laboratory, Cleveland, Ohio.

(j) Bowen, E.R., Westcott, V.C., "Wear Particle Atlas," Foxboro/Trans-Sonics, July 1976.

(k) Bowne, C.R., Siefert, W., "Ferrography - A New Tool for Analyzing Wear Conditions," Fluid Power Testing Symposium, 1976.

(l) Burwell, J.T., "Survey of Possible Wear Mechanisms," WEAR, 1 (1957-58) 119.

(m) Centers, P.W., Wright, R.W., "Ferrographic Nondestructive Inspection of Mechanical Assemblies." Presented at 23rd Department of Defense Conference on Nondestructive Inspection, September 1974, San Francisco, California.

(n) Chiu, Y.P., Liu, J.Y., "An Analytical Study of Stress Concentration Around a Furrow Shaped Surface Defect in Rolling Contact," TRANSACTIONS ASME, Journal Lubrication Technology (92), 1970, 258-263.

(o) Dahal, H., et al, "Final Technical Report on Progression of Surface Damage and Oil Wear Debris Accumulation in Rolling Contact Fatigue," Naval Air Engineering Center, Contract No. N00156-74-C-1634, SKF Report AL75T007, 1975.

(p) Dahal, H., et al, "Progression of Surface Damage in Rolling Contact Fatigue," Final Report, Contract N00014-73-C-0464, SKF Report AL74T002, 1974.

(q) Dalah, H., Senholzi, P.B., "Characteristics of Wear Particles Generated During Failure Progression of Roller Bearings," ASLE Paper Presented at ASLE Annual Meeting, 1976.

(r) "Effect of Lubricant Contaminants on Wear Rates of Lubricated Compoments," Final Report NAEC-92-132, Contract N68335-76-C-2280, Naval Air Engineering Center, October 1978.

(s) Eyre, T.S., Maynard, D., "Surface Aspects of Unlubricated Metal to Metal Wear," WEAR, 18 (1971) 301-310.

(t) "Failure Modes of Sliding Lubricated Concentrated Contacts," WEAR, 28 (1974) 95-101.

(u) "Ferrographic Lube Oil Analysis," Naval Ship Engineering Center, March 1977.

(v) Hofman, M.U., Johnson, J.H., "The Development of Ferrography as a Laboratory Wear Measurement Method for the Study of Engine Operating Conditions on Diesel Engine Wear," WEAR, 44 (1977) 183-199.

(w) Hogmark, S., Vingsbo, O., Fridstrom, S., "Mechanisms of Dry Wear of Some Martensitic Steels," WEAR, 31 (1975) 39-61.

(x) Howard, P.L., "Shock Pulse Instrumentation," Mechanical Failures Prevention Group 14th Meeting, 40-43, 1971.

(y) Johnson, J.H., "Monitoring of Machine Wear by Used Oil Analysis," MIT Conference - Fundamentals of Tribology, June 1978.

(z) Jones, W.R., Jr., "Ferrographic Analysis of Wear Debris from Boundary Lubrication Experiments with a Five Ring Polyphenyl Ether," NASA Technical Note NASA TND-7804. Lewis Research Center, Cleveland, Ohio.

(aa) Leonard, L., et al, "Analysis of Sliding Wear in a Test Diesel Engine," Naval Air Engineering Center, Final Report, Contract N00156-73-C-0764, Franklin Institute Research Laboratories Report, 1975.

(bb) Leonard, L., et al, "Structural Studies of Bearing Steel Undergoing Cyclic Stressing," Office of Naval Research, Final Summary Report, Contract Nonr 4433 (00), SKR Report AL70C005, 1970.

(cc) Maciejewski, A.S., "Oil Analysis Aspects of Tribology," Fluid Power Research Conference, 1979.

(dd) Mayer, T.C., et al, "Field Evaluation of Shock Pulse Technique to UH-1 Series Helicopters," Final Report, Contracts Nos. BOA DAAJ01,72-A-0027 and DO DAAJ01-72-A-0027-0002, June 1974.

(ee) "Mechanical Failure Prognosis Through Oil Debris Monitoring," USAAMRDL-TR-74-100, Exxon Research and Engineering Company, Linden, New Jersey, January 1975.

(ff) "Metallurgical Analysis of Wear Particles and Wearing Surfaces," Metallurgy Division, National Bureau of Standards, Washington, D.C., May 1975.

(gg) Middleton, J.L., Westcott, V.C., Wright, R.W., "Short Communication - The Number of Spherical Particles Emitted by Propagating Fatigue Cracks in Rolling Bearings," WEAR, 30 (1974) 275-277.

(hh) "Minutes of the Second Oil Analysis Project Quarterly Meeting," Naval Air Engineering Center, Philadelphia, Pennsylvania, October 1973.

(ii) "Navy Oil Analysis Program - Wear Mode Terminology Meeting," Franklin Institute Research Laboratories, January 1974.

(jj) "Oil Analysis Program," First Quarterly Report, Contract N00150-74-C-1682, Trans-Sonics, Inc., August 1974.

(kk) Oil Analysis Program Gear Bench Testing," Naval Air Propulsion Test Center, NAPTC-PE-90, Trenton, New Jersey, August 1976.

(ll) "Oil Analysis Program," Second Quarterly Report, Contract N00150-74-C-1682, Trans-Sonics, Inc., December 1974.

(mm) "Oil Analysis Project Quarterly Summary," Naval Air Engineering Center, Philadelphia, Pennsylvania, February 1974.

(nn) "Oil Analysis Project Semi-Annual Summary, A/T A3400000/051B/5F 53537401, Naval Air Engineering Center, Philadelphia, Pennsylvania, November 1974.

(oo) Palmgren, A., "Ball and Roller Bearing Engineering," SKF Industries, Inc., 1959.

(pp) Quinn, T.F.J., Wooley, J.L., "The Unlubricated Wear of 3% Cr - ½% Mo Steel," Lubrication Engineering, 26, 1970.

(qq) Reda, A.A., "A Note on the Investigation of Friction Polymer Rolling Pin Formation," A Short Communication, WEAR, 32 (1975) 115-116.

(rr) Reda, A.A., Bowen, E.R., Westcott, V.C., "Characteristics of Particles Generated at the Interface Between Sliding Steel Surfaces," WEAR, 34 (1975) 261-273.

(ss) "Sample Preparation/Ferrogram Procedure/Ferrogram Analysis," Report NAEC-MISC-92-0458, Naval Air Engineering Center, Philadelphia, Pennsylvania, August 1980.

(tt) Scott, D., Mills, G.H, "Debris Examination in the SEM: A Prognostic Approach to Failure Prevention," Proceedings of the Workshop on Failure Analysis and the SEM, IIT Research Institute, Chicago, Illinois, April 1974.

(uu) Scott, D., Seifert, W.W., Westcott, V.C., "Ferrography - An Advanced Design Aid for the 80's," WEAR, 34 (1974) 251-260.

(vv) Scott, D., Seifert, W.W., Westcott, V.C., "The Particles of Wear," SCIENTIFIC AMERICAN, Volume 230, No. 5, 88-97, May 1974.

(ww) Seifert, W.W., Westcott, V.C., "A Method for the Study of Wear Particles in Lubricating Oil," WEAR, 21, No. 1,.27-42.

(xx) Seifert, W.W., Westcott, V.C., "Investigation of Iron Content of Lubricating Oil Using Ferrograph and Emission Spectrometer," WEAR, 23, No. 2, 239-249.

(yy) Senholzi, P.B., "Oil Analysis/Wear Particle Analysis," Mechanical Failures Prevention Group, 1977.

(zz) Senholzi, P.B., "Oil Analysis/Wear Particle Analysis II," Institute of Mechanical Engineers, 1978.

(aaa) Senholzi, P.B., "System Health Monitoring Through Wear Particle Analysis," Mechanical Failures Prevention Group, October 1979.

(bbb) Senholzi, P.B., "Technical Approach to the Exploratory Development Oil Analysis Program," Naval Air Engineering Center, 1973.

(ccc) Senholzi, P.B., "Tri Service R&D Oil Analysis Program - Background, Description, and Results," Fluid Power Research Conference, October 1975.

(ddd) Senholzi, P.B., "Tri Service Oil Analysis R&D Program," Mechanical Failures Prevention Group, 1975.

(eee) Senholzi, P.B., Bowen, C.R., "Oil Analysis Research," National Conference on Fluid Power, October 1976.

(fff) Skerkat, M., "Spectrographic Oil Analysis Program at American Airlines," ATA Nondestructive Testing Forum, September 1977.

(ggg) "Studies of the Nature of Wear," Trans-Sonics, Inc., October 1974.

(hhh) Suh, N.P., "The Delamination Theory of Wear," WEAR, 25 (1973) 111-124.

(iii) "Technical Approach to the Exploratory (Cat. 6.2 R&D) Development Oil Analysis Program, " Naval Air Engineering Center, Philadelphia, Pennsylvania, January 1973.

(jjj) "The Investigations and Interpretation of the Nature of Wear Particles," Final Report, Contract NOOO14-73-C-0455, Foxboro/Trans-Sonics, Inc., March 1974.

(kkk) "Tribology Laboratory Analysis Report Twin Agent Unit 3, A/S 32, P16 Gearbox and Hydraulic Samples," Naval Air Engineering Center, Philadelphia, Pennsylvania, September 1977.

(lll) Tri Service Oil Analysis Research and Development Program, Report NAPTC-PE-90, Naval Air Engineering Center, Lakehurst, New Jersey, May 1976.

(mmm) "Wear Debris Analysis of Grease Lubricated Ball Bearings," Final Report NAEC-92-152, Naval Air Engineering Center, 1981.

(nnn) "Wear In Fluid Power Systems," Final Report ONR CR169-004-2, Contract NOOO14-75-C-1157, Fluid Power Research Center, June 1979.

(ooo) "Wear Particle Analysis of Grease Samples," Report NAEC-92-129, Contract N68335-76-C-2281, Naval Air Engineering Center, April 1979.

(ppp) "Wear Particle Formation Mechanisms," Annual Report, Massachusetts Institute of Technology (Koba, H., Cook, N.H.), May 1974.

(qqq) Westcott, V.C., "Ferrographic Oil and Grease Analysis as Applied to Earth-moving Machinery," presented at Earthmoving Industry Conference, Central Illinois Section, Peoria, Illinois, April 1975.

(rrr) Westcott, V.C., "Predicting and Determining Failures by Means of Ferrography," Paper given at Ninth Annual FAA International Aviation Maintenance Symposium, Washington, D.C.

(sss) Westcott, V.C., et al, "Oil Analysis Program," Final Report, Contract NOO156-74-C-1682, Naval Air Engineering Center, Foxboro/Trans-Sonics, Inc. Report, Revised November 1975.

(ttt) Westcott, V.C., Wright, R.W., and Succi, G.P., "Survey of Wear Processes and Particles from Wear by Means of a Ferrograph, Final Report, Contract NOOO14-72-C-0278, October 1972.

This page left blank

intentionally.

APPENDIX A
SLIDING CONTACT TEST SEQUENCE "SB"
FERROGRAPH DATA

NAEC-92-153

FERROGRAM ANALYSIS REPORT

Ferrogram No.: 182 Date: 5/20/75

Organization: Franklin Institute Sample No.: 4304

Equip. Type: 1-cyl. diesel (SB) Serial No.: Operating Time: Break in

Sample Date: Oil Type Time on Oil:

Replenishment Data: (diluted 10:1)

Volume of Sample passed along Ferrogram 2.0 cc

	Entry	54mm	50mm	10mm
Ferrogram Reading (% area covered)	29.2	19.5	15.3	1.4

Volume of Entry 1.15×10^6 um^3 Height of Entry Deposit 11 um

Types of Particles	None	Few	Moderate	Heavy
Normal Rubbing Wear			X	
Fatigue Chunks (Typical gear surface fatigue)		X		
Spheres (fatigue cracks in rolling bearings)	X			
Laminar Particles (gears or rolling bearings)	X			
Severe Wear Particles		X		
Cutting Wear Particles (high unit pressure)		X		
Corrosive Wear Particles	X			
Oxides Particles (includes rust)		X		
Dark Metallo-oxide Particles (typical hard steels)		X		
Non-ferrous Metallic			X	
Non-metallic, Crystalline		X		
Non-metallic, Amorphous (i.e. friction polymer)	X			

Considered Judgement of Wear Situation

Very Low	Normal	Caution	Very High (Red Alert)

Emission Spectrometer PPM

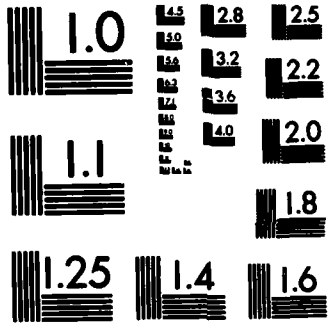
Al	Fe	Cr	Ag	Cu	Sn	Mg	Ti	Ni	Si

Comments: The entry deposit located at 56.5mm, contains rubbing wear, fatigue particles and oxides. The nonferrous metallic particles are bright white and some of them show signs of severe wear.

AD-A122 156 OIL ANALYSIS(U) NAVAL AIR ENGINEERING CENTER LAKEHURST 6/6
NJ SUPPORT EQUIPMENT ENGINEERING DEPT P B SENHOLZI
23 AUG 82 NAEC-92-153

UNCLASSIFIED F/G 11/8 NL





MICROCOPY RESOLUTION TEST CHART
NATIONAL BUREAU OF STANDARDS-1963-A

FERROGRAM ANALYSIS REPORT

Ferrogram No.: 183 Date: 5/20/75

Organization: Franklin Institute Sample No.: 4308

Equip. Type: 1-cyl. diesel (SB) Serial No.: Operating Time: 1 hr 50 min.

Sample Date: Oil Type Time on Oil:

Replenishment Data: (diluted 10:1)

Volume of Sample passed along Ferrogram _____ cc

	Entry	54mm	50mm	10mm
Ferrogram Reading (% area covered)	21.3	27.2	16.1	3.4

Volume of Entry $.69 \times 10^6$ um^3 Height of Entry Deposit 9 um

Types of Particles	None	Few	Moderate	Heavy
Normal Rubbing Wear			X	
Fatigue Chunks (Typical gear surface fatigue)		X		
Spheres (fatigue cracks in rolling bearings)	X			
Laminar Particles (gears or rolling bearings)	X			
Severe Wear Particles	X			
Cutting Wear Particles (high unit pressure)		X		
Corrosive Wear Particles	X			
Oxides Particles (includes rust)		X		
Dark Metallo-oxide Particles (typical hard steels)	X			
Non-ferrous Metallic		X		
Non-metallic, Crystalline	X			
Non-metallic, Amorphous (i.e. friction polymer)	X			

Considered Judgement of Wear Situation

	Very Low		Normal		Caution		Very High (Red Alert)

Emission Spectrometer PPM

Al	Fe	Cr	Ag	Cu	Sn	Mg	Ti	Ni	Si

Comments: The entry deposit, located at 55.1mm, contains rubbing wear, cutting wear and fatigue particles. Many of the rubbing wear particles from the shear mixed layer range in size up to 10um on the side. Some of the steel particles show evidence of high temperature at the wearing surface. The nonferrous metallic particles are bright white (silver) in color.

NAEC-92-153

FERROGRAM ANALYSIS REPORT

Ferrogram No.: 184 Date: 5/21/79

Organization: Franklin Institute Sample No.: 4319

Equip. Type: 1-cyl. diesel (SB) Serial No.: Operating Time: 17 hr. 35 mt

Sample Date: Oil Type Time on Oil:

Replenishment Date: (diluted 10:1)

Volume of Sample passed along Ferrogram ____ cc

	Entry	34mm	50mm	10mm
Ferrogram Reading (% area covered)	45.1	26.6	22.3	7.1

Volume of Entry 2.44×10^6 um^3 Height of Entry Deposit 15 um

Types of Particles	None	Few	Moderate	Heavy
Normal Rubbing Wear				X
Fatigue Chunks (Typical gear surface fatigue)		X		
Spheres (fatigue cracks in rolling bearings)	X			
Laminar Particles (gears or rolling bearings)	X			
Severe Wear Particles		X		
Cutting Wear Particles (high unit pressure)		X		
Corrosive Wear Particles	X			
Oxides Particles (includes rust)		X		
Dark Metallo-oxide Particles (typical hard steels)	X			
Non-ferrous Metallic			X..	
Non-metallic, Crystalline		X		
Non-metallic, Amorphous (i.e. friction polymer)				

Considered Judgement of Wear Situation

	Very Low		Normal		Caution		Very High (Red Alert)

Emission Spectrometer PPM

Al	Fe	Cr	Ag	Cu	Sn	Mg	Ti	Ni	Si

Comments: The entry deposit, located at 56.6mm, contains rubbing wear particles, cutting wear particles, severe wear particles and some fibrous particles. The rubbing wear particles range in size up to 15 um on the side and many show evidence of high temperature at the wearing surface. The nonferrous metallic particles are very thin (typically 1um thick) and they are bright white (silver).

FERROGRAM ANALYSIS REPORT

Ferrogram No.: 185 Date: 5/21/75

Organization: Franklin Institute Sample No.: 4323

Equip. Type: 1 cyl. diesel (SB) Serial No.: Operating Time: 33 hr. 25 min

Sample Date: Oil Type Time on Oil:

Replenishment Data: (dilute 10:1)

Volume of Sample passed along Ferrogram ____ cc

	Entry	54mm	50mm	10mm
Ferrogram Reading (% area covered)	23.4	20.0	16.6	7.0

Volume of Entry 0.84×10^6 um^3 Height of Entry Deposit 10 um

Types of Particles	None	Few	Moderate	Heavy
Normal Rubbing Wear			X	
Fatigue Chunks (Typical gear surface fatigue)	X			
Spheres (fatigue cracks in rolling bearings)	X			
Laminar Particles (gears or rolling bearings)	X			
Severe Wear Particles		X		
Cutting Wear Particles (high unit pressure)		X		
Corrosive Wear Particles	X			
Oxides Particles (includes rust)		X		
Dark Metallo-oxide Particles (typical hard steels)		X		
Non-ferrous Metallic			X	
Non-metallic, Crystalline		X		
Non-metallic, Amorphous (i.e. friction polymer)		X		

Considered Judgement of Wear Situation

	Very Low		Normal		Caution		Very High (Red Alert)

Emission Spectrometer PPM

Al	Fe	Cr	Ag	Cu	Sn	Mg	Ti	Ni	Si

Comments: The entry deposit, located at 55.1 mm, contains rubbing wear particles; cutting wear particles, oxides and severe wear particles. Many of the rubbing wear particles show evidence of high temperatures at the wearing surface.

NAEC-92-153

FERROGRAM ANALYSIS REPORT

Ferrogram No.: 186 Date: 5/21/75

Organization: Franklin Institute Sample No.: 4325

Equip. Type: 1 cyl diesel (SR) Serial No.: Operating Time: 48 hr. 25 min

Sample Date: Oil Type Time on Oil:

Replenishment Data: (dilute 10:1)

Volume of Sample passed along Ferrogram _____ cc

Ferrogram Reading (% area covered)	Entry	54mm	30mm	10mm
	37.0	21.5	21.2	8.4

Volume of Every 1.99×10^6 um^3 Height of Entry Deposit 15 um

Types of Particles	None	Few	Moderate	Heavy
Normal Rubbing Wear			X	
Fatigue Chunks (Typical gear surface fatigue)	X			
Spheres (fatigue cracks in rolling bearings)	X			
Laminar Particles (gears or rolling bearings)	X			
Severe Wear Particles	X			
Cutting Wear Particles (high unit pressure)		X		
Corrosive Wear Particles	X			
Oxides Particles (includes rust)		X		
Dark Metallic-oxide Particles (typical hard steels)		X		
Non-ferrous Metallic			X	
Non-metallic, Crystalline		X		
Non-metallic, Amorphous (i.e. friction polymer)	X			

Considered Judgement of Wear Situation

	Very Low		Normal		Caution		Very High (Red Alert)

Emission Spectrometer PPM

Al	Fe	Cr	Ag	Cu	Sn	Mg	Ti	Ni	Si

Comments: The entry deposit, located at 56.2 mm contains rubbing wear particles, cutting wear particles, a bright white nonmagnetic particle and oxides. Many of the rubbing wear particles show evidence of high temperatures (blue).

FERROGRAM ANALYSIS REPORT

Ferrogram No.: 187 Date: 5/21/75

Organization: Franklin Institute Sample No.: 4329

Equip. Type: 1 cyl. diesel (SB) Serial No.: Operating Time: 63 hr. 55 min

Sample Date: Oil Type Time on Oil:

Replenishment Data: (dilute 30:1)

Volume of Sample passed along Ferrogram ____ cc

	Entry	54mm	30mm	10mm
Ferrogram Reading (% area covered)	35.3	22.2	23.3	12.8

Volume of Entry 2.79×10^6 um^3 Height of Entry Deposit 22 um

Types of Particles	None	Few	Moderate	Heavy
Normal Rubbing Wear			X	
Fatigue Chunks (Typical gear surface fatigue)	X			
Spheres (fatigue cracks in rolling bearings)	X			
Laminar Particles (gears or rolling bearings)	X			
Severe Wear Particles		X		
Cutting Wear Particles (high unit pressure)		X		
Corrosive Wear Particles	X			
Oxides Particles (includes rust)		X		
Dark Metallo-oxide Particles (typical hard steels)		X		
Non-ferrous Metallic		X		
Non-metallic, Crystalline		X		
Non-metallic, Amorphous (i.e. friction polymer)	X			

Considered Judgement of Wear Situation

	Very Low		Normal		Caution		Very High (Red Alert)

Emission Spectrometer PPM

Al	Fe	Cr	Ag	Cu	Sn	Mg	Ti	Ni	Si

Comments: The entry deposit, located at 56.0 mm, contains rubbing wear particles, cutting wear and severe wear particles. Some of the rubbing wear particles show evidence of high temperatures (blue).

NAEC-92-153

FERROGRAM ANALYSIS REPORT

Ferrogram No.: 188 Date: 5/21/75

Organization: Franklin Institute Sample No.: 4337

Equip. Type: 1 cyl. diesel (SB) Serial No.: Operating Time: 95 hr. 50 min

Sample Date: Oil Type Time on Oil:

Replenishment Date: (dilute 10:1)

Volume of Sample passed along Ferrogram ____ cc

	Entry	54mm	90mm	10mm
Ferrogram Reading (% area covered)	30.2	40.8	39.7	22.5

Volume of Entry 2.17×10^6 um^3 Height of Entry Deposit 20 um

Types of Particles	None	Few	Moderate	Heavy
Normal Rubbing Wear			X	
Fatigue Chunks (Typical gear surface fatigue)	X			
Spheres (fatigue cracks in rolling bearings)	X			
Laminar Particles (gears or rolling bearings)	X			
Severe Wear Particles		X		
Cutting Wear Particles (high unit pressure)		X		
Corrosive Wear Particles	X			
Oxides Particles (includes rust)		X		
Dark Metallo-oxide Particles (typical hard steels)		X		
Non-ferrous Metallic			X	
Non-metallic, Crystalline		X		
Non-metallic, Amorphous (i.e. friction polymer)	X			

Considered Judgement of Wear Situation

	Very Low		Normal		Caution		Very High (Red Alert)

Emission Spectrometer PPM

Al	Fe	Cr	Ag	Cu	Sn	Mg	Ti	Ni	Si

Comments: The entry deposit, located at 55.0 mm, contains rubbing wear particles, cutting wear particles and oxides. Many of the rubbing wear particles show evidence of high temperatures at the wearing surface. Many of the bright white nonmagnetic particles are fatigue particles.

APPENDIX B
NAVAL AIR ENGINEERING CENTER
TRIBOLOGY LABORATORY
LUBRICANT SAMPLING PROCEDURE

NAEC-92-153

30 Sept. 1977

Naval Air Engineering
Center Tribology Laboratory
Lubricant Sampling Procedure

Introduction:

In order to establish the operating conditions and health of machines by the analysis of the particulate matter in their lubricating fluid, it is essential that the lubricant sample contain a representative cross section of particles. Since the particulate matter exists as a separate phase in the fluid, it cannot be assumed that a uniform distribution exists throughout the oil. Consequently, careful attention must be given to the method of sample extraction.

Scope:

To detail and standardize the procedure to be utilized in obtaining an equipment lubricant sample required for wear particle analysis.

Purpose:

To ensure that a representative lubricant sample be obtained for wear particle analysis.

Sample Container:

The sample container should be a clean glass bottle with a plastic cap containing a teflon seal/liner. The use of plastic bottles should be avoided due to their reaction with some lubricants. A standard SOAP sample bottle is recommended for use as a suitable container. If a recleaned bottle is not available, bottle cleaning can be accomplished by the following steps: Wash, rinse, wash, dry, and cap.

Sample Volume:

A sample volume of 100 ml should be withdrawn from the system for analysis. If as a result of the lubricant system design, this volume is impractical, the largest practical volume should be obtained. The sample volume should never be less than 15 ml. The withdrawn sample volume should be immediately replaced by an equal volume of clean compatible lubricant.

Sampling Interval:

The sampling interval will be a function of monitored equipment type and respective operating parameters. These factors will be analyzed by the NAEC Laboratory in each monitoring case and an applicable sample interval will be defined.

Sampling Technique:

The lubricant sample should be taken during equipment operating (after a "warm-up" period) or shortly after shutdown. A sample should never be taken more than one hour after shutdown. These measures serve to minimize the settling effect of particles in the lubricant.

Lubricant samples are withdrawn from a system by one of three basis tech niques; filler sampling, drain sampling, and valve sampling. For the sake of continuity, samples should be withdrawn utilizing the same technique and location throughout an equipment monitoring effort. The sample volume should never exceed 80% of the total sample container volume.

A. Filler Sampling

This technique involves inserting a sampling tube into the lubricant from the top of the sump. The tube should be extended into the lubricant a distance of at least half of the sump lubricant depth, but not more than one inch from the sump bottom. This location insures a representative sample and eliminates sampling sludge from the sump bottom. Once inserted, the lower end of the tube should be allowed to fill with lubricant. Upon filling, the upper tube end should be closed in order to hold the lubricant and the tube withdrawn. The resulting trapped lubricant can then be drained into the sample bottle. This procedure should be repeated until a desired sample volume is collected. Plastic or glass sampling tubes can be used according to the application. Sampling tube cleanliness is essential and should be checked before each sample is taken. If visually contaminated, the sampling tube should be flushed with filtered freon until the contamination is removed. Cap the sample bottle immediately after sampling.

B. Drain Sampling

This technique involves obtaining a sample from the bottom of the lubricant sump. The drain outlet in the sump should be opened and lubricant should be allowed to flow out (approximately 1/2 pint) in order to wash out any accumulated sediment. Once this wash out procedure has been accomplished, a sample bottle can be filled from the drain flow. Upon filling the bottle the drain should be reclosed. Cap the sample bottle immediately after sampling.

C. Valve Sampling

This technique involves the utilization of a permanently installed sampling valve. When using this technique, enough lubricant must be drained from the valve before sampling to thoroughly flush the sampling line. This flush volume will vary with respect to the sampling port design. As a general guide, the dead volume of lubricant in the sample system should be estimated and approximately twice that volume extracted before the actual sample is taken. Upon completion of the sampling process, immediately close the sampling valve and cap the sample bottle.

Sample Data:

In order to thoroughly and effectively perform an analysis on a lubricant sample, a comprehensive set of background information must be submitted with the sample. The following information is required:

A. Activity

- Name
- Address
- Code
- Contact Personnel
  - a. Responsible Party
  - b. Sampler
    Phone No./Autovon

B. Equipment

- Type (component)
- Model
- End Item
- Serial Number
- Operating Parameters
- Operating Environment
- Wear Components (lubricated)
- Wear Materials (vs. wear components)
- Time on Equipment (mileage/hours)
- Time Since Overhaul
- Recent Maintenance Actions

C. Lubricant

- Type
- Specification
- Capacity
- Additives
- Time Since Filter Change
- Time Since Lubricant Change
- Lubricant Added Since Change/Time
- Filter Size
  - a. Nominal Rating
  - b. Absolute Rating
- Filter Type

D. Sample

- Date/Time
- Number
- Technique
- Location with Respect to Filter
- Sample Frequency
- Time After Shutdown

E. Observations/Comments

Sample Packaging:

The top of each sample bottle should be securely tightened and sealed with teflon tape to prevent loosening and leakage. Bottles should be plainly labeled for correlation with respective data sheets. Care should be taken in bottle packaging in order to prevent breakage during shipment. Data sheets should be shipped with samples in a waterproof pouch to protect them from possible lubricant spills and leakage.

Sample Storage:

If a sample is to be stored for an extended period before shipment or analysis (more than a week), proper storage procedures must be followed. The sample/samples must be stored in a cold environment (approximately 0°F). Low temperatures will serve to retard any chemical reactions that may occur in the lubricant sample.

Extraneous Contamination:

Two main sources of possible contamination not previously mentioned are lubricant contamination and residual contamination. Each of these sources can seriously effect wear particle analysis and as such their effect must be minimized.

A. Lubricant Contamination:

This type of contamination is introduced into a system by the lubricant itself. Samples submitted to NAEC should be accompanied by an unused lubricant sample obtained from the same lubricant batch as that used in the equipment. This sample will be utilized to establish the baseline level of contamination contributed by the lubricant. This baseline will be taken into consideration during the analysis process.

B. Residual Contamination:

This type of contamination is introduced into the system by initial assembly of the equipment or by maintenance actions performed on the equipment. In the case of test equipment, residual/cross-contamination could carry over from previous test runs. This residual contamination effect can be minimized by proper flushing of the lubrication system before initial startup, after pertinent maintenance actions, and between selective test runs. Three flushes using clean lubricant, or a combination of appropriate solvents and clean lubricant, are sufficient to purge the lubricant system of the major portion of residual contamination.

References:

A. Wear Particle Atlas, Naval Air Engineering Center, 1976.

B. Navy Oil Analysis Program, NAVMAT INST 4731.1, 1972.

This page left blank

intentionally.

GLOSSARY OF TERMS

A. Participation in the Oil Analysis Program involved numerous organizations and numerous technical disciplines. While there are some differences in wear terminology between industries and disciplines, it is important for the purposes of this program to have a common set of terms by which various observers in the field can describe surface damage. In this classification system, the emphasis is placed on that type of damage which produces particles found in the lubricating oil. Normal wear occurs on all working surfaces and produces particles found in oil. After initial run-in, this wear may reach a stabilizing condition which does not alter the life or operating characteristics of the part. However, there will be particles found in the oil and the surfaces are modified.

B. It is generally accepted that there are four general classifications of surface damage, depending on the initiating cause. The following outline, followed by detailed descriptions, is a suggested list of surface damage classification.

1. Abnormal Wear

    a. Abrasion
    b. Corrosion
    c. Fretting Corrosion
    d. Scoring or Scuffing of Gear Tooth Surfaces
    e. Smearing
    f. Bearing Cage Wear

2. Fatigue

    a. Spalling
    b. Surface Distress: glazing, frosting, fine crack formation, surface flaking or peeling

3. Plastic Flow

   a. Rolling and peening, rippling and ridging of gear teeth
   b. Brinnelling of bearing surfaces

4. Gross Failure of the Part

   a. Fracture due to fatigue
   b. Cracking due to improper heat treat
   c. Cracking due to overload
   d. Case crushing
   e. Burnout

C. ABNORMAL WEAR. This is considerd to be surface damage, deterioration or a change in geometry to such an extent that life is shortened and the functioning of the part is impaired. The common causes are:

1. ABRASION. This is damage due to the intrusion of foreign particles between contacting surfaces. The size of the particles is greater than the separating oil film. Hardness of the particles has a great influence on the damage done. The damaging particles could have initiated at another failure location and be transported by the oil to the surfaces being observed. Analysis of the type of contaminant may determine this. The surfaces appear roughened and dented. A bearing or a set of gears may have excessive play.

2. CORROSION. This usually refers to attack of the surface by acids, moisture, lubricant contamination, or the use of overly active EP additives. It is very closely involved with the quality of the lubricant. Deterioration of the lubricant, because of high temperature, produces chemicals which attack metal. The surfaces have a pitted, rusted, and a generally discolored appearance.

3. FRETTING CORROSION. This type of damage will usually be found under conditions of severe vibration, poor lubrication, or absence of rotation. Slight relative movement with metal-to-metal contact will cause abrasion and oxidation

of the metal. This not only produces particles but causes surface wear. On bearing surfaces, it is sometimes called false brinnelling because the wear pattern produced on the raceway by the rolling element resembles that of a brinnelled surface. The most common location is on fitted surfaces such as between a bearing bore and its shaft seat or between the bearing outside diameter and its housing. Improper fitting can cause slight relative movement which initiates fretting. The condition becomes progressive as wear produces more looseness. A fretted surface will usually be rusted and discolored.

4. SCORING OR SCUFFING OF GEAR TEETH. A common type of gear damage characterized by long radial lines. It is attributed to the momentary welding and tearing of metal as two surfaces slide past each other. Since it can only occur during metal-to-metal contact, an inadequate lubricant film strength must also exist. Therefore, poor viscosity due to a momentary high temperature rise during mesh as well as surface finish and gear tooth geometry variation are all considered contributing factors. Because it occurs during sliding motion, the originating points are likely to be at the gear tip and pinion root, the pinion tip and gear root and highest and lowest point of pinion single tooth contact.

5. SMEARING. This type of damage is closely akin to gear tooth scoring since it involves metal-to-metal contact during sliding motion. There is a momentary welding and transferral of metal from one surface to another or to a new location. In bearings, it is usually attributed to skidding of rolling elements on raceway surfaces. Besides being smeared, the metal surfaces are also glazed and there may be light heat discoloration. Skidding occurs when there are inadequate tractive forces to overcome the inertial forces of rolling elements causing loss of rolling contact. Examples are high-speed, lightly loaded, angular contact ball bearings and lightly, non-uniformly loaded roller bearings. In other cases, there is always sliding motion such as at tapered roller bearing cone flanges. In every case, inadequate lubricant film strength is a contributing factor.

6. BEARING CAGE WEAR. Excessive cage wear usually occurs in the cage pockets or on the land riding surfaces. In the pockets, considerable force may be generated by differences in motion of the cage and the rolling elements. Wear on the land riding surfaces is usually due to inadequate lubrication during sliding motion. Cage surfaces will wear faster because they are softer. In many cases, they are made of brass or bronze, and therefore, nonferrous contamination will be found in the oil. When debris and other foreign metal are present, they will embed themselves in the cage material and then cause wear of the harder steel surfaces.

D. FATIGUE

1. When contacting surfaces are subjected to repeated cycles of stress, they will eventually fail in fatigue. This will occur even with proper lubrication, handling, cleanliness, mounting, and operating conditions. While both gear and bearing surfaces are subjected to fatigue, it is much more likely to occur on bearing surfaces because they usually experience much higher contact stresses and undergo many more stress cycles. Fatigue damage results in a loss of material from the surfaces. Although the fatigue life of no one bearing can be predicted, the bearing industry has done extensive research into the statistical dispersion of fatigue failures and have developed formulas relating fatigue life to load, speed, and bearing geometry. The most commonly accepted explanation is that a fatigue crack originates below the surface at a nonmetallic weak point and is influenced by the maximum shear stress and the depth at which it occurs. It is also possible for a fatigue crack to originate at the surface and travel below it. Lubrication is recognized to play a major role in the type of fatigue failure observed. When a lubricating film of sufficient strength exists so that complete separation of surfaces occurs, fatigue is usually of subsurface origin and results in a spall of some depth into the surface. Inadequate lubrication, in which metal-to-metal contact results, causes a surface distress type of fatigue failure. These then are the two categories of fatigue failure:

a. Spalling. A deep cavity produced on the working surface resulting from cracks which propagate until a piece of metal is broken off from the surface. The depth of the cavity is on the order of the depth of the max shear stress. Pitting is the term used by the gear industry to describe spalls which are usually found near the pitch line and are more likely on the pinion. The use of the work pitting in this present classification system is reserved to describe corrosive or electrical damage.

b. Surface Distress. A progressive appearance of glazing, frosting, fine crack formation, and finally, flaking or peeling of the surface. As previously mentioned, it is closely associated with bearing surface fatigue under conditions of inadequate lubrication. Under such conditions, failure will more likely be this type rather than deep spalling.

2. The occurrence of fatigue is greatly influenced by high stress concentrations such as edge loading, soft steel, and dirty steel. Improvements in these areas have lessened the incidence of fatigue failure except where lubrication distress occurs. A bearing, and especially a gear, can be expected to fail in some other manner before its fatigue limit is reached.

E. PLASTIC FLOW. This refers to surface deformation due to yielding under high stresses. Particulate matter need not necessarily accompany this form of damage, but in severe cases other wear mechanisms are also usually present and will cause particles to enter the lubricant.

1. When gear teeth undergo plastic deformation they have the appearance of being rolled and peened and having rippling and ridging lines. These terms are self descriptive.

2. Brinnelling. Flat spots or permanent dents on bearing surfaces. Permanent deformations will occur under any load but it is only when their magnitude has an influence on bearing operation and noise level do they become significant. The arbitrary design limit set for allowable denting at bearing contact point is a magnitude of less than .0001 of the rolling element diameter. It is on this basis that bearing static capacity is usually calculated.

F. GROSS FAILURE OF THE PART. Any failure which reduces the life and alters the operating conditions of a bearing or gear but does not necessarily involve the working surfaces.

1. Breakage or fracture due to fatigue. While it occurs to both gear teeth and bearing rings, fatigue fracture is more likely to happen to the former. Gear teeth fail in bending fatigue. The fracture surface is quite smooth and there is usually a focal point or eye. This can be in the form of a notch, a tear, an inclusion, or a heat treat crack. A red stain may be found in the crack because of fretting corrosion due to a slight amount of rubbing before the final break. Failure occurs near the root fillet. A tooth which fails in fatigue can initiate a series of tooth breakages because the resulting gap may cause dynamic overloading on subsequent teeth.

2. Cracking due to improper heat treatment. Improper quenching may cause excessive internal stresses which may lead to a series of hairline cracks throughout a gear tooth or bearing ring.

3. Cracking due to overload. This type of failure progresses to failure very rapidly. Like fatigue, it is more common in gear teeth than bearing rings. It may be due to shock or misalignment in which case a corner of the tooth tip is usually broken off. The fracture has a stringy appearance. There may be evidence of plastic yielding on the tooth surface. Bearing rings will crack due to excessive tensile or torsional stresses. These usually result from improper mounting such as too tight an inner ring fit on a shaft.

4. Case crushing. In carburized steel gears or bearing rings this results from a combination of too soft a core and a very heavy load. There is considerable flow and distortion of the part as the hard outside case collapses inward. In a gear tooth, it may cause shattering from the pitch line up.

5. Burnout. Thermal destruction of a part, usually a bearing, resulting from a thermal instability in which the heat generation exceeds the heat removal. The bearing undergoes various stages of discoloration, growth, seizure,

and finally softening and melting of the steel. Lubrication is usually the most significant factor in this occurrence whether it is inadequate or completely lacking. The adequacy of lubrication is influenced by load, speed, and environmental conditions. Not only must the lubricant help reduce friction but it is also the medium for transporting heat away from the part. Too much lubricant can cause thermal instability because of churning. When the lubricant itself fails, most likely due to temperature, it will leave a carbonized residue on the parts.

This page left blank

intentionally.

DISTRIBUTION LIST

NAVAIRENGCEN
- 1114 (2)
- 1115
- 9011
- 92A1C
- 92A3 (20)

NAVAIRSYSCOM
- AIR-00D4 (2)
- AIR-340E (3)
- AIR-552B
- AIR-417
- AIR-411

DTIC (12)

JOAP/TSC, PENSACOLA

AAMERADCOM, SAVDL-EV-MOR

NAVAIRDEVCEN, 3021

AFARL/LJ, WPAFB

ONR CODE 430

NAVMAT (MAT033)

REVISION LIST

REVISION	PAGES AFFECTED	DATE OF REVISION

END

FILMED

1-83

DTIC